frontiers | Research Topics

The adaptation and response of aquatic animals in the context of global climate change

Edited by
Hongsheng Yang, John I. Spicer, Juan D. Gaitan-Espitia and Da Huo

Coordinated by
Da Huo

Published in
Frontiers in Marine Science

ISSN 1664-8714
ISBN 978-2-8325-3061-0
DOI 10.3389/978-2-8325-3061-0

About Frontiers

Frontiers is more than just an open access publisher of scholarly articles: it is a pioneering approach to the world of academia, radically improving the way scholarly research is managed. The grand vision of Frontiers is a world where all people have an equal opportunity to seek, share and generate knowledge. Frontiers provides immediate and permanent online open access to all its publications, but this alone is not enough to realize our grand goals.

Frontiers journal series

The Frontiers journal series is a multi-tier and interdisciplinary set of open-access, online journals, promising a paradigm shift from the current review, selection and dissemination processes in academic publishing. All Frontiers journals are driven by researchers for researchers; therefore, they constitute a service to the scholarly community. At the same time, the *Frontiers journal series* operates on a revolutionary invention, the tiered publishing system, initially addressing specific communities of scholars, and gradually climbing up to broader public understanding, thus serving the interests of the lay society, too.

Dedication to quality

Each Frontiers article is a landmark of the highest quality, thanks to genuinely collaborative interactions between authors and review editors, who include some of the world's best academicians. Research must be certified by peers before entering a stream of knowledge that may eventually reach the public - and shape society; therefore, Frontiers only applies the most rigorous and unbiased reviews. Frontiers revolutionizes research publishing by freely delivering the most outstanding research, evaluated with no bias from both the academic and social point of view. By applying the most advanced information technologies, Frontiers is catapulting scholarly publishing into a new generation.

What are Frontiers Research Topics?

Frontiers Research Topics are very popular trademarks of the *Frontiers journals series*: they are collections of at least ten articles, all centered on a particular subject. With their unique mix of varied contributions from Original Research to Review Articles, Frontiers Research Topics unify the most influential researchers, the latest key findings and historical advances in a hot research area.

Find out more on how to host your own Frontiers Research Topic or contribute to one as an author by contacting the Frontiers editorial office: frontiersin.org/about/contact

The adaptation and response of aquatic animals in the context of global climate change

Topic editors

Hongsheng Yang — Institute of Oceanology, Chinese Academy of Sciences (CAS), China

John I. Spicer — University of Plymouth, United Kingdom

Juan D. Gaitan-Espitia — The University of Hong Kong, SAR China

Da Huo — Institute of Oceanology, Chinese Academy of Sciences (CAS), China

Topic Coordinator

Da Huo — Institute of Oceanology, Chinese Academy of Sciences (CAS), China

Citation

Yang, H., Spicer, J. I., Gaitan-Espitia, J. D., Huo, D., eds. (2023). *The adaptation and response of aquatic animals in the context of global climate change*.

Lausanne: Frontiers Media SA. doi: 10.3389/978-2-8325-3061-0

Table of contents

frontiers | Frontiers in Marine Science

TYPE Editorial
PUBLISHED 14 July 2023
DOI 10.3389/fmars.2023.1231099

OPEN ACCESS

EDITED AND REVIEWED BY
Gretchen E Hofmann,
University of California, Santa Barbara, United States

*CORRESPONDENCE
Hongsheng Yang
hshyang@qdio.ac.cn

RECEIVED 30 May 2023
ACCEPTED 29 June 2023
PUBLISHED 14 July 2023

CITATION
Huo D, Gaitán-Espitia JD, Spicer JI and Yang H (2023) Editorial: The adaptation and response of aquatic animals in the context of global climate change. *Front. Mar. Sci.* 10:1231099. doi: 10.3389/fmars.2023.1231099

Editorial: The adaptation and response of aquatic animals in the context of global climate change

Da Huo[1,2,3], Juan Diego Gaitán-Espitia[4], John I. Spicer[5] and Hongsheng Yang[1,2,3]*

[1]CAS Key Laboratory of Marine Ecology and Environmental Sciences, Institute of Oceanology, Chinese Academy of Sciences, Qingdao, China, [2]Laboratory for Marine Ecology and Environmental Science, Qingdao National Laboratory for Marine Science and Technology, Qingdao, China, [3]University of Chinese Academy of Sciences, Beijing, China, [4]The Swire Institute of Marine Science, School of Biological Sciences, The Hong Kong University, Hong Kong, Hong Kong SAR, China, [5]Marine Biology and Ecology Research Centre, School of Biological and Marine Sciences, University of Plymouth, Devon, United Kingdom

KEYWORDS

environmental stress, molecular mechanism, aquatic animal, phenotypic plasticity, adaptive evolution, stress response

Editorial on the Research Topic
The adaptation and response of aquatic animals in the context of global climate change

Anthropogenic climate change has brought on widespread changes in marine environments, including ocean warming, ocean acidification, the development and expansion of hypoxic zones. These environmental changes represent major threats to marine life, challenging the survival and adaptation of marine organisms. The adverse effects of these changes can interact in synergistic, additive or antagonistic ways (Huo et al., 2019a; Huo et al., 2019b; Small et al., 2020; Collins et al., 2021), evidencing different biological influence compared to their individual action (Huo et al., 2021a). Such influence can vary across populations and species as a consequence of differences in phenotypic plasticity and physiological tolerances shaped by their specific environmental and genetic backgrounds (Gaitán-Espitia et al., 2017a; Gaitán-Espitia et al., 2017b). These factors ultimately modulate the ecological response and evolutionary adaptation of marine organisms to climate change. From an ecological perspective, changes in the marine environment are likely to have significant negative phenotypic effects (e.g., physiology, behavior, gene/protein expression), across levels of biological organization (i.e., from individuals, populations, to species). These changes can alter the ingestion, digestion, respiration and growth of aquatic animals (Huo et al., 2018), potentially influencing demographic and genetic declines driven, for instance, by massive mortality (Huo et al., 2021b). From an adaptive evolution perspective, phenotypic plasticity appears to be a suitable strategy to cope with these changes, at least in the short-term, through behavioral,

physiological, life-history and morphological adjustments (Gaitán-Espitia et al., 2017b). However, there are limits for plastic adjustments beyond which populations and species require genetic and cellular modifications to adapt to the unfavorable environmental conditions. These adaptive responses include microevolutionary changes of transcriptional, translational and post-translational mechanisms underpinning phenotypic responses (Huo et al., 2021b). Through the study of these mechanisms, we can gain better understanding of the costs and trade-offs of adaptive evolution in marine animals under climate change.

Our aim for this Research Topic in *Frontiers in Marine Science* was to bring together studies that enhance our understanding of the potential biological, ecological and evolutionary impacts of extreme environmental changes (individual and compound) on marine animals. This Research Topic comprises 17 scientific papers, which included reviews, original research and data reports, covering diverse taxa from unicellular foraminifera to more complex multicellular animals such as bivalves (hard Clam *Mercenaria mercenaria*, eastern oyster *Crassostrea Virginica*, Yesso scallop *Patinopecten yessoensis*, Zhikong scallop *Chlamys farreri* and bay scallop *Argopecten irradians*, Chilean scallop *Argopecten purpuratus*), holothurians (sea cucumber *Apostichopus japonicus*), and fishes (e.g., silver carp *Hypophthalmichthys molitrix*, spotted sea bass *Lateolabrax maculatus*, loaches *Triplophysa bleekeri*). The main research focus of these papers was associated with changes of key environmental drivers (e.g., temperature, oxygen, pH) and stressors closely linked to global climate change (e.g., seasonal cooling, fishing, microplastics and cadmium).

One theme that emerges from this Research Topic is the importance of understanding the multiple biological levels involved in the ecological responses and adaptive evolution of marine organisms, here from genes to organismal phenotypes and population dynamics. Padilla-Gamiño et al. explored this issue by reviewing the impacts of ocean acidification on processes of sexual reproduction (e.g., gametogenesis, fertilization, and reproductive resource allocation) in five economically and ecologically important marine invertebrate groups, including cnidarians, crustaceans, echinoderms, molluscs and ascidians. They found that the fertilization rate declined as pH fell, indicating the negative impacts on future generations in the context of a rapidly changing oceans. Similar to ocean acidification, warming oceans are expected to induce detrimental effects on marine organisms. Yuan et al. found that increasing temperatures induce major metabolic reprogramming and lipid remodeling in loaches fish *Triplophysa bleekeri*, highlighting potential physiological costs induced by climate change. Another important driver modulating life in marine environments is oxygen availability. Li X. et al. demonstrated that low oxygen conditions (i.e., hypoxia stress) trigger tissue damage and changes in the immune defense and oxygen transport in the silver carp *Hypophthalmichthys molitrix*. In other fish species (e.g., spotted sea bass *Lateolabrax maculatus*), Ren et al. found that this type of environmental stress altered the HIF signal network system, suppressing the cell cycle process. Environmental drivers such as pH, temperature, and oxygen, however, do not change in isolation but co-vary among them and have interactive effects. For instance, Huo et al. showed that the immune system, digestion, and antioxidant levels in the sea cucumber *Apostichopus japonicus* were affected differently by individual and combined changes in temperature and dissolved oxygen. Similarly, Li C. et al. found that the interaction of air exposure and elevated temperatures, can ultimately influence the regulation of the cell cycle, apoptosis, and proline accumulation in the eastern oyster *Crassostrea virginica* as part of its adaptive response. The immune and apoptotic response has been also been documented in other marine animals such as scallops when limited oxygen interacts with transient heat (Mao et al.).

Although global warming is the dominant trend, there are regions in which temperatures are decreasing (e.g., upwelling areas along the East South Pacific coast). Ramajo et al. showed that populations of scallops (*Argopecten purpuratus*) in upwelling areas decreased their growth and gross calcification rates when exposed to cooling waters and low oxygen conditions. Such interactive effects directly impact traits that are relevant for the fitness and dynamics of natural populations of these marine invertebrates.

Temperature, dissolved oxygen and pH are environmental factors of great interest and discussion. In addition to those factors, global climate change has also exacerbated the effects of other stressors on marine organisms. For instance, toxic algal blooms of *Karenia mikimotoi* are more regularly impacting populations of the abalone *Haliotis discus*. These effects are exacerbated when hypoxic conditions are present, significantly reducing survival rate and the activation of oxidative stress (Zhang Y. et al.). Another important anthropogenic stressor that is more frequently documented in the literature is derived from marine and coastal pollution. Zhang C. et al. examined the effects of dietary ingestion of microplastics and cadmium in the sea cucumber *Apostichopus japonicus*, finding that the interactive exposure can lead to oxidative stress, the inflammatory response in the intestine, and the activation of the intestinal immune defense system. These studies contributed to the goal of expanding our understanding of how marine organisms respond to upcoming environmental challenges mainly from molecular and physiological aspects. The identified changes in biological processes in these studies provide fundamental information for deciphering the adaptive regulatory mechanisms employed by marine animals when exposed to environmental stress and climate change.

Another theme that emerged from this Research Topic is the importance of understanding the mechanisms underpinning adaptative evolution. As species face new and changing environments, they must evolve to avoid extinction. Hu Z. et al. emphasized the significance of heat shock protein 70 genes expansion as part of the adaptive evolutionary responses of the hard Clam *Mercenaria mercenaria* to heat and hypoxic environments. Mao et al. identified that heat shock proteins could

likely have helped in correct protein folding to aid the adaption of the scallops to the altered environment. Ren et al. suggested that alternative splicing events have been probably shaped by natural selection as part of the hypoxia adaptation in the spotted sea bass *Lateolabrax maculatus*. In addition to internal regulation at the molecular level, phenotypic change, mediated by natural selection, is also an important strategy for adaptation to environmental stress. Such phenotypic changes can show intra-specific variation due to genotype-by-environmental interactions. For example, the purple strain of the sea cucumber *A. japonicus* can tolerate a wider range of temperatures and higher salinity levels than those of the green morph (Bin et al., 2018). Yao et al. characterized the types, quantities and expression of TGFβ signaling pathway members in *A. japonicus* and provided information for pigmentation, as it is a key trait for understanding environmental adaptability and species stability. Hu W. et al. concentrated on the Oxudercinae fishes distributed in the intertidal mudflats, one of the ecosystems with the most drastic changes in salinity, temperature, and oxygen content. Hu W. et al. identified the morphological features of corneal epithelial cells as the visual adaptation mechanisms for Oxudercinae species to adjust to varied environments. Phenotypic evolution and gene regulation together enable species to better adapt to environmental stress and change.

Impacts of climate change are evident in natural systems all over the world (Gaitan-Espitia and Hobday, 2021). The studies in this Research Topic explored this context across diverse biogeographic backgrounds around the globe, from the poles to the tropics. As a result of climate change and other anthropogenic pressures, marine ecosystems have been strongly impacted, reducing their ecological stability (e.g., 75% in coral reefs globally) (Bruno and Selig, 2007; Hu et al., 2020). Zhang X. et al. used the Ecopath with Ecosim model to investigate the effects of ocean warming and fishing on the coral reef ecosystem surrounding the Xisha Islands in the South China Sea. According to their findings, ocean warming and fishing caused the overall catch to decline by 3.79% and 4.74%, respectively, by the middle of the century compared to 2009. Some groups (i.e., medium and large carnivorous fish), tend to be less affected by ocean warming when the fishing effort is reduced. Yu et al. explored the hypoxia avoidance behavior of six common reef-dependent species found in the northeastern sea areas of China (i.e., rockfishes *Sebastes schlegelii* and *Hexagrammos otakii*, filefish *Thamnacomus modestus*, flatfish *Pseudopleuronectes yokohamae*, sea cucumber *Stichopus japonicus*, and crab *Charybdis japonica*). The findings demonstrated that reduced DO levels enhanced the habitat affinity to preferred habitat types for the two habitat-specific rockfishes, decreased the usage of preferred habitats of sea cucumber and filefish, and had no effects on crab habitat usage. Similar to the tropics, the Antarctic region biota is currently facing major threats from complicated environmental changes (Convey and Peck, 2019). As Antarctic marine animals are facing a stable and limited range of low seawater temperatures (Carter et al.), slight variations in thermal environment can result in differences in the spatial distribution of species and populations (Bilyk and DeVries, 2011; Sandersfeld et al., 2017; Morley et al., 2020). Li Q. et al. presented the relationships between foraminiferal molecular diversity and environmental variables in the Antarctic region, discovering that both, water depth and temperature have distinct effects on abundant and rare foraminiferal subcommunities. Specifically, the foraminiferal alpha diversity of the most abundant subcommunity was positively correlated with water depth and negatively correlated with temperature, whereas the alpha diversity of the rarest subcommunity did not exhibit a linear relationship with any of these environmental factors. Carter et al. investigated the upper thermal limits (CTmax) of seven marine ectotherm Antarctic species (Chordata 3 spp., Arthropoda 2 spp., and Echinodermata 2 spp.) and discovered that basal mortality was influenced by seasonal temperature change in the intertidal zone, with echinoderms having greater CTmax than Chordata and Arthropod species. These papers help to our understanding of how future environmental changes will affect biodiversity from the tropics to the poles.

The study of ecological responses and adaptive evolution in marine animals facing environmental stress will unavoidably get more attention as global changes are increasing in frequency, magnitude and duration all across the globe. Each of the articles summarized in this Research Topic have made a major contribution to this area and contributed a piece of the puzzle to advance our comprehension. Moreover, this Research Topic points to new directions and highlights the many knowledge gaps that still remain to be addressed in this area of research. This Research Topic highlights the urgent need for continued investigation into these complex interactions. Future directions in this field include encouraging integrated evaluation of multiple environmental stressors, comparative multi-species research, cross-regional and cross-temporal investigations. This Research Topic also highlights that understanding the impact of climate change on aquatic animals requires interdisciplinary collaboration, including ecology, biology, genetics, oceanography, and climate science. Collaborations between researchers from different fields can provide a more comprehensive understanding of the complex interactions between climate change and aquatic ecosystems, as well as identify potential solutions and management strategies. We strongly hope that this topic will attract the attention of the broader scientific community interested in climate change biology, bringing together researchers with expertise in diverse and complementary fields.

Author contributions

All authors listed have made a substantial, direct and intellectual contribution to the work, and approved it for publication.

Funding

This work was financially supported by the National Natural Science Foundation of China (grant numbers No. 42261160378, 42106106), the Shandong Provincial Natural Science Foundation

(grant number ZR2021QD013), Postdoctoral Innovative Talents Support Program of Shandong Province (grant number SDBX2020006), Special Research Assistant Project of Chinese Academy of Sciences. JDGE was supported by the NSFC-RGC project N_HKU791/22 and the Research Grants Council (GRF 17113221) of Hong Kong.

Acknowledgments

We thank the editor Xinji Li for her help on this Research topic application, the authors for their contributions on this Research Topic, the journal for agreeing to its compilation, and the reviewers for their time and effort in improving manuscripts.

Conflict of interest

The authors declare that the research was conducted in the absence of any commercial or financial relationships that could be construed as a potential conflict of interest.

Publisher's note

References

Bilyk, K. T., and DeVries, A. L. (2011). Heat tolerance and its plasticity in Antarctic fishes. *Comp. Biochem. Physiol. Part A: Mol. Integr. Physiol.* 158, 382–390. doi: 10.1016/j.cbpa.2010.12.010

Bin, Z., Wei, H., and Chenglin, L. (2018). Effects of temperature and salinity on survival, growth, and coloration of juvenile apostichopus japonicus selenta. *Oceanologia Limnologia Sin.* 49, 700–706.

Bruno, J. F., and Selig, E. R. (2007). Regional decline of coral cover in the indo-pacific: timing, extent, and subregional comparisons. *PloS One* 2, e711. doi: 10.1371/journal.pone.0000711

Collins, M., Truebano, M., Verberk, W. C., and Spicer, J. I. (2021). Do aquatic ectotherms perform better under hypoxia after warm acclimation? *J. Exp. Biol.* 224, jeb232512. doi: 10.1242/jeb.232512

Convey, P., and Peck, L. S. (2019). Antarctic Environmental change and biological responses. *Sci. Adv.* 5, eaaz0888. doi: 10.1126/sciadv.aaz0888

Gaitán-Espitia, J. D., Bacigalupe, L. D., Opitz, T., Lagos, N. A., Osores, S., and Lardies, M. A. (2017a). Exploring physiological plasticity and local thermal adaptation in an intertidal crab along a latitudinal cline. *J. Therm Biol.* 68, 14–20. doi: 10.1016/j.jtherbio.2017.02.011

Gaitán-Espitia, J. D., and Hobday, A. J. (2021). Evolutionary principles and genetic considerations for guiding conservation interventions under climate change. *Global Change Biol.* 27, 475–488. doi: 10.1111/gcb.15359

Gaitán-Espitia, J. D., Villanueva, P. A., Lopez, J., Torres, R., Navarro, J. M., and Bacigalupe, L. D. (2017b). Spatio-temporal environmental variation mediates geographical differences in phenotypic responses to ocean acidification. *Biol. Lett.* 13, 20160865. doi: 10.1098/rsbl.2016.0865

Hu, W. J., Chen, B., Arnupap, P., Zhang, D., Liu, X. M., Gu, H. F., et al. (2020). Ecological vulnerability assessment of coral reef: a case study of Si Chang island, Thailand. *Chin. J. Ecol.* 39, 979.

Huo, D., Sun, L., Ru, X., Zhang, L., Lin, C., Liu, S., et al. (2018). Impact of hypoxia stress on the physiological responses of sea cucumber apostichopus japonicus: respiration, digestion, immunity and oxidative damage. *Peerj* 6, e4651. doi: 10.7717/peerj.4651

Huo, D., Sun, L., Sun, J., Lin, C., Liu, S., Zhang, L., et al. (2021a). Emerging roles of circRNAs in regulating thermal and hypoxic stresses in apostichopus japonicus (Echinodermata: holothuroidea). *Ecotoxicol Environ. Saf.* 228, 112994. doi: 10.1016/j.ecoenv.2021.112994

Huo, D., Sun, L., Sun, J., Zhang, L., Liu, S., Su, F., et al. (2021b). Sea Cucumbers in a high temperature and low dissolved oxygen world: roles of miRNAs in the regulation of environmental stresses. *Environ. Pollut.* 268, 115509. doi: 10.1016/j.envpol.2020.115509

Huo, D., Sun, L., Zhang, L., Ru, X., Liu, S., and Yang, H. (2019a). Metabolome responses of the sea cucumber apostichopus japonicus to multiple environmental stresses: heat and hypoxia. *Mar. Pollut. Bull.* 138, 407–420. doi: 10.1016/j.marpolbul.2018.11.063

Huo, D., Sun, L., Zhang, L., Ru, X., Liu, S., Yang, X., et al. (2019b). Global-warming-caused changes of temperature and oxygen alter the proteomic profile of sea cucumber apostichopus japonicus. *J. Proteomics* 193, 27–43. doi: 10.1016/j.jprot.2018.12.020

Morley, S. A., Abele, D., Barnes, D. K., Cárdenas, C. A., Cotté, C., Gutt, J., et al. (2020). Global drivers on southern ocean ecosystems: changing physical environments and anthropogenic pressures in an earth system. *Front. Mar. Sci.* 7, 547188. doi: 10.3389/fmars.2020.547188

Sandersfeld, T., Mark, F. C., and Knust, R. (2017). Temperature-dependent metabolism in Antarctic fish: do habitat temperature conditions affect thermal tolerance ranges? *Polar Biol.* 40, 141–149. doi: 10.1007/s00300-016-1934-x

Small, D. P., Calosi, P., Rastrick, S. P., Turner, L. M., Widdicombe, S., and Spicer, J. I. (2020). The effects of elevated temperature and p CO2 on the energetics and haemolymph pH homeostasis of juveniles of the European lobster, homarus gammarus. *J. Exp. Biol.* 223, jeb209221. doi: 10.1242/jeb.209221

frontiers | Frontiers in Marine Science

ORIGINAL RESEARCH
published: 16 May 2022
doi: 10.3389/fmars.2022.900200

Hypoxia Stress Induces Tissue Damage, Immune Defense, and Oxygen Transport Change in Gill of Silver Carp (*Hypophthalmichthys molitrix*): Evaluation on Hypoxia by Using Transcriptomics

Xiaohui Li[1,2], *Chen Ling*[1], *Qiaoxin Wang*[1], *Cui Feng*[1], *Xiangzhong Luo*[1], *Hang Sha*[1], *Guoyu He*[1], *Guiwei Zou*[1]* and *Hongwei Liang*[1,3]*

[1] Yangtze River Fisheries Research Institute, Chinese Academy of Fisheries, Wuhan, China, [2] State Key Laboratory of Developmental Biology of Freshwater Fish, College of Life Sciences, Hunan Normal University, Changsha, China, [3] Hubei Hongshan Laboratory, Huazhong Agricultural University, Wuhan, China

The silver carp (*Hypophthalmichthys molitrix*) is an economically, as well as environmentally, important fish that harbors low environmental hypoxia tolerance and frequently contributes to a loss of aquaculture productivity. The gill is the first tissue attacked by hypoxia; however, the response of the gills of *H. molitrix* to hypoxia stress at the tissue, cellular, and molecular levels has not been clearly established. The influence of hypoxia on histological features along with gene expression in silver carp gills were explored in this research. The hematoxylin and eosin-stained sections and electron microscopy examinations of gills indicated that the gill lamellae were seriously twisted, gill filaments were dehisced, and the swelling and shedding of epithelial cell layer in the gill tissue were intensified along with the degree of hypoxia. In the hypoxia, semi-asphyxia, and asphyxia groups, the gill transcriptomic assessment of shifts in key genes, as well as modulatory networks in response to hypoxic conditions revealed 587, 725, and 748 differentially expressed genes, respectively. These genes are abundant in immune response signaling cascades (e.g., complement and coagulation cascades, Nucleotide-binding and oligomerization domain (NOD)-like receptor signaling cascade, and differentiation of Th1 along with Th2 cells) and oxygen transport [e.g., MAPK, PI3K-Akt, and hypoxia-inducible factor 1 (HIF-1) signaling cascades]. Genes linked to immune response (e.g., *c2*, *c3*, *c6*, *klf4*, *cxcr4*, *cd45*, and *cd40*) and oxygen transport (e.g., *egln1*, *egln3*, *epo*, *ldh*, and *vegfa*) were additionally identified. According to our findings, the silver carp may be using "HIF-1" to obtain additional oxygen during hypoxia. These findings

OPEN ACCESS

Edited by:
Hongsheng Yang,
Institute of Oceanology (CAS), China

Reviewed by:
Shuming Zou,
Shanghai Ocean University, China
Fernando Diaz,
Center for Scientific Research and Higher Education in Ensenada (CICESE), Mexico

***Correspondence:**
Guiwei Zou
zougw@yfi.ac.cn
Hongwei Liang
lianghw@yfi.ac.cn

Specialty section:
This article was submitted to Global Change and the Future Ocean, a section of the journal Frontiers in Marine Science

Received: 20 March 2022
Accepted: 15 April 2022
Published: 16 May 2022

Citation:
Li X, Ling C, Wang Q, Feng C, Luo X, Sha H, He G, Zou G and Liang H (2022) Hypoxia Stress Induces Tissue Damage, Immune Defense, and Oxygen Transport Change in Gill of Silver Carp (Hypophthalmichthys molitrix): Evaluation on Hypoxia by Using Transcriptomics. Front. Mar. Sci. 9:900200. doi: 10.3389/fmars.2022.900200

illustrate that hypoxia stress might damage gill tissue, trigger an immunological response, and activate HIF-1 signaling to increase oxygen availability under hypoxic situations. The findings of this work will help scientists better understand the molecular mechanisms driving hypoxia responses in hypoxia-sensitive fish and speed up the development of hypoxia-resistant varieties.

Keywords: *Hypophthalmichthys molitrix*, hypoxia, gill, tissue damage, transcriptome

INTRODUCTION

Most of aerobic life on the planet need molecular oxygen to survive (Van der Meer et al., 2005). Fish interact directly with the aquatic environment, exhibiting significantly greater temporal, as well as spatial, fluctuations in oxygen contents relative to the terrestrial habitat (Zhu et al., 2013). Hypoxia is regarded as a low level of dissolved oxygen (DO) that adversely impacts fish behavioral, biochemical, and physiological activities consisting of reproduction, movement, respiration, development, and metabolism coupled with immunity (Jiang et al., 2017; Abdel-Tawwab et al., 2019). Conditions, for instance, high stocking density, organic matter buildup from unconsumed food, and feces accompanied with the blooms of algae in aquaculture habitats all contribute to the severity of the hypoxic situation (Gallage et al., 2016; Li et al., 2017). As a result, hypoxia occurs often in aquaculture, and the molecular responses of fish to hypoxic stress have generated considerable interest in recent years (Chen et al., 2017; Xia et al., 2018; Mu et al., 2020).

The silver carp is among the four main Chinese carp species that was responsible for 14.7% of total cultured freshwater fish production in 2020 alone (Yearbook, 2020). Silver carp feed on phytoplankton without additional feeding due to normal filter feeding; hence, silver carp aquaculture saves feeding costs. The silver carp has been introduced to or expanded across over 88 countries globally, not only to improve breeding benefits but also to prevent algal bloom and enhance water quality (Li et al., 2020). Nevertheless, *H. molitrix* harbors a low tolerance for hypoxia in the environment, which leads to higher pond turnover in high-density pond aquaculture (Li et al., 2021). As a result, studying the adaptive approaches of silver carp under hypoxia would be more beneficial.

Hypoxia causes fish to respond to stress in a chronic, as well as acute, manner, leading to diverse molecular, behavioral, morphological, and physiological alterations (Abdel-Tawwab et al., 2019). The principal site of gaseous exchange and the initial target in a hypoxic episode is the fish gill (Tiedke et al., 2015). The crucian carp (*Carassius carassius*) decreases the size of their inter-lamellar cell mass and exposed lamella, as well as increases the functional surface area of their gills in response to hypoxia (Sollid et al., 2003). When the fish are returned to a normoxic state, the gill structure caused by hypoxia would be changed (Sollid and Nilsson, 2006). As a result, the fish gill plays an indispensable role in the aquatic exchange of gases and may undergo dramatic remodeling as a response to variations in DO contents (Wu et al., 2017). Furthermore, the fish gill is an immune-competent organ with vast mucosal surfaces, referred to as gill-associated lymphoid tissue (Rebl et al., 2014). It is unclear how the gill of *H. molitrix* responds to hypoxic stress at the tissue, cellular, and molecular levels since it is the first tissue to be affected by hypoxia.

With its high-throughput precision coupled with reproducibility, transcriptome sequencing technology is a useful tool for studying aquatic animal growth along with development, disease-resistant immunological systems, stress physiology, and other functional processes (Zhang et al., 2009; Li and Dewey, 2011). The environmental stress adaption of various aquatic species, for instance, *Cyprinus carpio* (Xing et al., 2019), *Scylla paramamosain* (Cheng et al., 2019), *Rana chensinensis* (Ma et al., 2018), *Procambarus clarkia* (Zhang et al., 2022), and *Gambusia affinis* (Hou et al., 2019), has been studied *via* high-throughput transcriptome sequencing technology. To help comprehend the intrinsic molecular process in the response to hypoxia, the transcriptome alterations in the gill of *H. molitrix* were determined using the Illumina HiSeq 2500 sequencing technology, and the corresponding histomorphology alterations were also investigated in the current work. The findings of this research will be critical in furthering our understanding of the hypoxia adaptation mechanisms of aquatic species and in speeding up the breeding of hypoxia-resistant types. It also serves as a source of information and data for relevant studies.

MATERIALS AND METHODS

Fish Preparation and Maintenance

Healthy silver carp with a body weight of 52.86 ± 5.64 g and body length of 15.06 ± 1.23 cm were selected as the experimental fish. They were acquired from the Genetics and Breeding Center of Silver Carp, Ministry of Agriculture and Rural Affairs in Jingzhou city, Hubei province, China. The fish were introduced in a re-circulating freshwater system (with heating features and a capacity of 400 L) and given 2 weeks to acclimate before the experiment began. Throughout acclimation, the water was kept at the following parameters: 25.0 ± 0.5°C; pH, 7.5 ± 0.2; and DO, 7.0± 0.5 mg/L. Throughout the study, we maintained a natural photoperiod. The DO level was assessed *via* a DO meter (HACH, Loveland, CO, USA).

Experimental Design

Following acclimation, fish were relocated to indoor rectangular glass tanks measuring 46 cm by length, 33 cm by width, and 28 cm by height, with ten fish in every tank) and fasted for 24 h prior to the hypoxia test (**Figure 1A**). When the hypoxic stress

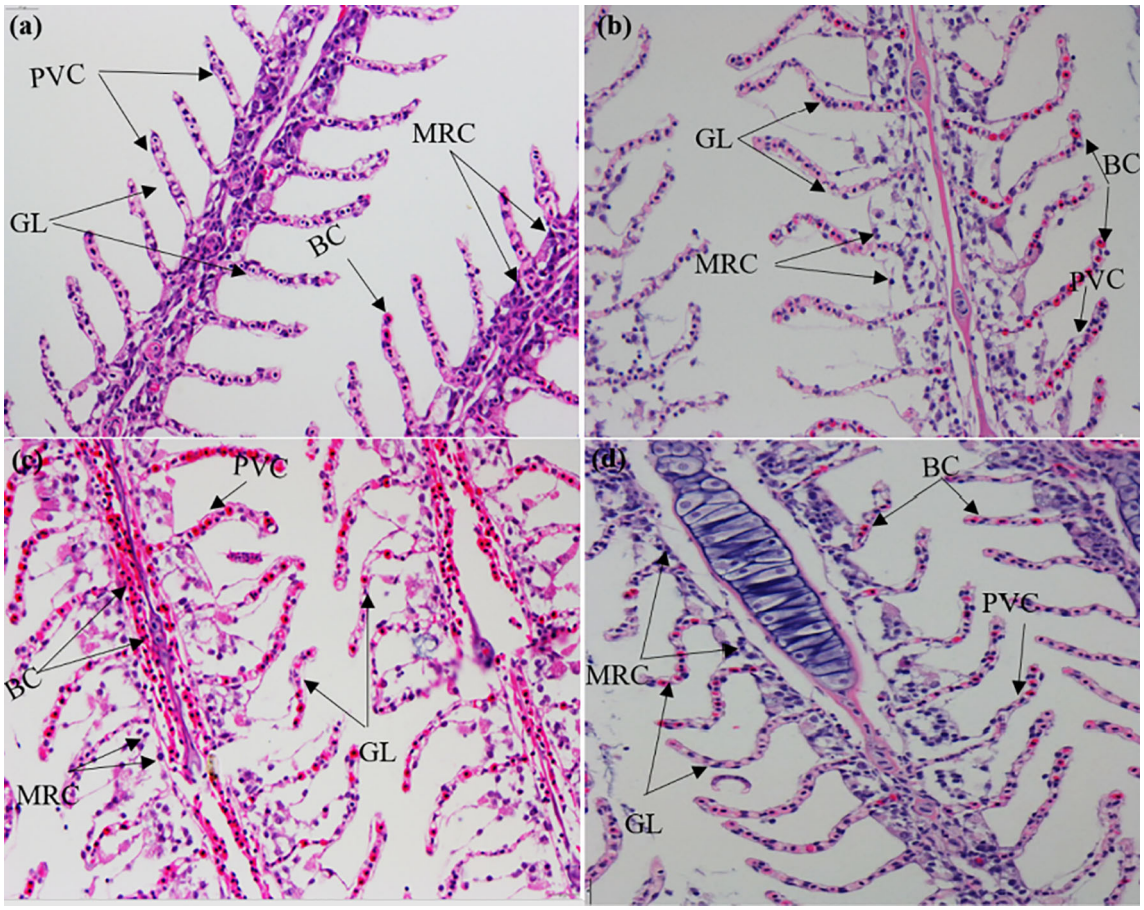

FIGURE 1 | Hematoxylin and eosin (H&E) staining of gill sections under **(A)** normoxia; **(B)** hypoxia; **(C)** demi-asphyxia; and **(D)** asphyxia stress in silver carp. GL, branch leaf; BC, blood cells; PVC, pavement cells; MRC, mitochondria-rich cells.

testing started, 12 glass tanks were employed. Three tanks of fish (n = 10) were used as the control group (CK) and were kept in normoxic conditions. The fish in the remaining nine tanks (n = 10) were deemed as the test groups (T1, T2, and T3). Hypoxia experiments were done by enclosing the water-filled tanks with plastic film, and the fish gradually consumed the oxygen in the aerated water *via* natural respiration (Chen et al., 2017; Jiang et al., 2020; Li et al., 2021) until the majority of fish attempted to breathe directly *via* their mouth (three tanks, designated as the hypoxia or T1 group, DO = 0.75 ± 0.04 mg/L), half of the fish lost their balance (three tanks, designated as semi-asphyxia or T2 group, DO = 0.58 ± 0.06 mg/L), and the other half of the fish sunk without the rhythmical opening and closing of the gill flaps (three tanks, designated as asphyxia or T3 group, DO = 0.27 ± 0.06 mg/L), similar to Feng et al. (2022).

Paraffin Section and Electron Microscopic Section

The fixed gill was dehydrated using a graded ethanol–xylol series and vacuum-embedded in paraffin. The sections (5~6 μm) of the specimens were cut and placed on polylysine-coated slides. hematoxylin and eosin (H&E) staining was done on the slices, and they were photographed under an Olympus microscope (Olympus CH2, Olympus, Japan).

Gill tissues were washed in PBS and preserved in 2.5% glutaraldehyde overnight. After being washed with PBS, the gill tissues were dehydrated using gradient alcohol (70%, 80%, 90%, 95%, and 100%) and then treated with isoamyl acetate for standard critical drying. Then, using a JEOL JSM 7800E field emission scanning electron microscopy (JEOL, Tokyo, Japan), a vacuum ion coating was applied to view and capture pictures.

Total RNA Isolation and Sequencing

The isolation of total RNA from the gills of CK, T1, T2, and T3 groups was done with the TRIzol Reagent (Invitrogen, Carlsbad, CA, USA). The processing of the complementary DNA (cDNA) along with the RNA sequencing was done at Frasergen Bioinformatics Co., Ltd (Wuhan, China), with sequencing run on the Illumina HiSeq™ 4000 system to generate 150 bp paired-end reads.

Analysis of RNA-Seq Data

The analyses of the RNA-seq data were done as documented previously (Li et al., 2021). FASTQC (v0.11.5) was employed to verify the quality of the fastq output files. Trimgalore (v0.4.3) was adopted to eliminate adapter sequences. The reads were mapped to the silver carp reference genome (unpublished data). HTSeq (v0.6.1) was utilized to produce raw counts (Anders et al., 2015). To identify DEGs (differentially expressed genes), a fold change (FC) > 2.0 along with a *P*-adjusted value < 0.05 cut-off (FDR) served as the threshold (Benjamini and Yekutieli, 2001). The R 'heatmap' package was adopted to conduct hierarchical DEG clustering. The Gene Ontology (GO) enrichment analysis along with the Kyoto Encyclopedia of Genes and Genomes (KEGG) enrichment analyses for DEGs were performed *via* the KOBAS program (v2.1.1), with a *P*-value of 0.05 signifying significant enrichment.

Real Time Quantitative PCR (RT-qPCR) Analysis

The oligonucleotide sequences of the primers are given in **Table 1**. The genes utilized to validate the RNA-seq data were the members of overlapping DEGs from CK versus T1, CK versus T2, and CK versus T3, and their primers were built using Primer 6. *B-actin* served as the control gene (Li et al., 2013; Li et al., 2016). qPCR was performed on samples that were not related to those utilized for RNA-seq. Following total RNA isolation, cDNA was synthesized using the FastKing RT Kit (TianGen, Beijing, China) and qPCR was done with a 2×SYBR Green MasterMix reagent (Takara, Kyoto, Japan) as previously documented (Zhang et al., 2022). The determination of gene expression was done *via* the $2^{-\triangle\triangle Ct}$ method (Livak and Schmittgen, 2001).

Statistical Analyses

All values were presented as SD ± mean. SPSS v15.0 (IBM Corp., USA) was used for data analyses. Before performing ANOVA, the Shapiro–Wilk test was performed to determine the normality of the data and the Levene test was used to determine the homoscedasticity of the data. When the data were homogeneous and met the normal distribution, a one-way ANOVA was used to determine the statistical differences between multiple testing, and $P < 0.05$ signified statistical significance.

RESULTS

Effect of Hypoxia Stress on Gill Tissue Structure of Silver Carp

The sections stained with H&E exhibited that the both sides of gill lamellae in the normoxia group were symmetrical and orderly arranged, the epithelial cells were flat and regularly arranged, the red blood cells (RBCs) were evenly distributed in the sinus, and the mitochondria-rich cells were elliptically distributed at the base of the lamellae (**Figure 1A**). Compared with the CK (normoxia) group, the gill tissue structure of T1 (hypoxia), T2 (semi-asphyxia), and T3 (asphyxia) groups began to be damaged in gradually lower DO. As shown in the T1 group (**Figure 1B**), the volume of cells with rich mitochondria became larger, the distribution of red blood cells was uneven, and the gill lamellae were gradually curved, thus increasing the gill respiratory area. At the T2 group (**Figure 1C**), most of the gill lamellae showed a disorder and an "S"-shape distortion, some gill filaments were dehisced in the middle, the RBCs in the blood sinuses were not uniformly distributed and piled up, and the phenomenon of cavitation was common. At the T3 group (**Figure 1D**), the volume and number of mitochondria-rich cells were increased and the whole gill lamellae were swollen and seriously curved, which deviated from the normal shape. In addition, the statistical analysis showed that the gill filament cracking proportion was higher in hypoxia groups (**Figure S1**). These results indicated that the severe hypoxia stress caused serious damage to the gill tissue.

The scanning electron microscope section showed that the gill tissue structure was complete and the gill lamellae were arranged

TABLE 1 | Information of the primers used in quantitative real-time PCR analysis.

Gene abbreviation	Gene description	Primer sequence (5'-3')	Length (bp)
cxcr4	C-X-C motif chemokine receptor 4	F: TCCTGGTGGACACTCTGGTGAC R: TGGAAGTACGCCAGTGCCTCA	106
gabarapl1	GABA type A receptor associated protein like 1	F: ACTCCCTTCCTCCATCCAGTTCC R: CCAATCCTTGCGTCCTCTGTCTC	131
irf7	Interferon regulatory factor 7	F: TGCTCAGCCAGGTGGAGACAA R: CGACTGACCGCACCGTAAGATTT	131
hspb1	Heat shock protein family B (small) member 1	F: TAACACAGGCAGCAGCACAGC R: GCAGTACGGCAATCCATCCTCTC	144
dusp2	Dual specificity phosphatase 2	F: TGAAGGTGGAGGACAGTCTAGCC R: TGTATGAGGTACGCCAGGCAGAT	157
ccng2	Cyclin G2	F: GCCAAGGAGCACAACCACCAA R: GCACAATGGCACCTCGCTGTA	145
ddit4	DNA damage-inducible transcript 4	F: ATGCCTCATCTGTGCTGCTGTG R: CCACTCCAACATCTGACGCTCC	120
egln1	egl-9 family hypoxia inducible factor 1	F: TGGCATCTGTGTGGTGGACAAC R: TCTTCTCGCATCCAGGCTCCTT	191
egln3	egl-9 family hypoxia inducible factor 3	F: TGGACACGCAGTTGGAGACTTT R: CCGTCGTTGAGAATCCCACAGTA	157

neatly without any damage at normoxia (**Figure 2A**). As shown in the T1 group (**Figure 2B**), the matrix of the gill lamellae became thin, some gill lamellae were damaged, and the surface of gill arch began to appear as a microridge. At the T2 group (**Figure 2C**), the arrangement of gill lamellae was disordered and the damage of the microridge on the surface of gill arch began to be obvious. At the T3 group (**Figure 2D**), the gill lamellae were seriously twisted, the matrix was thinned, and the number of microridge on the surface of the gill arch was greatly expanded.

Mapping of Reads Generated by RNA-seq of Gill to the Silver Carp Genome

We constructed a total of 12 cDNA libraries in this research. RNA-seq generated 21,228,388–29,007,113 million high-quality clean reads (**Table 2**). We mapped 16,801,436–22,573,384 reads (70.50%–80.27% of clean reads) to the genome of silver carp (unpublished), illustrating that the majority of clean reads generated by high-throughput sequencing were mapped (**Table 2**). Genes with count >1 were considered as highly expressed genes if they accounted for at least 75% of the 12 samples and were utilized for further differential expression assessment, giving a total of 25,319 genes in this research.

TABLE 2 | Statistics of sequencing.

Sample name	Mapped reads	Mapped reads	Mapping rate
CK-1	23,394,144	18,036,700	77.10
CK-2	23,190,974	18,584,187	80.14
CK-3	26,988,191	20,753,726	76.90
T1-1	21,228,388	16,801,436	79.15
T1-2	24,953,200	19,693,195	78.92
T1-3	25,851,796	20,638,869	79.84
T2-1	25,063,099	19,650,596	78.40
T2-2	25,232,520	17,787,773	70.50
T2-3	22,782,532	18,286,816	80.27
T3-1	29,007,113	22,573,384	77.82
T3-2	27,512,568	20,658,683	75.09
T3-3	22,440,988	17,897,520	79.75

Identification of Differentially Expressed Genes

To unveil the mechanism *via* which the silver carp responds to hypoxia, differential gene expression analyses were carried out in the CK gill relative to the T1, T2, and T3 gills ($P < 0.05$). In comparison to the normoxia group, the hypoxia group harbored 587 DEGs, consisting of 312 upregulated along with 275 downregulated DEGs (**Figure 3A**). A total of 725 DEGs were found in the semi-asphyxia group, consisting of 426 upregulated

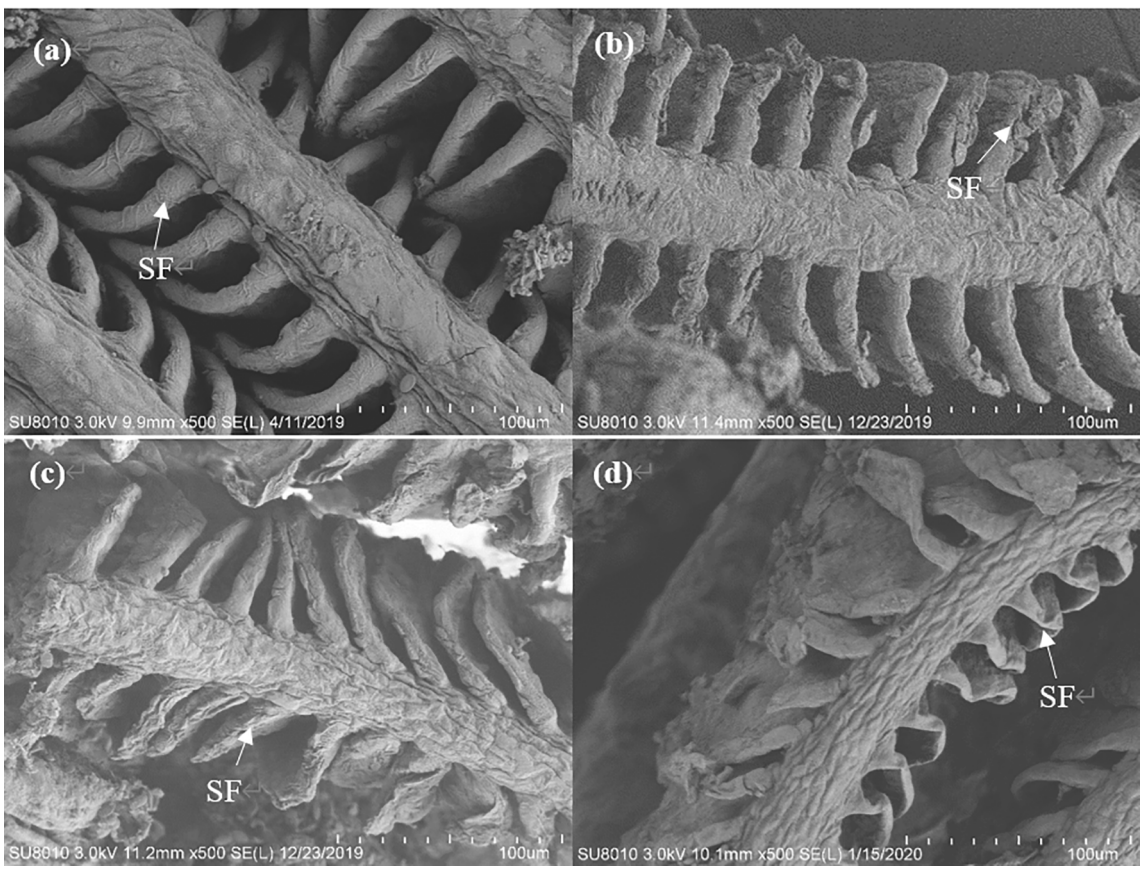

FIGURE 2 | Electron microscopy examinations of gill sections under **(A)** normoxia, **(B)** hypoxia, **(C)** semi-asphyxia, and **(D)** asphyxia stress in silver carp. SF: branch leaf.

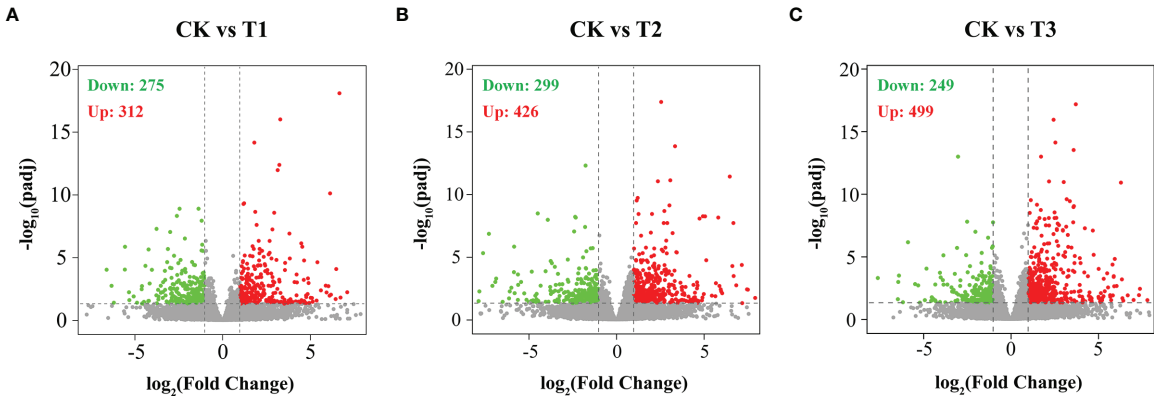

FIGURE 3 | Differentially expressed genes (DEGs) were identified by hypoxia in the gills of silver carp. Volcano plots of DEGs in **(A)** CK vs. T1, **(B)** CK vs. T2, and **(C)** CK vs. T3. Red dots designate upregulated genes, and green dots designate downregulated genes. CK: normoxia, T1: hypoxia, T2: semi-asphyxia, T3: asphyxia.

coupled with 299 downregulated genes (**Figure 3B**). In the asphyxia group, a total of 748 DEGs were identified, 499 of which were upregulated with 249 being downregulated (**Figure 3C**). A Venn diagram exhibited the common and specific DEGs obtained from differential gene expression analyses described above (**Figure 4A**), and **Figure 4B** depicted the 224 co-expressed genes' distinct expression trends in these four groups.

Gene Ontology Enrichment Analysis of Differentially Expressed Genes

The DEGs were analyzed using the GO term analyses to determine considerably ($P < 0.05$) enriched BPs (biological processes), CCs (cellular components), and MFs (molecular functions). GO analyses exhibited that DEGs in the T1 group were enriched for BPs containing the immune system process, antigen processing and presentation, immune system development, and oxidation–reduction process; for CCs containing MHC protein complex and extracellular region; for MF-containing oxidoreductase activity, iron ion binding, and endopeptidase inhibitor activity (**Figure 5A**). In the T2 group, the immune system process, the modulation of the immune system process, antigen processing along with presentation, and the response to lipid were enriched in BPs; the MHC protein complex and MHC class II protein complex were enriched in CCs; the oxidoreductase activity, iron ion binding, and MAP kinase phosphatase activity were enriched in MFs (**Figure 5B**). In the T3 group, immune system process, the response to oxygen-containing compound, the cellular response to chemical stimulus, and the modulation of immune system process were enriched in BPs; the MHC protein complex and MHC class II protein complex were enriched in CCs; and the oxidoreductase activity, iron ion binding, and phospholipase C activity were enriched in MFs (**Figure 5C**). For better clarity and concise presentation, we analyzed the intersection of significantly enriched GO terms among three comparisons. Genes induced by

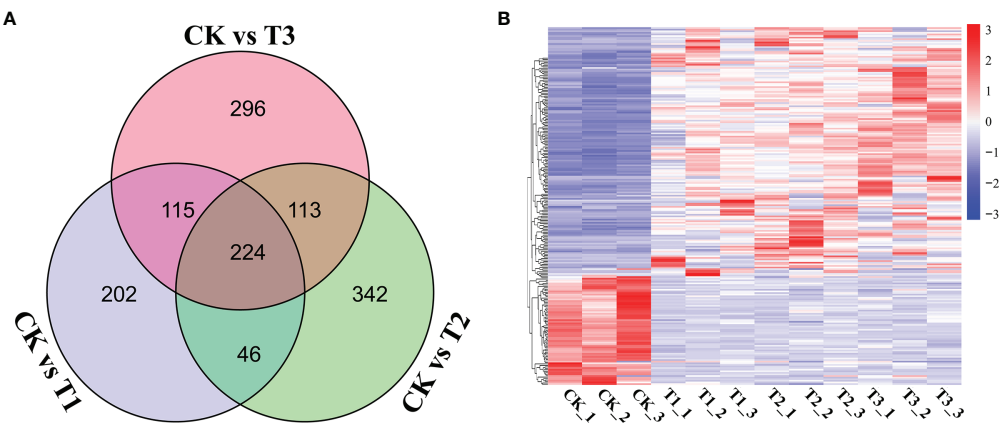

FIGURE 4 | Clustering analysis of DEGs between the three comparisons. **(A)** The DEGs in the three comparisons are exhibited in a Venn diagram. **(B)** The heatmap exhibits the variance in the expression of overlapping DEGs on the basis of the fragments per kilobase of transcript per million mapped read (FPKM) values. Genes with contents with greater than the mean are highlighted in red, while those with expression levels below the mean are highlighted in blue.

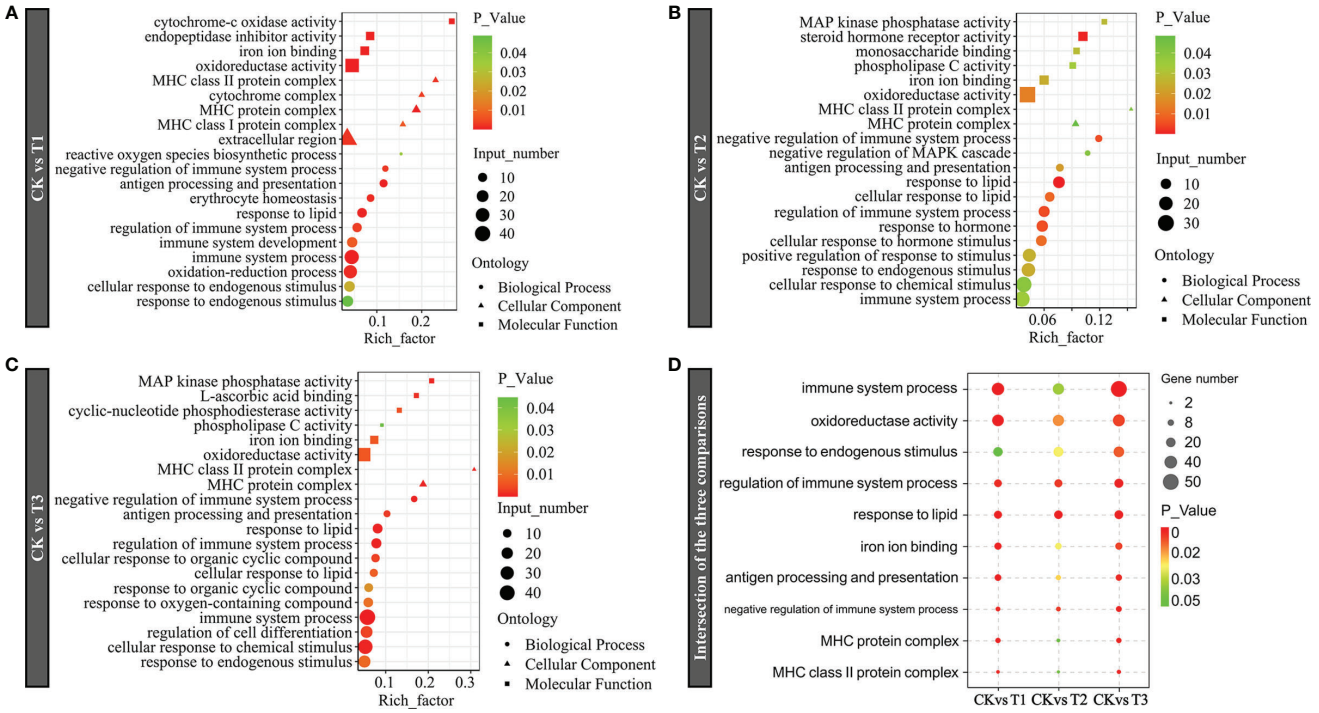

FIGURE 5 | Gene Ontology (GO) term enrichment of dramatically DEGs in **(A)** CK vs. T1, **(B)** CK vs. T2, and **(C)** CK vs. T3. **(D)** Intersection of the three comparisons. Bubble plots represent remarkably enriched GO terms within the DEGs. The *y*-axis designates GO terms, and the *x*-axis exhibits the rich factor. The P-value indicates the enrichment importance of the GO terms, with lower P-values suggesting higher intensity. CK: normoxia, T1: hypoxia, T2: semi-asphyxia, T3: asphyxia.

hypoxia were consistently enriched in GO terms including the immune system process, oxidoreductase activity, the response to endogenous stimulus, iron ion binding, and MHC protein complex (**Figure 5D**). It is worth mentioning that the numbers of the associated genes and the significance of the GO enrichments roughly increased with the degree of hypoxia stress (hypoxia, semi-asphyxia, and asphyxia).

Kyoto Encyclopedia of Genes and Genomes Enrichment Analysis of Differentially Expressed Genes

KEGG enrichment analysis was used to reveal the affected biological pathways. The DEGs induced by hypoxia stress (T1) were enriched in signaling pathways consisting of complement and coagulation, mTOR, Th1 and Th2 cell differentiation, HIF-1, and FoxO (**Figure 6A**). The genes induced by semi-asphyxia stress (T2) were enriched in signaling pathways including drug metabolism – cytochrome P450, complement and coagulation, and HIF-1 (**Figure 6B**). The genes induced by asphyxia stress (T3) were enriched in signaling pathways including vitamin B6 metabolism, the immune network for IgA production, antigen processing along with presentation, Th1 and Th2 cell differentiation, HIF-1, FoxO, and MAPK (**Figure 6C**). Given that the enrichment signaling cascades in T1, T2, and T3 were primarily related to the immune response and oxygen transport, the intersection of enriched KEGG cascades in these two functions was determined for better clarity and concise presentation. As a result, the signaling cascades linked to immune system (complement and coagulation cascades, NOD-like receptor signaling cascade, leukocyte transendothelial migration, and Th1 and Th2 cell differentiation), immune diseases (rheumatoid arthritis, asthma, inflammatory bowel disease, graft-versus-host disease, and systemic lupus erythematosus), as well as oxygen transport (MAPK, FoxO, PI3K-Akt, and HIF-1 signaling cascade) were enriched (**Figure 6D**). Moreover, the numbers of the associated genes and significance of the KEGG enrichments roughly increased with the degree of hypoxia stress (hypoxia, semi-asphyxia, and asphyxia). Furthermore, the DEGs linked to immune system (**Figure 7** and **Table 3**) as well as oxygen transport (**Figure 8**) were analyzed.

RT-qPCR Verification

To confirm the RNA-seq findings, we employed RT-qPCR to verify 18 DEGs from insulin signaling pathways. RT-qPCR data exhibited that cxcr4 and gabarapl1 (immune response related), hspb1, dusp2, ccng2, ddit4, egln1 and egln3 (oxygen transport related) were remarkably and gradually increased, while irf7

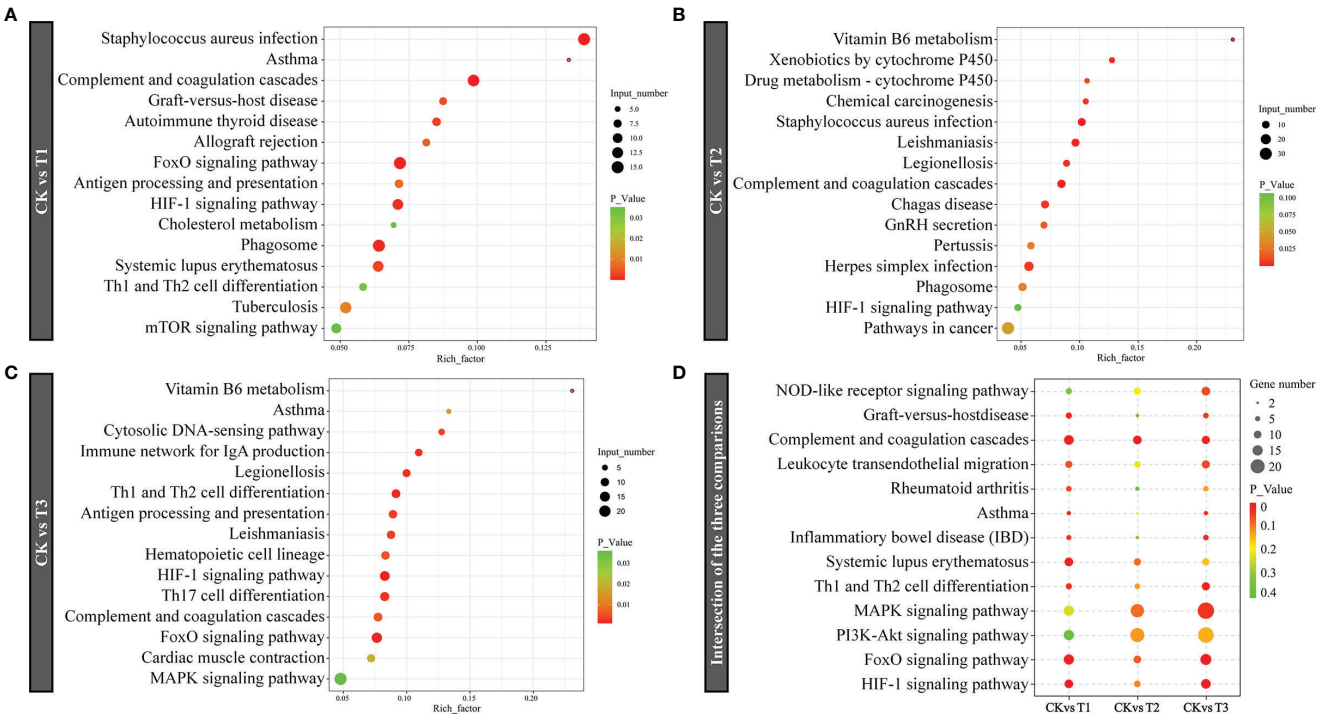

FIGURE 6 | KEGG pathway enrichment of dramatically DEGs in **(A)** CK vs. T1, **(B)** CK vs. T2, **(C)** CK vs. T3, **(D)** Intersection of the three comparisons in immune response and oxygen transport. The bubble plots highlight KEGG cascades that are considerably enriched in the remarkable DEGs. The *y*-axis exhibits KEGG cascades. The *x*-axis denotes the rich factor. The P result signifies the signaling cascades enrichment importance; the lower the *P*-value, the higher the intensity. CK: normoxia, T1: hypoxia, T2: semi-asphyxia, T3: asphyxia.

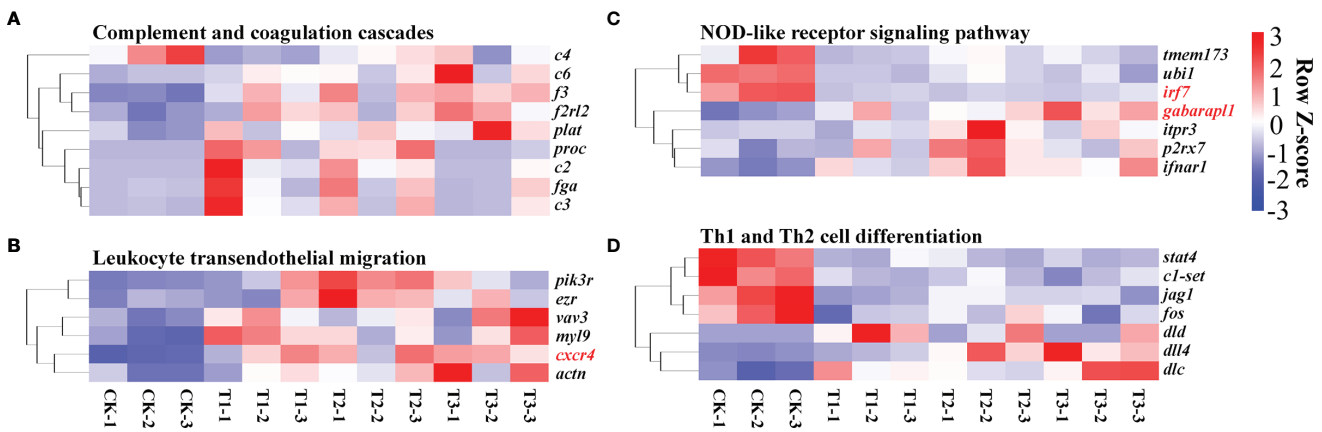

FIGURE 7 | Heat map exhibiting alterations in gene expression in the pathways related to immune response, like complement and coagulation cascades **(A)**, leukocyte transendothelial migration **(B)**, NOD-like receptor signaling cascade **(C)**, and Th1 and Th2 cell differentiation **(D)**. The evaluation criteria used the average RPKM value per gene. Genes with contents greater than the mean are colored red, while those with contents below the mean are colored blue.

(immune response related) were remarkably and gradually decreased in the hypoxia, semi-asphyxia, and asphyxia groups (**Figure 9**). These data were congruent with RNA-seq data in terms of the variation trend (**Table 4**), demonstrating the accuracy and reliability of the RNA-seq investigation.

4 DISCUSSION

Herein, the impacts of varying degrees of hypoxia stress (hypoxia, semi-asphyxia, and asphyxia) were evaluated on the histomorphological in the gill tissue of *H. molitrix*. Results

TABLE 3 | The representative immunity-related DEGs in the gills of *H. molitrix* in varying degrees of hypoxia.

Accession number	Gene name	Description	log_2 ratio		
			T1/CK	T2/CK	T3/CK
CAFS_HM_T_00082284	*abcb1*	ATP-binding cassette subfamily B member 1	-0.13	-1.95	-1.57
CAFS_HM_T_00022426	*brf1*	Transcription factor TFIIIB subunit BRF1	-1.40	-0.26	-1.51
CAFS_HM_T_00087508	*c2*	Complement C2	1.28	1.01	-1.16
CAFS_HM_T_00050307	*c6*	Complement component C6	1.29	1.31	2.21
CAFS_HM_T_00024133	*cd36*	CD36 molecule	-1.26	-1.05	-1.00
CAFS_HM_T_00037696	*cd40*	CD40 molecule	1.29	1.43	1.38
CAFS_HM_T_00005419	*cd45*	Receptor-type tyrosine-protein phosphatase C	0.68	1.57	1.70
CAFS_HM_T_00031558	*cited2*	Cbp/p300-interacting transactivator with Glu/Asp rich carboxy-terminal domain 2	1.63	1.84	2.20
CAFS_HM_T_00079400	*cxcr4*	C-X-C motif chemokine receptor 4	1.77	1.88	1.95
CAFS_HM_T_00088254	*dlc*	deltaC	-1.53	-1.34	-1.63
CAFS_HM_T_00020279	*dld*	Dihydrolipoamide dehydrogenase	-1.59	-1.62	-1.68
CAFS_HM_T_00045987	*epo*	Erythropoietin	0.46	-0.29	1.04
CAFS_HM_T_00046337	*etnppl*	Ethanolamine-phosphate phospho-lyase	2.24	2.69	2.36
CAFS_HM_T_00090703	*ezr*	Ezrin	0.45	1.45	0.75
CAFS_HM_T_00031270	*fos*	Fos proto-oncogene, AP-1 transcription factor subunit	1.56	3.17	3.38
CAFS_HM_T_00033733	*fyn*	Fyn proto-oncogene	0.47	1.38	0.91
CAFS_HM_T_00055839	*gata2*	GATA-binding protein 2	0.87	0.06	0.47
CAFS_HM_T_00079776	*ifnar1*	Interferon alpha and beta receptor subunit 1	0.94	1.50	1.31
CAFS_HM_T_00063373	*irf7*	Interferon regulatory factor 7	-1.51	-1.53	-1.40
CAFS_HM_T_00008734	*jagn1b*	Jagunal homolog 1b	-0.43	-1.22	-0.84
CAFS_HM_T_00076201	*klf4*	Kruppel like factor 4	2.83	2.59	2.99
CAFS_HM_T_00060378	*klf6*	Kruppel like factor 6	0.89	0.72	0.92
CAFS_HM_T_00040278	*lime1*	Lck-interacting transmembrane adaptor 1	4.16	-0.65	4.29
CAFS_HM_T_00065779	*nccrp1*	P1, F-box associated domain containing	1.08	-0.05	0.58
CAFS_HM_T_00029544	*ndrg1*	N-myc downstream regulated 1	0.66	0.58	0.89
CAFS_HM_T_00053358	*rpl22*	Ribosomal protein L22	0.25	0.58	0.61
CAFS_HM_T_00009090	*s1pr4*	Sphingosine-1-phosphate receptor 4	1.95	1.57	1.75
CAFS_HM_T_00018523	*sec23*	Secretory 23	1.21	1.47	1.84
CAFS_HM_T_00002602	*slc25a38*	Solute carrier family 25 member 38	-2.18	-1.59	-1.72
CAFS_HM_T_00072448	*smox*	Spermine oxidase	0.94	0.58	0.73
CAFS_HM_T_00063974	*snrk*	SNF-related kinase	0.76	0.66	0.86
CAFS_HM_T_00039980	*tfe3*	Transcription factor binding to IGHM enhancer 3	-1.55	-1.08	-1.09
CAFS_HM_T_00028261	*tgfbr2*	Transforming growth factor beta receptor 2	0.82	0.75	1.19
CAFS_HM_T_00035272	*tmem173*	Transmembrane protein 173	-2.63	-1.40	-2.05
CAFS_HM_T_00036122	*tsc22d3*	TSC22 domain family member 3	1.53	1.56	1.68
CAFS_HM_T_00080525	*znf148*	Zinc finger protein 148	-0.86	-1.04	-1.28

illustrated that the tissue damage in the gills becomes more and more severe with the increasingly low DO concentration. Using gill transcriptomic analysis, the effects of hypoxia on immune defense and oxygen transport-related genes and signaling cascades in *H. molitrix* were uncovered. As a result, the classified discussion is detailed below.

Effect of Hypoxia Stress on the Gill Tissue Structure of *H. molitrix*

Aquatic habitats have a range of oxygen contents, from anoxia to hyperoxia, which results in a corresponding range of tissue and cellular diversity in aquatic animals. Silver carp, being a somewhat hypoxia-sensitive freshwater fish, is susceptible to being harmed by a fall in DO levels caused by weather changes or eutrophication (Li et al., 2021). The gill is the main respiratory organ of fish, and its dominant functions are carrying out gas exchange, promoting metabolism, and regulating osmotic pressure. As the first organ that responds to rapid changes in the DO level of water, the functions of a gill were disrupted by hypoxia, including respiration, nitrogenous waste excretion, and osmoregulation (Khansari et al., 2018). Under hypoxia stress, a *Crucian carp* could increase its oxygen intake by increasing the number of gill lamellae (Sollid et al., 2003). Studies have also shown that *Gymnocypris przewalskii* (Matey et al., 2008) and *C. carassius* (Sollid et al., 2005) can adapt to the hypoxia environment by changing the shape and structure of gills to increase its oxygen intake. In this study, the volume of cells with rich mitochondria became larger and the gill lamellae was gradually curved in the hypoxia condition, thus possibly increasing the gill respiratory area to obtain more oxygen. The results were consistent with the changes of gill tissues of *Oncorhynchus mykiss* (Matey et al., 2011) and *G. przewalskii* (Matey et al., 2008) under hypoxia stress. Furthermore, the tissue section and scanning electron microscope section of the gills in silver carp showed that the swelling and shedding of the epithelial cell layer in the gill tissue were intensified, the gill lamellae were seriously twisted, the phenomenon of cavitation became common, and gill filaments were dehisced in the semi-asphyxia and asphyxia conditions. Therefore, the abovementioned results further illustrate that hypoxia would

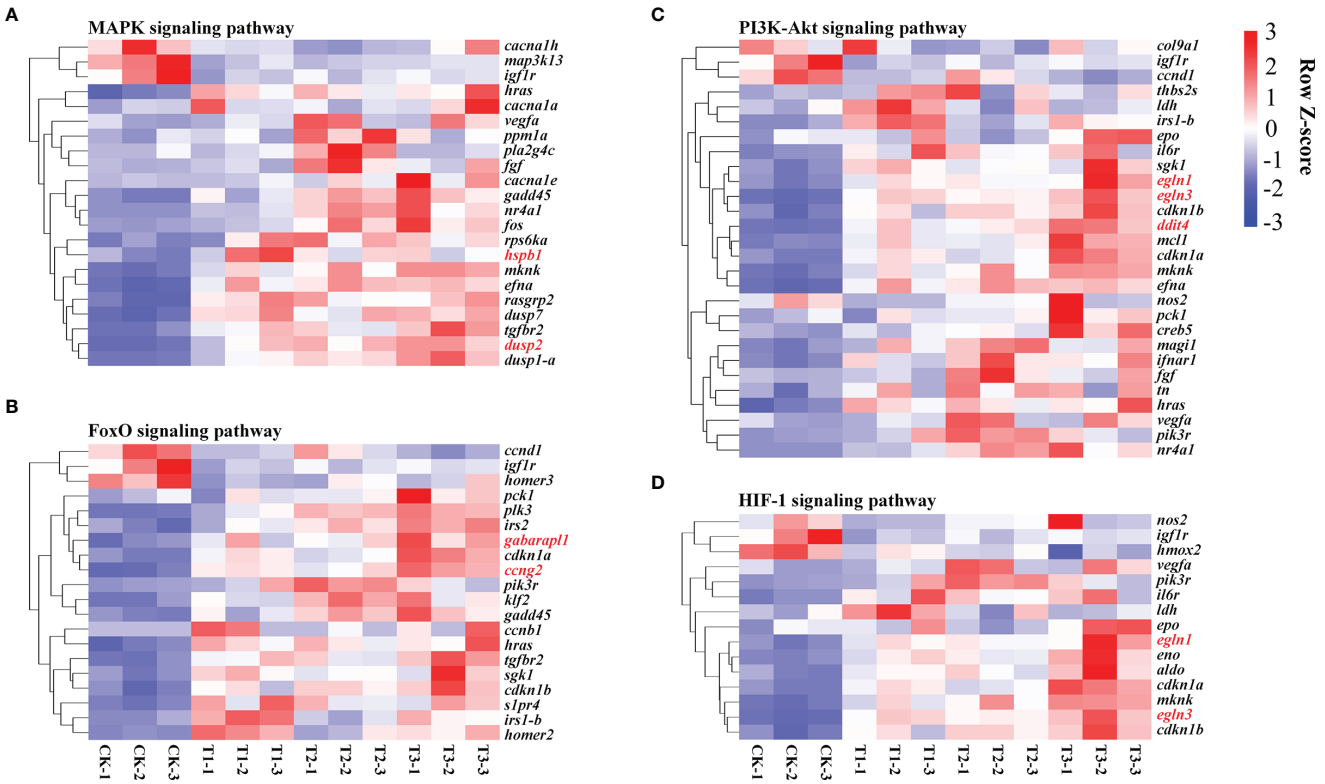

FIGURE 8 | Heat map exhibiting alterations in gene expression in the pathways related to oxygen transport, such as MAPK **(A)**, FoxO **(B)**, PI3K-Akt **(C)**, and HIF-1 signaling cascade **(D)**. The evaluation criteria used the average RPKM value per gene. Genes with contents greater than the mean are colored red, while those with contents below the mean are colored blue.

alter the structure of gills to adapt to environmental challenges and severe hypoxia condition could cause a more serious and irreversible tissue damage of the gills in *H. molitrix*.

Effect of Hypoxia Stress on the Immune Defense of *H. molitrix*

The majority of studies on the teleost immune response focused on changes in the expression of genes in the head, kidney, and spleen, which represent the primary hematopoietic along with secondary lymphoid organs of fish, respectively (Ewart et al., 2005; Overturf and LaPatra, 2006; Jørgensen et al., 2011). While the gill is primarily responsible for gas along with electrolyte exchange coupled with excretion (Evans et al., 2005), it has been considered as a key infection site, owing to its continual interaction with the aquatic environment (Dos Santos et al., 2001). Additionally, the fish gills, as a lymphoid tissue connected with the mucosa, contain a variety of leuklarki populations that are responsible for local immune responses, making them an immune-competent organ (Press and Evensen, 1999; Rebl et al., 2014). In this work, immunological cascades (complement and coagulation cascades, leukocyte transendothelial migration, NOD-like receptor signaling cascade, and the differentiation of Th1 and Th2 cells) were enriched in diverse degrees of hypoxic stress. Complement and coagulation systems are two closely linked plasma protein cascades that play critical roles in host defense and hemostasis, respectively (Berends et al., 2014). The complement system, a critical defender against invasive pathogenic microbes, may be triggered by traditional, alternative, or mannan-docking lectin cascades (Kemper et al., 2014). Complement C3 is a critical component of the complement system, and the activation of C3 converges the three complement activation cascades (Meng et al., 2019). C2 and C4 are two effector proteins that have the potential to initiate the classical complement cascade (Petersen et al., 2000). C6 is one of the terminal components of a complement system that, when coupled with other complement components, forms the membrane attack complex, which results in bacterial cell lysis (Shen et al., 2013). The upregulation of complement C2, C6, and C3 in **Figure 7A** demonstrated that hypoxic stress may trigger the *H. molitrix* immune defense response.

Atherogenesis and other inflammatory vascular disorders are complicated by leukocyte adherence and trans-endothelial migration (Zhang et al., 2011). The NOD-like receptor signaling cascade is responsible for the generation of innate immune responses and plays an indispensable role in inflammation (Viale-Bouroncle et al., 2012). Herein, leukocyte trans-endothelial migration and the NOD-like receptor signaling pathway were enriched in varying groups, indicating that hypoxia might initiate

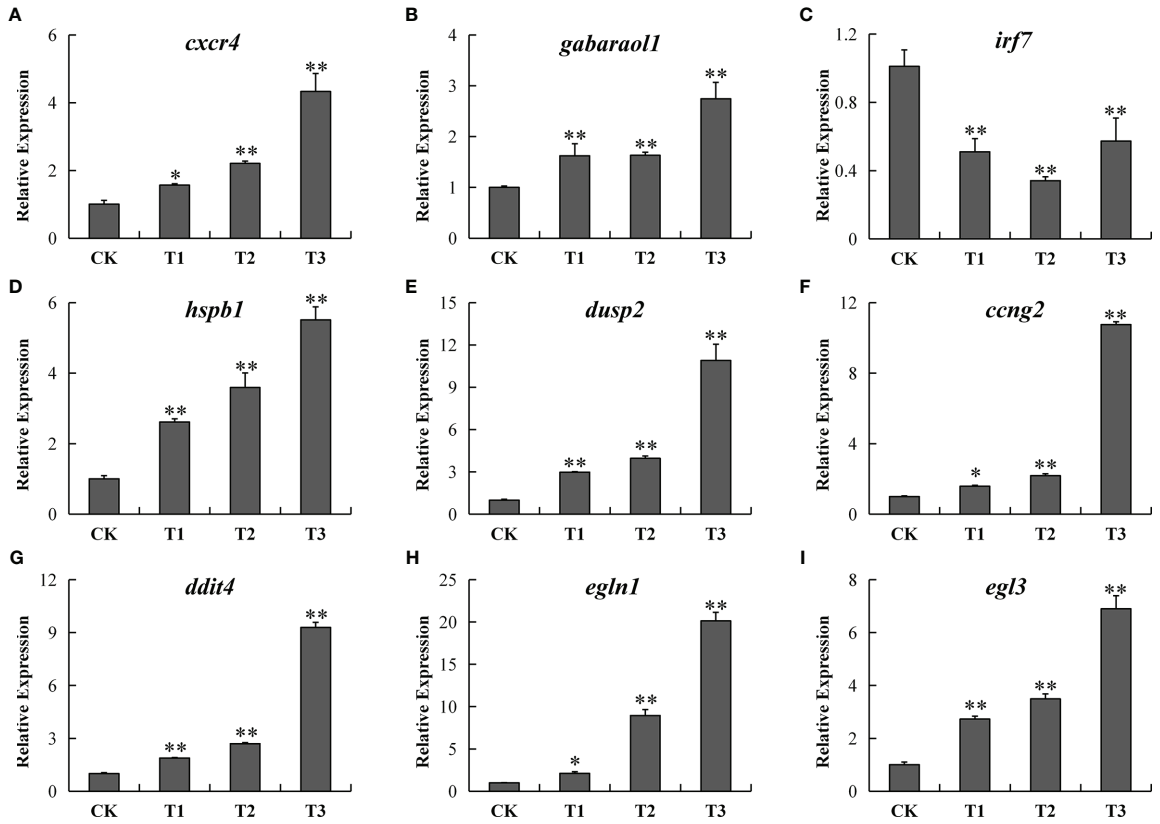

FIGURE 9 | RT-qPCR verification of 9 differentially expressed genes [cxcr4 **(A)**, gabarapl1 **(B)**, irf7 **(C)**, hspb1 **(D)**, dusp2 **(E)**, ccng2 **(F)**, ddit4 **(G)**, egln1 **(H)**, and egln3 **(I)**] in the CK, T1, T2, and T3 groups. *Y*-axis exhibits the relative fold change. * designates $P < 0.05$, ** designates $P < 0.01$.

TABLE 4 | Comparisons of RNA-seq and RT-qPCR results.

Gene abbreviation	Gene description	Fold-change (CK vs. T1)		Fold-change (CK vs. T2)		Fold-change (CK vs. T3)	
		qPCR	RNA-seq	qPCR	RNA-seq	qPCR	RNA-seq
cxcr4	C-X-C motif chemokine receptor 4	1.57	3.40	2.21	3.69	4.33	3.88
gabarapl1	GABA type A receptor associated protein like 1	1.62	1.75	1.63	1.80	2.74	2.38
irf7	Interferon regulatory factor 7	0.51	0.35	0.34	0.35	0.57	0.38
hspb1	Heat shock protein family B (small) member 1	2.62	3.66	3.59	2.53	5.51	2.39
dusp2	Dual-specificity phosphatase 2	2.98	3.10	3.96	3.85	10.90	4.35
ccng2	cyclin G2	1.59	2.24	2.19	2.08	10.75	2.89
ddit4	DNA damage-inducible transcript 4	1.89	3.48	2.70	3.63	9.30	5.23
egln1	egl-9 family hypoxia inducible factor 1	2.12	2.36	8.95	2.33	20.13	3.52
egln3	egl-9 family hypoxia inducible factor 3	2.73	8.23	3.49	7.42	6.90	10.81

an innate immune response and trigger inflammation processes. The Th1/Th2 balance is thought to be critical for good immunological responses, and an imbalance between the two may result in immune-linked diseases (Ohno et al., 2015). Patients with rheumatoid arthritis, type 1 diabetes, and multiple sclerosis have Th1-dominant immune responses, while those with type 1 hypersensitivity conditions including allergies or asthma exhibit Th2-dominant immune responses (Kidd, 2003). STAT4 is primarily involved in the induction of Th1 responses and suppresses Th2 responses (Chitnis et al., 2004; Cui et al., 2021). STAT4 activation is thought to have an inflammatory impact, and it is involved in the modulation of Th1/Th2 differentiation as well as the autoimmune conditions associated with this dysfunction (Cui et al., 2021). In this research, *stat4* was downregulated in hypoxia-treated groups, indicating that Th1 responses were inhibited and Th2 responses were induced in the hypoxia condition in *H. molitrix*. Furthermore, rheumatoid arthritis, asthma, and Th1 and Th2 cell differentiation were enriched in varying groups in

Figure 6D, suggesting that varying degrees of hypoxia would impact Th1/Th2 balance and further cause immune disease including rheumatoid arthritis and asthma in *H. molitrix*.

In addition to the aforementioned findings, a high number of functional DEGs were identified; and these DEGs have the potential to influence the immune system and various signaling cascades. KLF4 is implicated in the control of endothelial inflammation by dampening the activation of the NF-B cascade (Fang and Davies, 2012). CXCR4 is required for a variety of biological activities, consisting of immune cell trafficking and bone-marrow homeostasis (Lin et al., 2019). IRF7 functions as the pivotal modulator of type 1 IFN-triggered immune responses, which are required for viral immunity (Honda et al., 2005). CD45, the prototypical receptor-like protein tyrosine phosphatase gene, plays an indispensable role in immune cell signal transduction cascades (Ren et al., 2018). CD36 is a membrane-bound glycoprotein that participates in a variety of cellular activities including lipid transport, immunological modulation, coagulation, and atherosclerosis (Endemann et al., 1993). CD40 is a co-stimulatory immune receptor belonging to the TNF receptor superfamily that plays a pivotal role in Th1-cell-triggered immune responses (Cella et al., 1996; Reyes-Moreno et al., 2004). The downregulation of *irf7* and *cd36* as well as the upregulation of *klf4*, *cxcr4*, *cd45*, and *cd40* (**Table 3**) in hypoxia-treated groups suggested that the immune response ability of the gills in *H. molitrix* might be weakened by the varying degrees of hypoxia stress (hypoxia, semi-asphyxia, and asphyxia).

Effect of Hypoxia Stress on the Oxygen Transport of *H. molitrix*

The majority of aquatic animals have evolved a variety of molecular approaches for hypoxia modulation, consisting of increased oxygen delivery as well as decreased oxygen consumption (Sun et al., 2016). These processes are controlled by HIF-1 signaling cascade-modulated genes, for instance, erythropoietin, transferrin, transferrin receptor, hexokinase, and lactic dehydrogenase (Zhu et al., 2013). In many species, the HIF-1 signaling cascade induces identical or homologous gene expression, resulting in similar biochemical and physical consequences, such as angiogenesis, oxygen sensing, and erythropoiesis along with oxygen transport (Xiao, 2015).

MAPKs play a role in oxygen sensing as critical modulators of HIF-1 signaling. Hypoxia has been exhibited to change MAPK expression in the zebrafish heart (Marques et al., 2008). As a critical factor in HIF-1 signaling, HIF-1 is activated through the PI3K/Akt signaling (Jiang et al., 2001). The FoxO signaling cascade is remarkably linked to the PI3K/Akt signaling cascade (Farhan et al., 2017), suggesting that it may have an indirect influence on HIF-1 signaling. Furthermore, the HIF-1, MAPK, FoxO, and PI3K-Akt signaling were enriched, and the related genes were remarkably elevated (**Figure 8**). These findings illustrate that in response to hypoxia, *H. molitrix* activates these signaling cascades.

Numerous upregulated genes, consisting of *nos2*, *vegfa*, *igf1r*, *hmox2*, *pik3r*, *il6r*, *ldh*, *epo*, *egln1*, *eno*, *aldo*, *cdkn1a*, *mknk*, *egln3*, and *cdkn1b*, which are commonly linked with hypoxia response, were shown to be enriched in HIF-1 signaling. In zebrafish, the *egln1* gene, also known as *egln1b*, produces PHD2, which degrades HIF-1 by prolyl hydroxylation in an aerobic environment (Schofield and Ratcliffe, 2004). Additionally, the EGLN family genes EGLN2 and EGLN3 act as cellular oxygen sensors, catalyzing and hydroxylating HIF alpha proteins (Hu et al., 2019). The EGLN family has been implicated in EPO synthesis and erythropoiesis in murine zygotes (Fisher et al., 2009), and EGLN3 transcriptome and proteomic alterations have been connected to Tibetan pig adaptation to high-altitude hypoxia (Zhang et al., 2017). The induction of EPO at low oxygen levels results in an increase in red blood cell formation, which results in an increase in oxygen delivery in response to ischemia stress (Zhang et al., 2014). HIF activation increases LDH activity, which in turn promotes HIF activation further, implying a positive feedback loop between HIF and LDH (Lu et al., 2002). Hypoxia and a rise in the expression of oxygen-modulated HIF transcription factors are major inducers of VEGFA overexpression (Fang et al., 2019). In our study, the gene expression of *egln1*, *egln3*, *epo*, *ldh*, and *vegfa* had an overall increase trend in response to hypoxia, semi-asphyxia, and asphyxia (**Figure 8D**), indicating that *H. molitrix* may utilize "HIF-1" to obtain more oxygen to maintain active functions under varying degrees of hypoxia stress.

CONCLUSIONS

This study showed that varying degrees of hypoxia induce the tissue damage of gill in silver carp. The H&E sections and electron microscopy examinations of gills indicated that the swelling and shedding of the epithelial cell layer in the gill tissue were intensified, the gill lamellae were seriously twisted, and gill filaments were dehisced with the degree of hypoxia intensified. The present study is the first to use a transcriptome to reveal the response to hypoxia in the gill of *H. molitrix*. In total, 587, 725, and 748 DEGs were identified in hypoxia, semi-asphyxia, and asphyxia groups, respectively. Further analysis illustrated that *c2*, *c3*, *c6*, *klf4*, *cxcr4*, *cd45*, and *cd40* were upregulated as well as complement and coagulation cascades, NOD-like receptor signaling cascade, and Th1 and Th2 cell differentiation were enriched, which involved immune defense in the silver carp exposed to varying degrees of hypoxia. Moreover, *egln1*, *egln3*, *epo*, *ldh*, and *vegfa* were upregulated, and HIF-1, MAPK, and PI3K-Akt signaling pathways were enriched, which involved oxygen transport in the response of silver carp to hypoxia. These findings suggest that hypoxia stress may activate the *H. molitrix* immune defense system and that the HIF-1 signaling pathway is employed to increase oxygen transport in hypoxic situations. The results of this investigation will provide light on the molecular processes driving hypoxia responses in hypoxia-sensitive fish.

DATA AVAILABILITY STATEMENT

The datasets presented in this study can be found in online repositories. The names of the repository/repositories and

accession number(s) can be found below: https://www.ncbi.nlm.nih.gov/, PRJNA812079.

ETHICS STATEMENT

The animal study was reviewed and approved by the animal care regulations of the Yangtze River Fisheries Research Institute, Chinese Academy of Fishery Sciences.

AUTHOR CONTRIBUTIONS

XHL: Methodology, Formal analysis, Investigation, Data curation, Writing – original draft preparation, Funding acquisition. CL: Investigation, Formal analysis. QW and CF: Investigation, Data curation. XZL: Methodology. HS: Software. GH: Validation. GZ: Project administration, Resources, Funding acquisition. HL: Conceptualization, Supervision, Writing – review and editing, Funding acquisition. All authors contributed to the article and approved the submitted version.

FUNDING

This work was supported by the National Key Research and Development Program of China (NO. 2018YFD0900302); the Foundation of Hubei Hongshan Laboratory (NO. 2021hskf014); State Key Laboratory of Developmental Biology of Freshwater Fish (NO. 2021KF005); the Central Public-interest Scientific Institution Basal Research Fund, CAFS (NO. 2020TD33 and NO. YFI202211); and the Earmarked Fund for China Agriculture Research System of MOF and MARA (NO. CARS-45).

SUPPLEMENTARY MATERIAL

The Supplementary Material for this article can be found online at: https://www.frontiersin.org/articles/10.3389/fmars.2022.900200/full#supplementary-material

Supplementary Figure 1 | Quantified results of the gill filament cracking proportion in the CK, T1, T2, and T3 groups (mean ± SD, n = 9). *, $P < 0.05$.

REFERENCES

Abdel-Tawwab, M., Monier, M. N., Hoseinifar, S. H., and Faggio, C. (2019). Fish Response to Hypoxia Stress: Growth, Physiological, and Immunological Biomarkers. *Fish. Physiol. Biochem.* 45 (3), 997–1013. doi: 10.1007/s10695-019-00614-9

Anders, S., Pyl, P. T., and Huber, W. (2015). HTSeq—A Python Framework to Work With High-Throughput Sequencing Data. *Bioinformatics* 31 (2), 166–169. doi: 10.1093/bioinformatics/btu638

Benjamini, Y., and Yekutieli, D. (2001). The Control of the False Discovery Rate in Multiple Testing Under Dependency. *Ann. Stat* 29 (4), 1165–1188. doi: 10.1214/aos/1013699998

Berends, E. T., Kuipers, A., Ravesloot, M. M., Urbanus, R. T., and Rooijakkers, S. H. (2014). Bacteria Under Stress by Complement and Coagulation. *FEMS Microbiol. Rev.* 38 (6), 1146–1171. doi: 10.1111/1574-6976.12080

Cella, M., Scheidegger, D., Palmer-Lehmann, K., Lane, P., Lanzavecchia, A., and Alber, G. (1996). Ligation of CD40 on Dendritic Cells Triggers Production of High Levels of Interleukin-12 and Enhances T Cell Stimulatory Capacity: TT Help *via* APC Activation. *J. Exp. Med.* 184 (2), 747–752. doi: 10.1084/jem.184.2.747

Cheng, C.-H., Ma, H.-L., Su, Y.-L., Deng, Y.-Q., Feng, J., Xie, J.-W., et al. (2019). Ammonia Toxicity in the Mud Crab (Scylla Paramamosain): The Mechanistic Insight From Physiology to Transcriptome Analysis. *Ecotoxicol. Environ. Saf.* 179, 9–16. doi: 10.1016/j.ecoenv.2019.04.033

Chen, B.-X., Yi, S.-K., Wang, W.-F., He, Y., Huang, Y., Gao, Z.-X., et al. (2017). Transcriptome Comparison Reveals Insights Into Muscle Response to Hypoxia in Blunt Snout Bream (Megalobrama Amblycephala). *Gene* 624, 6–13. doi: 10.1016/j.gene.2017.04.023

Chitnis, T., Salama, A. D., Grusby, M. J., Sayegh, M. H., and Khoury, S. J. (2004). Defining Th1 and Th2 Immune Responses in a Reciprocal Cytokine Environment *In Vivo*. *J. Immunol.* 172 (7), 4260–4265. doi: 10.4049/jimmunol.172.7.4260

Cui, J., Tong, R., Xu, J., Tian, Y., Pan, J., Wang, N., et al. (2021). Association Between STAT4 Gene Polymorphism and Type 2 Diabetes Risk in Chinese Han Population. *BMC Med. Genomics* 14 (1), 1–16. doi: 10.1186/s12920-021-01000-2

Dos Santos, N. M., Taverne-Thiele, J., Barnes, A. C., van Muiswinkel, W. B., Ellis, A. E., and Rombout, J. H. (2001). The Gill Is a Major Organ for Antibody Secreting Cell Production Following Direct Immersion of Sea Bass (Dicentrarchus Labrax, L.) in a Photobacterium Damselae Ssp. Piscicida Bacterin: An Ontogenetic Study. *Fish. Shellfish. Immunol.* 11 (1), 65–74. doi: 10.1006/fsim.2000.0295

Endemann, G., Stanton, L. W., Madden, K. S., Bryant, C. M., White, R. T., and Protter, A. A. (1993). CD36 Is a Receptor for Oxidized Low Density Lipoprotein. *J. Biol. Chem.* 268 (16), 11811–11816. doi: 10.1016/S0021-9258(19)50272-1

Evans, D. H., Piermarini, P. M., and Choe, K. P. (2005). The Multifunctional Fish Gill: Dominant Site of Gas Exchange, Osmoregulation, Acid-Base Regulation, and Excretion of Nitrogenous Waste. *Physiol. Rev.* 85 (1), 97–177. doi: 10.1152/physrev.00050.2003

Ewart, K. V., Belanger, J. C., Williams, J., Karakach, T., Penny, S., Tsoi, S. C., et al. (2005). Identification of Genes Differentially Expressed in Atlantic Salmon (Salmo Salar) in Response to Infection by Aeromonas Salmonicida Using cDNA Microarray Technology. *Dev. Comp. Immunol.* 29 (4), 333–347. doi: 10.1016/j.dci.2004.08.004

Fang, Y., and Davies, P. F. (2012). Site-Specific microRNA-92a Regulation of Krüppel-Like Factors 4 and 2 in Atherosusceptible Endothelium. *Arteriosclerosis. Thrombosis. Vasc. Biol.* 32 (4), 979–987. doi: 10.1161/ATVBAHA.111.244053

Fang, P., Zhang, L., Zhang, X., Yu, J., Sun, J., Jiang, Q.-a., et al. (2019). Apatinib Mesylate in the Treatment of Advanced Progressed Lung Adenocarcinoma Patients With EGFR-TKI Resistance—A Multicenter Randomized Trial. *Sci. Rep.* 9 (1), 1–8. doi: 10.1038/s41598-019-50350-6

Farhan, M., Wang, H., Gaur, U., Little, P. J., Xu, J., and Zheng, W. (2017). FOXO Signaling Pathways as Therapeutic Targets in Cancer. *Int. J. Biol. Sci.* 13 (7), 815. doi: 10.7150/ijbs.20052

Feng, C., Li, X., Sha, H., Luo, X., Zou, G., and Liang, H. (2022). Comparative Transcriptome Analysis Provides Novel Insights Into the Molecular Mechanism of the Silver Carp (Hypophthalmichthys Molitrix) Brain in Response to Hypoxia Stress. *Comp. Biochem. Physiol. Part D.: Genomics Proteomics* 41, 100951. doi: 10.1016/j.cbd.2021.100951

Fisher, T. S., Lira, P. D., Stock, J. L., Perregaux, D. G., Brissette, W. H., Ozolinš, T. R., et al. (2009). Analysis of the Role of the HIF Hydroxylase Family Members in Erythropoiesis. *Biochem. Biophys. Res. Commun.* 388 (4), 683–688. doi: 10.1016/j.bbrc.2009.08.058

Gallage, S., Katagiri, T., Endo, M., Futami, K., Endo, M., and Maita, M. (2016). Influence of Moderate Hypoxia on Vaccine Efficacy Against Vibrio Anguillarum in Oreochromis Niloticus (Nile Tilapia). *Fish. Shellfish. Immunol.* 51, 271–281. doi: 10.1016/j.fsi.2016.02.024

Honda, K., Yanai, H., Negishi, H., Asagiri, M., Sato, M., Mizutani, T., et al. (2005). IRF-7 Is the Master Regulator of Type-I Interferon-Dependent Immune Responses. *Nature* 434 (7034), 772–777. doi: 10.1038/nature03464

Hou, L., Chen, S., Liu, J., Guo, J., Chen, Z., Zhu, Q., et al. (2019). Transcriptomic and Physiological Changes in Western Mosquitofish (Gambusia Affinis) After

Exposure to Norgestrel. *Ecotoxicol. Environ. Saf.* 171, 579–586. doi: 10.1016/j.ecoenv.2018.12.053

Hu, X.-J., Yang, J., Xie, X.-L., Lv, F.-H., Cao, Y.-H., Li, W.-R., et al. (2019). The Genome Landscape of Tibetan Sheep Reveals Adaptive Introgression From Argali and the History of Early Human Settlements on the Qinghai–Tibetan Plateau. *Mol. Biol. Evol.* 36 (2), 283–303. doi: 10.1093/molbev/msy208

Jørgensen, H., Sørensen, P., Cooper, G., Lorenzen, E., Lorenzen, N., Hansen, M., et al. (2011). General and Family-Specific Gene Expression Responses to Viral Hemorrhagic Septicaemia Virus Infection in Rainbow Trout (Oncorhynchus Mykiss). *Mol. Immunol.* 48 (8), 1046–1058. doi: 10.1016/j.molimm.2011.01.014

Jiang, B.-H., Jiang, G., Zheng, J. Z., Lu, Z., Hunter, T., and Vogt, P. K. (2001). Phosphatidylinositol 3-Kinase Signaling Controls Levels of Hypoxia-Inducible Factor 1. *Cell Growth Differ.* 12 (7), 363–370.

Jiang, J.-L., Mao, M.-G., Lü, H.-Q., Wen, S.-H., Sun, M.-L., Liu, R.-t., et al. (2017). Digital Gene Expression Analysis of Takifugu Rubripes Brain After Acute Hypoxia Exposure Using Next-Generation Sequencing. *Comp. Biochem. Physiol. Part D.: Genomics Proteomics* 24, 12–18. doi: 10.1016/j.cbd.2017.05.003

Jiang, M., Yang, H., Peng, R., Han, Q., and Jiang, X. (2020). 1h NMR-Based Metabolomic Analysis of Cuttlefish, SepiaLarkiaC (Ehrenberg 1831) Exposed to Hypoxia Stresses and Post-Anoxia Recovery. *Sci. Total. Environ.* 726, 138317. doi: 10.1016/j.scitotenv.2020.138317

Kemper, C., Pangburn, M. K., and Fishelson, Z. (2014). Complement Nomenclature 2014. *Mol. Immunol.* 61 (2), 56–58. doi: 10.1016/j.molimm.2014.07.004

Khansari, A. R., Balasch, J. C., Vallejos-Vidal, E., Parra, D., Reyes-López, F. E., and Tort, L. (2018). Comparative Immune-and Stress-Related Transcript Response Induced by Air Exposure and Vibrio Anguillarum Bacterin in Rainbow Trout (Oncorhynchus Mykiss) and Gilthead Seabream (Sparus Aurata) Mucosal Surfaces. *Front. Immunol.* 9, 856. doi: 10.3389/fimmu.2018.00856

Kidd, P. (2003). Th1/Th2 Balance: The Hypothesis, Its Limitations, and Implications for Health and Disease. *Altern. Med. Rev.* 8 (3), 223–246.

Li, B., and Dewey, C. N. (2011). RSEM: Accurate Transcript Quantification From RNA-Seq Data With or Without a Reference Genome. *BMC Bioinf.* 12 (1), 1–16. doi: 10.1186/1471-2105-12-323

Li, H. L., Lin, H. R., and Xia, J. H. (2017). Differential Gene Expression Profiles and Alternative Isoform Regulations in Gill of Nile Tilapia in Response to Acute Hypoxia. *Marine. Biotechnol.* 19 (6), 551–562. doi: 10.1007/s10126-017-9774-4

Li, X., Li, F., Zou, G., Feng, C., Sha, H., Liu, S., et al. (2021). Physiological Responses and Molecular Strategies in Heart of Silver Carp (Hypophthalmichthys Molitrix) Under Hypoxia and Reoxygenation. *Comp. Biochem. Physiol. Part D.: Genomics Proteomics* 40, 100908. doi: 1016/j.cbd.2021.100908

Li, X., Ma, J., Lei, W., Li, J., Zhang, Y., and Li, Y. (2013). Cloning of Cytochrome P450 3A137 Complementary DNA in Silver Carp and Expression Induction by Ionic Liquid. *Chemosphere* 92 (9), 1238–1244. doi: 10.1016/j.chemosphere.2013.04.055

Li, X., Ma, J., and Li, Y. (2016). Molecular Cloning and Expression Determination of P38 MAPK From the Liver and Kidney of Silver Carp. *J. Biochem. Mol. Toxicol.* 30 (5), 224–231. doi: 10.1002/jbt.21781

Li, C., Wang, J., Chen, J., Schneider, K., Veettil, R. K., Elmer, K. R., et al. (2020). Native Bighead Carp Hypophthalmichthys Nobilis and Silver Carp Hypophthalmichthys Molitrix Populations in the Pearl River Are Threatened by Yangtze River Introductions as Revealed by Mitochondrial DNA. *J. Fish. Biol.* 96 (3), 651–662. doi: 10.1111/jfb.14253

Lin, Y., Lin, Y., Lin, X., Sun, X., and Luo, K. (2019). Combination of PET and CXCR4-Targeted Peptide Molecule Agents for Noninvasive Tumor Monitoring. *J. Cancer* 10 (15), 3420–3426. doi: 10.7150/jca.31087

Livak, K. J., and Schmittgen, T. D. (2001). Analysis of Relative Gene Expression Data Using Real-Time Quantitative PCR and the 2– ΔΔCT Method. *Methods* 25 (4), 402–408. doi: 10.1006/meth.2001.1262

Lu, H., Forbes, R. A., and Verma, A. (2002). Hypoxia-Inducible Factor 1 Activation by Aerobic Glycolysis Implicates the Warburg Effect in Carcinogenesis. *J. Biol. Chem.* 277 (26), 23111–23115. doi: 10.1074/jbc.M202487200

Ma, Y., Li, B., Ke, Y., Zhang, Y., and Zhang, Y. (2018). Transcriptome Analysis of Rana Chensinensis Liver Under Trichlorfon Stress. *Ecotoxicol. Environ. Saf.* 147, 487–493. doi: 10.1016/j.ecoenv.2017.09.016

Marques, I. J., Leito, J. T., Spaink, H. P., Testerink, J., Jaspers, R. T., Witte, F., et al. (2008). Transcriptome Analysis of the Response to Chronic Constant Hypoxia in Zebrafish Hearts. *J. Comp. Physiol. B.* 178 (1), 77–92. doi: 10.1007/s00360-007-0201-4

Matey, V., Iftikar, F. I., De Boeck, G., Scott, G. R., Sloman, K. A., Almeida-Val, V. M., et al. (2011). Gill Morphology and Acute Hypoxia: Responses of Mitochondria-Rich, Pavement, and Mucous Cells in the AmazonianLark (Astronotus Ocellatus) and the Rainbow Trout (Oncorhynchus Mykiss), Two Species With Very Different Approaches to the Osmo-Respiratory Compromise. *Can. J. Zool.* 89 (4), 307–324. doi: 10.1139/z11-002

Matey, V., Richards, J. G., Wang, Y., Wood, C. M., Rogers, J., Davies, R., et al. (2008). The Effect of Hypoxia on Gill Morphology and Ionoregulatory Status in the Lake Qinghai Scaleless Carp, Gymnocypris Przewalskii. *J. Exp. Biol.* 211 (7), 1063–1074. doi: 10.1242/jeb.010181

Meng, X., Shen, Y., Wang, S., Xu, X., Dang, Y., Zhang, M., et al. (2019). Complement Component 3 (C3): An Important Role in Grass Carp (Ctenopharyngodon 17Larki) Experimentally Exposed to Aeromonas Hydrophila. *Fish. Shellfish. Immunol.* 88, 189–197. doi: 10.1016/j.fsi.2019.02.061

Mu, Y., Li, W., Wei, Z., He, L., Zhang, W., and Chen, X. (2020). Transcriptome Analysis Reveals Molecular Strategies in Gills and Heart of Large Yellow Croaker (Larimichthys Crocea) Under Hypoxia Stress. *Fish. Shellfish. Immunol.* 104, 304–313. doi: 10.1016/j.fsi.2020.06.028

Ohno, K., Sato, Y., Ohshima, K.-i., Takata, K., Miyata-Takata, T., Takeuchi, M., et al. (2015). A Subset of Ocular Adnexal Marginal Zone Lymphomas may Arise in Association With IgG4-Related Disease. *Sci. Rep.* 5 (1), 1–10. doi: 10.1038/srep13539

Overturf, K., and LaPatra, S. (2006). Quantitative Expression (Walbaum) of Immunological Factors in Rainbow Trout, Oncorhynchus Mykiss (Walbaum), After Infection With Either Flavobacterium Psychrophilum, Aeromonas Salmonicida, or Infectious Haematopoietic Necrosis Virus. *J. Fish. Dis.* 29 (4), 215–224. doi: 10.1111/j.1365-2761.2006.00707.x

Petersen, S. V., Thiel, S., Jensen, L., Vorup-Jensen, T., Koch, C., and Jensenius, J. C. (2000). Control of the Classical and the MBL Pathway of Complement Activation. *Mol. Immunol.* 37 (14), 803–811. doi: 10.1016/S0161-5890(01)00004-9

Press, C. M., and Evensen, Ø. (1999). The Morphology of the Immune System in Teleost Fishes. *Fish. Shellfish. Immunol.* 9 (4), 309–318. doi: 10.1006/fsim.1998.0181

Rebl, A., Korytář, T., Köbis, J. M., Verleih, M., Krasnov, A., Jaros, J., et al. (2014). Transcriptome Profiling Reveals Insight Into Distinct Immune Responses to Aeromonas Salmonicida in Gill of Two Rainbow Trout Strains. *Marine. Biotechnol.* 16 (3), 333–348. doi: 10.1007/s10126-013-9552-x

Ren, X., Deng, R., Zhang, K., Sun, Y., Teng, X., and Li, J. (2018). SpliceRCA: *In Situ* Single-Cell Analysis of mRNA Splicing Variants. *ACS Cent. Sci.* 4 (6), 680–687. doi: 10.1021/acscentsci.8b00081

Reyes-Moreno, C., Girouard, J., Lapointe, R., Darveau, A., and Mourad, W. (2004). CD40/CD40 Homodimers Are Required for CD40-Induced Phosphatidylinositol 3-Kinase-Dependent Expression of B7. 2 by Human B Lymphocytes. *J. Biol. Chem.* 279 (9), 7799–7806. doi: 10.1074/jbc.M313168200

Schofield, C. J., and Ratcliffe, P. J. (2004). Oxygen Sensing by HIF Hydroxylases. *Nat. Rev. Mol. Cell Biol.* 5 (5), 343–354. doi: 10.1038/nrm1366

Shen, Y., Zhang, J., Xu, X., Fu, J., and Li, J. (2013). A New Haplotype Variability in Complement C6 Is Marginally Associated With Resistance to Aeromonas Hydrophila in Grass Carp. *Fish. Shellfish. Immunol.* 34 (5), 1360–1365. doi: 10.1016/j.fsi.2013.02.011

Sollid, J., De Angelis, P., Gundersen, K., and Nilsson, G. (2003). Hypoxia Induces Adaptive and Reversible Gross Morphological Changes in Crucian Carp Gills. *J. Exp. Biol.* 206 (20), 3667–3673. doi: 10.1242/jeb.00594

Sollid, J., Kjernsli, A., De Angelis, P. M., Røhr, A. K., and Nilsson, G. E. (2005). Cell Proliferation and Gill Morphology in Anoxic Crucian Carp. *Am. J. Physiology-Regulatory. Integr. Comp. Physiol.* 289 (4), R1196–R1201. doi: 10.1152/ajpregu.00267.2005

Sollid, J., and Nilsson, G. E. (2006). Plasticity of Respiratory Structures—Adaptive Remodeling of Fish Gills Induced by Ambient Oxygen and Temperature. *Respir. Physiol. Neurobiol.* 154 (1-2), 241–251. doi: 10.1016/j.resp.2006.02.006

Sun, S., Xuan, F., Fu, H., Ge, X., Zhu, J., Qiao, H., et al. (2016). Comparative Proteomic Study of the Response to Hypoxia in the Muscle of Oriental River Prawn (Macrobrachium Nipponense). *J. Proteomics* 138, 115–123. doi: 10.1016/j.jprot.2016.02.023

Tiedke, J., Borner, J., Beeck, H., Kwiatkowski, M., Schmidt, H., Thiel, R., et al. (2015). Evaluating the Hypoxia Response of Ruffe and Flounder Gills by a Combined Proteome and Transcriptome Approach. *PloS One* 10 (8), e0135911. doi: 10.1371/journal.pone.0135911

Van der Meer, D. L., van den Thillart, G. E., Witte, F., de Bakker, M. A., Besser, J., Richardson, M. K., et al. (2005). Gene Expression Profiling of the Long-Term Adaptive Response to Hypoxia in the Gills of Adult Zebrafish. *Am. J. Physiology-Regulatory. Integr. Comp. Physiol.* 289 (5), R1512–R1519. doi: 10.1152/ajpregu.00089.2005

Viale-Bouroncle, S., Felthaus, O., Schmalz, G., Brockhoff, G., Reichert, T. E., and Morsczeck, C. (2012). The Transcription Factor DLX3 Regulates the Osteogenic Differentiation of Human Dental Follicle Precursor Cells. *Stem Cells Dev.* 21 (11), 1936–1947. doi: 10.1089/scd.2011.0422

Wu, C.-B., Liu, Z.-Y., Li, F.-G., Chen, J., Jiang, X.-Y., and Zou, S.-M. (2017). Gill Remodeling in Response to Hypoxia and Temperature Occurs in the Hypoxia Sensitive Blunt Snout Bream (Megalobrama Amblycephala). *Aquaculture* 479, 479–486. doi: 10.1016/j.aquaculture.2017.06.020

Xia, J. H., Li, H. L., Li, B. J., Gu, X. H., and Lin, H. R. (2018). Acute Hypoxia Stress Induced Abundant Differential Expression Genes and Alternative Splicing Events in Heart of Tilapia. *Gene* 639, 52–61. doi: 10.1016/j.gene.2017.10.002

Xiao, W. (2015). The Hypoxia Signaling Pathway and Hypoxic Adaptation in Fishes. *Sci. China Life Sci.* 58 (2), 148–155. doi: 10.1007/s11427-015-4801-z

Xing, H., Chen, J., Peng, M., Wang, Z., Liu, F., Li, S., et al. (2019). Identification of Signal Pathways for Immunotoxicity in the Spleen of Common Carp Exposed to Chlorpyrifos. *Ecotoxicol. Environ. Saf.* 182, 109464. doi: 10.1016/j.ecoenv.2019.109464

Yearbook, C. F. S. (2020). *China Fishery Statistical Yearbook* Vol. 2020 (Beijing, China: China Agriculture Press), 24–34.

Zhang, J., Alcaide, P., Liu, L., Sun, J., He, A., Luscinskas, F. W., et al. (2011). Regulation of Endothelial Cell Adhesion Molecule Expression by Mast Cells, Macrophages, and Neutrophils. *PloS One* 6 (1), e14525. doi: 10.1371/journal.pone.0014525

Zhang, B., Chamba, Y., Shang, P., Wang, Z., Ma, J., Wang, L., et al. (2017). Comparative Transcriptomic and Proteomic Analyses Provide Insights Into the Key Genes Involved in High-Altitude Adaptation in the Tibetan Pig. *Sci. Rep.* 7 (1), 1–11. doi: 10.1038/s41598-017-03976-3

Zhang, Z., Ju, Z., Wells, M. C., and Walter, R. B. (2009). Genomic Approaches in the Identification of Hypoxia Biomarkers in Model Fish Species. *J. Exp. Marine. Biol. Ecol.* 381, S180–S187. doi: 10.1016/j.jembe.2009.07.021

Zhang, L., Song, Z., Zhong, S., Gan, J., Liang, H., Yu, Y., et al. (2022). Acute Hypoxia and Reoxygenation Induces Oxidative Stress, Glycometabolism, and Oxygen Transport Change in Red Swamp Crayfish (ProcambarusLarkia): Application of Transcriptome Profiling in Assessment of Hypoxia. *Aquacult. Rep.* 23, 101029. doi: 10.1016/j.aqrep.2022.101029

Zhang, Y., Wang, L., Dey, S., Alnaeeli, M., Suresh, S., Rogers, H., et al. (2014). Erythropoietin Action in Stress Response, Tissue Maintenance and Metabolism. *Int. J. Mol. Sci.* 15 (6), 10296–10333. doi: 10.3390/ijms150610296

Zhu, C.-D., Wang, Z.-H., and Yan, B. (2013). Strategies for Hypoxia Adaptation in Fish Species: A Review. *J. Comp. Physiol. B.* 183 (8), 1005–1013. doi: 10.1007/s00360-013-0762-3

Conflict of Interest: The authors declare that the research was conducted in the absence of any commercial or financial relationships that could be construed as a potential conflict of interest.

Publisher's Note: All claims expressed in this article are solely those of the authors and do not necessarily represent those of their affiliated organizations, or those of the publisher, the editors and the reviewers. Any product that may be evaluated in this article, or claim that may be made by its manufacturer, is not guaranteed or endorsed by the publisher.

frontiers | Frontiers in Marine Science

ORIGINAL RESEARCH
published: 27 May 2022
doi: 10.3389/fmars.2022.898669

Massive Heat Shock Protein 70 Genes Expansion and Transcriptional Signatures Uncover Hard Clam Adaptations to Heat and Hypoxia

Zhi Hu[1,2,3,4,5,6], *Hao Song*[1,2,3,4,6], *Jie Feng*[1,2,3,4,6], *Cong Zhou*[1,2,3,4,5,6], *Mei-Jie Yang*[1,2,3,4,6], *Pu Shi*[1,2,3,4,5,6], *Zheng-Lin Yu*[7], *Yong-Ren Li*[8], *Yong-Jun Guo*[8], *Hai-Zhou Li*[9] *and Tao Zhang*[1,2,3,4,6]*

[1] Chinese Academy of Sciences (CAS) Key Laboratory of Marine Ecology and Environmental Sciences, Institute of Oceanology, Chinese Academy of Sciences, Qingdao, China, [2] Laboratory for Marine Ecology and Environmental Science, Qingdao National Laboratory for Marine Science and Technology, Qingdao, China, [3] Center for Ocean Mega-Science, Chinese Academy of Sciences, Qingdao, China, [4] CAS Engineering Laboratory for Marine Ranching, Institute of Oceanology, Chinese Academy of Sciences, Qingdao, China, [5] University of Chinese Academy of Sciences, Beijing, China, [6] Shandong Province Key Laboratory of Experimental Marine Biology, Qingdao, China, [7] Yantai Institute of Coastal Zone Research, Chinese Academy of Sciences, Yantai, China, [8] Tianjin Key Laboratory of Aqua-Ecology and Aquaculture, Fisheries College, Tianjin Agricultural University, Tianjin, China, [9] Shandong Fu Han Ocean Sci-Tech Co., Ltd, Haiyang, China

OPEN ACCESS

Edited by:
Juan D. Gaitan-Espitia,
The University of Hong Kong, China

Reviewed by:
Chase Smith,
University of Texas at Austin, United States
Tim Regan,
University of Edinburgh, United Kingdom

***Correspondence:**
Tao Zhang
tzhang@qdio.ac.cn

Specialty section:
This article was submitted to Global Change and the Future Ocean, a section of the journal Frontiers in Marine Science

Received: *17 March 2022*
Accepted: *02 May 2022*
Published: *27 May 2022*

Citation:
Hu Z, Song H, Feng J, Zhou C, Yang M-J, Shi P, Yu Z-L, Li Y-R, Guo Y-J, Li H-Z and Zhang T (2022) Massive Heat Shock Protein 70 Genes Expansion and Transcriptional Signatures Uncover Hard Clam Adaptations to Heat and Hypoxia. Front. Mar. Sci. 9:898669. doi: 10.3389/fmars.2022.898669

Heat shock protein 70 (HSP70) members participate in a wide range of housekeeping and stress-related activities in eukaryotic cells. In marine ecosystems, bivalves encounter abiotic stresses, including high temperatures and low dissolved oxygen. Here, 133 MmHSP70 genes were identified through combined methods including Blastp, HMM and manual filtration, based on the whole *Mercenaria mercenaria* genome. The MmHSP70 genes were unevenly distributed, and 41 genes (33.08%) were located on Chr 7. Phylogenetic analyses indicated that the MmHSP70 gene family mainly consisted of two clusters and the Hspa12 subfamily underwent lineage-specific expansion. A high-density collinear gene block was observed between *M. mercenaria* Chr 7 and *Cyclina sinensis* Chr 14. Tandem duplication MmHSP70 gene pairs experienced different levels of purifying selection, which could be an important source of sequence and functional constraints. MmHSP70 genes showed tissue-specific and stress-specific expression. Most tandem duplication HSP70 gene pairs had high expression under hypoxia stress. HSP70 B2 tandem duplication gene pairs showed significantly increased expression under heat plus severe hypoxia stress. This study provided a comprehensive understanding of the MmHSP70 gene family in the *M. mercenaria* and laid a significant foundation for further studies on the functional characteristics of MmHSP70 genes during exposure to heat and hypoxia stress.

Keywords: ***Mercenaria mercenaria*, HSP70, heat, hypoxia, adaptation**

INTRODUCTION

Heat shock proteins (HSPs) are a group of soluble intracellular proteins produced by cells in response to various environmental stresses (Welch, 1993). In the absence of stress, the content of HSPs is ~5% of the total intercellular protein content, but it can rapidly increase up to 15% or more after exposure to stress (Srivastava, 2002). Based on their molecular weights (MWs), HSPs can be divided into various families, such as small HSPs, HSP40, HSP70, HSP90, and HSP110 (Lindquist and Craig, 1988). HSP70, also known as HSPa, is an abundant heat-inducible 70 kDa HSP encoded by HSP70 and is evolutionarily conserved in terms of both structure and function (Lindquist and Craig, 1988; Daugaard et al., 2007). In general, HSP70 has three motifs: an N-terminal adenosine triphosphatase domain (ATPase; ~400 aa), a substrate-binding domain (SBD; ~180 aa), and a variable-length C-terminal domain (Nikolaidis and Nei, 2004). HSP70 first received attention for its role in the response to heat shock (Ritossa, 1962) and was also found to be critical for the folding and assembly of other cellular proteins (Gething and Sambrook, 1992). Some HSP70 genes are expressed only under stress conditions, but not all the members are induced under stress conditions; they are necessary for cell viability under normal conditions (Daugaard et al., 2007; Murphy, 2013). Due to their organelle- and tissue-specific expression, different members of the HSP70 family have distinct biological functions, although they might function redundantly in some cases (Daugaard et al., 2007; Murphy, 2013). In summary, the HSP70 family functions in buffering against extrinsic and intrinsic stress (Murphy, 2013).

The HSP70 gene family has been studied in humans (Brocchieri et al., 2008), bovines (Tripathy et al., 2021), fish (Song et al., 2016; Xu et al., 2018), the fruit fly *Drosophila melanogaster* (Gong and Golic, 2004), and nematodes (Heschl and Baillie, 1990; Nikolaidis and Nei, 2004; Guerin et al., 2019). Mollusca is the second largest phylum in Animalia, and as the largest group of species in the Lophotrochozoa, it is central to our understanding of the biology and evolution of this superphylum of protostomes (Zhang et al., 2012). Bivalves, which are the second class in the Mollusca, are among the oldest and evolutionarily most successful groups of invertebrates (Wang et al., 2013). They are widely distributed from intertidal areas to the deep sea and from polar to tropical regions (Li et al., 2017). Several members of HSP70 have been cloned in several bivalve species and were upregulated after exposure to heat stress and other stresses (Franzellitti and Fabbri, 2005; Liu et al., 2014; Cheng et al., 2019). As an increasing number of genomic resources, the genome-wide HSP70 gene family has been elementary studied in Pteriomorphia and Veneridae. HSP70 genes are expanded in the oysters *Crassostrea gigas* (Zhang et al., 2012) and *C. hongkongensis* (Peng et al., 2020) the Sydney rock oyster *Saccostrea glomerata* (Powell et al., 2018), the pearl oyster *Pinctada fucata* (Takeuchi et al., 2016), the scallop *Patinopecten yessoensis* (Cheng et al., 2016), the Manila clam *Ruditapes philippinarum* (Yan et al., 2019), *Cyclina sinensis* (Wei et al., 2020), the deep-sea vent mussel *Bathymodiolus platifrons* (Sun et al., 2017) and the shallow-water mussel *Modiolus philippinarum* (Sun et al., 2017), suggesting that these genes play important roles in adaptation to heat and other stress factors in dynamic environments with a wide variety of stress factors. As a case of molecular convergent evolution, HSP70 family members independently expanded across multiple lineages to mitigate environmental stress (Guerin et al., 2019). Phylogenetic analysis showed recent species-specific HSP70 expansions along with older mixed-species clusters dating to ancestral bivalve lineages, which was consistent with natural selection favouring the expansion (Guerin et al., 2019).

The hard clam, *Mercenaria mercenaria*, has a burrowing lifestyle typical of bivalves and naturally lives along the East Coast of the United States and Canada (Menzel, 2009). It has become an emerging pond culture species since being imported to China. During pond culture, warm water and low oxygen are major environmental stresses in the summer. Heat is commonly accompanied by hypoxia in the ponds. In our previous transcriptional study, most HSPa12 transcripts showed high expression in the hypoxia-stress groups, while other HSPa subfamilies (including B2, 4, 5, 8, 9 and 14) showed high expression in the heat combined hypoxia stress groups (Hu et al., 2022). These results indicated that HSP70 has a vital function in protecting cells against heat and hypoxia stress (Hu et al., 2022). However, the HSP70 gene family in this hardy species remains poorly understood.

In this study, we comprehensively analysed the chromosomal locations, duplication, structure and motif compositions of 133 HSP70 genes based on the recently completed genome sequence of the *M. mercenaria*. We also analysed the evolutionary relationships of HSP70 genes by performing phylogenetic and collinearity analyses. In addition, we studied the expression of HSP70 genes under thermal and hypoxia stress. This study provides a comprehensive understanding of the HSP70 gene family in the *M. mercenaria* and lays a significant foundation for further studies on the functional characteristics of MmHSP70 genes during exposure to acute thermal and hypoxia stress.

MATERIALS AND METHODS

Identification and Sequence Analysis of HSP70 Genes

The *M. mercenaria* genome was downloaded from the National Center for Biotechnology Information (BioProject number: PRJNA596049). Gene family identification methods include based on sequence homology (Blast) and conserved domain (HMMER). In this study, we used combined methods to identify *M. mercenaria* HSP70 gene family. Firstly, HSP70 protein sequences from the oyster *C. gigas*, which were downloaded from UniProt (https://www.uniprot.org/), were treated as a query database to perform Basic Local Alignment Search Tool algorithm program (BLASTP) search with an E-value ≤ e-5 and identity ≥ 30% against the *M. mercenaria* genome. These candidate genes were believed to have sequence similarities with *C. gigas* HSP70. Then, the candidate genes were filtered by conserved domain. HMMER is a common domain

prediction software. Cut_tc is the strictest option controlling model-specific thresholding. The hidden Markov model (HMM) profile of the HSP70 domain (PF00072) was downloaded from the Pfam protein family database (https://pfam.xfam.org/). The putative *M. mercenaria* HSP70 genes were filtered using HMMER with cut_tc algorithm. Finally, protein sequences with fewer than 300 amino acids were excluded from further analyses. The putative MmHSP70 genes functionally annotated as HSP70 in Swiss-prot database were manually selected as the final identified *M. mercenaria* HSP70. The ExPASy ProtParam tool (https://web.expasy.org/protparam/) was used to analyse molecular weights (MWs).

To study the evolution of HSP70 in Veneridae, another clam, *C. sinensis*, was used for comparison. Whole-genome proteins of *C. sinensis* were downloaded from CNGBdb (https://db.cngb.org/, CNA0003280) (Wei et al., 2020). The CsHSP70 genes were identified as described above.

Chromosomal Distribution, Gene Structure and Conserved Motif Characterization

HSP70 genes were mapped to the chromosomes and contigs according to the Generic Feature Format (GFF) file, and the results were visualized by gene location visualization of the GTF/GFF file in TBtools (Chen et al., 2020). Those genes were named according to their position on the chromosome. MCScanX was applied to search for gene duplicate types in the HSP70 family (Wang et al., 2012). The whole-genome protein sequences were compared in pairs by Diamond software with the parameters max-target-seqs 5 and evalue 1e-10 (Buchfink et al., 2015). Calculator 2.0 software was employed to calculate the Ka and Ks values of tandem HSP70s (Wang et al., 2010). HSP70 gene structure was investigated based on the coding sequence (exon), untranslated region, and intron data from the GFF file and visualized by TBtools (Chen et al., 2020). Conserved motif analysis of the HSP70 proteins was conducted by MEME (5.4.1), and the parameters were set to anr mode, an optimum mode width of 6 to 200 and a maximum number of motifs of 10 (Bailey et al., 2015).

Sequence Alignment and Phylogenetic Analyses

We perform two alignment process based on protein sequences. The first one was based on 133 *M. mercenaria* HSP70 protein sequences, the second one was based on 133 *M. mercenaria* HSP70 protein sequences and 60 C. *sinensis* HSP70 protein sequences. Multiple sequence alignment of HSP70 protein sequences was carried out with the ClustalW algorithm in MEGA 7.0 software (Kumar et al., 2016). Two phylogenetic trees (one was *M. mercenaria* HSP70 tree, the other was *M. mercenaria* and *C. sinensis* HSP70 tree) were constructed using the neighbour-joining (NJ) method and 1000 bootstrap replicates. Gap data Treatment was pairwise deletion.

Synteny Analysis

Diamond software was used to perform two-way BLASTP between the *M. mercenaria* whole-genome protein sequences and those of *C. sinensis* (Buchfink et al., 2015). In details, *M. mercenaria* whole-genome protein sequence file was firstly blastp with *C. sinensis* whole-genome protein sequence file. Then, *C. sinensis* whole-genome protein sequence file was blastp with *M. mercenaria* whole-genome protein sequence file. The blastp parameters were as following: max-target-seqs was 5 and evalue was 1e-10. The two blastp files were merged into one blast file named Mme_Csi.Blast. The *M. mercenaria* and *C. sinensis* whole genome GFF files were also merged into one GFF file named Mme_Csi.gff. MCScanX was used to search for duplicate genes between the *M. mercenaria* and *C. sinensis* (Wang et al., 2012). The Mme_Csi.Balst file and Mme_Csi.gff file were used as the input to MCScanX software. The results were visualized by JCVI. The syntenic HSP70 gene pairs were highlight in red lines.

Tissue Expression of MmHSP70 Genes

The healthy adult hard clam tissue transcriptome libraries were constructed in our previous study including testis, ovary, mantle, gill, foot, intestine, liver, stomach, adductor muscle, and hemolymph (Song et al., 2021). The raw data have been deposited in the SRA of NCBI with the accession number PRJNA596049. Raw data were filtered using in-house Perl scripts to remove adapter reads, poly-N sequences and low-quality reads. After quality control, clean reads were mapped to the hard clam genome by HISAT v 2.0.4 (default parameters). HTSeq v0.6.1 (union model) was used to calculate the numbers of reads mapped to each gene. The per kilobase per million mapped reads (FPKM) value of each gene was calculated. Transcript abundance was evaluated using FPKM values. A heatmap was generated using OmicShare tools, a free online platform for data analysis (http://www.omicshare.com/tools).

Expression Analysis of MmHSP70 Genes Under Heat and Hypoxia Stress

Transcriptome libraries of *M. mercenaria* exposed to heat, hypoxia, and heat combined with hypoxia were constructed in our previous study (Hu et al., 2022). In brief, heat, hypoxia and combined stress challenge experiments were carried out using a novel hypoxia simulation device (Li et al., 2019). The *M. mercenaria* were abruptly exposed to the experimental temperature and dissolved oxygen conditions and remained in these experimental conditions for 3 days. Six groups were established for the six treatments in the experiment: 20°C, 6 mg/L DO (control, C_6); 20°C, 2 mg/L DO (moderate hypoxia, C_2); 20°C, 0.2 mg/L DO (severe hypoxia, C_02); 35°C, 6 mg/L DO (heat, H_6); 35°C, 2 mg/L DO (heat plus moderate hypoxia, H_2); and 35°C, 0.2 mg/L DO (heat plus severe hypoxia, H_02). All *M. mercenaria* under all conditions were under stress for 3 days. Gills were selected as the target tissue for RNA-seq. RNA-seq data (PRJNA764366 and PRJNA764372) were used to examine MmHSP70 gene expression profiles in response to heat and hypoxia stress in the *M. mercenaria* (Hu et al., 2022). The similar methods were used to evaluate transcript abundance as above.

RESULTS

Identification and Sequence Analysis of HSP70 Genes

Compared to those of previously studied bivalves, including the oyster *C. gigas* (Zhang et al., 2012) and the scallops *P. yessoensis* (Cheng et al., 2016) and *C. farreri* (Hu et al., 2019), the genome of the *M. mercenaria* had more HSP70 genes. In the present study, 133 MmHSP70 genes were identified in the genome of *M. mercenaria* by BLASTP and HMM methods, which gives the *M. mercenaria* the largest HSP70 gene repertoire in bivalve, to the best of our knowledge. The *M. mercenaria* MmHSP70 genes included 4 HSPa B2 genes, 1 HSPa4 gene, 1 HSPa5 gene, 1 HSPa8 gene, 2 HSPa9 genes, 122 HSPa12 genes, 1 HSPa14 gene and 1 HSPa17 gene. The expanded HSP70 genes mainly included 122 (91.73%) HSPa12 genes, in accordance with findings in the oyster *C. gigas* (Zhang et al., 2012) and the scallops *P. yessoensis* (Cheng et al., 2016) and *C. farreri* (Hu et al., 2019). Information including genome location, amino acid length, annotation and MW is summarized in **Supplementary File 1**. The encoded proteins ranged from 303 aa (MmHSPa12_90) to 1387 aa (MmHSPa12_65). The predicted MWs of the HSP70 proteins varied from 33.78 kDa (MmHSPa12_90) to 156.41 kDa (MmHSPa12_65). Moreover, 60 CsHSP70 genes were identified in the *C. sinensis* genome, 47 (78.33%) of which were HSPa12 genes.

Chromosomal Distribution and Duplication of HSP70 Genes

A total of 133 MmHSP70 genes were unevenly distributed among 19 *M. mercenaria* chromosomes and 4 scaffolds (**Figure 1**). Among the 133 HSP70 genes, 41 (33.08%) were located on Chr 7. There were fewer than 11 HSP70 genes on other chromosomes and contigs. Only one HSP70 gene was observed on Chr 6, Chr 10 and Chr 19. Similarly, 60 CsHSP70 genes were distributed on 14 chromosomes, and 28 genes were located on Chr 14.

Forty-five and thirty-five MmHSP70 genes were tandemly duplicated and proximally duplicated, respectively, which accounted for 60.15% of the HSP70 gene family. Twenty-six and seven CsHSP70 genes were tandemly duplicated and proximally duplicated, respectively. In total, 17 tandemly duplicated HSP70 gene pairs were found. There were two groups of three tandemly duplicated gene pairs on Chr 2 and Chr 4. Genes in the same tandemly duplicated pairs had short physical distances. The Ka and Ks values of tandemly duplicated HSP70 gene pairs were calculated by Calculator 2.0 with the MA method (Wang et al., 2010) to determine if they experienced various selection pressures (Song et al., 2021). The Ka/Ks values of all tandem duplication HSP70 gene pairs were significantly less than 1 (ranging from 0.0548205 to 0.417659, $P < 0.05$, **Table 1**). All tandem pair HSP70 genes had multiple exons. MmHSPa B2_1, MmHSPa B2_2 and MmHSPa B2_3 had similar gene structures (**Figure 2**). A total of 10 conserved motifs were detected in tandem pair HSP70 genes, whose length ranged from 29 to 200 aa. Highly similar conserved motifs were found in the same pairs of tandem duplicated genes (**Figure 3**). Moreover, the tandemly duplicated gene pairs on Chr 7 also had a similar motif pattern (**Figure 3**).

Phylogenetic Analysis of HSP70 Genes

To study the evolutionary relationships of HSP70, two NJ phylogenetic trees were constructed based on the protein sequences. In **Figure 4**, the tree showed that the *M. mercenaria* HSP70 gene family mainly had two clusters, including the HSPa12 subfamily and other subfamilies. One ancestral branch consisted of 11 HSP70 genes, including HSPa4, HSPa5, HSPa8, HSPa9, HSPa14, HSPa17 and HSPa B2. The *M. mercenaria* HSPa B2s were first clustered together. The tandemly duplicated HSPa9 gene pairs were also clustered together. The other branch consisted of 122 HSPa12 subfamily members (**Figure 4**). Another NJ phylogenetic tree of HSP70 protein sequences from the *M. mercenaria* and *C. sinensis* was also constructed (**Figure 5**). These two trees had similar topological structures. The ancestral branch consisted of 24 HSP70 genes, including HSPa4, HSPa5, HSPa8, HSPa9, HSPa14, HSPa17 and HSPa B2. The clam HSPa4, HSPa5, HSPa8, HSPa9, HSPa14, HSPa17 and HSPa B2 were clustered together. The expanded HSPa12 branch consist of 122 *M. mercenaria* HSPa12 genes and 47 C. *sinensis* HSPa12 genes. Species-specific HSPa12 expansions could also be observed.

Synteny Analysis of HSP70 Genes Between the *M. Mercenaria* and *C. Sinensis*

We performed synteny analysis of the HSP70 genes between the *M. mercenaria* and *C. sinensis*. The HSP70 genes in the *M. mercenaria* were homologous to genes in *C. sinensis*, and syntenic conservation was observed in *C. sinensis* (22 pairs of orthologous gene pairs distributed on several chromosomes). Interestingly, a high-density collinear gene block on Chr 7 could be clearly seen (**Figure 6**). Most MmHSP70 genes located on Chr 7 were HSPa12 genes. These results indicated that the *M. mercenaria* HSP70 gene family was conserved and that the HSPa12 genes expanded on Chr 7 of the *M. mercenaria* genome might have evolved from those of a common ancestor with *C. sinensis*.

Expression Patterns of MmHSP70 Genes in Different Tissues

RNA-seq data of ten tissues, namely, the testis, ovary, mantle, gill, foot, intestine, hepatopancreas, stomach, adductor muscle, and hemolymph, from healthy adult *M. mercenaria* were used to characterize the expression profiles of MmHSP70s (Song et al., 2021). The expression data was shown in **Supplementary File 2**. In general, the average expression of HSP70 genes was highest in the hemolymph and gill and lowest in the foot and adductor muscle. Based on FPKM values, a heatmap of HSP70 genes in various tissues was created (**Figure 7**). Interestingly, the expression pattern of HSP70s in the gill was different from that in the other tested tissues. Some HSP70 genes showed highly

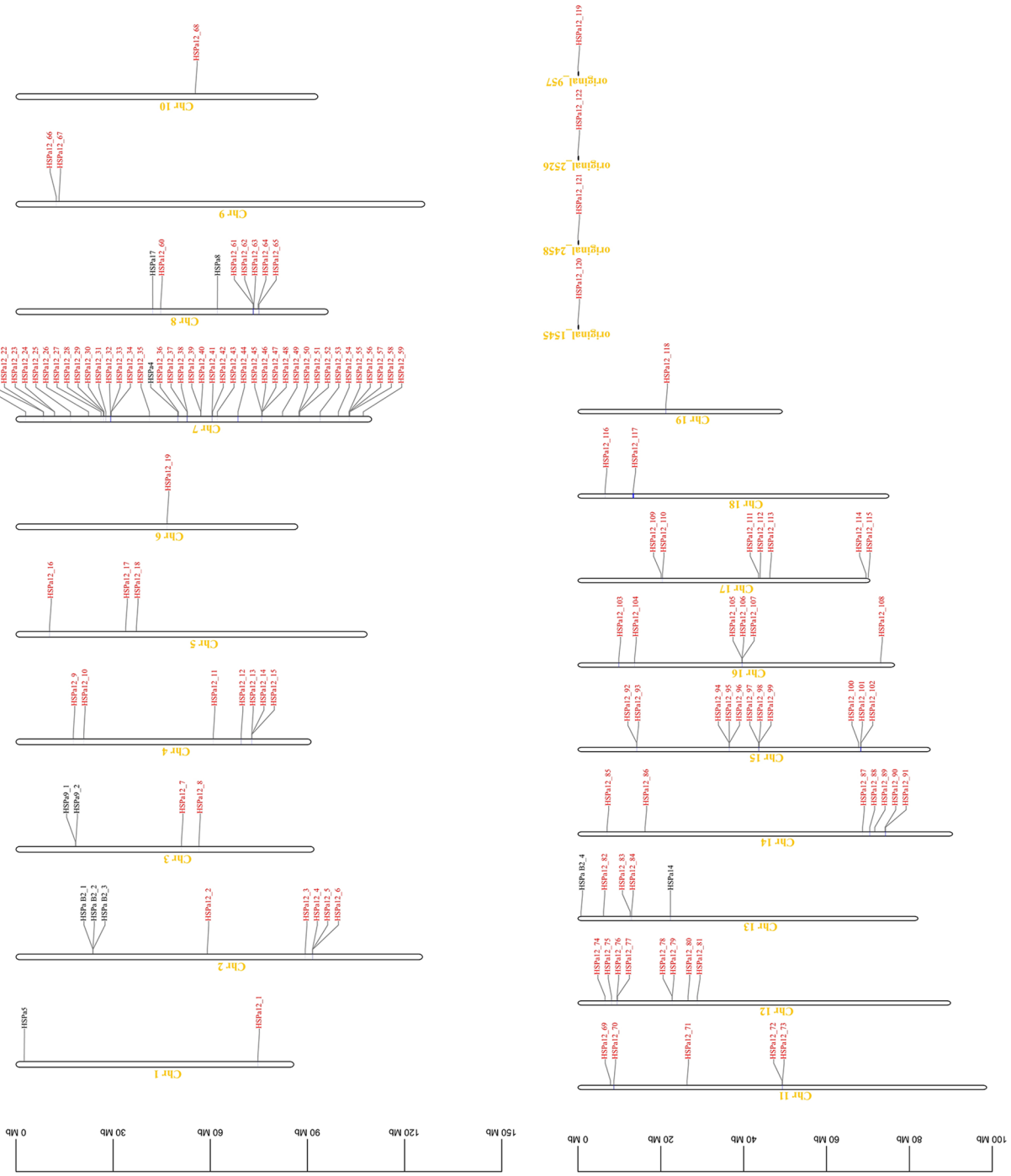

FIGURE 1 | Chromosomal distribution of *Mercenaria mercenaria* HSP70 genes. The HSPa12 genes were highlight in red.

TABLE 1 | Selection pressure on the tandem duplication HSP70 gene pairs.

	Ka	Ks	Ka/Ks	P-Value
MmHSPa12_77 vs MmHSPa12_76	0.113353	0.414677	0.273352	1.39E-25
MmHSPa12_99 vs MmHSPa12_98	0.142116	0.815801	0.174205	3.44E-78
MmHSPa12_102 vs MmHSPa12_101	0.048744	0.295194	0.165126	6.73E-31
MmHSPa12_93 vs MmHSPa12_92	0.040509	0.619088	0.065434	1.09E-49
MmHSPa12_96 vs MmHSPa12_95	0.46246	3.0997	0.149195	0
MmHSPa B2_2 vs MmHSPa B2_1	0.012861	0.157544	0.081635	2.00E-27
MmHSPa B2_3 vs MmHSPa B2_1	0.011003	0.14957	0.073562	9.87E-27
MmHSPa12_106 vs MmHSPa12_105	0.132287	0.473412	0.279434	1.32E-28
MmHSPa9_2 vs MmHSPa9_1	0.022449	0.05375	0.417659	0.010988
MmHSPa12_14 vs MmHSPa12_13	0.419676	3.07451	0.136502	0
MmHSPa12_15 vs MmHSPa12_13	0.336695	3.29855	0.102074	0
MmHSPa12_38 vs MmHSPa12_37	0.147352	0.9504	0.155042	7.39E-99
MmHSPa12_40 vs MmHSPa12_39	0.061806	0.259192	0.238457	1.29E-21
MmHSPa12_48 vs MmHSPa12_47	0.215566	3.93222	0.054821	0
MmHSPa12_51 vs MmHSPa12_50	0.229313	3.52074	0.065132	0
MmHSPa12_24 vs MmHSPa12_23	0.206561	3.76189	0.054909	0
MmHSPa12_30 vs MmHSPa12_29	0.264318	3.64983	0.072419	0
MmHSPa12_34 vs MmHSPa12_33	0.304513	3.70911	0.082099	0
MmHSPa12_63 vs MmHSPa12_62	0.095559	0.280466	0.340714	5.80E-15

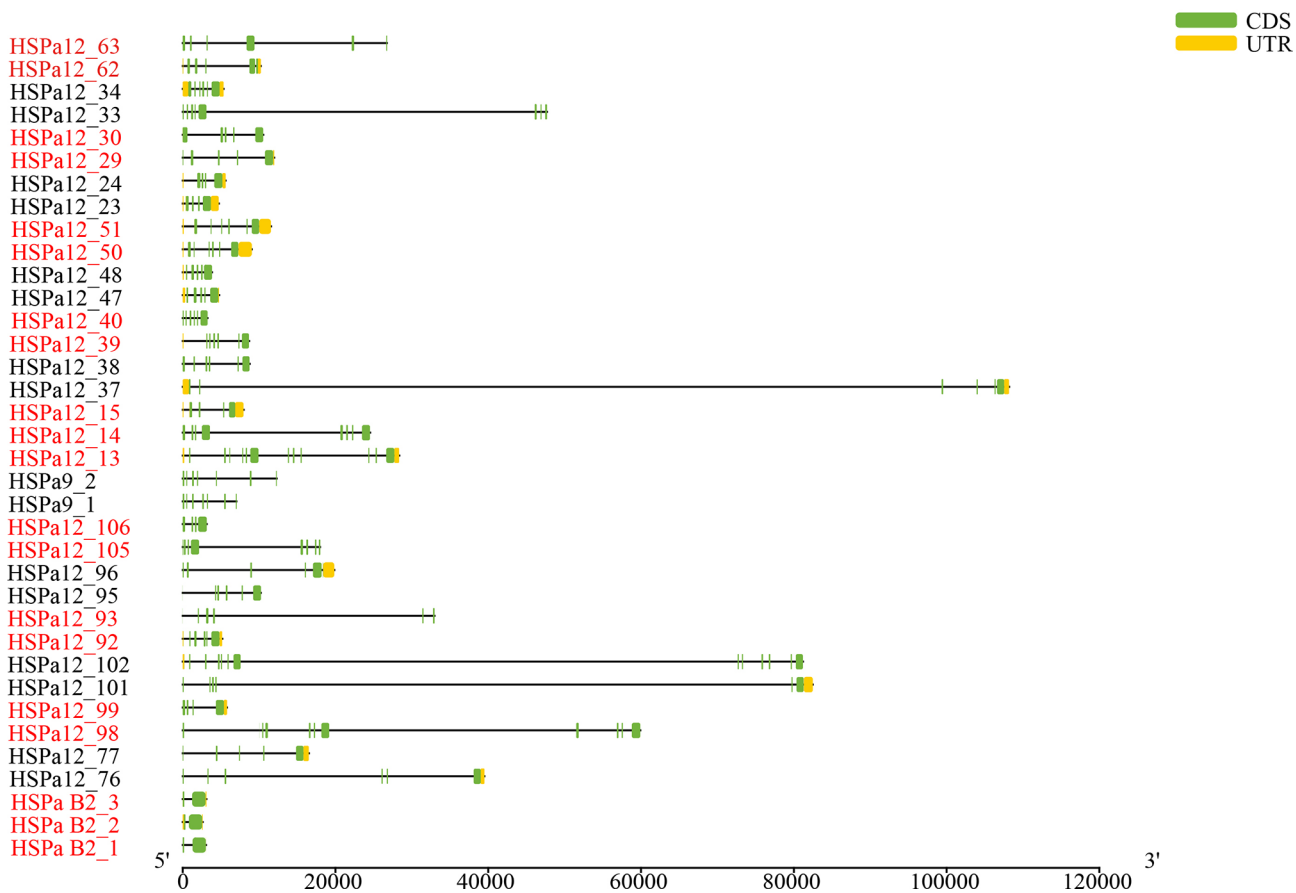

FIGURE 2 | Gene structure of *M. mercenaria* tandem duplication MmHSP70 gene pairs. Green boxes, black lines and yellow boxes represent exons, introns and untranslated region (UTR), respectively. The tandemly duplicated gene pairs were shown by adjacent two or three genes with the same colours.

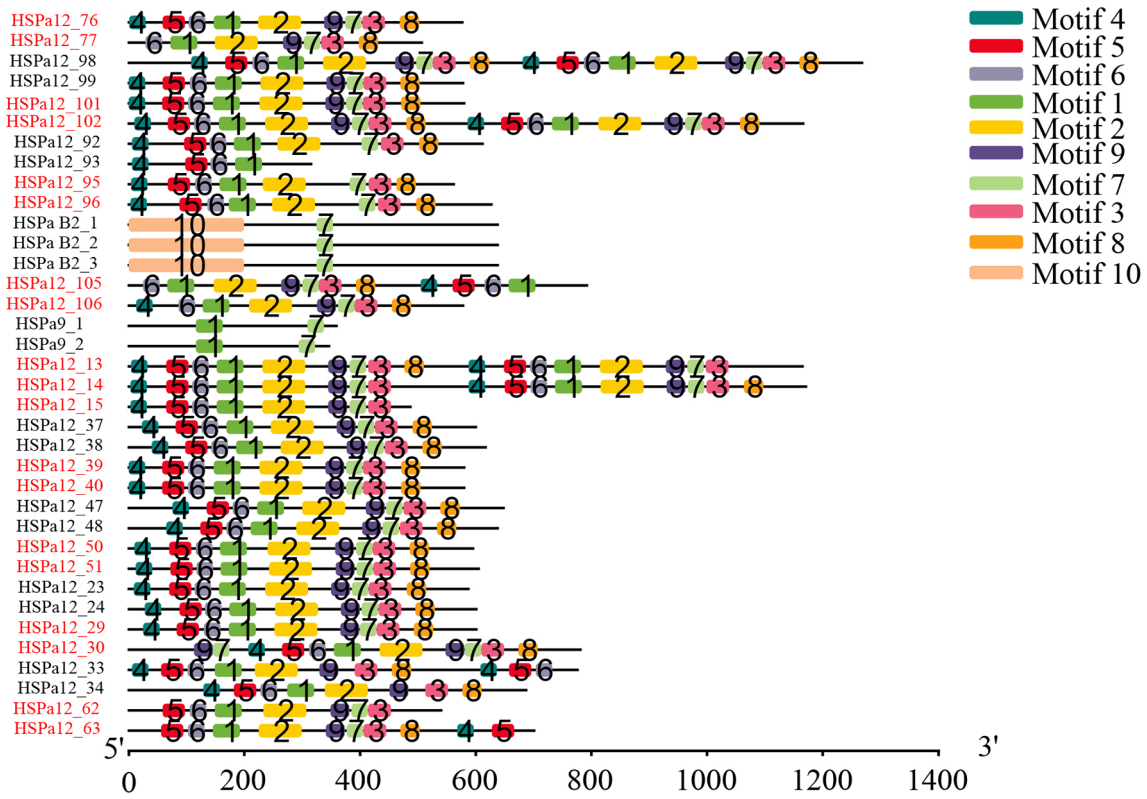

FIGURE 3 | Distribution of conserved motifs in tandem duplication MmHSP70 gene pairs. The tandemly duplicated gene pairs were shown by adjacent two or three genes with the same colours.

tissue-specific expression. For example, MmHSPa12_67, MmHSPa_81 et al. had high expression in the gill. MmHSPa12_10, MmHSPa12_105 et al. showed high expression in the hemolymph. MmHSPa12_64, MmHSPa12_54 et al. showed high expression in the hepatopancreas. Most HSP70 genes were expressed in at least one tissue.

Expression Profiles of Tandem Duplication MmHSP70 Genes in Response to Heat and Hypoxia Stress

The tightly linked gene modules formed by tandem duplication play an important role in adaptation to environmental stress in bivalves (Zhang et al., 2012; Song et al., 2021; Li et al., 2021). To provide insight into the functions of tandem duplication HSP70 genes in the *M. mercenaria*, we determined the expression profiles of such genes by using RNA-seq data. The expression data was shown in **Supplementary File 3**. The tandem duplication HSP70 gene pairs seemed to have similar expression patterns (**Figure 8**). Most of the gene pairs had high expression under hypoxic stress (C_2, C_02). The gene pairs consisting of MmHSPa B2_1, MmHSPa B2_2 and MmHSPa B2_3 had high expression under heat plus extreme hypoxia stress (H_02). Moreover, the gene pair consisting of MmHSPa12_92 and MmHSPa12_93 also had high expression in the H_02 group.

DISCUSSION

The HSP70 gene family functions in a wide range of housekeeping and stress-related activities (Rosenzweig et al., 2019). The function of HSP70 family members has been investigated in some bivalves (Zhang et al., 2012; Cheng et al., 2016; Hu et al., 2019), but to date, no detailed analysis of the HSP70 family has been reported in the *M. mercenaria*. In this study, we performed exhaustive research on the *M. mercenaria* genome, conducted phylogenetic and synteny analyses with selected bivalve species, and determined expression patterns by examining RNA-seq datasets for *M. mercenaria* under heat and hypoxia stress. This study provided a comprehensive understanding of the HSP70 gene family in the *M. mercenaria* and laid a significant foundation for further studies on the functional characteristics of MmHSP70 genes during exposure to heat and hypoxia stress.

HSP70 genes are widespread in all domains of life, and the copy number varies among species. Compared with those in other representative animals, HSP70 genes exhibit expansion in

FIGURE 4 | Phylogenetic analysis of 133 *M. mercenaria* HSP70 protein sequences. The phylogenetic tree was created with MEGA 7.0 software using the Neighbor-Joining method. The HSPa12s were highlight in red. Support value was assessed using bootstrapping (100 pseudoreplicates), if value was less than 50, the data was not shown.

bivalves (Guerin et al., 2019; Hu et al., 2019). In this study, a total of 133 and 60 HSP70 genes were identified in the *M. mercenaria* and *C. sinensis* genomes, respectively. Compared with other bivalve species, for example, *C. gigas* (88) (Zhang et al., 2012), *P. yessoensis* (61) (Cheng et al., 2016) and *C. farreri* (65) (Hu et al., 2019), the *M. mercenaria* had the largest HSP70 gene repertoire, to the best of our knowledge. The HSP70 gene copy number varied greatly among bivalves, which might be a reflection of regulatory variation affecting physiological differences in response to fluctuations in environmental factors, especially temperature (Zhang et al., 2012). There were 8 subfamilies of *M. mercenaria* HSP70 genes. Among these, 122 HSPa12 genes accounted for the vast majority of HSP70 members, which was consistent with the results of previous reports (Zhang et al., 2012; Cheng et al., 2016; Hu et al., 2019). In both previous studies and our study, HSPa1, HSPa2, HSPa6

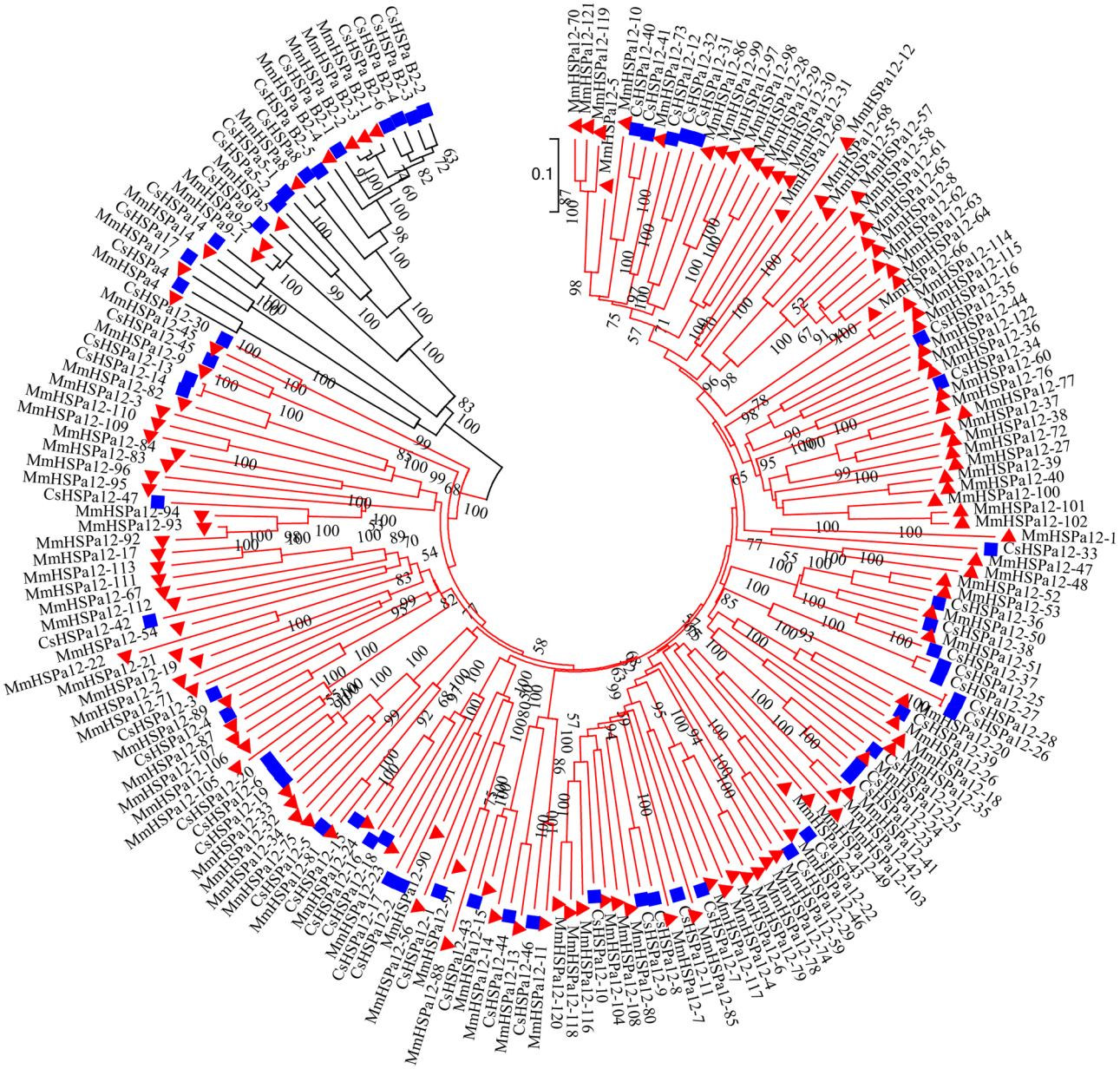

FIGURE 5 | Phylogenetic analysis of 193 clam HSP70 protein sequences (133 *M. mercenaria* HSP70 and 60 *Cyclina sinensis* HSP70 protein sequences). *M. mercenaria* HSP70s and *C. sinensis* HSP70s were marked with red triangles and blue squares, respectively. The HSPa12 branches were highlight in red. Support value was assessed using bootstrapping (100 pseudoreplicates), if value was less than 50, the data was not shown.

and HSPa7 were absent in the bivalve genome, suggesting species-specific loss (Fu et al., 2021). Notably, we identified the HSPa17 gene in the *M. mercenaria* and *C. sinensis* genomes, which was not reported in the oyster (Zhang et al., 2012) and scallop genomes (Cheng et al., 2016; Hu et al., 2019). The HSPa17 gene was also identified in the human (Brocchieri et al., 2008), bovine (Tripathy et al., 2021), channel catfish (Song et al., 2016), large yellow croaker (Xu et al., 2018), rainbow trout (Ma and Luo, 2020), and ascidian (Fujikawa et al., 2010) genomes. However, we did not identify HSPa13 in the *M. mercenaria* genome. MmHSP70 genes were unevenly located on 19 chromosomes and 4 scaffolds, and 41 were located on Chr 7 (**Figure 1**). In addition, 46.67% of CsHSP70 genes were located on Chr 14. It might be a common phenomenon for members of large gene families to be unequally distributed on chromosomes. For example, 19 (a total of 66) transient receptor potential channel genes were located on Chr 2 in an oyster (Fu et al., 2021), and 59 (a total of 159) inhibitors of apoptosis genes

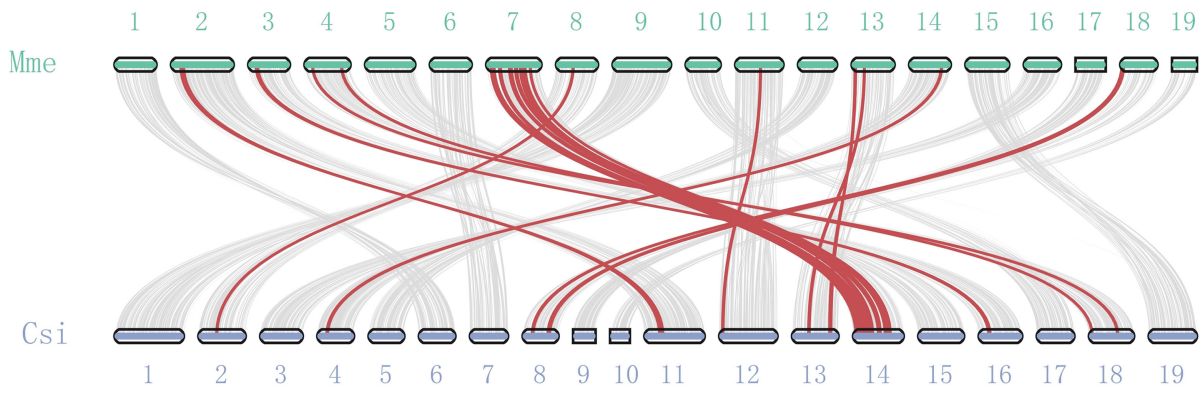

FIGURE 6 | Synteny analyses between the HSP70 genes of the *M. mercenaria* and *C. sinensis*. Grey lines in the background indicate collinear blocks in the *M. mercenaria* and *C. sinensis* genomes, while red lines highlight syntenic HSP70 gene pairs.

were densely tandemly linked on Chr 5 in the *M. mercenaria* (Song et al., 2021).

Gene duplication can provide materials for evolutionary novelty (Zhang, 2003; Roth et al., 2007; Song et al., 2021). Tandem duplication is an important driving force of gene duplication (Chen et al., 2013; Long et al., 2013). After tandem duplication, dose-sensitive genes are lost through selective sweeps to ensure normal organismal function, and environmental stress-related genes tend to be amplified. The HSPa2 gene has undergone tandem duplication in several teleost fishes (Evgen'Ev et al., 2014; Metzger et al., 2016). Tandem duplication was responsible for the expansion of the oyster and scallop HSP70 gene families (Zhang et al., 2012; Cheng et al., 2016; Hu et al., 2019). Forty-five MmHSP70 genes were tandemly duplicated in the *M. mercenaria* genome, while twenty-six CsHSP70 genes were tandemly duplicated in the *C. sinensis* genome. Differences in the number of tandemly duplicated HSP70 genes between species may be explained by tandemly duplicated genes having independent origins or there having been some genomic rearrangement in this region (Metzger et al., 2016). In our study, the same pairs of tandemly duplicated HSP70 genes seemed to have highly similar conserved motifs (**Figure 3**). Moreover, all HSPa B2 tandem duplication pair genes (MmHSPa B2_1, MmHSPa B2_2 and MmHSPa B2_3) had the same number of exons (**Figure 2**). In the early phase of evolution, the function of duplicated genes is retained through purifying selection (Kondrashov et al., 2002). The Ka/Ks values of all tandemly duplicated HSP70 gene pairs were significantly less than 1 (ranging from 0.0548205 to 0.417659, $P < 0.05$, **Table 1**). Moreover, the tandemly duplicated HSP70 gene pairs seemed to have similar expression patterns under heat and hypoxia stress (**Figure 8**). These results indicated that duplicated MmHSP70 genes had experienced different levels of purifying selection and that purifying selection could be an important source of sequence and functional constraints (Song et al., 2021).

In the present study, MmHSP70 genes were expressed in a tissue-specific and stress-specific pattern. Specifically, most MmHSP70 genes were expressed in at least one tissue, while some MmHSP70s showed tissue-specific expression. Some HSP70 genes were highly expressed in gills in the Manila clam (Liu et al., 2015; Nie et al., 2017) and scallops (Cheng et al., 2019). In our present study, the expression pattern of HSP70 in the gill was different from that in the other tested tissues, and some MmHSP70 genes had high expression in the gill. Bivalve gills are sensitive to environmental stress, and high HSP70 expression promotes the regulation of the environmental stress response (Cheng et al., 2019). In marine ecosystems, bivalves always encounter stresses such as high temperature, low osmotic pressure, low dissolved oxygen, heavy metals, toxic dinoflagellates and bacterial invasion, and numerous studies have shown that HSP70 genes play a vital role in maintaining cellular homeostasis to defend against abiotic and biotic stresses (Piano et al., 2002; Franzellitti and Fabbri, 2005; Liu et al., 2014; Cheng et al., 2016; Nie et al., 2017; Nie et al., 2018; Cheng et al., 2019; Clark et al., 2021; Hu et al., 2022). In our previous study, many HSP70 genes were differentially expressed under heat, hypoxia and combined stress (Hu et al., 2022). Tandemly duplicated gene pairs played vital roles in stress adaptation in bivalves (Zhang et al., 2012; Li et al., 2021; Song et al., 2021). In the present study, we determined the expression profiles of tandemly duplicated HSP70 genes by analysing RNA-seq data. As shown in **Figure 8**, the tandemly duplicated HSP70 gene pairs seemed to have similar expression patterns. MmHsp70s exhibited diverse expression patterns in the gill when bivalves were exposed to heat, hypoxia and combined stress. This could be partly explained by HSP70 subfunctionalization after gene duplication (Ramsøe et al., 2020). Most tandemly duplicated HSP70 gene pairs had higher expression under hypoxic stress. Interestingly, the tandemly duplicated HSPa B2 gene pairs (MmHSPa B2_1, MmHSPa B2_2 and MmHSPa B2_3) showed significantly high expression under heat plus severe hypoxia stress. Above all, the considerable expansion of HSP70 genes may enhance transcriptional complexity and play an important role in adaptation to diverse temperatures and dissolved oxygen conditions in the *M. mercenaria*.

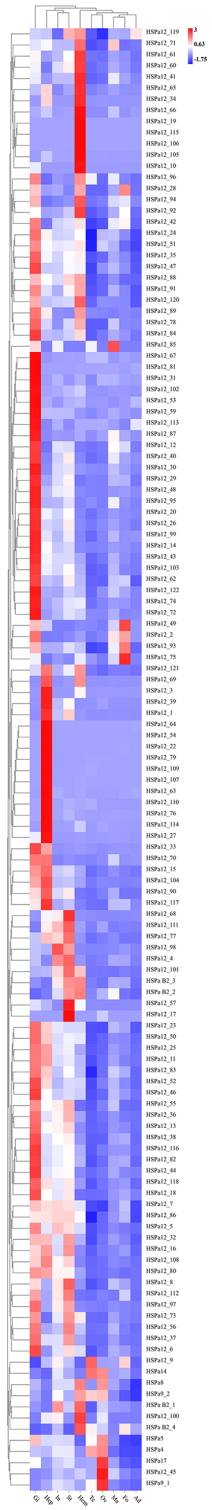

FIGURE 7 | Heatmap analysis of MmHSP70 in ten tissues of adult *M. mercenaria* based on the FPKM. The name of tissues was abbreviated as Te, testis; Ov, ovary; Ma, mantle; Gi, gill; Fo, foot; In, intestine; Hep, hepatopancreas; St, stomach; Ad, adductor muscle; and Hem, hemolymph. The colour scale represented Z-score.

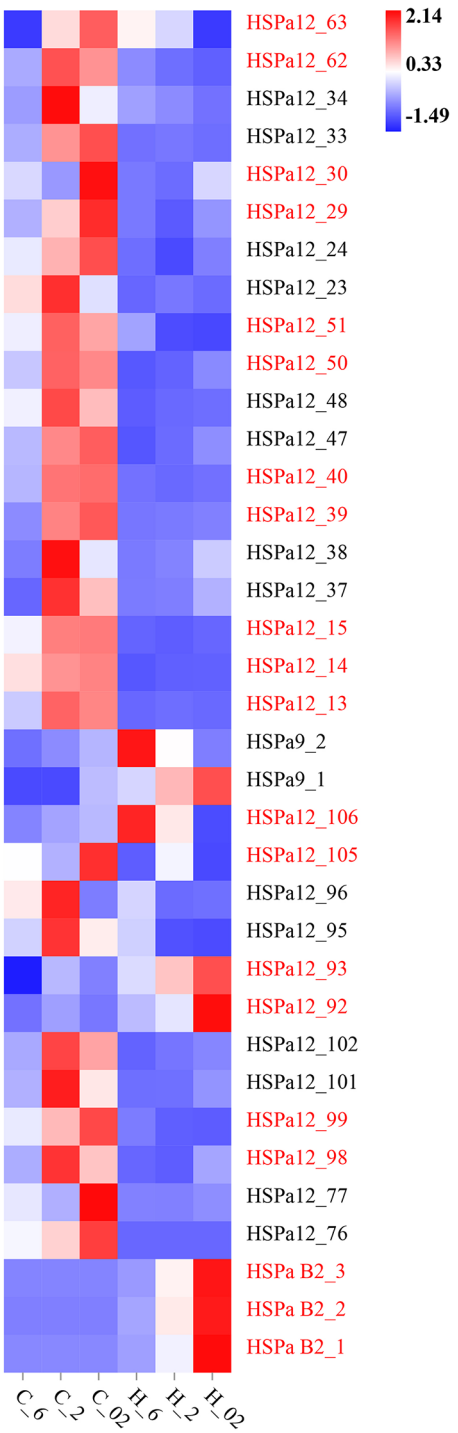

FIGURE 8 | *In silico* gene expression analysis of *M. mercenaria* tandem duplication MmHSP70 genes under heat, hypoxia and combined stress. The colour scale represented Z-score. C_6: 20°C, 6 mg/L DO, control; C_2: 20° C, 2 mg/L DO, moderate hypoxia stress; C_02: 20°C, 0.2 mg/L DO, severe hypoxia stress; H_6: 35°C, 6 mg/L DO, heat stress; H_2: 35°C, 2 mg/L DO, heat plus moderate hypoxia stress; H_02: 35°C, 0.2 mg/L DO, heat plus severe hypoxia stress. The tandemly duplicated gene pairs were shown by adjacent two or three genes with the same colours.

DATA AVAILABILITY STATEMENT

The datasets presented in this study can be found in online repositories. The names of the repository/repositories and accession number(s) can be found below: https://www.ncbi.nlm.nih.gov/, PRJNA596049, https://www.ncbi.nlm.nih.gov/, PRJNA764366, https://www.ncbi.nlm.nih.gov/, PRJNA764372.

AUTHOR CONTRIBUTIONS

ZH contributed to Data curation, Software, Formal analysis, Writing - original draft and Writing - review and editing. HS contributed to Data curation, Formal analysis, Writing - review and editing. JF contributed to Formal analysis, Writing - review and editing. CZ contributed to Data curation, Formal analysis. M-JY contributed to Formal analysis, Software. PS contributed to Formal analysis, Software. Z-LY contributed to Visualization. Y-RL contributed to Resources. Y-JG contributed to Resources. H-ZL contributed to Resources. TZ contributed to Supervision, Funding acquisition, Writing - review and editing. All authors read and approved the final manuscript.

FUNDING

This research was supported by the China National Key R & D Program (2019YFD0900800), Tianjin science and technology commission project (20YFZCSN00240), Tianjin Agricultural Committee Project (202103010), the China Agriculture Research System of MOF and MARA, Shandong Province Agricultural Major Applied Technology Innovation Project (Grant No. SF1405303301), Taishan Industrial Leading Talents Project (Grant No. LJNY201704, Recipient: Tao Zhang), the 'Double Hundred' Blue Industry Leader Team of Yantai (Recipient: Tao Zhang), and the Creative Team Project of the Laboratory for Marine Ecology and Environmental Science, Qingdao Pilot National Laboratory for Marine Science and Technology (Grant No. LMEES-CTSP-2018-1). The funders had no role in the study design, data collection or analysis, decision to publish, or preparation of the manuscript.

ACKNOWLEDGMENTS

The authors thanked Novogene Bioinformatics Institute for bioinformatics analysis. The authors also thanked the AJE (https://www.aje.cn/) for editing the language of the manuscript.

SUPPLEMENTARY MATERIAL

The Supplementary Material for this article can be found online at: https://www.frontiersin.org/articles/10.3389/fmars.2022.898669/full#supplementary-material

REFERENCES

Bailey, T. L., Johnson, J., Grant, C. E., and Noble, W. S.. (2015). The MEME Suite. *Nucleic Acids Res.* 43 (W1), W39–W49. doi: 10.1093/nar/gkv416

Brocchieri, L., De Macario, E. C., and Macario, A. J. (2008). Hsp70 Genes in the Human Genome: Conservation and Differentiation Patterns Predict a Wide Array of Overlapping and Specialized Functions. *BMC Evol. Biol.* 8 (1), 19–19. doi: 10.1186/1471-2148-8-19

Buchfink, B., Xie, C., and Huson, D. H. (2015). Fast and Sensitive Protein Alignment Using DIAMOND. *Nat. Methods* 12 (1), 59–60. doi: 10.1038/nmeth.3176

Chen, C., Chen, H., Zhang, Y., Thomas, H. R., Frank, M. H., He, Y, et al. (2020). TBtools: An Integrative Toolkit Developed for Interactive Analyses of Big Biological Data. *Mol. Plant* 13 (8), 1194–1202. doi: 10.1016/j.molp.2020.06.009

Cheng, D., Liu, H., Zhang, H., Soon, T. K., Ye, T., Li, S., et al. (2019). Differential Expressions of HSP70 Gene Between Golden and Brown Noble Scallops *Chlamys Nobilis* Under Heat Stress and Bacterial Challenge. *Fish Shellfish Immunol.*, 94 , 924–933. doi: 10.1016/j.fsi.2019.10.018

Cheng, J., Xun, X., Kong, Y., Wang, S., Yang, Z., Li, Y., et al. (2016). Hsp70 Gene Expansions in the Scallop *Patinopecten Yessoensis* and Their Expression Regulation After Exposure to the Toxic Dinoflagellate *Alexandrium Catenella*. *Fish Shellfish Immunol.*, 58, 266–273. doi: 10.1016/j.fsi.2016.09.009

Chen, S., Krinsky, B. H., and Long, M. (2013). New Genes as Drivers of Phenotypic Evolution. *Nat. Rev. Genet.* 14 (9), 645–660. doi: 10.1038/nrg3521

Clark, M. S., Peck, L. S., and Thyrring, J. (2021). Resilience in Greenland Intertidal *Mytilus*: The Hidden Stress Defense. *Sci. Total Environ.* 767, 144366. doi: 10.1016/j.scitotenv.2020.144366

Daugaard, M., Rohde, M., and Jaattela, M. (2007). The Heat Shock Protein 70 Family: Highly Homologous Proteins With Overlapping and Distinct Functions. *FEBS Lett.* 581 (19), 3702–3710. doi: 10.1016/j.febslet.2007.05.039

Evgen'Ev, M. B., Garbuz, D. G., and Zatsepina, O. G. (2014). *Heat Shock Proteins and Whole Body Adaptation to Extreme Environments* (Switzerland: Springer).

Franzellitti, S., and Fabbri, E. (2005). Differential HSP70 Gene Expression in the Mediterranean Mussel Exposed to Various Stressors. *Biochem. Biophys. Res. Commun.* 336 (4), 1157–1163. doi: 10.1016/j.bbrc.2005.08.244

Fu, H., Jiao, Z., Li, Y., Tian, J., Ren, L., Zhang, F., et al. (2021). Transient Receptor Potential (TRP) Channels in the Pacific Oyster (*Crassostrea Gigas*): Genome-Wide Identification and Expression Profiling After Heat Stress Between C. Gigas and *C. Angulata*. *Int. J. Mol. Sci.* 22 (6), 3222. doi: 10.3390/ijms22063222

Fujikawa, T., Munakata, T., Kondo, S. I., Satoh, N., and Wada, S.. (2010). Stress Response in the Ascidian *Ciona Intestinalis*: Transcriptional Profiling of Genes for the Heat Shock Protein 70 Chaperone System Under Heat Stress and Endoplasmic Reticulum Stress. *Cell Stress Chaperones* 15 (2), 193–204. doi: 10.1007/s12192-009-0133-x

Gething, M., and Sambrook, J. (1992). Protein Folding in the Cell. *Nature* 355 (6355), 33–45. doi: 10.1038/355033a0

Gong, W. J., and Golic, K. G. (2004). Genomic Deletions of the *Drosophila Melanogaster* Hsp70 Genes. *Genetics* 168 (3), 1467–1476. doi: 10.1534/genetics.104.030874

Guerin, M. N., Weinstein, D. J., and Bracht, J. R. (2019). Stress Adapted Mollusca and Nematoda Exhibit Convergently Expanded Hsp70 and AIG1 Gene Families. *J. Mol. Evol.* 87 (9), 289–297. doi: 10.1007/s00239-019-09900-9

Heschl, M. F., and Baillie, D. L. (1990). The Hsp70 Multigene Family of *Caenorhabditis Elegans*. *Comp. Biochem. Physiol. B* 96 (4), 633–637. doi: 10.1016/0305-0491(90)90206-9

Hu, Z., Feng, J., Song, H., Zhou, C., Yu, Z. L., Yang, M. J., et al. (2022). Mechanisms of Heat and Hypoxia Defense in Hard Clam: Insights From Transcriptome Analysis. *Aquaculture*, 549, 737792. doi: 10.1016/j.aquaculture.2021.737792

Hu, B., Li, M., Yu, X., Xun, X., Lu, W., Li, X., et al. (2019). Diverse Expression Regulation of Hsp70 Genes in Scallops After Exposure to Toxic *Alexandrium*

Dinoflagellates. *Chemosphere* 234, 62–69. doi: 10.1016/j.chemosphere.2019.06.034

Kondrashov, F. A., Rogozin, I. B., Wolf, Y. I., and Koonin, E. V.. (2002). Selection in the Evolution of Gene Duplications. *Genome Biol.* 3 (2), 1–9. doi: 10.1186/gb-2002-3-2-research0008

Kumar, S., Stecher, G., and Tamura, K. (2016). MEGA7: Molecular Evolutionary Genetics Analysis Version 7.0 for Bigger Datasets. *Mol. Biol. Evol.* 33 (7), 1870–1874. doi: 10.1093/molbev/msw054

Li, A., Dai, H., Guo, X., Zhang, Z., Zhang, K., Wang, C., et al. (2021). Genome of the Estuarine Oyster Provides Insights Into Climate Impact and Adaptive Plasticity. *Commun. Biol.* 4 (1), 1–12. doi: 10.1038/s42003-021-02823-6

Lindquist, S., and Craig, E. A. (1988). The Heat-Shock Proteins. *Annu. Rev. Genet.* 22 (1), 631–677. doi: 10.1146/annurev.ge.22.120188.003215

Li, Y., Sun, X., Hu, X., Xun, X., Zhang, J., Guo, X., et al. (2017). Scallop Genome Reveals Molecular Adaptations to Semi-Sessile Life and Neurotoxins. *Nat. Commun.* 8 (1), 1–11. doi: 10.1038/s41467-017-01927-0

Li, Q., Sun, S., Zhang, F., Wang, M., Li, M., et al. (2019). Effects of Hypoxia on Survival, Behavior, Metabolism and Cellular Damage of Manila Clam (*Ruditapes Philippinarum*). *PloS One* 14 (4), e0215158. doi: 10.1371/journal.pone.0215158

Liu, H., He, J., Chi, C. F., and Shao, J. (2014). Differential HSP70 Expression in *Mytilus Coruscus* Under Various Stressors. *Gene* 543 (1), 166–173. doi: 10.1016/j.gene.2014.04.008

Liu, T., Pan, L., Cai, Y., and Miao, J. (2015). Molecular Cloning and Sequence Analysis of Heat Shock Proteins 70 (HSP70) and 90 (HSP90) and Their Expression Analysis When Exposed to Benzo (a) Pyrene in the Clam *Ruditapes Philippinarum*. *Gene* 555 (2), 108–118. doi: 10.1016/j.gene.2014.10.051

Long, M., VanKuren, N. W., Chen, S., and Vibranovski, M. D.. (2013). New Gene Evolution: Little did We Know. *Annu. Rev. Genet.* 47, 307–333. doi: 10.1146/annurev-genet-111212-133301

Ma, F., and Luo, L. (2020). Genome-Wide Identification of Hsp70/110 Genes in Rainbow Trout and Their Regulated Expression in Response to Heat Stress. *PeerJ* 8, e10022. doi: 10.7717/peerj.10022

Menzel, R. W. (2009). Quahog Clams and Their Possible Mariculture. *Proc. Annu. Workshop - World Mariculture Soc.* 2 (1-4), 21–36. doi: 10.1111/j.1749-7345.1971.tb00029.x

Metzger, D. C., Hemmer-Hansen, J., and Schulte, P. M. (2016). Conserved Structure and Expression of Hsp70 Paralogs in Teleost Fishes. *Comp. Biochem. Physiol. Part D: Genomics Proteomics* 18, 10–20. doi: 10.1016/j.cbd.2016.01.007

Murphy, M. E. (2013). The HSP70 Family and Cancer. *Carcinogenesis* 34 (6), 1181–1188. doi: 10.1093/carcin/bgt111

Nie, H., Liu, L., Huo, Z., Chen, P., Ding, J., Yang, F., et al. (2017). The HSP70 Gene Expression Responses to Thermal and Salinity Stress in Wild and Cultivated Manila Clam *Ruditapes Philippinarum*. *Aquaculture* 470, 149–156. doi: 10.1016/j.aquaculture.2016.12.016

Nie, H., Liu, L., Wang, H., Huo, Z., and Yan, X. (2018). Stress Levels Over Time in *Ruditapes Philippinarum*: The Effects of Hypoxia and Cold Stress on Hsp70 Gene Expression. *Aquacul. Rep.* 12, 1–4. doi: 10.1016/j.aqrep.2018.08.003

Nikolaidis, N., and Nei, M. (2004). Concerted and Nonconcerted Evolution of the Hsp70 Gene Superfamily in Two Sibling Species of Nematodes. *Mol. Biol. Evol.* 21 (3), 498–505. doi: 10.1093/molbev/msh041

Peng, J., Li, Q., Xu, L., Wei, P., He, P., Zhang, X., et al. (2020). Chromosome-Level Analysis of *Crassostrea Hongkongensis* Genome Reveals Extensive Duplication of Immune-Related Genes in Bivalves. *Mol. Ecol. Resources* 00, 1–15. doi: 10.1111/1755-0998.13157

Piano, A., Asirelli, C., Caselli, F., and Fabbri, E. (2002). Hsp70 Expression in Thermally Stressed *Ostrea Edulis*, a Commercially Important Oyster in Europe. *Cell Stress Chaperones* 7 (3), 250. doi: 10.1379/1466-1268(2002)007<0250:HEITSO>2.0.CO;2

Powell, D., Subramanian, S., Suwansaard, S., Zhao, M., O'Connor, W., Raftos, D., et al. (2018). The Genome of the Oyster *Saccostrea* Offers Insight Into the Environmental Resilience of Bivalves. *DNA Res.* 25 (6), 655–665. doi: 10.1093/dnares/dsy032

Ramsøe, A., Clark, M. S., and Sleight, V. A. (2020). Gene Network Analyses Support Subfunctionalization Hypothesis for Duplicated Hsp70 Genes in the Antarctic Clam. *Cell Stress Chaperones* 25, 1111–1116. doi: 10.1007/s12192-020-01118-9

Ritossa, F. (1962). A New Puffing Pattern Induced by Temperature Shock and DNP in *Drosophila*. *Experientia* 18 (12), 571–573. doi: 10.1007/BF02172188

Rosenzweig, R., Nillegoda, N. B., Mayer, M. P., and Bukau, B. (2019). The Hsp70 Chaperone Network. *Nat. Rev. Mol. Cell Biol.* 20 (11), 665–680. doi: 10.1038/s41580-019-0133-3

Roth, C., Rastogi, S., Arvestad, L., Dittmar, K., Light, S., and Ekman, D. (2007). Evolution After Gene Duplication: Models, Mechanisms, Sequences, Systems, and Organisms. *J. Exp. Zool. Part B: Mol. Dev. Evol.* 308 (1), 58–73. doi: 10.1002/jez.b.21124

Song, H., Guo, X., Sun, L., Wang, Q., Han, F., Wang, H., et al. (2021). The Hard Clam Genome Reveals Massive Expansion and Diversification of Inhibitors of Apoptosis in Bivalvia. *BMC Biol.* 19 (1), 1–20. doi: 10.1186/s12915-020-00943-9

Song, L., Li, C., Xie, Y., Liu, S., Zhang, J., Yao, J., et al. (2016). Genome-Wide Identification of Hsp70 Genes in Channel Catfish and Their Regulated Expression After Bacterial Infection. *Fish Shellfish Immunol.* 49, 154–162. doi: 10.1016/j.fsi.2015.12.009

Srivastava, P. K. (2002). Roles of Heat-Shock Proteins in Innate and Adaptive Immunity. *Nat. Rev. Immunol.* 2 (3), 185–194. doi: 10.1038/nri749

Sun, J., Zhang, Y., Xu, T., Zhang, Y., Mu, H., Zhang, Y., et al. (2017). Adaptation to Deep-Sea Chemosynthetic Environments as Revealed by Mussel Genomes. *Nat. Ecol. Evol.* 1 (5), 1–7. doi: 10.1038/s41559-017-0121

Takeuchi, T., Koyanagi, R., Gyoja, F., Kanda, M., Hisata, K., Fujie, M., et al. (2016). Bivalve-Specific Gene Expansion in the Pearl Oyster Genome: Implications of Adaptation to a Sessile Lifestyle. *Zool. Lett.* 2 (1), 1–13. doi: 10.1186/s40851-016-0039-2

Tripathy, K., Sodhi, M., Kataria, R. S., Chopra, M., and Mukesh, M.. (2021). *In Silico* Analysis of HSP70 Gene Family in Bovine Genome. *Biochem. Genet.* 59 (1), 134–158. doi: 10.1007/s10528-020-09994-7

Wang, S., Hou, R., Bao, Z., Du, H., He, Y., Su, H., et al. (2013). Transcriptome Sequencing of Zhikong Scallop (*Chlamys Farreri*) and Comparative Transcriptomic Analysis With Yesso Scallop (*Patinopecten Yessoensis*). *PloS One* 8 (5), e63927. doi: 10.1371/journal.pone.0063927

Wang, Y., Tang, H., DeBarry, J. D., Tan, X., Li, J., Wang, X., et al. (2012). MCScanX: A Toolkit for Detection and Evolutionary Analysis of Gene Synteny and Collinearity. *Nucleic Acids Res.* 40 (7), e49. doi: 10.1093/nar/gkr1293

Wang, D., Zhang, Y., Zhang, Z., Zhu, J., Yu, J., et al. (2010). KaKs_Calculator 2.0: A Toolkit Incorporating Gamma-Series Methods and Sliding Window Strategies. *Genomics Proteomics Bioinf.* 8 (1), 77–80. doi: 10.1016/S1672-0229(10)60008-3

Wei, M., Ge, H., Shao, C., Yan, X., Nie, H., Duan, H., et al. (2020). Chromosome-Level Clam Genome Helps Elucidate the Molecular Basis of Adaptation to a Buried Lifestyle. *iScience* 23, 101148. doi: 10.1016/j.isci.2020.101148

Welch, W. J. (1993). How Cells Respond to Stress. *Sci. Am.* 268 (5), 56–56. doi: 10.1038/scientificamerican0593-56

Xu, K., Xu, H., and Han, Z. (2018). Genome-Wide Identification of Hsp70 Genes in the Large Yellow Croaker (*Larimichthys Crocea*) and Their Regulated Expression Under Cold and Heat Stress. *Genes* 9 (12), 590. doi: 10.3390/genes9120590

Yan, X., Nie, H., Huo, Z., Ding, J., Li, Z., Yan, L., et al. (2019). Clam Genome Sequence Clarifies the Molecular Basis of Its Benthic Adaptation and Extraordinary Shell Color Diversity. *iScience*, 19,1225–1237. doi: 10.1016/j.isci.2019.08.049

Zhang, J. (2003). Evolution by Gene Duplication: An Update. *Trends Ecol. Evol.* 18 (6), 292–298. doi: 10.1016/S0169-5347(03)00033-8

Zhang, G., Fang, X., Guo, X., Li, L., Luo, R., Xu, F., et al. (2012). The Oyster Genome Reveals Stress Adaptation and Complexity of Shell Formation. *Nature* 490 (7418), 49–54. doi: 10.1038/nature11413

Conflict of Interest: Author H-ZL was employed by Shandong Fu Han Ocean Sci-Tech Co., Ltd.

The remaining authors declare that the research was conducted in the absence of any commercial or financial relationships that could be construed as a potential conflict of interest.

this article, or claim that may be made by its manufacturer, is not guaranteed or endorsed by the publisher.

frontiers | Frontiers in Marine Science

ORIGINAL RESEARCH
published: 17 June 2022
doi: 10.3389/fmars.2022.921877

Regulation of the Cell Cycle, Apoptosis, and Proline Accumulation Plays an Important Role in the Stress Response of the Eastern Oyster *Crassostrea Virginica*

Cui Li[1,2,3], *Haiyan Wang*[2,3] *and Ximing Guo*[1*]

[1] Haskin Shellfish Research Laboratory, Department of Marine and Coastal Sciences, Rutgers University, Port Norris, NJ, United States, [2] Department of Marine Organism Taxonomy and Phylogeny, Institute of Oceanology, Chinese Academy of Sciences, Qingdao, China, [3] Center for Ocean Mega-Science, Chinese Academy of Sciences, Qingdao, China

OPEN ACCESS

Edited by:
Juan D. Gaitan-Espitia,
The University of Hong Kong,
Hong Kong, SAR China

Reviewed by:
Joanna Griffiths,
University of California, Davis,
United States
Norma Estrada,
Centro de Investigación Biológica del Noroeste (CIBNOR), Mexico

***Correspondence:**
Ximing Guo
xguo@hsrl.rutgers.edu

Specialty section:
This article was submitted to Global Change and the Future Ocean, a section of the journal Frontiers in Marine Science

Received: 16 April 2022
Accepted: 24 May 2022
Published: 17 June 2022

Citation:
Li C, Wang H and Guo X (2022) Regulation of the Cell Cycle, Apoptosis, and Proline Accumulation Plays an Important Role in the Stress Response of the Eastern Oyster Crassostrea Virginica. Front. Mar. Sci. 9:921877. doi: 10.3389/fmars.2022.921877

Background: Understanding how organisms respond and adapt to environmental changes is central to evolutionary biology. As a sessile organism that has adapted to life in estuaries and intertidal zones, the eastern oyster *Crassostrea virginica* can tolerate wide fluctuations in temperature and salinity and survive for weeks out of water. To understand the molecular mechanisms underlying the remarkable stress tolerance of the eastern oyster, we studied the transcriptomic changes induced by exposure to air and cold stress. Eastern oysters were maintained for 7 days under four conditions, namely, in seawater (normal) at 22°C, in air at 22°C, in seawater at 5°C and in air at 5°C, and then sampled for RNA sequencing.

Results: Transcriptomic analysis revealed that many genes involved in cell cycle progression and DNA replication were downregulated in oysters exposed to air and cold, which indicates that stress inhibits cell division. Exposure to air at 22°C induced a concerted inhibition of apoptosis through the upregulation of expanded *inhibitors of apoptosis* and the downregulation of *caspases*. Interactions between TNF and NF-κB signalling implied a reduction in the inflammatory response and immune functions. Key genes for proline production, fatty acid synthesis and chromosomal proteins were upregulated during exposure to low temperatures, which suggested that proline accumulation, energy conservation, and epigenetic modification of chromosomes are important for coping with cold stress. The upregulation of melatonin, FMRFamide, and neural acetylcholine receptors indicate the significance of the neurohormonal regulation of homeostasis.

Conclusion: These results show that air exposure and cold stress alter the expression of key genes for cell division, apoptosis, proline accumulation, fatty acid metabolism, neurohormonal signalling, and epigenetic modifications, suggesting regulation of these processes plays an important role in the stress response of the eastern oyster and

possibly other marine molluscs. This study provides new insights into molecular mechanisms of stress response that are essential for understanding the adaptive potential of marine organisms under climate change.

Keywords: stress, transcriptome, cell cycle control, apoptosis, growth, immune function, epigenetic modification

1 INTRODUCTION

The mechanism through which organisms respond and adapt to environmental shifts is a fundamental question of evolutionary biology. As climate change causes significant shifts in the oceanic environment, understanding its effects on marine organisms and ecosystems is critical. The eastern oyster (*Crassostrea virginica*) is a marine bivalve widely distributed along the Atlantic coast of America, ranging from the Gulf of St. Lawrence in Canada to the Gulf of Mexico and extending to West Indies, and an important fishery and aquaculture species in the US and Canada. Due to its adaptation to estuarine and intertidal environments across a wide latitudinal range, the eastern oyster is remarkably resilient and can tolerate wide fluctuations in salinity and temperature as well as long periods of exposure to air. In the intertidal zone, the eastern oyster may face icy conditions in the winter and 45°C in the summer (Galtsoff, 1964; Shumway, 1996). This species can survive well for at least a month during exposure to air at 4°C (Kawabe et al., 2010). This remarkable resilience makes the eastern oyster an interesting model for studying stress adaptation.

Among all environmental challenges, prolonged exposure to air may be very stressful for oysters and can cause heavy mortalities during summer months (Malek, 2010; Clements et al., 2018). As observed in field experiments, increases in intertidal air exposure increase disease prevalence and mortality and reduce growth (Malek, 2010). Genomic analyses have provided some insights into the molecular mechanisms of the stress response and adaptation of oysters. Transcriptomic analyses of the eastern oyster have identified genes and pathways related to the immune responses of the species and its responses to salinity and crude oil (Eierman and Hare, 2014; McDowell et al., 2014; Zhang et al., 2014a; López-Landavery et al., 2019; Modak and Gomez-Chiarri, 2020). Transcriptomic studies of Pacific oysters *Crassostrea gigas* subjected to thermal, salinity, air exposure and heavy metal stresses have shown that air exposure induces transcriptional changes in the largest number of genes (Zhang et al., 2012). These changes include strong upregulation of the expression of *heat shock proteins* (*HSPs*) and *inhibitor of apoptosis* (*IAPs*), which suggests that these proteins play key roles in stress response and adaptation (Zhang et al., 2012; Guo et al., 2015). A proteomic study of Pacific oysters under desiccation stress revealed increases in ubiquinone synthesis, reductions in reactive oxygen species (ROS), and downregulation of the expression of proteins involved in metabolism, ion transport, DNA replication and protein synthesis (Zhang et al., 2014b). In the eastern oyster, air exposure induces the upregulation and alternative splicing of *alternative oxidases* that participate in ROS removal (Liu and Guo, 2017).

Few studies have examined the relationship between air exposure and the innate immune system. Allen and Burnett (2008) found that hypoxia and high temperatures reduce the ability of haemocytes to kill bacteria in *C. gigas* under air exposure. Air exposure may result in reduced oxygen levels in oysters or hypoxia. Alvarez and Friedl (1992) reported that hypoxia and anoxia have no effects on phagocytosis and particle clearance in the eastern oyster, whereas another study (Boyd and Burnett, 1999) in the same species showed that the respiratory burst function (ROS production) of haemocytes is reduced under hypoxic conditions. Environmental stressors exert immunosuppressive effects in *Pinctada imbricata* (Kuchel et al., 2010). The eastern oyster populations are seriously impacted by two lethal diseases, MSX caused by *Haplosporidium nelsoni* and Dermo caused by *Perkinsus marinus* (Guo and Ford, 2016). The effects of air exposure on the immune function of the eastern oyster are unclear.

Compared with air exposure, cold exposure is a relatively mild stressor for oysters. The LT50 (median lethal time to reach 50% mortality) values for oysters exposed to air at temperatures of 4°C, 15°C and 20°C are 47.8, 15.9 and 12.2 days, respectively (Kawabe et al., 2010). The regulation of energy storage and consumption is crucial for the survival of animals during long periods of cold conditions (Storey and Storey, 1990). During cold periods, bivalves can enter a state of metabolic rate depression (MRD) (Saucedo et al., 2004; Xiao et al., 2014). An analysis of the physiological states of oysters at low temperatures has suggested that the metabolic pathways in oysters change after one week of exposure (Kawabe et al., 2010), although most of the regulatory networks at the protein and transcriptomic levels are largely unknown.

Abbreviations: ABCD, ATP-binding cassette subfamily D; ACAA1, 3-ketoacyl-CoA thiolase A, peroxisomal; ACOX1, peroxisomal acyl-coenzyme A oxidase 1; ARG, arginase; CASP, caspase; CDC, cell division cycle-related protein kinase; CDK, cyclin-dependent kinase; CEBP, CCAAT/enhancer-binding protein; CROT, peroxisomal carnitine O-octanoyltransferase; CYP450, cytochrome P450; E2F, transcription factor E2F3; ER, endoplasmic reticulum; GADD 45, growth arrest and DNA damage-inducible protein 45; GST, glutathione S-transferase; IAP, inhibitor of apoptosis; JUN, AP-1 transcription factor; MAP2K6, dual specificity mitogen-activated protein kinase 6; MCM2-7, minichromosome maintenance proteins; NFKB, nuclear factor NF-kappa-B p105; NFKBIA, NF-kappa-B inhibitor alpha-like; NUDT19, nucleoside diphosphate-linked moiety X motif 19; OAT, ornithine aminotransferase; P5CS, delta-1-pyrroline-5-carboxylate synthase; PCNA, proliferating cell nuclear antigen; PECR, peroxisomal trans-2-enoyl-CoA reductase-like; PEX, peroxin protein; PIK3, phosphatidylinositol-4,5-bisphosphate 3-kinase; PYCR, pyrroline-5-carboxylate reductase; RFC, replication factor C; ROS, reactive oxygen species; RPA, replication protein A; TNF, tumour necrosis factor; TNFAIP3, tumour necrosis factor alpha-induced protein 3; TNFR, tumour necrosis factor receptor.

The availability of the *C. virginica* genome and high-throughput next-generation sequencing technology has allowed accurate measurement of transcriptional levels of all genes, which provided a valuable tool for studying molecular mechanisms of stress response in oysters (Zhang et al., 2012; Gómez-Chiarria et al., 2015; Guo et al., 2015; Guo and Ford, 2016). In this study, we used the reference genome (GCA_002022765.4 C_virginica-3.0) and transcriptomic sequencing to characterize transcriptional changes in eastern oysters subjected to air exposure and cold stress and thus elucidate the molecular mechanisms or regulatory pathways underlying stress response in this species.

2 MATERIALS AND METHODS

2.1 Air Exposure and Cold Stress

Hatchery-produced eastern oysters of the same age (18 months) and similar shell lengths (5–8 cm) were used in this study. The oysters were obtained from the Haskin Shellfish Research Laboratory, Rutgers University, Port Norris, New Jersey, USA. The oysters were maintained in ambient seawater at 9°C ~ 12°C and then acclimated to 22°C for 3 days for this experiment in April. To elicit a strong response to chronic air exposure and cold stress, oysters were exposed to air and cold (5°C) for 7 days. The low temperature of 5°C was selected because it is the lowest possible temperature above freezing that can be stably maintained in the lab. The duration of 7 days was selected based on a previous study (Zhang et al., 2012), where oysters exposed to 5°C for 7 days and to air for 7-9 days exhibited the strongest responses. Although 7-day exposure is rare in the field (only experienced by oysters at extremely high tidal positions), this extreme length helps to identify key genes responding to air exposure stress. Also, eastern oysters are often stored in cold rooms without water for 1-2 weeks before being consumed live. Taking all these factors into account, we subjected oysters to 7 days of air exposure. In winter, the coldest month in New Jersey is January when the average temperature ranged from -6.7°C to 3.3°C. The oysters may be covered by ice for several days at a time in the field. The low temperate tested in this study is quite common for eastern oysters in NJ and the northeastern US. The average ambient temperature in April was 10°C. The control oysters were maintained in seawater at 22°C with heaters, an optimal temperature that is routinely used for oyster conditioning in our lab. Accordingly, the oysters were divided into 4 groups (7 per group): one group was maintained in seawater at 22°C with aeration and served as the control group (hereafter the 22SW group), one group was exposed to air in an incubator with temperature set at 22°C (the 22AE group), one group was maintained in seawater at 5°C (the 5SW group), and one group was exposed to air at 5°C (the 5AE group). The cold treatment was conducted in a cold storage room with both water and air temperature set at 5°C. The temperature decreased from 22°C to 5°C over approximately one day. The oysters exposed to air were covered with a wet towel to keep them moist, and the towel was rewetted daily. The oysters kept in seawater were not fed to ensure consistency with those exposed to air. The salinity of the seawater was 32 parts per thousand.

2.2 Transcriptome Analysis

2.2.1 Total RNA Extraction

After 7 days of treatment, 6 oysters were sampled from each group. Gill tissue from each oyster was flash-frozen in liquid nitrogen and used for transcriptome sequencing. Gills were used for this study because gills are the organ needed for respiration and are important for maintaining homeostasis. Total RNA was extracted from the gill tissue using TRIzol reagent (Invitrogen, USA) following the manufacturer's protocol. The quantity and quality of the extracted total RNA were assessed with a NanoDrop 2000 (Thermo Scientific, USA) and agarose gel electrophoresis. For each group, RNA was extracted from six oysters, and equal amounts of RNA from each oyster were combined into one sample. A total of 3 μg of RNA per group was used for library preparation.

2.2.2 Library Preparation and Bulk RNA Sequencing

Sequencing libraries were generated using an NEBNext® Ultra™ RNA Library Prep Kit for Illumina® (NEB, USA) following the manufacturer's recommendations, and unique index codes were utilised to distinguish the samples. Briefly, mRNA was purified from total RNA using poly-T oligo-attached magnetic beads. Fragmentation was performed using divalent cations under elevated temperature in NEBNext First Strand Synthesis Reaction Buffer (5X). First-strand cDNA was synthesized using random hexamer primers and M-MuLV reverse transcriptase (RNase H^-). Second-strand cDNA synthesis was performed using DNA polymerase I and RNase H. The remaining overhangs were converted into blunt ends by exonuclease/polymerase. After adenylation of the 3' ends, NEBNext adaptors with hairpin loop structures were ligated to the fragments to prepare them for hybridization. To preferentially select cDNA fragments with a length of 150~200 bp, the library fragments were purified with an AMPure XP System (Beckman Coulter, USA). The size-selected, adaptor-ligated cDNA was then incubated with 3 μl of USER Enzyme at 37°C for 15 min and then at 95°C for 5 min before PCR. PCR was performed with Phusion High-Fidelity DNA polymerase, universal PCR primers and the Index (X) Primer. The PCR products were purified (AMPure XP System), and the library quality was assessed with an Agilent Bioanalyzer 2100 system. Clustering of the index-coded samples was performed using a cBot Cluster Generation System with a TruSeq PE Cluster Kit v3-cBot-HS (Illumina) according to manufacturer's instructions. After cluster generation, the libraries were sequenced on an Illumina HiSeq 2000 platform to generate 100-bp paired-end reads.

2.3 Bioinformatic Analysis

2.3.1 Mapping of Reads Against the *C. Virginica* Genome

Raw sequence data in fastq format were first processed through in-house Perl scripts. Clean reads were obtained by removing reads containing adapters or poly-N sequences (for which the proportion

of N bases was > 10%) and reads containing more than 50% of low quality (Q-value ≤ 20) bases. The *C. virginica* reference genome and gene model annotation files were downloaded from NCBI (https://www.ncbi.nlm.nih.gov/genome/398). An index of the reference genome was built, and clean paired-end reads were mapped to the reference genome using HISAT2.2.4 (Kim et al., 2015) with the "-rna-strandness RF" setting and default settings for other parameters.

2.3.2 Gene Expression Analysis

The mapped reads of each sample were assembled with StringTie v1.3.1 (Pertea et al., 2015; Pertea et al., 2016) using a reference-based approach. For each transcription region, fragments per kilobase of transcript per million mapped reads (FPKM) values were calculated to quantify transcript abundance of each gene using StringTie software. Differential expression between two samples was analysed with edgeR (Robinson et al., 2010; McCarthy et al., 2012). P-values were obtained using the exactTest function with normalized counts and assuming a negative binomial distribution. Correction for multiple testing was performed by applying the Benjamini–Hochberg method to the p-values to control the false discovery rate (FDR) (Benjamini and Hochberg, 1995). To reduce false positives due to the lack of replication, a fold-change threshold was also applied. Genes with a false discovery rate (FDRs) < 0.001 and absolute fold change ≥ 2 were considered DEGs. A hierarchical cluster analysis of the top 1000 DEGs was performed to assess transcriptional variations among oysters exposed to different stresses using in-house R scripts.

2.3.3 Screening of Stress Response Genes

Gene Ontology (GO) enrichment analysis of the DEGs was performed with the GOseq R package (Young et al., 2010). We used the Kyoto Encyclopedia of Genes and Genomes (KEGG) Orthology-Based Annotation System (KOBAS) (Mao et al., 2005) to test the significance of the enrichment of DEGs in KEGG (Kanehisa et al., 2008) pathways. KOBAS uses the whole genome as the default background distribution. For each pathway that occurs in a geneset, it counts the number of genes in the geneset that belong to the pathway and compares it against the whole-genome background. The calculating formula of P-value is:

$$P = 1 - \sum_{i=0}^{m-1} \frac{\binom{M}{i}\binom{N-M}{n-i}}{\binom{N}{n}}$$

where N is the number of all genes that with KEGG annotation, n is the number of DEGs in N, M is the number of all genes annotated to specific pathways, and m is number of DEGs in M. The calculated p-values were corrected for FDR (Benjamini and Hochberg, 1995) with FDR ≤ 0.05 as the threshold. Pathways meeting this condition were defined as significantly enriched pathways in DEGs.

2.4 qPCR Validation of the RNA-seq Results

Before combining RNA from 6 oysters for library construction, 2 μg of total RNA from each oyster was removed and separately reverse-transcribed into cDNA for qPCR validation. Complementary DNA (cDNA) was prepared using a FastQuant RT kit (with gDNase) (Tiangen, Beijing, China).

We selected eight genes for qPCR validation rather arbitrarily to cover genes with different expression levels. Most of the eight genes were significantly expressed in at least one treatment group, but not all of them were DEGs, such as *EC-SOD (Extracellular superoxide dismutaseare)*. They were chosen to show the correlation between the read counts obtained by RNA-seq and the relative expression levels obtained by qPCR. Some genes were abundantly expressed (*KLF5*) and some were not (*EEF2*). At the same time, they may or may not be key genes or in important pathways analyzed. Primers for the eight genes were designed with Primer-BLAST online (http://www.ncbi.nlm.nih.gov/tools/primer-blast/) (**Supplementary Table 2**). The expression of the selected genes and the housekeeping gene *β-actin* (Ivanina et al., 2010) was quantified by qPCR using a 7500 Fast Real-time PCR System (Applied Biosystems, USA). The cycle threshold (CT) values of each gene were normalized to those of *β-actin*, and the relative amount of mRNA specific to each of the selected genes was calculated using the $2^{-\Delta\Delta Ct}$ method (Livak and Schmittgen, 2001). Validation analyses were performed by comparing the read count of each gene obtained from the RNA-seq data (adjusted by edgeR software using one scaling normalized factor) with the mean $2^{-\Delta\Delta Ct}$ value from the qPCR results.

3 RESULTS AND DISCUSSION

3.1 Transcriptome Mapping and General Patterns of Gene Expression

A total of 247,921,390 clean paired-end reads were generated from the four groups of oysters, and these numbers ranged from 55.2 to 67.9 million per group (**Supplementary Table 1**). The raw sequence data have been submitted to NCBI under the accession numbers SRR5643669, SRR5643668, SRR5643671 and SRR5643670. For all the groups, approximately 80% of the reads were successfully mapped to the reference genome, covering 84.30% to 86.73% of the genes (**Supplementary Table 1**). For the eight genes selected for validation (**Supplementary Table 2**), a highly significant correlation ($p < 0.0001$, $r = 0.8553$) was found between the read counts obtained by RNA-seq and the relative expression levels obtained by qPCR (**Supplementary Figure 1**), which indicated that the RNA-seq data are reliable due to the pooling of six individuals and a high read coverage. Further, we applied more stringent selection criteria (FDR < 0.001 plus fold-change ≥ 2) to DEG identification to compensate for the lack of sequencing replication, and identified affected pathways based on concerted regulation of multiple protagonist and antagonist genes (see below) so that the conclusions are not affected by random false positives. Nevertheless, it should be noted that the inclusion of independent samples or sample pools would increase the statistical power and detect more DEGs with small fold changes that could not be identified in this study. Additionally, findings of this study should be viewed with

caution due to the lack of treatment replicates. Finally, the response to stress is a temporal process, and our observations are limited to the response at day 7, which may differ from the responses at other time points.

Differential expression analysis revealed large numbers of DEGs among the four groups. Compared with the control condition (22SW), exposure to air at 22°C resulted in the largest number of DEGs (2488), which suggested that air at 22°C is the harshest of the tested conditions for the eastern oyster (**Figure 1A**). Exposure to air at 5°C produced 1969 DEGs, and exposure to seawater at 5°C produced 1802 DEGs, which indicated that these conditions are relatively less stressful. The two conditions at 5°C shared 987 DEGs (**Figure 1B**). Under all three stress conditions, a higher number of genes were downregulated than upregulated. These results indicate that all three stress conditions depressed the transcriptional activities of the eastern oyster and that air exposure at 22°C was the most stressful. This finding is consistent with the results obtained for the Pacific oyster, in which air exposure also induces the highest number (4420) of DEGs (Zhang et al., 2012).

The three stress conditions differed among the types of DEGs induced. Although the three conditions shared 636 DEGs, they also had large numbers of unique DEGs: 1296 in 22AE, 713 in 5AE and 528 in 5SW (**Figure 1B**). Among the four groups, the expression profiles obtained for 5AE and 5SW were most similar but differed significantly from that obtained for 22AE, as indicated by the clustering heatmap (**Figure 1C**). As low temperature tends to reduce metabolic activity, oysters might be less susceptible to air exposure at low temperature than at normal or high temperatures. All DEGs revealed by pairwise comparisons are shown in **Supplementary Table 3**.

Enrichment analysis revealed that the following KEGG pathways were overrepresented in the DEGs between the 22AE and 22SW control groups: DNA replication, cell cycle control, retinol metabolism, apoptosis, nuclear factor kappa B (NF-κB) signalling, lipid metabolism, peroxisome and tumour necrosis factor (TNF) signalling (P-value < 0.05, **Table 1**). The main processes affected in the 5SW and 5AE groups were lipid metabolism and DNA replication. The only GO term significantly enriched in DEGs between 22AE and 5AE was DNA metabolism (0006259), and these DEGs included genes involved in DNA replication and cell cycle control. Some of the significantly enriched pathways and processes are highlighted below. For brevity, the gene IDs from the reference genome were shortened by omitting the string "OC1111", which is shared by all the genes (i.e., L00001 for LOC111100001).

3.2 Cell Cycle Control Under Stress

One of the most significantly affected processes in the eastern oyster under stress is cell division, as evidenced by the identification of large number of DEGs related to DNA replication and cell cycle control under all three stressors at day 7, particularly in the 22AE group (**Table 1**). Cell cycle progression, a process that is conserved in metazoans, is regulated by cyclin-dependent kinases (CDKs) and their specific cyclin partners, positive and negative regulators, and downstream targets (Morgan, 1997). In this study, *cyclin A* (*L22860, L22939*), *cyclin D* (*L03611*), *cyclin E* (*L32839, L99092*), and *CDK2* (*L21435*), which are expressed at the G1 phase and determine whether cells proceed through the G1 phase into the S phase, were all downregulated under air

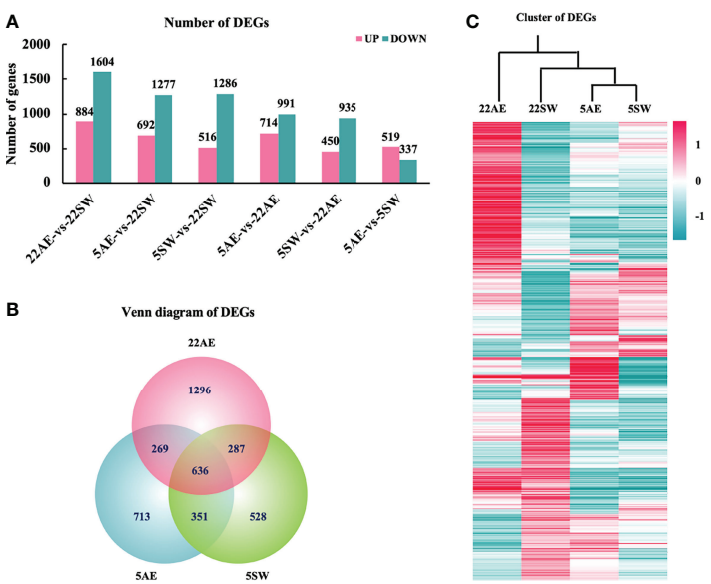

FIGURE 1 | Differentially expressed genes (DEGs) among the four experimental groups of eastern oysters. **(A)**, Number of DEGs between pairs of four groups: seawater at 22°C (22SW, control), exposure to air at 22°C (22AE), seawater at 5°C (5SW) and exposure to air at 5°C (5AE); **(B)**, Venn diagram of DEGs between the three stress conditions and the control 22SW condition; **(C)**, hierarchical clustering of the expression of the top 1000 DEGs in the four groups. The colour range indicates the $log_{10}^{normalized\ (read\ count+1)}$ values from high (red, the maximum value is 8.14) to low (green, the minimum value is -6.82).

TABLE 1 | KEGG pathways enriched in differentially expressed genes induced by stressors in the eastern oyster.

KEGG ID	Pathway	Gene number	Backgroundnumber	P-value
22°C air exposure vs. 22°C seawater				
Ko03030	DNA replication	24	44	1.16E-07
Ko04110	Cell cycle	41	133	0.000529
Ko00830	Retinol metabolism	20	51	0.000532
Ko04215	Apoptosis, cell growth and death	44	151	0.001249
Ko04064	NF-kappa B signalling pathway	40	137	0.001953
Ko00592	Lipid alpha-linolenic acid metabolism	13	31	0.002447
Ko04146	Peroxisome, transport and catabolism	35	127	0.009693
Ko04668	TNF signalling pathway	41	158	0.015759
5°C seawater vs. 22°C seawater				
Ko00061	Lipid fatty acid biosynthesis	11	23	0.000171
Ko00592	Lipid alpha-linolenic acid metabolism	13	31	0.000229
Ko00140	Lipid steroid hormone biosynthesis	12	33	0.001790
Ko03030	DNA replication	14	44	0.003277
5°C air exposure vs. 22°C seawater				
Ko00592	Lipid alpha-linolenic acid metabolism	16	31	1.51E-06
Ko03030	DNA replication	15	44	0.001052

Background number is the number of all genes annotated to specific pathways. Gene number is the number of DEGs belonging to specific pathways.

exposure and cold stress (**Supplementary Table 4** and **Figure 2**). During the S phase, DNA replication starts with the building of replication complexes, where minichromosome maintenance (MCM) proteins are loaded onto chromatin to "licence" DNA for replication (Blow and Laskey, 1988). Six *MCM2-7* complex genes (*L09564*, *L24297*, *L35545*, *L31693*, *L03623*, *L36042*), the associated component *MCMBP* (*L00880*) and *CDC7* (*L22674*), which can phosphorylate *MCM2* and *MCM3*, were significantly downregulated in oysters under the 22AE conditions (**Supplementary Table 4**). All six genes under cold stress showed reduced expression, although the reduction in the expression of some of the genes was not significant. Once replication complexes are built and activated, a series of replicating forks form along the chromosome, generating bubbles that eventually fuse together to complete DNA replication (Alberts et al., 2010). Genes associated with the replication protein A complex, such as replication protein A (*L20888*), DNA polymerase (*L12959*, *L30346*, *L37485*, *L30057*, *L26184*, *L28010*), DNA primase (*L26192*, *L21347*) and DNA clamp proteins (*RFC* and *PCNA*, *L08767*, *L31355*, *L32381*, *L34900*, *L22897*, *L35799*, *L20673*), were downregulated (**Supplementary Table 4**). Genes encoding cyclins and CDKs that promote the progression of cells from the G2 phase to the M phase, such as G2/mitotic-specific cyclin-A (*L22860*, *L22939*) and M-phase inducer phosphatase (*CDC25A*, *L32091*, *L32548*, *L35070*), which function as dosage-dependent inducers of mitotic progression (Nilsson and Hoffmann, 2000), were also downregulated (**Figure 2**). Other genes, such as *CDK7* (L25401), involved in transcription initiation and DNA repair were also downregulated. These results strongly suggest that exposure of the eastern oyster to air and cold stress suppresses the transcription of key genes needed for cell cycle progression or cell division, which is crucial for growth and immune functions. The discovery of the downregulation of key genes needed for cell division provides molecular support for the well-known negative effects of stress on growth and the immune response (Malek, 2010; Guo et al., 2015; Guo and Ford, 2016; Clements et al., 2018; La Peyre et al., 2018).

Cell cycle arrest may be induced by DNA damage, and cells attempt to repair this damage during cell cycle arrest (Pucci et al., 2000). In this study, genes that are induced by DNA damage, such as the growth arrest and DNA damage-inducible protein GADD45 (*L18431*, *L18444*, *L18682*, *L21109*), which is induced by p53 and arrests the cell cycle at the G2/M checkpoint (Papa et al., 2004), were upregulated. High-mobility group proteins

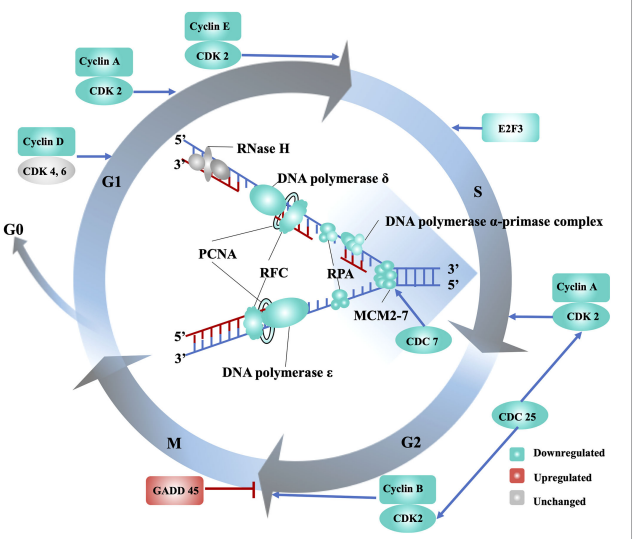

FIGURE 2 | Transcriptional regulation of the cell cycle and DNA replication in eastern oysters under stress. The gene names are the following: CDC, cell division cycle-related protein kinase; CDK, cyclin-dependent kinase; E2F, transcription factor E2F3; GADD 45, growth arrest and DNA damage-inducible protein 45; MCM2-7, minichromosome maintenance proteins; PCNA, proliferating cell nuclear antigen; RFC, replication factor C; RPA, replication protein A.

(*L09677*, *L09703*, *L12806*, *L17359*, *L25762*, *L26226*), which respond to DNA damage and oxidative stress in yeast (Reeves and Adair, 2005; Lange et al., 2008), were also upregulated. In addition, sestrin1 (*L03315*), which is induced by the p53 tumour suppressor protein and has the ability to arrest cell growth and decrease ROS production, was also upregulated (Sun et al., 2014). It is widely accepted that p53 mediates cell cycle arrest, apoptotic cell death, and/or cellular senescence (Li et al., 2012). Although the transcription level of p53 did not change significantly under stress in this study, it is possible that p53 activity, a key event in the cell cycle arrest process, is controlled by a diverse array of posttranslational modifications (Kruse and Gu, 2009). Additionally, because this study only provides a snapshot in time, p53 and its regulators may be differentially expressed at other time points. It should be noted that in addition to DNA damage repair, stress and nutritional limitations may also lead to cell cycle arrest and growth arrest (Yanagida et al., 2011; Rossi and Antonangeli, 2015).

Although the underlying mechanisms are not completely defined, cell cycle arrest is an active response to stress that enables organisms to survive under challenging environmental conditions. The results of this study demonstrate that the exposure of eastern oyster to air and cold stress suppresses the transcription of genes promoting cell cycle progression, which may lead to cell cycle arrest and in turn affect growth, immune responses and other biological processes. Growth retardation inferred from cell cycle arrest is consistent with the results from field experiments conducted by Malek (2010), who found that the growth of eastern oysters decreased with increases in the duration of intertidal air exposure, and La Peyre et al. (2018), who found that a lower growth rate among oysters that experienced daily air exposure. Air exposure in the field may also reduce the time dedicated to feeding and increase the use of glycogen storage, which contribute to reduced growth.

3.3 Evasion of Cell Death during Exposure to Air at 22°C

Exposure to air at 22°C triggers the inhibition of apoptosis and related regulatory pathways. Inhibitors of apoptosis (IAPs) play important roles in promoting cell survival. IAP family members inhibit programmed cell death by binding to and/or directly inhibiting caspases (LaCasse et al., 1998). The *C. gigas* genome exhibits an expanded IAP family (48 genes), members of which are highly expressed after air exposure and pathogen infection, which indicates that IAPs play crucial roles in anti-apoptotic processes in oysters (Zhang et al., 2012; Green et al., 2015). We identified 58 *IAPs* in the eastern oyster genome; 8 and 4 of these *IAPs* were highly and significantly upregulated and slightly downregulated, respectively, in the 22AE group, resulting in an overall upregulation of *IAPs* (**Supplementary Table 4**). Furthermore, genes encoding caspases, *CASP7* (*L3317*, *L2489*, *L24891*) and *CASP10* (*L04823*, *L33185*, *L33189*), were slightly downregulated in the 22AE group. These results suggest the existence of a concerted effort to inhibit apoptosis in oysters under stress (**Figure 3** and **Supplementary Table 4**).

Exposure to air at 22°C affected signalling pathways such as the TNF signalling and NF-kappa B signalling pathways (**Table 1** and **Supplementary Table 4**). These pathways play important roles in the responses to biotic and abiotic stresses in the Pacific oyster (Zhang et al., 2015) and other molluscs, such as the

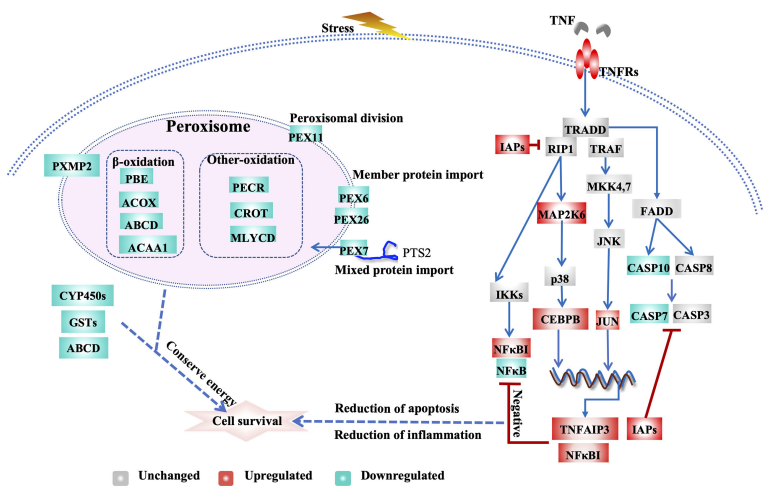

FIGURE 3 | Transcriptional regulation of apoptosis, TNF signalling and peroxisomal activity in eastern oysters during exposure to air. The key genes are the following: ABCD, ATP-binding cassette subfamily D; ACAA1, 3-ketoacyl-CoA thiolase A, peroxisomal; ACOX1, peroxisomal acyl-coenzyme An oxidase 1; NUDT19, nucleoside diphosphate-linked moiety X motif 19; JUN, Jun proto-oncogene, AP-1 transcription factor subunit; CASP7, caspase-7; CASP10, caspase-10; CEBP, CCAAT/enhancer-binding protein; CYP450s, cytochrome P450s; CROT, peroxisomal carnitine O-octanoyltransferase; GSTs, glutathione S-transferases; IAP, inhibitor of apoptosis; TNFR, tumour necrosis factor receptor; MAP2K6, dual specificity mitogen-activated protein kinase 6; NFKBIA, NF-kappa-B inhibitor alpha-like; NFKB, nuclear factor NF-kappa-B p105; PEX7, peroxisomal targeting signal 2 receptor; PEX26, peroxisome assembly protein 26; PEX6, peroxisome assembly factor 2; PEX11, peroxisomal membrane protein 11; PXMP2, peroxisomal membrane protein 2; PECR, peroxisomal trans-2-enoyl-CoA reductase-like; PIK3, phosphatidylinositol-4,5-bisphosphate 3-kinase; TNFAIP3, tumour necrosis factor alpha-induced protein 3.

European flat oyster *Ostrea edulis* (Martín-Gómez et al., 2012), disk abalone *Haliotis discus* (De Zoysa et al., 2009), and Chinese scallop *Chlamys farreri* (Li et al., 2009). Depending on which downstream genes are activated, the TNF signalling pathway can induce apoptosis or necroptosis or promote cell survival (Baud and Karin, 2001; Sabio and Davis, 2014). TNF signalling may induce apoptosis *via* TNFα-TNFR-(TRADD/RIP1/TRAF2 complex)-FADD-CASP signalling (Rath and Aggarwal, 1999). However, the upregulation of *IAPs* and the downregulation of *CASPs* may have a negative feedback effect on TNF signalling. The TNF signalling pathway induces inflammation *via* TNFα-TNFR-(TNFR1 complex I)-TAB/TAK1-IKK-NF-κB signalling (Bantel and Schulze-Osthoff, 2012). The major pathway for the systemic inflammatory responses depends on NF-κB. The strong upregulation of NF-κB inhibitor alpha-like genes (*NFκBIA*, *L31108*, *L31219*) and the downregulation of NF-κB (*L21590*) suggest that the NF-κB signalling pathway is inhibited by stress (De Martin et al., 1993). Notably, genes encoding TNF alpha-induced protein 3 (*TNFAIP3*, *L04432*, *L34417*) (**Figure 3** and **Supplementary Table 4**) induced by TNF were highly upregulated, and these genes inhibit NF-κB activation and TNF-mediated apoptosis and thereby negatively regulate downstream cell death signalling (Song et al., 1996; Jiang et al., 1999). The prostaglandin E receptor 4 (*EP4*, *L17914*, *L20936*, *L18192*, *L22415*) interacts with prostaglandin E receptor 4-associated protein (EPRAP) to inhibit the activation of NF-κB (Minami et al., 2008). Other genes that negatively regulate the inflammatory response, such as *suppressor of cytokine signalling* (*SOCS2*, *L17924*), were also upregulated, which could limit the cytokine response by inhibiting Janus kinase 2 (JAK2) activity (Rico-Bautista et al., 2006; Posselt et al., 2011). These processes inhibit apoptosis through TNF signalling pathways and attenuate the inflammatory response by inhibiting NFκB activation. Inhibition of the inflammatory response may lead to weakened immune responses, which explains the susceptibility and mortality of oysters under stress (Malek, 2010; Guo et al., 2015; Guo and Ford, 2016; Clements et al., 2018). In addition, Jun proto-oncogene (*JUN*, *L20138*) and CEBP-beta (*CEBPB*, *L36304*), which regulate a number of cellular processes, including differentiation, proliferation, apoptosis and the immune response, were upregulated, which indicated their potential role in the stress response and the complex crosstalk among signalling pathways.

Overall, these transcriptomic changes indicate that an orchestrated response involving the upregulation of expanded *IAPs* and the downregulation of *caspases* through interactions with TNF and NF-κB signalling work in concert to help stressed oyster cells evade apoptosis, whereas the downregulation of NF-κB signalling may suppress inflammatory responses and impair immune functions.

3.4 Xenobiotic and Lipid Metabolism During Exposure to Air at 22°C

The key genes and pathways involved in xenobiotic biotransformation and lipid metabolism were affected during exposure to air at 22°C (**Table 1**). The xenobiotic biotransformation system helps oysters cope with environmental contaminants (Zhang et al., 2016). Genes that are known to be important for xenobiotic biotransformation, such as *cytochrome P450s* (*CYP450s*, 11 genes), *myeloperoxidase* (*MPO*, *L099927*, *L01491*, *L01639*, *L01744*), *GSTs* (*L02975*, *L04070*), and *ATP-binding cassette subfamily D member* (*L30560*) (**Supplementary Table 4**), were significantly downregulated under 22AE conditions.

Genes related to fatty acid synthesis, particularly the key gene *fatty acid synthase* (*FAS*, *L18924*, *L21707*), were highly upregulated under 22AE conditions. Moreover, genes playing key roles in fatty acid oxidation in peroxisomes, such as *peroxisomal acyl-coenzyme A oxidase 1* (*ACOX1*, *L13840*, *L15085*, *L32545*, *MSTRG.2967*), which is the first enzyme in the fatty acid beta-oxidation pathway that produces hydrogen peroxide (Inestrosa et al., 1979), were downregulated. The *3-ketoacyl-CoA thiolase* (*ACAA1*, *L15744*, *L15745*), which catalyses the final step in the β-oxidation cycle, was also downregulated. The upregulation and downregulation of these key genes were also observed in the groups exposed to cold stress, albeit at a small magnitude, which suggested similar regulation of fatty acid metabolism under cold stress (**Supplementary Table 4**). Maintaining the energy balance is critical for stress tolerance (Sokolova et al., 2012), and our results indicate the involvement of lipid metabolism in coping with air exposure and cold stress. Additionally, organisms in cold environments often have more unsaturated fatty acids for membrane fluidity (Dey et al., 1993).

Peroxisomes play particularly important roles in lipid metabolism, ether-phospholipid biosynthesis, and reactive oxygen species (ROS) metabolism (Fransen et al., 2012; Jo and Cho, 2019). Moreover, peroxisomes are signalling platforms for antiviral innate immune responses (Dixit et al., 2010). More peroxisomal genes were downregulated during exposure to air at 22°C than under cold stress conditions. Proteins that control peroxisome assembly, division, and inheritance, such as peroxins or peroxisome biogenesis factors (*PEXs*, *L03004*, *L08788*, *L31586*, *L17608*, *L28390*, *L35112*) (Ma et al., 2011), were downregulated (**Figure 3** and **Supplementary Table 4**), which indicated that peroxisome biogenesis is downregulated during exposure to air at 22°C.

The downregulation of xenobiotic biotransformation and peroxisome-related genes may decrease fatty acid oxidation (Mayer et al., 1995), whereas the upregulation of *fatty acid synthase* increases the *de novo* synthesis of fatty acids; altogether, these effects alter the fatty acid composition. These results all indicate that fatty acid metabolism plays a critical role in mediating the responses of oysters to air exposure.

3.5 Proline Accumulation and Histone Upregulation Under Cold Stress

The proline accumulation pathway was activated in oysters under cold stress (**Figure 4**). The synthesis of proline is mediated by two pathways: the L-glutamic acid pathway and the ornithine pathway (Verbruggen and Hermans, 2008). Delta-1-pyrroline-5-carboxylate synthase (*P5CS*, *L36221*), a

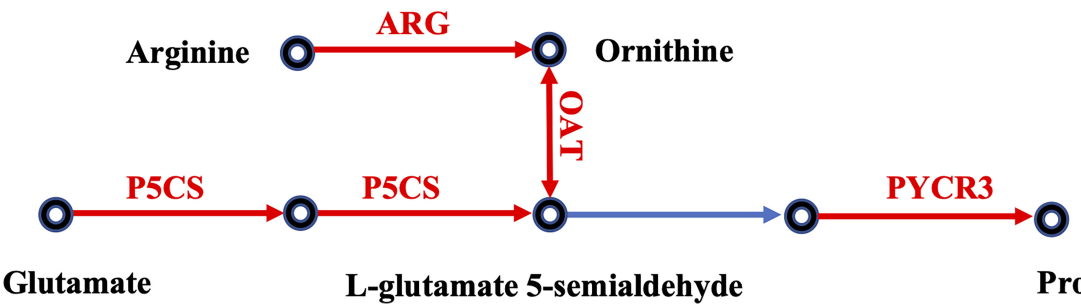

FIGURE 4 | Effects of cold stress on the proline accumulation pathway in eastern oysters. The genes in red exhibit upregulated expression. The gene names are the following: P5CS, delta-1-pyrroline-5-carboxylate synthase; PYCR, pyrroline-5-carboxylate reductase; ARG, arginase; OAT, ornithine aminotransferase.

key enzyme responsible for the synthesis of L-glutamate 5-semialdehyde from L-glutamate in steps 1 and 2 of the subpathway, was significantly upregulated (**Figure 4** and **Supplementary Table 4**). Arginase (*ARG*, L30979), which transforms arginine to ornithine, and ornithine aminotransferase (*OAT*, L36290), which catalyses the transformation of ornithine into L-glutamate 5-semialdehyde, were both upregulated by cold stress. The enzyme pyrroline-5-carboxylate reductase (*PYCR2*, *L28747*, *PYCR3*, *L28753*), which catalyses the last step in proline biosynthesis, was also upregulated. Together, these results suggest that the proline accumulation pathway is activated or upregulated under cold stress. The accumulation of proline has been observed in oysters under hyperosmotic stress (Meng et al., 2013) and is a key mechanism for cold tolerance in plants (Szabados and Savoure, 2010). The activation of the proline accumulation pathway observed in this study implies that a large proline pool is important for the survival of oysters under cold stress conditions.

Nine genes for histone H4 and four genes for histone H2B were highly upregulated under cold stress, particularly under 5SW conditions. The upregulation of some but not all histone subunits was also observed in the Pacific oyster under stress (Zhang et al., 2012). Canonical histones are synthesized during the S phase for the packaging of newly synthesized DNA. Because genes that promote cell division were downregulated under stress, the upregulation of some histone genes is intriguing and begs other explanations. Moving, ejecting or restructuring nucleosomes is one of the strategies for maintaining chromatin stability (Cedar and Bergman, 2009; Clapier and Cairns, 2009). The high-mobility groups (HMGs) of proteins (*L09677*, *L09703*, *L12806*, *L17359*, *L25762*, *L26226*), another group of major chromatin architectural components of eukaryotes, were also highly upregulated under cold stress (**Supplementary Table 4**). Although preliminary and to be confirmed through further studies, these results indicate that genes encoding chromosomal proteins are upregulated under cold stress, probably for repairing or stabilizing DNA under stress or as epigenetic modifications that regulate transcription. In plants, stress induces dramatic epigenetic changes, such as DNA methylation, histone modifications and changes in the composition of different histone variants, which regulate gene expression and enable stress responses and memory (Chinnusamy and Zhu, 2009). We hypothesize that the upregulation of the expression of certain chromosomal structural protein genes observed in this study is involved in the epigenetic modifications of chromatin that are needed for regulating the transcriptional response to stress and facilitating epigenetic memory in oysters.

3.6 Upregulation of Hormone and Neurotransmitter Receptors

Several genes encoding hormone and neurotransmitter receptors were upregulated in oysters under air exposure and cold stress conditions. The melatonin receptor (*MTNR*, *L03709*, *L04987*, *L03710*) and the FMRFamide receptor (*FMRFAR*, *L22789*, *L22537*, *L21307*) were upregulated under all three conditions, particularly under 22AE conditions (**Supplementary Table 4**). FMRFamide and FMRFamide-related neuropeptides are abundant in invertebrates and have several important functions. FMRFamide-related peptides (FaRPs) in gastropods are involved in movement, feeding, defecation, and reproduction (López-Vera et al., 2008). Melatonin is involved in circadian and seasonal timing (Reppert et al., 1994; Dubocovich et al., 2003) and was highly upregulated under all stresses in this study. In addition, genes encoding atrial natriuretic peptide receptor A and neuronal acetylcholine receptor were also upregulated under 5AE conditions. The up regulation of these hormone and neurotransmitter receptors may be critical for activating physiological responses or inducing physiological state transitions as in a circadian system shift (Ottaviani and Franceschi, 1996; Fuentes-Pardo et al., 2013; Lenz et al., 2015). In *C. gigas*, many GPCR genes, including those encoding prostaglandin E2 receptors, FMRFamide receptors, cholecystokinin receptors, melatonin receptors, prolactin-releasing peptide receptors, adenosine receptors and dopamine D2-like receptors, are upregulated by OsHV-1 infection (He et al., 2015). It has been shown that neuronal acetylcholine receptors are greatly expanded in bivalve

molluscs and are important for adaptation to stationary life under variable environments (Jiao et al., 2019).

4 CONCLUSIONS

The remarkable resilience of the eastern oyster is not well understood at the molecular level. The results obtained in this study clearly demonstrate that exposure to air and cold stress induce significant changes in the transcription of large numbers of genes that are likely crucial for the response and tolerance of the eastern oyster to stress. The observed suppression of genes promoting cell cycle progression suggests that cell division may be arrested in oysters under stress. The upregulation of anti-apoptosis genes and the downregulation of pro-apoptosis genes and regulatory pathways indicate a concerted effort to evade cell death. The inhibition of key signalling pathways that activate the immune response suggests that immune defence is impaired by stress. Receptors for hormones and neurotransmitters were found to be upregulated in response to stress. The upregulation of genes for proline synthesis and chromosome structural proteins indicates that proline accumulation and epigenetic modifications of chromosomes are important for coping with cold stress. Although it is well known that stress depresses growth and immune responses, which often lead to disease outbreaks and mass summer mortalities in molluscs (Guo and Ford, 2016), the underlying molecular mechanisms are not well understood. By revealing the downregulation of genes involved in cell cycle progression and the inflammatory response under stress, this study provides transcriptomic evidence for the negative effects of stress on growth and immune functions. This study reveals several previously undescribed responses to stress in oysters and other molluscs. The genes and pathways implicated in this study provide useful resources for further studies on the stress response and adaptation in molluscs and other marine invertebrates. Knowing how stress affects growth and immune response at molecular levels is essential for understanding stress impact and assessing the adaptive potential of marine organisms under climate change. Oysters are economically important and support major aquaculture industries worldwide. The sustainable development of the oyster aquaculture industry depends on genetic improvement of cultured stocks (Guo, 2021). The candidate genes and their polymorphisms can be used for marker-assisted selection for the breeding of more resilient oysters.

AUTHORS CONTRIBUTIONS

XG and CL conceived and designed the study. CL performed the experiments and analysed the data. CL, XG and HW interpreted the data and wrote the manuscript. All authors have read and approved the manuscript. All authors contributed to the article and approved the submitted version.

DATA AVAILABILITY STATEMENT

The datasets presented in this study can be found in online repositories. The names of the repository/repositories and accession number(s) can be found below: https://www.ncbi.nlm.nih.gov/, PRJNA378873.

FUNDING

This work was partly supported by grants from the National Science Foundation of China (No. 41906083), the Taishan Overseas Scholar Project of Shandong, the US National Oceanic and Atmospheric Agency (NA18NMF4720321) and the Department of Agriculture Animal Health (NJ32920). The statements, findings, conclusions, and recommendations are those of the authors and do not necessarily reflect the views of the National Oceanic and Atmospheric Administration or the Department of Commerce.

ACKNOWLEDGMENTS

We thank Baoyu Huang for helping with the sampling.

SUPPLEMENTARY MATERIAL

The Supplementary Material for this article can be found online at: https://www.frontiersin.org/articles/10.3389/fmars.2022.921877/full#supplementary-material

REFERENCES

Alberts, B., Johnson, A., Lewis, J., Raff, M., Roberts, K., and Walter, P. (2002). "The Initiation and Completion of DNA Replication in Chromosomes," in *Molecular Biology of the Cell* 4th edition. (New York, NY: Garland Science), 377–392.

Allen, S. M., and Burnett, L. E. (2008). The Effects of Intertidal Air Exposure on the Respiratory Physiology and the Killing Activity of Hemocytes in the Pacific Oyster, *Crassostrea Gigas* (Thunberg). *J. Exp. Mar. Biol. Ecol.* 357, 165–171. doi: 10.1016/j.jembe.2008.01.013

Alvarez, M. R., and Friedl, F. E. (1992). Effects of a Fungicide on *In Vitro* Hemocyte Viability, Phagocytosis and Attachment in the American Oyster, *Crassostrea Virginica*. *Aquaculture* 107, 135–140. doi: 10.1016/0044-8486(92)90058-S

Bantel, H., and Schulze-Osthoff, K. (2012). Mechanisms of Cell Death in Acute Liver Failure. *Front. Physiol.* 3. doi: 10.3389/fphys.2012.00079

Baud, V., and Karin, M. (2001). Signal Transduction by Tumor Necrosis Factor and its Relatives. *Trends Cell Biol.* 11, 372–377. doi: 10.1016/S0962-8924(01)02064-5

Benjamini, Y., and Hochberg, Y. (1995). Controlling the False Discovery Rate: A Practical and Powerful Approach to Multiple Testing. *J. R. Stat. Soc. B Methodol.* 57, 289–300. doi: 10.1111/j.2517-6161.1995.tb02031.x

Blow, J. J., and Laskey, R. A. (1988). A Role for the Nuclear Envelope in Controlling DNA Replication Within the Cell Cycle. *Nature* 332, 546–548. doi: 10.1038/332546a0

Boyd, J. N., and Burnett, L. E. (1999). Reactive Oxygen Intermediate Production by Oyster Hemocytes Exposed to Hypoxia. *J. Exp. Biol.* 202 (22), 3135–3143. doi: 10.1242/jeb.202.22.3135

Cedar, H., and Bergman, Y. (2009). Linking DNA Methylation and Histone Modification: Patterns and Paradigms. *Nat. Rev. Genet.* 10, 295–304. doi: 10.1038/nrg2540

Chinnusamy, V., and Zhu, J. K. (2009). Epigenetic Regulation of Stress Responses in Plants. *Curr. Opin. Plant Biol.* 12, 133–139. doi: 10.1016/j.pbi.2008.12.006

Clapier, C. R., and Cairns, B. R. (2009). The Biology of Chromatin Remodeling Complexes. *Annu. Rev. Biochem.* 78, 273–304. doi: 10.1146/annurev.biochem.77.062706.153223

Clements, J. C., Davidson, J. D. P., McQuillan, J. G., and Comeau, L. A. (2018). Increased Mortality of Harvested Eastern Oysters (*Crassostrea Virginica*) is Associated With Air Exposure and Temperature During a Spring Fishery in Atlantic Canada. *Fish. Res.* 206, 27–34. doi: 10.1016/j.fishres.2018.04.022

De Martin, R., Vanhove, B., Cheng, Q., Hofer, E., Csizmadia, V., Winkler, H., et al. (1993). Cytokine-Inducible Expression in Endothelial Cells of an I Kappa B Alpha-Like Gene is Regulated by NF Kappa B. *EMBO J.* 12, 2773–2779. doi: 10.1002/j.1460-2075.1993.tb05938.x

Dey, I., Buda, C., Wiik, T., Halver, J. E., and Farkas, T. (1993). Molecular and Structural Composition of Phospholipid Membranes in Livers of Marine and Freshwater Fish in Relation to Temperature. *Proc. Natl. Acad. Sci. U.S.A.* 90, 7498–7502. doi: 10.1073/pnas.90.16.7498

De Zoysa, M., Jung, S., and Lee, J. (2009). First Molluscan TNF-α Homologue of the TNF Superfamily in Disk Abalone: Molecular Characterization and Expression Analysis. *Fish Shellfish Immunol.* 26, 625–631. doi: 10.1016/j.fsi.2008.10.004

Dixit, E., Boulant, S., Zhang, Y., Lee, A. S., Odendall, C., Shum, B., et al. (2010). Peroxisomes are Signaling Platforms for Antiviral Innate Immunity. *Cell* 141, 668–681. doi: 10.1016/j.cell.2010.04.018

Dubocovich, M. L., Rivera-Bermudez, M. A., Gerdin, M. J., and Masana, M. I. (2003). Molecular Pharmacology, Regulation and Function of Mammalian Melatonin Receptors. *Front. Biosci.* 8, d1093–d1108. doi: 10.2741/1089

Eierman, L. E., and Hare, M. P. (2014). Transcriptomic Analysis of Candidate Osmoregulatory Genes in the Eastern Oyster *Crassostrea Virginica*. *BMC Genom.* 15, 503. doi: 10.1186/1471-2164-15-503

Fransen, M., Nordgren, M., Wang, B., and Apanasets, O. (2012). Role of Peroxisomes in ROS/RNS-Metabolism: Implications for Human Disease. Biochim. *Biophys. Acta* 1822, 1363–1373. doi: 10.1016/j.bbadis.2011.12.001

Fuentes-Pardo, B., Barriga-Montoya, C., and de la O-Martínez, A. (2013). ""Melatonin as a Circadian Hormone in Invertebrates,"," in *New Developments in Melatonin Research*. Eds. D. Acuna-Castroviejo, I. Rusanova and G. Escames (New York, NY: Nova Science Publishers, Inc), 27–38.

Galtsoff, P. S. (1964). "The American Oyster, Crassostrea Virginica Gmelin," in *Fishery Bulletin* (Washington, D.C.: US Government Printing Office), 1–480.

Gómez-Chiarria, M., Warrenb, W. C., Guo, X., and Proestoud, D. (2015). Developing Tools for the Study of Molluscan Immunity: The Sequencing of the Genome of the Eastern Oyster, *Crassostrea Virginica*. *Fish Shellfish Immunol.* 46, 2–4. doi: 10.1016/j.fsi.2015.05.004

Green, T. J., Rolland, J. L., Vergnes, A., Raftos, D., and Montagnani, C. (2015). OsHV-1 Countermeasures to the Pacific Oyster's Anti-Viral Response. *Fish Shellfish Immunol.* 47, 435–443. doi: 10.1016/j.fsi.2015.09.025

Guo, X. (2021). "Genetics in Shellfish Culture," in *Molluscan Shellfish Aquaculture: A Practical Guide*. Ed. S. Shumway (Essex, UK: 5m Books Ltd), 393–413.

Guo, X., and Ford, S. E. (2016). Infectious Diseases of Marine Molluscs and Host Responses as Revealed by Genomic Tools. *Philos. Trans. R. Soc Lond. B Biol. Sci.* 371, 20150206. doi: 10.1098/rstb.2015.0206

Guo, X., He, Y., Zhang, L., Lelong, C., and Jouaux, A. (2015). Immune and Stress Responses in Oysters With Insights on Adaptation. *Fish Shellfish Immunol.* 46, 107–119. doi: 10.1016/j.fsi.2015.05.018

He, Y., Jouaux, A., Ford, S. E., Lelong, C., Sourdaine, P., Mathieu, M., et al. (2015). Transcriptome Analysis Reveals Strong and Complex Antiviral Response in a Mollusc. *Fish Shellfish Immunol.* 46, 131–144. doi: 10.1016/j.fsi.2015.05.023

Inestrosa, N. C., Bronfman, M., and Leighton, F. (1979). Detection of Peroxisomal Fatty Acyl-Coenzyme A Oxidase Activity. *Biochem. J.* 182, 779–788. doi: 10.1042/bj1820779

Ivanina, A. V., Sokolov, E. P., and Sokolova, I. M. (2010). Effects of Cadmium on Anaerobic Energy Metabolism and mRNA Expression During Air Exposure and Recovery of an Intertidal Mollusk *Crassostrea Virginica*. *Aquat. Toxicol.* 99, 330–342. doi: 10.1016/j.aquatox.2010.05.013

Jiang, Y., Woronicz, J. D., Liu, W., and Goeddel, D. V. (1999). Prevention of Constitutive TNF Receptor 1 Signaling by Silencer of Death Domains. *Science* 283, 543–546. doi: 10.1126/science.283.5401.543

Jiao, Y., Cao, Y., Zheng, Z., Liu, M., and Guo, X. (2019). Massive Expansion and Diversity of Nicotinic Acetylcholine Receptors in Lophotrochozoans. *BMC Genom.* 20, 937. doi: 10.1186/s12864-019-6278-9

Jo, D. S., and Cho, D. H. (2019). Peroxisomal Dysfunction in Neurodegenerative Diseases. *Arch. Pharm. Res.* 42, 393–406. doi: 10.1007/s12272-019-01131-2

Kanehisa, M., Araki, M., Goto, S., Hattori, M., Hirakawa, M., Itoh, M., et al. (2008). KEGG for Linking Genomes to Life and the Environment. *Nucleic Acids Res.* 36, D480–D484. doi: 10.1093/nar/gkm882

Kawabe, S., Takada, M., Shibuya, R., and Yokoyama, Y. (2010). Biochemical Changes in Oyster Tissues and Hemolymph During Long-Term Air Exposure. *Fish. Sci.* 76, 841–855. doi: 10.1007/s12562-010-0263-1

Kim, D., Langmead, B., and Salzberg, S. L. (2015). HISAT: A Fast Spliced Aligner With Low Memory Requirements. *Nat. Methods* 12, 357–360. doi: 10.1038/nmeth.3317

Kruse, J. P., and Gu, W. (2009). Modes of P53 Regulation. *Cell* 137, 609–622. doi: 10.1016/j.cell.2009.04.050

Kuchel, R. P., Raftos, D. A., and Nair, S. (2010). Immunosuppressive Effects of Environmental Stressors on Immunological Function in *Pinctada Imbricata*. *Fish Shellfish Immunol.* 29, 930–936. doi: 10.1016/j.fsi.2010.07.033

LaCasse, E. C., Baird, S., Korneluk, R. G., and MacKenzie, A. E. (1998). The Inhibitors of Apoptosis (IAPs) and Their Emerging Role in Cancer. *Oncogene* 17, 3247–3259. doi: 10.1038/sj.onc.1202569

Lange, S. S., Mitchell, D. L., and Vasquez, K. M. (2008). High Mobility Group Protein B1 Enhances DNA Repair and Chromatin Modification After DNA Damage. *Proc. Natl. Acad. Sci. U.S.A.* 105, 10320–10325. doi: 10.1073/pnas.0803181105

La Peyre, J. F., Casas, S. M., and Supan, J. E. (2018). Effects of Controlled Air Exposure on the Survival, Growth, Condition, Pathogen Loads and Refrigerated Shelf Life of Eastern Oysters. *Aquac. Res.* 49, 19–29. doi: 10.1111/are.13427

Lenz, O., Xiong, J., Nelson, M. D., Raizen, D. M., and Williams, J. A. (2015). FMRFamide Signaling Promotes Stress-Induced Sleep in Drosophila. *Brain Behav. Immun.* 47, 141–148. doi: 10.1016/j.bbi.2014.12.028

Li, T., Kon, N., Jiang, L., Tan, M., Ludwig, T., Zhao, Y., et al. (2012). Tumor Suppression in the Absence of P53-Mediated Cell-Cycle Arrest, Apoptosis, and Senescence. *Cell* 149, 1269–1283. doi: 10.1016/j.cell.2012.04.026

Li, L., Qiu, L., Song, L., Song, X., Zhao, J., Wang, L., et al. (2009). First Molluscan TNFR Homologue in Zhikong Scallop: Molecular Characterization and Expression Analysis. *Fish Shellfish Immunol.* 27, 625–632. doi: 10.1016/j.fsi.2009.07.009

Liu, M., and Guo, X. (2017). A Novel and Stress Adaptive Alternative Oxidase Derived From Alternative Splicing of Duplicated Exon in Oyster *Crassostrea Virginica*. *Sci. Rep.* 7, 10785. doi: 10.1038/s41598-017-10976-w

Livak, K. J., and Schmittgen, T. D. (2001). Analysis of Relative Gene Expression Data Using Real-Time Quantitative PCR and the 2(-Delta Delta C(T)) Method. *Methods* 25, 402–408. doi: 10.1006/meth.2001.1262

López-Landavery, E. A., Amador-Cano, G., Alejandri, N., Ramirez-Álvarez, N., Montelongo, I., Díaz, F., et al. (2019). Transcriptomic Response and Hydrocarbon Accumulation in the Eastern Oyster (*Crassostrea Virginica*) Exposed to Crude Oil. *Comp. Biochem. Physiol. C Toxicol. Pharmacol.* 225, 108571. doi: 10.1016/j.cbpc.2019.108571

López-Vera, E., Aguilar, M. B., and Heimer de la Cotera, E. P. (2008). FMRFamide and Related Peptides in the Phylum Mollusca. *Peptides* 29, 310–317. doi: 10.1016/j.peptides.2007.09.025

Ma, C., Agrawal, G., and Subramani, S. (2011). Peroxisome Assembly: Matrix and Membrane Protein Biogenesis. *J. Cell Biol.* 193, 7–16. doi: 10.1083/jcb.201010022

Malek, J. C. (2010). *The Effects of Intertidal Exposure on Disease, Mortality, and Growth of the Eastern Oyster, Crassostrea Virginica* (Maryland, College Park, MD: College Park, MD: ProQuest Dissertations Publishing, University of Maryland).

Mao, X., Cai, T., Olyarchuk, J. G., and Wei, L. (2005). Automated Genome Annotation and Pathway Identification Using the KEGG Orthology (KO) as a Controlled Vocabulary. *Bioinformatics* 21, 3787–3793. doi: 10.1093/bioinformatics/bti430

Martín-Gómez, L., Villalba, A., and Abollo, E. (2012). Identification and Expression of Immune Genes in the Flat Oyster Ostrea Edulis in Response to Bonamiosis. *Gene* 492, 81–93. doi: 10.1016/j.gene.2011.11.001

Mayer, J. M., Testa, B., Roy-de Vos, M., Audergon, C., and Etter, J. C. (1995). ""Interactions Between the In Vitro Metabolism of Xenobiotics and Fatty

Acids,"," in *Toxicology in Transition*. Eds. G. H. Degen, J. P. Seiler and P. Bentley (Berlin, Heidelberg: Springer), 499–513.
McCarthy, D. J., Chen, Y., and Smyth, G. K. (2012). Differential Expression Analysis of Multifactor RNA-Seq Experiments With Respect to Biological Variation. *Nucleic Acids Res.* 40, 4288–4297. doi: 10.1093/nar/gks042
McDowell, I. C., Nikapitiya, C., Aguiar, D., Lane, C. E., Istrail, S., and Gomez-Chiarri, M. (2014). Transcriptome of American Oysters, *Crassostrea Virginica*, in Response to Bacterial Challenge: Insights Into Potential Mechanisms of Disease Resistance. *PLoS One* 9, e105097. doi: 10.1371/journal.pone.0105097
Meng, J., Zhu, Q., Zhang, L., Li, C., Li, L., She, Z., et al. (2013). Genome and Transcriptome Analyses Provide Insight Into the Euryhaline Adaptation Mechanism of *Crassostrea Gigas*. *PLoS One* 8, e58563. doi: 10.1371/journal.pone.0058563
Minami, M., Shimizu, K., Okamoto, Y., Folco, E., Ilasaca, M. L., Feinberg, M. W., et al. (2008). Prostaglandin E Receptor Type 4-Associated Protein Interacts Directly With NF-κb1 and Attenuates Macrophage Activation. *J. Biol. Chem.* 283, 9692–9703. doi: 10.1074/jbc.M709663200
Modak, T. H., and Gomez-Chiarri, M. (2020). Contrasting Immunomodulatory Effects of Probiotic and Pathogenic Bacteria on Eastern Oyster, *Crassostrea Virginica*, Larvae. *Vaccines (Basel)* 8, 588. doi: 10.3390/vaccines8040588
Morgan, D. O. (1997). Cyclin-Dependent Kinases: Engines, Clocks, and Microprocessors. *Annu. Rev. Cell Dev. Biol.* 13, 261–291. doi: 10.1146/annurev.cellbio.13.1.261
Nilsson, I., and Hoffmann, I. (2000). Cell Cycle Regulation by the Cdc25 Phosphatase Family. *Prog. Cell Cycle Res.* 4, 107–114. doi: 10.1007/978-1-4615-4253-7_10
Ottaviani, E., and Franceschi, C. (1996). The Neuroimmunology of Stress From Invertebrates to Man. *Prog. Neurobiol.* 48, 421–440. doi: 10.1016/0301-0082(95)00049-6
Papa, S., Zazzeroni, F., Bubici, C., Jayawardena, S., Alvarez, K., Matsuda, S., et al. (2004). Gadd45β Mediates the NF-κb Suppression of JNK Signalling by Targeting MKK7/JNKK2. *Nat. Cell Biol.* 6, 146–153. doi: 10.1038/ncb1093
Pertea, M., Kim, D., Pertea, G. M., Leek, J. T., and Salzberg, S. L. (2016). Transcript-Level Expression Analysis of RNA-Seq Experiments With HISAT, StringTie and Ballgown. *Nat. Protoc.* 11, 1650–1667. doi: 10.1038/nprot.2016.095
Pertea, M., Pertea, G. M., Antonescu, C. M., Chang, T. C., Mendell, J. T., and Salzberg, S. L. (2015). StringTie Enables Improved Reconstruction of a Transcriptome From RNA-Seq Reads. *Nat. Biotechnol.* 33, 290–295. doi: 10.1038/nbt.3122
Posselt, G., Schwarz, H., Duschl, A., and Horejs-Hoeck, J. (2011). Suppressor of Cytokine Signaling 2 is a Feedback Inhibitor of TLR-Induced Activation in Human Monocyte-Derived Dendritic Cells. *J. Immunol.* 187, 2875–2884. doi: 10.4049/jimmunol.1003348
Pucci, B., Kasten, M., and Giordano, A. (2000). Cell Cycle and Apoptosis. *Neoplasia* 2, 291–299. doi: 10.1038/Sj.Neo.7900101
Rath, P. C., and Aggarwal, B. B. (1999). TNF-Induced Signaling in Apoptosis. *J. Clin. Immunol.* 19, 350–364. doi: 10.1023/A:1020546615229
Reeves, R., and Adair, J. E. (2005). Role of High Mobility Group (HMG) Chromatin Proteins in DNA Repair. *DNA Repair (Amst.)* 4, 926–938. doi: 10.1016/j.dnarep.2005.04.010
Reppert, S. M., Weaver, D. R., and Ebisawa, T. (1994). Cloning and Characterization of a Mammalian Melatonin Receptor That Mediates Reproductive and Circadian Responses. *Neuron* 13, 1177–1185. doi: 10.1016/0896-6273(94)90055-8
Rico-Bautista, E., Flores-Morales, A., and Fernández-Pérez, L. (2006). Suppressor of Cytokine Signaling (SOCS) 2, A Protein With Multiple Functions. *Cytokine Growth Factor Rev.* 17, 431–439. doi: 10.1016/j.cytogfr.2006.09.008
Robinson, M. D., McCarthy, D. J., and Smyth, G. K. (2010). Edger: A Bioconductor Package for Differential Expression Analysis of Digital Gene Expression Data. *Bioinformatics* 26, 139–140. doi: 10.1093/bioinformatics/btp616
Rossi, M. N., and Antonangeli, F. (2015). Cellular Response Upon Stress: P57 Contribution to the Final Outcome. *Mediat. Inflamm.* 2015, 259325. doi: 10.1155/2015/259325
Sabio, G., and Davis, R. J. (2014). TNF and MAP Kinase Signalling Pathways. *Semin. Immunol.* 26, 237–245. doi: 10.1016/j.smim.2014.02.009
Saucedo, P. E., Ocampo, L., Monteforte, M., and Bervera, H. (2004). Effect of Temperature on Oxygen Consumption and Ammonia Excretion in the Calafia Mother-of-Pearl Oyster, *Pinctada Mazatlanica* (Hanley 1856). *Aquaculture* 229, 377–387. doi: 10.1016/S0044-8486(03)00327-2
Shumway, S. E. (1996). "Natural Environmental Factors," in *The Eastern Oyster Crassostrea Virginica*. Eds. V. S. Kennedy, R. I. E. Newell and A. F. Eble (Maryland, College Park, MD: Maryland Sea Grant College), 467–513.
Sokolova, I. M., Frederich, M., Bagwe, R., Lannig, G., and Sukhotin, A. A. (2012). Energy Homeostasis as an Integrative Tool for Assessing Limits of Environmental Stress Tolerance in Aquatic Invertebrates. *Mar. Environ. Res.* 79, 1–15. doi: 10.1016/j.marenvres.2012.04.003
Song, H. Y., Rothe, M., and Goeddel, D. V. (1996). The Tumor Necrosis Factor-Inducible Zinc Finger Protein A20 Interacts With TRAF1/TRAF2 and Inhibits NF-kappaB Activation. *Proc. Natl. Acad. Sci. U.S.A.* 93, 6721–6725. doi: 10.1073/pnas.93.13.6721
Storey, K. B., and Storey, J. M. (1990). Metabolic Rate Depression and Biochemical Adaptation in Anaerobiosis, Hibernation and Estivation. *Q. Rev. Biol.* 65, 145–174. doi: 10.1086/416717
Sun, G., Xue, R., Yao, F., Liu, D., Huang, H., Chen, C., et al. (2014). The Critical Role of Sestrin 1 in Regulating the Proliferation of Cardiac Fibroblasts. *Arch. Biochem. Biophys.* 542, 1–6. doi: 10.1016/j.abb.2013.11.011
Szabados, L., and Savoure, A. (2010). Proline: A Multifunctional Amino Acid. *Trends Plant Sci.* 15, 89–97. doi: 10.1016/j.tplants.2009.11.009
Verbruggen, N., and Hermans, C. (2008). Proline Accumulation in Plants: A Review. *Amino Acids* 35, 753–759. doi: 10.1007/s00726-008-0061-6
Xiao, B. C., Li, E. C., Du, Z. Y., Jiang, R. L., Chen, L. Q., and Yu, N. (2014). Effects of Temperature and Salinity on Metabolic Rate of the Asiatic Clam *Corbicula Fluminea* (Müller 1774). *SpringerPlus* 3, 455. doi: 10.1186/2193-1801-3-455
Yanagida, M., Ikai, N., Shimanuki, M., and Sajiki, K. (2011). Nutrient Limitations Alter Cell Division Control and Chromosome Segregation Through Growth-Related Kinases and Phosphatases. *Philos. Trans. R. Soc Lond. B Biol. Sci.* 366, 3508–3520. doi: 10.1098/rstb.2011.0124
Young, M. D., Wakefield, M. J., Smyth, G. K., and Oshlack, A. (2010). Gene Ontology Analysis for RNA-Seq: Accounting for Selection Bias. *Genome Biol.* 11, R14. doi: 10.1186/gb-2010-11-2-r14
Zhang, G., Fang, X., Guo, X., Li, L., Luo, R., Xu, F., et al. (2012). The Oyster Genome Reveals Stress Adaptation and Complexity of Shell Formation. *Nature* 490, 49–54. doi: 10.1038/nature11413
Zhang, L., Li, L., Guo, X., Litman, G. W., Dishaw, L. J., and Zhang, G. (2015). Massive Expansion and Functional Divergence of Innate Immune Genes in a Protostome. *Sci. Rep.* 5, 8693. doi: 10.1038/srep08693
Zhang, G., Li, L., Meng, J., Qi, H., Qu, T., Xu, F., et al. (2016). Molecular Basis for Adaptation of Oysters to Stressful Marine Intertidal Environments. *Annu. Rev. Anim. Biosci.* 4, 357–381. doi: 10.1146/annurev-animal-022114-110903
Zhang, L., Li, L., Zhu, Y., Zhang, G., and Guo, X. (2014a). Transcriptome Analysis Reveals a Rich Gene Set Related to Innate Immunity in the Eastern Oyster (*Crassostrea Virginica*). *Mar. Biotechnol.* 16, 17–33. doi: 10.1007/s10126-013-9526-z
Zhang, Y., Sun, J., Mu, H., Li, J., Zhang, Y., Xu, F., et al. (2014b). Proteomic Basis of Stress Responses in the Gills of the Pacific Oyster *Crassostrea Gigas*. *J. Proteome Res.* 14, 304–317. doi: 10.1021/pr500940s

Conflict of Interest: The authors declare that the research was conducted in the absence of any commercial or financial relationships that could be construed as a potential conflict of interest.

frontiers | Frontiers in Marine Science

TYPE Original Research
PUBLISHED 12 September 2022
DOI 10.3389/fmars.2022.971796

OPEN ACCESS

EDITED BY
Juan D. Gaitan-Espitia,
The University of Hong Kong,
Hong Kong SAR, China

REVIEWED BY
Jesús Antonio López-Carvallo,
Center for Scientific Research and Higher Education in Ensenada (CICESE), Mexico
Deevesh Ashley Hemraj,
The University of Hong Kong,
Hong Kong SAR, China

*CORRESPONDENCE
Jun Ding
dingjun1119@dlou.edu.cn
Yaqing Chang
changlab@hotmail.com

SPECIALTY SECTION
This article was submitted to Global Change and the Future Ocean, a section of the journal Frontiers in Marine Science

RECEIVED 17 June 2022
ACCEPTED 22 August 2022
PUBLISHED 12 September 2022

CITATION
Mao J, Huang X, Sun H, Jin X, Guan W, Xie J, Wang Y, Wang X, Yin D, Hao Z, Tian Y, Song J, Ding J and Chang Y (2022) Transcriptome analysis provides insight into adaptive mechanisms of scallops under environmental stress. *Front. Mar. Sci.* 9:971796. doi: 10.3389/fmars.2022.971796

Transcriptome analysis provides insight into adaptive mechanisms of scallops under environmental stress

Junxia Mao, Xiaofang Huang, Hongyan Sun, Xin Jin, Wenjuan Guan, Jiahui Xie, Yiying Wang, Xubo Wang, Donghong Yin, Zhenlin Hao, Ying Tian, Jian Song, Jun Ding* and Yaqing Chang*

Key Laboratory of Mariculture and Stock Enhancement in North China's Sea, Ministry of Agriculture and Rural Affairs, Dalian Ocean University, Dalian, China

High temperature and hypoxia greatly threaten marine life and aquaculture. Scallops, a diverse and ecologically important group of high economic value, mostly thrive in fluctuating environments, and are vulnerable to environmental stress. In the present study, the molecular response mechanism of scallops to a combination of environmental stressors was investigated *via* transcriptome analysis of the gill tissues in three scallop species, the Yesso scallop (*Patinopecten yessoensis*), Zhikong scallop (*Chlamys farreri*) and bay scallop (*Argopecten irradians*) that were exposed to transient heat, hypoxia and a combination thereof. The Yesso scallop had the most differentially expressed genes (DEGs) compared with the other two scallop species, indicating the highest sensitivity of the Yesso scallop to environmental stress. With increased temperature and decreased dissolved oxygen, the number of DEGs was greatly increased in the three scallop species, indicative of the enhancement in gene expression regulation in scallops in response to severe environmental changes. Heat and hypoxia had a synergistic effect on scallops. GO and KEGG enrichment analysis of DEGs under different stressors revealed overlapping molecular mechanisms of response in scallops following exposure to heat and hypoxia. Several immune and apoptosis-related pathways were highly enriched in the upregulated DEGs of the three scallops, suggesting that immune system activation and apoptosis promotion occurred in scallops in response to environmental stress. *Heat shock proteins* (*HSPs*) were significantly upregulated under heat and hypoxia, which likely assisted in correct protein folding to facilitate the adaption of the scallops to the altered environment. Additionally, the HIF-1 signaling pathway—the key pathway associated with hypoxia response—was triggered by extremely acute environmental changes. Comparative transcriptome analysis revealed 239 positively selected genes among the different scallops, including those involved in immune system and environmental adaptation, suggesting a long-term mechanism of environmental adaptation. The present study provides new insights into the molecular response mechanism in scallops to multiple environmental stressors

and improves our understanding of the adaptive mechanisms of marine organisms under changing global climate conditions.

KEYWORDS

scallops, heat, hypoxia, transcriptome, response mechanism

Introduction

Water temperature and dissolved oxygen (DO) are two important environmental factors for marine organisms. The changing global climate has increased the ocean temperatures, which in turn has led to a decline in the DO levels in coastal zones (Vaquer-Sunyer and Duarte, 2008; Keeling et al., 2010; Vaquer-Sunyer and Duarte, 2011; Doney et al., 2012). High ocean temperatures have been proven to be a major driver of hypoxia (Vaquer-Sunyer and Duarte, 2011). Over the past decades, global warming and marine eutrophication have increased the number of coastal hypoxic zones, as well as their extension, severity and duration, which has been a major threat to coastal ecosystems, globally (Vaquer-Sunyer and Duarte, 2011; Sun et al., 2021). High temperature and hypoxia decrease the feeding, growth, reproduction and even survival of marine species (Levin et al., 2009; Hoegh-Guldberg and Bruno, 2010; Doney et al., 2012; Gobler et al., 2014; Li et al., 2020). Particularly, hypoxia caused by high temperatures resulted in high mortality in benthic marine organisms, leading to a major loss of marine biodiversity and also impacting aquaculture (Breitburg, 2002; Vaquer-Sunyer and Duarte, 2011). High temperatures in summer and hypoxia due to global warming, algal blooms and high-density aquaculture have led to frequent outbreaks of disease and the large-scale death of aquatic species, resulting in huge economic losses (Kemp et al., 2009; Pörtner, 2010; Pörtner, 2012; Stevens and Gobler, 2018). Thus, uncovering the molecular response mechanism of marine life to environmental stress (heat and hypoxia) is of priority concern to better comprehend the effects of the changing climate on marine organisms. Recently, the adaptive responses of marine organisms to heat and hypoxia have been widely investigated at molecular, metabolic, and cellular levels. However, most studies focused on only a single stressor (Truebano et al., 2010; Artigaud et al., 2014; Huo et al., 2019; Sun et al., 2020; Sun et al., 2021), whereas the two environmental stressors (heat and hypoxia) often affect marine life concurrently (Parthasarathy et al., 1992; Pörtner, 2010). Although the physiological effects of combined environmental stressors have been reported in some marine species (Pörtner and Knust, 2007; Pörtner and Farrell, 2008; Stevens and Gobler, 2018), the molecular response mechanism in marine organisms, including scallops, remains largely unknown.

Scallops, a diverse group of animals, consist of more than 300 extant marine species distributed worldwide. They play an important role in the structure and function of local benthic ecosystems (Brand, 2016). As filter-feeding bivalves, they are recognized for their ability to mitigate eutrophication, improve light availability, and recycle nutrients and organic matter, which reduces the risk of algal blooms in the coastal ecosystems (Officer et al., 1982; Cerrato et al., 2004; Gobler et al., 2005; Carroll et al., 2008; Wall et al., 2008). Additionally, many scallop species are of great economic value and support both commercial fisheries and mariculture. However, most of the commercially valuable species live and are farmed in shallow water, where environmental conditions are fluctuating, making scallops vulnerable to heat and hypoxia stresses (Guo and Luo, 2016; Stevens and Gobler, 2018). Therefore, elucidating the response and adaptive mechanism of scallops to heat, hypoxia and multiple environmental stressors is imperative to understanding the ecology of scallops and improving aquaculture strategies. Studies have shown that individual or combined environmental stressors could have different physiological effects on bivalve species with different environmental sensitivities (Stevens and Gobler, 2018). However, comparisons of molecular response mechanisms of different scallop species remain poorly studied, limiting our knowledge of their evolutionary adaptation to environmental changes.

Particularly, the Yesso scallop (*Patinopecten yessoensis*), Zhikong scallop (*Chlamys farreri*) and bay scallop (*Argopecten irradians*) are the three most important aquaculture scallop species in northern China with varying degrees of temperature tolerance. The Yesso scallop is a cold-water species that is naturally distributed along the coastlines of northern Japan, the far east of Russia, and the northern Korean Peninsula (Kosaka, 2016). The tolerable temperature range of the Yesso scallop is 4 to 23°C with the optimum temperature for growth ranging from 10 to 15°C (Kosaka, 2016). Since it was introduced into China in the 1980s, the aquaculture of the Yesso scallop has been growing rapidly due to its large size (Guo and Luo, 2016). However, the high summer water temperatures of the Bohai Sea, which can reach 25 to 28°C, are a challenge (Guo and Luo, 2016). The Zhikong scallop is a local species of China, which thrives

mainly in the southern Liaoning Peninsula and the north and south coasts of the Shandong Peninsula (Guo and Luo, 2016). Although the Zhikong scallop can tolerate a wide range of water temperatures (about -1.5°C to 30°C, with rapid growth at temperatures ranging from 16 to 18°C), growth decreases sharply when the water temperature exceeds 23°C (Yang et al., 1999; Guo and Luo, 2016). The large-scale mortality of cultured individuals has occurred each summer in most areas of northern China since 1996 (Xiao et al., 2005). In contrast to Yesso and Zhikong scallops, the bay scallop is a native of the east coast of the United States, occurring from Cape Cod to around New Jersey and Maryland (Clarke, 1965; Shumway and Castagna, 1994). It was successfully introduced into China in 1982 and can tolerate higher temperatures (the tolerable temperature range of adults is about -1 to 31°C with the optimum temperature for growth ranging from 18 to 28°C), growing fast in summer (Wang et al., 2011; Robinson et al., 2016). In addition to being impacted by the high temperatures, these three scallop species often suffer from hypoxia caused by environmental changes and intensive culture (Chen et al., 2007; Li et al., 2020; Silina, 2019; Gurr et al., 2021). For example, a decline in the growth rate of a Yesso scallop population in the coastal waters of Amur Bay off Vladivostok was found to be due to the lower oxygen saturation of water (Silina, 2019). A large-scale mortality event for the Zhikong scallop was caused by severe hypoxia resulting from eutrophication (Chen et al., 2007). Low DO also significantly increases the heartbeat rates and respiration rates of the bays scallop during hypoxia (Gurr et al., 2021; Yang et al., 2021). Therefore, to elucidate the molecular response mechanism of scallops with different thermal tolerance to combined environmental stressors, transcriptome analysis of the three scallops exposed to heat, hypoxia and heat plus hypoxia was first performed in the present study. Next, comparative transcriptome analysis was performed and positively selected genes were identified. This study provides new insights into the molecular response mechanism of scallops under multiple environmental stressors and improves our understanding of the adaptive mechanism of marine organisms in response to a changing global climate.

Results

Transcriptome sequencing, assembly and annotation of the three scallop species

To elucidate the response mechanism of scallops to high temperature and hypoxia, a total of 63 RNA-seq libraries were constructed to analyze the gill tissues of the Yesso scallop, Zhikong scallop, and bay scallop under normal and stressed conditions (heat or/and hypoxia). After eliminating adaptors and low-quality reads, a total of 3023.51 million reads (~424.64 Gb) with an average of 47.99 million reads (~6.74 Gb) for each sample were obtained, and the detailed sequencing information for each library is presented in Supplementary Table S1 and summarized in Table 1. A *de novo* assembly was separately carried out for each species using the Trinity method to construct the reference sequences for the analysis of differential gene expression and comparative transcriptome analysis. Finally, a total of 94,592, 112,109 and 83,299 unigenes with an average length of 1351.12 bp, 1174.67 bp and 1254.20 bp were obtained for the Yesso scallop, Zhikong scallop and bay scallop, respectively. The assembly information for the three scallops is summarized in Supplementary Table S2. The unigenes for each scallop were annotated by searching the sequences against the Nr, Swiss-Prot, GO, KOG, eggNOG and KEGG databases using BLASTX with a cut-off Evalue ≤ 1e-5 to describe their functions at different levels. The annotation information is summarized in Supplementary Table S3 and Figures S1-3.

Gene regulation of the three scallop species exposed to heat stress

The expression of the assembled unigenes was analyzed *via* the FPKM method. Analysis of differential gene expression was conducted in the three individual scallop species exposed to heat stress (HIG1: 22°C, HIG2: 25°C) and under normal (NOR: 15°C) conditions. At 22°C, there were 5231 differentially expressed genes (DEGs) detected in the Yesso scallop (PY_HIG1 vs PY_NOR), 3838 DEGs in the Zhikong scallop (CF_HIG1 vs CF_NOR) and 3227 DEGs in the bay scallop (AI_HIG1 vs AI_NOR) (Figure 1). After the temperature was increased to 25°C, a total of 8713 unigenes in the Yesso scallop (PY_HIG2 vs PY_NOR), 4018 unigenes in the Zhikong scallop (CF_HIG2 vs CF_NOR), and 3882 unigenes in the bay scallop (AI_HIG2 vs AI_NOR) were found be differentially expressed (Figure 1). Overall, the number of DEGs in the three scallops increased as the temperature increased. The Yesso scallop had more DEGs than the other two scallops.

GO enrichment analysis was performed to elucidate the functions of the DEGs. At 22°C and 25°C, a total of 288 and 444 GO terms in the Yesso scallop (Tables S4, 5), 165 and 179 GO terms in the Zhikong scallop (Tables S6, 7), and 192 and 177 GO terms in the bay scallop (Tables S8, 9) were significantly enriched, respectively. Among these GO terms, many immune response-related functions—such as 'immune response', 'innate immune response', and 'regulation of immune response' —and apoptosis-related functions—such as 'regulation of apoptotic process' and 'regulation of necroptotic process' —were enriched at both temperatures for the three scallop species. GO functions related to heat response, such as 'cellular response to heat', 'regulation of cellular response to heat', and 'Hsp 70 (heat shock protein 70) protein binding', were significantly enriched at 25 °C, indicating the obvious cellular response processes to severe heat stress. Additionally, protein

TABLE 1 Summary of transcriptome sequencing of scallop gill tissue.

Species	Group	Conditions	Sample number	CleanReads (Million)	CleanBases (Gb)
P. yessoensis	PY_NOR	Normal (15°C, 8 mg/L)	3	143.10	20.23
	PY_HIG1	Heat (22°C, 8 mg/L)	3	140.91	19.93
	PY_HIG2	Heat (25°C, 8 mg/L)	3	144.74	20.28
	PY_LOW1	Hypoxia (15°C, 6 mg/L)	3	144.02	20.15
	PY_LOW2	Hypoxia (15°C, 4 mg/L)	3	140.73	19.84
	PY_LOW3	Hypoxia (15°C, 2 mg/L)	3	138.60	19.51
	PY_UNI	Heat plus hypoxia (25°C, 2 mg/L)	3	141.69	19.93
C. farreri	CF_NOR	Normal (15°C, 8 mg/L)	3	137.38	19.36
	CF_HIG1	Heat (22°C, 8 mg/L)	3	147.59	20.66
	CF_HIG2	Heat (25°C, 8 mg/L)	3	144.15	20.28
	CF_LOW1	Hypoxia (15°C, 6 mg/L)	3	141.57	19.84
	CF_LOW2	Hypoxia (15°C, 4 mg/L)	3	144.74	20.25
	CF_LOW3	Hypoxia (15°C, 2 mg/L)	3	144.60	20.22
	CF_UNI	Heat plus hypoxia (25°C, 2 mg/L)	3	143.50	20.16
A. irradians	AI_NOR	Normal (15°C, 8 mg/L)	3	145.48	20.39
	AI_HIG1	Heat (22°C, 8 mg/L)	3	146.48	20.64
	AI_HIG2	Heat (25°C, 8 mg/L)	3	148.80	20.95
	AI_LOW1	Hypoxia (15°C, 6 mg/L)	3	147.45	20.68
	AI_LOW2	Hypoxia (15°C, 4 mg/L)	3	146.45	20.51
	AI_LOW3	Hypoxia (15°C, 2 mg/L)	3	144.12	20.21
	AI_UNI	Heat plus hypoxia (25°C, 2 mg/L)	3	147.41	20.62
	SUM		63.00	3023.51	424.64

processing-related GO functions, such as 'response to unfolded protein', 'protein refolding', 'chaperone cofactor-dependent protein refolding', 'misfolded protein binding', and 'regulation of proteolysis', were much more enriched at the higher temperature. This was indicative of heat damage to the structures of many proteins in cells and the organisms' activated response mechanisms to repair or eliminate these abnormal proteins. Additionally, GO functions associated with the oxidative stress response, such as 'regulation of cellular response to oxidative stress' and 'response to hypoxia', were also enriched at higher temperatures, which probably resulted from the hypoxia caused by high temperature. Overall, the above

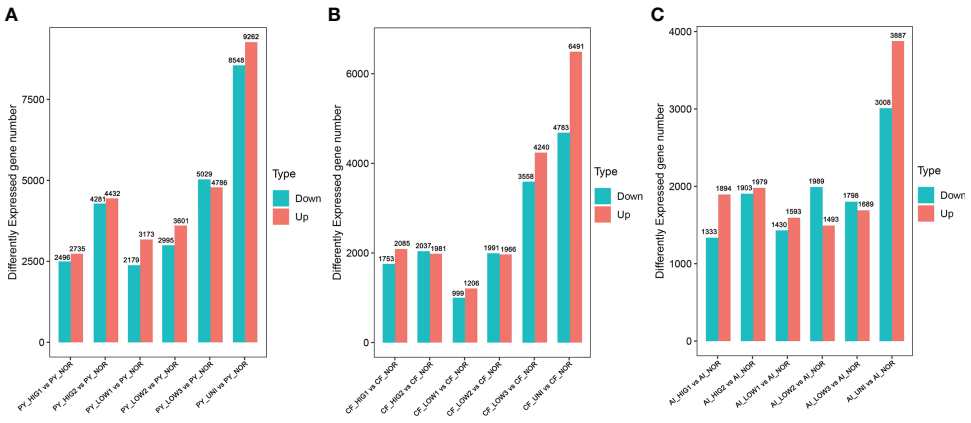

FIGURE 1
Number of DEGs for the Yesso scallop **(A)**, Zhikong scallop **(B)**, and bay scallop **(C)** exposed to heat, hypoxia and heat combined with hypoxia. (PY, *Patinopecten yessoensis*; CF, *Chlamys farreri*; AI, *Argopecten irradians*; HIG1 and HIG2, heat stress at 22 and 25°C, respectively; LOW1-LOW3, hypoxia at DO levels of 6 mg/L, 4 mg/L, and 2 mg/L, respectively; UNI, heat plus hypoxia at 25°C and the 2 mg/L DO; NOR, normal conditions at 15°C and 8 mg/L DO).

related GO terms were found much more enriched in the Yesso scallop, as highlighted in Supplementary Tables S4-S9.

KEGG enrichment analysis was further performed for all DEGs as well as up- and downregulated DEGs to identify the important molecular pathways involved in heat stress. The results showed that, at 22°C and 25°C, a total of 40 and 76 pathways in the Yesso scallop, 19 and 24 pathways in the Zhikong scallop, and 17 and 14 pathways in the bay scallop were significantly enriched for all the DEGs, respectively. Notably, the most significantly enriched pathways were those related to immune response and apoptosis, which were significantly upregulated at two heat stresses in the three scallops (Figure 2). However, many more related pathways were found in the Yesso scallop (Supplementary Tables S10-S15). Among these pathways, 'TNF (tumor necrosis factor) signaling pathway', 'Toll and Imd (immune deficiency) signaling pathway', 'NF (nuclear factor)-kappa B signaling pathway', 'NOD (nucleotide oligomerization domain)-like receptor signaling pathway', 'Apoptosis-multiple species' and 'Necroptosis' were simultaneously enriched at both heat stress groups for the three scallop species (Figure 2; Tables S10-S15). The pathways of 'Protein processing in endoplasmic reticulum' and 'Ubiquitin mediated proteolysis', which were involved in protein processing, were also significantly enriched in the three scallop species. 'Ubiquitin mediated proteolysis' was upregulated in all the heat-treated groups of the three scallop species; and 'Protein processing in endoplasmic reticulum' was upregulated in both two treated groups of the Yesso scallop and HIG2 group of the Zhikong scallop, but downregulated in HIG2 group of the bay scallop (Tables S10-S15; Figure S4). With the temperature

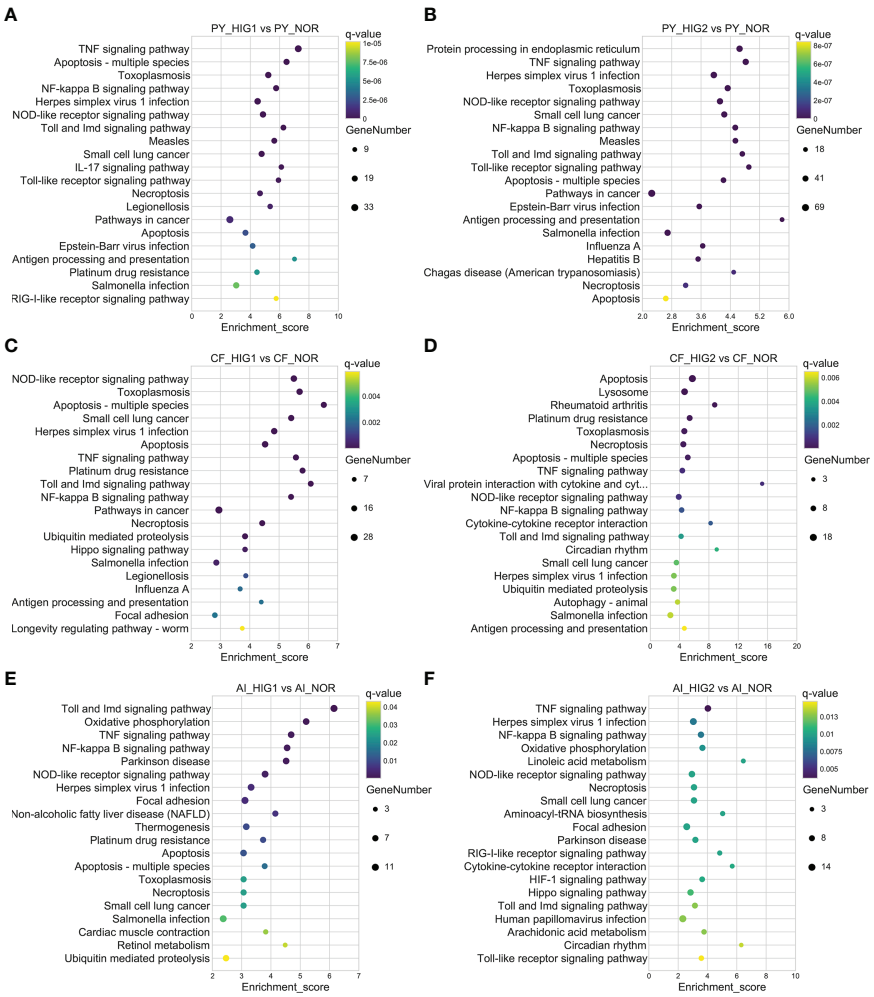

FIGURE 2
Top 20 significantly enriched KEGG pathways of upregulated DEGs in the Yesso scallop **(A, B)**, Zhikong scallop **(C, D)**, and bay scallop **(E, F)** exposed to different heat stressors. (PY, *Patinopecten yessoensis*; CF, *Chlamys farreri*; AI, *Argopecten irradians*; HIG1 and HIG2, heat stress at 22 and 25°C, respectively; NOR, normal conditions at 15°C and 8 mg/L DO).

increase, the 'HIF-1 signaling pathway' was significantly upregulated in the Yesso and bay scallops at 25°C (Tables S11, 15).

Gene regulation of the three scallop species exposed to hypoxia stress

Changes in transcriptomic expression in the three scallop species exposed to different levels of hypoxia (LOW1: 6 mg/L, LOW2: 4 mg/L, LOW3: 2 mg/L) were then determined by comparison with scallops under normal conditions (NOR: 8 mg/L). A total of 5552, 6596, and 9815 DEGs were identified in the Yesso scallop at DO concentrations of 6 mg/L (PY_LOW1 vs PY_NOR), 4 mg/L (PY_LOW2 vs PY_NOR), and 2 mg/L (PY_LOW3 vs PY_NOR), respectively (Figure 1A). In the Zhikong scallop, a total of 2205, 3957 and 7828 DEGs were detected at DO concentrations of 6 mg/L (CF_LOW1 vs CF_NOR), 4 mg/L (CF_LOW2 vs CF_NOR), and 2 mg/L (CF_LOW3 vs CF_NOR), respectively (Figure 1B). In the bay scallop, the number of DEGs were 3023, 3482 and 3487 at different DO levels (AI_LOW1 vs AI_NOR, AI_LOW2 vs AI_NOR and AI_LOW3 vs AI_NOR) (Figure 1C). Under hypoxia stress, the Yesso scallop exhibited the most DEGs among the three scallop species, followed by the Zhikong scallop, and the bay scallop. Generally, the number of DEGs increased with the decrease in DO among the three scallop species, but especially in the Yesso and Zhikong scallops.

GO enrichment analysis of the DEGs in the three scallop species showed that a total of 319, 353 and 527 GO terms in the Yesso scallop (Tables S16-S18), 89, 163 and 390 GO terms in the Zhikong scallop (Tables S19-S21), and 204, 196 and 228 GO terms in the bay scallop (Tables S22-S24) were significantly enriched under different levels of hypoxia stress (LOW1 to LOW3). A variety of functions were affected. Among these GO terms, functions related to immune response, apoptosis, protein folding, and hypoxia response (highlighted with different colors in Tables S16-S24) were significantly enriched in three scallop species, especially in the Yesso scallop. Some related GO functions were also found in the Zhikong and bay scallops, but fewer than in the Yesso scallop.

KEGG enrichment analysis revealed that, at different degrees of hypoxia (LOW1, LOW2, and LOW3), a total of 47, 42 and 91 pathways in the Yesso scallop, 38, 45 and 51 pathways in the Zhikong scallop, and 31, 18 and 11 pathways in the bay scallop, were significantly enriched, respectively. Like in response to heat stress, the most significantly enriched pathways in the three scallop species were those related to immune response and apoptosis. This was most pronounced in the Yesso scallop, with all pathways upregulated simultaneously in all the three hypoxia groups, including 'TNF signaling pathway', 'Toll and Imd signaling pathway', 'Toll-like receptor signaling pathway', 'NF-kappa B signaling pathway', 'NOD-like receptor signaling pathway', 'IL (interleukin)-17 signaling pathway', 'RIG (retinoic acid-inducible gene)-I-like receptor signaling pathway', 'Apoptosis', 'Apoptosis-multiple species', and 'Necroptosis' (Figures 3A-C; Figures S5A-C; Tables S25-S27). In the Zhikong scallop, some of these immune and apoptosis-related pathways were downregulated or both up- and downregulated (Figures 3D-F; Figures S5D-F; Tables S28-30). In the bay scallop, some of these pathways were upregulated in the LOW1 and LOW2 groups but not in the LOW3 group, except for the downregulated pathway of 'Apoptosis' (Figures 3G-I; S5G-I; Tables S31-S33). Additionally, protein processing-related pathways of 'Protein processing in endoplasmic reticulum' and 'Ubiquitin mediated proteolysis' were upregulated at all hypoxia levels for the Yesso scallop and at most for the Zhikong scallop, but were not enriched in the bay scallop except for the upregulatation of 'Ubiquitin mediated proteolysis' in the LOW2 group. Following decreased DO, the 'HIF-1 signaling pathway' was found to be significantly upregulated in the severe hypoxia groups of the three scallop species, i.e., the LOW3 group of the Yesso and Zhikong scallops and the LOW2 and LOW3 groups of the bay scallop (Figure 3). DNA replication- and repair-associated pathways, such as 'DNA replication', 'Mismatch repair', 'Base excision repair', and 'Nucleotide excision repair', were also found to be significantly enriched, but were downregulated, in severe hypoxia groups of the Yesso (LOW2 and LOW3) and Zhikong scallops (LOW3) (Figure S5).

Gene regulation of the three scallop species exposed to combined heat and hypoxia

The regulation of gene expression in the three scallop species following exposure to a combination of heat hypoxia (UNI: 25 °C and 2 mg/L) was analyzed. A total of 17810 (PY_UNI vs PY_NOR), 11174 (CF_UNI vs CF_NOR) and 6885 unigenes were differentially expressed in the Yesso, Zhikong, and bay scallops, respectively (Figure 1). This was much higher than that induced by each stressor individually. GO enrichment analysis of the DEGs showed that a total of 481, 501, and 280 GO terms were significantly enriched in the Yesso, Zhikong and bay scallops, respectively (Tables S34-S36), which covered a variety of functions, including those related to immune response, apoptosis, and stress response (highlighted with different colors in Tables S34-S36). KEGG enrichment analysis showed that a total of 84, 50 and 25 pathways were significantly enriched in the Yesso, Zhikong, and bay scallops, respectively. As expected, the pathways involved in immune response, apoptosis, and protein processing were most significantly enriched in the three scallop species All were upregulated under combined stress, with significant upregulation of 'TNF signaling pathway', 'Toll and Imd signaling pathway', 'NF-kappa B signaling pathway', 'NOD-like receptor signaling pathway', 'Apoptosis', 'Apoptosis-multiple species', 'Necroptosis', as well as 'Ubiquitin mediated proteolysis'

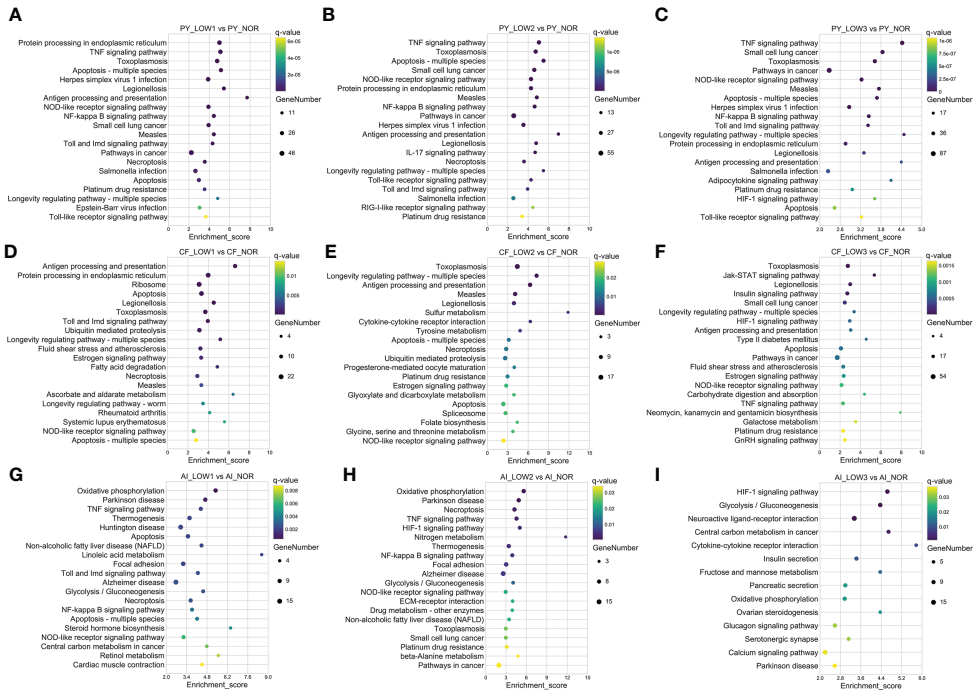

FIGURE 3
Top 20 significantly enriched KEGG pathways of upregulated DEGs in the Yesso scallop **(A–C)**, Zhikong scallop **(D–F)**, and bay scallop **(G–I)** exposed to different levels of hypoxia stress. (PY, *Patinopecten yessoensis*; CF, *Chlamys farreri*; AI, *Argopecten irradians*; LOW1-LOW3, hypoxia stress associated with DO levels of 6 mg/L, 4 mg/L, and 2 mg/L, respectively; NOR, normal conditions at 15°C and 8 mg/L DO).

and 'HIF-1 signaling pathway', in the three scallop species (Tables S37-S39; Figure 4). Like the downregulated pathways of the severe hypoxia groups, DNA replication- and repair-associated pathways were mainly enriched in the downregulated DEGs of the Yesso and Zhikong scallops (Figure S6).

Finally, a Venn analysis of the DEGs was performed in all the treatment groups (HIG1, HIG2, LOW1, LOW2, LOW3, and UNI). Following exposure to heat and hypoxia, the number of non-redundant DEGs in the three scallops was 14019, 10787, and 6466 for the Yesso, Zhikong, and bay scallops, respectively (Figures 7A-C). Additionally, 722, 71, and 164 DEGs were shared by all the separate treatment groups of the Yesso, Zhikong, and bay scallops (Figure 5). Due to the relatively few shared DEGs—including several non-annotated ones—that were identified in the Zhikong and bay scallops, a significant enrichment of GO functions and pathways was mainly observed in the Yesso scallop. A total of 91 GO terms, including those related to immune response, apoptosis, heat and hypoxia response were significantly enriched in the Yesso scallop (Table S40). KEGG enrichment analysis showed 51 significantly enriched pathways, including some associated with immune response and apoptosis (Table S41). Furthermore, among the enriched GO functions and pathways for the Yesso scallop, several key candidate genes involved in stress response were detected, including *TNF receptor-associated factor 3*, *TNF receptor superfamily member 11B*, *TNF receptor superfamily member 27*, *HSP 70B2*, *Heat shock cognate 71 kDa protein*, *HSP 90-beta*, *HSP 90 co-chaperone Cdc37*, *Putative tyrosinase-like protein-3*, *Cell division cycle and apoptosis regulator protein 1*, and *Cytochrome P450 2C38* (Figure 6).

Comparative transcriptome analysis of different scallop species

The transcriptome sequences of the king scallop (*Pecten maximus*) reported by Kenny et al. (2020) were used because at least four species were required for phylogenetic analysis. A total of 5693 single-copy orthologs were detected with the CDS sequences of the four scallop species. Phylogenetic analysis of these orthologs indicated clusters of Yesso and Zhikong scallops, followed by the bay scallop and king scallop, which was consistent with their species phylogeny (Figure 7A). The color of each branch indicated the dN/dS value of the 'super gene' and was generated by directly connecting all the orthologs of each species. The distribution of dN/dS in each species is shown in Figure 7B. Overall, the dN/dS value of the Yesso scallop was the largest among the three scallop species, followed by the Zhikong and bay scallops, suggesting a relatively rapid evolutionary speed of the Yesso scallop compared with that of the other two

10.3389/fmars.2022.971796

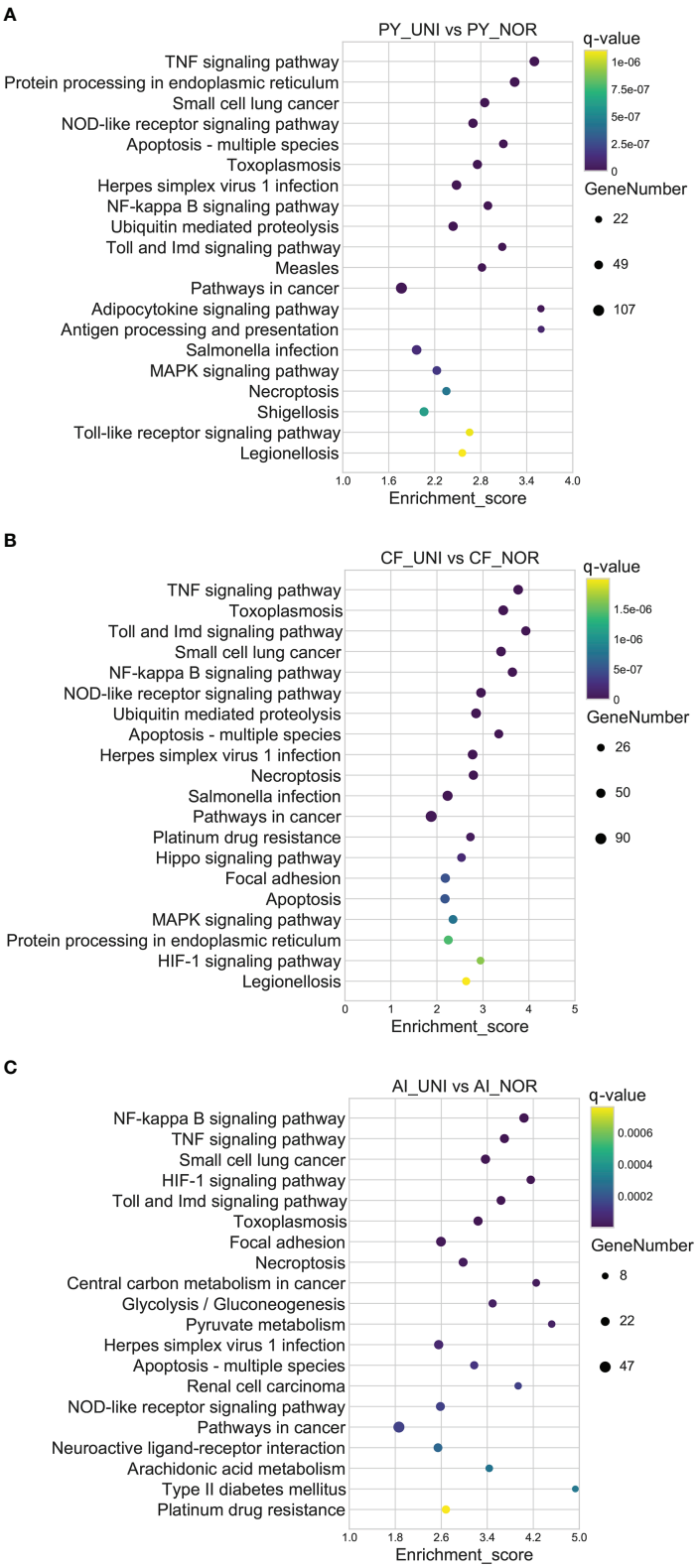

FIGURE 4
Top 20 significantly enriched KEGG pathways of upregulated DEGs in the Yesso scallop **(A)**, Zhikong scallop **(B)**, and bay scallop **(C)** exposed to heat and hypoxia. (PY, *Patinopecten yessoensis*; CF, *Chlamys farreri*; AI, *Argopecten irradians*; UNI, heat + hypoxia stress at 25°C and 2 mg/L DO; NOR, normal conditions at 15°C and 8 mg/L DO).

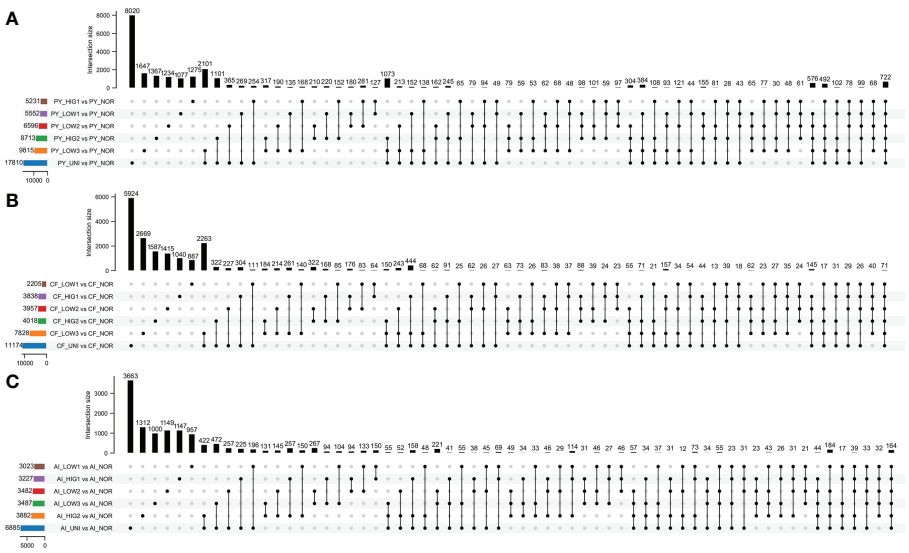

FIGURE 5
Venn diagrams representing DEGs in the Yesso scallop **(A)**, Zhikong scallop **(B)**, and bay scallop **(C)** under stress. (PY, *Patinopecten yessoensis*; CF, *Chlamys farreri*; AI, *Argopecten irradians*; HIG1 and HIG2, heat stress at 22 and 25°C; LOW1-LOW3, hypoxia stress induced by DO levels of 6 mg/L, 4 mg/L, and 2 mg/L, respectively; UNI, stress induced by heat and hypoxia at 25°C and 2 mg/L DO; NOR, normal conditions at 15°C and 8 mg/L DO).

scallops. A total of 239 positively selected genes were identified using the branch-site model of the PAML software ($p < 0.05$). These genes may be associated with positive selection. GO enrichment analysis of these positively selected genes indicated enrichment of 44 GO functions (level 2), including 'response to stimulus' and 'immune system process' (Figure 7C). KEGG enrichment showed that pathways related to 'immune system', 'infectious disease' and 'environmental adaptation' were also significantly enriched (Figure 7D). Positively selected genes that were possibly involved in stress adaptation are listed in Table 2.

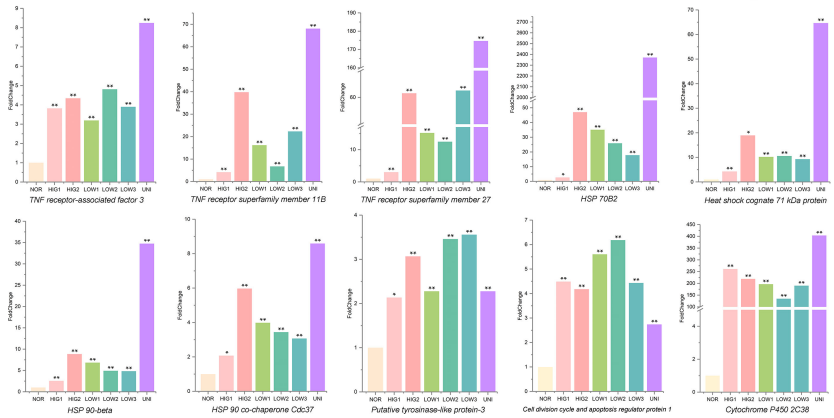

FIGURE 6
Levels of mRNA expression associated with key candidate genes involved in stress response in the Yesso scallop. (Values marked with an asterisk indicate significant differences, *p-value < 0.05, **p-value < 0.01; HIG1and HIG2, heat stress at 22 and 25°C; LOW1-LOW3, hypoxia stress at DO levels of 6 mg/L, 4 mg/L, and 2 mg/L; UNI, stress due to heat and hypoxia at 25°C and 2 mg/L DO; NOR, normal conditions at 15°C and 8 mg/L DO).

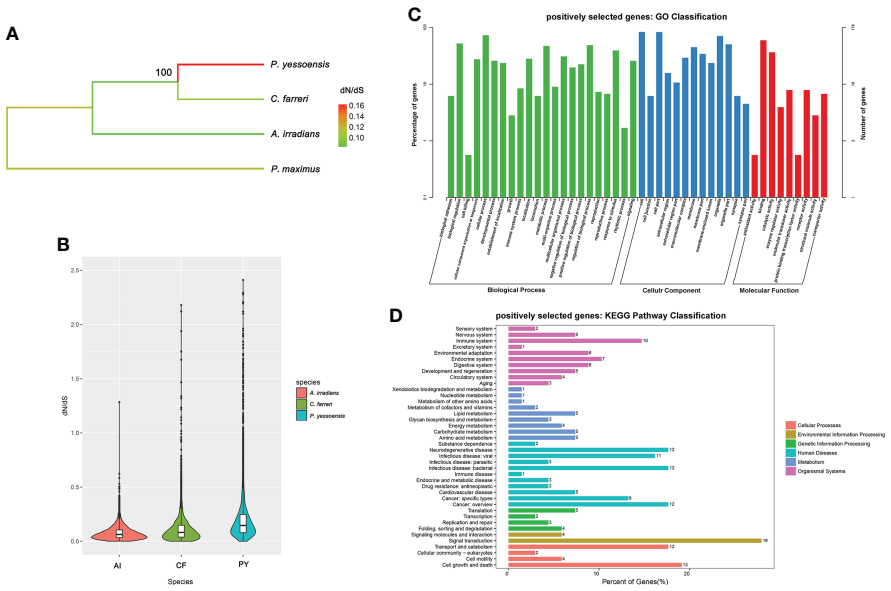

FIGURE 7
Comparative transcriptome analysis of different scallops. **(A)** Phylogenetic analysis of different scallop species with single-copy orthologs. The color of the branch indicates the dN/dS value of the 'super gene' connected by all orthologs of the species. **(B)** Distribution of dN/dS values in different scallops. **(C)** GO enrichment analysis of positively selected genes. **(D)** KEGG enrichment analysis of positively selected genes.

TABLE 2 Positively selected genes associated with stress adaptation.

Ortholog ID	Annotation Description	*p* (< 0.05)
OG2311	protein toll-like	3.37E-03
OG4032	Toll-like receptor 3	4.25E-02
OG3293	Toll-like receptor 6	4.27E-03
OG1353	C-type lectin domain family 4 member K-like, partial	8.85E-03
OG2977	proto-oncogene tyrosine-protein kinase receptor Ret-like	2.25E-06
OG1437	Cytochrome c oxidase subunit 6B1	1.65E-07
OG229	Sulfhydryl oxidase 2	3.25E-05
OG3492	amiloride-sensitive amine oxidase (copper-containing)-like	2.86E-02
OG1437	Cytochrome c oxidase subunit 6B1	1.65E-07
OG4631	sulfite oxidase, mitochondrial	4.87E-02
OG3689	Cytochrome P450 2C40	4.92E-02
OG3013	cytochrome c-like	5.42E-03
OG5521	Insoluble matrix shell protein 5	2.54E-02
OG2729	chitinase-3-like protein 1	1.71E-02
OG1700	Temptin	4.23E-02
OG4894	Calmodulin	7.83E-03
OG2143	Calmodulin	1.39E-02
OG3529	calcium/calmodulin-dependent protein kinase type 1-like	9.92E-03
OG2568	Calcium uniporter protein, mitochondrial	4.35E-02
OG1575	calexcitin-2-like isoform X1	3.48E-02
OG4652	cadherin-23-like	3.71E-02

Discussion

High temperature and hypoxia have become common stress factors that pose a great threat to marine life and aquaculture. Although some studies have explored the influence of each of these stressors on aquatic animals individually, the combined effects of the two stressors remain largely unknown, especially in scallops. In the present study, three scallop species—Yesso, Zhikong and bay scallops— were exposed to short-time heat and hypoxia, both individually and combined. Then, an analysis of transcriptome regulation was performed to elucidate the molecular response mechanism of the scallops under environmental stress, especially under combined stress. The key molecular pathways of scallops involved in the response of the scallops to heat, hypoxia and heat plus hypoxia were obtained. Comparative transcriptome analysis among the different scallop species was also performed to reveal an evolutionary mechanism of the scallops' adaptation to environmental changes. This study provides insights into the response mechanisms of scallops exposed to multiple environmental stressors and improves our understanding of adaptive mechanisms in marine organisms in response to a changing global climate.

Effects of different environmental stressors on scallops

Environmental stress can damage macromolecules within cells, such as DNA and proteins, which induces a response mechanism by the organisms to maintain cellular homeostasis (Halliwell and Cross, 1994; Visick and Clarke, 1995; Chen and Jin, 2019). Accumulated DNA damages and unrepaired abnormal proteins will activate apoptosis or cell death (Franco et al., 2009; Erguler et al., 2013). In the present study, heat, hypoxia, and their combination resulted in high levels of protein disorder. Many protein folding-related GO functions—such as "protein folding", "chaperone-mediated protein folding", "protein refolding", "chaperone cofactor-dependent protein refolding", "response to unfolded protein", "unfolded protein binding", and "misfolded protein binding"—were significantly enriched in the three scallop species, especially the Yesso scallop, in response to the different environmental stressors. However, it appeared that DNA damages mainly occurred under acute hypoxia stress, as DNA replication and repair-related pathways—such as "DNA replication", "mismatch repair", "base excision repair", and "nucleotide excision repair"—were significantly downregulated in the acute hypoxia groups of the Yesso (LOW 2, LOW3 and UNI) and Zhikong scallops (LOW3 and UNI). These effects would lead to a high mutation ratio (Artigaud et al., 2015). Acute hypoxia probably caused high levels of reactive oxygen species (ROS) in scallops, which would lead to DNA damage and, ultimately, cell death (de Almeida et al., 2007).

Exposure to single stressors—increased temperature and decreased DO—increased the number of DEGs in the three scallop species. This was consistent with results for the hard clam (*Mercenaria mercenaria*); that is, the number of DEGs increased with an increase in the severity of heat and hypoxia stresses (Hu et al., 2022). Heat often accompanies hypoxia, as high temperatures decrease the solubility of oxygen, while increasing the metabolic and respiratory rates of organisms, thus enhancing oxygen requirements in warmer water that holds less DO (Vaquer-Sunyer and Duarte, 2011). However, the combined impact of heat and hypoxia on scallops was unclear before this study. Multiple stressors interact in unpredictable ways (Stevens and Gobler, 2018). Environmental stressors are more likely to act synergistically or antagonistically than additively (Crain et al., 2008). In the present study, the number of DEGs in the three scallop species following exposure to combined stress (heat plus hypoxia) was significantly higher than for either single stressor and was also greater than the summation of non-redundant DEGs under heat and hypoxia individually. This was suggestive of a synergistic effect of the two stressors. GO and KEGG enrichment analysis revealed the simultaneous enrichment of multiple functions and pathways related to immune response, apoptosis, and protein processing in response to different stressors (Figure 8). This suggested shared molecular responses, that is, activation of the immune system and promotion of apoptosis, to heat and hypoxia in scallops. Similar results were reported in small abalone (*Haliotis diversicolor*), suggesting a similar molecular response to thermal stress and hypoxia (Zhang et al., 2014).

Activation of immune pathways in response to environmental changes

Environment stress has been shown to significantly alter the immunity of several marine organisms (Chen et al., 2007; Malagoli et al., 2007; Sun et al., 2020). Immune regulation can be activated by the exposure to environmental stressors to increase the immune defenses of organisms in adverse environments (Huo et al., 2019; Zhang et al., 2019; Nie et al., 2020). In the current study, several innate immune-related GO functions and pathways were significantly enriched in the three scallop species following exposure to heat, hypoxia, and heat plus hypoxia. Most of these pathways were upregulated and included in the most significantly enriched pathways, which indicated the activation of the immune response of the scallops to the different environmental stresses. The TNF signaling pathway, NF-kappa B signaling pathway, Toll and Imd signaling pathway, and NOD-like receptor signaling pathway were significantly upregulated under different levels of heat stress and the combination of heat and hypoxia in all the three

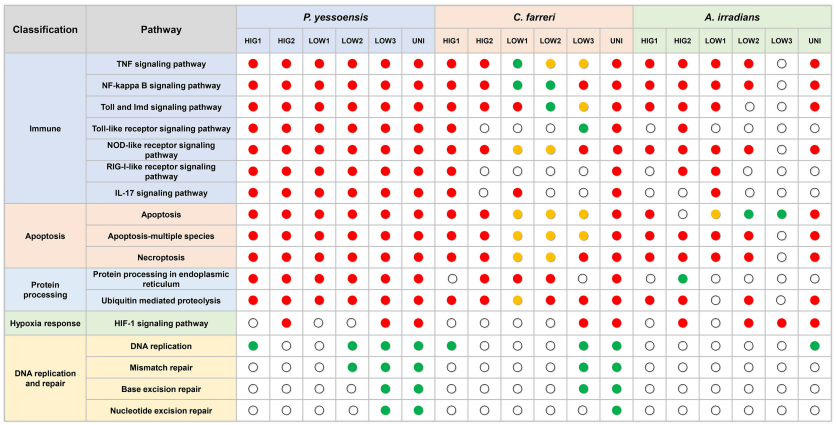

FIGURE 8
Key pathways in the three scallop species in response to different kinds of environmental stresses. Red dot represent enriched pathways in upregulated DEGs, green dots represent enriched pathways in downregulated DEGs, and yellow dots represent enriched pathways in both up- and downregulated DEGs.

scallop species, and were significantly enriched in all the hypoxia groups of the Yesso scallop (all upregulated) and at least one hypoxia group of the Zhikong and bay scallops (Figure 8). These findings indicated the important role of these pathways in the immune response of the scallops to heat, hypoxia and heat plus hypoxia.

Similar immune pathways were also detected in response to environmental stressors in several other bivalves. For example, both the NF-kappa B signaling pathway and TNF signaling pathway were significantly enriched in ark shells (*Scapharca subcrenata*) for DEGs under heat and hypoxia stresses (Ning et al., 2021). In the Manila clam (*Ruditapes philippinarum*), KEGG analyses of the DEGs showed that the TNF signaling pathway, NOD-like receptor signaling pathway, RIG-I-like receptor signaling pathway, and NF-kappa B signaling pathway were significantly enriched under hypoxia stress (Nie et al., 2020), and the TNF signaling pathway and NF-kappa B signaling pathway were highly enriched after aerial exposure stress (Nie et al., 2020). Similar results have also been found in hard clams under aerial exposure; that is, the NF-kappa B signaling pathway, NOD-like receptor signaling pathway, and RIG-I-like receptor signaling pathway were significantly enriched (Zhou et al., 2021). Therefore, mollusks may have developed sophisticated immune regulatory mechanisms to sense the environmental changes and orchestrate appropriate signaling pathways to facilitate adaptation in the marine environment.

The TNF family members and their receptors are important pleiotropic cytokines that mediated inflammatory signaling in infectious diseases (Wajant et al., 2003). TNF can coordinate with Imd, Toll, and JNK pathways to regulate the innate immune response through controlling the capacity of phenoloxidase and the expression of antimicrobial peptide genes synergistically (Tang et al., 2019), while the NF-kappa B signaling pathway is crucial for mediating cellular TNF responses (Tanji and Ip, 2005). NF-kappa B is prominently involved in the regulation of immune and inflammatory responses, typically by inducing antiapoptotic gene expression to promote cell survival (Mattson and Meffert, 2006). NOD-like receptors have emerged as pivotal intracellular sensors in innate and adaptive immunity, which can integrate positive and negative incoming signals and stimulate other signaling pathways, such as the NF-kappa B signaling pathway (Shaw et al., 2010; Liu et al., 2019). Therefore, these immune pathways do not function alone. The simultaneous regulation of these pathways in the three scallop species under different environmental stressors is also indicative that the pathways can interact to protect organisms from stresses. Among these pathways, the TNF signaling pathway may represent a key environmental response mechanism in the Yesso scallop, given the significant upregulation of several TNF receptor superfamily genes (*TNF receptor-associated factor 3, TNF receptor superfamily member 11B, TNF receptor superfamily member 27*) in all the stressed groups of the Yesso scallop. Additionally, TNF is also a crucial regulator of the generation of ROS, and high ROS concentrations in cells ultimately lead to DNA damage and cell death (Blaser et al., 2016).

Induction of apoptosis in response to environmental changes

Apoptosis, or programmed cell death, plays a vital role in organ development, tissue homeostasis regulation, elimination of abnormal or damaged cells, and the immune response (Jacobson et al., 1997; Ameisen, 2002; Sokolova, 2009).

Environmental stressors are well known to induce apoptotic cell death (Franco et al., 2009). In the present study, the apoptotic GO functions and pathways were highly enriched for DEGs in all the three scallop species following exposure to heat, hypoxia, and heat plus hypoxia, indicating the key role of apoptosis in response to environmental stress. Furthermore, these apoptosis-related pathways, such as "Apoptosis", "Apoptosis-multiple species", and "Necroptosis", were significantly upregulated and mostly involved in the top enriched pathways, suggesting the induction of apoptosis under environmental stress. Similar conclusions were also obtained for the Manila clam in response to hypoxia and aerial exposure stresses (Nie et al., 2020; Nie et al., 2020), the king scallop in response to aeration stress (Pauletto et al., 2018), the Pacific oyster (*Crassostrea gigas*) in response to heat stress (Yang et al., 2017) and the Pacific abalone (*H. discus hannai*) in response to hypoxia stress (Shen et al., 2019).

Apoptosis can be induced *via* the unfolded protein response (UPR), which is a major signaling cascade controlling the quality of protein folding in the endoplasmic reticulum (ER) (Hetz, 2012; Erguler et al., 2013; Sun et al., 2020). If the unfolded or misfolded proteins in cells are not repaired within a certain period, the UPR triggers cellular apoptosis (Sun et al., 2020). In the present study, many protein folding-related GO functions were significantly enriched, suggesting that an active UPR occurred in scallop gill cells in response to environmental changes. Protein quality control is critical in maintaining cellular homeostasis under environmental stress, and the ER has quality control systems that ensure the correct folding of proteins (Ellgaard et al., 1999). In this study, the pathway of "protein processing in endoplasmic reticulum" was significantly upregulated in most of the Yesso and Zhikong scallop treatment groups; this would recognize and selectively direct misfolded proteins to be either refolded or degraded. "Ubiquitin mediated proteolysis", which plays an important role in degrading irreparable proteins (Hampton, 2002), was another significantly upregulated pathway in nearly all of the treated groups of the three scallop species. This indicated that abnormal proteins induced by environmental stress in scallops may be eliminated by ubiquitin-mediated proteolysis. Similar conclusions have also been reported in the hard clam, with these same two pathways being the most significantly enriched under heat and hypoxia stresses. These results suggest that bivalves employ a strict quality control system to guarantee correct protein folding and the elimination of irreparable proteins, thereby alleviating cytotoxicity and maintaining cell homeostasis under environmental stress (Hu et al., 2022). However, even in the presence of a quality control system, incorrectly folded proteins will accumulate in the ER under severe stress (Ma and Hendershot, 2004). Therefore, as exposure to heat or hypoxia may induce considerable protein disorder in scallops, apoptosis could eventually result despite the attempts at maintaining homeostasis *via* the UPR.

HSPs mediation of acute environmental stress response

HSPs are highly conserved proteins that act as biomarkers of environmental stress (Kregel, 2002; Sørensen et al., 2003). Most studies on HSPs, such as HSPs 70 and 90, have mainly focused on thermal tolerance in mollusks; however, these genes are widely involved in several other environmental stresses responses, including hypoxia and aerial exposure (Delaney and Klesius, 2004; Mohindra et al., 2015; Huo et al., 2019; Nie et al., 2020; Nie et al., 2020). In the hard clam, the elevated expression of two HSP 90 genes and some HSP 70 members was induced by heat and hypoxia stresses (Hu et al., 2022). In the present study, the GO functions of "HSP 70 protein binding" were significantly enriched in the HIG2, LOW1, LOW2, LOW3, and UNI groups of the Yesso scallop and the UNI group of the Zhikong scallop. The GO functions of "HSP binding" were significantly enriched in the LOW1, LOW2, and LOW3 groups of the bay scallop and the LOW1 group of the Yesso scallop. Furthermore, for DEGs shared by all stressed groups in the Yesso scallop, the "HSP binding" GO functions were also highly enriched, and the involved genes *HSP 70B2, Heat shock cognate 71 kDa protein, HSP 90-beta, and Hsp 90 co-chaperone Cdc37* were significantly upregulated in all the heat, hypoxia, and heat plus hypoxia groups. These results suggested that HSPs play an important role in response to different types of environmental stress in scallops. HSPs have extensive functions associated with apoptosis, including enhanced cell survival by inhibiting apoptosis (Roberts et al., 2010; Artigaud et al., 2015). Acting as molecular chaperones, HSPs can catalyze protein folding and refolding, stabilize normal proteins to prevent degeneration, eliminate irreversibly damaged proteins, and maintain cellular homeostasis. HSP 90 and HSP 70 are two major chaperone classes (Frydman, 2001; Sørensen et al., 2003; Liu et al., 2019). Therefore, given the highly enriched protein folding and apoptosis-related functions and pathways in the present study, it is likely that HSPs inhibited apoptosis by interacting with abnormal proteins to facilitate the adaption of scallops to environmental changes.

HIF-1 signaling pathway mediates severe heat and hypoxia stress

The ability of marine organisms to adapt to changing levels of DO is important for their survival. Several studies have suggested that the modulation of oxygen homeostasis in animals greatly depends on HIF-1 signaling. This induces similar biochemical and physiological responses in different organisms, including oxygen sensor mobilization and oxygen transport, to facilitate cellular or tissue adaptation to low oxygen levels (Semenza, 1999; Zhang et al., 2017). The important role of

the HIF-1 signaling pathway in environmental stress tolerance and resistance has been reported in some mollusks. In the Pacific oyster, the expression of *HIF-α* was significantly increased by air exposure and heat shock (Kawabe and Yokoyama, 2012). The HIF-1 signaling pathway was significantly enriched in the Manila clam and small abalone under hypoxia stress (Sun et al., 2019; Nie et al., 2020). In the Yesso scallop, Kotsyuba reported that the activity of HIF-1α depended on the duration of anoxia and the temperature (Kotsyuba, 2017). In the present study, the HIF-1 signaling pathway was significantly enriched for the upregulated DEGs under severe heat and hypoxia. The pathway was significantly enriched in the HIG2 groups of the Yesso and bay scallops, and the LOW3 and UNI groups of all the three scallop species, suggesting that the HIF-1 signaling pathway was triggered by extreme and acute environmental changes. Thus, the activation of the HIF-1 signaling pathway in scallops depends on the intensity of stress. A few GO functions related to the hypoxia response were also significantly enriched at increased temperatures, suggesting that the activation of the HIF-1 signaling pathway under acute heat stress was probably due to a sharp decrease in DO at high temperatures.

Comparative transcriptome analysis of the three scallop species in response to environmental stressors

Different numbers of DEGs in the three scallop species were induced by individual and combined stressors, which were associated with their susceptibility to environmental stress. This is perhaps the first study to simultaneously analyze the gene expression regulation induced by environmental stress in more than one bivalve species. In the present study, many more DEGs were observed in the Yesso scallop compared with the other two scallop species in response to both the individual and combined stressors. This suggested the higher sensitivity of the Yesso scallop to environmental changes (heat and hypoxia), followed by the Zhikong scallop, and then the bay scallop. Consistent with the DEGs numbers, more immune response and apoptosis-related GO functions and pathways were enriched in the Yesso scallop. This indicated that the Yesso scallop likely enhanced its gene expression related to the biological processes of immune response and apoptosis in response to environmental stresses. As a tropical species, the bay scallop has a higher thermal tolerance than the other two scallop species. Therefore, the environmental stresses used in this study were likely mild for the bay scallop, resulting in the least DEGs being induced. It is probable that fewer cytotoxic effects—such as DNA and proteins damages—were caused by the environmental stressors in the bay scallop: the DNA repair-related pathways and the protein processing in endoplasmic reticulum pathway were virtually unaffected this species following exposure to any environmental stressor but were down- or upregulated in the other two scallop species (Figure 8). As a result, fewer molecular pathways—such as immune response-related pathways—were induced in the bay scallop in response to environmental changes.

The extent of impacts of environmental stressors varies among taxa, depending on their physiological strategies, life stages, and motility, but also depending on the capacity of microevolutionary processes to increase the resistance of organisms (Vaquer-Sunyer and Duarte, 2011). Intriguingly, different dN/dS ratios, indicating different evolutionary ratio, were discovered among the three scallop species and were consistent with their sensitivity to environmental stress. The highest dN/dS ratio was for the Yesso scallop, followed by the Zhikong and then the bay scallops, This result indicated that scallops with higher environmental sensitivity may experience ongoing accelerated evolution to enable the species to better cope with the changing environment.

Bivalves are mostly weak-swimming or stationary filter-feeders. Many live in intertidal zones or shallow waters where there are wide fluctuations in environmental conditions. Thus, bivalves may have evolved mechanisms such as high genetic diversity and expansion of key stress response genes to adapt to diverse and highly variable environments (Guo et al., 2015). A growing body of evidence shows that environmental stress can affect genome stability in eukaryotes (Galhardo et al., 2007). For instance, hypoxia can suppress DNA repair pathways and cause an increase in mutagenesis in mammalian cells (Yuan et al., 2000; Mihaylova et al., 2003), and yeast regulates mutagenesis in response to environmental stress (Shor et al., 2013). In mollusks, downregulated genes involved in DNA replication and/or repair were detected in the king scallop and Pacific abalone under different environmental stresses (Artigaud et al., 2015; Shen et al., 2019). Consistently, pathways associated with DNA replication and repair were also suppressed in the Yesso and Zhikong scallops under severe hypoxia and combined stresses, which indicated that these individuals might experience increased mutation rates under different environmental stresses (Artigaud et al., 2015).

Evolutionary pressures of various kinds have often been hypothesized to cause active and rapid evolutionary changes, which occasionally generate fitter mutants and potentially accelerate adaptive evolution (Galhardo et al., 2007). Positive selection is a form of natural selection that influences the process by which new advantageous genetic variants sweep across populations (Wang et al., 2010). In Tibetan Schizothoracinae fish (*Gymnocypris przewalskii*), significant signals of positive selection were discovered on genes controlling innate immunity (Tong et al., 2017). In oysters, some members of expanded immune-related gene families diverged in function at different temperatures and salinities or assumed new roles in abiotic stress responses (Guo et al., 2015), and a positive selection pressure on immune-related genes has also been documented (Yu et al., 2011). In the present study, a total of 239 positively selected

genes were identified among four different scallop species, including those involved in immune system and environmental adaptation such as the *toll-like, toll-like receptor, c-type lectin, cytochrome c oxidase, and cytochrome P450 genes*. The selection of these genes represents an important adaptive mechanism in response to the long-term environmental changes. Further study is needed to investigate the molecular functions of these genes that are associated with environmental adaptation.

Conclusion

In the present study, a transcriptome analysis of the gill tissues of three scallop species—the Yesso, Zhikong, and bay scallops—was performed following short-term exposure to heat, hypoxia, and heat plus hypoxia. The molecular response mechanism of the scallops under environmental stress, especially under combined stress was explored. The DEGs under different types of stress were determined and important functional pathways in environmental stress were identified *via* GO and KEGG analyses. Comparative transcriptome analysis was performed and positively selected genes were identified, suggesting possible mechanisms of long-term environmental adaptation. The present study provides new insights into the molecular response mechanisms of scallops exposed to combined environmental stressors and improves our understanding of adaptive mechanisms in marine organisms in response to the changing global climate.

Materials and methods

Experimental design and scallop collection

Healthy Yesso, Zhikong, and bay scallops with an average shell size of 71.33 ± 0.72 mm, 63.07 ± 0.85 mm and 54.87 ± 1.13 mm, respectively, were obtained from culture populations in the Lvshun Sea area in Dalian, Liaoning Province. The scallops were then cultured under laboratory conditions in the Key Laboratory of Mariculture & Stock Enhancement in North China's Sea for one week, with filtered and aerated seawater at 15°C, and a twice-daily mixed algal diet of *Chlorella* sp. and *Spirulina platensis*. The individual scallop species were divided into the following groups: normal control (NOR) at a water temperature of 15°C and adequate DO (8 mg/L); heat stress at a water temperature of 22°C (HIG1) and 25°C (HIG2) under adequate DO (8 mg/L); hypoxia stress with decreased DO at 6 mg/L (LOW1), 4 mg/L (LOW2), and 2 mg/L (LOW3) at a water temperature of 15°C; and combined stress (UNI) at a water temperature of 25°C and low DO of 2 mg/L. Although the three types of scallops thrive at different temperature ranges, 15 °C is within the optimum temperature range of all the three scallop species and was selected as the control temperature. The temperatures of 22 °C and 25 °C were to indicate the tolerance of the Yesso scallop. The lowest DO of 2 mg/L would be stressful but not lethal for the scallops and has been used in previous studies on hypoxia stress in scallops (Chen et al., 2007; Stevens and Gobler, 2018). The three levels of DO were set as low (6 mg/L), moderate (4 mg/L), and high (2 mg/L) levels of hypoxia compared with the control group of 8 mg/L.

A total of 105 individuals of each species with similar size and good activity were divided into the above seven groups and cultured in 70 L tanks. There were three replicates for each group. For heat stress, the temperature was controlled by a thermostatic heating rod (RS Electrical®, China). For hypoxia stress, the scallops were cultured in closed tanks in which the DO was controlled by pumping nitrogen or air into the seawater with adjustment of the nitrogen flow to maintain the DO level (Sun et al., 2020; Nie et al., 2020). The temperature and DO levels were constantly monitored with a thermometer and O_2 sensing probe (YSI ProPlus, USA), respectively, and adjusted whenever necessary. All the scallops from each group were exposed to stress for 36 h. Due to the use of short-term stress treatments in the present study, to avoid the effects of feeding on the culture environment and physiology of the scallops, the scallops were not fed during the experiment. Following treatment, the gill tissues of scallops from each group were sampled, immediately frozen in liquid nitrogen, and stored at -80°C. Three individuals from different tanks of each group (three biological replicates) were selected for transcriptome sequencing. The experimental design is presented in Figure 9. No specific permits were needed for the described field studies. All the Yesso, Zhikong, and bay scallops utilized in this study were cultured marine species that are commercially available and are not endangered or protected species. All experiments were conducted in accordance with the regulations of the local and central governments.

RNA extraction, library construction and sequencing

The total RNA of each sample was isolated with the RNAprep pure tissue kit (Tiangen, China) according to the manufacturer's protocol. The quantity and quality of total RNA were determined using an NV3000 micro-spectrophotometer (Vastech, US), and the integrity was determined by agarose gel electrophoresis. The mRNA was purified from total RNA using oligo(dT) magnetic beads. The RNA-seq libraries were constructed using the TruSeq Stranded mRNA LTSample Prep Kit (Illumina, San Diego, CA, USA) following the manufacturer's instructions. The quality of the libraries was evaluated using the Agilent 2100 Bioanalyzer (Agilent Technologies, Santa Clara, CA, USA). Finally, a total of 63 libraries were subjected to 150 bp paired-end sequencing on the Illumina Hiseq X TEN sequencing platform.

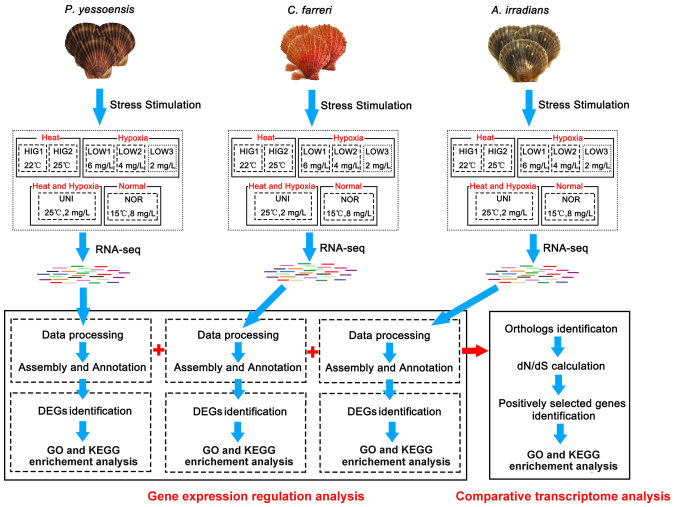

FIGURE 9
Experimental design.

Data processing, *de novo* assembly and annotation

Raw sequencing data were processed utilizing Trimmomatic (Bolger et al., 2014) to remove reads containing poly-N and low-quality reads. The high-quality clean reads of each scallop species were combined and used for *de novo* transcriptome assembly using the Trinity software (version: 2.4) (Grabherr et al., 2011) with the paired-end method and a kmer size of 32. The longest transcript was selected as the unigene based on the similarity and length of a sequence for subsequent analysis. The functions of the unigenes in each scallop species were separately annotated by aligning the unigene sequences to the NCBI non-redundant protein (Nr) database, Swiss-Prot database, Gene Ontology (GO) database, Eukaryotic Orthologous Groups (KOG) protein database and Kyoto Encyclopedia of Genes and Genomes (KEGG) pathway database (Kanehisa et al., 2007) using BLASTX with an E-value of 10^{-5}.

Analysis of differentially expressed genes

The expression of unigenes was determined by mapping the reads from each sample to the assembled references using Bowtie 2 (Langmead and Salzberg, 2012) and the fragments per kilobase per million mapped reads (FPKM) method, which eliminated the effects of gene length and sequencing depth on the calculation of gene expression. Differentially expressed genes (DEGs) in stressed and normal groups were identified by DESeq (Anders and Huber, 2012). The negative binomial distribution hypothesis was tested to determine the significance of differential expression. A fold change > 2 or < 0.5 and unadjusted p-value < 0.05 was set as the threshold for statistically significant differential expression. GO and KEGG enrichment analysis of DEGs were carried out using the clusterProfiler package in R (Yu et al., 2012) based on the hypergeometric distribution test. GO functions or pathways with q-values (calibrated p-values *via* the Benjamini-Hochberg method) < 0.05 and gene numbers ≥ 3 were considered to be enriched.

Comparative transcriptome analysis

The transcripts of the three scallop species and the king scallop (Kenny et al., 2020) were subjected to comparative transcriptome analysis. The transcript coding region sequences (CDS) were predicted by ESTScan software (Iseli et al., 1999). The CDS were then translated into amino acid sequences *via* standard genetic coding. The orthologous gene clusters were constructed with the CDS sequences of four scallop species using OrthoMCL software (Li et al., 2003) with BLASTP (E-value < 10^{-10}). Single-copy genes with clear one-to-one orthologs between species were used for subsequent analysis. The putative orthologous pairs were then aligned using MUSCLE software (Edgar, 2004) with the default parameters. The polygenetic tree of the four scallops was constructed using RAxML software (Stamatakis, 2014) using the maximum likelihood (ML) method. The dN, dS, and dN/dS values of the orthologs were calculated using the CodeML program of the PAML package (Yang, 2007). The positively selected genes were identified using the branch-site model of PAML with the threshold p-value < 0.05. GO and KEGG enrichment analyses were performed to determine the function of these positively selected genes using the method described in the previous section.

Data availability statement

The datasets presented in this study can be found in online repositories. The names of the repository/repositories and accession number(s) can be found below: https://www.ncbi.nlm.nih.gov/, PRJNA786240.

Ethics statement

Ethical review and approval was not required for the animal study because no specific permits were needed for the described field studies. All the Yesso, Zhikong and bay scallops utilized in this study were cultured marine species available commercially, and were not part of an endangered or protected species. All experiments were conducted in accordance with the regulations of the local and central government.

Author contributions

JD and YC conceived and designed the experiments. XH, XJ, WG, JX, YW, DY, and JS prepared the samples. XH, HS, XJ, WG, and JX performed the experiments. JM, XH, XW, ZH, and YT analyzed the data. JM wrote the paper. JD, ZH, and YC reviewed and revised the paper. and JM, JD, and YC acquired the funding. All authors contributed to manuscript revision, read, and approved the submitted version.

Funding

This project was supported by the Science and Technology Foundation of Dalian (2021JB11SN035), the University Innovation Team and Innovation Talent Support Plan of Liaoning Province (LT2019003), Dalian High-level Talent Innovation Support Program (2019RQ143), Scientific Research Fund of Liaoning Provincial Department of Education (LJKZ0705), and the National Natural Science Foundation of China (31702342).

Conflict of interest

The authors declare that the research was conducted in the absence of any commercial or financial relationships that could be construed as a potential conflict of interest.

Publisher's note

All claims expressed in this article are solely those of the authors and do not necessarily represent those of their affiliated organizations, or those of the publisher, the editors and the reviewers. Any product that may be evaluated in this article, or claim that may be made by its manufacturer, is not guaranteed or endorsed by the publisher.

Supplementary material

The Supplementary Material for this article can be found online at: https://www.frontiersin.org/articles/10.3389/fmars.2022.971796/full#supplementary-material

References

Ameisen, J. C. (2002). On the origin, evolution, and nature of programmed cell death: a timeline of four billion years. *Cell Death Differentiation* 9 (4), 367–393. doi: 10.1038/sj.cdd.4400950

Anders, S., and Huber, W. (2012). *Differential expression of RNA-seq data at the gene level-the DESeq package* Vol. 10 (Heidelberg, Germany: European Molecular Biology Laboratory (EMBL), f1000research.

Artigaud, S., Lacroix, C., Pichereau, V., and Flye-Sainte-Marie, J.. (2014). Respiratory response to combined heat and hypoxia in the marine bivalves *Pecten maximus* and *Mytilus* spp. *Comp. Biochem. Physiol. Part A: Mol. Integr. Physiol.* 175, 135–140. doi: 10.1016/j.cbpa.2014.06.005

Artigaud, S., Richard, J., Thorne, M. A. S., Lavaud, R., Flye-Sainte-Marie, J., Jean, F., et al. (2015). Deciphering the molecular adaptation of the king scallop (*Pecten maximus*) to heat stress using transcriptomics and proteomics. *BMC Genomics* 16, 1–14. doi: 10.1186/s12864-015-2132-x

Blaser, H., Dostert, C., Mak, T. W., and Brenner, D.. (2016). TNF and ROS crosstalk in inflammation. *Trends Cell Biol.* 26 (4), 249–261. doi: 10.1016/j.tcb.2015.12.002

Bolger, A. M., Lohse, M., and Usadel, B. (2014). Trimmomatic: a flexible trimmer for illumina sequence data. *Bioinformatics* 30 (15), 2114–2120. doi: 10.1093/bioinformatics/btu170

Brand, A. R. (2016). "Scallop ecology: distributions and behaviour," in *Scallops: biology, ecology and aquaculture*. Eds. S. Shumway and G. J. Parsons (Amsterdam, Netherlands:Elsevier), pp:469–pp:533.

Breitburg, D. (2002). Effects of hypoxia, and the balance between hypoxia and enrichment, on coastal fishes and fisheries. *Estuaries* 25, 767–781. doi: 10.1007/BF02804904

Carroll, J., Gobler, C. J., and Peterson, B. J. (2008). Resource-restricted growth of eelgrass in new York estuaries: light limitation, and alleviation of nutrient stress by hard clams. *Mar. Ecol. Prog. Ser.* 369, 51–62. doi: 10.3354/meps07593

Cerrato, R. M., Caron, D. A., Lonsdale, D. J., Rose, J. M., and Schaffner, R. A.. (2004). Effect of the northern quahog *Mercenaria mercenaria* on the development of blooms of the brown tide alga aureococcus anophagefferens. *Mar. Ecol. Prog. Ser.* 281, 93–108. doi: 10.3354/meps281093

Chen, D., and Jin, C. (2019). Histone variants in environmental-stress-induced DNA damage repair. *Mutat. Res.* 780, 55–60. doi: 10.1016/j.mrrev.2017.11.002

Chen, J., Mai, K., Ma, H., Wang, X., Deng, D., Liu, X., et al. (2007). Effects of dissolved oxygen on survival and immune responses of scallop (*Chlamys farreri* Jones et Preston). *Fish Shellfish Immunol.* 22 (3), 272–281. doi: 10.1016/j.fsi.2006.06.003

Chen, M., Yang, H., Delaporte, M., Zhao, S., and Xing, K.. (2007). Immune responses of the scallop *Chlamys farreri* after air exposure to different temperatures. *J. Exp. Mar. Biol. Ecol.* 345 (1), 52–60. doi: 10.1016/j.jembe.2007.01.007

Clarke, H. (1965). The scallop superspecies *Aequipecten irradians* (Lamarck). *Malacologia* 2, 161–188.

Crain, C. M., Kroeker, K., and Halpern, B. S. (2008). Interactive and cumulative effects of multiple human stressors in marine systems. *Ecol. Lett.* 11 (12), 1304–1315. doi: 10.1111/j.1461-0248.2008.01253.x

de Almeida, E. A., Bainy, A. C. D., de Melo Loureiro, A. P., Martinez, G. R., Miyamoto, S., Onuki, J., et al. (2007). Oxidative stress in *Perna perna* and other bivalves as indicators of environmental stress in the Brazilian marine environment: antioxidants, lipid peroxidation and DNA damage. *Comp. Biochem. Physiol. Part A: Mol. Integr. Physiol.* 146 (4), 588–600. doi: 10.1016/j.cbpa.2006.02.040

Delaney, M. A., and Klesius, P. H. (2004). Hypoxic conditions induce Hsp70 production in blood, brain and head kidney of juvenile Nile tilapia *Oreochromis niloticus* (L.). *Aquaculture* 236 (1-4), 633–644. doi: 10.1016/j.aquaculture.2004.02.025

Doney, S. C., Ruckelshaus, M., Emmett Duffy, J., Barry, J. P., Chan, F., English, C. A., et al. (2012). Climate change impacts on marine ecosystems. *Annu. Rev. Mar. Sci.* 4, 11–37. doi: 10.1146/annurev-marine-041911-111611

Edgar, R. C. (2004). MUSCLE: multiple sequence alignment with high accuracy and high throughput. *Nucleic Acids Res.* 32 (5), 1792–1797. doi: 10.1093/nar/gkh340

Ellgaard, L., Molinari, M., and Helenius, A. (1999). Setting the standards: quality control in the secretory pathway. *Science* 286 (5446), 1882–1888. doi: 10.1126/science.286.5446.1882

Erguler, K., Pieri, M., and Deltas, C. (2013). A mathematical model of the unfolded protein stress response reveals the decision mechanism for recovery, adaptation and apoptosis. *BMC Syst. Biol.* 7 (1), 1–18. doi: 10.1186/1752-0509-7-16

Franco, R., Sánchez-Olea, R., Reyes-Reyes, E. M., and Panayiotidis, M. I.. (2009). Environmental toxicity, oxidative stress and apoptosis: Ménage à trois. *Mutation* 674 (1-2), 3–22. doi: 10.1016/j.mrgentox.2008.11.012

Frydman, J. (2001). Folding of newly translated proteins *in vivo*: the role of molecular chaperones. *Annu. Rev. Biochem.* 70 (1), 603–647. doi: 10.1146/annurev.biochem.70.1.603

Galhardo, R. S., Hastings, P. J., and Rosenberg, S. M. (2007). Mutation as a stress response and the regulation of evolvability. *Crit. Rev. Biochem. Mol. Biol.* 42 (5), 399–435. doi: 10.1080/10409230701648502

Gobler, C. J., DePasquale, E. L., Griffith, A. W., and Baumann, H.. (2014). Hypoxia and acidification have additive and synergistic negative effects on the growth, survival, and metamorphosis of early life stage bivalves. *PLoS One* 9 (1), e83648. doi: 10.1371/journal.pone.0083648

Gobler, C. J., Lonsdale, D. J., and Boyer, G. L. (2005). A review of the causes, effects, and potential management of harmful brown tide blooms caused by *Aureococcus anophagefferens* (Hargraves et sieburth). *Estuaries* 28, 726–749. doi: 10.1007/BF02732911

Grabherr, M. G., Haas, B. J., Yassour, M., Levin, J. Z., Thompson, D. A., Amit, I., et al. (2011). Trinity: reconstructing a full-length transcriptome without a genome from RNA-seq data. *Nat. Biotechnol.* 29 (7), 644. doi: 10.1038/nbt.1883

Guo, X., He, Y., Zhang, L., Lelong, C., and Jouaux, A.. (2015). Immune and stress responses in oysters with insights on adaptation. *Fish shellfish Immunol.* 46 (1), 107–119. doi: 10.1016/j.fsi.2015.05.018

Guo, X., and Luo, Y. (2016). "Scallops and scallop aquaculture in China," in . *scallops: biology, ecology and aquaculture*. Eds. S. Shumway and G. J. Parsons (Amsterdam, Netherlands:Elsevier), pp: 937–952.

Gurr, S. J., Dwyer, I. P., Goleski, J., Lima, F. P., Seabra, R., and Gobler, C. J.. (2021). Acclimatization in the bay scallop *Argopecten irradians* along a eutrophication gradient: insights from heartbeat rate measurements during a simulated hypoxic event. *Mar. Freshw. Behav. Physiol.* 54, 23–49. doi: 10.1080/10236244.2020.1867477

Halliwell, B., and Cross, C. E. (1994). Oxygen-derived species: their relation to human disease and environmental stress. *Environ. Health Perspect.* 102 (suppl 10), 5–12. doi: 10.1289/ehp.94102s105

Hampton, R. Y. (2002). ER-associated degradation in protein quality control and cellular regulation. *Curr. Opin. Cell Biol.* 14 (4), 476–482. doi: 10.1016/S0955-0674(02)00358-7

Hetz, C. (2012). The unfolded protein response: controlling cell fate decisions under ER stress and beyond. *Nat. Rev. Mol. Cell Biol.* 13 (2), 89–102. doi: 10.1038/nrm3270

Hoegh-Guldberg, O., and Bruno, J. F. (2010). The impact of climate change on the world's marine ecosystems. *Science* 328 (5985), 1523–1528. doi: 10.1126/science.1189930

Hu, Z., Feng, J., Song, H., Zhou, C., Yu, Z., Yang, M., et al. (2022). Mechanisms of heat and hypoxia defense in hard clam: Insights from transcriptome analysis. *Aquaculture* 549, 737792. doi: 10.1016/j.aquaculture.2021.737792

Huo, D., Sun, L., Zhang, L., Ru, X., Liu, S., Yang, X., et al. (2019). Global-warming-caused changes of temperature and oxygen alter the proteomic profile of sea cucumber *Apostichopus japonicus*. *J. Proteomics* 193, 27–43. doi: 10.1016/j.jprot.2018.12.020

Iseli, C., Jongeneel, C. V., and Bucher, P. (1999). ESTScan: a program for detecting, evaluating, and reconstructing potential coding regions in EST sequences. *ISMB.* 99, 138–148.

Jacobson, M. D., Weil, M., and Raff, M. C. (1997). Programmed cell death in animal development. *Cell* 88 (3), 347–354. doi: 10.1016/S0092-8674(00)81873-5

Kanehisa, M., Araki, M., Goto, S., Hattori, M., Hirakawa, M., Itoh, M., et al. (2007). KEGG for linking genomes to life and the environment. *Nucleic Acids Res.* 36 (suppl_1), D480–D484. doi: 10.1093/nar/gkm882

Kawabe, S., and Yokoyama, Y. (2012). Role of hypoxia-inducible factor α in response to hypoxia and heat shock in the pacific oyster *Crassostrea gigas*. *Mar. Biotechnol.* 14 (1), 106–119. doi: 10.1007/s10126-011-9394-3

Keeling, R. F., Körtzinger, A., and Gruber, N. (2010). Ocean deoxygenation in a warming world. *Annu. Rev. Mar. Sci.* 2, 199–229. doi: 10.1146/annurev.marine.010908.163855

Kemp, W. M., Testa, J. M., Conley, D. J., Gilbert, D., and Hagy, J. D.. (2009). Temporal responses of coastal hypoxia to nutrient loading and physical controls. *Biogeosciences* 6 (12), 2985–3008. doi: 10.5194/bg-6-2985-2009

Kenny, N. J., McCarthy, S. A., Dudchenko, O., James, K., Betteridge, E., Corton, C., et al. (2020). The gene-rich genome of the scallop *Pecten maximus*. *GigaScience* 9 (5), giaa037. doi: 10.1093/gigascience/giaa037

Kosaka, Y. (2016). "Scallop fisheries and aquaculture in Japan," in *scallops: biology, ecology and aquaculture*. Eds. S. Shumway and G. J. Parsons (Amsterdam, Netherlands:Elsevier), pp: 891–936.

Kotsyuba, E. P. (2017). Hypoxia-inducible factor 1α in the central nervous system of the scallop *Mizuhopecten yessoensis* jay, 1857 (Bivalvia: Pectinidae) during anoxia and elevated temperatures. *Russian J. Mar. Biol.* 43 (4), 293–301. doi: 10.1134/S1063074017040071

Kregel, K. C. (2002). Invited review: heat shock proteins: modifying factors in physiological stress responses and acquired thermotolerance. *J. Appl. Physiol.* 92 (5), 2177–2186. doi: 10.1152/japplphysiol.01267.2001

Langmead, B., and Salzberg, S. L. (2012). Fast gapped-read alignment with bowtie 2. *Nat. Methods* 9 (4), 357. doi: 10.1038/nmeth.1923

Levin, L. A., Ekau, W., Gooday, A. J., Jorissen, F., Middelburg, J. J., Naqvi, S. W.A., et al. (2009). Effects of natural and human-induced hypoxia on coastal benthos. *Biogeosciences* 6 (10), 2063–2098. doi: 10.5194/bg-6-2063-2009

Li, L., Stoeckert, C. J., and Roos, D. S. (2003). OrthoMCL: identification of ortholog groups for eukaryotic genomes. *Genome Res.* 13 (9), 2178–2189. doi: 10.1101/gr.1224503

Liu, Y., Li, L., Huang, B., Wang, W., and Zhang, G.. (2019). RNAi based transcriptome suggests genes potentially regulated by HSF1 in the pacific oyster *Crassostrea gigas* under thermal stress. *BMC Genomics* 20 (1), 1–15. doi: 10.1186/s12864-019-6003-8

Liu, P., Lu, Z., Liu, L., Li, R., Liang, Z., Shen, M., et al. (2019). NOD-like receptor signaling in inflammation-associated cancers: from functions to targeted therapies. *Phytomedicine* 64, 152925. doi: 10.1016/j.phymed.2019.152925

Li, Q., Zhang, F., Wang, M., Li, M., and Sun, S.. (2020). Effects of hypoxia on survival, behavior, and metabolism of Zhikong scallop *Chlamys farreri* Jones et Preston 1904. *J. Ocean. Limnol.* 38(2), 351–363. doi: 10.1007/s00343-019-9074-0.

Ma, Y., and Hendershot, L. M. (2004). ER chaperone functions during normal and stress conditions. *J. Chem. Neuroanat.* 28 (1-2), 51–65. doi: 10.1016/j.jchemneu.2003.08.007

Malagoli, D., Casarini, L., Sacchi, S., and Ottaviani, E.. (2007). Stress and immune response in the mussel mytilus galloprovincialis. *Fish Shellfish Immunol.* 23 (1), 171–177. doi: 10.1016/j.fsi.2006.10.004

Mattson, M. P., and Meffert, M. K. (2006). Roles for NF-κB in nerve cell survival, plasticity, and disease. *Cell Death Differentiation* 13 (5), 852–860. doi: 10.1038/sj.cdd.4401837

Mihaylova, V. T., Bindra, R. S., Yuan, J., Yuan, J., Campisi, D., Narayanan, L., Jensen, R., et al. (2003). Decreased expression of the DNA mismatch repair gene Mlh1 under hypoxic stress in mammalian cells. *Mol. Cell. Biol.* 23 (9), 3265–3273. doi: 10.1128/MCB.23.9.3265-3273.2003

Mohindra, V., Tripathi, R. K., Yadav, P., Singh, R. K., and Lal, K. K.. (2015). Hypoxia induced altered expression of heat shock protein genes (Hsc71, Hsp90α and Hsp10) in Indian catfish, *Clarias batrachus* (Linnaeus, 1758) under oxidative stress. *Mol. Biol. Rep.* 42 (7), 1197–1209. doi: 10.1007/s11033-015-3855-0

Nie, H., Jiang, K., Li, N., and Yan, X.. (2020). Transcriptomic analysis of *Ruditapes philippinarum* under aerial exposure and reimmersion reveals genes involved in stress response and recovery capacity of the Manila clam. *Aquaculture* 524, 735271. doi: 10.1016/j.aquaculture.2020.735271

Nie, H., Wang, H., Jiang, K., and Yan, X.. (2020). Transcriptome analysis reveals differential immune related genes expression in *Ruditapes philippinarum* under hypoxia stress: potential HIF and NF-κB crosstalk in immune responses in clam. *BMC Genomics* 21 (1), 1–16. doi: 10.1186/s12864-020-6734-6

Ning, J., Zou, D., Lu, X., Cao, W., Chen, M., Liu, B., et al. (2021). Transcriptomic analyses provide insights into the adaptive responses to heat stress in the ark shells,

Scapharca subcrenata. *Comp. Biochem. Physiol. Part D: Genomics Proteomics* 38, 100813. doi: 10.1016/j.cbd.2021.100813

Officer, C. B., Smayda, T. J., and Mann, R. (1982). Benthic filter feeding: a natural eutrophication control. *Mar. Ecol. Prog. Ser.* 9, 203–210. doi: 10.3354/meps009203

Parthasarathy, A., Srinivasan, S., Appleby, A. J., and Martin, C. R.. (1992). Temperature dependence of the electrode kinetics of oxygen reduction at the platinum/Nafion® interface-a microelectrode investigation. *J. Electrochemical Soc.* 139 (9), 2530. doi: 10.1149/1.2221258

Pauletto, M., Di Camillo, B., Miner, P., Huvet, A., Quillien, V., Milan, M., et al. (2018). Understanding the mechanisms involved in the high sensitivity of *Pecten maximus* larvae to aeration. *Aquaculture* 497, 189–199. doi: 10.1016/j.aquaculture.2018.07.059

Pörtner, H. O. (2010). Oxygen-and capacity-limitation of thermal tolerance: a matrix for integrating climate-related stressor effects in marine ecosystems. *J. Exp. Biol.* 213 (6), 881–893. doi: 10.1242/jeb.037523

Pörtner, H. O. (2012). Ntegrating climate-related stressor effects on marine organisms: unifying principles linking molecule to ecosystem-level changes. *Mar. Ecol. Prog. Ser.* 470, 273–290. doi: 10.3354/meps10123

Pörtner, H. O., and Farrell, A. P. (2008). Physiology and climate change. *Science*, 322(5902)690–692. doi: 10.1126/science.1163156

Pörtner, H. O., and Knust, R. (2007). Climate change affects marine fishes through the oxygen limitation of thermal tolerance. *science* 315 (5808), 95–97. doi: 10.1126/science.1135471

Roberts, R. J., Agius, C., Saliba, C., Bossier, P., and Sung, Y. Y.. (2010). Heat shock proteins (chaperones) in fish and shellfish and their potential role in relation to fish health: a review. *J. fish Dis.* 33 (10), 789–801. doi: 10.1111/j.1365-2761.2010.01183.x

Robinson, S. M. C., Parsons, G. J., Davidson, L. A., Shumway, S. E., and Blake, N. J.. (2016). "Scallop aquaculture and fisheries in Eastern north America," in *Scallops: biology, ecology and aquaculture*. Eds. S. Shumway and G. J. Parsons (Amsterdam, Netherlands:Elsevier), pp: 737–779.

Sørensen, J. G., Kristensen, T. N., and Loeschcke, V. (2003). The evolutionary and ecological role of heat shock proteins. *Ecol. Lett.* 6 (11), 1025–1037. doi: 10.1046/j.1461-0248.2003.00528.x

Semenza, G. L. (1999). Regulation of mammalian O2 homeostasis by hypoxia-inducible factor 1. *Annu. Rev. Cell Dev. Biol.* 15 (1), 551–578. doi: 10.1146/annurev.cellbio.15.1.551

Shaw, P. J., Lamkanfi, M., and Kanneganti, T. D. (2010). NOD-like receptor (NLR) signaling beyond the inflammasome. *Eur. J. Immunol.* 40 (3), 624–627. doi: 10.1002/eji.200940211

Shen, Y., Huang, Z., Liu, G., Ke, C., and You, W.. (2019). Hemolymph and transcriptome analysis to understand innate immune responses to hypoxia in pacific abalone. *Comp. Biochem. Physiol. Part D: Genomics Proteomics* 30, 102–112. doi: 10.1016/j.cbd.2019.02.001

Shor, E., Fox, C. A., and Broach, J. R. (2013). The yeast environmental stress response regulates mutagenesis induced by proteotoxic stress. *PLoS Genet.* 9 (8), e1003680. doi: 10.1371/journal.pgen.1003680

Shumway, S. E., and Castagna, M. (1994). Scallop fisheries, culture and enhancement in the united states. *Memoirs Queensland Museum* 36 (2), 283–298.

Silina, A. V. (2019). A yesso scallop population exposed to climate-induced and anthropogenic habitat changes in amur bay, Sea of Japan. *Oceanology* 59, 75–85. doi: 10.1134/S000143701901020X

Sokolova, I. M. (2009). Apoptosis in molluscan immune defense. *Invertebrate Survival J.* 6 (1), 49–58.

Stamatakis, A. (2014). RAxML version 8: a tool for phylogenetic analysis and post-analysis of large phylogenies. *Bioinformatics* 30 (9), 1312–1313. doi: 10.1093/bioinformatics/btu033

Stevens, A. M., and Gobler, C. J. (2018). Interactive effects of acidification, hypoxia, and thermal stress on growth, respiration, and survival of four north Atlantic bivalves. *Mar. Ecol. Prog. Ser.* 604, 143–161. doi: 10.3354/meps12725

Sun, X., Tu, K., Li, L., Wu, B., Wu, L., Liu, Z., et al. (2021). Integrated transcriptome and metabolome analysis reveals molecular responses of the clams to acute hypoxia. *Mar. Environ. Res.* 168, 105317. doi: 10.1016/j.marenvres.2021.105317

Sun, Y., Zhang, X., Wang, Y., Day, R., Yang, H., and Zhang, Z., et al. (2019). Immunity-related genes and signaling pathways under hypoxic stresses in *Haliotis diversicolor*: a transcriptome analysis. *Sci. Rep.* 9 (1), 1–15. doi: 10.1038/s41598-019-56150-2

Sun, J. L., Zhao, L. L., Liao, L., Tang, X., Cui, C., Liu, Q., et al. (2020). Interactive effect of thermal and hypoxia on largemouth bass (*Micropterus salmoides*) gill and liver: Aggravation of oxidative stress, inhibition of immunity and promotion of cell apoptosis. *Fish shellfish Immunol.* 98, 923–936. doi: 10.1016/j.fsi.2019.11.056

Tang, T., Li, W., Wang, X., Wu, Y., and Liu, F.. (2019). A house fly TNF ortholog eiger regulates immune defense *via* cooperating with toll and imd pathways. *Dev. Comp. Immunol.* 90, 21–28. doi: 10.1016/j.dci.2018.08.016

Tanji, T., and Ip, Y. T. (2005). Regulators of the toll and imd pathways in the drosophila innate immune response. *Trends Immunol.* 26 (4), 193–198. doi: 10.1016/j.it.2005.02.006

Tong, C., Fei, T., Zhang, C., and Zhao, K. (2017). Comprehensive transcriptomic analysis of Tibetan schizothoracinae fish *Gymnocypris przewalskii* reveals how it adapts to a high altitude aquatic life. *BMC evolutionary Biol.* 17 (1), 1–11. doi: 10.1186/s12862-017-0925-z

Truebano, M., Burns, G., Thorne, M. A. S., Hillyard, G., Peck, L. S., Skibinski, D. O.F., et al. (2010). Transcriptional response to heat stress in the Antarctic bivalve laternula elliptica. *J. Exp. Mar. Biol. Ecol.* 391, 65–72. doi: 10.1016/j.jembe.2010.06.011

Vaquer-Sunyer, R., and Duarte, C. M. (2008). Thresholds of hypoxia for marine biodiversity. *Proc. Natl. Acad. Sci.* 105 (40), 15452–15457. doi: 10.1073/pnas.0803833105

Vaquer-Sunyer, R., and Duarte, C. M. (2011). Temperature effects on oxygen thresholds for hypoxia in marine benthic organisms. *Global Change Biol.* 17 (5), 1788–1797. doi: 10.1111/j.1365-2486.2010.02343.x

Visick, J. E., and Clarke, S. (1995). Repair, refold, recycle: how bacteria can deal with spontaneous and environmental damage to proteins. *Mol. Microbiol.* 16 (5), 835–845. doi: 10.1111/j.1365-2958.1995.tb02311.x

Wajant, H., Pfizenmaier, K., and Scheurich, P. (2003). Tumor necrosis factor signaling. *Cell Death Differentiation* 10 (1), 45–65. doi: 10.1038/sj.cdd.4401189

Wall, C. C., Peterson, B. J., and Gobler, C. J. (2008). Facilitation of seagrass zostera marina productivity by suspension-feeding bivalves. *Mar. Ecol. Prog. Ser.* 357, 165–174. doi: 10.3354/meps07289

Wang, C., Liu, B., Li, J., Liu, S., Li, J., Hu, L., et al. (2011). Introduction of the Peruvian scallop and its hybridization with the bay scallop in China. *Aquaculture* 310 (3-4), 380–387. doi: 10.1016/j.aquaculture.2010.11.014

Wang, J. R., Wei, Y. M., Deng, M., Nevo, E., Yan, Z. H., and Zheng, Y. L.. (2010). The impact of single nucleotide polymorphism in monomeric alpha-amylase inhibitor genes from wild emmer wheat, primarily from Israel and golan. *BMC Evolutionary Biol.* 10 (1), 1–13. doi: 10.1186/1471-2148-10-170

Xiao, J., Ford, S. E., Yang, H., Zhang, G., Zhang, F., and Guo, X.. (2005). Studies on mass summer mortality of cultured zhikong scallops (*Chlamys farreri* Jones et Preston) in China. *Aquaculture* 250, 602–615. doi: 10.1016/j.aquaculture.2005.05.002

Yang, Z. (2007). PAML 4: phylogenetic analysis by maximum likelihood. *Mol. Biol. Evol.* 24 (8), 1586–1591. doi: 10.1093/molbev/msm088

Yang, C., Gao, Q., Wang, L., Zhou, Z., Gong, C., et al. (2017). The transcriptional response of the pacific oyster *Crassostrea gigas* against acute heat stress. *Fish Shellfish Immunol.* 68, 132–143. doi: 10.1016/j.fsi.2017.07.016

Yang, B., Gao, X., Zhao, J., Liu, Y., Xie, L., Lv, X., et al. (2021). Summer deoxygenation in a bay scallop (*Argopecten irradians*) farming area: The decisive role of water temperature, stratification and beyond. *Mar. pollut. Bull.* 173, 113092. doi: 10.1016/j.marpolbul.2021.113092

Yang, H. S., Zhang, T., Wang, J., Wang, P., He, Y., and Zhang, F.. (1999). Growth characteristics of *Chlamys farreri* and its relation with environmental factors in intensive raft-culture areas of sishiliwan bay, yantai. *J. Shellfish Res.* 18 (1), 71–83.

Yuan, J., Narayanan, L., Rockwell, S., and Glazer, P. M.. (2000). Diminished DNA repair and elevated mutagenesis in mammalian cells exposed to hypoxia and low pH. *Cancer Res.* 60 (16), 4372–4376.

Yu, H., He, Y., Wang, X., Zhang, Q., Bao, Z., and Guo, X.. (2011). Polymorphism in a serine protease inhibitor gene and its association with disease resistance in the eastern oyster (*Crassostrea virginica* gmelin). *Fish shellfish Immunol.* 30 (3), 757–762. doi: 10.1016/j.fsi.2010.12.015

Yu, G., Wang, L. G., Han, Y., and He, Q. Y.. (2012). clusterProfiler: an r package for comparing biological themes among gene clusters. *Omics: J. Integr. Biol.* 16 (5), 284–287. doi: 10.1089/omi.2011.0118

Zhang, X., Huang, Y., Cai, X., Zou, Z., Wang, G., Wang, S., et al. (2014). Identification and expression analysis of immune-related genes linked to Rel/NF-κB signaling pathway under stresses and bacterial challenge from the small abalone *Haliotis diversicolor*. *Fish shellfish Immunol.* 41 (2), 200–208. doi: 10.1016/j.fsi.2014.08.022

Zhang, X., Shi, J., Sun, Y., Habib, Y. J., Yang, H., Zhang, Z., et al. (2019). Integrative transcriptome analysis and discovery of genes involving in immune response of hypoxia/thermal challenges in the small abalone *Haliotis diversicolor*. *Fish Shellfish Immunol.* 84, 609–626. doi: 10.1016/j.fsi.2018.10.044

Zhang, G., Zhao, C., Wang, Q., Gu, Y., Li, Z., Tao, P., et al. (2017). Identification of HIF-1 signaling pathway in *Pelteobagrus vachelli* using RNA-seq: effects of acute hypoxia and reoxygenation on oxygen sensors, respiratory metabolism, and hematology indices. *J. Comp. Physiol. B* 187 (7), 931–943. doi: 10.1007/s00360-017-1083-8

Zhou, C., Song, H., Feng, J., Hu, Z., Yu, Z., Yang, M., et al. (2021). RNA-Seq analysis and WGCNA reveal dynamic molecular responses to air exposure in the hard clam *Mercenaria mercenaria*. *Genomics* 113 (4), 2847–2859. doi: 10.1016/j.ygeno.2021.06.025

frontiers | Frontiers in Marine Science

TYPE Original Research
PUBLISHED 03 October 2022
DOI 10.3389/fmars.2022.1024218

OPEN ACCESS

EDITED BY
Hongsheng Yang,
Chinese Academy of Sciences (CAS), China

REVIEWED BY
Changxu Tian,
Guangdong Ocean University, China
Qiao Liu,
Sichuan Agricultural University, China

*CORRESPONDENCE
Yun Li
yunli0116@ouc.edu.cn

†These authors have contributed equally to this work

SPECIALTY SECTION
This article was submitted to Global Change and the Future Ocean, a section of the journal Frontiers in Marine Science

RECEIVED 21 August 2022
ACCEPTED 20 September 2022
PUBLISHED 03 October 2022

CITATION
Ren Y, Tian Y, Mao X, Wen H, Qi X, Li J, Li J and Li Y (2022) Acute hypoxia changes the gene expression profiles and alternative splicing landscape in gills of spotted sea bass (*Lateolabrax maculatus*). *Front. Mar. Sci.* 9:1024218. doi: 10.3389/fmars.2022.1024218

Acute hypoxia changes the gene expression profiles and alternative splicing landscape in gills of spotted sea bass (*Lateolabrax maculatus*)

Yuhang Ren†, Yuan Tian†, Xuebin Mao, Haishen Wen, Xin Qi, Jinku Li, Jifang Li and Yun Li*

Key Laboratory of Mariculture, Ocean University of China, Ministry of Education, Qingdao, China

Hypoxia is one of the most important environmental stressors in aquatic ecosystems. To deal with the hypoxia environment, fishes exhibit a series of physiological and molecular responses to maintain homeostasis and organism functions. In the present study, hypoxia-induced changes in gene expression profiles and alternative splicing (AS) events in spotted sea bass (*Lateolabrax maculatus*), a promising marine-culture fish species in China, were thoroughly investigated by RNA-Seq analysis. A total of 1,242, 1,487 and 1,762 differentially expressed genes (DEGs) were identified at 3 h, 6 h and 12 h in gills after hypoxia stress. Functional enrichment analysis by KEGG and GSEA demonstrated that HIF signal network system was significantly activated and cell cycle process was remarkably suppressed in response to hypoxia. According to the temporal gene expression profiles, six clusters were generated and protein-protein interaction (PPI) networks were constructed for the two clusters that enriched with hypoxia-induced (cluster 2) or -suppressed genes (cluster 5), respectively. Results showed that HIF signaling related genes including *vegfa*, *igf1*, *edn1*, *cox2b*, *cxcr4b*, *ctnnb1*, and *slc2a1a*, were recognized as hubs in cluster 2, while *mcm2*, *chek1*, *pole*, *mcm5*, *pola1*, and *rfc4*, that tightly related to cell cycle, were down-regulated and considered as hubs in cluster 5. Furthermore, a total of 410 differential alternative splicing (DAS) genes were identified after hypoxia, which were closely associated with spliceosome. Of them, 63 DAS genes also showed differentially expressed levels after hypoxia, suggesting that their expression changes might be regulated by AS mechanism. This study revealed the key biological pathways and AS events affected by hypoxia, which would help us to better understand the molecular mechanisms of hypoxia response in spotted sea bass and other fish species.

KEYWORDS

RNA-Seq, hypoxia-inducible factor, cell cycle, alternative splicing, hypoxia

Introduction

Fish are frequently exposed to variations in oxygen levels due to the rapid fluctuations in patterns of oxygen production and consumption in aquatic environment (Nikinmaa and Rees, 2005). As one of the most important environmental stressors in aquatic ecosystems, hypoxia is usually defined as the dissolved oxygen (DO) levels of less than 2.0 mg/L, which is low enough to negatively influence the normal physiological conditions of fishes (Hrycik et al., 2017). If severe hypoxia persists, fish will eventually die and result in serious yield losses (Abdel-Tawwab et al., 2019). Hypoxia occurres with temperature, seasonal and compositional changes in water (Xiao, 2015). In aquaculture system, hypoxia can be accelerated by several factors such as high stocking density, water pollution, excessive nutrient enrichment and human activities (Ng and Chiu, 2020). To deal with the hypoxia environment, fishes exhibit a number of behavioral, morphological, physiological and molecular responses to maintain homeostasis and organism functions. For example, in order to get more oxygen, they try to breathe directly by emerging at the water surface (Xiao, 2015), or enlarge the respiratory surface area by remodeling their gills (Sollid et al., 2005). Some fishes make a rapid reorganization of cellular metabolism to suppress ATP and O_2 consumption (Richards, 2011), and increase the number of red blood cells to improve oxygen-carrying capacity (Claireaux et al., 1988). Moreover, hypoxia response is always correlated with the activation of anaerobic metabolism and the increase of anaerobic glycolysis, in order to meet the high energy demand during hypoxia (Abdel-Tawwab et al., 2019).

At the molecular level, several proteins and signaling pathways have been reported to involve in hypoxia response. Among them, hypoxia-inducible factor 1 (HIF-1) is recognized as master regulator of the cellular responses to hypoxia by promoting target genes transcription under hypoxia (Déry et al., 2005). HIF-1 is a heterodimeric DNA-binding complex consisting of an oxygen-labile α-subunit (HIF-1α) and a stably expressed β-subunit (HIF-1β). Under normoxia (normal oxygen condition), HIF-1α is hydroxylated by prolyl hydroxylase domain-containing enzymes (PHDs) whose activities are closely related with oxygen levels, and eventually degraded by proteasome. In contrast, when exposed to hypoxia conditions, HIF-1α is not hydroxylated because of the catalytic activity of PHD is inhibited by the lack of oxygen. Meantime, HIF-1 heterodimers rapidly accumulate and bind to hypoxia response elements (HREs) contained in the promoter or enhancer regions of the hypoxia-inducible genes (Bartoszewski et al., 2019). These HIF-1 target genes were demonstrated to involve in numbers of signaling pathways such as redox status (Semenza, 2001), AMPK (Bohensky et al., 2010), MAPK (Zhang et al., 2013), PI3K-Akt (Zhang et al., 2018), mTOR (Wei et al., 2019), and VEGF (Kajimura et al., 2006), which affect multiple aspects of the physiological responses including proliferation, apoptosis, and differentiation (Zhu et al., 2013). Moreover, it has recently become clear that HIF-1 pathway is not a linear cascade of signal transduction but a multi-level regulatory network representing a high degree of complexity (Bárdos and Ashcroft, 2005; Yee Koh et al., 2008; Zheng et al., 2008; Agani and Jiang, 2013; Fábián et al., 2016).

Investigation into the hypoxia responses of fish will not only help us to understand the strategies and mechanisms for environmental stress adaptation in fish, but will also guide us in improving fish hypoxia tolerance capabilities and preventing economic losses in aquaculture, and artificial breeding of hypoxia-tolerant fish strain/species in the future. In recent years, with the rapid development of high-throughput sequencing technology, RNA-Seq tool has been successfully used in studying the molecular responses to hypoxia in various fish species, and several known and novel hypoxia-related genes and pathways have been identified in different tissues. For examples, in large yellow croaker (*Larimichthys crocea*), genes involved in innate immunity, ion transport and glycolytic pathways were significantly differentially expressed in the gill and/or heart under hypoxia, indicating they may contribute to maintain cellular energy balance during hypoxia (Mu et al., 2020). In bighead carp (*Hypophthalmichthys nobilis*), the cardiac transcriptomic analysis identified that MAPK signaling pathway played a key role in cardiac tolerance after acute hypoxia treatment (Zhou et al., 2020). In the gill of Nile tilapia (*Oreochromis niloticus*), the hypoxia responsive genes were significantly enriched in energy and immune-related pathways including glycolysis, metabolic process and antigen processing and presentation (Li et al., 2017). For channel catfish (*Ictalurus punctatus*), RNA-Seq analysis with swimbladder samples revealed that many genes affected by hypoxia were enriched in the HIF, MAPK, PI3K/Akt/mTOR, VEGF and Ras signaling pathways (Yang et al., 2018). Moreover, liver transcriptomes under hypoxia have been widely studied in aquaculture fishes such as large yellow croaker (Ding et al., 2020), silver sillago (*Sillago sihama*) (Tian et al., 2020a), largemouth bass (*Micropterus salmoides*) (Sun et al., 2020), golden pompano (*Trachinotus blochii*) (Sun et al., 2021b), rainbow trout (*Oncorhynchus mykiss*) (Hou et al., 2020) and Nile tilapia (*Oreochromis niloticus*) (Ma et al., 2021).

Alternative splicing (AS) mechanism are widely existed in eukaryotes that could generate multiple transcripts and enables different proteins to be synthesized from one single gene (Nilsen and Graveley, 2010). This regulatory mechanism significantly expands transcript variability and proteome diversity, servicing as an enhancing ability to cope with biotic or abiotic stresses in eukaryotes, including fishes (Mastrangelo et al., 2012; Lee and Rio, 2015). It has been documented that there are changes in splicing patterns for a set of functional genes that play central roles in cold-acclimation responses in Atlantic killifish (*Fundulus heteroclitus*), threespine stickleback (*Gasterosteus*

aculeatus) and zebrafish (*Danio rerio*) (Healy and Schulte, 2019). AS events of several RNA-binding proteins are significantly induced by different salinity environments in turbot (*Scophthalmus maximus*), tongue sole (*Cynoglossus semilaevis*) and steelhead trout (*Oncorhynchus mykiss*), which may affect the splicing decisions of many downstream target genes in response to osmoregulation (Tian et al., 2022). However, the AS events related to hypoxia adaptation are only reported in Nile tilapia until now. A total of 103 genes undergo differential usage of exons and splice junction events after acute hypoxia stress in the heart of Nile tilapia, the biological function of which are tightly associated with structural constituent of ribosome, structural molecule activity and ribosomal protein (Xia et al., 2017).

Spotted sea bass (*Lateolabrax maculatus*), also known as Chinese sea bass, is a euryhaline and eurythermic fish species which broadly distributed along the coasts of China and Indo-China Peninsula (Chen et al., 2019). Because of its fast growth, high nutritive value and pleasant taste, the industry of spotted sea bass is considered as one of the leading aquaculture marine fish in China (Wen et al., 2016; Liu et al., 2020), with the production capacity of 195,000 tons last year (Yearbook, 2021). However, spotted sea bass is threatened by hypoxia in natural watersheds resulted from ongoing global warming and environmental pollution, as well as in cultured conditions due to the sustained high temperature in summer and high-density farming (Dong et al., 2020). To date, studies about hypoxia responses of spotted sea bass remains largely unknown. The fish gill is the dominant organ responsible for physiological exchanges with the surrounding environment, playing a primary role in gas exchange and is the first target under hypoxia (Evans et al., 2005), but the underlying molecular basis has not been explored in spotted sea bass. Therefore, in this study, hypoxia-induced changes in gene expression profiles and AS events in gills were investigated by RNA-Seq analysis in spotted sea bass. Our results revealed the key biological pathways and AS events affected by hypoxia, and candidate regulatory hub genes involving in hypoxia response, which will provide new insights into the elucidation of the responses and adaption mechanism to environmental stress in fish.

Materials and methods

Ethics statement

This study was carried out in accordance with the rules and approval of the respective Animal Research and Ethics Committees of Ocean University of China (Permit Number: 20141201), and was not involved in any endangered or protected species.

Fish maintenance and hypoxia exposure

A total of 60 healthy spotted sea bass (body length: 48.76 ± 4.26 cm, body weight: 178.25 ± 18.56 g) were obtained from Shuangying Aquatic Seeding Co., Ltd. (Lijin, Shandong, China). Before hypoxia experiment, the individuals were acclimated in the square tank (5 m × 5 m × 1 m, L × W × H) for two weeks. All the water was obtained from the natural sea area in Bohai, China (38.04°N, 118.58°E), followed by plain sedimentation, sand filtration and UV sterilization. During the periods of acclimation, the water quality conditions were kept relatively constant and suitable for the culture of spotted sea bass, including temperature (17.0 ± 1.0°C), dissolved oxygen saturation (7.0 ± 0.5 mg/L), salinity (27 - 30) and pH (6.5 - 7.5).

After acclimation, fish individuals were transferred to three tanks (0.5 m × 0.5 m × 1 m, L × W × H) for hypoxia challenge experiment and the density was set as 20 individuals per tank. The oxygen level in each tank was quickly reduced to 1.1 ± 0.14 mg/L within ~ 1h by bubbling nitrogen gas. Then, the hypoxia experiment started and lasted for 12 h. During the periods of experiment, dissolved oxygen levels were maintained relatively constant by pumping the mixture of air and nitrogen gas and continuously monitored using YSI DO200 oxygen meter (YSI EcoSense, OH, USA) every ten minutes. 3 individuals per tank (a total of 9 individuals for each time point) were anesthetized and euthanized with MS-222, and collected for gill tissues at 0 h (before hypoxia experiment), 3 h, 6 h and 12 h after hypoxia (named as T0, T3, T6 and T12 groups, respectively). Then gill tissues were quickly frozen in liquid nitrogen until RNA extraction.

RNA extraction, library construction and Illumina sequencing

Total RNA of gill tissues was extracted using TRIzol reagents (Invitrogen, USA). The concentration of total RNA was determined by NanoDrop 2000 (Thermo Scientific, Waltham, MA), and RNA integrity was checked by the Agilent 2100 Bioanalyzer (Agilent Technologies, USA). Equal quantity of high-quality RNA from the 3 individuals each tank was pooled as one sample, and 3 replicated samples were generated for each time point to minimize the individual differences. A total of 12 sequencing libraries (3 replicated samples × 4 time points), named T0 (T0-1, T0-2, T0-3), T3 (T3-1, T3-2, T3-3), T6 (T6-1, T6-2, T6-3), and T12 (T12-1, T12-2, T12-3), were generated using NEBNext® Ultra™ RNA Library Prep Kit for Illumina® (NEB, USA), respectively. Sequencing was conducted on the Illumina Novaseq platform, generating 150 bp paired-end reads.

Identification of differential expressed genes

Raw reads were treated to discard adapter sequences and ambiguous nucleotides using fastp v0.20.1 software to generate the clean reads. The reference genome file of spotted sea bass (Assembly ID: GCA_004028665.1) was used for the following bioinformatics analysis. Index of the reference genome was built using "hisat2-build" function of Hisat2 v2.1.0 software (Kim et al., 2015) and paired-end clean reads were mapped to the reference genome using Hisat2 with the default parameters. The count matrixes were constructed using featureCounts software from Subread v1.6.4 program, which were then transformed into fragments per kilobase of transcript per million fragments mapped (FPKM) for the normalization of gene expression levels. DEGs among the three comparisons (T3 vs. T0, T6 vs. T0 and T12 vs. T0) were calculated using the scripts run_DE_analysis.pl in Trinity program (Grabherr et al., 2011), and the calculation method was performed using the DESeq2 package. The threshold of DEGs were set as false discovery rate (FDR)-$p < 0.05$ and $|\log_2 (\text{fold change})| \geq 1$. Expression cluster analysis of time-series data was performed based on fuzzy c-means using Mfuzz v2.48.0 R package (Kumar and Futschik, 2007) and the number of centers was set as 6.

Functional enrichment analysis

Kyoto Encyclopedia of Genes and Genomes (KEGG) enrichment analysis of DEGs were implemented using clusterProfiler v4.2.2 R package (Yu et al., 2012) and FDR-$p <$ 0.05 was considered as statistically significant. Additionally, Gene Set Enrichment Analysis (GSEA) (Subramanian et al., 2005) was performed to interpret expression matrix from RNA-Seq data. The FPKMs of all genes in gill transcriptome were used for the calculation of normalized enrichment score (NES) in GSEA. |NES|>1, FDR-$p < 0.25$ and Nominal (NOM) p-value < 0.05 were regarded as the significant threshold.

Protein-protein interaction network construction and hub gene identification

The PPI network was constructed *via* STRING v11.5 (Szklarczyk et al., 2016). Minimum required interaction score was settled as 0.4. The predicted network was analyzed and visualized by Cytoscape v3.8.0 software. The highly connected protein nodes were determined by Cyto-Hubba v0.1, a plug-in of Cytoscape software. Significant modules in PPI network were identified by MCODE (Bader and Hogue, 2003) v1.6.1 of Cytoscape, which meet the following parameters: MCODE score ≥ 5, degree cut-off = 2, node score cut-off = 0.2, max depth = 100, and k-score = 2.

Identification of differential alternative splicing events

rMATS v4.0.1 (Shen et al., 2014) was utilized to determine DAS events by computing the inclusion level from two-group RNA-Seq data with replicates. Five classical types of DAS events were identified including exon skipping (ES), intron retention (IR), alternative 3' splice sites (A3SS), alternative 5' splice sites (A5SS), and mutually exclusive exon (ME). In details, rMATS applied a hierarchical framework to simultaneously model the variability among replicates, and estimated uncertainty of inclusion and exclusion isoform proportions in individual replicates. Mature mRNAs including or excluding additional sequences were regarded as inclusion or exclusion isoforms, respectively (Ding et al., 2017). A likelihood-ratio test was used to calculate the p-value and FDR-p of the inclusion levels between two sets of RNA-Seq datasets. FDR-$p < 0.05$ was set as the threshold for significant DAS events. DAS genes were determined and their KEGG functional enrichment analysis was performed by the same procedures as for DEGs.

Validation experiments by quantitative real-time PCR and RT-PCR

To validate the gene expression results of DEGs generated from RNA-Seq analysis, qPCR was performed to detect the relative expression levels of several DEGs among different pairwise comparisons. In details, total RNA of gills collected from hypoxia experiment was reverse-transcribed to cDNA using PrimeScript RT reagent kit (Takara, Shiga, Japan) following the manufacturer's instructions. 10 × diluted cDNA (~100ng/μl) was served as the template for PCR amplification, which was conducted using FastPfu reagent kit (TransGen, Beijing, China). The gene specific primers used in qPCR were designed using Primer 5 software and listed in Supplementary Table 1. qPCR was performed on the StepOne Plus Real-Time PCR system (Applied Biosystems, CA, USA) using the SYBR Premix Ex Taq^{TM} Kit (Takara, Shiga, Japan). qPCR reaction system consisted of 2 μl of cDNA, 10 μl SYBR premix Ex Taq, 0.4 μl forward primers, 0.4 μl reverse primers, 0.4 μl ROX reference dye, and 6.8 μl ddH_2O in a final volume of 20 μl, which was repeated in triplicate and was run in accordance with the following procedure: 95°C for 30 s, then 40 cycles of 95°C for 10 s and 55°C for 30 s, and finally 72°C for 30 s. The 18S ribosomal RNA was considered as the internal reference gene (Strepparava et al., 2014). The expression levels were calculated using the $2^{-\Delta\Delta Ct}$ method.

The cDNA samples were subsequently used as templates for following RT-PCR experiment, which was performed to validate the identified DAS events. Transcript-specific primers were designed to span the predicted splicing events using Primer 5 software and Primer-BLAST (https://www.ncbi.nlm.nih.gov/tools/primer-blast/) (Supplementary Table 1). PCR condition was set as follows: 94°C for 5 min, following by 35 cycles of 94°C for 30 s, melting temperature for 30 s, 72°C for a time period that depends on the product sizes, and finally extended at 72°C for 10 min. PCR products were monitored on 1% agarose gel stained by GelStain (TransGen, Beijing, China).

Statistical analysis

In the present study, all the data are shown as the mean ± standard deviation (SD). Correlation coefficient between the results of DEGs in RNA-Seq and qPCR were determined by SPSS 22.0 software (SPSS Inc., Chicago, USA). One-way ANOVA was conducted followed by Duncan's multiple tests to identify significance differences when $P < 0.05$.

Results

Overview of high-throughput sequencing data

In the present study, RNA-Seq analysis was performed on the gill tissues of spotted sea bass at 0 h, 3 h, 6 h and 12 h after hypoxia. As a result, a total of 655,653,966 raw reads were generated respectively, on average, 99.12% of which were considered as clean reads after quality control. Then, all clean reads were aligned to the reference genome of spotted sea bass with mapping ratio ranging from 83.14% to 92.50%, and the unique mapping ratios were different between 80.91% and 89.91% (Supplementary Table 2).

The expression profiles of DEGs

As results showed, the total number of DEGs increased as the hypoxia-treating time was prolonged (Figure 1). In details, a total of 1,242, 1,487 and 1,762 DEGs were identified through the comparisons of T3 vs. T0, T6 vs. T0 and T12 vs. T0, respectively. In those comparison groups, 914 DEGs were significantly up-regulated and 328 DEGs were down-regulated in T3 vs. T0 group (Figure 1A), and 853 up-regulated DEGs and 634 down-regulated DEGs were identified in T6 vs. T0 group (Figure 1B), as well as 1,254 up-regulated and 508 down-regulated DEGs were discovered in T12 vs. T0 group (Figure 1C). The number of DEGs were greatly increased with the prolongation of hypoxia stress from 3 h to 12 h. Notably, 607 DEGs were shared among all three comparison groups, and 181 (overlapped between T3 vs. T0 and T6 vs. T0), 205 (overlapped between T6 vs. T0 and T3 vs. T0), and 247 (overlapped between T6 vs. T0 and T12 vs. T0) DEGs were coexisted in two comparison groups, respectively. Meantime, 249 (T3 vs. T0), 452 (T6 vs. T0) and 703 (T12 vs. T0) DEGs was only appeared in unique comparison group (Supplementary Figure 1).

To confirm the accuracy of our bioinformatic analysis results for gene expression pattern of RNA-Seq data, the expression levels of 10 randomly selected genes were detected by qPCR experiment at 0 h, 3 h, 6 h and 12 h after hypoxia, including *hif-1α*, *L-lactate dehydrogenase A chain* (*ldha*), *hexokinase-1* (*hk1*), *glyceraldehyde-3-phosphate dehydrogenase* (*gapdh*), *pyruvate kinase M1/2* (*pkm*), *aldolase, fructose-bisphosphate A* (*aldoa*), *insulin like growth factor binding protein 1* (*igfbp1*), *insulin like growth factor binding protein 4* (*igfbp4*), *ephrin A2* (*epha2*) and *transforming growth factor beta 3* (*tgfβ–3*). As shown in Supplementary Figure 2, expression patterns determined by qPCR were consistent with the results of RNA-Seq analysis with the $R^2 =$ 0.87, 0.93 and 0.89 in the pairwise comparisons of T3 vs. T0, T6 vs. T0 and T12 vs. T12, respectively. The results indicated the accuracy and reliability of our bioinformatic analysis results.

KEGG enrichment analysis for DEGs

KEGG enrichment analysis was conducted to investigate the potential biology function of DEGs. Results revealed that a total of 31 (T3 vs. T0), 17 (T6 vs. T0) and 26 (T12 vs. T0) pathways were significantly enriched (FDR-$p < 0.05$) in the three comparison groups, respectively. The top 20 KEGG pathways (ranked by FDR-*p*) in each comparison group were displayed in Figures 1D–F, which were categorized into distinct KEGG orthology classes including environmental information processing, organismal systems, cellular processes, metabolism, genetic information processing and human disease. Among them, the two functional classes, environmental information processing and metabolism, which harbored a large number of significantly enriched pathways in our study, were recognized playing essential roles in sensing stress associated with changes in environmental dissolved oxygen and intracellular transduction. For example, at 3 h after hypoxia, the significantly enriched pathways were concentrated in signaling transduction and signaling molecules and interactions, such as ECM-receptor interaction, PI3K-Akt signaling pathway, Calcium signaling pathway, Cytokine-cytokine receptor interaction, Apelin signaling pathway, cGMP-PKG signaling pathway, and HIF-1 signaling pathway (Figure 1D). At 6 h, DEGs involved in four carbohydrate metabolism processes including Glycolysis/Gluconeogenesis, Fructose and mannose metabolism, Galactose metabolism, Starch and sucrose metabolism, as well as two lipid metabolism processes

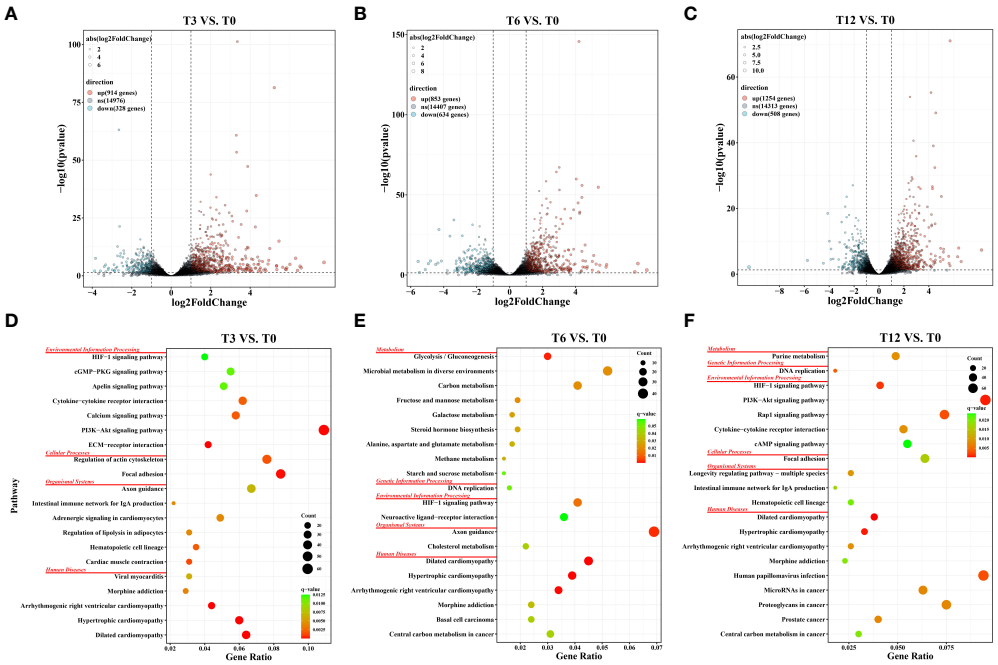

FIGURE 1
Statistics of differentially expressed genes (DEGs) and KEGG pathway enrichment analysis in gills of spotted sea bass at different time points after hypoxia. **(A)** Volcano plot of DEGs in the comparison group of T3 vs. T0; **(B)** Volcano plot of DEGs in the comparison group of T6 vs. T0; **(C)** Volcano plot of DEGs in the comparison group of T12 vs. T0; **(D)** KEGG pathway enrichment analysis of DEGs in the comparison group of T3 vs. T0; **(E)** KEGG pathway enrichment analysis of DEGs in the comparison group of T6 vs. T0; **(F)** KEGG pathway enrichment analysis of DEGs in the comparison group of T12 vs. T0;.

including Steroid hormone biosynthesis and Alanine, aspartate and glutamate metabolism, were significantly enriched (Figure 1E). At 12 h, the DEGs were also significantly enriched in signaling pathways like PI3K-Akt signaling pathway, HIF-1 signaling pathway, Rap1 signaling pathway, Cytokine-cytokine receptor interaction, and cAMP signaling pathway. Notably, the HIF-1 signaling pathway was enriched in all three tested time points after hypoxia (Figure 1F), confirming the key roles of HIF pathway in the response to hypoxia.

GSEA analysis for functional gene sets enriched in the whole gene lists

In addition to determine the KEGG enrichment information of these DEGs, we performed GSEA analysis for interpreting gene expression data of the gills under hypoxia at the level of gene sets, by using canonical pathways (CP) collection in the Molecular Signatures Database (MSigDB). We identified the significant gene sets within each comparison group (T3 vs. T0, T6 vs. T0, T12 vs. T0), and the top 20 most significant enrichments (ranked in descending order of the |NES-value|) were listed in Supplementary Table 3. Overall, the most significantly enriched gene sets positively correlated with all the hypoxia-treatment groups (gene sets that up-regulated in T3, T6 and T12) included HIF-1-alpha transcription factor network, HIF-2-alpha transcription factor network, Glycolysis and Gluconeogenesis, and Cori cycle (Figure 2 and Supplementary Table 3). Additionally, signal transduction associated pathways such as signaling by Type 1 Insulin-like Growth Factor 1 Receptor (IGF1R), Insulin receptor, VEGF, as well as metabolism pathways including Oxidative phosphorylation and Respiratory electron transport, were also enriched in the gill after hypoxia (Supplementary Table 3). Alternatively, the most significant enriched gene sets positively correlated with the control group (gene sets that up-regulated in T0) were mainly concentrated in cell cycle and DNA replication related processes such as Cell Cycle Mitotic, Cell Cycle Checkpoints, Mitotic G1 phase and G1/S transition, G2/M Checkpoints, DNA Replication Pre-Initiation, Activation of the pre-replicative complex, and other associated pathways (Figure 2 and Supplementary Table 3).

Dynamic gene expression patterns

A total of 2,796 DEGs were assigned to six clusters, the gene number of which varied from 422 to 541 (Figure 3). The six

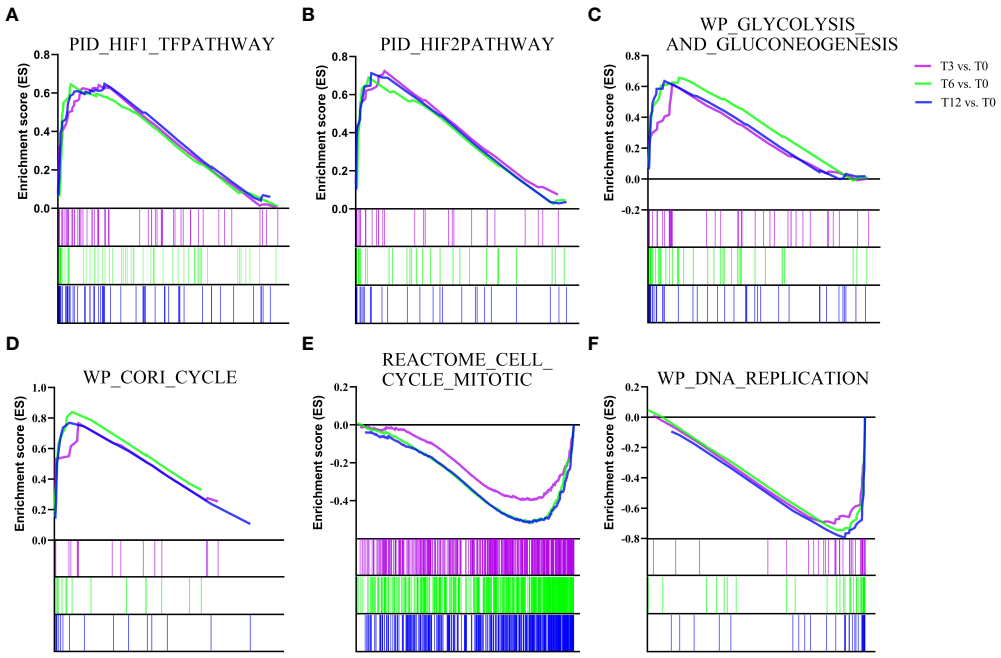

FIGURE 2
Gene Set Enrichment analysis (GSEA) plots showing the most enriched gene sets in hypoxia treatment groups (T3, T6 and T12) and control group (T0). The most significant enriched gene sets positively correlated with hypoxia treatment groups (T3, T6 and T12) are **(A)** PID_HIF1_TFPATHWAY, **(B)** PID_HIF2PATHWAY, **(C)** WP_GLYCOLYSIS_AND_GLUCONEOGENESIS, and **(D)** WP_CORI_CYCLE. The most significant enriched gene sets positively correlated with control group (T0) are **(E)** REACTOME_CELL_CYCLE_MITOTIC and **(F)** WP_DNA_REPLICATION. The enrichment score of each comparison is showed with different color lines.

clusters represented six distinct patterns of expression trajectories in the time course, and the detected clusters of co-expressed genes indicated co-regulation. As we mainly focus on the most relevant regulation networks (genes) interacted with hypoxia environment, the two clusters including cluster 2 and cluster 5, which enriched with hypoxia-responsive genes and pathways, were further analyzed. As shown in Figure 3A, with the prolonging of hypoxia time, the expression pattern of DEGs in cluster 2 showed a general upward trend, while expression of DEGs in cluster 5 exhibited the overall downward trend. KEGG enrichment analysis showed that DEGs in cluster 2 were significantly enriched in signal transduction pathways including HIF-1 signaling pathway, MAPK signaling pathway, AMPK signaling pathway, PI3K-Akt signaling pathway and Insulin signaling pathway, as well as carbohydrate metabolism pathways such as Glycolysis/Gluconeogenesis, Fructose and mannose metabolism, and Galactose metabolism (Figure 3B). The DEGs in cluster 5 were enriched in 1) replication and repair related pathways containing DNA replication, Base excision repair, Mismatch repair, Homologous recombination, and Fanconi anemia pathway; 2) Cell cycle; and 3) several nucleotide metabolism and lipid metabolism pathways (Figure 3C).

PPI network construction, hub genes recognition and module analysis

PPI networks were constructed and hub genes were identified for co-expression genes of cluster 2 and cluster 5. STRING analysis identified 206 nodes and 240 edges for cluster 2, as well as 246 nodes and 817 edges for cluster 5. Their networks were visualized using Cytoscape software, showing in Figures 4A, B. Cyto-Hubba of Cytoscape was used for determining highly connected protein nodes (hubs) by four algorithms (MCC, MNC, Degree and EPC). The ranks and names for top 10 hub genes of each algorithm were shown in Supplementary Table 4. The results showed that for cluster 2, all four methods identified *vascular endothelial growth factor A* (*vegfa*), *insulin-like growth factor 1* (*igf1*), *endothelin 1* (*edn1*), *cyclooxygenase 2b* (*cox2b*), *chemokine (C-X-C motif) receptor 4b* (*cxcr4b*), *catenin beta 1* (*ctnnb1*), and *solute carrier family 2 member 1a* (*slc2a1a*) as hub genes, and *hk1* was considered as hub gene by three of the four algorithms (Supplementary Table 4). For cluster 5, six hub genes, that were *minichromosome maintenance 2* (*mcm2*), *replication factor C subunit 4* (*rfc4*), *minichromosome maintenance 5* (*mcm5*), *DNA polymerase alpha 1 catalytic subunit* (*pola1*), *DNA*

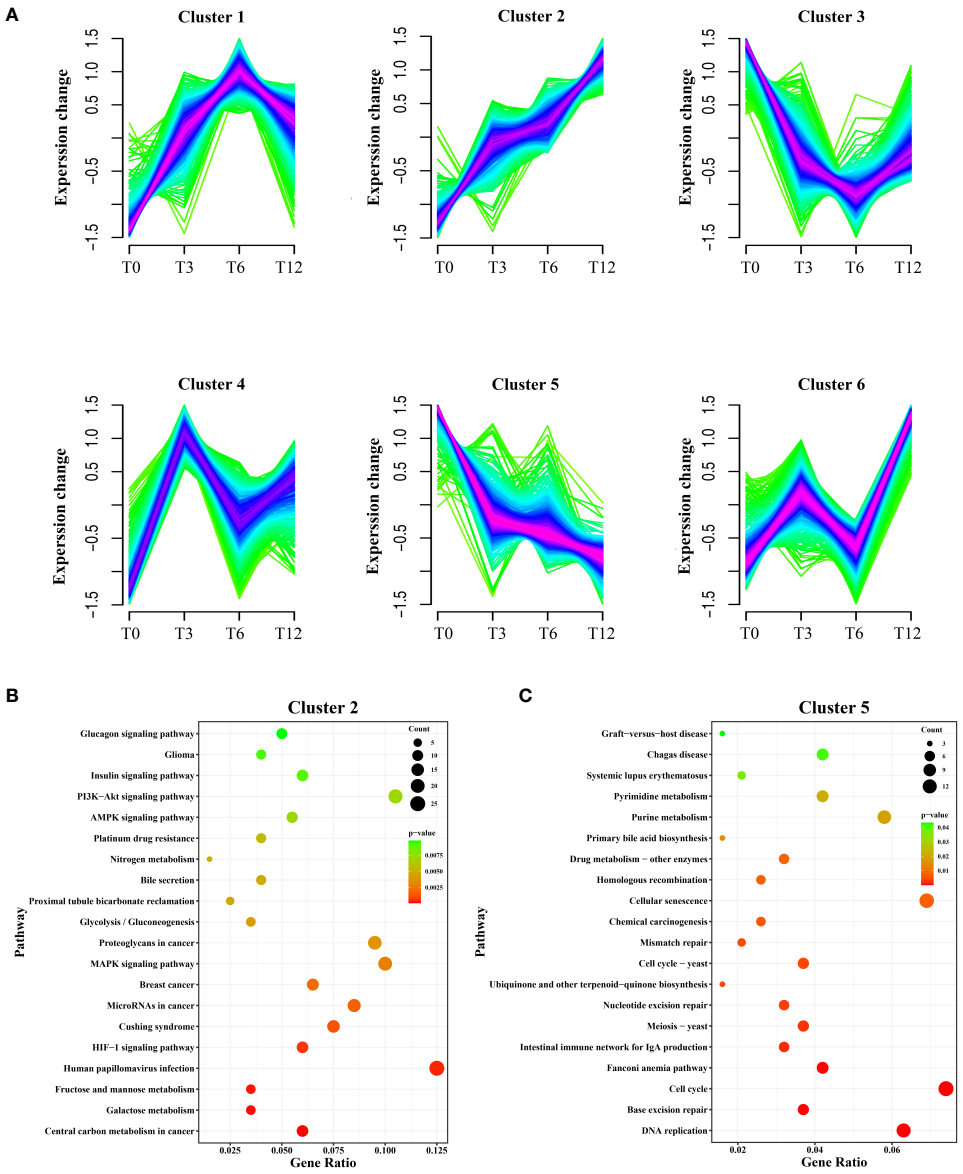

FIGURE 3
Soft clustering profiles of DEGs after hypoxia. **(A)** The dynamic expression patterns of the DEGs were analyzed by Mfuzz R package. Six clusters (cluster 1-6) were identified based on the similarity in expression patterns. Different colors indicate the match degrees between changes of genes and the major changes of the clusters. Fuchsia, blue and green represent high, moderate and low match degrees, respectively. **(B)** KEGG enrichment analysis of DEGs in cluster 2. **(C)** KEGG enrichment analysis of DEGs in cluster 5.

polymerase epsilon catalytic subunit A (*pole*), and *HK1 checkpoint homolog* (*chek1*), were identified by all four algorithms. Additionally, *cell division cycle 20* (*cdc20*), *recombinase rad51* (*rad51*), *replication protein A1* (*rpa1*) and *gins complex subunit 2* (*gins2*) were suggested as hub genes by three algorithms (Supplementary Table 4).

MCODE defined one and three significant modules from the PPI networks of cluster 2 and cluster 5, respectively. For cluster 2, the five genes in the significant module (*vegfa*, *igf1*, *edn1*, *cox2b*, *cxcr4b*) all belonged to hub genes with top-ranking obtained from the Cyto-Hubba analysis (Figure 4C). For cluster 5, the identified hub genes including *mcm2*, *mcm5*, *pola*, *pole*, *chek1*, *rfc4* were also included in the most significant module (Figures 4D–F).

Taken together, from the enrichment analysis results generated by above methods, the genes and pathways involved in HIF signal network system were induced most significantly in response to hypoxia, meanwhile the cell cycle related genes and

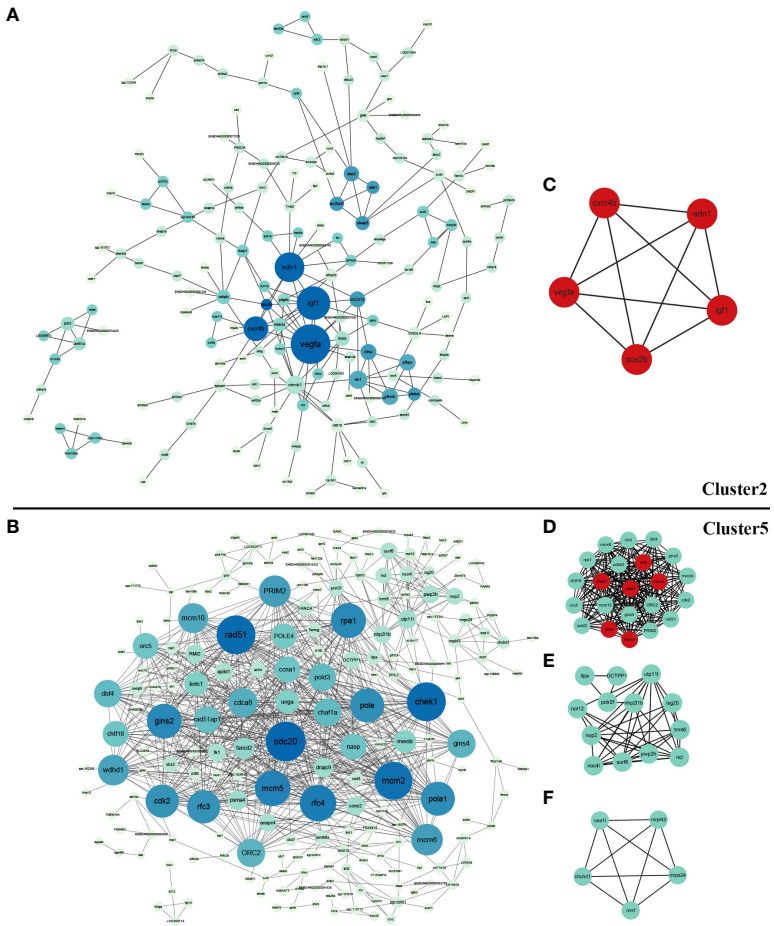

FIGURE 4
Protein-protein interaction (PPI) network and significant module of DEGs in cluster 2 and cluter 5. **(A)** PPI network of DEGs in cluster 2 created by STRING and visualized using Cytoscape software; **(B)** PPI network of DEGs in cluster 5 created by STRING and visualized using Cytoscape software; **(C)** The significant module of cluster 2 identified by MCODE (score = 5.000). The hub genes identified by Cyto-Hubba analysis were shown in red; **(D)** The most significant module of cluster 5 identified by MCODE (score =20.286); **(E)** The second significant module of Cluster 5 identified by MCODE (score =7.167); **(F)** The third significant module of Cluster 5 identified by MCODE (score =5.000). The hub genes identified by Cyto-Hubba analysis are shown in red.

pathways were dramatically suppressed by hypoxia. Putative pathways and genes involved in low oxygen response in spotted sea bass gills were illustrated in Figure 5, and their gene expression levels were shown in Supplementary Tables 5, 6. In addition, their potential biological functions were discussed in detail in the Discussion section.

DAS events in gill tissues under hypoxia

In order to survey AS events in genes associated with hypoxia response in gills, DAS events were determined between two sets of RNA-Seq samples within each comparison group using rMATS. As a result, a total of 400 DAS events were identified after hypoxia including 166, 176 and 295 DASs in comparison group of T3 vs. T0, T6 vs. T0 and T12 vs. T0, which were derived from 153, 158 and 262 genes, respectively (Table 1). Among the five types of AS events (ES, IR, A3SS, A5SS, and ME), ES was the most abundant type, accounting for more than 80% of the total DAS events (Table 1). To validate the reliability of the bioinformatic analysis results for AS, four predicted DAS genes with ES type (*slc6a13, zmym2, tnip1, msrb3*) were selected, and specific primers of the inclusion isoforms were designed and the sizes were validated by RT-PCR. The results demonstrated that the amplified product sizes were consistent with predicted target fragments (Supplementary Figure 3).

The KEGG functional enrichment analysis result for the DAS genes indicated the most significant pathway was spliceosome (Figure 6A), which is directly related to the occurrence of DAS events. Notably, 63 DAS genes were also

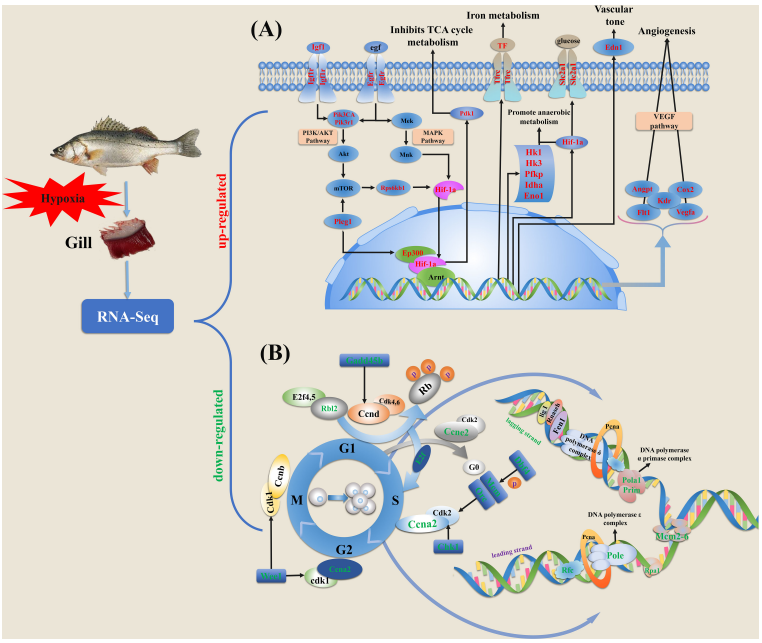

FIGURE 5
Schematic diagram of key genes and pathways in response to hypoxia based on the expression profiles in gills of spotted sea bass. **(A)** The genes involved in HIF-1 signal network system were significantly induced by hypoxia. **(B)** The genes involved in cell cycle progression were significantly suppressed by hypoxia stress. Cell cycle is generally consisted of four different phases, including M, S, G1 and G2. DEGs in HIF-1 signal network system and cell cycle progression were labeled with red and green texts, respectively. The detailed information of these genes involved in HIF-1 signaling pathway and cell cycle are given in Supplementary Tables 3, 4, respectively.

determined as DEGs after hypoxia (Figure 6B and Supplementary Table 7), suggesting that the hypoxia-response expression of these genes might be regulated by the alternative splicing mechanism.

Discussion

Fish are often challenged to survive in hypoxia environments caused by various factors such as high temperature, low atmospheric pressure and eutrophication in water (Abdel-Tawwab et al., 2019; Sun et al., 2020). Although fishes are capable to make quickly reactions to hypoxia to maintain normal physical activity, a lack of oxygen will have detrimental effects on growth, reproduction and survival (Wang et al., 2017). Therefore, to prevent yield loss, increasing attention should be taken into account on DO levels and elucidating the mechanisms of fish reaction under hypoxia. Over the past decade, the profound changes in gene expression profiles were generated based on transcriptomic datasets, which have been widely employed in investigating the molecular basis for hypoxia-responsive and -adaptive mechanisms in a number of fish species. Fish gills play dominant roles in aquatic gas exchange and are responsible for making behavioral, morphological and physiological adaptions to hypoxia conditions (Wu et al., 2017; Abdel-

TABLE 1 Statistics of DAS events detected in gills after hypoxia.

Alternative splicing types	T3 vs. T0	T6 vs. T0	T12 vs. T0
Exon skipping	147 (61:86)	156 (58:98)	278 (72:206)
Mutually exclusive exons	15 (8:7)	17 (8:9)	12 (4:8)
Alternative 3' splice site	2 (1:1)	2 (1:1)	4 (2:2)
Alternative 5' splice site	1 (0:1)	0 (0:0)	0 (0:0)
Intron retention	1 (1:0)	1 (1:0)	1 (1:0)
Total DAS events /DAS gene	166/153	176/158	295/262

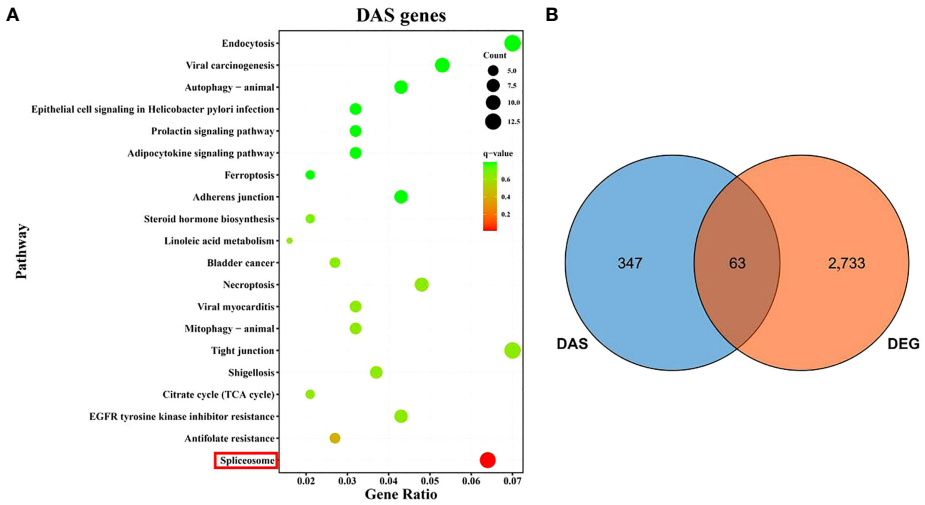

FIGURE 6
An overview of differential alternative splicing (DAS) events in gills of spotted sea bass after hypoxia. **(A)** KEGG enrichment analysis of DAS genes. **(B)** Venn diagram showing the overlap of DEGs and DAS genes.

Tawwab et al., 2019). Previous studies have characterized the plastic hypoxia-induced changes in gill morphology and cellular ultrastructure in several fish species (Sollid et al., 2003; Sollid and Nilsson, 2006; Matey et al., 2008; Wu et al., 2017), but the underlying molecular basis in gills was still lacking. In this study, we performed the in-depth analysis of transcriptomic datasets of spotted sea bass gills to better understand the molecular changes affected by hypoxia and the underlying adaptive mechanisms. It was noted that the number of DEGs were greatly increased with the prolongation of hypoxia stress from 3 h to 12 h. It suggested that a series of adaptive mechanisms may be gradually activated to deal with hypoxia stress and maintain homeostasis in gills of spotted sea bass.

The HIF signal network system is induced in gills under hypoxia

Several proteins and signaling pathways have been reported to function in hypoxia adaptation in fishes, and the changes of their expressions can trigger a great number of biological processes (Zhu et al., 2013). In our study, through function enrichment annotation analysis by DEGs-based KEGG, or GSEA analysis based on all the gene expression data under hypoxia in spotted sea bass, the transcriptional inducible genes and pathways in gills were significantly enriched in HIF signal network (Figures 1D–F and 2). This evolutionarily conserved signal network included HIF homologs and their targets, and hypoxia adaptation signaling pathways such as PI3K-Akt, MAPK, AMPK, VEGF and calcium signaling pathway, which have been extensively reported in vertebrate species (Xiao, 2015; Xie et al., 2019).

HIF-α is recognized as a key modulator for the regulation of the hypoxia signaling pathway. Among the three isoforms of HIF-α (HIF-1α, HIF-2α and HIF-3α) that have been identified in vertebrates, HIF-1α and HIF-2α are widely studied and considered particular critical for hypoxia response. They share similar domain structures, heterodimerize with the stable HIF-1β and bind to hypoxia responsive element (HRE), but their regulations on the expression of genes may be different (Loboda et al., 2010). In mammals, HIF-1α is expressed ubiquitously in all cells, whereas HIF-2α are selectively expressed in certain tissues (Majmundar et al., 2010). For the central adaptation to hypoxia that shift towards non-oxidative forms of carbon metabolism and ATP production, both HIF-1α and HIF-2α play essential functions in modulating cellular metabolisms and controlling redox homeostasis, but through distinct transcriptional programs (Majmundar et al., 2010). For example, glucose consumption and glycolysis were reported to be promoted primarily by HIF-1α, while fatty acid storage was promoted by HIF-2α (Loboda et al., 2010; Majmundar et al., 2010). In our results, both HIF-1α and HIF-2α were identified to be expressed in gills of spotted sea bass, and their mRNA expressions were regulated by hypoxia (Supplementary Table 5). In addition, several KEGG pathways related to carbohydrate and lipid metabolism processes were significantly induced by hypoxia exposure (Figures 1D–F). The related up-regulated DEGs potentially to be targeted by HIF-α included genes encoding *pdk1* that represses the flux of pyruvate into acetyl-CoA and suppresses O_2 consumption (Simon, 2006), *edn1*

used for vasomotor control (Koltsova et al., 2014), *slc2a1* that facilitate cellular glucose uptake, *cox2b* that promotes angiogenesis, *hk1*, *hk3*, *ldha*, *pfkp*, *gapdh*, and *eno1* as metabolic enzymes that reduce oxygen consumption and promote anaerobic glycolysis (Rye and LaMarr, 2015) (Figure 5A and Supplementary Table 5). However, the specific targets regulated by HIF-1α and HIF-2α in fish gills couldn't be distinguished based on expression patterns, which need to be further investigated. In addition, we performed GSEA analysis as it could provide valuable information based on expression levels of all the genes in an experiment instead of only considering those DEGs (Subramanian et al., 2005). Our results also indicated that hypoxia-treatment groups (T3, T6 and T12) were most positively correlated with enriched gene sets, like HIF-1-alpha transcription factor network, HIF-2-alpha transcription factor network, Glycolysis and Gluconeogenesis and Cori cycle (Figure 2).

As the master regulator of the transcriptional response to hypoxia, HIF is not merely a transducer but an integrator of multiple signaling pathways (Fábián et al., 2016). Numerous signaling pathways have been reported to function in hypoxia adaptation. VEGF has been demonstrated as the common target gene shared by HIF-1α and HIF-2α (Loboda et al., 2010), and the HIF-α/VEGF signaling pathway showed to play a crucial role in angiogenesis which stimulates the proliferation of blood vessels to increase oxygen supply (Zhu et al., 2013). In our study, the mRNA expression levels of numerous genes involved in signaling by VEGF was significantly induced by hypoxia, such as *vegfa*, *fms-related tyrosine kinase 1* (*flt1*), *kinase insert domain receptor* (*kdr*), *angiopoietin-like 4* (*angpt*) and *cox2b* (Figure 5A and Supplementary Table 5). Although not detected by KEGG enrichment analysis based on DEGs, we noted that the gene sets of VEGF and angiogenesis were positively correlated with hypoxia treatment groups (T3 and T12) by GSEA analysis (Supplementary Table 3). In addition, PI3K/Akt, MAPK and AMPK pathways have been reported to play important roles in hypoxia response in both higher vertebrates and fish species (Zhu et al., 2013). The PI3K/Akt signaling pathway is activated by IGF1, which increase synthesis and transcriptional activity of HIF-1α by preventing its ubiquitination and degradation (Yang et al., 2018). The MAPK signaling pathway is essential for controlling the production of reactive oxygen species (ROS) and oxygen homeostasis (Seifried et al., 2007), and has been proved to be implicated in regulating the activity of HIF (Bracken et al., 2003). For AMPK signaling pathway, hypoxia can lead to the activation of AMPK, which initiates various adaptive responses to decreased ATP levels or reduced oxygen levels (Zhu et al., 2013). Moreover, in brain of mammals, PI3K and MAPK pathways have been reported to be involved in stimulating HIF in angiogenesis and could be activated by the insulin signaling pathway, which suggested that PI3K and MAPK pathways might act as cross-talk between the insulin signaling pathway and the angiogenesis pathway (Zeng et al., 2016). Correspondingly, in our study, we found that insulin, PI3K/AKt, MAPK and AMPK signaling pathways were all enriched based on the expression patterns of genes in cluster 2, which showed a general upward trend towards hypoxia (Figure 3) The identified DEGs involved in these pathways included *insulin receptor* (*insr*), *hk1* in the insulin signaling pathway, *platelet-derived growth factor receptor beta-like* (*pdgfrb*), *CREB binding protein* (*creb*), *growth hormone receptor 2* (*ghr*) in the PI3K/AKt signaling pathway, *transcription factor jun-D* (*jund*), *igf1* in the MAPK signaling pathway and ATP-dependent 6-phosphofructokinase, platelet type (*pfkp*), *cyclin, C-terminal domain* (*cycd*) in the AMPK signaling pathway (Supplementary Table 5). This result indicated the potential critical involvement and conservative functions of these genes and signaling pathways in gills of spotted sea bass after hypoxia stress, and future studies are required to elucidate how the hypoxia signaling cascade can integrate information from many other signaling pathways.

Furthermore, we performed PPI analysis and identified hub genes in cluster 2, which showed continuously induced expression patterns by hypoxia in our study. Notably, the identified hub genes in cluster 2 (*vegfa*, *igf1*, *edn1*, *cox2b*, *cxcr4b*, *slc2a1*) were all related to HIF signal network system and supposed to be targeted by HIF-α (Figure 4 and Supplementary Table 4). The significant module identified by MCODE included five hub genes (*vegfa*, *igf1*, *edn1*, *cox2b* and *slc2a1*), and their potential roles in response to hypoxia have been mentioned above. In addition, hypoxia enhances *cxcr4* expression by activating HIF-1α in several types of tumor cells (Korbecki et al., 2021). Moreover, there are extensive interactions among those hub genes (Figure 4). For example, *cox2* was reported to play a critical role in VEGF induction and stimulation of angiogenesis (Kaidi et al., 2006), meanwhile VEGF was proved to be one of the principal factors produced by hypoxia myocytes that is responsible for the induction of endothelial cell *cox2* expression (Wu et al., 2003). Overall, in line with expectations, the HIF signal network system plays the most important roles in response to hypoxia in gills of spotted sea bass, and the functions of HIF target genes and related pathways may highly conserved from teleost to mammals.

The cell cycle progression is inhibited in gills under hypoxia

In mammals, it have been demonstrated that hypoxia served as a stimulus for cell cycle arrest, which might be mediated through the non-transcriptional role as an inhibitor of MCM helicase activity of HIF-1α (Hubbi et al., 2013). MCM helicase is

composed of six protein subunits termed MCM2-7 and is a principal component of the prereplicative complex, which assemble at origins of replication during G1 before the onset of DNA replication. Under hypoxia, the HIF-1α protein may bind to the MCM proteins, maintaining the complex in a loaded but inactive state (Hubbi and Semenza, 2015). Moreover, evidence showed that MCM mRNA expression was inhibited in a HIF-1α-dependent manner (Semenza, 2011). Conversely, individual MCM subunit such as MCM2, MCM3, MCM5 or MCM7 can inhibit the activity of HIF-1α, which functions as negative regulators of HIF activity (Hubbi et al., 2011). Thus HIF and MCM proteins act in a mutually antagonistic manner, however, the ability of HIF-1α to inhibit cell cycle progression under severe hypoxia may be dominant over the ability of MCMs to promote cell cycle progression by inhibiting HIF-1α (Semenza, 2011).

Although the relationship of hypoxia and cell cycle arrest has not revealed in teleosts, in our study, it can be obviously observed that numerous cell cycle related genes and pathways were significantly suppressed in gills of spotted sea bass under hypoxia (Figures 1D–F and 2). Consistent with the findings in mammals, genes encoding MCM proteins (*mcm2-6* and *mcm10*) were dramatically down-regulated in the hypoxia treatment groups than that in the control group (Supplementary Table 6). Besides MCM helicase, several other types of DEGs which are functioning for DNA replication at the S phase showed down-regulation, such as genes encoding: 1) the different catalytic subunits of DNA polymerase complex (*pola1, DNA polymerase delta 3 subunit 3* (*pold3*), *pole, DNA polymerase epsilon 4 subunit* (*pole4*)); 2) the replication factor C (*replication factor C subunit 3* (*rfc3*) and *replication factor C subunit 4* (*rfc4*)) which act as an activator of DNA polymerases; 3) the replication protein A complex (*rpa1*) that binds to single-stranded DNA; 4) the subunits of the origin recognition complex (*origin recognition complex subunit 1-2, 4-5* (*orc1-2, orc4-5*)) that form a core complex and bind specifically to origins of replication; 5) the subunit of DNA primase (*DNA primase large subunit 2* (*prim2*)) which forms a heterodimer to function as RNA polymerase to synthesize small RNA primers that are used to create Okazaki fragments on the lagging strand of the DNA. In addition, the expression levels of genes function in other cell cycle stages, including G1 phase and G1/S transition (*ccne2, rbl2, anapc4-5*), cell cycle checkpoints (*cell division cycle associated 8* (*cdca8*), *chek1, protein DBF4 homolog A* (*dbf4*), *wee1-like protein kinase* (*wee1*), *DNA excision repair protein ERCC-6-like* (*ercc6l*)), and chromosome maintenance (*centromere protein H* (*cenph*), *centromere protein K* (*cenpk*), *telomeric repeat-binding factor 1* (*terf1*)) exhibited remarkably downregulation under hypoxia (Figure 5B and Supplementary Table 6). Overall, a large numbers of cell cycle related genes were suppressed significantly by hypoxia in our study, indicating hypoxia may mediate severely inhibition of cell cycle progression in fish gills.

AS mechanism plays regulatory roles in gills under hypoxia

AS plays critical roles at the post-transcriptional level of gene regulation by producing structurally and functionally distinct mRNA and protein variants (Blencowe, 2006). In recent years, accumulating studies have showed that AS in teleost species served as the tightly regulated processes to cope with environmental stresses. For example, through transcriptome analysis, AS has been demonstrated as important regulator in channel catfish and rainbow trout in response to heat stress (Tan et al., 2019; Sun et al., 2021a), in common carp (*Cyprinus carpio*) and Atlantic killifish during cold acclimation (Healy and Schulte, 2019; Long et al., 2020), in spotted sea bass during salinity adaptation (Tian et al., 2020b), as well as in Nile tilapia after hypoxia stress (Li et al., 2017; Xia et al., 2017). In our study, for the first time, the hypoxia stress induced AS changes in gills of spotted sea bass has been investigated by transcriptome analysis. We found that among the typical patterns of AS (ES, IR, A3SS, A5SS, and ME), ES was the most abundant type, accounting for more than 80% of the total DAS events in gills under hypoxia (Table 1). Moreover, in our previous study, ES was proved to be the most enriched type of AS event in spotted sea bass based on the RNA-Seq data generated by pooling tissues (Tian et al., 2020b). The similar result was also reported in rainbow trout, catfish and common carp (Tan et al., 2018; Long et al., 2020; Ali et al., 2021). It has been demonstrated that animals have higher rates of ES than other eukaryotes (Patthy, 2019). Besides, ES is reported to be the most common AS event leading to a variety of human diseases, due to the loss of functional domains/sites or shifting of the open reading frame (ORF) (Kim et al., 2020). Since the correct processing for the production of a mature mRNA requires specialized interaction with the splicing machinery, we hypothesized that hypoxia stress may induce alteration of the communication between the transcriptional and splicing machinery, which may result in widespread ES and play important role in response to hypoxia (Dutertre et al., 2010).

Notably, KEGG functional analyses revealed that the genes undergoing hypoxia-induced DAS in gills of spotted sea bass were mainly involved in spliceosome (Figure 6). In consistence with our findings, DAS involved in spliceosome were significantly enriched in the brain of common carp during cold adaption (Long et al., 2020), in both gill and liver of spotted sea bass during salinity acclimation (Tian et al., 2020b), and in the liver of catfish after heat stress (Tan et al., 2019). Spliceosome is known as a large and ribonucleoprotein complex, which are differently assembled at distinct introns and accomplishes the feat of intron removal from the messenger RNA precursors (pre-mRNA) of eukaryotic cells (Jenkins and Kielkopf, 2017; Yan et al., 2019). It suggested that some important elements in spliceosome, RNA splicing regulators, underwent different splicing events between normoxia and

hypoxia, which may alter their function in pre-mRNA splicing and affect the splicing decisions of numerous downstream target genes to deal with hypoxia stress and maintain homeostasis in gills of spotted sea bass. The results were largely consistent with the previous observation that splicing factors themselves often undergo auto- or cross-regulation by AS in response to environmental and developmental cues (Staiger and Brown, 2013; Tian et al., 2022). However, the underlying mechanism need to be investigated further in the future.

Conclusions

In the current study, the in-depth analysis of transcriptomic datasets of spotted sea bass gills have been performed to study the molecular changes including the gene expression patterns and AS profiles affected by hypoxia, which provided further insights into the underlying adaptive mechanisms. As results, a total of 1,242, 1,487 and 1,762 DEGs were identified through the comparisons of T3 vs. T0, T6 vs. T0 and T12 vs. T0, respectively. KEGG enrichment analysis based on these DEGs and GSEA analysis performed with the whole gene expression datasets indicated that HIF signal network system was significantly activated and cell cycle related genes and pathways were suppressed in response to hypoxia in gills of spotted sea bass. Six clusters were generated based on dynamic gene expression patterns, and PPI networks were constructed and hub genes were recognized for the cluster 2 and cluster 5, which enriched mostly with hypoxia-responsive genes and pathways. *Vegfa*, *igf1*, *edn1*, *cox2b*, *cxcr4b*, *ctnnb1*, and *slc2a1a* were identified as hubs for hypoxia-induced genes (cluster 2), and *mcm2*, *chek1*, *pole*, *mcm5*, *pola1*, *rfc4* were considered as hubs for down-regulated genes (cluster 5). Besides, a total of 153, 158 and 262 DAS genes were identified in comparison group of T3 vs. T0, T6 vs. T0 and T12 vs. T0, which were mainly enriched in spliceosome. Of them, 63 DAS genes also showed differentially expressed levels after hypoxia, suggesting that the expression changes of these genes might be regulated by the AS mechanism. Our results will lay the valuable basis for elucidated the molecular mechanisms that contribute to short-term hypoxia acclimation in spotted sea bass and other fish species.

Data availability statement

The data presented in the study are deposited in the NCBI Sequence Read Archive (SRA) repository, accession number SRR17822288-SRR17822299.

Ethics statement

The animal study was reviewed and approved by Animal Research and Ethics Committees of Ocean University of China (Permit Number: 20141201).

Author contributions

YR: Methodology, Software, Visualization, Validation and Original draft. YT: Conceptualization and Formal analysis. XM: Data curation. HW: Funding acquisition, Resources and Investigation. XQ: Resources and Investigation. JL: Methodology and Validation. YL: Project administration, Supervision and Writing - review & editing. All authors contributed to the article and approved the submitted version.

Funding

This work was supported by the National Key R&D Program of China [grant numbers 2018YFD0900101]; the National Natural Science Foundation of China [grant numbers 32072947]; and the China Agriculture Research System of MOF and MARA [grant numbers CARS-47].

Conflict of interest

The authors declare that the research was conducted in the absence of any commercial or financial relationships that could be construed as a potential conflict of interest.

Publisher's note

Supplementary material

The Supplementary Material for this article can be found online at: https://www.frontiersin.org/articles/10.3389/fmars.2022.1024218/full#supplementary-material

References

Abdel-Tawwab, M., Monier, M. N., Hoseinifar, S. H., and Faggio, C. J. (2019). Fish response to hypoxia stress: Growth, physiological, and immunological biomarkers. *Fish Physiol. Biochem.* 45, 997–1013. doi: 10.1007/s10695-019-00614-9

Agani, F., and Jiang, B. H. (2013). Oxygen-independent regulation of HIF-1: Novel involvement of PI3K/AKT/mTOR pathway in cancer. *Curr. Cancer Drug Targets* 245, 51. doi: 10.2174/1568009611313030003

Ali, A., Thorgaard, G. H., and Salem, M. (2021). PacBio iso-seq improves the rainbow trout genome annotation and identifies alternative splicing associated with economically important phenotypes. *Front. Genet.* 12. doi: 10.3389/fgene.2021.683408

Bader, G. D., and Hogue, C. (2003). An automated method for finding molecular complexes in large protein interaction networks. *BMC Bioinf.* 4, 1–27. doi: 10.1186/1471-2105-4-2

Bárdos, J. I., and Ashcroft, M. (2005). Negative and positive regulation of HIF-1: A complex network. *Biochim. Biophys. Acta* 1755, 107–120. doi: 10.1016/j.bbcan.2005.05.001

Bartoszewski, R., Moszyńska, A., Serocki, M., Cabaj, A., Polten, A., Ochocka, R., et al. (2019). Primary endothelial cell-specific regulation of hypoxia-inducible factor (HIF)-1 and HIF-2 and their target gene expression profiles during hypoxia. *FASEB J.* 33, 7929–7941. doi: 10.1096/fj.201802650RR

Blencowe, B. (2006). Alternative splicing: New insights from global analyses. *Cell* 126, 37–47. doi: 10.1016/j.cell.2006.06.023

Bohensky, J., Leshinsky, S., Srinivas, V., and Shapiro, I. (2010). Chondrocyte autophagy is stimulated by HIF-1 dependent AMPK activation and mTOR suppression. *Pediatr. Nephrol.* 25, 633–642. doi: 10.1007/s00467-009-1310-y

Bracken, C. P., Whitelaw, M. L., and Peet, D. J. (2003). The hypoxia-inducible factors: Key transcriptional regulators of hypoxic responses. *Cell. Mol. Life Sci.* 60, 1376–1393. doi: 10.1007/s00018-003-2370-y

Chen, B., Li, Y., Peng, W., Zhou, Z., Shi, Y., Pu, F., et al. (2019). Chromosome-level assembly of the Chinese seabass (*Lateolabrax maculatus*) genome. *Front. Genet.* 10. doi: 10.3389/fgene.2019.00275

Claireaux, G., Thomas, S., Fievet, B., and Motais, R. (1988). Adaptive respiratory responses of trout to acute hypoxia. II. blood oxygen carrying properties during hypoxia. *Respir. Physiol.* 74, 91–98. doi: 10.1016/0034-5687(88)90143-0

Déry, M. A., Michaud, M. D., and Richard, D. E. (2005). Hypoxia-inducible factor 1: Regulation by hypoxic and non-hypoxic activators. *Int. J. Biochem. Cell Biol.* 37, 535–540. doi: 10.1016/j.biocel.2004.08.012

Ding, J., Liu, C., Luo, S., Zhang, Y., Gao, X., Wu, X., et al. (2020). Transcriptome and physiology analysis identify key metabolic changes in the liver of the large yellow croaker (*Larimichthys crocea*) in response to acute hypoxia. *Ecotoxicol. Environ. Saf.* 189, 109957. doi: 10.1016/j.ecoenv.2019.109957

Ding, L., Rath, E., and Bai, Y. (2017). Comparison of alternative splicing junction detection tools using RNA-seq data. *Curr. Genomics* 18, 268–277. doi: 10.2174/1389202918666170215125048

Dong, H., Sun, Y., Duan, Y., Li, H., Li, Y., Liu, Q., et al. (2020). The effect of teprenone on the intestinal morphology and microbial community of Chinese sea bass (*Lateolabrax maculatus*) under intermittent hypoxic stress. *Fish Physiol. Biochem.* 46, 1873–1882. doi: 10.1007/s10695-020-00838-0

Dutertre, M., Sanchez, G., De Cian, M. C., Barbier, J., Dardenne, E., Gratadou, L., et al. (2010). Cotranscriptional exon skipping in the genotoxic stress response. *Nat. Struct. Mol. Biol.* 17, 1358–1366. doi: 10.1038/nsmb.1912

Evans, D. H., Piermarini, P. M., and Choe, K. (2005). The multifunctional fish gill: Dominant site of gas exchange, osmoregulation, acid-base regulation, and excretion of nitrogenous waste. *Physiol. Rev.* 85, 97–177. doi: 10.1152/physrev.00050.2003

Fábián, Z., Taylor, C. T., and Nguyen, L. (2016). Understanding complexity in the HIF signaling pathway using systems biology and mathematical modeling. *J. Cell. Mol. Med.* 94, 377–390. doi: 10.1007/s00109-016-1383-6

Grabherr, M. G., Haas, B. J., Yassour, M., Levin, J. Z., Thompson, D. A., Amit, I., et al. (2011). Full-length transcriptome assembly from RNA-seq data without a reference genome. *Nat. Biotechnol.* 29, 644–652. doi: 10.1038/nbt.1883

Healy, T. M., and Schulte, P. S. (2019). Patterns of alternative splicing in response to cold acclimation in fish. *J. Exp. Biol.* 222, jeb193516. doi: 10.1242/jeb.193516

Hou, Z., Wen, H., Li, J., He, F., Li, Y., and Qi, X. (2020). Environmental hypoxia causes growth retardation, osteoclast differentiation and calcium dyshomeostasis in juvenile rainbow trout (*Oncorhynchus mykiss*). *Sci. Total Environ.* 705, 135272. doi: 10.1016/j.scitotenv.2019.135272

Hrycik, A. R., Almeida, L. Z., and Höök, T. O. (2017). Sub-Lethal effects on fish provide insight into a biologically-relevant threshold of hypoxia. *Oikos* 126, 307–317. doi: 10.1111/oik.03678

Hubbi, M. E., Kshitiz Gilkes, D. M., Rey, S., Wong, C. C., Luo, W., Kim, D., et al. (2013). A nontranscriptional role for HIF-1α as a direct inhibitor of DNA replication. *Sci. Signal.* 6, ra10–ra10. doi: 10.1126/scisignal.2003417

Hubbi, M. E., Luo, W., Baek, J. H., and Semenza, G. L. (2011). MCM proteins are negative regulators of hypoxia-inducible factor 1. *Mol. Cell.* 42, 700–712. doi: 10.1016/j.molcel.2011.03.029

Hubbi, M. E., and Semenza, G. L. (2015). An essential role for chaperone-mediated autophagy in cell cycle progression. *Autophagy* 11, 850–851. doi: 10.1080/15548627.2015.1037063

Jenkins, J. L., and Kielkopf, C. L. (2017). Splicing factor mutations in myelodysplasias: Insights from spliceosome structures. *Trends Genet.* 33, 336–348. doi: 10.1016/j.tig.2017.03.001

Kaidi, A., Qualtrough, D., Williams, A. C., and Paraskeva, C. (2006). Direct transcriptional up-regulation of cyclooxygenase-2 by hypoxia-inducible factor (HIF)-1 promotes colorectal tumor cell survival and enhances HIF-1 transcriptional activity during hypoxia. *Cancer Res.* 66, 6683–6691. doi: 10.1158/0008-5472.CAN-06-0425

Kajimura, S., Aida, K., and Duan, C. (2006). Understanding hypoxia-induced gene expression in early development: *In vitro* and *in vivo* analysis of hypoxia-inducible factor 1-regulated zebra fish insulin-like growth factor binding protein 1 gene expression. *Mol. Cell Biol.* 26, 1142–1155. doi: 10.1128/MCB.26.3.1142-1155.2006

Kim, D., Langmead, B., and Salzberg, S. L. (2015). HISAT: a fast spliced aligner with low memory requirements. *Nat. Methods* 12, 357–360. doi: 10.1038/nmeth.3317

Kim, P., Yang, M., Yiya, K., Zhao, W., and Zhou, X. (2020). ExonSkipDB: functional annotation of exon skipping event in human. *Nucleic Acids Res.* 48, D896–D907. doi: 10.1093/nar/gkz917

Koltsova, S. V., Shilov, B., Birulina, J. G., Akimova, O. A., Haloui, M., Kapilevich, L. V., et al. (2014). Transcriptomic changes triggered by hypoxia: Evidence for HIF-1α-independent,[Na^+] i/[K^+] i-mediated, excitation-transcription coupling. *PloS One* 9, e110597. doi: 10.1371/journal.pone.0110597

Korbecki, J., Kojder, K., Kapczuk, P., Kupnicka, P., Gawrońska-Szklarz, B., Gutowska, I., et al. (2021). The effect of hypoxia on the expression of CXC chemokines and CXC chemokine receptors-a review of literature. *Int. J. Mol. Sci.* 22, 843. doi: 10.3390/ijms22020843

Kumar, L., and Futschik, M. E. (2007). Mfuzz: a software package for soft clustering of microarray data. *Bioinformation* 2, 5–7. doi: 10.6026/97320630002005

Lee, Y., and Rio, D. C. (2015). Mechanisms and regulation of alternative pre-mRNA splicing. *Annu. Rev. Biochem.* 84, 291–323. doi: 10.1146/annurev-biochem-060614-034316

Li, H. L., Lin, H. R., and Xia, J. (2017). Differential gene expression profiles and alternative isoform regulations in gill of Nile tilapia in response to acute hypoxia. *Mar. Biotechnol.* 19, 551–562. doi: 10.1007/s10126-017-9774-4

Liu, Y., Wang, H., Wen, H., Shi, Y., Zhang, M., Qi, X., et al. (2020). First high-density linkage map and QTL fine mapping for growth-related traits of spotted sea bass (*Lateolabrax maculatus*). *Mar. Biotechnol.* 22, 526–538. doi: 10.1007/s10126-020-09973-4

Loboda, A., Jozkowicz, A., and Dulak, J. (2010). HIF-1 and HIF-2 transcription factors-similar but not identical. *Mol. Cells* 29, 435–442. doi: 10.1007/s10059-010-0067-2

Long, Y., Li, X., Li, F., Ge, G., Liu, R., Song, G., et al. (2020). Transcriptional programs underlying cold acclimation of common carp (*Cyprinus carpio* l.). *Front. Genet.* 111122. doi: 10.3389/fgene.2020.556418

Majmundar, A. J., Wong, W. J., and Simon, M. C. (2010). Hypoxia-inducible factors and the response to hypoxic stress. *Mol. Cell.* 40, 294–309. doi: 10.1016/j.molcel.2010.09.022

Ma, J., Qiang, J., Tao, Y., Bao, J., Zhu, H., Li, L., et al. (2021). Multi-omics analysis reveals the glycolipid metabolism response mechanism in the liver of genetically improved farmed tilapia (GIFT, *Oreochromis niloticus*) under hypoxia stress. *BMC Genomics* 22, 1–16. doi: 10.1186/s12864-021-07410-x

Mastrangelo, A. M., Marone, D., Laidò, G., De Leonardis, A. M., and De Vita, P. (2012). Alternative splicing: Enhancing ability to cope with stress *via* transcriptome plasticity. *Plant Sci.* 186, 40–49. doi: 10.1016/j.plantsci.2011.09.006

Matey, V., Richards, J. G., Wang, Y., Wood, C. M., Rogers, J., Davies, R., et al. (2008). The effect of hypoxia on gill morphology and ionoregulatory status in the lake qinghai scaleless carp, *Gymnocypris przewalskii*. *J. Exp. Biol.* 211, 1063–1074. doi: 10.1242/jeb.010181

Mu, Y., Li, W., Wei, Z., He, L., Zhang, W., and Chen, X. (2020). Transcriptome analysis reveals molecular strategies in gills and heart of large yellow croaker

(*Larimichthys crocea*) under hypoxia stress. *Fish Shellfish Immunol.* 104, 304–313. doi: 10.1016/j.fsi.2020.06.028

Nikinmaa, M., and Rees, B. B. (2005). Oxygen-dependent gene expression in fishes. *Am. J. Physiol. Regul. Integr. Comp. Physiol.* 288, R1079–R1090. doi: 10.1152/ajpregu.00626.2004

Ng, J. C., and Chiu, J. M. (2020). Changes in biofilm bacterial communities in response to combined effects of hypoxia, ocean acidification and nutrients from aquaculture activity in three fathoms cove. *Mar. Pollut. Bull.* 156, 111256. doi: 10.1016/j.marpolbul.2020.111256

Nilsen, T. W., and Graveley, B. R. (2010). Expansion of the eukaryotic proteome by alternative splicing. *Nature* 463, 457–463. doi: 10.1038/nature08909

Patthy, L. (2019). Exon skipping-rich transcriptomes of animals reflect the significance of exon-shuffling in metazoan proteome evolution. *Biol. Direct.* 14, 1–4. doi: 10.1186/s13062-019-0231-3

Richards, J. G. (2011). Physiological, behavioral and biochemical adaptations of intertidal fishes to hypoxia. *J. Exp. Biol.* 214, 191–199. doi: 10.1242/jeb.047951

Rye, P. T., and LaMarr, W. A. (2015). Measurement of glycolysis reactants by high-throughput solid phase extraction with tandem mass spectrometry: Characterization of pyrophosphate-dependent phosphofructokinase as a case study. *Anal. Biochem.* 482, 40–47. doi: 10.1016/j.ab.2015.03.029

Seifried, H. E., Anderson, D. E., Fisher, E. I., and Milner, J. A. (2007). A review of the interaction among dietary antioxidants and reactive oxygen species. *J. Nutr. Biochem.* 18, 567–579. doi: 10.1016/j.jnutbio.2006.10.007

Semenza, G. L. (2001). HIF-1 and mechanisms of hypoxia sensing. *Curr. Opin. Cell Biol.* 13, 167–171. doi: 10.1016/s0955-0674(00)00194-0

Semenza, G. L. (2011). Hypoxia. cross talk between oxygen sensing and the cell cycle machinery. *Am. J. Physiol. Cell Physiol.* 301, C550–C552. doi: 10.1152/ajpcell.00176.2011

Shen, S., Park, J. W., Lu, Z., Lin, L., Henry, M. D., Wu, Y. N., et al. (2014). rMATS: Robust and flexible detection of differential alternative splicing from replicate RNA-seq data. *Proc. Natl. Acad. Sci. U. S. A.* 111, E5593–E5601. doi: 10.1073/pnas.1419161111

Simon, M. C. (2006). Coming up for air: HIF-1 and mitochondrial oxygen consumption. *Cell Metab.* 3, 150–151. doi: 10.1016/j.cmet.2006.02.007

Sollid, J., De Angelis, P., Gundersen, K., and Nilsson, G. E. (2003). Hypoxia induces adaptive and reversible gross morphological changes in crucian carp gills. *J. Exp. Biol.* 206, 3667–3673. doi: 10.1242/jeb.00594

Sollid, J., and Nilsson, G. E. (2006). Plasticity of respiratory structures-adaptive remodeling of fish gills induced by ambient oxygen and temperature. *Respir. Physiol. Neurobiol.* 154, 241–251. doi: 10.1016/j.resp.2006.02.006

Sollid, J., Weber, R. E., and Nilsson, G. E. (2005). Temperature alters the respiratory surface area of crucian carp *Carassius carassius* and goldfish *Carassius auratus*. *J. Exp. Biol.* 208, 1109–1116. doi: 10.1242/jeb.01505

Staiger, D., and Brown, J. W. (2013). Alternative splicing at the intersection of biological timing, development, and stress responses. *Plant Cell.* 25, 3640–3656. doi: 10.1105/tpc.113.113803

Strepparava, N., Wahli, T., Segner, H., and Petrini, O. J. (2014). Detection and quantification of *Flavobacterium psychrophilum* in water and fish tissue samples by quantitative real time PCR. *BMC Microbiol.* 14, 1–10. doi: 10.1186/1471-2180-14-105

Subramanian, A., Tamayo, P., Mootha, V. K., Mukherjee, S., Ebert, B. L., Gillette, M. A., et al. (2005). Gene set enrichment analysis: A knowledge-based approach for interpreting genome-wide expression profiles. *Proc. Natl. Acad. Sci. U. S. A.* 102, 15545–15550. doi: 10.1073/pnas.0506580102

Sun, J., Liu, Y., Jiang, T., Li, Y., Song, F., Wen, X., et al. (2021b). Golden pompano (*Trachinotus blochii*) adapts to acute hypoxic stress by altering the preferred mode of energy metabolism. *Aquaculture* 542, 736842. doi: 10.1016/j.aquaculture.2021.736842

Sun, J., Liu, Z., Quan, J., Li, L., Zhao, G., and Lu, J. (2021a). RNA-Seq analysis reveals alternative splicing under heat stress in rainbow trout (*Oncorhynchus mykiss*). *Mar. Biotechnol.* 17, 1–13. doi: 10.1007/s10126-021-10082-z

Sun, J., Zhao, L., Wu, H., Liu, Q., Liao, L., Luo, J., et al. (2020). Acute hypoxia changes the mode of glucose and lipid utilization in the liver of the largemouth bass (*Micropterus salmoides*). *Sci. Total Environ.* 713, 135157. doi: 10.1016/j.scitotenv.2019.135157

Szklarczyk, D., Morris, J. H., Cook, H., Kuhn, M., Wyder, S., Simonovic, M., et al. (2016). The STRING database in 2017: quality-controlled protein–protein association networks, made broadly accessible. *Nucleic Acids Res.* 45, 362–368. doi: 10.1093/nar/gkw937

Tan, S., Wang, W., Tian, C., Niu, D., Zhou, T., Jin, Y., et al. (2019). Heat stress induced alternative splicing in catfish as determined by transcriptome analysis. *Comp. Biochem. Physiol. Part D Genomics Proteomics.* 29, 166–172. doi: 10.1016/j.cbd.2018.11.008

Tan, S., Wang, W., Zhong, X., Tian, C., Niu, D., Bao, L., et al. (2018). Increased alternative splicing as a host response to *Edwardsiella ictaluri* infection in catfish. *Mar. Biotechnol.* 20, 729–738. doi: 10.1007/s10126-018-9844-2

Tian, Y., Gao, Q. F., Dong, S. L., Zhou, Y. G., Yu, H., Liu, D., et al. (2022). Genome-wide analysis of alternative splicing (AS) mechanism provides insights into salinity adaptation in the livers of three euryhaline teleosts, including *Scophthalmus maximus*, *Cynoglossus semilaevis* and *Oncorhynchus mykiss*. *Biology* 11, 222. doi: 10.3390/biology11020222

Tian, C., Lin, X., Saetan, W., Huang, Y., Shi, H., Jiang, D., et al. (2020a). Transcriptome analysis of liver provides insight into metabolic and translation changes under hypoxia and reoxygenation stress in silver sillago (*Sillago sihama*). *Comp. Biochem. Physiol. Part D Genomics Proteomics.* 36, 100715. doi: 10.1016/j.cbd.2020.100715

Tian, Y., Wen, H., Qi, X., Zhang, X., Sun, Y., Li, J., et al. (2020b). Alternative splicing (AS) mechanism plays important roles in response to different salinity environments in spotted sea bass. *Int. J. Biol. Macromol.* 155, 50–60. doi: 10.1016/j.ijbiomac.2020.03.178

Wang, Q., Shen, W., Hou, C., Liu, C., Wu, X., and Zhu, J. (2017). Physiological responses and changes in gene expression in the large yellow croaker *Larimichthys crocea* following exposure to hypoxia. *Chemosphere* 169, 418–427. doi: 10.1016/j.chemosphere.2016.11.099

Wei, X., Ai, K., Li, H., Zhang, Y., Li, K., and Yang, J. (2019). Ancestral T cells in fish require mTORC1-coupled immune signals and metabolic programming for proper activation and function. *J. Immunol.* 203, 1172–1188. doi: 10.4049/jimmunol.1900008

Wen, H. S., Zhang, M., He, F., and Li, J. (2016). Research progress of aquaculture industry and its seed engineering in spotted sea bass (*Lateolabrax maculatus*) of China. *Fish Inf. Strategy* 31, 105–111. doi: 10.13233/j.cnki.fishis.2016.02.005

Wu, C., Liu, Z., Li, F., Chen, J., Jiang, X., and Zou, S. (2017). Gill remodeling in response to hypoxia and temperature occurs in the hypoxia sensitive blunt snout bream (*Megalobrama amblycephala*). *Sci. Total Environ.* 479, 479–486. doi: 10.1016/j.scitotenv.2019.135157

Wu, G., Mannam, A. P., Wu, J., Kirbis, S., Shie, J., Chen, C., et al. (2003). Hypoxia induces myocyte-dependent COX-2 regulation in endothelial cells: role of VEGF. *Am. J. Physiol. Heart Circ. Physiol.* 285, H2420–H2429. doi: 10.1152/ajpheart.00187.2003

Xia, J., Li, H., Li, B., Gu, X., and Lin, H. (2017). Acute hypoxia stress induced abundant differential expression genes and alternative splicing events in heart of tilapia. *Gene* 639, 52–61. doi: 10.1016/j.gene.2017.10.002

Xiao, W. (2015). The hypoxia signaling pathway and hypoxic adaptation in fishes. *Sci. China Life Sci.* 58, 148–155. doi: 10.1007/s11427-015-4801-z

Xie, Y., Shi, X., Sheng, K., Han, G., Li, W., Zhao, Q., et al. (2019). PI3K/Akt signaling transduction pathway, erythropoiesis and glycolysis in hypoxia. *Mol. Med. Rep.* 19, 783–791. doi: 10.3892/mmr.2018.9713

Yang, Y., Fu, Q., Wang, X., Liu, Y., Zeng, Q., Li, Y., et al. (2018). Comparative transcriptome analysis of the swimbladder reveals expression signatures in response to low oxygen stress in channel catfish, *Ictalurus punctatus*. *Physiol. Genomics* 50, 636–647. doi: 10.1152/physiolgenomics.00125.2017

Yan, C., Wan, R., and Shi, Y. (2019). Molecular mechanisms of pre-mRNA splicing through structural biology of the spliceosome. *Cold Spring Harb. Perspect. Biol.* 11, a032409. doi: 10.1101/cshperspect.a032409

Yearbook. (2021). *China Fishery statistical yearbook*. Beijing: China Agriculture Press.

Yee Koh, M., Spivak-Kroizman, T. R., and Powis, G. (2008). HIF-1 regulation: Not so easy come, easy go. *Trends Biochem. Sci.* 33, 526–534. doi: 10.1016/j.tibs.2008.08.002

Yu, G., Wang, L., Han, Y., and He, Q. (2012). clusterProfiler: an r package for comparing biological themes among gene clusters. *OMICS* 16, 284–287. doi: 10.1089/omi.2011.0118

Zeng, Y., Zhang, L., and Hu, Z. (2016). Cerebral insulin, insulin signaling pathway, and brain angiogenesis. *Neurol. Sci.* 37, 9–16. doi: 10.1007/s10072-015-2386-8

Zhang, Q., Cui, B., Li, H., Li, P., Hong, L., Liu, L., et al. (2013). MAPK and PI3K pathways regulate hypoxia-induced atrial natriuretic peptide secretion by controlling HIF-1 alpha expression in beating rabbit atria. *Biochem. Biophys. Res. Commun.* 438, 507–512. doi: 10.1016/j.bbrc.2013.07.106

Zhang, Z., Yao, L., Yang, J., Wang, Z., and Du, G. (2018). PI3K/Akt and HIF–1 signaling pathway in hypoxia–ischemia. *Mol. Med. Rep.* 18, 3547–3554. doi: 10.3892/mmr.2018.9375

Zheng, X., Linke, S., Dias, J. M., Zheng, X., Gradin, K., Wallis, T. P., et al. (2008). Interaction with factor inhibiting HIF-1 defines an additional mode of cross-

coupling between the notch and hypoxia signaling pathways. *Proc. Natl. Acad. Sci. U. S. A.* 105, 3368–3373. doi: 10.1073/pnas.0711591105

Zhou, Y., Luo, W., Yu, X., Wang, J., Feng, Y., and Tong, J. (2020). Cardiac transcriptomics reveals that MAPK pathway plays an important role in hypoxia tolerance in bighead carp (*Hypophthalmichthys nobilis*). *Animals* 101483. doi: 10.3390/ani10091483

Zhu, C., Wang, Z., and Yan, B. (2013). Strategies for hypoxia adaptation in fish species: A review. *J. Comp. Physiol. B.* 183, 1005–1013. doi: 10.1007/s00360-013-0762-3

frontiers | Frontiers in Marine Science

TYPE Original Research
PUBLISHED 18 October 2022
DOI 10.3389/fmars.2022.1017142

OPEN ACCESS

EDITED BY
Hongsheng Yang,
Institute of Oceanology (CAS), China

REVIEWED BY
Mohammad Abdul Momin Siddique,
Noakhali Science and Technology University, Bangladesh
Tianming Wang,
Zhejiang Ocean University, China

*CORRESPONDENCE
Shijun Xiao
shijun_xiao@163.com
Zhijian Wang
wangzj1969@126.com

†These authors have contributed equally to this work and share first authorship

SPECIALTY SECTION
This article was submitted to Global Change and the Future Ocean, a section of the journal Frontiers in Marine Science

RECEIVED 11 August 2022
ACCEPTED 04 October 2022
PUBLISHED 18 October 2022

CITATION
Yuan D, Wang H, Liu X, Wang S, Shi J, Cheng X, Gu H, Xiao S and Wang Z (2022) High temperature induced metabolic reprogramming and lipid remodeling in a high-altitude fish species, *Triplophysa bleekeri*. *Front. Mar. Sci.* 9:1017142. doi: 10.3389/fmars.2022.1017142

High temperature induced metabolic reprogramming and lipid remodeling in a high-altitude fish species, *Triplophysa bleekeri*

Dengyue Yuan[1†], Haoyu Wang[1†], Xiaoqin Liu[1], Siya Wang[1], Jinfeng Shi[1], Xinkai Cheng[1], Haoran Gu[1], Shijun Xiao[2*] and Zhijian Wang[1*]

[1]Integrative Science Center of Germplasm Creation in Western China (Chongqing) Science City & Southwest University, Chongqing, China, [2]Jiaxing Key Laboratory for New Germplasm Breeding of Economic Mycology, Jiaxing, Zhejiang, China

The effect of thermal changes on the physiology and behavior of fish is a major research focus in the face of ongoing global warming. There is little information about the effects of temperature increase on fish in the wild. However, the consequences of temperature increase on fish in controlled laboratory conditions can provide insights into what can be expected in the wild. *Triplophysa bleekeri*, a high-plateau fish, exhibits high sensitivity to high temperatures, suggesting it to be a good model to investigate the impact of temperature increase on fish. In this study, we analyzed the effect of gradual temperature increase on transcriptional and metabolic levels of *T. bleekeri* subjected to a gradual temperature change of 0.5°C/day until temperatures of 10°C, 13°C, 16°C, and 19°C were reached. Transcriptomics results of the liver, gut, spleen, and trunk kidney showed that metabolic pathways are widely involved in the response to increased temperatures in *T. bleekeri*. Lipidomics results further indicated that the lipid composition was altered by increased temperatures, and three lipids (PC 14:0e/22:1, PC 18:0e/22:5, and TAG 14:3-21:2-21:2) were identified as potential biomarkers of heat stress in *T. bleekeri*. Moreover, a decline in unsaturated fatty acid levels was observed in *T. bleekeri* under high temperatures. These results suggest that high temperatures modify the metabolomic pathways. Overall, our results help improve the understanding of physiological responses in fish to increased temperatures, and provide valuable information predicting the consequences of global warming on fish.

KEYWORDS

temperature change, heat stress response, lipid metabolism, metabolic reprogramming, high-plateau fish

Introduction

Temperature acts as an important abiotic factor that constrains the geographical distribution and controls the physiological and behavioral parameters of fish (Nilsson et al., 2009; Dadras et al., 2017; Forgati et al., 2017). Fish have evolved the ability to adapt to a certain range of temperature variations in nature, such as seasonal variations and diurnal fluctuations (Crozier and Hutchings, 2014). However, the magnitude of temperature change approaching or beyond the thermal tolerance range of fish can lead to severe sublethal disturbances and mortality (Donaldson et al., 2008). In the context of ongoing global warming, threats for over one-third freshwater fish species have increased considerably (Barbarossa et al., 2021). Fish populations, biodiversity, and distribution have been altered by rising temperature coupled with increased extreme climate events around the world, and some fish species even face local extinction (Free et al., 2019; Punzón et al., 2016). Hence, there is a need to better understand the impact of temperature increase on fish physiology for predicting the consequences of global warming on fish.

The capacity of fish to cope with temperature changes is closely related to the degree of phenotypic plasticity (Norin et al., 2016; Keen et al., 2017). Phenotypic plasticity is defined as the ability of a genotype to produce different phenotypes in response to different environmental conditions (Pigliucci et al., 2006). When fishes face a challenge caused by temperature changes, they attempt to alter their physiological and behavioral traits through producing a cascade of plastic responses (e.g., neuroendocrine, metabolic, cellular, and immunological responses), a process termed acclimation, to resist sublethal and lethal effects (Donaldson et al., 2008; Alfonso et al., 2021). Increasing evidence shows that transcriptional variabilities are key contributors to phenotypic plasticity, allowing organisms to adapt to a changing environment (Smith et al., 2013; Wellband and Heath, 2017; Ecker et al., 2018; Li et al., 2021). Understanding the transcriptional variability of fish to altered temperature is critical for assessing the heat/cold acclimation ability in the face of climate change. Coincident with the advancement of sequencing, RNA-seq offers opportunities to explore transcriptional responses as well as molecular mechanisms underlying responses (Oomen and Hutchings, 2017). The transcriptional plasticity to temperature decrease has been described in multiple teleosts using RNA-seq (Long et al., 2012; Zhou et al., 2019; Liu et al., 2020; Long et al., 2020). However, there is little information to explain the transcriptional responses to temperature increase in fishes (Alfonso et al., 2021). Both acute and chronic exposures to high temperature are regarded as a stress by fish, inducing transcriptional changes in processes including stress response, signal transduction, metabolism, and immune response (Smith et al., 2013; Guo et al., 2016; Huang et al., 2018; Chen et al., 2021). With respect to long-term heat stress, the number of differentially expressed genes (DEGs) involved in stress and immune response decreased comparing to that of short-term challenge studies (Narum and Campbell, 2015; Li et al., 2017), which suggests that fishes acclimate to temperature increase after chronic heat stress.

Stenothermal high-plateau fishes are expected to be vulnerable to global warming. However, the mechanism underlying the response of high-plateau fish to temperature increase is still largely unknown. *Triplophysa bleekeri*, an endemic fish inhabiting the peripheral areas of Qinghai-Tibetan Plateau, is widely distributed at elevations of 200–3,000 m (Wang, 2013). The optimal temperature range of *T. bleekeri* is 14–15°C, and this fish can spawn even in December (approximately 10°C) (Wang et al., 2013). However, *T. bleekeri* dies as a result of long-term exposure to temperatures exceeding 21°C. This means that *T. bleekeri* is very sensitive to high temperatures. Therefore, *T. bleekeri* is an ideal model for studying the impact on fish due to temperature increase. To gain a comprehensive understanding of transcriptional responses to temperature increases, we detected the transcriptional variations in multiple tissues (liver, gut, trunk kidney, and spleen) under four temperature conditions (10°C, 13°C, 16°C, and 19°C). This approach differs from those in previously reported studies on transcriptional responses to temperature changes in fish in that previous studies used a single or two tissues for RNA-seq. The transcriptional change of genes involved energy metabolism is a critical part of the plasticity response to temperature increases (Veilleux et al., 2015; Jeffries et al., 2016). Hence, we hypothesized that the transcriptional levels of metabolism pathways are affected by temperature increases in *T. bleekeri*, resulting in changes in metabolites. Liver tissue is a lynchpin in metabolic reprogramming in response to temperature changes (Barat et al., 2016; Lyu et al., 2018; Paul et al., 2021). In this study, we characterized the lipid metabolite changes in the liver of *T. bleekeri* at high temperatures using a hybrid quadrupole time-of-flight mass spectrometry (UHPLC-QTOF-MS) and gas chromatography-mass spectrometry (GC-MS) analysis. To the best of our knowledge, only a few studies have examined the metabolic profile of fish at high temperatures. Our findings reveal the transcriptional and metabolic response of *T. bleekeri* exposed to high temperatures, and provide valuable information for understanding how fish biology will be affected by global warming.

Materials and methods

Animals and sampling

Fish were caught from a tributary of the Yangtze River using brails and were then transferred to the laboratory. Fish were

maintained in indoor tanks (50 × 40 × 30 cm) with a water-circulating system at 15°C under a 14L:10D lighting cycle. All fish were fed tubificid worms twice daily. Fish were acclimated under these conditions for 3 weeks before the formal experiment. After acclimation, fish (weight 5.6 ± 0.8 g, length 7.1 ± 0.6 cm) were randomly split into four groups, i.e., 10°C group (3 tanks, n = 9/tank), 13°C group (3 tanks, n = 9/tank), 16°C group (3 tanks, n = 9/tank), and 19°C group (3 tanks, n = 9/tank). The temperatures were gradually declined/increased from 15°C to four temperature conditions (10°C, 13°C, 16°C, and 19°C) at a rate of approximately 0.5°C/day using a thermostat. Fish were maintained at aforementioned temperature conditions for 2 weeks. Thereafter, fish were anesthetized by immersion in ice-cold water and were immediately dissected to collect the liver, gut, trunk kidney, and spleen samples. These tissues were quickly frozen in liquid nitrogen for 1 h and then stored at −80°C.

All experimental protocols were approved by Southwest University, and the study was carried out under the protocols of the Institutional Animal Care and Use Committee of Southwest University.

RNA sequencing

Total RNA was extracted from the liver, gut, trunk kidney, and spleen using an Animal Total RNA Isolation Kit (Foregene, China). The quality and quantity of RNA were detected as our previous study (Yuan et al., 2020). Samples with a total RNA concentration ≥ 10 μg and RIN ≥ 8 were used for sequencing. The RNA sequence library was constructed using a paired-end sample preparation kit (Illumina Inc., USA), and the library was sequenced on an Illumina HiSeq 2000 sequencer.

RNA-seq data analysis

A quality control step was conducted on the raw sequencing reads of each sample before bioinformatics analysis. The raw reads were filtered, and then clean reads were aligned to the reference genome of *T. Bleekeri* (Yuan et al., 2020) using HISAT (Kim et al., 2015). The differentially expressed genes (DEGs) between the low-temperature and high-temperature groups were analyzed using DESeq2 (Love et al., 2014). The DEGs of each group were identified and compared with the other group in *T. Bleekeri*. Genes with p-value < 0.01 and $|\log_2 FC| > 1$ were considered as DEGs. GO enrichment and KEGG pathway analyses for DEGs were performed using Tbtools (Chen et al., 2020). R packages ggplot and cytoscape were used for visualization of the Go and KEGG enrichment results. The Short Time-series Expression Miner (STEM) analysis based on FPKM values was conducted to cluster, compare, and visualize gene expression data from the four temperature groups. Genes which had similar expression patterns were clustered into a profile (Ernst and Bar-Joseph, 2006).

Validation of RNA-Seq results using real-time PCR

Total RNA was extracted from the tissue samples, viz., liver, gut, trunk kidney, and spleen, as described above. The synthesis of cDNA was conducted as described in our previous study (Yuan et al., 2021). Real-time PCR (RT-PCR) was performed on the LightCycle 96 (Roche, USA). Primers for the target genes were designed based on the genomic and transcriptomic data of *T. bleekeri* (Yuan et al., 2020) and are listed in Supplementary Table A.1. *β-actin* was used as the reference gene, and the relative gene expression was analyzed as described in our previous study (Yuan et al., 2021).

Lipid extraction for UHPLC-QTOF-MS and GC-MS analysis

Lipid extraction was carried out on liver samples, and six liver samples each were sampled from fish of 10°C, 13°C, 16°C, and 19°C groups. Into an EP tube, 25 mg of each liver sample, 200 μL of water, and 480 μL of extracting solution (V_{MTBE}: V_{MeOH} = 5: 1) were added sequentially. This mixture was homogenized (35 Hz, 4 min) and sonicated for 10 min. After repeating this process three times, the mixture was incubated (1 h) at -40°C and centrifuged at 4°C (3,000 rpm, 15 min), and then the supernatant (350 μL) was dried at 37°C. The dried sample was then reconstituted in 50% methanol in DCM (200 μL) by sonication for 10 min. The mixture was centrifuged at 4°C (13,000 rpm, 15min). Subsequently, the 75 μL of supernatant was used for UHPLC-QTOF-MS analysis.

Similarly, each liver sample (50 mg) was extracted with 460 μL of extracting solution ($V_{Isopropanol}$: $V_{n\text{-}Hexane}$ = 2: 3), and then mixed with 40 μL of Octadecanoic-D35 acid (1 mg/L). The mixture was placed in an ice-water bath for 5 min and then centrifuged at 4°C (12,000 rpm, 15 min). The supernatant was transferred to a fresh tube. Next, the extracting solution (500 μL) was added to the mixture, which was then placed in an ice-water bath and centrifuged for 15 min, as mentioned above. The supernatant was collected and mixed with the previously obtained supernatant. The resulting supernatant (400 μL) was then added to a fresh tube, dried under nitrogen, and mixed with 200 μL of methanol and 100 μL of (trimethylsilyl) diazomethane and maintained for 15 min. This mixture was dried under nitrogen, reconstituted in 160 μL of n-hexane, and then centrifuged at 4°C (12,000 rpm, 5 min). The resulting supernatant was used for GC-MS analysis.

UHPLC-QTOF-MS analysis of lipids

The lipid analysis was performed by an UHPLC System (AB Sciex, USA), coupled with a high-resolution mass spectrometer (Triple TOF 5600, AB Sciex). Lipid species were separated using mobile phases A and B. The mobile phase A consisted of 40% water, 60% ACN, and 10 mmol/L $HCOONH_4$, and the mobile phase B consisted of 10% ACN and 90% IPA. The mobile phase was carried out as described previously (Zhang et al., 2021). The injection volume was 1 μL for the positive ionization (POS) model and negative ionization (NEG) model, respectively. MS/MS spectra were acquired on an information-dependent acquisition (IDA) model using the Triple TOF 5600 mass spectrometer. In the IDA model, the full scan survey MS data was continuously evaluated using analyst TF 1.7 (AB Sciex).

GC-MS analysis of free fatty acids

The free fatty acid (FFA) profiles in the liver samples were analyzed using an Agilent 7890 B gas chromatography system coupled with an Agilent 5977B mass spectrometer and an Agilent DB-FastFAME capillary column (Agilent Technologies, USA). Helium was used as the carrier gas (flow rate: 3.0 mL/min). The temperature program conditions were as follows: the initial temperature was maintained at 75°C for 1 min, raised to 200°C (rate: 50°C/min), and maintained at 200°C for 15 min. The temperature was then increased to 210°C (rate: 2°C/min) for 1 min, finally increased to 230°C (rate: 10°C/min) and maintained at 230°C for 16.5 min. The analytes were ionized by electron impact (EI) at -70 eV. Subsequently, the mass spectrometry data were obtained in Scan/SIM mode with continuous scanning ions from m/z 33 to 400.

Lipid data processing

The format of raw data files (.wiff format) was converted to special format (mzXML) (Holman et al., 2014). Then, the XCMS software (parameters: minfrac=0.5; cutoff=0.3) was used to generate the peak information of MS1, including the retention time (RT), peak area, and m/z values (Tautenhahn et al., 2012). Lipids were identified using the LipidBlast library based on RT and m/z values in the MS/MS spectra (Kind et al., 2013). The principal component analysis (PCA) and orthogonal projections to latent structures discriminant analysis (OPLS-DA) were performed as previous study (Wen et al., 2018), and the VIP was obtained using OPLS-DA. The SPSS 23 was used to analyze data using Student's t-test. The lipids with p-values < 0.05, and VIP > 1 were considered significantly different. The GraphPad Prism 9 software was used for visualization of lipids. The differential lipids were normalized by Z-score following the equation:

$$Z = (x-\mu)/\sigma$$

in which, z is the value of Z-score, x is a value of data, μ is a mean of data, and σ is a number of standard deviation of data. The normalized differential lipids were analyzed by K-means clustering using fpc and cluster package in R to illustrate pattern in lipids with the increasing temperature.

Results

RNA-seq analysis reveals metabolic reprogramming under high temperatures

To comprehensively investigate the transcriptional response to temperature variations, 48 samples from the liver, gut, spleen, and trunk kidney at 10°C, 13°C, 16°C, and 19°C were used for library construction and sequenced. In total, 2,176 Mb of raw reads were obtained. All raw reads were deposited in the NCBI SRA database. After filtering the raw reads, approximately 2,133 Mb clean reads were obtained from each library. The average Q20 and Q30 of the clean reads were 98.14% and 94.24%, respectively. Approximately 92.47% of the clean reads from each library were mapped to the reference genome of *T. bleekeri* (Supplementary Table A.2).

A total of 1,150, 1,709, 1,243, and 510 DEGs were identified in the gut, spleen, trunk kidney, and liver among the four temperature groups (10°C, 13°C, 16°C, and 19°C) through pairwise transcriptome comparison. The largest number of DEGs was observed in the aforementioned tissues between 19°C group and 10°C group (Supplementary Table A.3). The functional enrichment analysis on the KEGG and GO parameters for DEGs was conducted to elucidate molecular pathways involved in transcriptional response to temperature variations. DEGs (19°C group *vs.* 10°C group) were mainly enriched in categories related to energy metabolism, such as lipid metabolic process, lipid biosynthetic process, steroid metabolic process, fatty acid metabolic process, cellular carbohydrate metabolic process, and glucose metabolic process (Figure 1; Supplementary Table A.4). Besides, DEGs were also significantly enriched in signal transduction, immune response, stress response (Supplementary Table A.4). Carnitine palmitoyltransferase 1A (CPT1A) was shared as a DEG by all four tissues, and was upregulated in the 19°C group (Supplementary Figure A.1; Supplementary Table A.4).

To validate the RNA-seq results, DEGs in the liver, gut, spleen, and trunk kidney of four groups were randomly selected and analyzed by RT-PCR. The expression patterns of DEGs detected using RT-PCR were highly consistent with RNA-seq data (Supplementary Figure A.2).

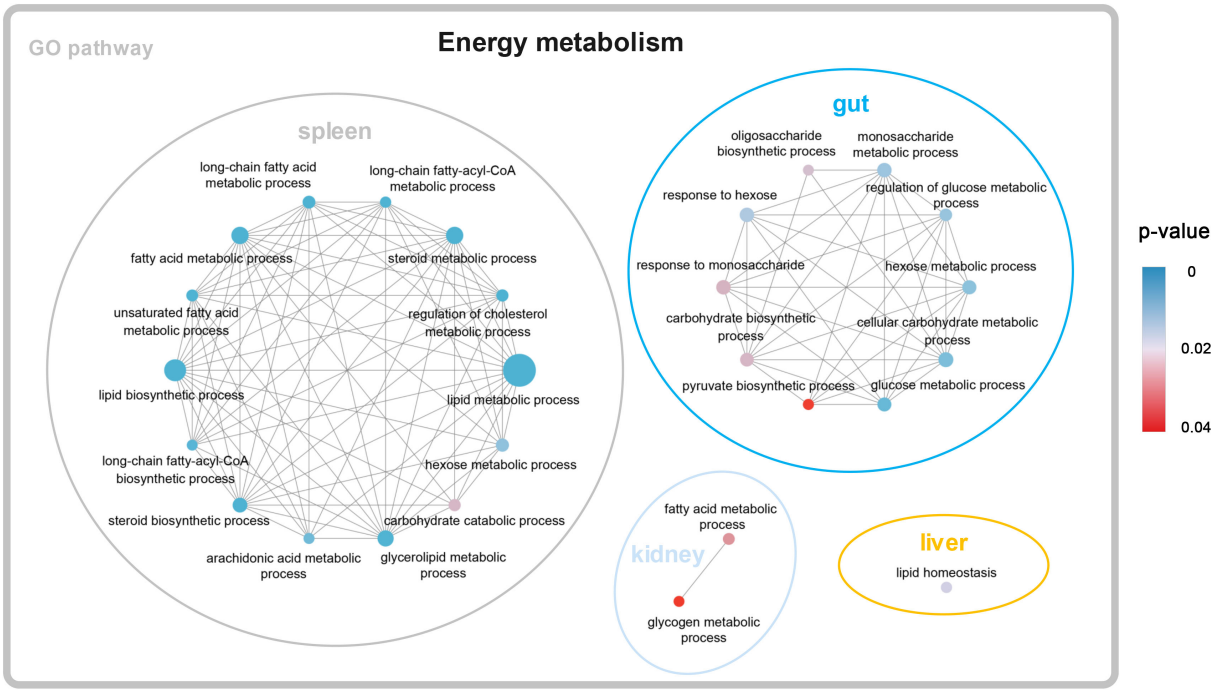

FIGURE 1
Significantly enriched KEGG items of DEGs (19°C group vs. 10°C group).

Clustering analysis reveals dynamic expression profiles of genes with increasing temperature

A clustering analysis (STEM) was conducted to investigate the dynamic expression patterns of genes with increasing temperature. A total of 10, 9, 9, and 8 significant expression profiles ($P < 0.01$) were identified in the gut, spleen, trunk kidney, and liver, respectively (Supplementary Figure A.3). The clustered profile 25 and 0 reflect responsive genes that consistently increase or decrease along with increasing temperature, respectively. The biological functions of genes in profile 25 and 0 ($P < 0.01$) were further analyzed through GO and KEGG assignments. Genes in profile 25 mainly enriched in arachidonic acid metabolism, Hedgehog signaling pathway, Fanconi anemia pathway, DNA repair and recombination pathway, mTOR signaling pathway, thyroid hormone signaling pathway, insulin signaling pathway, metabolic process, and response to stimulus (Figure 2). The majority of genes in profile 0 were involved in ribosome biogenesis, glycosylphosphatidylinositol (GPI)-anchored proteins, adipocytokine signaling pathway, glucagon signaling pathway, signal transduction, and cellular response to stimulus (Figure 2).

Untargeted lipidomics shows lipid remodeling along with increasing temperature

Twenty-four liver samples from the 10°C, 13°C, 16°C, and 19°C groups were processed for UHPLC-QTOF-MS analysis in the POS and NEG modes. PCA and OPLS-DA analysis indicated that aforementioned groups achieved good separation of lipid extracts (Figure 3; Supplementary Figure A.4). Finally, 2,560 lipids were identified based on existing databases. These detected lipids were further analyzed to identify differential lipids. In total, 265 differential lipids were identified among the four temperature groups. These differential lipids were predominantly attributable to phosphatidylcholine (PC, 12.08%), triacylglycerol (TAG, 10.57%), and phosphatidylethanolamine (PE, 7.55%) (Figure 3).

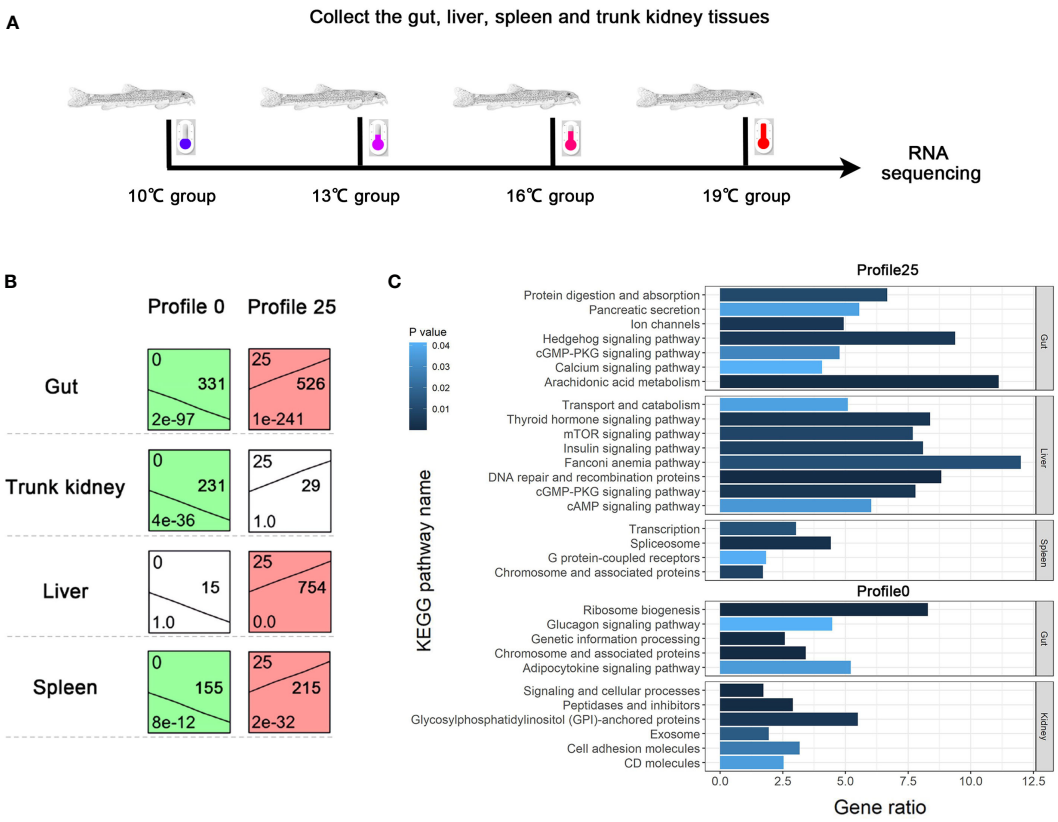

FIGURE 2
Dynamic expression profiles of genes with increasing temperature. **(A)** Temperature conditions and sample collections. **(B)** Expression patterns of consistently increasing and decreasing genes identified by STEM analysis. **(C)** KEGG enrichment results of genes belonging to profile 0 and 25.

The largest number of differential lipids was observed in the 19°C group vs. 13°C group (142), followed by the 19°C group vs. 10°C group (105) (Supplementary Table A.5). The differential lipids with high fold change in 19°C group vs. 13°C group, and 19°C group vs. 10°C group are showed in the Figure 3.

Clustering analysis reveals potential markers of heat stress

To investigate the dynamic change of differential lipids with increasing temperature, the K-means analysis was conducted. The total of nine clusters was obtained (Figure 4), and the list of differential lipids from each cluster is shown in Supplementary Table A.6. The clusters 1 and 9 contain consistently decreasing and increasing lipids with increasing temperature, respectively. PC 14:0e/22:1, PC 18:0e/22:5, and TAG 14:3-21:2-21:2, which belong cluster 9, have a high content under temperature 19°, suggesting that these three lipids can be used as potential biomarkers of heat stress in *T. bleekeri* (Figure 4; Supplementary Table A.6).

Targeted lipidomics reveals decreased concentration of unsaturated fatty acids under high temperature

The targeted lipidomics was conducted using a GC-MS platform to evaluate the effect of high temperature on free fatty acids (FFAs). 49 FFAs were detected, and 14 FFAs were significantly altered in 19°C group compared to that of 10°C group (Figure 5). Among these 14 FFAs, only heneicosanoic acid was significantly elevated in the 19°C group. Unsaturated fatty acids, such as 9-elaidic acid, 9-palmitelaidic acid, 10-pentadecenoic acid, 11-octadecenoic acid, 11-eicosenoic acid, 6,9,12-linolenic acid, 7,10,13,16-docosatetraenoic acid, and 4,7,10,13,16-docosapentaenoic acid, were significantly decreased in the 19°C group.

Discussion

In this study, we used two postgenomic approaches, transcriptomics and lipidomics, to reveal the transcriptional and

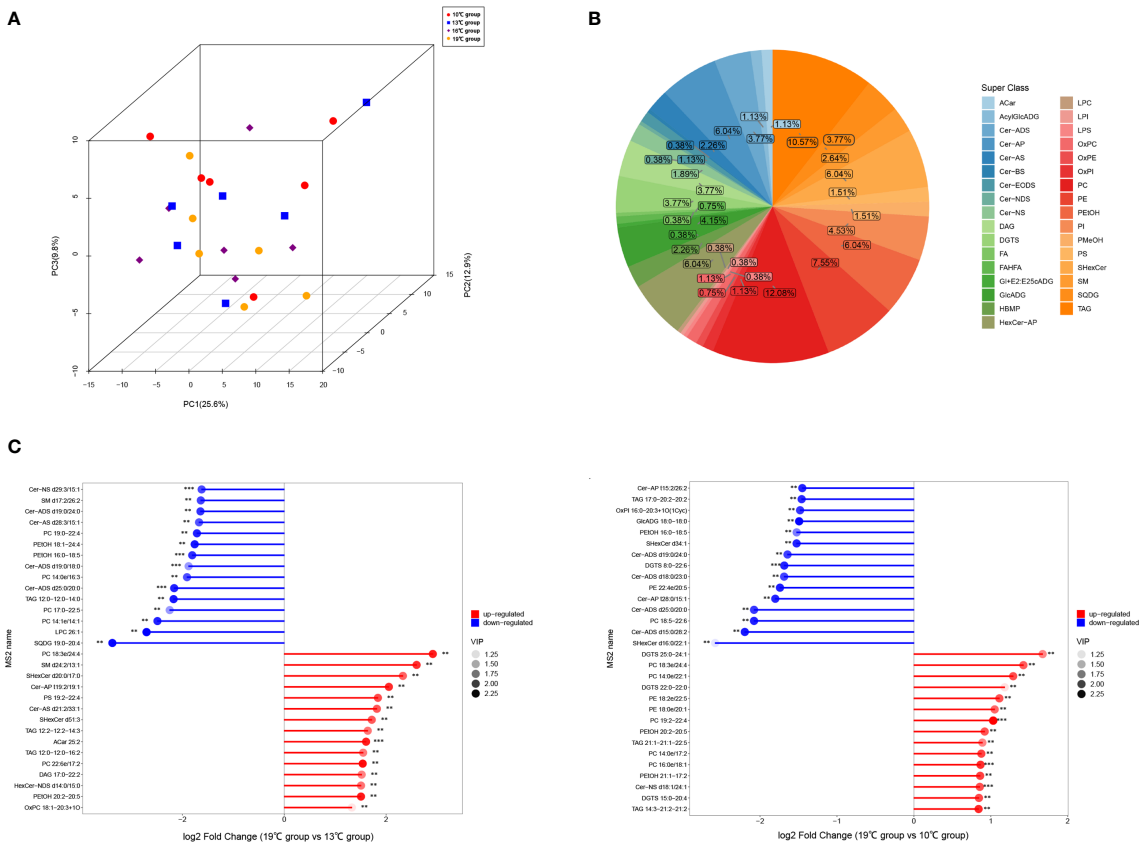

FIGURE 3
Results of untargeted lipidomics based on UHPLC-QTOF-MS analysis. **(A)** PCA plots of the samples. **(B)** Classification of differential lipids among four temperature groups. **(C)** Differential lipids with high fold change in 19°C group vs. 13°C group, and 19°C group vs. 10°C group.

lipid alterations in *T. bleekeri* with increasing temperature. RNA-seq analysis reveals that metabolic pathways are widely involved in the response to temperature changes. In *T. bleekeri*, DEGs (19°C *vs.* 10°C) were significantly enriched in the lipid metabolic process, lipid biosynthetic process, steroid metabolic process, and fatty acid metabolic process. This observation is similar to the results observed in other fish. The expressions of genes involved in lipid metabolism category were significantly changed in response to elevated temperature in *Sparus aurata* (Balbuena-Pecino et al., 2019), and *Scophthalmus maximus* (Zhao et al., 2021). In *Acanthochromis polyacanthus*, a tropical damselfish, lipid metabolism genes were among the most upregulated transgenerationally at elevated temperatures (Veilleux et al., 2015). These results suggest that lipid metabolism has a critical role in heat resistance in fish, which is a conservation mechanism for responding to high temperatures.

To explore the role of lipid metabolism in temperature acclimation of *T. bleekeri*, mass spectrometry-based lipidomics was used in this study. As the liver is a central player in lipid metabolism, the differences in lipid profiles of the liver among 10°C, 13°C, 16°C, and 19°C groups were investigated. Significant lipid remodeling was observed in *T. bleekeri* with increasing temperature. The contents of PC, TAG, and PE account for the majority of differential lipids. PC and PE, which act as structural lipids, are an essential component of the cellular membrane (Coskun and Simons, 2011). In fish, the phospholipid composition of the cell membrane was altered by temperature (Farkas et al., 2001; Grim et al., 2010). In rainbow trout (*Oncorhynchus mykiss*), the levels of PC and lysophosphatidylcholine (LysoPC) in the liver were reduced after exposure to high temperatures (Li et al., 2022). Here, most of the glycerophospholipids containing polyunsaturated fatty acids (PUFAs), such as PC 18:5-22:6 and PE 22:4e-20:5, were downregulated in the 19°C group (Supplementary Table A.5.). It suggests that these PUFAs play an imporatnt role in lipid remodeling in *T. bleekeri* under high temperatures, since the proportion of saturated and unsaturated acyl chains in membrane lipids is closely related to membrane viscosity and fluidity (Ernst et al., 2016). Fatty acids are also an important component of membrane phospholipids as well as a major energy source that play crucial physiological roles in various tissues (Wakil and Abu-Elheiga, 2009). The previous studies

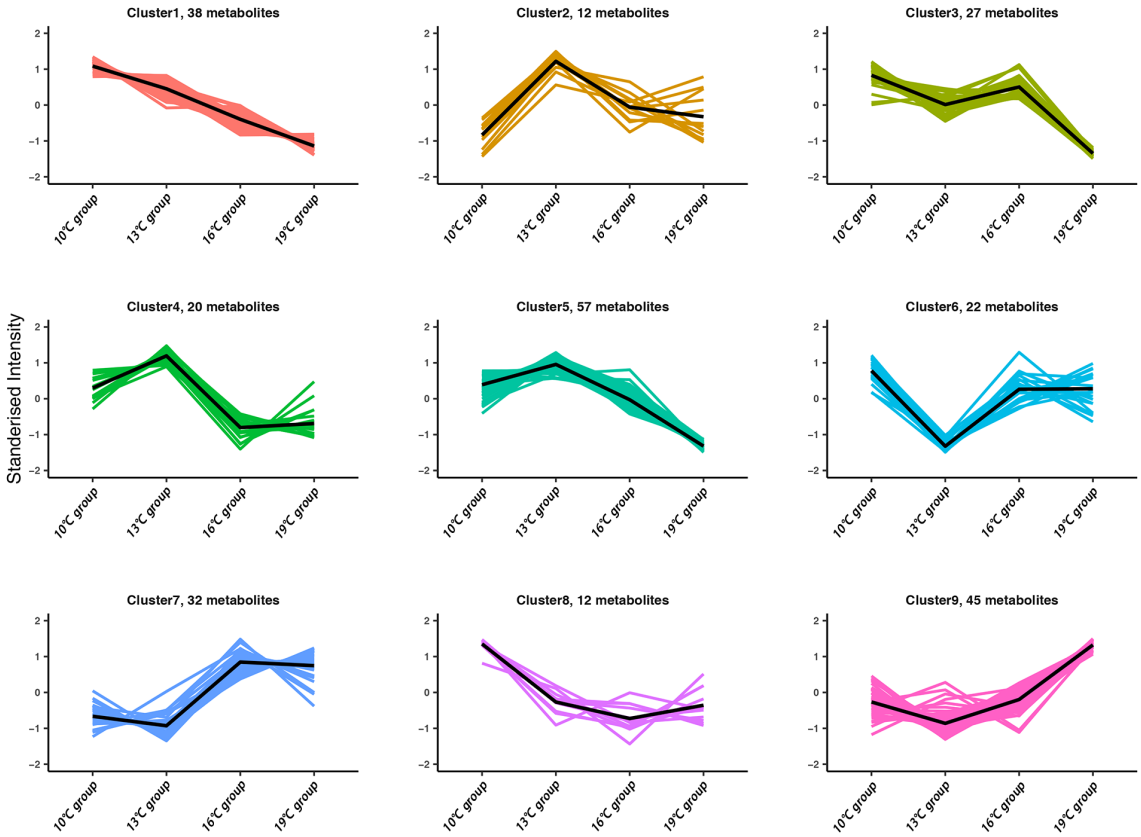

FIGURE 4
Dynamic change of differential lipids with increasing temperature.

showed that fatty acids are involved in metabolic response to temperature changes. In Antarctic notothenioid fish, high temperature (6°C) induced the saturated fatty acids, and reduced the unsaturated fatty acids (Malekar et al., 2018). Conversely, the content of unsaturated fatty acids increased to maintain membrane fluidity in fish at low temperatures (Grim et al., 2010; He et al., 2015). In this study, PUFAs, such as linolenic acid (C18:3, n-6), docosatetraenoic acid (C22:4, n-6), and docosapentaenoic acid (C22:5, n-3), were significantly decreased in the 19°C group. To sum up, altered lipid saturation in response to temperature change is a major thermal acclimation mechanism. Except above-mentioned n-3/n-6 PUFAs, palmitic acid (C16:0), palmitoleic acid (C16:1), and octadecenoic acid (C18:1) significantly decreased in the 19°C group. Accumulation of fatty acyls containing either n-3 or n-6 indicates the reduced utility of these fatty acids through oxidation, whereas an increase in 16:0, 16:1, 18:0, and 18:1 fatty acids indicates their increased *de novo* biosynthesis under physiological conditions (Han, 2016). Hence, we speculated that high temperatures decrease lipid biosynthesis but enhance fatty acid oxidation in *T. bleekeri*. RNA-seq results also support the hypothesis that the genes involved in the biosynthesis of phospholipids and TAG, such as *phosphatidate phosphatase-1* (*lipin-1*) (Bou Khalil et al., 2009), were downregulated in the 19° C group (Supplementary Table A.3). Conversely, *phospholipase B1* (*PLB1*), which is involved in the degradation of phospholipids (Wright et al., 2007), was upregulated in the 19° C group (Supplementary Table A.4). Besides, the expression of *CPT1A* in the liver, gut, spleen, and trunk kidney was upregulated at 19°C (Supplementary Table A.4). CPT1A, a major rate-limiting enzyme, participates in the fatty acid β-oxidation process and plays an essential role in maintaining energy homeostasis (Schlaepfer and Joshi, 2020). The similar results also observed in *Salmo salar* that increasing temperature significantly reduced levels of genes (*fas*, *cpla2*, and *elovl2*) related to fatty acid biosynthesis, and increased levels of *CPT1A* and *pparα* involved in fatty acid β-oxidation (Norambuena et al., 2015). Hence, lipid biosynthesis were suppressed, whereas fatty acid β-oxidation was enhanced in fish at high temperature.

High temperatures affect lipid metabolism and influence carbohydrate metabolism. A previous study showed that the

concentrations of glycogen in *Notothenia coriiceps* rapidly increased, followed by a decline, in response to varying glucose-6-phosphatase (G6Pase) levels after exposure to high temperatures (Forgati et al., 2017). The acute increase in temperature reduced glycolysis in the heart of *Notothenia rossii*, while the opposite result was observed in the muscle (Souza et al., 2018). In *Scophthalmus maximus*, high temperatures increased expression levels of *G6Pase*, a key

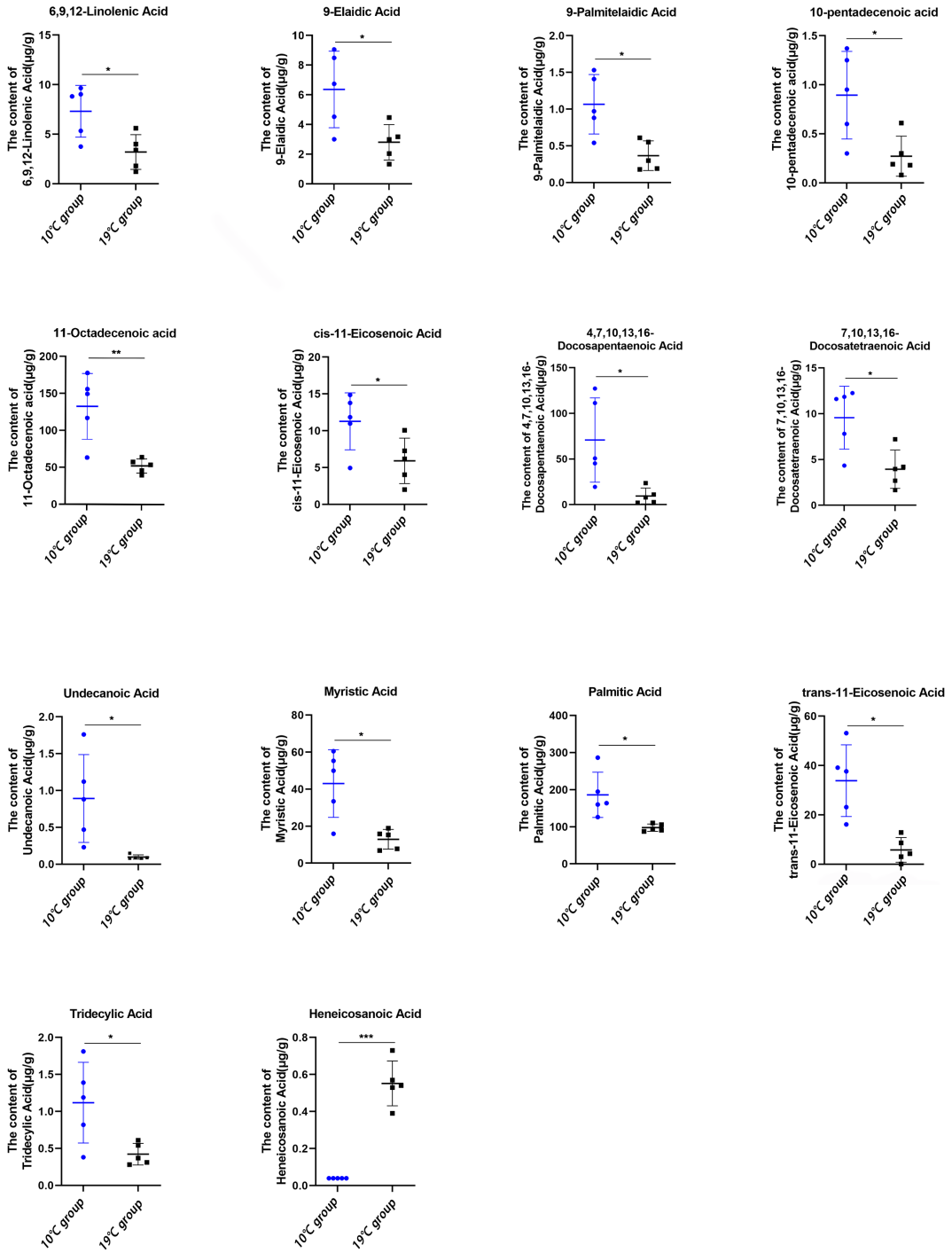

FIGURE 5
Absolute concentration of free fatty acids in the liver between the 10°C and 19°C groups. *p < 0.05, **p < 0.01, ***p < 0.001.

enzyme of gluconeogenesis, suggesting that gluconeogenesis was activated to cope with thermal stress (Yang et al., 2020). In this study, our results showed that DEGs were significantly enriched in the glycogen, glucose, hexose, oligosaccharide, and monosaccharide metabolic process. Further, the expression level of *glucose-6-phosphate dehydrogenase* (*G6PD*), which catalyzes the first step in the pentose phosphate pathway, was significantly increased, whereas the expression level of *6-phosphofructokinase* (*Pfk*), a critical rate-limiting enzyme in the process of glycolysis, was significantly decreased in the 19°C group. We speculated that high temperatures decrease glycolysis, but enhance the pentose phosphate pathway in *T. bleekeri*.

Apart from energy metabolism, many key physiological processes, such as immune, stress resistance, and DNA repair systems are strongly affected by high temperatures. In *Oreochromis mossambicus*, the immune parameters such as leucocyte count, phagocytic activity, and phagocytic index decreased when fish was transferred to high temperatures, suggesting that high temperatures reduced the immune capability of fish (Ndong et al., 2007). In *Salmo salar*, temperature increase negatively affected complement bacteriolytic activity (Jokinen et al., 2011). In *T. Bleekeri*, DEGs were significantly enriched in the Hippo signal pathway, NOD-like receptors signal pathway, and RIG-I-like receptor signaling pathway (Supplementary Table A.4). All these pathways play an indispensable role in the innate immune system (Fritz et al., 2006; Zeng et al., 2010; Zhang et al., 2018). Further, genes related to innate immune function, such as *interferon regulatory factor 3* (*IRF3*) and *CXC chemokine receptor 1* (*CXCR1*) were significantly downregulated in the 19°C group. Therefore, we speculated that the innate immunity of *T. Bleekeri* was diminished by high temperatures. Arachidonic acid (ARA) not only takes part in modulation of lipid metabolism, but also act an esstensial role in stress resistance (Xu et al., 2022). The STEM analysis showed the expression of genes involved in arachidonic acid metabolism significantly increased in *T. bleekeri* with increasing temperature.The previous study showed that *Solea senegalensis* prefers to select a diet rich in ARA with the seasonal temperature changes (Norambuena et al., 2012). In *Morone saxatilis*, higher dietary ARA improved the productive performance under sub-optimal temperatures (Araújo et al., 2021). These results suggest ARA act roles in thermal stress resistance. High temperatures induced the generation of reactive oxygen species (ROS) and antioxidant proteins (Devireddy et al., 2021). In *T. bleekeri*, we found that the expression level of glutathione peroxidase (GPX) increased under high temperatures. GPX, a key enzymes in the antioxidant system, protect organisms from oxidative stresses (Srikanth et al., 2013). It suggests that *T. bleekeri* initiates the expression of GPX to reduce the negative effects of oxidative damage induced by high temperature. Furthermore, increased DNA damage was observed in many species of fish exposed to high temperatures (Cheng et al., 2018; Castro et al., 2020). Here, STEM analysis showed that the expression levels of genes involved in Fanconi anemia pathway and DNA repair and recombination pathway constantly increased along with increasing temperature. These pathways all participate in DNA repair (Kim and D'andrea, 2012), which suggests that *T. bleekeri* may exhibit functional acclimation to increased temperatures.

Conclusion

In this study, transcriptomics and lipidomics approaches were used to comprehensively study effects of high temperatures on the transcriptional and metabolic levels of *T. bleekeri*. High temperatures induced a series of transcriptional plasticity responses in *T. bleekeri*, which resulted in altered levels of lipid metabolites. The decreased unsaturated fatty acid levels found in the lipidomics analysis were consistent with the downregulated genes involved in the lipid biosynthesis pathway found by RNA sequencing. Our results thus suggest that lipid metabolism was altered by temperature increase. Further, three lipids (PC 14:0e/22:1, PC 18:0e/22:5, and TAG 14:3-21:2-21:2) which showed rising content with increasing temperature and consequently, high content under high temperatures were identified as potential biomarkers of heat stress in *T. bleekeri*. However, further studies should be explored to identify whether these lipids can also be used as biomarkers of heat stress in other fishes. Overall, our results help improve the understanding of transcriptional and metabolic variations in fish in response to high temperatures, and provide essential information for forecasting potential impacts of global warming on fish biology.

Data availability statement

The datasets presented in this study can be found in online repositories. The names of the repository/repositories and accession number(s) can be found in the article/Supplementary Material.

Ethics statement

The animal study was reviewed and approved by Institutional Animal Care and Use Committee of Southwest University.

Author contributions

ZW and DY conceived and designed the study. DY, XC, HG, and SW collected the samples. DY, XL, and JS performed the molecular experiments. HW, DY, and SX performed the bioinformatics analysis. DY, SX, and ZW wrote the

manuscript. All authors contributed to the article and approved the submitted version.

Funding

This work was supported by the Fundamental Research Funds for the Central Universities (Grant No. SWU-KQ22016), and the National Natural Science Foundation of China (Grant No. 32072980).

Acknowledgments

We gratefully acknowledge the assistance of Biotree Bio-Technique Co., Ltd. (Shanghai, China) in metabolomics analysis.

Conflict of interest

The authors declare that the research was conducted in the absence of any commercial or financial relationships that could be construed as a potential conflict of interest.

Publisher's note

All claims expressed in this article are solely those of the authors and do not necessarily represent those of their affiliated organizations, or those of the publisher, the editors and the reviewers. Any product that may be evaluated in this article, or claim that may be made by its manufacturer, is not guaranteed or endorsed by the publisher.

Supplementary material

The Supplementary Material for this article can be found online at: https://www.frontiersin.org/articles/10.3389/fmars.2022.1017142/full#supplementary-material

SUPPLEMENTARY TABLE 3
Differentially expressed genes in the liver, gut, spleen, and trunk kidney among four temperature groups.

SUPPLEMENTARY TABLE 4
KEGG and GO enrichment results of differentially expressed genes between the 19°C and 10°C groups.

SUPPLEMENTARY TABLE 5
The differential lipids in the liver among four temperature groups.

SUPPLEMENTARY TABLE 6
The differential lipids of each cluster identified by k-means analysis.

SUPPLEMENTARY FIGURE 1
Significantly differentially expressed genes. **(A)** The shared differentially expressed genes of 4 tissues between the 19°C and 10°C groups. **(B)** Significantly differentially expressed genes involved in energy metabolism and immune response.

SUPPLEMENTARY FIGURE 2
Comparisons between RNA-seq and qPCR results.

SUPPLEMENTARY FIGURE 3
Expression patterns of genes identified by STEM analysis.

SUPPLEMENTARY FIGURE 4
Score scatter plot of the OPLS-DA model.

References

Alfonso, S., Gesto, M., and Sadoul, B. (2021). Temperature increase and its effects on fish stress physiology in the context of global warming. *J. Fish. Biol.* 98, 1496–1508. doi: 10.1111/jfb.14599

Araújo, B. C., Rodriguez, M., Honji, R. M., Rombenso, A. N., Rio-Zaragoza, O. B., and Cano, A. (2021). Arachidonic acid modulated lipid metabolism and improved productive performance of striped bass (*Morone saxatilis*) juvenile under sub-to optimal temperatures. *Aquaculture.* 364-365, 198–205. doi: 10.1016/j.aquaculture.2020.735939

Balbuena-Pecino, S., Riera-Heredia, N., Vélez, E. J., Gutiérrez, J., Navarro, I., Riera-Codina, M., et al. (2019). Temperature affects musculoskeletal development and muscle lipid metabolism of gilthead sea bream (*Sparus aurata*). *Front. Endocrinol.* 10. doi: 10.3389/fendo.2019.00173

Barat, A., Sahoo, P. K., Kumar, R., Goel, C., and Singh, A. K. (2016). Transcriptional response to heat shock in liver of snow trout (*Schizothorax richardsonii*)–a vulnerable Himalayan cyprinid fish. *Funct. Integr. Genomics* 16, 203–213. doi: 10.1007/s10142-016-0477-0

Barbarossa, V., Bosmans, J., Wanders, N., King, H., Bierkens, M. F. P., Huijbregts, M. A. J., et al. (2021). Threats of global warming to the world's freshwater fishes. *Nat. Commun.* 12, 1701. doi: 10.1038/s41467-021-21655-w

Bou Khalil, M., Sundaram, M., Zhang, H. Y., Links, P. H., Raven, J. F., Manmontri, B., et al. (2009). The level and compartmentalization of phosphatidate phosphatase-1 (lipin-1) control the assembly and secretion of hepatic VLDL. *J. Lipid Res.* 50, 47–58. doi: 10.1194/jlr.M800204-JLR200

Castro, J. S., Braz-Mota, S., Campos, D. F., Souza, S. S., and Val, A. L. (2020). High temperature, pH, and hypoxia cause oxidative stress and impair the spermatic performance of the Amazon fish *Colossoma macropomum*. *Front. Physiol.* 11. doi: 10.3389/fphys.2020.00772

Chen, C., Chen, H., Zhang, Y., Thomas, H. R., Frank, M. H., He, Y., et al. (2020). TBtools: an integrative toolkit developed for interactive analyses of big biological data. *Mol. Plant* 13, 1194–1202. doi: 10.1016/j.molp.2020.06.009

Cheng, C. H., Guo, Z. X., Luo, S. W., and Wang, A. L. (2018). Effects of high temperature on biochemical parameters, oxidative stress, DNA damage and apoptosis of pufferfish (*Takifugu obscurus*). *Ecotoxicol. Environ. Saf.* 150, 190–198. doi: 10.1016/j.ecoenv.2017.12.045

Chen, Y., Liu, E., Li, C., Pan, C., Zhao, X., Wang, Y., et al. (2021). Effects of heat stress on histopathology, antioxidant enzymes, and transcriptomic profiles in gills of pikeperch *Sander lucioperca*. *Aquaculture* 534, 736277. doi: 10.1016/j.aquaculture.2020.736277

Coskun, U., and Simons, K. (2011). Cell membranes: The lipid perspective. *Structure.* 19, 1543–1548. doi: 10.1016/j.str.2011.10.010

Crozier, L. G., and Hutchings, J. A. (2014). Plastic and evolutionary responses to climate change in fish. *Evol. Appl.* 7, 68–87. doi: 10.1111/eva.12135

Dadras, H., Dzyuba, B., Cosson, J., Golpour, A., Siddique, M. A. M., and Linhart, O. (2017). Effect of water temperature on the physiology of fish spermatozoon function: a brief review. *Aquac. Res.* 48, 729–740. doi: 10.1111/are.13049

Devireddy, A. R., Tschaplinski, T. J., Tuskan, G. A., Muchero, W., and Chen, J. G. (2021). Role of reactive oxygen species and hormones in plant responses to temperature changes. *Int. J. Mol. Sci.* 22 (16), 8843. doi: 10.3390/ijms22168843

Donaldson, M. R., Cooke, S. J., Patterson, D. A., and Macdonald, J. S. (2008). Cold shock and fish. *J. Fish. Biol.* 73, 1491–1530. doi: 10.1111/j.1095-8649.2008.02061.x

Ecker, S., Pancaldi, V., Valencia, A., Beck, S., and Paul, D. S. (2018). Epigenetic and transcriptional variability shape phenotypic plasticity. *BioEssays* 40, 1700148. doi: 10.1002/bies.201700148

Ernst, J., and Bar-Joseph, Z. (2006). STEM: A tool for the analysis of short time series gene expression data. *BMC Bioinf.* 7, 191. doi: 10.1186/1471-2105-7-191

Ernst, R., Ejsing, C. S., and Antonny, B. (2016). Homeoviscous adaptation and the regulation of membrane lipids. *J. Mol. Biol.* 428, 4776–4791. doi: 10.1016/j.jmb.2016.08.013

Farkas, T., Fodor, E., Kitajka, K., and Halver, J. (2001). Response of fish membranes to environmental temperature. *Aquac. Res.* 32, 645–655. doi: 10.1046/j.1365-2109.2001.00600.x

Forgati, M., Kandalski, P. K., Herrerias, T., Zaleski, T., Machado, C., Souza, M. R. D. P., et al. (2017). Effects of heat stress on the renal and branchial carbohydrate metabolism and antioxidant system of Antarctic fish. *J. Comp. Physiol. B.* 187, 1137–1154. doi: 10.1007/s00360-017-1088-3

Free, C. M., Thorson, J. T., Pinsky, M. L., Oken, K. L., Wiedenmann, J., and Jensen, O. P. (2019). Impacts of historical warming on marine fisheries production. *Science.* 363, 979–983. doi: 10.1126/science.aau1758

Fritz, J. H., Ferrero, R. L., Philpott, D. J., and Girardin, S. E. (2006). Nod-like proteins in immunity, inflammation and disease. *Nat. Immunol.* 7, 1250–1257. doi: 10.1038/ni1412

Grim, J. M., Miles, D. R., and Crockett, E. L. (2010). Temperature acclimation alters oxidative capacities and composition of membrane lipids without influencing activities of enzymatic antioxidants or susceptibility to lipid peroxidation in fish muscle. *J. Exp. Biol.* 213, 445–452. doi: 10.1242/jeb.036939

Guo, L., Wang, Y., Liang, S., Lin, G., Chen, S., and Yang, G. (2016). Tissue-overlapping response of half-smooth tongue sole (*Cynoglossus semilaevis*) to thermostressing based on transcriptome profiles. *Gene* 586, 97–104. doi: 10.1016/j.gene.2016.04.020

Han, X. (2016). *Lipidomics: Comprehensive mass spectrometry of lipids* (Hoboken, NJ: John Wiley & Sons). doi: 10.1002/9781119085263.ch5

He, J., Qiang, J., Yang, H., Xu, P., Zhu, Z. X., and Yang, R. Q. (2015). Changes in the fatty acid composition and regulation of antioxidant enzymes and physiology of juvenile genetically improved farmed tilapia *Oreochromis niloticus* (L.), subjected to short-term low temperature stress. *J. Therm. Biol.* 53, 90–97. doi: 10.1016/j.jtherbio.2015.08.010

Holman, J. D., Tabb, D. L., and Mallick, P. (2014). Employing ProteoWizard to convert raw mass spectrometry data. *Curr. Protoc. Bioinf* 46, 13.24.1–13.24.9. doi: 10.1002/0471250953.bi1324s46

Huang, J., Li, Y., Liu, Z., Kang, Y., and Wang, J. (2018). Transcriptomic responses to heat stress in rainbow trout *Oncorhynchus mykiss* head kidney. *Fish. Shellfish. Immunol.* 82, 32–40. doi: 10.1016/j.fsi.2018.08.002

Jeffries, K. M., Connon, R. E., Davis, B. E., Komoroske, L. M., Britton, M. T., Sommer, T., et al. (2016). Effects of high temperatures on threatened estuarine fishes during periods of extreme drought. *J. Exp. Biol.* 219, 1705–1716. doi: 10.1242/jeb.134528

Jokinen, I. E., Salo, H. M., Markkula, E., Rikalainen, K., Arts, M. T., and Browman, H. I. (2011). Additive effects of enhanced ambient ultraviolet b radiation and increased temperature on immune function, growth and physiological condition of juvenile (parr) Atlantic salmon, *Salmo salar*. *Fish. Shellfish. Immunol.* 30, 102–108. doi: 10.1016/j.fsi.2010.09.017

Keen, A. N., Klaiman, J. M., Shiels, H. A., and Gillis, T. E. (2017). Temperature-induced cardiac remodelling in fish. *J. Exp. Biol.* 220, 147–160. doi: 10.1242/jeb.128496

Kim, D., Langmead, B., and Salzberg, S. L. (2015). HISAT: a fast spliced aligner with low memory requirements. *Nat. Methods* 12, 357–360. doi: 10.1038/nmeth.3317

Kind, T., Liu, K. H., Lee, D. Y., DeFelice, B., Meissen, J. K., and Fiehn, O. (2013). LipidBlast in silico tandem mass spectrometry database for lipid identification. *Nat. Methods* 10, 755–758. doi: 10.1038/nmeth.2551

Li, Y., Huang, J., Liu, Z., Zhou, Y., Xia, B., Wang, Y., et al. (2017). Transcriptome analysis provides insights into hepatic responses to moderate heat stress in the rainbow trout (*Oncorhynchus mykiss*). *Gene* 619, 1–9. doi: 10.1016/j.gene.2017.03.041

Li, L., Liu, Z., Quan, J., Lu, J., Zhao, G., and Sun, J. (2022). Metabonomics analysis reveals the protective effect of nano−selenium against heat stress of rainbow trout (*Oncorhynchus mykiss*). *J. Proteomics.* 259, 104545. doi: 10.1016/j.jprot.2022.104545

Li, A., Li, L., Zhang, Z. Y., Li, S. M., Wang, W., Guo, X. M., et al. (2021). Noncoding variation and transcriptional plasticity promote thermal adaptation in oysters by altering energy metabolism. *Mol. Biol. Evol.* 38, 5144–5155. doi: 10.1093/molbev/msab241

Liu, L., Zhang, R., Wang, X., Zhu, H., and Tian, Z. (2020). Transcriptome analysis reveals molecular mechanisms responsive to acute cold stress in the tropical stenothermal fish tiger barb (*Puntius tetrazona*). *BMC Genomics* 21, 1–14. doi: 10.1186/s12864-020-07139-z

Long, Y., Li, X., Li, F., Ge, G., Liu, R., Song, G., et al. (2020). Transcriptional programs underlying cold acclimation of common carp (*Cyprinus carpio* l.). *Front. Genet.* 11. doi: 10.3389/fgene.2020.556418

Long, Y., Li, L., Li, Q., He, X., and Cui, Z. (2012). Transcriptomic characterization of temperature stress responses in larval zebrafish. *PLoS. One* 7, e37209. doi: 10.1371/journal.pone.0037209

Love, M. I., Huber, W., and Anders, S. (2014). Moderated estimation of fold change and dispersion for RNA-seq data with DESeq2. *Genome Biol.* 15, 550. doi: 10.1186/s13059-014-0550-8

Lyu, L., Wen, H., Li, Y., Li, J., Zhao, J., Zhang, S., et al. (2018). Deep transcriptomic analysis of black rockfish (*Sebastes schlegelii*) provides new insights on responses to acute temperature stress. *Sci. Rep.* 8, 9113. doi: 10.1038/s41598-018-27013-z

Malekar, V. C., Morton, J. D., Hider, R. N., Cruickshank, R. H., Hodge, S., and Metcalf, V. J. (2018). Effect of elevated temperature on membrane lipid saturation in Antarctic notothenioid fish. *PeerJ* 6, e4765. doi: 10.7717/peerj.4765

Narum, S. R., and Campbell, N. R. (2015). Transcriptomic response to heat stress among ecologically divergent populations of redband trout. *BMC Genomics* 16, 103. doi: 10.1186/s12864-015-1246-5

Ndong, D., Chen, Y. Y., Lin, Y. H., Vaseeharan, B., and Chen, J. C. (2007). The immune response of tilapia *Oreochromis mossambicus* and its susceptibility to *Streptococcus iniae* under stress in low and high temperatures. *Fish. Shellfish. Immunol.* 22, 686–694. doi: 10.1016/j.fsi.2006.08.015

Nilsson, G. E., Crawley, N., Lunde, I. G., and Munday, P. L. (2009). Elevated temperature reduces the respiratory scope of coral reef fishes. *Global Change Biol.* 15, 1405–1412. doi: 10.1111/j.1365-2486.2008.01767.x

Norambuena, F., Estévez, A., Sánchez-Vázquez, F. J., Carazo, I., and Duncan, N. (2012). Self-selection of diets with different contents of arachidonic acid by Senegalese sole (*Solea senegalensis*) broodstock. *Aquaculture.* 364, 198–205. doi: 10.1016/j.aquaculture.2012.08.016

Norambuena, F., Morais, S., Emery, J. A., and Turchini, G. M. (2015). Arachidonic acid and eicosapentaenoic acid metabolism in juvenile Atlantic salmon as affected by water temperature. *PloS One* 10, e0143622. doi: 10.1371/journal.pone.0143622

Norin, T., Malte, H., and Clark, T. D. (2016). Differential plasticity of metabolic rate phenotypes in a tropical fish facing environmental change. *Funct. Ecol.* 30, 369–378. doi: 10.1111/1365-2435.12503

Oomen, R. A., and Hutchings, J. A. (2017). Transcriptomic responses to environmental change in fishes: Insights from RNA sequencing. *Facets.* 2, 610–641. doi: 10.1139/facets-2017-0015

Paul, N., Novais, S. C., Silva, C. S. E., Mendes, S., Kunzmann, A., and Lemos, M. F. L. (2021). Global warming overrides physiological anti-predatory mechanisms in intertidal rock pool fish *Gobius paganellus*. *Sci. Total Environ.* 776, 145736. doi: 10.1016/j.scitotenv.2021.145736

Pigliucci, M., Murren, C. J., and Schlichting, C. D. (2006). Phenotypic plasticity and evolution by genetic assimilation. *J. Exp. Biol.* 209, 2362–2367. doi: 10.1242/jeb.02070

Punzón, A., Serrano, A., Sánchez, F., Velasco, F., Preciado, I., González-Irusta, J. M., et al. (2016). Response of a temperate demersal fish community to global warming. *J. Mar. Syst.* 161, 1–10. doi: 10.1016/j.jmarsys.2016.05.001

Schlaepfer, I. R., and Joshi, M. (2020). CPT1A-mediated fat oxidation, mechanisms, and therapeutic potential. *Endocrinology.* 161, bqz046. doi: 10.1210/endocr/bqz046

Smith, S., Bernatchez, L., and Beheregaray, L. B. (2013). RNA-Seq analysis reveals extensive transcriptional plasticity to temperature stress in a freshwater fish species. *BMC Genomics* 14, 375. doi: 10.1186/1471-2164-14-375

Souza, M. R. D. P., Herrerias, T., Zaleski, T., Forgati, M., Kandalski, P. K., Machado, C., et al. (2018). Heat stress in the heart and muscle of the Antarctic fishes *Notothenia rossii* and *Notothenia coriiceps*: carbohydrate metabolism and antioxidant defence. *Biochimie* 146, 43–55. doi: 10.1016/j.biochi.2017.11.010

Srikanth, K., Pereira, E., Duarte, A. C., and Ahmad, I. (2013). Glutathione and its dependent enzymes' modulatory responses to toxic metals and metalloids in fish–a review. *Environ. Sci. pollut. Res.* 20, 2133–2149. doi: 10.1007/s11356-012-1459-y

Tautenhahn, R., Patti, G. J., Rinehart, D., and Siuzdak, G. (2012). XCMS online: a web-based platform to process untargeted metabolomic data. *Anal. Chem.* 84, 5035–5039. doi: 10.1021/ac300698c

Veilleux, H. D., Ryu, T., Donelson, J. M., van Herwerden, L. V., Seridi, L., Ghosheh, Y., et al. (2015). Molecular processes of transgenerational acclimation to a warming ocean. *Nat. Clim. Change.* 5, 1074–1078. doi: 10.1038/nclimate2724

Wakil, S. J., and Abu-Elheiga, L. A. (2009). Fatty acid metabolism: target for metabolic syndrome. *J. Lipid Res.* 50 Supplement, S138–S143. doi: 10.1194/jlr.R800079-JLR200

Wang, Z. J. (2013). *The reproductive biology and hematology of triplophysa bleekeri from daning river (Southwest university)*.

Wang, Z., Huang, J., and Zhang, Y. (2013). The reproductive traits of *Triplophysa bleekeri* in the daning river. *Freshw. Fish.* (Chongqing, China: Southwest University) 43, 8–12. doi: 10.3969/j.issn.1000-6907.2013.05.002

Wellband, K. W., and Heath, D. D. (2017). Plasticity in gene transcription explains the differential performance of two invasive fish species. *Evol. Appl.* 10, 563–576. doi: 10.1111/eva.12463

Wen, B., Jin, S. R., Chen, Z. Z., and Gao, J. Z. (2018). Physiological responses to cold stress in the gills of discus fish (*Symphysodon aequifasciatus*) revealed by conventional biochemical assays and GC-TOF-MS metabolomics. *Sci. Total Environ.* 640–641, 1372–1381. doi: 10.1016/j.scitotenv.2018.05.401

Wright, L. C., Santangelo, R. M., Ganendren, R., Payne, J., Djordjevic, J. T., and Sorrell, T. C. (2007). Cryptococcal lipid metabolism: phospholipase B1 is implicated in transcellular metabolism of macrophage-derived lipids. *Eukaryot. Cell.* 6, 37–47. doi: 10.1128/EC.00262-06

Xu, H., Meng, X., Wei, Y., Ma, Q., Liang, M., and Turchini, G. M. (2022). Arachidonic acid matters. *Rev. Aquacult.* 1, 1–33. doi: 10.1111/raq.12679

Yang, S., Zhao, T., Ma, A., Huang, Z., Liu, Z., Cui, W., et al. (2020). Metabolic responses in *Scophthalmus maximus* kidney subjected to thermal stress. *Fish. Shellfish. Immunol.* 103, 37–46. doi: 10.1016/j.fsi.2020.04.003

Yuan, D., Chen, X., Gu, H., Zou, M., Zou, Y., Fang, J., et al. (2020). Chromosomal genome of *Triplophysa bleekeri* provides insights into its evolution and environmental adaptation. *GigaScience* 9, giaa132. doi: 10.1093/gigascience/giaa132

Yuan, D. Y., Wang, B., Tang, T., Lei, L., Zhou, C. W., Li, Z. Q., et al. (2021). Characterization and evaluation of the tissue distribution of CRH, apelin, and GnRH2 reveal responses to feeding states in *Schizothorax davidi*. fish physiol. *Biochem.* 47, 421–438. doi: 10.1007/s10695-020-00922-5

Zeng, W., Sun, L., Jiang, X., Chen, X., Hou, F., Adhikari, A., et al. (2010). Reconstitution of the RIG-I pathway reveals a signaling role of unanchored polyubiquitin chains in innate immunity. *Cell* 141, 315–330. doi: 10.1016/j.cell.2010.03.029

Zhang, X., Liu, L., Wang, L., Pan, Y., Hao, X., Zhang, G., et al. (2021). Comparative lipidomics analysis of human milk and infant formulas using UHPLC-Q-TOF-MS. *J. Agric. Food Chem.* 69, 1146–1155. doi: 10.1021/acs.jafc.0c06940

Zhang, Y., Zhang, H., and Zhao, B. (2018). Hippo signaling in the immune system. *Trends Biochem. Sci.* 43, 77–80. doi: 10.1016/j.tibs.2017.11.009

Zhao, T., Ma, A., Huang, Z., Liu, Z., Sun, Z., Zhu, C., et al. (2021). Transcriptome analysis reveals that high temperatures alter modes of lipid metabolism in juvenile turbot (Scophthalmus maximus) liver. *Comp. Biochem. Physiol. Part D. Genomics Proteomics.* 40, 100887. doi: 10.1016/j.cbd.2021.100887

Zhou, T., Gui, L., Liu, M., Li, W., Hu, P., Duarte, D. F., et al. (2019). Transcriptomic responses to low temperature stress in the Nile tilapia, *Oreochromis niloticus*. *Fish. Shellfish. Immunol.* 84, 1145–1156. doi: 10.1016/j.fsi.2018.10.023

frontiers | Frontiers in Marine Science

TYPE Review
PUBLISHED 28 October 2022
DOI 10.3389/fmars.2022.977754

OPEN ACCESS

EDITED BY
Hongsheng Yang,
Institute of Oceanology (CAS), China

REVIEWED BY
Gael John Lecellier,
Université de Versailles Saint-Quentin-en-Yvelines, France
Alessandra Gallo,
Stazione Zoologica Anton Dohrn Napoli, Italy

*CORRESPONDENCE
Jacqueline L. Padilla-Gamiño
jpgamino@uw.edu

†These authors have contributed equally to this work

SPECIALTY SECTION
This article was submitted to Global Change and the Future Ocean, a section of the journal Frontiers in Marine Science

RECEIVED 24 June 2022
ACCEPTED 28 September 2022
PUBLISHED 28 October 2022

CITATION
Padilla-Gamiño JL, Alma L, Spencer LH, Venkataraman YR and Wessler L (2022) Ocean acidification does not overlook sex: Review of understudied effects and implications of low pH on marine invertebrate sexual reproduction.
Front. Mar. Sci. 9:977754.
doi: 10.3389/fmars.2022.977754

Ocean acidification does not overlook sex: Review of understudied effects and implications of low pH on marine invertebrate sexual reproduction

Jacqueline L. Padilla-Gamiño[1*†], Lindsay Alma[1,2†], Laura H. Spencer[1,3†], Yaamini R. Venkataraman[1,4†] and Leah Wessler[1,5†]

[1]School of Aquatic and Fishery Sciences, College of the Environment, University of Washington, Seattle, WA, United States, [2]Bodega Marine Laboratory, Coastal and Marine Sciences Institute, College of Biological Sciences, University of California, Davis, Bodega Bay, CA, United States, [3]Alaska Fisheries Science Center, National Marine Fisheries Service, National Oceanic and Atmospheric Administration, Seattle, WA, United States, [4]Department of Biology, Woods Hole Oceanographic Institution, Woods Hole, MA, United States, [5]Land and Food Systems, University of British Columbia, Vancouver, BC, Canada

Sexual reproduction is a fundamental process essential for species persistence, evolution, and diversity. However, unprecedented oceanographic shifts due to climate change can impact physiological processes, with important implications for sexual reproduction. Identifying bottlenecks and vulnerable stages in reproductive cycles will enable better prediction of the organism, population, community, and global-level consequences of ocean change. This article reviews how ocean acidification impacts sexual reproductive processes in marine invertebrates and highlights current research gaps. We focus on five economically and ecologically important taxonomic groups: cnidarians, crustaceans, echinoderms, molluscs and ascidians. We discuss the spatial and temporal variability of experimental designs, identify trends of performance in acidified conditions in the context of early reproductive traits (gametogenesis, fertilization, and reproductive resource allocation), and provide a quantitative meta-analysis of the published literature to assess the effects of low pH on fertilization rates across taxa. A total of 129 published studies investigated the effects of ocean acidification on 122 species in selected taxa. The impact of ocean acidification is dependent on taxa, the specific reproductive process examined, and study location. Our meta-analysis reveals that fertilization rate decreases as pH decreases, but effects are taxa-specific. Echinoderm fertilization appears more sensitive than molluscs to pH changes, and while data are limited, fertilization in cnidarians may be the most sensitive. Studies with echinoderms and bivalve molluscs are prevalent, while crustaceans and cephalopods are among the least studied species even though they constitute some of the largest fisheries worldwide. This lack of information has important implications for commercial aquaculture, wild

fisheries, and conservation and restoration of wild populations. We recommend that studies expose organisms to different ocean acidification levels during the entire gametogenic cycle, and not only during the final stages before gametes or larvae are released. We argue for increased focus on fundamental reproductive processes and associated molecular mechanisms that may be vulnerable to shifts in ocean chemistry. Our recommendations for future research will allow for a better understanding of how reproduction in invertebrates will be affected in the context of a rapidly changing environment.

KEYWORDS

sperm, egg, fertilization, gametogenesis, fecundity, brooding, spawning, climate change

Introduction

Global climate change is impacting physical, biological, and chemical processes in the marine environment (Hoegh-Guldberg and Bruno, 2010; Howes et al., 2015; Shukla et al., 2019). Absorption of excess carbon dioxide by seawater lowers pH and reduces carbonate ion concentration and aragonite saturation state (Doney et al., 2009). These alterations in water chemistry are referred to as ocean acidification (OA) and can impact marine organisms at multiple levels of biological organization (Melzner et al., 2019). At the organismal level, changing chemistry can influence physiological processes (e.g., calcification, internal pH control, respiration and nutrient uptake), affecting performance and survival (Kroeker et al., 2010; Howes et al., 2015; Melzner et al., 2019). Although there is extensive research on the effects of OA in marine invertebrates, gaps in our understanding of how OA affects sexual reproductive processes (Figure 1) constrain predictions of species persistence, evolutionary adaptation, and biodiversity. For example, acidification could result in decoupling of biological and environmental cues, leading to reproductive failure with significant consequences for population dynamics in marine ecosystems (Shlesinger and Loya, 2019; Olischläger and Wild, 2020) (Figure 2).

Reproduction is a complex process that relies on numerous mechanisms (Figure 1, Box 1); using multiple parameters to evaluate reproductive performance is fundamental to predict how fitness may be impacted by future environmental conditions. OA research has centered around processes during early-life history stages (embryos, larvae, and juveniles), and previous reviews have synthesized trends in organismal responses to OA (Kurihara et al., 2008; Dupont et al., 2010; Albright, 2011b; Ross et al., 2011; Byrne and Przeslawski, 2013; Przeslawski et al., 2015; Ross et al., 2016; Foo and Byrne, 2017). While larval or juvenile performance can be indicative of successful reproduction, an appropriate chemical and physical environment for gamete development, spawning, mating behavior, and fertilization success is also crucial.

In 2016, nearly 26 million tons of invertebrates were produced for consumption *via* commercial aquaculture, comprising 32% of global aquaculture and 77% of marine and coastal aquaculture that year (FAO, 2018). Invertebrate aquaculture is increasingly leveraged by restoration groups to enhance wild populations that are struggling to recover naturally (Froehlich et al., 2017; Wasson et al., 2020). Both commercial and restoration aquaculture depend upon reliable sources of viable gametes or larvae, which are either produced in controlled hatchery conditions or collected from the wild (Helm et al., 2004; Washington Sea Grant, 2015). Aquaculture production could be hampered if acidification decreases reproductive capacity (Figure 2). In contrast to aquaculture, wild fisheries depend upon an organism's ability to reproduce in the natural environment; any impact of acidification on reproduction will directly influence wild stock available for fisheries. Threatened and endangered marine invertebrates increasingly require human interventions to conserve and restore populations (Elliott et al., 2007). Success of these programs is contingent upon a population's ability to persist naturally and successfully reproduce once interventions cease. Therefore, it is critical that aquaculture, fisheries, and conservation groups identify whether reproductive processes will be impacted by low pH, and how that will impact their focal species' abundance and distribution (Figure 2).

In this review we synthesize the literature to date that has explored how OA impacts reproductive processes of five ecologically, economically, and culturally important marine invertebrate taxa: cnidarians, crustaceans, echinoderms, molluscs, and ascidians. These groups play important roles as keystone species, ecological engineers, aquaculture and fishery products, and model organisms in developmental biology. Our synthesis identifies important gaps in knowledge of the physiological mechanisms involved in reproduction in response to OA in invertebrate taxa important to aquaculture,

fisheries, and conservation efforts. In addition to fertilization and brooding, we focus on pre-fertilization processes (Figure 1) that are poorly understood both mechanistically and in the context of climate change. Finally, we provide recommendations for future research to better understand how invertebrate sexual reproduction will be affected in the context of a rapidly changing environment.

Methods

To identify empirical studies for this review, we searched the literature databases ProQuest, Web of Science, Google Scholar, and European Project on Ocean Acidification (EPOCA) for articles published in English-language journals through the end of 2021 that examined the effects of OA on reproduction in our focal taxa (Table 1). Keywords included British and American spelling for each taxonomic group. We used Boolean search operators to specify or expand our search results. ProQuest, Web of Science, and Google Scholar queries were sorted by relevance and at minimum 350 results were manually reviewed. We searched all available papers on EPOCA. Google Scholar limits word count for each search, so we broke searches down into several iterations, using the list of common terms in each search and alternating through the taxa-specific terms. We included studies featuring experiments in laboratory and field conditions that included several spatial (m to km) and temporal (minutes to years) scales. We did not include gray literature or observational studies. Throughout the manuscript we will refer to ocean acidification, OA, low pH, or acidification interchangeably.

For each study, the effect of OA on reproduction was determined for the following processes: 1) sex determination, differentiation, and ratio, 2) gametogenesis and gamete quality, 3) fecundity and reproductive output, 4) timing of reproduction and synchronization, 5) mating behavior, and 6) fertilization (Figure 1). While we acknowledge that reproductive processes are linked, we define specific metrics associated with individual processes used to categorize all findings (Box 1). The number of independent findings per reproductive process was summarized

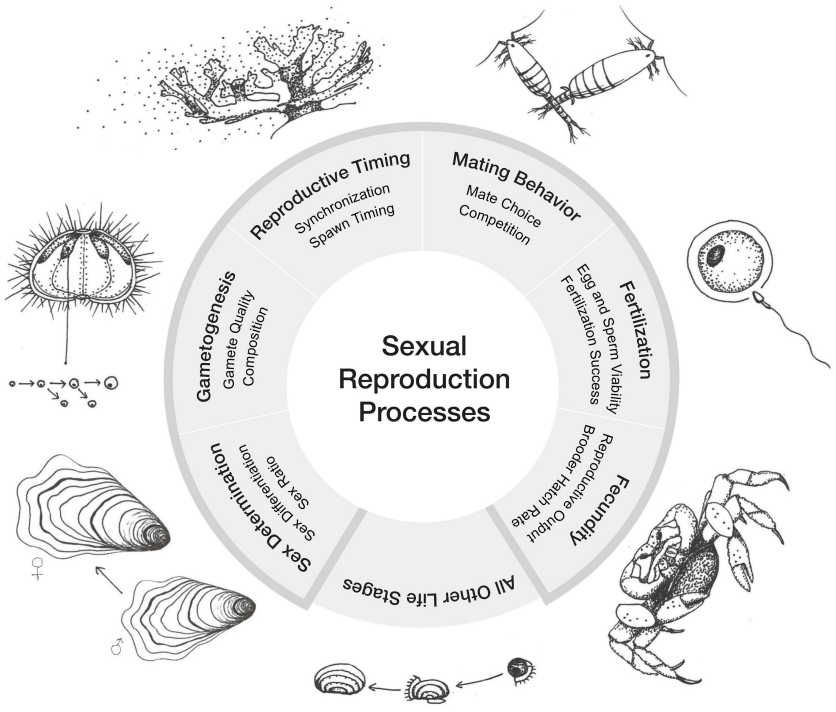

FIGURE 1
Sexual reproduction processes in marine invertebrates. The six processes discussed in this review are presented clockwise beginning with Sex Determination. Sex determination is the initial event that determines whether the gonads will develop as testes or ovaries and has great importance to the consideration of sex ratios, particularly for non-hermaphroditic species. Mechanisms for sex determination can be genetic or environmental. Sex differentiation is the development of sex differences after determination. Gametogenesis is the process of gamete formation which can lead to gametes with different characteristics (i.e., size, reserves, viability). Reproductive timing includes synchronization of gamete development, spawning, and any other reproductive process. Mate selection, courtship display, and mate guarding are common mating behaviors. Fertilization success depends on gamete quality, reproductive timing, mating behavior and synchronization. Fecundity is a measure of reproductive potential of an organism.

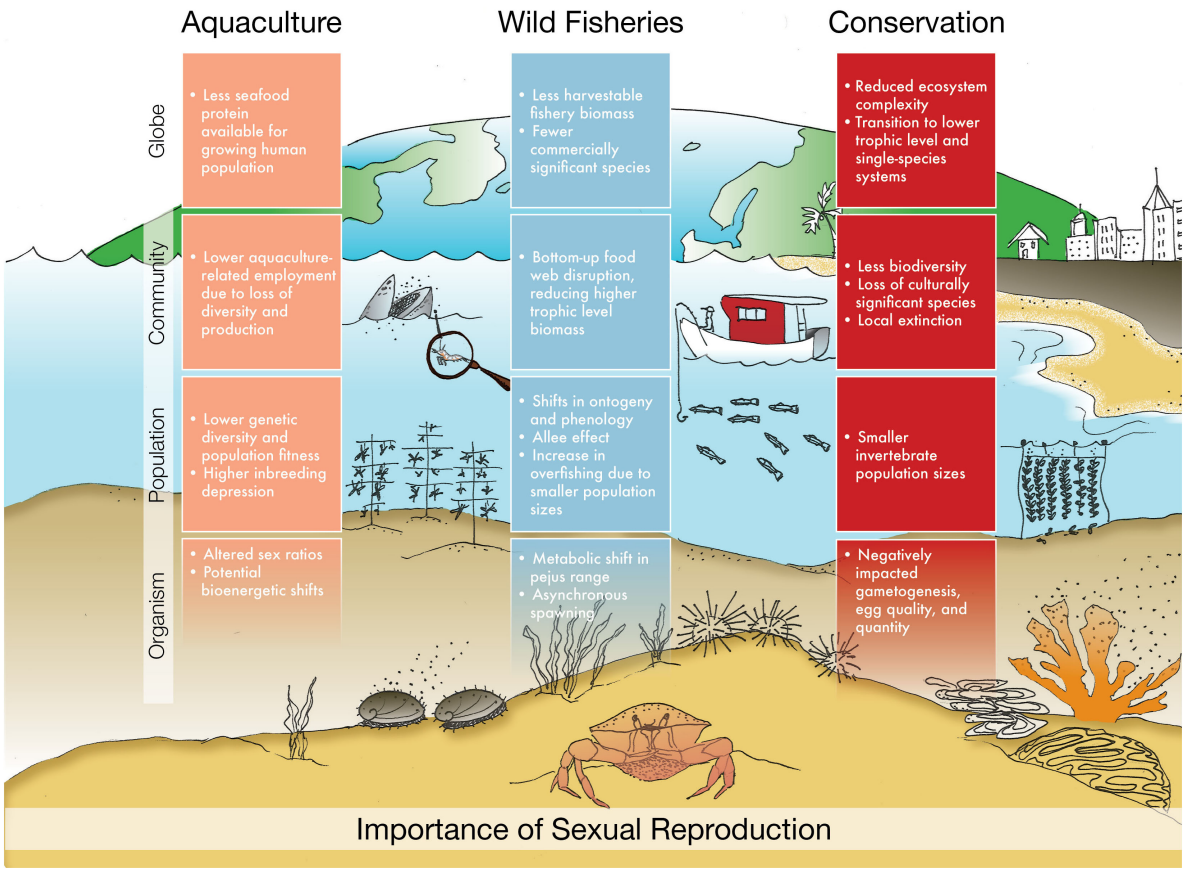

FIGURE 2
Potential effects of OA-caused changes in reproductive processes at the organism, population, community, and global level for commercial and restoration aquaculture, wild fisheries, and conservation and restoration of wild populations. Implications mentioned are not necessarily exclusive to one category.

for each taxonomic group. If a study examined multiple reproductive processes, they were categorized independently. Studies that investigated multiple response variables within a single reproductive process (e.g., fertilization rate and sperm motility) and reported an effect of OA on at least one response variable were classified as showing an effect on reproduction.

To characterize geographic location of research, study site and collection site were assigned to one of the 12 Marine Realms of the World (Spalding et al., 2007). If organisms were collected from a different marine realm than where the experiment took place, only the collection location was considered.

Given the extensive literature that quantified and reported fertilization rate in varying pH conditions, we conducted a meta-analysis to explore the response of fertilization to reduced pH in cnidarians, echinoderms, and molluscs. Crustaceans and ascidians were excluded as no studies have directly measured fertilization rate in varying pH treatments. A generalized linear mixed model was developed to estimate fertilization rate by pH using a logit-linked beta distribution. When reported, the following metrics were extracted from publications, then tested as candidate predictor variables for fertilization success with Analysis of Deviance and chi-squared statistics: 1) difference between experimental and control pH (ΔpH), 2) phylum, 3) lower taxonomic group (e.g. urchin, oyster, coral), 4) incubation time, 5) sperm concentration, 6) sperm:egg ratio, 7) number of sires, 8) number of dams, and 9) pH of the control treatment (Supplemental Table 3). Analysis of covariance (ANCOVA) and the Akaike Information Criterion (AIC) were used to identify the maximal predictive model using variables that significantly affected fertilization rate as sole predictors or as covariates with ΔpH. Significance of intercepts and slope estimates were determined using *z*-tests. Fertilization data from multiple stressor studies were included in the analysis for all treatments (i.e., all temperature, dissolved oxygen, and salinity treatments) to capture the effect of pH on fertilization rate across a range of environmental conditions. Data from treatments that combined OA and secondary metal contaminants and cocaine byproduct stressors were excluded. When necessary, fertilization rate

BOX 1 Glossary of key reproduction terms.

Egg fertilization mechanisms: molecular processes in eggs involved in successful fertilization, including release of egg-derived chemicals, egg-sperm fusion, egg activation and polyspermy prevention

Egg receptivity: the length of time an egg can be fertilized by a sperm cell

Exogenous vs. endogenous reproductive cues: external environmental cues vs. cues originating within the organism

F1: first filial generation comprised of offspring resulting from a cross between two individuals from parental generation

Fecundity: number of eggs (or embryos) per individual. For colonial organisms, the number or eggs or sperm per module (i.e., polyp) or number of fecund modules per weight unit, body length or projected area

Fertilization: union of male and female gametes during sexual reproduction to form a zygote

Gamete quality: size, composition, and developmental stage of gametes

Gametogenesis: process by which gametes are produced through meiosis and cell differentiation. Formation of ova occurs through oogenesis and spermatozoa through spermatogenesis

Gonad condition: Assessment of gonad development via histological examination

Gonad Index (GI) or Gonadosomatic Index (GSI): gonad mass as a proportion of the total body mass [(gonad weight / total tissue weight) X 100]

Gravid: carrying eggs or young offspring

Hatching success: percentage of eggs which produce viable offspring

Indeterminate vs. determinate sex: ability to change sex during an organism's lifetime vs having a defined sex at birth

Mating behavior: social interaction that prepares for, or increases the success of, copulation and fertilization

Mass spawning: synchronous release of gametes by many species or the majority of a mating aggregation

Oocyte: cell in an ovary which may undergo meiotic division to form an ovum

Oosorption (atresia): process of resorbing vitellogenic eggs under stress to reuse lipids for other physiological processes

Phenology: study of periodic events in biological life cycles and how they are influenced by local, seasonal, and interannual environmental variation

Polyspermy: occurs when an egg is fertilized by more than one sperm

Reproductively inactive vs. sexually immature: sexually mature individual not presently breeding vs. one not old or big enough to undergo gametogenesis

Reproductive output: number of reproductive elements (spermary or egg) per unit body volume. Can also be measured by counting embryos per unit body volume. In colonial organisms, reproductive output is the total amount of gametes released by the colony. In some cases, fecundity and reproductive output are used interchangeably

Resource allocation: proportion of an organism's energy budget allocated to reproduction

Sex determination: initial event before sex differentiation that determines whether gonads will develop as male or female

Sex differentiation: events after sex determination that ultimately produce either the male or female sexual phenotype

Sire and dam: father and mother of a genetic line

Spawned bundle: sperm and/or egg clusters released to the water column for external fertilization

Sperm activity: sperm swimming behavior, including motility, velocity or speed, and path linearity

Sperm linearity: how straight the sperm is swimming, as calculated by the ratio of average velocity on a straight line from start to endpoint of the sperm's path to the curvilinear velocity along the sperm's path

Sperm velocity: defined by (1) curvilinear velocity along the sperm's path, (2) smoothed average sperm path velocity, (3) average velocity on a straight line from start to endpoint of the sperm's path

Spermatocyte: male gametocyte from which spermatozoa develop

Standardized Gonad Index (SGI): reproductive cycle indicator based on the differences between the observed and expected weights of the gonads for an individual of a given size. Takes into account allometric gonadal growth

Synchronization: coordination of reproductive events to increase mating potential, fertilization, and offspring success

Timing of reproduction: milestones that rely on environmental and chronological cues

Vitellogenins: principal precursors to the yolk proteins (the vitellins) of egg-laying animals, but not present in all marine invertebrates

Volitional vs. strip or induced spawning: release of gametes via natural or hormonal means vs artificially releasing gametes through anthropogenic means

estimates were extracted from published figures using WebPlotDigitizer v4.2. In addition to exploring fertilization rates across all experimental pH levels (6.0 - 8.5), we also examined the response of fertilization to pH using conditions more relevant to OA (pH >7.6) (IPCC, 2022). For all models tested, study was included as a random effect. Data were weighted by the inverse of one plus the sampling variance squared ($1/(1+\sigma^2)^2$), which was determined from the fertilization mean, error rate (standard deviation), and number of trials conducted at each pH level. The value 1 was added to every sampling variance to prevent overinflation of low variances (between 0-1) in models (Fiorenza et al., 2020). Resultant p-values were considered significant if they were less than $\alpha = 0.05$.

Of the 70 studies that experimentally tested fertilization rates in multiple pH conditions, six were omitted (one, four, and one

in echinoderms, molluscs, and cnidarians, respectively) due to missing error rates (corresponding authors were contacted). The resulting meta-analysis included data from 35, 23, and 6 studies in echinoderms, molluscs, and cnidarians, respectively. We recognize that the fertilization rate reported by some studies may represent both fertilization rate and early embryonic development success. Other reproductive processes included in this review (Figure 1) were not considered for meta-analyses given the inconsistent metrics reported and/or the limited number of studies (Figure 3C).

Results and discussion

We identified a total of 129 studies (16 cnidarian studies, 25 crustacean studies, 69 echinoderm studies, and 56 molluscan studies) that investigated the effects of OA on reproduction in 122 species total (19 cnidarian species, 38 crustacean species, 30 echinoderm species, and 35 mollusc species; Supplemental Table 1). Only two studies examining OA impacts on ascidian reproduction were identified. In ascidian *Ciona robusta*, OA significantly decreased sperm motility, mitochondrial membrane potential (MMP), and intracellular pH (pH_i) (Gallo et al., 2019) but did not affect sperm intracellular reactive oxygen species (ROS), lipid peroxidation, nor viability (Gallo et al., 2019; Esposito et al., 2020). *In situ* and microcosm experiments showed that in *C. robusta*, OA initially decreased sperm motility, viability, MMP, pH_i, and morphology, but sperm underwent rapid recovery after within one week of exposure, suggesting that ascidian spermatozoa is resilient to OA (Gallo et al., 2019). Given the lack of ascidian studies, the remainder of this review will focus on the remaining four taxa.

Echinoderm research comprises the majority (53.5%) of OA and reproduction studies, followed by research in molluscs (43.4%) (Figures 3A, B). The same echinoderm and mollusc species are examined in multiple studies, while cnidarian and crustacean studies tend to study unique species (Supplementary Table 1). Except for one echinoderm study published in 1924, all OA and reproduction research highlighted in this review was conducted between 2004 and 2021 (Figure 3B). The majority of the studies were performed under laboratory conditions (Supplementary Table 2) highlighting the need for more research in mesocosms and the natural environment. Life stages exposed to OA and duration of experiments were variable among taxa (Supplementary Table 2). Most studies collected organisms from the Temperate Northern Atlantic Marine Realms (Spalding et al., 2007), followed by Temperate Northern Pacific and Temperate Australasia (Figure 3A). Collection sites are reported in Figure 3A, and study sites (which in some instances differ from collection location) are included in Supplemental Table 1.

Published research suggests that the effects of OA depend on the taxa and the specific process studied (Figure 3C). Within each taxon, OA studies focus on a handful of species. Copepods dominated crustacean literature, while urchin species were prominent in echinoderm studies. All cnidarian studies examined corals. There was only one cephalopod study within molluscan research.

Impacts of ocean acidification on sexual reproduction processes

In this section, we summarize ocean acidification studies for cnidarians, crustaceans, echinoderms, and molluscs by reproductive process (Supplemental Table 1). See the Supplementary Materials for a more comprehensive synthesis of results.

Sex determination, differentiation, and ratio

The sex of many invertebrate species is sensitive to environmental conditions, which can skew populations' sex ratios (Korpelainen, 1990; Yusa, 2007). Changes to the number and proportion of mature females and males at a given time can alter a population's reproductive capacity, its effective population size, and its genetic diversity. There are no studies

TABLE 1 This review utilized specific keywords to search several literature databases.

Keywords	
All Taxa	climate change, ocean acidification, carbonate chemistry, CO_2, hypercapnia, aragonite saturation state, reproduction, gamete*, sperm*, egg*, ovary, oocyte*, fertilization, fertilization, fecund*, mating behavior, behavior, gametogenesis, reproductive output, synchronization, brood*, hatch*, spawn*, spawning, sex*, determination, differentiation, gonad development
Cnidaria	coral*, jelly*, hydroid, zoanthid*, sea pen, gorgonian, siphonophore, anemone, cnidaria*, cubozoa*, anthozoa*, scyphozoa*, hydrozoa*, myxozoa*, medusa*, medusozoa*, polipodiozoa*, staurozoa*, hexacorallia*, octocorallia*, hydromedusae*, scleractinia*, zoantharia*, corallimorpharia*
Crustacea	crustacean*, arthropod*, malacostraca*, crab*, lobster*, shrimp*, amphipod*, copepod*, barnacle*, decapod*, brachyura*, artemia*, ostracoda*, dendrobranchiata*, isopod*, branchiopoda*, mysid*, hermit*, zoea*, krill*, cyst*, prawn*
Echinodermata	echinoderm*, sea star*, starfish*, urchin*, sand dollar*, brittle star*, sea cucumber*, feather star*, crinoidea*, echinozoa*, holothuroidea*, echinoidea*, asterozoa*, ophiuroidea*, asteroidea*
Ascidiacea	ascidian*, sea squirt, tunicate, tunicata, urochordata, sea tulip, sea liver, sea pork, ascidiacea, thaliacea, appendicularia, salp, doliolid

Each taxonomic group used a common list of words, which were followed by a list of taxa-specific words. Keywords unique to each taxa included both common names and Latin nomenclature for major classifications. The Boolean search operator asterisk (*) was used as a "wildcard operator" to search for words or phrases that may contain parts of that truncated word. In addition to the general terms, all taxa specific terms were given an asterisk.

that have directly examined effects of acidification on sex determination or differentiation in individuals of any taxa covered in this review. However, we identified several studies that examined effects of acidification on sex ratios. The sole crustacean study did not find differences in sex ratios in copepods when reared in OA conditions (Kita et al., 2013). Two studies that exposed oysters to low pH prior to and during gametogenesis also reported no impact on gonad sex ratios (Venkataraman et al., 2019; Clements et al., 2020). In contrast, three oyster studies indicated that acidification exposure during gametogenesis may alter populations' sex ratios by impacting egg and sperm development unequally. Sex-specific impacts of OA on gametogenesis therefore reduce the proportion of females (Boulais et al., 2017) or males (Parker et al., 2018; Spencer et al., 2020) capable of breeding in a population, thereby reducing the effective population size. These studies are challenging due to the difficulty of identifying sex without harming or destroying the organisms being investigated (Ellis et al., 2017), the lack of sex biomarkers, and the limited understanding of hormonal control on reproductive processes in marine invertebrates.

Gametogenesis and gamete quality

Environmental conditions during gametogenesis can influence population dynamics through changes to gamete development and quality. Several metrics are associated with gametogenesis, including gamete size, stage, biocomposition, integrity, viability, developmental rate, maturation, and spawning capability. In cnidarians, OA negatively affected octocoral egg size (Rossin et al., 2019), while hexacoral studies showed no effect of OA on gamete size (Fine and Tchernov, 2007; Gizzi et al., 2017; Caroselli et al., 2019; Marchini et al., 2021) or maturation stage (Fine and Tchernov, 2007; Gizzi et al., 2017; Caroselli et al., 2019). However, Marchini et al. (2021) showed a delay in spermary development due to OA. In crustaceans, OA resulted in delayed gametogenesis and smaller spermatophores (Fitzer et al., 2012a; Cripps et al., 2014; Meseck et al., 2016; Conradi et al., 2019). OA did not affect copepod egg viability, oogenesis (Vehmaa et al., 2013; Thor et al., 2018), or barnacle and copepod gametogenesis (Smith et al., 2017; Pansch et al., 2018).

OA had negative effects on gonad growth, maturation, egg size, and gamete development in some echinoderm species (Siikavuopio et al., 2007; Kurihara, 2008; Stumpp et al., 2012; Kurihara et al., 2013; Suckling et al., 2014; Suckling et al., 2015; Verkaik et al., 2016; Dworjanyn and Byrne, 2018; Hu et al., 2018; Hue et al., 2020; Marčeta et al., 2020; Anand et al., 2021), while other studies reported no change in gamete development and quality (Wood et al., 2008; Uthicke et al., 2013; Hazan et al.,

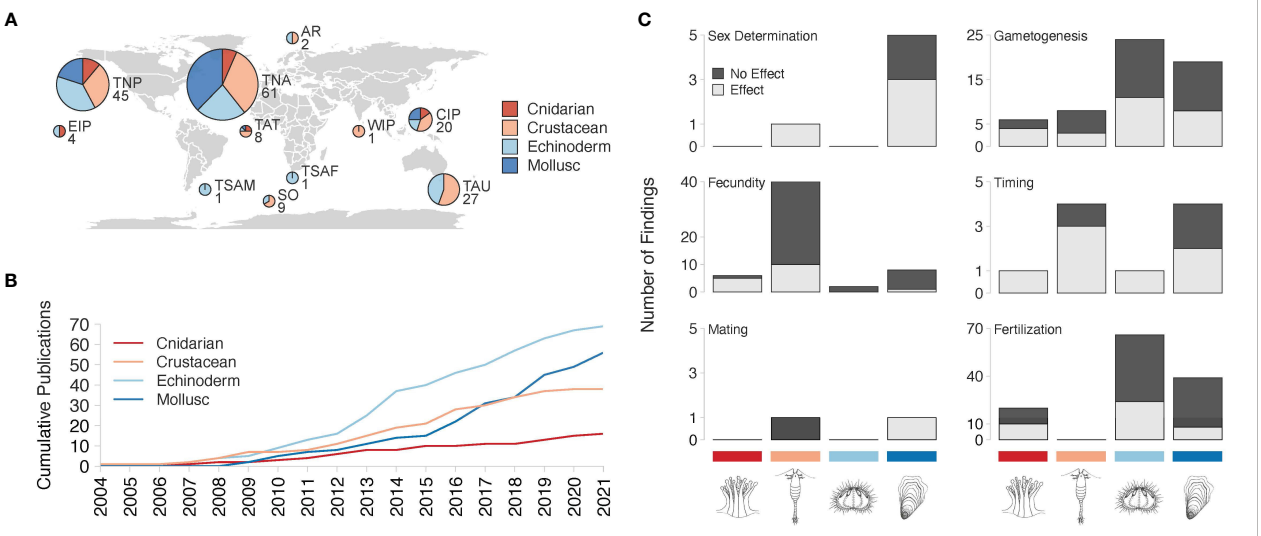

FIGURE 3
Summary of study locations, number of publications, and effects of Ocean Acidification on Reproductive Processes across taxa. **(A)** Graphical description of published studies used in this review. Pie charts for each geographic study locations are labeled with initials and the number of studies from that realm: Eastern Indo-Pacific (4), Temperate Northern Pacific (45), Temperate South America (1), Temperate Northern Atlantic (61), Tropical Atlantic (8), Southern Ocean (9), Temperate Southern Africa (1), Arctic (2), Western Indo-Pacific (1), Central Indo-Pacific (20), and Temperate Australasia (27). There were no studies from Tropical Eastern Pacific. Pie charts represent the proportion of taxa-specific studies in which study organisms were collected in each region, and pie size and numbers underneath the pies represent the total number of studies in that region. Studies may be represented more than once in a pie chart if the study examined multiple taxa. **(B)** Cumulative number of papers published for each taxon from 2004 to 2021. One echinoderm study was published in 1924 but was not included in this figure. Studies may be represented more than once per year if the study examined multiple taxa. **(C)** Number of findings that reported an OA effect (either positive or negative, light gray) or no effect (black) for various reproductive processes by taxa (from left to right: cnidarians, crustaceans, echinoderms, molluscs).

2014; Uthicke et al., 2014; Dell'Acqua et al., 2019; Karelitz et al., 2019; Wong et al., 2019; Hue et al., 2020; Uthicke et al., 2020). One study reported a positive effect on gonad protein storage after low pH exposure (Challener et al., 2014). Suckling et al. (2015) suggests egg size is plastic in response to OA, and longer exposure to low pH can lead to larger eggs due to increased maternal provisioning.

Most studies in molluscs indicate that low pH exposure affects the rate of gametogenesis, typically by decreasing gamete development or spawning rates (Xu et al., 2016; Boulais et al., 2017; Parker et al., 2018; Zhao et al., 2019; Spencer et al., 2020; Wang et al., 2021), or less commonly by accelerating gamete development (Dell'Acqua et al., 2019; Clements et al., 2020). However, no impact of OA on molluscan gametogenesis has also been reported (Le Moullac et al., 2016; Venkataraman et al., 2019). Molluscan egg quality may be resilient to OA, as most studies report no impact to egg size or lipid content (Parker et al., 2017; Parker et al., 2018; Scanes et al., 2018; Parker et al., 2021; Reed et al., 2021; Gibbs et al., 2021a) (but see Spady et al., 2020, the sole non-bivalve study). Two studies do report increased egg size or lipid content in response to OA (Zhao et al., 2019; Gibbs et al., 2021b), which can be indicative of higher energy content and egg quality (Moran and McAlister, 2009). While other egg quality parameters are possibly vulnerable (e.g., egg rupture rate, Omoregie et al., 2019), most studies indicate that molluscan species prioritize per-egg maternal investment when exposed to low pH, in some cases over gametogenic rate. In one of the few studies utilizing naturally low pH environments, *Bathymodiolus septemdierum* mussels were collected from hydrothermal vents, which reach conditions as low as pH 5.2. These mussels can maintain similar egg sizes and gametogenic cycles compared to those living in higher pH sites, possibly at the expense of calcification (Rossi and Tunnicliffe, 2017). This study provides evidence that OA-adapted populations are capable of gametogenesis despite extreme pH conditions. Given the variable responses in gametogenesis and gamete quality across phyla, species, and even populations, broader characterizations are needed to better understand how OA will impact physiological performance and allocation to energy expensive processes such as gamete development.

Fecundity and reproductive output

The fecundity and reproductive output of individuals and populations can vary along environmental gradients. In this section we highlight studies that assess fecundity and reproductive output in varying OA conditions. We considered hatch rate as a proxy for fecundity and reproductive success in brooding organisms. Cnidarian studies report no effect of OA on fecundity in hexacorals. The number of eggs, sperm, or gamete bundles were not affected by OA in four hexacoral species (Jokiel et al., 2008; Gizzi et al., 2017; Caroselli et al., 2019; Marchini et al., 2021). Most of these studies report reduced adult growth under OA, suggesting resources may have been allocated towards reproduction over growth. In the sole octocoral study, exposure to OA reduced the number of eggs per polyp (Rossin et al., 2019). In echinoderms, OA negatively affected egg production (Dupont et al., 2013). Three molluscan studies report negative effects of OA across reproductive modes, with decreased pH reducing fecundity and spawn rate in a broadcast spawner (Parker et al., 2018), and reducing clutch size and egg masses in two oviparous species (Dionísio et al., 2017; Spady et al., 2020). Two studies reveal the complexity of responses to OA in molluscs, including reduced fecundity but more frequent spawn events (Manno et al., 2016), and unaffected spawn frequency and number of egg capsules (Kita et al., 2013).

Studies that measure hatch rate in brooders were limited to crustaceans and molluscs, as hatch rate was not reported for brooding species in any other taxa. Several brooding crustacean species held at low pH were found to have differences in fecundity, hatch success, or number of offspring (Kurihara et al., 2004; Mayor et al., 2007; Kurihara et al., 2008; Findlay et al., 2009; Zhang et al., 2011; Vehmaa et al., 2012; Weydmann et al., 2012; Kita et al., 2013; Long et al., 2013; McConville et al., 2013; Zervoudaki et al., 2013; Cripps et al., 2014; Cao et al., 2015; Swiney et al., 2015; Thor and Dupont, 2015; Choi et al., 2016; Miller et al., 2016; Vehmaa et al., 2016; Borges et al., 2018a; Cardoso et al., 2018; Gravinese, 2018; Pansch et al., 2018; Thor et al., 2018; Lee et al., 2020). One study in copepods found that OA reduced the number of brooding females (Lee et al., 2019). Several crustacean studies, however, showed that fecundity or hatch rate were unaffected by OA (Kurihara et al., 2004; Mayor et al., 2007; Kurihara and Ishimatsu, 2008; Egilsdottir et al., 2009; Zhang et al., 2011; Weydmann et al., 2012; McConville et al., 2013; Vehmaa et al., 2013; Cripps et al., 2014; Cao et al., 2015; Isari et al., 2015; Almén et al., 2016; Rains et al., 2016; Zervoudaki et al., 2017; Thor et al., 2018; Langer et al., 2019). One study found that OA can increase fecundity, and another found that low pH increased reproductive output, but at the cost of body size and shell integrity (Fitzer et al., 2012b; Engström-Öst et al., 2014). In molluscs, OA exposure during breeding reduced bivalve brood size (Wippel, 2017; Maboloc and Chan, 2021), while a previous OA exposure resulted in increased brood size but no effect to overall larval production (Spencer et al., 2020). Instances where reproductive output increases may be a short-term stress response or may indicate adaptive potential to pH change (Engström-Öst et al., 2014). Overall, research to date suggests that OA negatively affects fecundity and reproductive output in molluscs and echinoderms, while some cnidarians appear to be less sensitive, and responses in crustaceans are variable.

Timing of reproduction and synchronization

Synchronicity and timing of reproductive maturation, spawning, hatching, and planulation are important to ensure reproductive success. In a brooding coral, OA conditions delayed planulation timing (Putnam et al., 2020). OA may

affect the timing at which brooding crustaceans reach milestones associated with hatching. When female copepods and crabs were acclimated to OA conditions, copepod hatching occurred earlier and crabs hatched for a longer duration (Long et al., 2013; Langer et al., 2019). However, there was no effect of OA on egg onset time in the barnacles (McDonald et al., 2009). On the other hand, OA did not affect the number of days that copepods needed to form mating pairs, successfully copulate, and spawn (Kita et al., 2013). A volitional spawning experiment in sea cucumbers reported no effect of OA on spawn timing (Verkaik et al., 2016). In molluscs, studies that induced spawning found reductions in spawning success in acidified conditions (Xu et al., 2016; Parker et al., 2018). Two studies examined impacts of OA on volitional spawning in a brooding molluscan species: one reported no effects to larval release timing (Spencer et al., 2020), and another reported delayed larval release onset in one of three trials (Wippel, 2017). More studies that incorporate natural spawning and planulation conditions are needed. Studies that monitor the number and timing of naturally breeding males and females would improve our understanding of ecologically relevant impacts of acidification on spawn timing and synchronicity.

Mating behavior

Marine species are diverse in their mating behaviors. However, there is a very limited number of OA studies to date examining mating behavior, limiting the number of observable behavioral metrics. We summarize two studies that measure mate selection, courtship display, and mate guarding. Male mate tracking and guarding behavior in amphipods were disrupted under OA conditions, which may have negative consequences for fertilization (Borges et al., 2018b). The ability for amphipods to detect and orient toward female pheromone cues through chemotaxis was greatly reduced under OA, suggesting potential disruptions in chemosensory cues related to food acquisition, defense, and predator avoidance behaviors under low pH. Squid mating pair behavior was unaffected by OA, even though females laid denser egg clutches after the pair were exposed to low pH (Spady et al., 2020). More studies are needed to explore the impacts of OA on invertebrate mating behavior, particularly in cephalopod, gastropod, and crustacean species with sophisticated mating behaviors (e.g., changing body patterns and textures, parallel swimming, male-male fighting, and mate guarding). It is critical that we expand our understanding of mating behavior in invertebrates exposed to OA because disruptions may have rippling effects on population fitness and ultimately, the future of the species.

Fertilization

Many marine invertebrates broadcast spawn and undergo external fertilization, which exposes gametes to the surrounding environment prior to and during fertilization. Acidification may affect fertilization success by altering chemosensory and biochemical egg-sperm interactions, therefore directly influencing gamete activation, sperm activity, egg biochemistry and polyspermy defense (Mortensen and Mortensen, 1921; Nakajima et al., 2005; Miyazaki, 2006; Lymbery et al., 2019). The impact of OA on fertilization and gametes has been reviewed previously (Byrne, 2011; Byrne, 2012; Byrne and Przeslawski, 2013; Foo and Byrne, 2017). Here we provide an updated review of 92 studies that have assayed fertilization, sperm quality, and/or egg biochemical processes under OA conditions, the majority of which were published since prior reviews. Additionally, we conducted a meta-analysis to evaluate general trends across and within echinoderms, molluscs, and cnidarians. Crustaceans were not included in the meta-analysis as no studies have directly measured fertilization rate in varying pH treatment, likely because they undergo internal fertilization.

Fertilization rate

Reviews by Byrne (2011; 2012) found that fertilization rate is robust in pH above ~7.6. However, discrepancies were noted among studies of the same species and conspecifics from different habitats. The authors encouraged researchers to examine other taxa with standardized experimental designs. Since then, an additional 51 studies have assessed fertilization rate in varying pH conditions.

The majority of studies, which predominantly evaluate echinoderms (largely urchins) and bivalve molluscs, conclude that acidification negatively affects fertilization rate when gametes are directly exposed (Smith and Clowes, 1924; Kurihara and Shirayama, 2004; Havenhand et al., 2008; Parker et al., 2009; Ericson, 2010; Parker et al., 2010; Kimura et al., 2011; Moulin et al., 2011; Schlegel et al., 2012; Van Colen et al., 2012; Barros et al., 2013; Gonzales-Bernat et al., 2013; Uthicke et al., 2013; Foo et al., 2014; Frieder, 2014; Scanes et al., 2014; Suckling et al., 2014; Sung et al., 2014; Riba et al., 2016; Boch et al., 2017; Shi et al., 2017a; Shi et al., 2017b; Szalaj et al., 2017; Zhan et al., 2017; Basallote et al., 2018; García et al., 2018; Świeżak et al., 2018; Zhan et al., 2018; Smith et al., 2019; Sui et al., 2019; Wang et al., 2020), or parents are exposed prior to fertilization (Graham et al., 2015). The pH level at which fertilization rate becomes compromised varies considerably across taxa, and also depends on factors such as sperm and egg concentration (Ericson, 2010; Albright, 2011a; Ericson et al., 2012; Albright and Mason, 2013; Gonzales-Bernat et al., 2013; Ho et al., 2013; Frieder, 2014), gamete incubation time (Bechmann et al., 2011; Gianguzza et al., 2014; García et al., 2018; Kong et al., 2019), inter-individual and mating pair variability (Schlegel et al., 2012; Foo et al., 2014; White et al., 2014; Smith et al., 2019), collection location and time of year (Martin et al., 2011; Cohen-Rengifo et al., 2013; Pecorino et al., 2014; Riba et al., 2016; Basallote et al., 2018; García et al., 2018; da Silva Souza et al., 2019; Pereira et al., 2020; Caetano et al., 2021), and species hybridization (Striewski,

2012). Parental acclimatization to low or highly variable conditions (including pH) can either increase (Moulin et al., 2011; Suckling et al., 2014; Kapsenberg et al., 2017) or decrease fertilization rates in low pH (Graham et al., 2015).

Negative effects of OA were not universally reported (Byrne et al., 2009; Byrne et al., 2010a; Byrne et al., 2010b; Schlegel et al., 2012; Byrne et al., 2013; Chua et al., 2013; Kamya et al., 2014; Onitsuka et al., 2014; Stavroff, 2014; Bylenga et al., 2015; Iguchi et al., 2015; Schutter et al., 2015; Foo et al., 2016; Zhan et al., 2016; Boulais et al., 2017; García et al., 2018; Armstrong et al., 2019; Lenz et al., 2019; Smith et al., 2019; Guo et al., 2020; Hue et al., 2020; Pitts et al., 2020), which indicates that fertilization in some species may be more resilient than others to the effects of acidification. Several studies report that *Mytilus* spp. mussels, for example, are capable of maintaining high fertilization rates across a broad pH range (Bechmann et al., 2011; Eads et al., 2016; Riba et al., 2016; Gallo et al., 2020). Fertilization in some molluscan and echinoderm species can persist at severely low pH (e.g., ~23% of *Crassostrea gigas* eggs were successfully fertilized at pH 6.0, Riba et al., 2016).

In rare instances, low pH can increase fertilization rate. Higher fertilization rates occur in *Mytilus galloprovincialis* when sperm are pre-exposed to low pH conditions in the presence of egg-derived chemicals (Lymbery et al., 2019). These results could be explained by a stronger attraction of sperm to egg-derived chemicals under low pH conditions, resulting in increased fertilization rates. As suggested by Lymbery et al. (2019), increased fertilization rates are not necessarily beneficial to population fitness. OA could alter chemical cues that would typically only occur among genetically compatible sperm and eggs, resulting in higher rates of fertilization among incompatible genotypes, and ultimately decreasing the overall population fitness (Lymbery et al., 2019).

Fertilization rate meta-analysis

Studies that reported fertilization rates across multiple pH levels were leveraged to perform a meta-analysis to quantify broad-scale impacts of pH on fertilization rate in cnidarians, echinoderms, and molluscs. Change in pH ($\Delta pH = pH_{experimental} - pH_{control}$) across all taxa significantly predicts fertilization success as a sole predictor ($X^2 = 22.0$, $p = 2.7e^{-6}$). Using ANCOVA we modeled fertilization rate by ΔpH and other candidate covariates. The most parsimonious model was selected using AIC criterion, and retained only the interaction between ΔpH and phylum (phylum:ΔpH, $X^2 = 34.3$, $p = 1.7e^{-7}$), and phylum as a main effect ($X^2 = 3.4$, $p = 0.18$), indicating that the response of fertilization rate is phylum-specific. The probability of successful fertilization is estimated by:

$$p(\textit{fertilization success, cnidarians}) = \frac{e^{(0.92 + 2.43 * \Delta pH)}}{1 + e^{(0.92 + 2.43 * \Delta pH)}}$$

$$p(\textit{fertilization success, echinoderms}) = \frac{e^{(1.16 + 1.92 * \Delta pH)}}{1 + e^{(1.16 + 1.92 * \Delta pH)}}$$

$$p(\textit{fertilization success, molluscs}) = \frac{e^{(1.13 + 0.32 * \Delta pH)}}{1 + e^{(1.13 + 0.32 * \Delta pH)}}$$

where the ΔpH coefficient estimates for cnidarians, echinoderms, and molluscs are 2.43 (z-score = 1.24, $p = 0.22$), 1.92 (z-score = 5.75, $p = 9.0e^{-9}$), and 0.32 (z-score=0.71, $p = 0.48$), respectively (Figure 4). The positive ΔpH coefficients indicate that fertilization rate decreases with pH in all phyla; however, ΔpH only significantly predicts fertilization for echinoderms. While pH is not a significant factor in the cnidarian model, likely due to limited data (6 studies), the model does suggest high pH sensitivity (Figure 4) and underlines the need for more cnidarian fertilization studies. The large number of studies in the echinoderm (35) and mollusc (23) models enables more confident predictions in those two taxa. Echinoderm fertilization appears to be more sensitive than molluscs to pH changes, which could reflect habitat differences in most species studied to date (largely subtidal echinoderms and intertidal molluscs).

Using the phylum-specific models, we estimate that under the Shared Socioeconomic Pathways (SSPs) SSP1-2.6, SSP2-4.5, SSP3-7.0 and SSP5-8.5 predicted for the end of the 21st century (Cooley et al., 2022; IPCC, 2022), fertilization rate will decrease by 2.9%-15.1% for echinoderms, and by a non-significant amount for molluscs (0.5%-2.3%), relative to 1995–2014 (Figure 4). Our low-confidence predictions for cnidarians estimate a decrease of 4.1%-21.0%.

Since many studies included pH levels beyond those predicted under SSP5-8.5, we reconstructed our meta-analysis using data from experimental pH ≥ 7.6. This reduced the dataset by ~20% for echinoderms and molluscs but did not affect the cnidarian data due to the narrower range of experimental pH levels tested for cnidarians (Figure 4). In the revised analysis, ΔpH remains significant but is less predictive of fertilization rate ($X^2 = 4.39$, p = 0.036). The best fit model includes ΔpH only and predicts a decrease in fertilization rate across all taxa by 2.0%, 4.3%, 7.1%, and 9.9% under SSP1-2.6, SSP2-4.5, SSP3-7.0 and SSP5-8.5, respectively. Predictions from this more conservative approach support previous conclusions that marine invertebrate fertilization is more robust — albeit still negatively impacted — at pH 7.6 and above (Byrne, 2011; Byrne, 2012), which may better reflect relevant open ocean pH projections. However, many species covered in this review are coastal and periodically experience pH levels below 7.6; therefore, the full model should not be disregarded.

As noted by Byrne (2011; 2012), there are many factors found to influence fertilization success that vary across studies. Given the diversity of species and secondary variables tested (e.g.

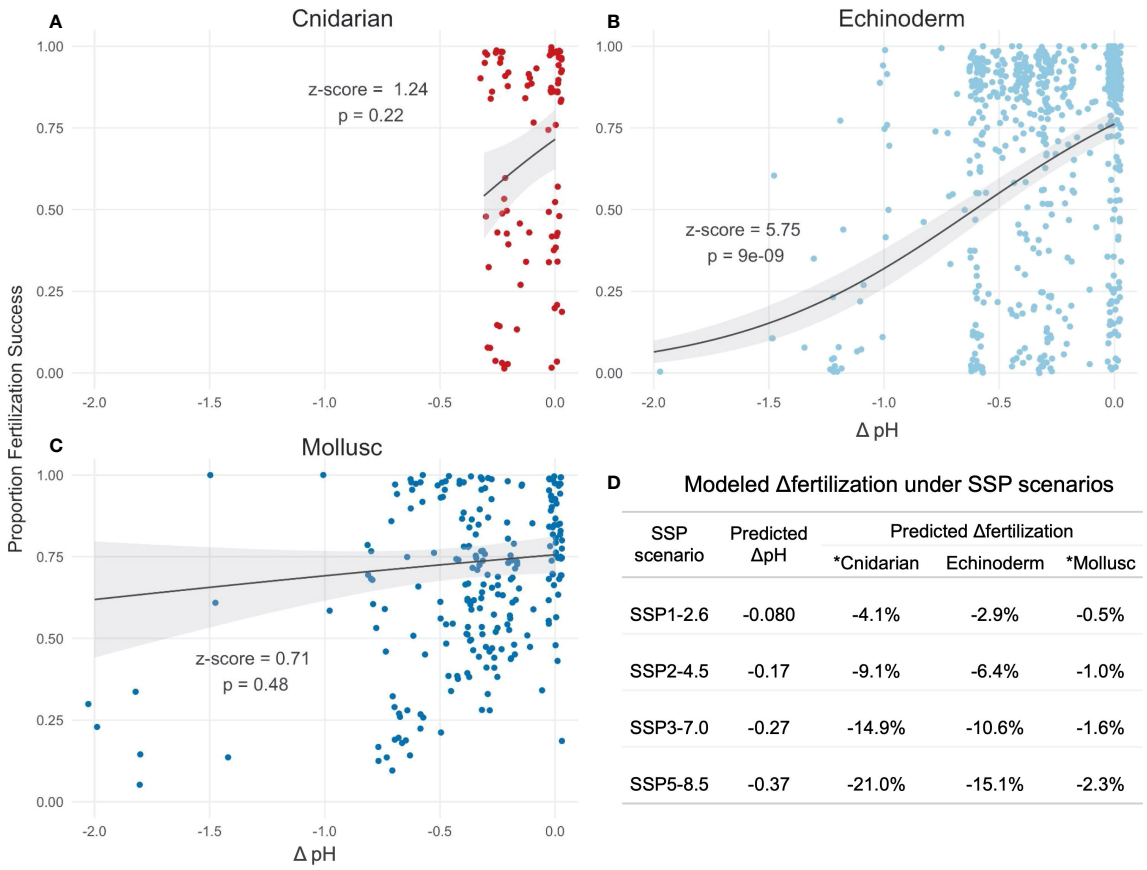

D Modeled Δfertilization under SSP scenarios

SSP scenario	Predicted ΔpH	Predicted Δfertilization		
		*Cnidarian	Echinoderm	*Mollusc
SSP1-2.6	-0.080	-4.1%	-2.9%	-0.5%
SSP2-4.5	-0.17	-9.1%	-6.4%	-1.0%
SSP3-7.0	-0.27	-14.9%	-10.6%	-1.6%
SSP5-8.5	-0.37	-21.0%	-15.1%	-2.3%

FIGURE 4
Fertilization success by ΔpH (the difference between experimental pH and control) for **(A)** cnidarians (6 studies), **(B)** echinoderms (35 studies), and **(C)** molluscs (23 studies). Control pH (ΔpH = 0) is defined separately by each experimental study, and typically represents present-day ambient pH at experimental location. The meta-analysis was performed using a beta regression model, and indicates that the effect of pH on fertilization rate is phylum-dependent (phylum:ΔpH interaction, X^2 = 34.3, p = 1.7e^{-7}). In all figures, each point reflects the average percent fertilization reported by one study at each ΔpH and secondary variable tested, curves indicate the fitted models, ribbons indicate 95% confidence intervals, and z-scores and p-values indicate the significance of the ΔpH coefficient estimates for each phylum. **(D)** Models were used to predict the change in fertilization rate under four Shared Socioeconomic Pathways (SSPs) for each phylum, which predict the pH change for the end of the 21st century (IPCC, 2022) relative to 1995–2014. *The pH coefficient was not a significant factor in the mollusc or cnidarian models, therefore these predictions should be considered descriptive, particularly for cnidarians for which there is limited data. No fertilization studies were found for crustaceans or ascidians.

warming), limiting the meta-analysis to only studies that used the same procedures was not possible. Instead, we took a broader approach, including all studies with a variety of secondary variables (Supplemental Table 3). We then tested for effects of six additional experimental variables (when reported, see Methods and Supplemental Table 3). We found that experimental sperm concentration significantly affects fertilization rates as a sole predictor but does not interact with ΔpH alone or as an additional covariate with phylum. Given that only five of the 34 studies that reported sperm concentration included multiple concentrations in the experimental design (Supplemental Table 3), the model was likely unable to fully characterize the interaction between pH and sperm concentration. In the natural environment, sperm levels can be considerably more dilute than the optimal levels used in most studies. Whenever possible, studies should test effects of pH on fertilization across a range of sperm concentrations.

Other experimental variables that are not commonly reported or considered may interact with pH to affect fertilization rate, making it difficult to fully describe the impacts of OA. For instance, given the rapid pace of ocean change, many experimental animals likely already experienced OA, which could have affected fertilization rates through changes to their gametes (e.g. maternal effects, epigenetic changes). This is particularly pertinent because control pH levels applied by researchers often reflected conditions entering their experimental systems or the historical pH for a given region, which could differ dramatically from conditions at

the animal collection site. Future studies should strive to characterize their focal species' current and future environments to determine pH treatment levels, as they will provide the most ecologically relevant results.

In summary, our meta-analysis indicates that OA will reduce fertilization rates in many marine invertebrates, and effects are taxa specific. Fertilization rates are likely to decrease in echinoderms but remain relatively similar in molluscs. More studies are needed for cnidarians, but preliminary work indicates that their fertilization rates may be the most affected.

Gamete mechanisms that influence fertilization rate

There are five major events that typically occur during fertilization: 1) sperm chemoattraction to the egg, 2) sperm binding to the egg envelope, 3) sperm acrosomal reaction, 4) sperm penetration through the egg envelope, and 5) gamete fusion (Vacquier, 1998). Successful fertilization therefore involves a cascade of biochemical processes in both sperm and eggs, many of which include intracellular pH and calcium ion changes (Morisawa and Yoshida, 2005; Nakajima et al., 2005; Byrne, 2011; Sherwood et al., 2012). OA could alter fertilization rates through changes to chemoattractants, surface receptors, jelly coat, polyspermy defense system, and activation processes in eggs, and/or activation, motility, velocity, mitochondrial activity, chemotaxis, and fusion reactions in sperm.

Several studies examined the impact of acidification on egg fertilization mechanisms. In urchins, low pH increased the percentage of abnormally fertilized eggs (Zhan et al., 2018), polyspermy frequency, and time to completely block polyspermy (Reuter et al., 2011; Sewell et al., 2014). In molluscs, polyspermy rates increased as pH decreased when clam *Tegillarca granosa* eggs were pre-exposed to various pH treatments (Han et al., 2021). The inability to block polyspermy may be related to low pH reducing the protective egg jelly coat area, which can subsequently impair sperm chemotaxis (Foo, 2015; Foo et al., 2018). These impacts are likely species- and population-specific, with some urchins exhibiting no impact of low pH on egg jelly coat area, and populations exhibiting varied impacts depending on prior pH exposure (Foo et al., 2018). Egg intracellular pH adjusts according to the external chemical environment (Ciapa and Philippe, 2013; Bögner et al., 2014), which may also hamper egg activation by interfering with calcium signaling and actin dynamics (Limatola et al., 2020). Indeed, Shi et al. (2017b) observed that low pH disrupts the intracellular calcium ion (Ca^{2+}) activity in *T. granosa* eggs, which was associated with reduced fertilization rates.

The influence of low pH on sperm activity varies. Three cnidarian (hexacoral) studies report negative effects of pH on sperm activity (Morita et al., 2010; Albright, 2011a; Nakamura and Morita, 2012). Albright's initial examination of OA impacts on hexacoral sperm velocity showed no effect, but results from a second experiment suggested a negative effect (Albright, 2011a). OA reduced sperm swimming speed, motility, and linearity in some echinoderms (Havenhand et al., 2008; Morita et al., 2010; Uthicke et al., 2013; Campbell et al., 2016; Caballes et al., 2017), but had no effect or positively impacted sperm swimming speed in others (Caldwell et al., 2011; Sung et al., 2014; Graham et al., 2015). Similarly, pH negatively affected sperm swimming speed, velocity, motility, and mitochondrial activity in some molluscs (Vihtakari et al., 2013; Vihtakari et al., 2016; Shi et al., 2017a; Shi et al., 2017b; Omoregie et al., 2019; Esposito et al., 2020), but had no effect on sperm motility in others (Havenhand and Schlegel, 2009; Vihtakari et al., 2016). In one population of *C. gigas* oysters, low pH increased sperm motility (Falkenberg et al., 2019).

Contrasting impacts on sperm activity could be due to varied sensitivities among genotypes within species (Schlegel et al., 2015; Campbell et al., 2016; Vihtakari et al., 2016; Falkenberg et al., 2019; Smith et al., 2019). Individual sperm characteristics can also respond differently to low pH (Schlegel et al., 2012; Graham et al., 2015). For instance, OA had a negative effect on the proportion of motile sperm, but not sperm swimming speed, in urchin *Heliocidaris erythrogramma* sperm (Schlegel et al., 2012). Impacts on sperm activity can also be influenced by experimental conditions, such as the exposure duration (e.g. Eads et al., 2016) or the method used to prepare experimental pH levels (pCO_2 vs. HCl, Shi et al., 2017b).

Implications

Our synthesis of the OA reproduction literature to date reveals the complexity of responses across and within species. For all reproductive processes there are studies that report effects of OA, while others found no effect (Figure 3C). Predicting future community-level changes at this stage is therefore not possible. There are, however, some observable trends for those well-studied reproductive processes (gametogenesis, fecundity, fertilization): for all phyla, negative effects were observed in at least one species (and typically many more), and reports of positive effects were rare. Echinoderm fertilization is quite sensitive to pH changes while molluscs are not. Gametogenesis is delayed and fecundity is reduced in many echinoderms and molluscs, but those processes are less sensitive in crustaceans. Cnidarian and ascidian studies are limited. Cnidarian studies suggest that gametogenesis and fecundity are relatively robust to OA, and fertilization may be quite sensitive. These observations provide the basis for hypotheses of the potential challenges faced by those in the aquaculture, fisheries, and conservation sectors. Not all reproductive processes will be affected in all species, but for those that are, here are some considerations.

Aquaculture

Impacts of OA on reproduction have the potential to negatively affect our marine food systems. Aquaculture programs may need to adjust their hatchery culturing

techniques to accommodate effects of OA. For example, gametogenesis in many species is delayed in OA, so conditioning them in buffered seawater could ensure or expedite gamete development. This may also improve synchronization of mature males and females in some species, as unequal impacts of acidification on oogenesis and spermatogenesis have been observed in oysters (e.g. Boulais et al., 2017). Seawater may also need to be buffered during fertilization to maintain high fertilization rates, particularly for some echinoderms and possibly cnidarian species. Alternatively, fertilization conditions could be re-optimized at a lower pH, such as by adjusting sperm concentrations. Should these measures be needed, larger facilities with more complex seawater treatment systems, more resources, and increased handling will be required, thus increasing the overall cost of production.

Wild fisheries

Wild fisheries do not have the capability of modulating the environment during reproduction, and may therefore be more susceptible to the effects of OA. Acidification may impact invertebrate fishery stocks by slowing gametogenesis, and reducing fecundity and fertilization, which could ultimately reduce reproductive output. While not covered in this review, there are many other possible indirect effects of OA on reproduction that could impact fisheries. Reproduction-related mortality may increase, as acidification can alter immune and stress-response functions, increasing vulnerability to pathogens and secondary stressors during and after reproduction (Mackenzie et al., 2014; Liu et al., 2016; Wang et al., 2016). In many invertebrates, reproductive capacity is closely tied to food availability before or during gametogenesis (Bernard et al., 2011). Changes to prey species dynamics due to acidification, such as altered phytoplankton communities' composition, abundance, and bloom timing (Cheung et al., 2011; Gao et al., 2012), may result in asynchronous invertebrate reproductive processes such that larval production and quality decreases.

Conservation and restoration

Conservation and restoration programs may need to update their strategic plans to account for impacts of acidification on reproduction. For instance, natural recovery of wild populations following removal of stressors (e.g., creation of a marine protected area following overharvest) could be impeded by decreased larval supply due to reduced reproductive success. Populations may take longer to recover, requiring programs to allocate more time and resources for longer-term interventions. Conservation and restoration approaches may need to change altogether, such as moving from passive strategies (e.g., removing disturbances and allowing succession to occur naturally), to active strategies (e.g., transplanting or augmenting wild populations) (Figure 2). For instance, programs may need to incorporate restoration aquaculture and gamete cryopreservation to rebuild threatened populations. While preliminary studies in coral report a variety of response, some aspects of coral reproduction may be uniquely vulnerable to acidification due to their sexual reproduction strategies (Richmond and Hunter, 1990; Burke et al., 2011). In many coral species, gametes take several months to develop, and spawning occurs only a few nights a year over a few hours (Babcock et al., 1986). If OA interferes with these highly coordinated spawning events (Olischläger and Wild, 2020), sexual reproduction could be severely inhibited in the wild, but this has yet to be tested.

Genetic considerations

Genetic diversity, an important factor for species resilience to environmental stressors (Bernhardt and Leslie, 2013; Timpane-Padgham et al., 2017), could shift as a consequence of acidification-induced changes to reproduction and effective population size. Many invertebrate species are r-strategists with highly fecund females (Ramirez Llodra, 2002). Should acidification reduce the number of individuals that reproduce each season due, for instance, to delayed gametogenesis, populations could still be sustained by a few individuals that "win the reproduction lottery" (Hedgecock and Pudovkin, 2011; Sanford and Kelly, 2011). It may therefore be important for programs to actively facilitate genetic diversity and/or resistance to acidification. For commercial and restoration aquaculture facilities, broodstock may need to be collected later or conditioned longer in the hatchery to increase the number of breeding individuals. Conservation programs may need to design marine protected areas that encompass a variety of current and projected pH conditions, not just buffered areas, to enable both diversity and selection for low pH-resilient individuals. To build resilient populations and lines, restoration and breeding programs could leverage standing genetic variability to target genotypes that are reproductively viable in acidified conditions (Parker et al., 2011; Rossi and Tunnicliffe, 2017). This may include careful consideration of broodstock collection sites, such as areas with naturally low or variable pH conditions. Should the number of individuals contributing gametes become dangerously low, programs may need to begin cryopreserving gametes to preserve allelic diversity in a "seed bank" for future use (Figure 2).

Within- and inter-generational acclimatization have been observed in some species in response to acidification (Ross et al., 2016). Adult exposure to acidification may result in beneficial carryover effects for offspring and future generations (Parker et al., 2012; Wong et al., 2019; Zhao et al., 2019; Spencer et al., 2020), which could mitigate some of the negative effects to reproduction reviewed here. While additional research is needed and there may be limitations to inter-generational acclimatization (Byrne et al., 2019), these beneficial carryover effects may be leveraged to improve offspring fitness for production and breeding purposes (Parker et al., 2011; Durland et al., 2019).

Gaps in understanding for OA impacts on reproduction mechanisms

In addition to the critical need to know more about the basic biology and natural history of reproduction in marine invertebrate communities (Box 2), the most pressing need is for increased mechanistic knowledge of reproductive processes to gauge the impact of OA on marine invertebrates (Figure 5). In this section we outline mechanisms that should be explored with future research.

Fertilization mechanisms

Fertilization mechanisms are the most studied reproductive processes in marine invertebrates. Even so, there are still considerable knowledge gaps, particularly in how changes to gamete quality and sperm-egg interactions will affect fertilization (Figure 5). As a model organism for developmental biology, urchin fertilization has been well-studied, with cellular processes potentially impacted by OA reviewed in Bögner (2016). Compared to the numerous echinoderm and molluscan bivalve studies, only a handful of studies have explored OA and fertilization in cnidarians (none in non-hexacoral cnidarians) and crustaceans, and there are none in cephalopods. Considerable research on fertilization mechanisms has come from ascidians (Sawada and Saito, 2022); however, only two studies have examined ascidian fertilization under OA conditions. More studies are clearly needed for these ecologically and economically important taxa.

Gamete quality depends on maintaining an optimal intracellular pH (pH_i). Reductions in extracellular pH are thought to affect pH_i, suppress motility, and impact fertilization success (Christen et al., 1983; Alavi and Cosson, 2005; Morita et al., 2006; Boulais et al., 2018). In certain species, an increase in pH may be required for sperm activation (Nakajima et al., 2005). Explicit measurements of sperm pH_i, including those taken in the field, can help uncover the mechanism behind pH_i activation of sperm motility and its vulnerability to environmental pH conditions.

The impact of acidification on spawned eggs likely depends on their composition, structure, and intracellular conditions. Egg size is used as a proxy for well-provisioned eggs, but few studies empirically test this assumption with lipid analyses. Intracellular egg calcium content can also impact fertilization. Calcium triggers the second meiotic division in eggs, readying it to unite with sperm to complete the fertilization process (Miyazaki, 2006), and is part of the polyspermy defense (Epel, 1978). Egg calcium content can also be influenced by environmental pH (Ciapa and Philippe, 2013). More research should be conducted on energy allocation, maternal provisioning, and egg lipid and calcium content in low pH conditions.

Other structural components that could be influenced by acidification include the egg jelly coat and gamete recognition proteins. Present in echinoderms and molluscs, the jelly coat protects the egg from intense wave action and prevents polyspermy and increases the likelihood of fertilization by increasing the size of the egg (Farley and Levitan, 2001; Podolsky, 2004). Additionally, the jelly coat is known to contain chemoattractants that activate and guide sperm or prevent polyspermy and harbor protective chaperone and gamete recognition proteins (Evans and Sherman, 2013). The dissolution of the jelly coat by low pH conditions observed in echinoderms can reduce percent fertilization, with jelly coats in some populations and species resilient to low pH. Cnidarian eggs do not have jelly coats, and similar structures have not been described in crustaceans. A general survey of gamete accessory structures in marine invertebrates will be beneficial to determine how low pH will impact eggs.

Mechanisms beyond fertilization

Mechanisms controlling pre-fertilization reproductive processes are understudied generally and in the context of OA. In many marine invertebrates, gametogenesis, spawn timing, and synchronicity is influenced by exogenous signals such as temperature, photoperiod, food, and pheromones from conspecific gametes (Galtsoff, 1938; Lawrence and Soame, 2004), and by endogenous signals such as hormones or neuropeptides (Tanabe et al., 2010; Jouaux et al., 2012). Applying knowledge of how these environmental cues are registered and acted upon by organisms may elucidate how low pH will affect these pathways.

Future studies should examine whether OA impacts biochemical cues involved in gametogenesis, coordinated spawning events, and mating behavior. Since many invertebrates are osmoconformers with open circulatory systems, reproductive hormones that circulate through the hemolymph are likely to be exposed to environmental pH changes (Tarrant, 2007; Treen et al., 2012). Structural changes have been observed in signaling peptides outside of the reproductive context (Tarrant, 2007; Roggatz et al., 2016). Exposure to acidification, for instance, resulted in protonation of three peptide signaling molecules, which was associated with behavioral impairment in shore crabs (Roggatz et al., 2016). Whether acidification alters marine invertebrate reproductive hormones is not yet known. This framework could be extended to pheromones involved in mating. Pheromones come in direct contact with the environment, and may be important for spawning synchrony, long-distance mate searches, mate guarding, and copulation dances. Out of all marine invertebrates, reproductive pheromones are best understood in decapod crustaceans. Pheromones released by female crabs instigate courtship displays and guarding behaviors in males (Kamio et al., 2022). Male crabs can distinguish female molting stages and copulation readiness based on pheromone detection (Kamio et al., 2022). Alteration of pheromone chemical composition, molecule shape, and residence time in low pH conditions could impact necessary mating behaviors and successful reproduction (Roggatz et al., 2016; Kamio et al.,

BOX 2 Experimental considerations for future OA and reproduction studies

Improve field research capability

- Spawning timing, duration, and intensity in natural settings are not easily predictable, and we lack baseline reproduction knowledge for most marine species. Additionally, physiological and reproductive responses of laboratory-raised organisms may be compromised by stress associated with captivity.
- Research initiatives should collect baseline knowledge. Technologies should be developed and integrated with biophysical models to track gametes and larvae in the natural environment.

Measure multiple reproductive traits simultaneously

- Reproduction is a complex process. It is important to examine multiple reproductive traits simultaneously to get a better understanding of overall reproductive performance.
- Reporting measures of reproductive success that integrate multiple traits will improve the predictability of demographic models (ex. fecundity and survival of mother, survival of offspring).

Incorporate diversity in test subjects and experimental design

- Studies should maximize genetic variation, as organism origin (i.e., field site, hatchery) and genotype can affect sperm and egg compatibility and confound findings.
- Future work should incorporate taxonomic diversity and multiple stressors to expand the breadth of species and conditions studied.

Account for length of gametogenic cycles

- Gametogenic cycles vary between species. Many studies only expose organisms to OA when gametes are almost fully developed.
- Accounting for gametogenic cycle length improves understanding of OA effects on gamete development and parental effects.

Test multiple sperm concentrations

- The probability of detecting a treatment effect may be dependent upon sperm concentrations. "Optimal" sperm concentration may be higher than ecologically relevant concentrations. Low sperm concentrations can exacerbate OA effects.
- Experiments should use multiple sperm concentrations and gamete incubation times, as these factors may alter the probability of fertilization and/or polyspermy.

Understand limitations of intergenerational studies

- Artificially induced fertilization methods (i.e., strip spawning, chemical/hormonal injection, etc.) used in intergenerational studies may cause organisms to release gametes before complete gametogenesis.
- Many intergenerational OA studies inherently include adult exposure during reproduction, so those studies should formally measure and report reproduction metrics.
- Future research should differentiate between within-generation carryover effects, cross-generational impacts (F0-F1), and multigenerational plasticity (F1-F2 +), and determine how reproductive conditioning may impact each facet of plasticity.

See previous reviews for additional challenges in the design and execution of ocean acidification experiments (Albright et al., 2011b; Grazer and Martin, 2012; Prezeslawski et al., 2017).

2022). Additionally, the ability of invertebrates to produce and detect these compounds may be impacted by low pH (Roggatz et al., 2016; Kamio et al., 2022). A recent hypothesis developed by Olischläger and Wild (2020) suggests that gamete release timing during periods of low water motion is possibly regulated by the carbon concentrating mechanism in corals and/or their symbionts, which may make the synchronized spawning of organisms with photo-symbionts vulnerable to OA. Future work should examine hormones, pheromones, and other factors governing reproductive cues and behavior to identify molecular signals vulnerable to OA.

For a more comprehensive understanding of changes to reproductive resource allocation in acidified conditions, future studies should examine multiple physiological metrics. OA-induced changes in sex-specific growth, tissue regeneration, and energy allocation could impact reproductive resource allocation. While there are no studies correlating internal pH at the site of gametogenesis and environmental pH, organisms that regulate their internal environment may have increased metabolic demand in low pH conditions, and less energy available for reproductive processes (Sokolova et al., 2012). In corals, tissue damage caused a reduction in coral fecundity (Rinkevich and Loya, 1989; Van Veghel and Bak, 1994; Rinkevich, 1996) and tissue regenerated at a lower rate under OA in various hexacorals (Horwitz and Fine, 2014). When exposed to acidified conditions, the intracellular fluid of the crab *Chionoecetes bairdi* did not change in low pH. However, there were significantly more dead hemolymph cells and less granular cells within acidified treatments. This suggests that metabolic demands related to increased cell apoptosis, immune response, and phagocytosis may be diverting energy away from reproduction (Meseck et al., 2016). If organisms can buffer extracellular pH to promote somatic growth or maintenance, the diversion of energetic resources to this task may impact reproduction.

There is a lack of research on how OA affects on brooding behavior in cnidarians, echinoderms, and molluscs. Brooding echinoderms may be disproportionately impacted by OA in the Southern Ocean, based on predicted changes to aragonite and calcite saturations at depths where these species are found (Sewell and Hofmann, 2011). Recent studies show that internal brooding itself may impart tolerance in these taxa. For example, pH conditions in the brood chambers of *Ostrea* spp. oysters are lower than the surrounding water (Gray et al., 2019; Gray et al., 2022). Naturally lower pH in brood chambers could make fertilization

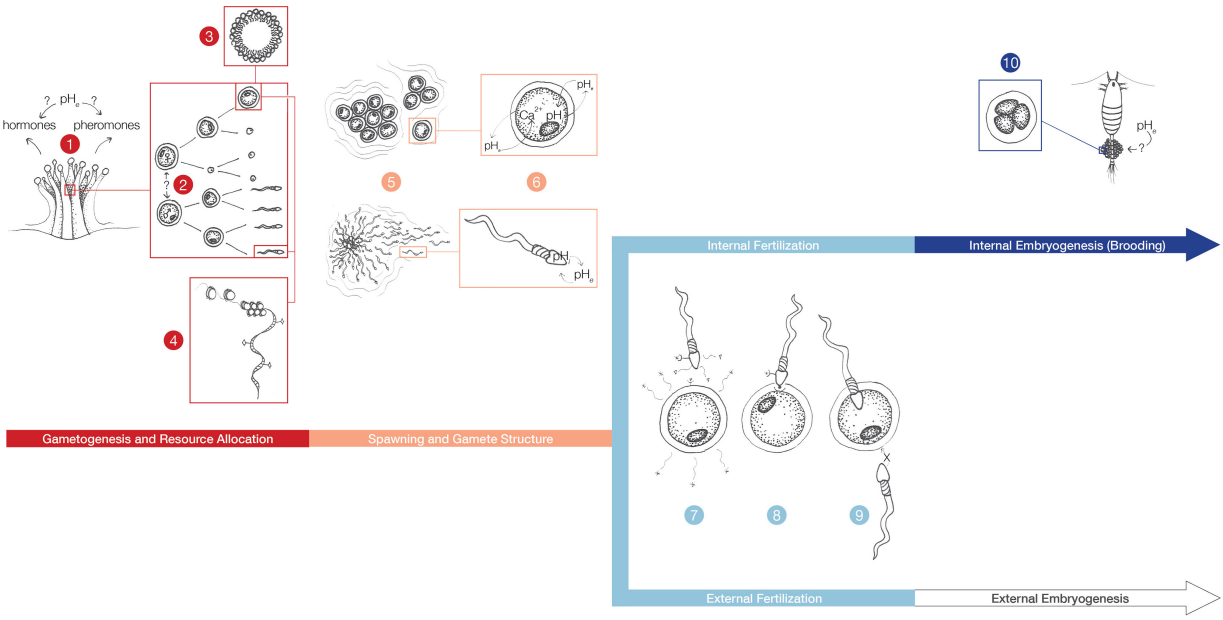

FIGURE 5
Sexual reproduction mechanisms that may be compromised by OA. Changes in the chemical environment can impact the release of hormones and pheromones that trigger gametogenesis, or gamete release in broadcast spawning species (1). Sex determination and differentiation processes (2), gametogenesis timing, and energy allocation (specifically maternal provisioning) (3) can be impacted by low pH. Gametes undergo substantial chromatin reorganization and DNA methylation (4) that can impact how gametes and subsequent offspring respond to acidified conditions. Spawn timing may be affected by OA (5). Gamete bundles undergo breakage, further exposing gamete intracellular conditions to changes in extracellular pH (pH_e) (6). To begin the fertilization process internally or externally, chemoattractants are released from eggs and sperm (7). A single sperm binds to the egg with the aid of gamete recognition proteins (8). Successful fertilization triggers calcium release or an egg jelly coat to prevent polyspermy (9). Internal embryogenesis can be affected by OA (10). For organisms with internal fertilization, brooding may shield embryo development from changes in pHe or expose embryos to more extreme conditions.

more resilient to OA (Lucey et al., 2015; Gray et al., 2019; Gray et al., 2022), thereby providing a potential evolutionary advantage. Potential advantages from brood chambers may not apply to external brooding species like the octocoral *Rhytisma fulvum* (Liberman et al., 2021). Further research should compare low pH impacts on external and internal brooding to determine if both reproductive strategies provide similar evolutionary advantages.

Genomic regulation of reproduction in marine invertebrates is a crucial, yet understudied, area. Determining how OA affects baseline genetic processes related to reproduction is imperative for understanding if processes can be phenotypically plastic or evolve in response to stressors. Genes specific to sex, maturation stage, early gametogenesis, sex determination, and differentiation have been identified for the oyster *C. gigas* (Dheilly et al., 2012; Cavelier et al., 2017; Yue et al., 2018). In other economically-important and edible species like the urchin *P. lividus* and scallop *Pecten maximus*, transcriptome information has been used to identify markers for sex determination (Machado et al., 2022) and gamete quality (Pauletto et al., 2017), respectively. Expressed transcriptomes of reproductively active individuals at various time points may elucidate genetic regulation of reproduction in low pH conditions. In fish, miRNA molecules regulate oogenesis genes; similar analyses should be conducted in invertebrate species to understand other regulators of gametogenesis (Juanchich et al., 2013). If organisms experience low pH during reproductive conditioning, environmental cues may be integrated in the germline through DNA methylation and other epigenetic modifications (Bell and Hellmann, 2019). Sex-associated methylation differences have been documented in *C. gigas*, and OA exposure modified the reproductive tissue methylome in *C. gigas and C. virginica* (Venkataraman et al., 2020; Sun et al., 2022; Venkataraman et al., 2022). Changes to DNA methylation due to low pH may impact successful reproduction or explain intergenerational effects of these conditions on marine invertebrates. Analysis of DNA methylation enzymes during the maternal-to-zygotic transition in coral *M. capitata* embryos exposed to OA suggests that methylome programming occurs within 4 hours of fertilization (Chille et al., 2021), further emphasizing the vulnerability of molecular machinery to OA and its influence on carryover effects. Beyond DNA methylation, changes to chromatin organization may influence reproduction and carryover effects. Gametes, particularly sperm, are subject to significant chromatin reorganization and packaging that can affect the availability of genes for methylation or expression (Eirin-Lopez and Putnam, 2018). As successful reproduction hinges on the survival of offspring, understanding genetic and epigenetic

mechanisms that drive reproduction is important to elucidate changes to reproductive processes and offspring performance.

Conclusion

Despite the large body of research examining the effects of OA on reproduction, there are notable gaps in the literature (Box 2). In addition to the mechanisms described in the previous section, long-term ecological baselines for reproduction are missing for most organisms. This information is essential for understanding the impacts of OA on organismal phenology and the resilience and plasticity of reproductive processes. More ecologically relevant experimental designs are also needed. For instance, knowledge of acidification effects on spawn timing and synchronicity is, to date, largely based on rates of spawning when induced or other metrics that approximate spawn readiness, such as the number of gravid individuals. Moving forward, it will be important to monitor natural spawn rates and timing in variable pH conditions. Studies on how OA affect mating behavior and sex determination and differentiation are very limited, and additional research into the effects of OA and additional environmental stressors on reproduction are also needed (for a summary of multi-stressor studies to date, see Supplemental Materials).

It is crucial that we expand OA studies to include a more diverse set of species with aquaculture, fisheries, and conservation importance. Of the taxa discussed in this review, those that constitute the largest fisheries and cultured species are among the least studied. Crustaceans are notably underrepresented. In wild fisheries, crustacean taxa represent the largest wild-caught group (6.31 billion tons in 2017), with over half of the fishery comprising shrimp and prawn species (3.60 billion tons combined, FAO, 2019), and to date there are no studies that have looked at the effects of OA on the top farmed marine crustaceans worldwide (FAO, 2018). Cephalopods are another overlooked group. Despite 3.77 billion tons of squid, cuttlefish, and octopus harvested globally in 2017 (FAO, 2019), we identified only one cephalopod study in this review that exposed adults to OA and monitored reproductive activity (Spady et al., 2020). Finally, while cnidarians are among the most threatened by changing oceanic conditions (Hoegh-Guldberg et al., 2017), they are also among the least studied. It will be important for future studies to prioritize impacts of acidification on reproduction in species that support aquaculture and fishing communities, restoration, and those species of conservation concern.

Author contributions

JLP-G, LA, LHS, YRV, and LW contributed to conception and design of the study. LA, LHS, YRV, and LW organized the data base. LS performed statistical analyses. LW and YRV produced the illustrations. JLP-G, LA, LHS, YRV, and LW wrote the manuscript. All authors contributed to manuscript revision, read, and approved the submitted version.

Funding

Alfred P. Sloan Research Fellowship, NOAA-Saltonstall Kennedy, NOAA Ocean Acidification Program (NA21OAR4170315), Kenneth K. Chew Endowed Professorship in Aquaculture, Washington Sea Grant, NSF IOS-IEP (1655682) and NSF CAREER BIO-OCE (2044840) awarded to JLP-G. The Joint Institute for the Study of the Atmosphere and Ocean (JISAO), University of Washington Victor and Tamara Loosanoff Endowed Fellowship awarded to LA. National Science Foundation Graduate Research Fellowship, WHOI Postdoctoral Scholar Program awarded to YRV. National Science Foundation Graduate Research Fellowship, NOAA INTERN program, University of Washington Victor and Tamara Loosanoff Endowed Fellowship awarded to LHS. This work was supported by the School of Aquatic and Fishery Sciences at University of Washington.

Acknowledgments

We would like to thank Nùria Viladrich, Paul McElhany and Eileen Bates for their helpful comments with earlier versions of this manuscript and Evan Fiorenza for guidance on the meta-analysis.

Conflict of interest

The authors declare that the research was conducted in the absence of any commercial or financial relationships that could be construed as a potential conflict of interest.

Publisher's note

Supplementary material

The Supplementary Material for this article can be found online at: https://www.frontiersin.org/articles/10.3389/fmars.2022.977754/full#supplementary-material

References

Alavi, S. M. H., and Cosson, J. (2005). Sperm motility in fishes. i. effects of temperature and pH: a review. *Cell Biol. Int.* 29, 101–110. doi: 10.1016/j.cellbi.11.021

Albright, R. (2011a). Effects of ocean acidification on early life history stages of Caribbean scleractinian corals. *Hindawi Publishing Corporation, Journal of Marine Biology* . Available at: https://scholarship.miami.edu/esploro/outputs/991031447465902976. 2011, 14 doi: 10.1155/2011/473615

Albright, R. (2011b). Reviewing the effects of ocean acidification on sexual reproduction and early life history stages of reef-building corals. *J. Mar. Biol* (Hindawi Publishing Corporation) 2011, 14. doi: 10.1155/2011/473615

Albright, R., and Mason, B. (2013). Projected near-future levels of temperature and pCO_2 reduce coral fertilization success. *PloS One* 8, e56468. doi: 10.1371/journal.pone.0056468

Almén, A.-K., Vehmaa, A., Brutemark, A., Bach, L., Lischka, S., Stuhr, A., et al. (2016). Negligible effects of ocean acidification on *Eurytemora affinis* (Copepoda) offspring production. *Biogeosciences* 13, 1037–1048. doi: 10.5194/bg-13-1037-2016

Anand, M., Rangesh, K., Maruthupandy, M., Jayanthi, G., Rajeswari, B., and Priya, R. J. (2021). Effect of CO_2 driven ocean acidification on calcification, physiology and ovarian cells of tropical sea urchin *Salmacis virgulata* – a microcosm approach. *Heliyon* 7 (1), e05970. doi: 10.1016/j.heliyon.2021.e05970

Armstrong, E. J., Dubousquet, V., Mills, S. C., and Stillman, J. H. (2019). Elevated temperature, but not acidification, reduces fertilization success in the small giant clam, *Tridacna maxima*. *Mar. Biol.* 167, 8. doi: 10.1007/s00227-019-3615-0

Babcock, R. C., Bull, G. D., Harrison, P. L., Heyward, A. J., Oliver, J. K., Wallace, C. C., et al. (1986). Synchronous spawnings of 105 scleractinian coral species on the great barrier reef. *Mar. Biol.* 90, 379–394. doi: 10.1007/BF00428562

Barros, P., Sobral, P., Range, P., Chícharo, L., and Matias, D. (2013). Effects of sea-water acidification on fertilization and larval development of the oyster *Crassostrea gigas*. *J. Exp. Mar. Bio. Ecol.* 440, 200–206. doi: 10.1016/j.jembe.2012.12.014

Basallote, M. D., Rodríguez-Romero, A., De Orte, M. R., Del Valls, T. Á., and Riba, I. (2018). CO_2 leakage simulation: effects of the pH decrease on fertilisation and larval development of *Paracentrotus lividus* and sediment metals toxicity. *Chem. Ecol.* 34, 1–21. doi: 10.1080/02757540.2017.1396319

Bechmann, R. K., Taban, I. C., Westerlund, S., Godal, B. F., Arnberg, M., Vingen, S., et al. (2011). Effects of ocean acidification on early life stages of shrimp (*Pandalus borealis*) and mussel (*Mytilus edulis*). *J. Toxicol. Environ. Health A* 74, 424–438. doi: 10.1080/15287394.2011.550460

Bell, A. M., and Hellmann, J. K. (2019). An integrative framework for understanding the mechanisms and multigenerational consequences of transgenerational plasticity. *Annu. Rev. Ecology Evolution Systematics* 50, 97–118. doi: 10.1146/annurev-ecolsys-110218-024613

Bernard, I., de Kermoysan, G., and Pouvreau, S. (2011). Effect of phytoplankton and temperature on the reproduction of the pacific oyster *Crassostrea gigas*: Investigation through DEB theory. *J. Sea Res.* 66, 349–360. doi: 10.1016/j.seares.2011.07.009

Bernhardt, J. R., and Leslie, H. M. (2013). Resilience to climate change in coastal marine ecosystems. *Ann. Rev. Mar. Sci.* 5, 371–392. doi: 10.1146/annurev-marine-121211-172411

Boch, C. A., Litvin, S. Y., Micheli, F., De Leo, G., Aalto, E. A., Lovera, C., et al. (2017). Effects of current and future coastal upwelling conditions on the fertilization success of the red abalone (*Haliotis rufescens*). *ICES J. Mar. Sci.* 74, 1125–1134. doi: 10.1093/icesjms/fsx017

Bögner, D. (2016). Life under climate change scenarios: Sea urchins' cellular mechanisms for reproductive success. *J. Mar. Sci. Eng.* 4, 28. doi: 10.3390/jmse4010028

Bögner, D., Bickmeyer, U., and Köhler, A. (2014). CO_2-induced fertilization impairment in *Strongylocentrotus droebachiensis* collected in the Arctic. *Helgol. Mar. Res.* 68, 341–356. doi: 10.1007/s10152-014-0394-3

Borges, F. O., Figueiredo, C., Sampaio, E., Rosa, R., and Grilo, T. F. (2018a). Transgenerational deleterious effects of ocean acidification on the reproductive success of a keystone crustacean (*Gammarus locusta*). *Mar. Environ. Res.* 138, 55–64. doi: 10.1016/j.marenvres.2018.04.006

Borges, F. O., Sampaio, E., Figueiredo, C., Rosa, R., and Grilo, T. F. (2018b). Hypercapnia-induced disruption of long-distance mate-detection and reduction of energy expenditure in a coastal keystone crustacean. *Physiol. Behav.* 195, 69–75. doi: 10.1016/j.physbeh.2018.07.023

Boulais, M., Chenevert, K. J., Demey, A. T., Darrow, E. S., Robison, M. R., Roberts, J. P., et al. (2017). Oyster reproduction is compromised by acidification experienced seasonally in coastal regions. *Sci. Rep.* 7, 13276. doi: 10.1038/s41598-017-13480-3

Boulais, M., Suquet, M., Arsenault-Pernet, E. J., Malo, F., Queau, I., Pignet, P., et al. (2018). pH controls spermatozoa motility in the pacific oyster (*Crassostrea gigas*). *Biol. Open* 7 (3), bio031427. doi: 10.1242/bio.031427

Burke, L., Reytar, K., Spalding, M., and Perry, A. (2011). *Reefs at risk revisited* (Washington DC: World Resources Institute). Available at: https://hdl.handle.net/20.500.12348/1107.

Bylenga, C. H., Cummings, V. J., and Ryan, K. G. (2015). Fertilisation and larval development in an Antarctic bivalve, *Laternula elliptica*, under reduced pH and elevated temperatures. *Mar. Ecol. Prog. Ser.* 536, 187–201. doi: 10.3354/meps11436

Byrne, M. (2011). Impact of ocean warming and ocean acidification on marine invertebrate life history stages: vulnerabilities and potential for persistence in a changing ocean. *Oceanogr. Mar. Biol. Annu. Rev.* 49, 1–42. doi: 10.1201/b11009-2

Byrne, M. (2012). Global change ecotoxicology: Identification of early life history bottlenecks in marine invertebrates, variable species responses and variable experimental approaches. *Mar. Environ. Res.* 76, 3–15. doi: 10.1016/j.marenvres.2011.10.004

Byrne, M., Foo, S. A., Ross, P. M., and Putnam, H. M. (2019). Limitations of cross and multigenerational plasticity for marine invertebrates faced with global climate change. *Glob. Change Biol.* 26, 80–102. doi: 10.1111/gcb.14882

Byrne, M., Gonzalez-Bernat, M., Doo, S., Foo, S., Soars, N., and Lamare, M. (2013). Effects of ocean warming and acidification on embryos and non-calcifying larvae of the invasive sea star *Patiriella regularis*. *Mar. Ecol. Prog. Ser.* 473, 235–246. doi: 10.3354/meps10058

Byrne, M., Ho, M., Selvakumaraswamy, P., Nguyen, H. D., Dworjanyn, S. A., and Davis, A. R. (2009). Temperature, but not pH, compromises sea urchin fertilization and early development under near-future climate change scenarios. *Proc. Biol. Sci.* 276, 1883–1888. doi: 10.1098/rspb.2008.1935

Byrne, M., and Przeslawski, R. (2013). Multistressor impacts of warming and acidification of the ocean on marine invertebrates' life histories. *Integr. Comp. Biol.* 53, 582–596. doi: 10.1093/icb/ict049

Byrne, M., Soars, N. A., Ho, M. A., Wong, E., McElroy, D., Selvakumaraswamy, P., et al. (2010a). Fertilization in a suite of coastal marine invertebrates from SE Australia is robust to near-future ocean warming and acidification. *Mar. Biol.* 157, 2061–2069. doi: 10.1007/s00227-010-1474-9

Byrne, M., Soars, N., Selvakumaraswamy, P., Dworjanyn, S. A., and Davis, A. R. (2010b). Sea Urchin fertilization in a warm, acidified and high pCO_2 ocean across a range of sperm densities. *Mar. Environ. Res.* 69, 234–239. doi: 10.1016/j.marenvres.2009.10.014

Caballes, C. F., Pratchett, M. S., Raymundo, M. L., and Rivera-Posada, J. A. (2017). Environmental tipping points for sperm motility, fertilization, and embryonic development in the crown-of-Thorns starfish. *Diversity* 9, 10. doi: 10.3390/d9010010

Caetano, L. S., Pereira, T. M., Envangelista, J. D., Cabral, D. S., Carvalho Coppo, G., de Souza, L. A., et al. (2021). Impact on fertility rate and embryo-larval development due to the association acidification, ocean warming and lead contamination of a Sea urchin *Echinometra lucunter* (Echinodermata: Echinoidea). *Bull. Environ. Contam. Toxicol.* 106, 923–928. doi: 10.1007/s00128-021-03225-4

Caldwell, G. S., Fitzer, S., Gillespie, C. S., Pickavance, G., Turnbull, E., and Bentley, M. G. (2011). Ocean acidification takes sperm back in time. *Invertebrate Reprod. Dev.* 55, 217–221. doi: 10.1080/07924259.2011.574842

Campbell, A. L., Levitan, D. R., Hosken, D. J., and Lewis, C. (2016). Ocean acidification changes the male fitness landscape. *Sci. Rep.* 6, 31250. doi: 10.1038/srep31250

Cao, Z., Mu, F., Wei, X., and Sun, Y. (2015). Influence of CO_2-induced seawater acidification on the development and lifetime reproduction of *Tigriopus japonicus* Mori1931 938. *J. Nat. Hist.* 49, 2813–2826. doi: 10.1080/00222933.2015.1034213

Cardoso, P. G., Loganimoce, E. M., Neuparth, T., Rocha, M. J., Rocha, E., and Arenas, F. (2018). Interactive effects of increased temperature, pCO_2 and the synthetic progestin levonorgestrel on the fitness and breeding of the amphipod *Gammarus locusta*. *Environ. pollut.* 236, 937–947. doi: 10.1016/j.envpol.2017.10.065

Caroselli, E., Gizzi, F., Prada, F., Marchini, C., Airi, V., Kaandorp, J., et al. (2019). Low and variable pH decreases recruitment efficiency in populations of a temperate coral naturally present at a CO_2 vent. *Limnology Oceanography* 64, 1059–1069. doi: 10.1002/lno.11097

Cavelier, P., Cau, J., Morin, N., and Delsert, C. (2017). Early gametogenesis in the pacific oyster: new insights using stem cell and mitotic markers. *J. Exp. Biol.* 220, 3988–3996. doi: 10.1242/jeb.167734

Challener, R. C., Watts, S. A., and McClintock, J. B. (2014). Effects of hypercapnia on aspects of feeding, nutrition, and growth in the edible sea urchin

Lytechinus variegatus held in culture. *Mar. Freshw. Behav. Physiol.* 47, 41–62. doi: 10.1080/10236244.2013.875273

Cheung, W. W. L., Dunne, J., Sarmiento, J. L., and Pauly, D. (2011). Integrating ecophysiology and plankton dynamics into projected maximum fisheries catch potential under climate change in the northeast Atlantic. *ICES J. Mar. Sci.* 68, 1008–1018. doi: 10.1093/icesjms/fsr012

Chille, E., Strand, E., Neder, M., Schmidt, V., Sherman, M., Mass, T., et al. (2021). Developmental series of gene expression clarifies maternal mRNA provisioning and maternal-to-zygotic transition in the reef-building coral *Montipora capitata*. *BMC Genomics* 22, 1–17. doi: 10.1186/s12864-021-08114-y

Choi, K.-H., Jang, M.-C., Shin, H. H., Lee, W.-J., and Shin, K. (2016). *In situ* hatching success of calanoid copepod eggs in hypoxic sediments of a coastal bay. *J. Coast. Res.* 32, 333–338. doi: 10.2112/JCOASTRES-D-14-00096.1

Christen, R., Schackmann, R. W., and Shapiro, B. M. (1983). Metabolism of sea urchin sperm. interrelationships between intracellular pH, ATPase activity, and mitochondrial respiration. *J. Biol. Chem.* 258, 5392–5399. doi: 10.1016/S0021-9258(20)81902-4

Chua, C., Leggat, W., Moya, A., and Baird, A. H. (2013). Temperature affects the early life history stages of corals more than near future ocean acidification. *Mar. Ecol. Prog. Ser.* 475, 85–92. doi: 10.3354/meps10077

Ciapa, B., and Philippe, L. (2013). Intracellular and extracellular pH and Ca are bound to control mitosis in the early sea urchin embryo *via* ERK and MPF activities. *PloS One* 8, e66113. doi: 10.1371/journal.pone.0066113

Clements, J. C., Carver, C. E., Mallet, M. A., Comeau, L. A., and Mallet, A. L. (2020). CO_2-induced low pH in an eastern oyster (*Crassostrea virginica*) hatchery positively affects reproductive development and larval survival but negatively affects larval shape and size, with no intergenerational linkages. *ICES J. Mar. Sci.* 78, 349–359. doi: 10.1093/icesjms/fsaa089

Cohen-Rengifo, M., Garcia, E., Hernandez, C. A., Hernandez, J. C., and Clemente, S. (2013). Global warming and ocean acidification affect fertilization and early development of the sea urchin *Paracentrotus lividus*. *Cah. Biol. Mar.* 54, 667–675.

Conradi, M., Sánchez-Moyano, J. E., Galotti, A., Jiménez-Gómez, F., Jiménez-Melero, R., Guerrero, F., et al. (2019). CO_2 leakage simulation: Effects of the decreasing pH to the survival and reproduction of two crustacean species. *Mar. pollut. Bull.* 143, 33–41. doi: 10.1016/j.marpolbul.2019.04.020

Cooley, S., Schoeman, D., Bopp, L., Boyd, P., Donner, S., Ghebrehiwet, D. Y., et al. (2022). Oceans and Coastal Ecosystems and Their Services. In: Climate Change 2022: Impacts, Adaptation and Vulnerability. *Contribution of Working Group II to the Sixth Assessment Report of the Intergovernmental Panel on Climate Change* H.-O. Pörtner, D.C. Roberts, M. Tignor, E.S. Poloczanska and K. Mintenbeck. (eds.) Cambridge, UK and New York, NY, USA: Cambridge University Press, pp. 379–550. doi: 10.1017/9781009325844.005

Cripps, G., Lindeque, P., and Flynn, K. (2014). Parental exposure to elevated pCO_2 influences the reproductive success of copepods. *J. Plankton Res.* 36, 1165–1174. doi: 10.1093/plankt/fbu052

da Silva Souza, L., Pusceddu, F. H., Cortez, F. S., de Orte, M. R., Seabra, A. A., Cesar, A., et al. (2019). Harmful effects of cocaine byproduct in the reproduction of sea urchin in different ocean acidification scenarios. *Chemosphere* 236, 124284. doi: 10.1016/j.chemosphere.2019.07.015

Dell'Acqua, O., Ferrando, S., Chiantore, M., and Asnaghi, V. (2019). The impact of ocean acidification on the gonads of three key Antarctic benthic macroinvertebrates. *Aquat. Toxicol.* 210, 19–29. doi: 10.1016/j.aquatox.2019.02.012

Dheilly, N. M., Lelong, C., Huvet, A., Kellner, K., Dubos, M.-P., Riviere, G., et al. (2012). Gametogenesis in the pacific oyster *Crassostrea gigas*: a microarrays-based analysis identifies sex and stage specific genes. *PloS One* 7, e36353. doi: 10.1371/journal.pone.0036353

Dionísio, G., Faleiro, F., Bilan, M., Rosa, I. C., Pimentel, M., Serôdio, J., et al. (2017). Impact of climate change on the ontogenetic development of "solar-powered" sea slugs. *Mar. Ecol. Prog. Ser.* 578, 87–97. doi: 10.3354/meps12227

Doney, S. C., Fabry, V. J., Feely, R. A., and Kleypas, J. A. (2009). Ocean acidification: the other CO_2 problem. *Ann. Rev. Mar. Sci.* 1, 169–192. doi: 10.1146/annurev.marine.010908.163834

Dupont, S., Dorey, N., Stumpp, M., Melzner, F., and Thorndyke, M. (2013). Long-term and trans-life-cycle effects of exposure to ocean acidification in the green sea urchin *Strongylocentrotus droebachiensis*. *Mar. Biol.* 160, 1835–1843. doi: 10.1007/s00227-012-1921-x

Dupont, S., Ortega-Martínez, O., and Thorndyke, M. (2010). Impact of near-future ocean acidification on echinoderms. *Ecotoxicology* 19, 449–462. doi: 10.1007/s10646-010-0463-6

Durland, E., Waldbusser, G., and Langdon, C. (2019). Comparison of larval development in domesticated and naturalized stocks of the pacific oyster *Crassostrea gigas* exposed to high pCO_2 conditions. *Mar. Ecol. Prog. Ser.* 621, 107–125. doi: 10.3354/meps12983

Dworjanyn, S. A., and Byrne, M. (2018). Impacts of ocean acidification on sea urchin growth across the juvenile to mature adult life-stage transition is mitigated by warming. *Proc. Biol. Sci.* 285 (1876), 20172684. doi: 10.1098/rspb.2017.2684

Eads, A. R., Kennington, W. J., and Evans, J. P. (2016). Interactive effects of ocean warming and acidification on sperm motility and fertilization in the mussel *Mytilus galloprovincialis*. *Mar. Ecol. Prog. Ser.* 562, 101–111. doi: 10.3354/meps11944

Egilsdottir, H., Spicer, J. I., and Rundle, S. D. (2009). The effect of CO_2 acidified sea water and reduced salinity on aspects of the embryonic development of the amphipod *Echinogammarus marinus* (Leach). *Mar. pollut. Bull.* 58, 1187–1191. doi: 10.1016/j.marpolbul.2009.03.017

Eirin-Lopez, J. M., and Putnam, H. M. (2019). Marine environmental epigenetics. *Ann. Rev. Mar. Sci.* 11, 335–368. doi: 10.1146/annurev-marine-010318-095114

Elliott, M., Burdon, D., Hemingway, K. L., and Apitz, S. E. (2007). Estuarine, coastal and marine ecosystem restoration: confusing management and science–a revision of concepts. *Estuar. Coast. Shelf Sci.* 74, 349–366. doi: 10.1016/j.ecss.2007.05.034

Ellis, R. P., Davison, W., Queirós, A. M., Kroeker, K. J., Calosi, P., Dupont, S., et al. (2017). Does sex really matter? explaining intraspecies variation in ocean acidification responses. *Biol. Lett.* 13 (2), 20160761. doi: 10.1098/rsbl.2016.0761

Engström-Öst, J., Holmborn, T., Brutemark, A., Hogfors, H., Vehmaa, A., and Gorokhova, E. (2014). The effects of short-term pH decrease on the reproductive output of the copepod *Acartia bifilosa* – a laboratory study. *Mar. Freshw. Behav. Physiol.* 47, 173–183. doi: 10.1080/10236244.2014.919096

Epel, D. (1978). Chapter 7 mechanisms of activation of sperm and egg during fertilization of Sea urchin gametes. *Curr. Topics Dev. Biol.*, 12, 185–246. doi: 10.1016/s0070-2153(08)60597-9

Ericson, J. (2010). *Effects of ocean acidification on fertilisation and early development in polar and temperate marine invertebrates* ([Dunedin (New Zealand: University of Otago). Available at: http://hdl.handle.net/10523/2945.

Ericson, J. A., Ho, M. A., Miskelly, A., King, C. K., Virtue, P., Tilbrook, B., et al. (2012). Combined effects of two ocean change stressors, warming and acidification, on fertilization and early development of the Antarctic echinoid *Sterechinus neumayeri*. *Polar Biol.* 35, 1027–1034. doi: 10.1007/s00300-011-1150-7

Esposito, M. C., Boni, R., Cuccaro, A., Tosti, E., and Gallo, A. (2020). Sperm motility impairment in free spawning invertebrates under near-future level of ocean acidification: uncovering the mechanism. *Front. Mar. Science.* 6, 794 doi: 10.3389/fmars.2019.00794

Evans, J. P., and Sherman, C. D. H. (2013). Sexual selection and the evolution of egg-sperm interactions in broadcast-spawning invertebrates. *Biol. Bull.* 224, 166–183. doi: 10.1086/BBLv224n3p166

Falkenberg, L. J., Styan, C. A., and Havenhand, J. N. (2019). Sperm motility of oysters from distinct populations differs in response to ocean acidification and freshening. *Sci. Rep.* 9, 7970. doi: 10.1038/s41598-019-44321-0

FAO (2018). *The state of world fisheries and Aquaculture2012, 018 - meeting the sustainable development goals* (Rome: License: CC). Available at: https://www.fao.org/3/i9540en/i9540en.pdf.

FAO (2019). FAO yearbook. fishery and aquaculture Statistics2012, 017/FAO annuaire. statistiques des pêches et de l'aquaculture2012, 017/FAO anuario. estadísticas de pesca y acuicultura2012, 017. *Food Agric. Org.* 82.

Farley, G. S., and Levitan, D. R. (2001). The role of jelly coats in sperm-egg encounters, fertilization success, and selection on egg size in broadcast spawners. *Am. Nat.* 157, 626–636. doi: 10.1086/320619

Findlay, H. S., Kendall, M. A., Spicer, J. I., and Widdicombe, S. (2009). Future high CO_2 in the intertidal may compromise adult barnacle *Semibalanus balanoides* survival and embryonic development rate. *Mar. Ecol. Prog. Ser.* 389, 193–202. doi: 10.3354/meps08141

Fine, M., and Tchernov, D. (2007). Scleractinian coral species survive and recover from decalcification. *Science* 315, 1811. doi: 10.1126/science.1137094

Fiorenza, E. A., Wendt, C. A., Dobkowski, K. A., King, T. L., Pappaionou, M., Rabinowitz, P., et al. (2020). It's a wormy world: Meta-analysis reveals several decades of change in the global abundance of the parasitic nematodes anisakis spp. and *Pseudoterranova* spp. in marine fishes and invertebrates. *Glob. Change Biol.* 26, 2854–2866. doi: 10.1111/gcb.15048

Fitzer, S. C., Bishop, J. D. D., Caldwell, G. S., Clare, A. S., Upstill-Goddard, R. C., and Bentley, M. G. (2012a). Visualisation of the copepod female reproductive system using confocal laser scanning microscopy and two-photon microscopy. *J. Crustacean Biol.* 32, 685–692. doi: 10.1163/193724012X639788

Fitzer, S. C., Caldwell, G. S., Close, A. J., Clare, A. S., Upstill-Goddard, R. C., and Bentley, M. G. (2012b). Ocean acidification induces multi-generational decline in copepod naupliar production with possible conflict for reproductive resource allocation. *J. Exp. Mar. Bio. Ecol.* 418-419, 30–36. doi: 10.1016/j.jembe.2012.03.009

Foo, S. A. (2015). "Acclimatisation and adaptive capacity of sea urchins in a changing ocean: Effects of ocean warming and acidification on early development and the potential to persist," (Sydney (Australia: University of Sydney). Available at: http://hdl.handle.net/2123/14988.

Foo, S. A., and Byrne, M. (2017). Marine gametes in a changing ocean: Impacts of climate change stressors on fecundity and the egg. *Mar. Environ. Res.* 128, 12–24. doi: 10.1016/j.marenvres.2017.02.004

Foo, S. A., Deaker, D., and Byrne, M. (2018). Cherchez la femme - impact of ocean acidification on the egg jelly coat and attractants for sperm. *J. Exp. Biol.* 221 (13), jeb177188. doi: 10.1242/jeb.177188

Foo, S. A., Dworjanyn, S. A., Khatkar, M. S., Poore, A. G. B., and Byrne, M. (2014). Increased temperature, but not acidification, enhances fertilization and development in a tropical urchin: potential for adaptation to a tropicalized eastern Australia. *Evol. Appl.* 7, 1226–1237. doi: 10.1111/eva.12218

Foo, S. A., Dworjanyn, S. A., Poore, A. G. B., Harianto, J., and Byrne, M. (2016). Adaptive capacity of the sea urchin *Heliocidaris erythrogramma* to ocean change stressors: responses from gamete performance to the juvenile. *Mar. Ecol. Prog. Ser.* 556, 161–172. doi: 10.3354/meps11841

Frieder, C. A. (2014). Present-day nearshore pH differentially depresses fertilization in congeneric sea urchins. *Biol. Bull.* 226, 1–7. doi: 10.1086/BBLv226n1p1

Froehlich, H. E., Gentry, R. R., and Halpern, B. S. (2017). Conservation aquaculture: Shifting the narrative and paradigm of aquaculture's role in resource management. *Biol. Conserv.* 215, 162–168. doi: 10.1016/j.biocon.2017.09.012

Gallo, A., Boni, R., Buia, M. C., Monfrecola, V., Esposito, M. C., and Tosti, E. (2019). Ocean acidification impact on ascidian *Ciona robusta* spermatozoa: New evidence for stress resilience. *Sci. Total Environ.* 697, 134100. doi: 10.1016/j.scitotenv.2019.134100

Gallo, A., Esposito, M. C., Cuccaro, A., Buia, M. C., Tarallo, A., Monfrecola, V., et al. (2020). Adult exposure to acidified seawater influences sperm physiology in *Mytilus galloprovincialis*: Laboratory and *in situ* transplant experiments. *Environ. pollut.* 265, 115063. doi: 10.1016/j.envpol.2020.115063

Galtsoff, P. S. (1938). Physiology of reproduction of *Ostrea virginica*. *Biol. Bull.* 75, 286–307. doi: 10.2307/1537736

Gao, K., Xu, J., Gao, G., Li, Y., Hutchins, D. A., Huang, B., et al. (2012). Rising CO_2 and increased light exposure synergistically reduce marine primary productivity. *Nat. Climate Change* 2, 519–523. doi: 10.1038/nclimate1507

García, E., Hernández, J. C., and Clemente, S. (2018). Robustness of larval development of intertidal sea urchin species to simulated ocean warming and acidification. *Mar. Environ. Res.* 139, 35–45. doi: 10.1016/j.marenvres.2018.04.011

Gianguzza, P., Visconti, G., Gianguzza, F., Vizzini, S., Sarà, G., and Dupont, S. (2014). Temperature modulates the response of the thermophilous sea urchin *Arbacia lixula* early life stages to CO_2-driven acidification. *Mar. Environ. Res.* 93, 70–77. doi: 10.1016/j.marenvres.2013.07.008

Gibbs, M. C., Parker, L. M., Scanes, E., Byrne, M., O'Connor, W. A., and Ross, P. M. (2021a). Adult exposure to ocean acidification and warming leads to limited beneficial responses for oyster larvae. *ICES J. Mar. Sci.* 78, 2017–2030. doi: 10.1093/icesjms/fsab071

Gibbs, M. C., Parker, L. M., Scanes, E., Byrne, M., O'Connor, W. A., and Ross, P. M. (2021b). Adult exposure to ocean acidification and warming remains beneficial for oyster larvae following starvation. *ICES J. Mar. Sci.* 78, 1587–1598. doi: 10.1093/icesjms/fsab066

Gizzi, F., de Mas, L., Airi, V., Caroselli, E., Prada, F., Falini, G., et al. (2017). Reproduction of an azooxanthellate coral is unaffected by ocean acidification. *Sci. Rep.* 7, 13049. doi: 10.1038/s41598-017-13393-1

Gonzales-Bernat, M. J., Lamare, M., Uthicke, S., and Byrne, M. (2013). Fertilization, embryogenesis and larval development in the tropical intertidal sand dollar *Arachnoides placenta* in response to reduced seawater pH. *Mar. Biol.* 160, 1927–1194. doi: 10.1007/s00227-012-2034-2

Graham, H., Rastrick, S. P. S., Findlay, H. S., Bentley, M. G., Widdicombe, S., Clare, A. S., et al. (2015). Sperm motility and fertilisation success in an acidified and hypoxic environment. *ICES J. Mar. Sci.* 73, 783–790. doi: 10.1093/icesjms/fsv171

Gravinese, P. M. (2018). Ocean acidification impacts the embryonic development and hatching success of the Florida stone crab, *Menippe mercenaria*. *J. Exp. Mar. Bio. Ecol.* 500, 140–146. doi: 10.1016/j.jembe.2017.09.001

Gray, M. W., Chaparro, O., Huebert, K. B., O'Neill, S. P., Couture, T., Moreira, A., et al. (2019). Life history traits conferring larval resistance against ocean acidification: The case of brooding oysters of the genus *Ostrea*. *J. Shellfish Res.* 38, 751. doi: 10.2983/035.038.0326

Gray, M. W., Salas-Yanquin, L. P., Bűchner-Miranda, J. A., and Chaparro, O. R. (2022). The *Ostrea chilensis* pallial cavity: nursery, prison, and time machine. *Mar. Biol.* 169, 25. doi: 10.1007/s00227-021-04015-6

Grazer, V. M., and Martin, C. (2012). Investigating climate change and reproduction: experimental tools from evolutionary biology. *Biology*, 1(2), 411–438.

Guo, X., Huang, M., Shi, B., You, W., and Ke, C. (2020). Effects of ocean acidification on toxicity of two trace metals in two marine molluscs in their early life stages. *Aquac. Environ. Interact.* 12, 281–296. doi: 10.3354/aei00362

Han, Y., Shi, W., Tang, Y., Zhao, X., Du, X., Sun, S., et al. (2021). Ocean acidification increases polyspermy of a broadcast spawning bivalve species by hampering membrane depolarization and cortical granule exocytosis. *Aquat. Toxicol.* 231, 105740. doi: 10.1016/j.aquatox.2020.105740

Havenhand, J. N., Buttler, F.-R., Thorndyke, M. C., and Williamson, J. E. (2008). Near-future levels of ocean acidification reduce fertilization success in a sea urchin. *Curr. Biol.* 18, R651–R652. doi: 10.1016/j.cub.2008.06.015

Havenhand, J. N., and Schlegel, P. (2009). Near-future levels of ocean acidification do not affect sperm motility and fertilization kinetics in the oyster *Crassostrea gigas*. *Biogeosciences* 6, 3009–3015. doi: 10.5194/bg-6-3009-2009

Hazan, Y., Wangensteen, O. S., and Fine, M. (2014). Tough as a rock-boring urchin: adult *Echinometra* sp. EE from the red Sea show high resistance to ocean acidification over long-term exposures. *Mar. Biol.* 161, 2531–2545. doi: 10.1007/s00227-014-2525-4

Hedgecock, D., and Pudovkin, A. I. (2011). Sweepstakes reproductive success in highly fecund marine fish and shellfish: A review and commentary. *Bull. Mar. Sci.* 87, 971–1002. doi: 10.5343/bms.2010.1051

Helm, M. M., Bourne, N., and Lovatelli, A. (2004). *Hatchery culture of bivalves: a practical manual* (FAO, Rome). Available at: http://www.sidalc.net/cgi-bin/wxis.exe/?IsisScript=UACHBC.xis&method=post&formato=2&cantidad=1&expresion=mfn=102646.

Hoegh-Guldberg, O., and Bruno, J. F. (2010). The impact of climate change on the world's marine ecosystems. *Science* 328, 1523–1528. doi: 10.1126/science.1189930

Hoegh-Guldberg, O., Poloczanska, E. S., Skirving, W., and Dove, S. (2017). Coral reef ecosystems under climate change and ocean acidification. *Front. Mar. Sci.* 4. doi: 10.3389/fmars.2017.00158

Ho, M. A., Price, C., King, C. K., Virtue, P., and Byrne, M. (2013). Effects of ocean warming and acidification on fertilization in the Antarctic echinoid *Sterechinus neumayeri* across a range of sperm concentrations. *Mar. Environ. Res.* 90, 136–141. doi: 10.1016/j.marenvres.2013.07.007

Horwitz, R., and Fine, M. (2014). High CO_2 detrimentally affects tissue regeneration of red Sea corals. *Coral Reefs* 33, 819–829. doi: 10.1007/s00338-014-1150-5

Howes, E., Joos, F., Eakin, M., and Gattuso, J.-P. (2015). An updated synthesis of the observed and projected impacts of climate change on the chemical, physical and biological processes in the oceans. *Front. Mar. Sci.* 2. doi: 10.3389/fmars.2015.00036

Hue, T., Chateau, O., Lecellier, G., Kayal, M., Lanos, N., Gossuin, H., et al. (2020). Temperature affects the reproductive outputs of coral-eating starfish acanthaster spp. after adult exposure to near-future ocean warming and acidification. *Mar. Environ. Res.* 162, 105164. doi: 10.1016/j.marenvres.2020.105164

Hu, M. Y., Lein, E., Bleich, M., Melzner, F., and Stumpp, M. (2018). Trans-life cycle acclimation to experimental ocean acidification affects gastric pH homeostasis and larval recruitment in the sea star *Asterias rubens*. *Acta Physiol.* 224, e13075. doi: 10.1111/apha.13075

Iguchi, A., Suzuki, A., Sakai, K., and Nojiri, Y. (2015). Comparison of the effects of thermal stress and CO_2-driven acidified seawater on fertilization in coral *Acropora digitifera*. *Zygote* 23, 631–634. doi: 10.1017/S0967199414000185

IPCC (2022). *Climate Change2022, 022: Impacts, adaptation, and vulnerability. contribution of working group II to the sixth assessment report of the intergovernmental panel on climate change*. Eds. H.-O. Pörtner, D. C. Roberts, M. Tignor, E. S. Poloczanska, K. Mintenbeck, A. Alegría, M. Craig, S. Langsdorf, S. Löschke, V. Möller, A. Okem and B. Rama (Cambridge, UK and New York, NY, USA: Cambridge University Press). 3056.

Isari, S., Zervoudaki, S., Peters, J., Papantoniou, G., Pelejero, C., and Saiz, E. (2015). Lack of evidence for elevated CO_2-induced bottom-up effects on marine copepods: a dinoflagellate–calanoid prey–predator pair. *ICES J. Mar. Sci.* 73, 650–658. doi: 10.1093/icesjms/fsv078

Jokiel, P. L., Rodgers, K. S., Kuffner, I. B., Andersson, A. J., Cox, E. F., and Mackenzie, F. T. (2008). Ocean acidification and calcifying reef organisms: a mesocosm investigation. *Coral Reefs* 27, 473–483. doi: 10.1007/s00338-008-0380-9

Jouaux, A., Franco, A., Heude-Berthelin, C., Sourdaine, P., Blin, J. L., Mathieu, M., et al. (2012). Identification of ras, pten and p70S6K homologs in the pacific oyster *Crassostrea gigas* and diet control of insulin pathway. *Gen. Comp. Endocrinol.* 176, 28–38. doi: 10.1016/j.ygcen.2011.12.008

Juanchich, A., Le Cam, A., Montfort, J., Guiguen, Y., and Bobe, J. (2013). Identification of differentially expressed miRNAs and their potential targets during fish ovarian development. *Biol. Reprod.* 88, 128. doi: 10.1095/biolreprod.112.105361

Kamio, M., Yambe, H., and Fusetani, N. (2022). Chemical cues for intraspecific chemical communication and interspecific interactions in aquatic environments:

applications for fisheries and aquaculture. *Fish. Sci.* 88, 203–239. doi: 10.1007/s12562-021-01563-0

Kamya, P. Z., Dworjanyn, S. A., Hardy, N., Mos, B., Uthicke, S., and Byrne, M. (2014). Larvae of the coral eating crown-of-thorns starfish, *Acanthaster planci* in a warmer-high CO_2 ocean. *Glob. Change Biol.* 20, 3365–3376. doi: 10.1111/gcb.12530

Kapsenberg, L., Okamoto, D. K., Dutton, J. M. , and Hofmann, G. (2017). Sensitivity of sea urchin fertilization to pH varies across a natural pH mosaic. *Ecol. Evol.* 7, 1737–1750. doi: 10.1002/ece3.2776

Karelitz, S., Lamare, M. D., Mos, B., De Bari, H., Dworjanyn, S. A., and Byrne, M. (2019). Impact of growing up in a warmer, lower pH future on offspring performance: transgenerational plasticity in a pan-tropical sea urchin. *Coral Reefs* 38, 1085–1095. doi: 10.1007/s00338-019-01855-z

Kimura, R., Takami, H., Ono, T., Onitsuka, T., and Nojiri, Y. (2011). Effects of elevated pCO_2 on the early development of the commercially important gastropod, ezo abalone *Haliotis discus hannai*. *Fish. Oceanogr.* 20, 357–366. doi: 10.1111/j.1365-2419.2011.00589.x

Kita, J., Kikkawa, T., Asai, T., and Ishimatsu, A. (2013). Effects of elevated pCO_2 on reproductive properties of the benthic copepod *Tigriopus japonicus* and gastropod *Babylonia japonica*. *Mar. pollut. Bull.* 73, 402–408. doi: 10.1016/j.marpolbul.2013.06.026

Kong, H., Jiang, X., Clements, J. C., Wang, T., Huang, X., Shang, Y., et al. (2019). Transgenerational effects of short-term exposure to acidification and hypoxia on early developmental traits of the mussel *Mytilus edulis*. *Mar. Environ. Res.* 145, 73–80. doi: 10.1016/j.marenvres.2019.02.011

Korpelainen, H. (1990). Sex ratios and conditions required for environmental sex determination in animals. *Biol. Rev. Camb. Philos. Soc* 65, 147–184. doi: 10.1111/j.1469-185x.1990.tb01187.x

Kroeker, K. J., Kordas, R. L., Crim, R. N., and Singh, G. G. (2010). Meta-analysis reveals negative yet variable effects of ocean acidification on marine organisms. *Ecol. Lett.* 13, 1419–1434. doi: 10.1111/j.1461-0248.2010.01518.x

Kurihara, H. (2008). Effects of CO_2-driven ocean acidification on the early developmental stages of invertebrates. *Mar. Ecol. Prog. Ser.* 373, 275–284. doi: 10.3354/meps07802

Kurihara, H., and Ishimatsu, A. (2008). Effects of high CO_2 seawater on the copepod (*Acartia tsuensis*) through all life stages and subsequent generations. *Mar. pollut. Bull.* 56, 1086–1090. doi: 10.1016/j.marpolbul.2008.03.023

Kurihara, H., Matsui, M., Furukawa, H., Hayashi, M., and Ishimatsu, A. (2008). Long-term effects of predicted future seawater CO_2 conditions on the survival and growth of the marine shrimp *Palaemon pacificus*. *J. Exp. Mar. Bio. Ecol.* 367, 41–46. doi: 10.1016/j.jembe.2008.08.016

Kurihara, H., Shimode, S., and Shirayama, Y. (2004). Effects of raised CO_2 concentration on the egg production rate and early development of two marine copepods (*Acartia steueri* and *Acartia erythraea*). *Mar. pollut. Bull.* 49, 721–727. doi: 10.1016/j.marpolbul.2004.05.005

Kurihara, H., and Shirayama, Y. (2004). Effects of increased atmospheric CO_2 on sea urchin early development. *Mar. Ecol. Prog. Ser.* 274, 161–169. doi: 10.3354/meps274161

Kurihara, H., Yin, R., Nishihara, G. N., Soyano, K., and Ishimatsu, A. (2013). Effect of ocean acidification on growth, gonad development and physiology of the sea urchin *Hemicentrotus pulcherrimus*. *Aquat. Biol.* 18, 281–292. doi: 10.3354/ab00510

Langer, J. A. F., Meunier, C. L., Ecker, U., Horn, H. G., Schwenk, K., and Boersma, M. (2019). Acclimation and adaptation of the coastal calanoid copepod *Acartia tonsa* to ocean acidification: a long-term laboratory investigation. *Mar. Ecol. Prog. Ser.* 619, 35–51. doi: 10.3354/meps12950

Lawrence, A. J., and Soame, J. M. (2004). The effects of climate change on the reproduction of coastal invertebrates. *Ibis* 146, 29–39. doi: 10.1111/j.1474-919X.2004.00325.x

Lee, E. H., Choi, S. Y., Seo, M. H., Lee, S. J., and Soh, H. Y. (2020). Effects of temperature and pH on the egg production and hatching success of a common Korean copepod. *Diversity* 12, 372. doi: 10.3390/d12100372

Lee, Y. H., Kang, H.-M., Kim, M.-S., Wang, M., Kim, J. H., Jeong, C.-B., et al. (2019). Effects of ocean acidification on life parameters and antioxidant system in the marine copepod *Tigriopus japonicus*. *Aquat. Toxicol.* 212, 186–193. doi: 10.1016/j.aquatox.2019.05.007

Le Moullac, G., Soyez, C., Vidal-Dupiol, J., Belliard, C., Fievet, J., Sham-Koua, M., et al. (2016). Impact of pCO_2 on the energy, reproduction and growth of the shell of the pearl oyster *Pinctada margaritifera*. *Estuar. Coast. Shelf Sci.* 182, 274–282. doi: 10.1016/j.ecss.2016.03.011

Lenz, B., Fogarty, N. D., and Figueiredo, J. (2019). Effects of ocean warming and acidification on fertilization success and early larval development in the green sea urchin *Lytechinus variegatus*. *Mar. pollut. Bull.* 141, 70–78. doi: 10.1016/j.marpolbul.2019.02.018

Liberman, R., Fine, M., and Benayahu, Y. (2021). Simulated climate change scenarios impact the reproduction and early life stages of a soft coral. *Mar. Environ. Res.* 163, 105215. doi: 10.1016/j.marenvres.2020.105215

Limatola, N., Chun, J. T., and Santella, L. (2020). Effects of salinity and pH of seawater on the reproduction of the Sea urchin *Paracentrotus lividus*. *Biol. Bull.* 239, 13–23. doi: 10.1086/710126

Liu, S., Shi, W., Guo, C., Zhao, X., Han, Y., Peng, C., et al. (2016). Ocean acidification weakens the immune response of blood clam through hampering the NF-kappa β and toll-like receptor pathways. *Fish Shellfish Immunol.* 54, 322–327. doi: 10.1016/j.fsi.2016.04.030

Long, C. W., Swiney, K. M., and Foy, R. J. (2013). Effects of ocean acidification on the embryos and larvae of red king crab, *Paralithodes camtschaticus*. *Mar. pollut. Bull.* 69, 38–47. doi: 10.1016/j.marpolbul.2013.01.011

Lucey, N. M., Lombardi, C., DeMarchi, L., Schulze, A., Gambi, M. C., and Calosi, P. (2015). To brood or not to brood: Are marine invertebrates that protect their offspring more resilient to ocean acidification? *Sci. Rep.* 5, 12009. doi: 10.1038/srep12009

Lymbery, R. A., Kennington, W. J., Cornwall, C. E., and Evans, J. P. (2019). Ocean acidification during prefertilization chemical communication affects sperm success. *Ecol. Evol.* 49, 1. doi: 10.1002/ece3.5720

Maboloc, E. A., and Chan, K. Y. K. (2021). Parental whole life cycle exposure modulates progeny responses to ocean acidification in slipper limpets. *Glob. Change Biol.* 27, 3272–3281. doi: 10.1111/gcb.15647

Machado, A. M., Fernández-Boo, S., Nande, M., Pinto, R., Costas, B., and Castro, L. F. C. (2022). The male and female gonad transcriptome of the edible sea urchin, *Paracentrotus lividus*: Identification of sex-related and lipid biosynthesis genes. *Aquaculture Rep.* 22, 100936. doi: 10.1016/j.aqrep.2021.100936

Mackenzie, C. L., Lynch, S. A., Culloty, S. C., and Malham, S. K. (2014). Future oceanic warming and acidification alter immune response and disease status in a commercial shellfish species, *Mytilus edulis* l. *PloS One* 9, e99712. doi: 10.1371/journal.pone.0099712

Manno, C., Peck, V. L., and Tarling, G. A. (2016). Pteropod eggs released at high pCO_2 lack resilience to ocean acidification. *Sci. Rep.* 6, 25752. doi: 10.1038/srep25752

Marčeta, T., Matozzo, V., Alban, S., Badocco, D., Pastore, P., and Marin, M. G. (2020). Do males and females respond differently to ocean acidification? an experimental study with the sea urchin *Paracentrotus lividus*. *Environ. Sci. Pollut. Res. Int.* 27 (31), 39516–39530. doi: 10.1007/s11356-020-10040-7

Marchini, C., Gizzi, F., Pondrelli, T., Moreddu, L., Marisaldi, L., Montori, F., et al. (2021). Decreasing pH impairs sexual reproduction in a Mediterranean coral transplanted at a CO_2 vent. *Limnology Oceanography* 66, 3990–4000. doi: 10.1002/lno.11937

Martin, S., Richier, S., Pedrotti, M.-L., Dupont, S., Castejon, C., Gerakis, Y., et al. (2011). Early development and molecular plasticity in the Mediterranean sea urchin *Paracentrotus lividus* exposed to CO_2-driven acidification. *J. Exp. Biol.* 214, 1357–1368. doi: 10.1242/jeb.051169

Mayor, D. J., Matthews, C., Cook, K., Zuur, A. F., and Hay, S. (2007). CO_2-induced acidification affects hatching success in *Calanus finmarchicus*. *Mar. Ecol. Prog. Ser.* 350, 91–97. doi: 10.3354/meps07142

McConville, K., Halsband, C., Fileman, E. S., Somerfield, P. J., Findlay, H. S., and Spicer, J. I. (2013). Effects of elevated CO_2 on the reproduction of two calanoid copepods. *Mar. pollut. Bull.* 73, 428–434. doi: 10.1016/j.marpolbul.2013.02.010

McDonald, M. R., McClintock, J. B., Amsler, C. D., Rittschof, D., Angus, R. A., Orihuela, B., et al. (2009). Effects of ocean acidification over the life history of the barnacle *Amphibalanus amphitrite*. *Mar. Ecol. Prog. Ser.* 385, 179–187. doi: 10.3354/meps08099

Melzner, F., Mark, F. C., Seibel, B. A., and Tomanek, L. (2020). Ocean acidification and coastal marine invertebrates: Tracking CO_2 effects from seawater to the cell. *Ann. Rev. Mar. Sci.* 12, 499–523 doi: 10.1146/annurev-marine-010419-010658

Meseck, S. L., Alix, J. H., Swiney, K. M., Long, W. C., Wikfors, G. H., and Foy, R. J. (2016). Ocean acidification affects hemocyte physiology in the tanner crab (*Chionoecetes bairdi*). *PloS One* 11, e0148477. doi: 10.1371/journal.pone.0148477

Miller, J. J., Maher, M., Bohaboy, E., Friedman, C. S., and McElhany, P. (2016). Exposure to low pH reduces survival and delays development in early life stages of dungeness crab (*Cancer magister*). *Mar. Biol.* 163 (5), 1–11. doi: 10.1007/s00227-016-2883-1

Miyazaki, S. (2006). Thirty years of calcium signals at fertilization. *Semin. Cell Dev. Biol.* 17, 233–243. doi: 10.1016/j.semcdb.2006.02.007

Moran, A. L., and McAlister, J. S. (2009). Egg size as a life history character of marine invertebrates: Is it all it's cracked up to be? *Biol. Bull.* 216 (3), 226–242. doi: 10.1086/BBLv216n3p226

Morisawa, M., and Yoshida, M. (2005). Activation of motility and chemotaxis in the spermatozoa: From invertebrates to humans. *Reprod. Med. Biol.* 4, 101–114. doi: 10.1111/j.1447-0578.2005.00099.x

Morita, M., Nishikawa, A., Nakajima, A., Iguchi, A., Sakai, K., Takemura, A., et al. (2006). Eggs regulate sperm flagellar motility initiation, chemotaxis and inhibition in the coral *Acropora digitifera*, *A. gemmifera* and *A. tenuis*. *J. Exp. Biol.* 209, 4574–4579. doi: 10.1242/jeb.02500

Morita, M., Suwa, R., Iguchi, A., Nakamura, M., Shimada, K., Sakai, K., et al. (2010). Ocean acidification reduces sperm flagellar motility in broadcast spawning reef invertebrates. *Zygote* 18, 103–107. doi: 10.1017/S0967199409990177

Mortensen, T., and Mortensen, T. (1921). Studies of the development and larval forms of echinoderms. *GEC Gad.* doi: 10.5962/bhl.title.11376

Moulin, L., Catarino, A. I., Claessens, T., and Dubois, P. (2011). Effects of seawater acidification on early development of the intertidal sea urchin *Paracentrotus lividus* (Lamarck1811, 816). *Mar. pollut. Bull.* 62, 48–54. doi: 10.1016/j.marpolbul.2010.09.012

Nakajima, A., Morita, M., Takemura, A., Kamimura, S., and Okuno, M. (2005). Increase in intracellular pH induces phosphorylation of axonemal proteins for activation of flagellar motility in starfish sperm. *J. Exp. Biol.* 208, 4411–4418. doi: 10.1242/jeb.01906

Nakamura, M., and Morita, M. (2012). Sperm motility of the scleractinian coral *Acropora digitifera* under preindustrial, current, and predicted ocean acidification regimes. *Aquat. Biol.* 15, 299–302. doi: 10.3354/ab00436

Olischläger, M., and Wild, C. (2020). How does the sexual reproduction of marine life respond to ocean acidification? *Diversity* 12, 241. doi: 10.3390/d12060241

Omoregie, E., Mwatilifange, N. S. I., and Liswaniso, G. (2019). Futuristic ocean acidification levels reduce growth and reproductive viability in the pacific oyster (*Crassostrea gigas*). *J. Appl. Sci. Environ. Manage.* 23, 1747–1754. doi: 10.4314/jasem.v23i9.21

Onitsuka, T., Kimura, R., Ono, T., Takami, H., and Nojiri, Y. (2014). Effects of ocean acidification on the early developmental stages of the horned turban, *Turbo cornutus*. *Mar. Biol.* 161, 1127–1138. doi: 10.1007/s00227-014-2405-y

Pansch, C., Hattich, G. S. I., Heinrichs, M. E., Pansch, A., Zagrodzka, Z., and Havenhand, J. N. (2018). Long-term exposure to acidification disrupts reproduction in a marine invertebrate. *PloS One* 13, e0192036. doi: 10.1371/journal.pone.0192036

Parker, L. M., O'Connor, W. A., Byrne, M., Coleman, R. A., Virtue, P., Dove, M., et al. (2017). Adult exposure to ocean acidification is maladaptive for larvae of the Sydney rock oyster *Saccostrea glomerata* in the presence of multiple stressors. *Biol. Lett.* 13 (2), 20160798. doi: 10.1098/rsbl.2016.0798

Parker, L. M., O'Connor, W. A., Byrne, M., Dove, M., Coleman, R. A., Pörtner, H.-O., et al. (2018). Ocean acidification but not warming alters sex determination in the Sydney rock oyster, *Saccostrea glomerata*. *Proc. R. Soc B* 285, 20172869. doi: 10.1098/rspb.2017.2869

Parker, L. M., Ross, P. M., and O'connor, W. A. (2009). The effect of ocean acidification and temperature on the fertilization and embryonic development of the Sydney rock oyster *Saccostrea glomerata* (Gould1851, 850). *Glob. Change Biol.* 15, 2123–2136. doi: 10.1111/j.1365-2486.2009.01895.x

Parker, L. M., Ross, P. M., and O'Connor, W. A. (2010). Comparing the effect of elevated pCO_2 and temperature on the fertilization and early development of two species of oysters. *Mar. Biol.* 157, 2435–2452. doi: 10.1007/s00227-010-1508-3

Parker, L. M., Ross, P. M., and O'Connor, W. A. (2011). Populations of the Sydney rock oyster, *Saccostrea glomerata*, vary in response to ocean acidification. *Mar. Biol.* 158, 689–697. doi: 10.1007/s00227-010-1592-4

Parker, L. M., Ross, P. M., O'Connor, W. A., Borysko, L., Raftos, D. A., and Pörtner, H.-O. (2012). Adult exposure influences offspring response to ocean acidification in oysters. *Glob. Change Biol.* 18, 82–92. doi: 10.1111/j.1365-2486.2011.02520.x

Parker, L. M., Scanes, E., O'Connor, W. A., and Ross, P. M. (2021). Transgenerational plasticity responses of oysters to ocean acidification differ with habitat. *J. Exp. Biol.* 224 (12), 12. doi: 10.1242/jeb.239269

Pauletto, M., Milan, M., Huvet, A., Corporeau, C., Suquet, M., Planas, J. V., et al. (2017). Transcriptomic features of *Pecten maximus* oocyte quality and maturation. *PloS One* 12, e0172805. doi: 10.1371/journal.pone.0172805

Pecorino, D., Barker, M. F., Dworjanyn, S. A., Byrne, M., and Lamare, M. D. (2014). Impacts of near future sea surface pH and temperature conditions on fertilisation and embryonic development in *Centrostephanus rodgersii* from northern new Zealand and northern new south Wales, Australia. *Mar. Biol.* 161, 101–110. doi: 10.1007/s00227-013-2318-1

Pereira, T. M., Gnocchi, K. G., Merçon, J., Mendes, B., Lopes, B. M., Passos, L. S., et al. (2020). The success of the fertilization and early larval development of the tropical sea urchin *Echinometra lucunter* (Echinodermata: Echinoidea) is affected by the pH decrease and temperature increase. *Mar. Environ. Res.* 161, 105106. doi: 10.1016/j.marenvres.2020.105106

Pitts, K. A., Campbell, J. E., Figueiredo, J., and Fogarty, N. D. (2020). Ocean acidification partially mitigates the negative effects of warming on the recruitment of the coral, *Orbicella faveolata*. *Coral Reefs* 39, 281–292. doi: 10.1007/s00338-019-01888-4

Podolsky, R. D. (2004). Life-history consequences of investment in free-spawned eggs and their accessory coats. *Am. Nat.* 163, 735–753. doi: 10.1086/382791

Prezeslawski, R., Byrne, M., and Mellin, C. (2017). A review and meta-analysis of the effects of multiple abiotic stressors on marine embryos and larvae. *Glob. Change Biol.* 21, 2122–2140. doi: 10.1111/gcb.12833

Putnam, H. M., Ritson-Williams, R., Cruz, J. A., Davidson, J. M., and Gates, R. D. (2020). Environmentally-induced parental or developmental conditioning influences coral offspring ecological performance. *Sci. Rep.* 10, 13664. doi: 10.1038/s41598-020-70605-x

Rains, S. A. M., Wilberg, M. J., and Miller, T. J. (2016). Sex ratios and average sperm per female blue crab *Callinectes sapidus* in six tributaries of Chesapeake bay. *Mar. Coast. Fish.* 8, 492–501. doi: 10.1080/19425120.2016.1208126

Ramirez Llodra, E. (2002). Fecundity and life-history strategies in marine invertebrates. *Adv. Mar. Biol.* 43, 87–170. doi: 10.1016/s0065-2881(02)43004-0

Reed, A. J., Godbold, J. A., Solan, M., and Grange, L. J. (2021). Invariant gametogenic response of dominant infaunal bivalves from the Arctic under ambient and near-future climate change conditions. *Front. Mar. Sci.* 8. doi: 10.3389/fmars.2021.576746

Reuter, K. E., Lotterhos, K. E., Crim, R. N., Thompson, C. A., and Harley, C. D. G. (2011). Elevated pCO_2 increases sperm limitation and risk of polyspermy in the red sea urchin *Strongylocentrotus franciscanus*. *Glob. Change Biol.* 17, 163–171. doi: 10.1111/j.1365-2486.2010.02216.x

Riba, I., Gabrielyan, B., Khosrovyan, A., Luque, A., and Del Valls, T. A. (2016). The influence of pH and waterborne metals on egg fertilization of the blue mussel (*Mytilus edulis*), the oyster (*Crassostrea gigas*) and the sea urchin (*Paracentrotus lividus*). *Environ. Sci. pollut. Res. Int.* 23, 14580–14588. doi: 10.1007/s11356-016-6611-7

Richmond, R. H., and Hunter, C. L. (1990). Reproduction and recruitment of corals: comparisons among the Caribbean, the tropical pacific, and the red Sea. *Mar. Ecol. Prog. Ser.* 60, 185–203. doi: 10.3354/meps060185

Rinkevich, B. (1996). Do reproduction and regeneration in damaged corals compete for energy allocation? *Mar. Ecol. Prog. Ser.* 143, 297–302. doi: 10.3354/meps143297

Rinkevich, B., and Loya, Y. (1989). Reproduction in regenerating colonies of the coral *Stylophora pistillata*. *Environ. Qual. ecosystem stability* 4, 257–265.

Roggatz, C. C., Lorch, M., Hardege, J. D., and Benoit, D. M. (2016). Ocean acidification affects marine chemical communication by changing structure and function of peptide signaling molecules. *Glob. Change Biol.* 22, 3914–3926. doi: 10.1111/gcb.13354

Rossin, A. M., Waller, R. G., and Stone, R. P. (2019). The effects of *in-vitro* pH decrease on the gametogenesis of the red tree coral, *Primnoa pacifica*. *PloS One* 14, e0203976. doi: 10.1371/journal.pone.0203976

Rossi, G. S., and Tunnicliffe, V. (2017). Trade-offs in a high CO_2 habitat on a subsea volcano: condition and reproductive features of a bathymodioline mussel. *Mar. Ecol. Prog. Ser.* 574, 49–64. doi: 10.3354/meps12196

Ross, P. M., Parker, L., and Byrne, M. (2016). Transgenerational responses of molluscs and echinoderms to changing ocean conditions. *ICES J. Mar. Sci.* 73, 537–549. doi: 10.1093/icesjms/fsv254

Ross, P. M., Parker, L., O'Connor, W. A., and Bailey, E. A. (2011). The impact of ocean acidification on reproduction, early development and settlement of marine organisms. *Water* 3, 1005–1030. doi: 10.3390/w3041005

Świeżak, J., Borrero-Santiago, A. R., Sokołowski, A., and Olsen, A. J. (2018). Impact of environmental hypercapnia on fertilization success rate and the early embryonic development of the clam *Limecola balthica* (Bivalvia, tellinidae) from the southern Baltic Sea - a potential CO_2 leakage case study. *Mar. pollut. Bull.* 136, 201–211. doi: 10.1016/j.marpolbul.2018.09.007

Sanford, E., and Kelly, M. W. (2011). Local adaptation in marine invertebrates. *Ann. Rev. Mar. Sci.* 3, 509–535. doi: 10.1146/annurev-marine-120709-142756

Sawada, H., and Saito, T. (2022). Mechanisms of sperm-egg interactions: What ascidian fertilization research has taught us. *CElls.* 11, 2096. doi: 10.3390/cells11132096

Scanes, E., Parker, L. M., O'Connor, W. A., Gibbs, M. C., and Ross, P. M. (2018). Copper and ocean acidification interact to lower maternal investment, but have little effect on adult physiology of the Sydney rock oyster *Saccostrea glomerata*. *Aquat. Toxicol.* 203, 51–60. doi: 10.1016/j.aquatox.2018.07.020

Scanes, E., Parker, L. M., O'Connor, W. A., and Ross, P. M. (2014). Mixed effects of elevated pCO_2 on fertilisation, larval and juvenile development and adult responses in the mobile subtidal scallop *Mimachlamys asperrima* (Lamarck1811 819). *PloS One* 9, e93649. doi: 10.1371/journal.pone.0093649

Schlegel, P., Binet, M. T., Havenhand, J. N., Doyle, C. J., and Williamson, J. E. (2015). Ocean acidification impacts on sperm mitochondrial membrane potential

bring sperm swimming behaviour near its tipping point. *J. Exp. Biol.* 218, 1084–1090. doi: 10.1242/jeb.114900

Schlegel, P., Havenhand, J. N., Gillings, M. R., and Williamson, J. E. (2012). Individual variability in reproductive success determines winners and losers under ocean acidification: a case study with sea urchins. *PloS One* 7, e53118. doi: 10.1371/journal.pone.0053118

Schutter, M., Nozawa, Y., and Kurihara, H. (2015). The effect of elevated CO_2 and increased temperature on *in vitro* fertilization success and initial embryonic development of single male: female crosses of broad-cast spawning corals at mid- and high-latitude locations. *J. Mar. Sci. Eng.* 3, 216–239. doi: 10.3390/jmse3020216

Sewell, M. A., and Hofmann, G. E. (2011). Antarctic Echinoids and climate change: a major impact on the brooding forms. *Glob. Change Biol.* 17, 734–744. doi: 10.1111/j.1365-2486.2010.02288.x

Sewell, M. A., Millar, R. B., Yu, P. C., Kapsenberg, L., and Hofmann, G. E. (2014). Ocean acidification and fertilization in the Antarctic sea urchin *Sterechinus neumayeri*: the importance of polyspermy. *Environ. Sci. Technol.* 48, 713–722. doi: 10.1021/es402815s

Sherwood, L., Klandorf, H., and Yancey, P. (2012). *Animal physiology: From genes to organisms* (Brooks/Cole, Belmont, California USA: Cengage Learning).

Shi, W., Han, Y., Guo, C., Zhao, X., Liu, S., Su, W., et al. (2017a). Ocean acidification hampers sperm-egg collisions, gamete fusion, and generation of Ca^{2+} oscillations of a broadcast spawning bivalve, *Tegillarca granosa*. *Mar. Environ. Res.* 130, 106–112. doi: 10.1016/j.marenvres.2017.07.016

Shi, W., Zhao, X., Han, Y., Guo, C., Liu, S., Su, W., et al. (2017b). Effects of reduced pH and elevated pCO_2 on sperm motility and fertilisation success in blood clam, *Tegillarca granosa*. *N. Z. J. Mar. Freshw. Res.* 51, 543–554. doi: 10.1080/00288330.2017.1296006

Shlesinger, T., and Loya, Y. (2019). Breakdown in spawning synchrony: A silent threat to coral persistence. *Science* 365, 1002–1007. doi: 10.1126/science.aax0110

Shukla, P. R., Skea, J., Calvo Buendia, E., Masson-Delmotte, V., Pörtner, H. O., Roberts, D. C., et al. (2019). *IPCC2012 019: Climate change and land: an IPCC special report on climate change, desertification, land degradation, sustainable land management, food security, and greenhouse gas fluxes in terrestrial ecosystems* (Geneva, Switzerland: Intergovernmental Panel on Climate Change (IPCC). Available at: https://spiral.imperial.ac.uk/bitstream/10044/1/76618/2/SRCCL-Full-Report-Compiled-191128.pdf.

Siikavuopio, S. I., Mortensen, A., Dale, T., and Foss, A. (2007). Effects of carbon dioxide exposure on feed intake and gonad growth in green sea urchin, *Strongylocentrotus droebachiensis*. *Aquaculture* 266, 97–101. doi: 10.1016/j.aquaculture.2007.02.044

Smith, K. E., Byrne, M., Deaker, D., Hird, C. M., Nielson, C., Wilson-McNeal, A., et al. (2019). Sea Urchin reproductive performance in a changing ocean: poor males improve while good males worsen in response to ocean acidification. *Proc. Biol. Sci.* 286, 20190785. doi: 10.1098/rspb.2019.0785

Smith, H. W., and Clowes, G. H. A. (1924). The influence of hydrogen ion concentration on the fertilization process in *Arbacia, asterias* and *Chaetopterus* eggs. *Biol. Bull.* 47, 333–344. doi: 10.2307/1536693

Smith, J. N., Richter, C., Fabricius, K. E., and Cornils, A. (2017). Pontellid copepods, *Labidocera* spp., affected by ocean acidification: A field study at natural CO_2 seeps. *PloS One* 12, e0175663. doi: 10.1371/journal.pone.0175663

Sokolova, I. M., Frederich, M., Bagwe, R., Lannig, G., and Sukhotin, A. A. (2012). Energy homeostasis as an integrative tool for assessing limits of environmental stress tolerance in aquatic invertebrates. *Mar. Environ. Res.* 79, 1–15. doi: 10.1016/j.marenvres.2012.04.003

Spady, B. L., Munday, P. L., and Watson, S.-A. (2020). Elevated seawater pCO_2 affects reproduction and embryonic development in the pygmy squid, *Idiosepius pygmaeus*. *Mar. Environ. Res.* 153, 104812. doi: 10.1016/j.marenvres.2019.104812

Spalding, M. D., Fox, H. E., Allen, G. R., Davidson, N., Ferdaña, Z. A., Finlayson, M., et al. (2007). Marine ecoregions of the world: A bioregionalization of coastal and shelf areas. *Bioscience* 57, 573–583. doi: 10.1641/B570707

Spencer, L. H., Venkataraman, Y. R., Crim, R., Ryan, S., Horwith, M. J., and Roberts, S. B. (2020). Carryover effects of temperature and pCO_2 across multiple Olympia oyster populations. *Ecol. Appl.* 30, e02060. doi: 10.1002/eap.2060

Stavroff, L.-A. (2014). *Effects of ocean acidification combined with multiple stressors on early life stages of the pacific purple sea urchin* (Colwood (BC: Royal Roads University). Available at: http://hdl.handle.net/10170/702.

Striewski, S. (2012). *Impact of ocean acidification on the reproduction, recruitment and growth of scleractinian corals* (Bochum (Germany: Ruhr-University Bochum). Available at: https://nbn-resolving.org/urn:nbn:de:hbz:294-46934.

Stumpp, M., Trübenbach, K., Brennecke, D., Hu, M. Y., and Melzner, F. (2012). Resource allocation and extracellular acid–base status in the sea urchin *Strongylocentrotus droebachiensis* in response to CO_2 induced seawater acidification. *Aquat. Toxicol.* 110-111, 194–207. doi: 10.1016/j.aquatox.2011.12.020

Suckling, C. C., Clark, M. S., Beveridge, C., Brunner, L., Hughes, A. D., Harper, E. M., et al. (2014). Experimental influence of pH on the early life-stages of sea urchins II: increasing parental exposure times gives rise to different responses. *Invertebr. Reprod. Dev.* 58, 161–175. doi: 10.1080/07924259.2013.875951

Suckling, C. C., Clark, M. S., Richard, J., Morley, S. A., Thorne, M. A. S., Harper, E. M., et al. (2015). Adult acclimation to combined temperature and pH stressors significantly enhances reproductive outcomes compared to short-term exposures. *J. Anim. Ecol.* 84, 773–784. doi: 10.1111/1365-2656.12316

Sui, Y., Zhou, K., Lai, Q., Yao, Z., and Gao, P. (2019). Effects of seawater acidification on early development of clam *Cyclina sinensis*. *J. Ocean Univ. China* 18, 913–918. doi: 10.1007/s11802-019-3942-2

Sung, C.-G., Kim, T. W., Park, Y.-G., Kang, S.-G., Inaba, K., Shiba, K., et al. (2014). Species and gamete-specific fertilization success of two sea urchins under near future levels of pCO_2. *J. Mar. Syst.* 137, 67–73. doi: 10.1016/j.jmarsys.2014.04.013

Sun, D., Li, Q., and Yu, H. (2022). DNA Methylation differences between male and female gonads of the oyster reveal the role of epigenetics in sex determination. *Gene* 820,146260. doi: 10.1016/j.gene.2022.146260

Swiney, K. M., Long, W. C., and Foy, R. J. (2015). Effects of high pCO_2 on tanner crab reproduction and early life history–part I: long-term exposure reduces hatching success and female calcification, and alters embryonic development. *ICES J. Mar. Sci.* 73, 825–835. doi: 10.1093/icesjms/fsv201

Szalaj, D., De Orte, M. R., Goulding, T. A., Medeiros, I. D., DelValls, T. A., and Cesar, A. (2017). The effects of ocean acidification and a carbon dioxide capture and storage leak on the early life stages of the marine mussel *Perna perna* (Linneaus1751 758) and metal bioavailability. *Environ. Sci. pollut. Res. Int.* 24, 765–781. doi: 10.1007/s11356-016-7863-y

Tanabe, T., Yuan, Y., Nakamura, S., Itoh, N., Takahashi, K. G., and Osada, M. (2010). The role in spawning of a putative serotonin receptor isolated from the germ and ciliary cells of the gonoduct in the gonad of the Japanese scallop, *Patinopecten yessoensis*. *Gen. Comp. Endocrinol.* 166, 620–627. doi: 10.1016/j.ygcen.2010.01.014

Tarrant, A. M. (2007). Hormonal signaling in cnidarians: do we understand the pathways well enough to know whether they are being disrupted? *Ecotoxicology* 16, 5–13. doi: 10.1007/s10646-006-0121-1

Thor, P., and Dupont, S. (2015). Transgenerational effects alleviate severe fecundity loss during ocean acidification in a ubiquitous planktonic copepod. *Glob. Change Biol.* 21, 2261–2271. doi: 10.1111/gcb.12815

Thor, P., Vermandele, F., Carignan, M.-H., Jacque, S., and Calosi, P. (2018). No maternal or direct effects of ocean acidification on egg hatching in the Arctic copepod *Calanus glacialis*. *PloS One* 13, e0192496. doi: 10.1371/journal.pone.0192496

Timpane-Padgham, B. L., Beechie, T., and Klinger, T. (2017). A systematic review of ecological attributes that confer resilience to climate change in environmental restoration. *PloS One* 12, e0173812. doi: 10.1371/journal.pone.0173812

Treen, N., Itoh, N., Miura, H., Kikuchi, I., Ueda, T., Takahashi, K. G., et al. (2012). Mollusc gonadotropin-releasing hormone directly regulates gonadal functions: a primitive endocrine system controlling reproduction. *Gen. Comp. Endocrinol.* 176, 167–172. doi: 10.1016/j.ygcen.2012.01.008

Uthicke, S., Liddy, M., Nguyen, H. D., and Byrne, M. (2014). Interactive effects of near-future temperature increase and ocean acidification on physiology and gonad development in adult pacific sea urchin, *Echinometra* sp. a. *Coral Reefs* 33, 831–845. doi: 10.1007/s00338-014-1165-y

Uthicke, S., Patel, F., Karelitz, S., Luter, H. M., Webster, N. S., and Lamare, M. (2020). Key biological responses over two generations of the sea urchin *Echinometra* sp. a under future ocean conditions. *Mar. Ecol. Prog. Ser.* 637, 87–101. doi: 10.3354/meps13236

Uthicke, S., Pecorino, D., Albright, R., Negri, A. P., Cantin, N., Liddy, M., et al. (2013). Impacts of ocean acidification on early life-history stages and settlement of the coral-eating sea star *Acanthaster planci*. *PloS One* 8, e82938. doi: 10.1371/journal.pone.0082938

Vacquier, V. D. (1998). Evolution of gamete recognition proteins. *Science* 281 (5385), 1995–1998. doi: 10.1126/science.281.5385.1995

Van Colen, C., Debusschere, E., Braeckman, U., Van Gansbeke, D., and Vincx, M. (2012). The early life history of the clam *Macoma balthica* in a high CO_2 world. *PloS One* 7, e44655. doi: 10.1371/journal.pone.0044655

Van Veghel, M. L. J., and Bak, R. P. M. (1994). Reproductive characteristics of the polymorphic Caribbean reef building coral *Montastrea annularis*. III. reproduction in damaged and regenerating colonies. *Mar. Ecol. Prog. Ser.* 109, 229–233. doi: 10.3354/meps109229

Vehmaa, A., Almén, A.-K., Brutemark, A., Paul, A., Riebesell, U., Furuhagen, S., et al. (2016). Ocean acidification challenges copepod reproductive plasticity. *Biogeosciences.* 13, 6171–6182. doi: 10.5194/bgd-12-18541-2015

Vehmaa, A., Brutemark, A., and Engström-Öst, J. (2012). Maternal effects may act as an adaptation mechanism for copepods facing pH and temperature changes. *PloS One* 7, e48538. doi: 10.1371/journal.pone.0048538

Vehmaa, A., Hogfors, H., Gorokhova, E., Brutemark, A., Holmborn, T., and Engström-Öst, J. (2013). Projected marine climate change: effects on copepod oxidative status and reproduction. *Ecol. Evol.* 3, 4548–4557. doi: 10.1002/ece3.839

Venkataraman, Y. R., Downey-Wall, A. M., Ries, J., Westfield, I., White, S. J., Roberts, S. B., et al. (2020). General DNA methylation patterns and environmentally-induced differential methylation in the eastern oyster (*Crassostrea virginica*). *Front. Mar. Sci.* 225 doi: 10.3389/fmars.2020.00225

Venkataraman, Y. R., Spencer, L. H., and Roberts, S. B. (2019). Larval response to parental low pH exposure in the pacific oyster *Crassostrea gigas*. *J. Shellfish Res.* 38, 743–750. doi: 10.2983/035.038.0325

Venkataraman, Y. R., White, S. J., and Roberts, S. B.. (2022). Differential DNA methylation in pacific oyster reproductive tissue in response to ocean acidification. *BMC Genomics*. 23 (1), 1–16. doi: 10.1186/s12864-022-08781-5

Verkaik, K., Hamel, J. F., and Mercier, A. (2016). Carry-over effects of ocean acidification in a cold-water lecithotrophic holothuroid. *Mar. Ecol. Prog. Ser.* 557, 189–206. doi: 10.3354/meps11868

Vihtakari, M., Havenhand, J., Renaud, P. E., and Hendriks, I. E. (2016). Variable individual- and population- level responses to ocean acidification. *Front. Mar. Sci.* 3. doi: 10.3389/fmars.2016.00051

Vihtakari, M., Hendriks, I. E., Holding, J., Renaud, P. E., Duarte, C. M., and Havenhand, J. N. (2013). Effects of ocean acidification and warming on sperm activity and early life stages of the Mediterranean mussel (*Mytilus galloprovincialis*). *Water* 5, 1890–1915. doi: 10.3390/w5041890

Wang, Q., Cao, R., Ning, X., You, L., Mu, C., Wang, C., et al. (2016). Effects of ocean acidification on immune responses of the pacific oyster *Crassostrea gigas*. *Fish Shellfish Immunol.* 49, 24–33. doi: 10.1016/j.fsi.2015.12.025

Wang, T., Kong, H., Shang, Y., Dupont, S., Peng, J., Wang, X., et al. (2021). Ocean acidification but not hypoxia alters the gonad performance in the thick shell mussel *Mytilus coruscus*. *Mar. pollut. Bull.* 167, 112282. doi: 10.1016/j.marpolbul.2021.112282

Wang, X., Shang, Y., Kong, H., Hu, M., Yang, J., Deng, Y., et al. (2020). Combined effects of ocean acidification and hypoxia on the early development of the thick shell mussel *Mytilus coruscus*. *Helgol. Mar. Res.* 74, 1–9. doi: 10.1186/s10152-020-0535-9

Washington Sea Grant (2015) *Shellfish aquaculture in Washington state. final report to the Washington state legislature*. Available at: https://pdfs.semanticscholar.org/b833/e0fcb8a0459697f94fd86b9848ee0e59c0a2.pdf.

Wasson, K., Gossard, D. J., Gardner, L., Hain, P. R., Zabin, C. J., Fork, S., et al. (2020). A scientific framework for conservation aquaculture: A case study of oyster restoration in central California. *Biol. Conserv.* 250, 108745. doi: 10.1016/j.biocon.2020.108745

Weydmann, A., Søreide, J. E., Kwasniewski, S., and Widdicombe, S. (2012). Influence of CO_2-induced acidification on the reproduction of a key Arctic copepod *Calanus glacialis*. *J. Exp. Mar. Bio. Ecol.* 428, 39–42. doi: 10.1016/j.jembe.2012.06.002

White, M. M., Mullineaux, L. S., McCorkle, D. C., and Cohen, A. L. (2014). Elevated pCO_2 exposure during fertilization of the bay scallop *Argopecten irradians* reduces larval survival but not subsequent shell size. *Mar. Ecol. Prog. Ser.* 498, 173–186. doi: 10.3354/meps10621

Wippel, B. J. T. (2017). *Potential transgenerational effects of ocean acidification and hypoxia on the Olympia oyster ostrea lurida: A three-part experimental study* (Seattle (WA: University of Washington). Available at: http://hdl.handle.net/1773/40227

Wong, J. M., Kozal, L. C., Leach, T. S., Hoshijima, U., and Hofmann, G. E. (2019). Transgenerational effects in an ecological context: Conditioning of adult sea urchins to upwelling conditions alters maternal provisioning and progeny phenotype. *J. Exp. Mar. Bio. Ecol.* 517, 65–77. doi: 10.1016/j.jembe.2019.04.006

Wood, H. L., Spicer, J. I., and Widdicombe, S. (2008). Ocean acidification may increase calcification rates, but at a cost. *Proc. Biol. Sci.* 275, 1767–1773. doi: 10.1098/rspb.2008.0343

Xu, X., Yang, F., Zhao, L., and Yan, X. (2016).). seawater acidification affects the physiological energetics and spawning capacity of the Manila clam *Ruditapes philippinarum* during gonadal maturation. *Comp. Biochem. Physiol. A Mol. Integr. Physiol.* 196, 20–29. doi: 10.1016/j.cbpa.2016.02.014

Yue, C., Li, Q., and Yu, H. (2018). Gonad transcriptome analysis of the pacific oyster *Crassostrea gigas* identifies potential genes regulating the sex determination and differentiation process. *Mar. Biotechnol.* 20, 206–219. doi: 10.1007/s10126-018-9798-4

Yusa, Y. (2007). Causes of variation in sex ratio and modes of sex determination in the Mollusca–an overview*. *Am. Malacol. Bull.* 23, 89–98. doi: 10.4003/0740-2783-23.1.89

Zervoudaki, S., Frangoulis, C., Giannoudi, L., and Krasakopoulou, E. (2013). Effects of low pH and raised temperature on egg production, hatching and metabolic rates of a Mediterranean copepod species (*Acartia clausi*) under oligotrophic conditions. *Mediterr. Mar. Sci.* 15, 74. doi: 10.12681/mms.553

Zervoudaki, S., Krasakopoulou, E., Moutsopoulos, T., Protopapa, M., Marro, S., and Gazeau, F. (2017). Copepod response to ocean acidification in a low nutrient-low chlorophyll environment in the NW Mediterranean Sea. *Estuar. Coast. Shelf Sci.* 186, 152–162. doi: 10.1016/j.ecss.2016.06.030

Zhang, D., Li, S., Wang, G., and Guo, D. (2011). Impacts of CO_2-driven seawater acidification on survival, egg production rate and hatching success of four marine copepods. *Acta Oceanologica Sin.* 30, 86–94. doi: 10.1007/s13131-011-0165-9

Zhan, Y., Hu, W., Duan, L., Liu, M., Zhang, W., Chang, Y., et al. (2017). Effects of seawater acidification on early development of the sea urchin *Hemicentrotus pulcherrimus*. *Aquac. Int.* 25, 655–678. doi: 10.1007/s10499-016-0064-3

Zhan, Y., Hu, W., Duan, L., Liu, M., Zhang, W., Chang, Y., et al. (2018). Effects of seawater acidification on the early development of sea urchin *Glyptocidaris crenularis*. *J. Oceanology Limnology* 36, 1442–1454. doi: 10.1007/s00343-018-6317-4

Zhan, Y., Hu, W., Zhang, W., Liu, M., Duan, L., Huang, X., et al. (2016). The impact of CO_2-driven ocean acidification on early development and calcification in the sea urchin *Strongylocentrotus intermedius*. *Mar. pollut. Bull.* 112, 291–302. doi: 10.1016/j.marpolbul.2016.08.003

Zhao, L., Liu, B., An, W., Deng, Y., Lu, Y., Liu, B., et al. (2019). Assessing the impact of elevated pCO_2 within and across generations in a highly invasive fouling mussel (*Musculista senhousia*). *Sci. Total Environ.* 689, 322–331. doi: 10.1016/j.scitotenv.2019.06.466

frontiers | Frontiers in Marine Science

TYPE Original Research
PUBLISHED 14 November 2022
DOI 10.3389/fmars.2022.1046106

OPEN ACCESS

EDITED BY
Juan D. Gaitan-Espitia,
The University of Hong Kong,
Hong Kong SAR, China

REVIEWED BY
Jimmy Argüelles,
Universidad Veracruzana, Mexico
Stuart James Kininmonth,
The University of Queensland,
Australia

*CORRESPONDENCE
Jianguo Du
dujianguo@tio.org.cn
Bin Chen
chenbin@tio.org.cn

SPECIALTY SECTION
This article was submitted to Global Change and the Future Ocean, a section of the journal Frontiers in Marine Science

RECEIVED 16 September 2022
ACCEPTED 28 October 2022
PUBLISHED 14 November 2022

CITATION
Zhang X, Li Y, Du J, Qiu S, Xie B, Chen W, Wang J, Hu W, Wu Z and Chen B (2022) Effects of ocean warming and fishing on the coral reef ecosystem: A case study of Xisha Islands, South China Sea. *Front. Mar. Sci.* 9:1046106. doi: 10.3389/fmars.2022.1046106

Effects of ocean warming and fishing on the coral reef ecosystem: A case study of Xisha Islands, South China Sea

Xinyan Zhang[1,2], Yuanchao Li[3], Jianguo Du[1,4,5]*, Shuting Qiu[1], Bin Xie[1], Weilin Chen[1,6], Jianjia Wang[1], Wenjia Hu[1], Zhongjie Wu[3] and Bin Chen[1]*

[1]Third Institute of Oceanography, Ministry of Natural Resources, Xiamen, China, [2]College of Ocean and Earth Sciences, Xiamen University, Xiamen, China, [3]Hainan Academy of Ocean and Fisheries Sciences, Haikou, China, [4]Key Laboratory of Marine Ecological Conservation and Restoration, Ministry of Natural Resources, Xiamen, China, [5]Fujian Provincial Key Laboratory of Marine Ecological Conservation and Restoration, Xiamen, China, [6]Fisheries College, Jimei University, Xiamen, China

Global change has generated challenges for oceans, from individuals to the entire ecosystem, and has raised contemporary issues related to ocean conservation and management. Specifically, coral reef ecosystems have been exposed to various environmental and human disturbances. In this study, the Ecopath with Ecosim model was used to explore the impacts of ocean warming and fishing on Xisha Islands coral reef ecosystem in the South China Sea. The variables in this model included two ocean warming scenarios and three fishing scenarios. The model consisted of 23 functional groups including algae, coral, sea birds, and sharks. Our results showed that by the middle of the century, ocean warming and fishing led to a 3.79% and 4.74% decrease in total catch compared with 2009, respectively. In addition, the combined effects of ocean warming and fishing caused a 4.79% decrease in total catch, and the mean trophic level of catch was predicted to decrease by 6.01% under the SSP585-High fishing scenario. Reducing the fishing effort mitigates the effects of ocean warming on some species, such as large carnivorous fish and medium carnivorous fish; however, under low fishing effort, some functional groups, such as small carnivorous and omnivorous fish, have low biomass because of higher predation mortality.

KEYWORDS

climate change, fishing effort, Xisha Islands coral reef ecosystem, food web simulations, Ecopath with Ecosim

1 Introduction

Coral reefs are ecosystems with rich biodiversity and high service value, and are referred to as "marine rainforests." (Smith, 1978; Reaka-Kudla., 1997; Miloslavich et al., 2005; Hughes et al., 2017; Williams et al., 2019). The coral reef ecosystem provides food, medicine, tourism, aesthetics and coastal zone protection, and it is of great significance for the socio-economic, cultural, and security of the country and region, playing an irreplaceable role in regulating the global climate and ecosystem balance (Pilling et al., 2017; Zheng et al., 2021). Although coral reefs only account for approximately 0.2% of the world's ocean area (Spalding et al., 2001; Fisher et al., 2015), they support nearly one-third of the world's marine fish species and approximately 10% of the marine fishery catch (Smith, 1978; Zheng et al., 2021).

However, in recent decades, coral reefs worldwide have faced various threats, and a series of climate change impacts and human activities have led to the degradation of coral reefs, with 75% of global coral reefs seriously threatened (Bruno et al., 2007; Hu et al., 2020). The service value of coral reef ecosystems is declining at an alarming rate owing to global and local pressures (Eddy et al., 2021). Moreover, some studies have shown that 50% of tropical coral reefs will lose their basic ecological and fishery functions by 2050 (Bellwood et al., 2004; Bruno et al., 2007). Ocean warming and fishing are the most important threat factors that affect the coral reef ecosystem, which may cause widespread degradation of the ecosystem (David et al., 2011), reducing the stability of tropical coral reefs (Zhang et al., 2017; Gibert, 2019; Inagaki et al., 2020), and increasing ecosystem vulnerability (Hughes et al., 2003; Pandolfi et al., 2003; Bellwood et al., 2006; Hughes et al., 2007).

Ecosystem models are generally used to examine ecological issues and one of their applications is assessing the impacts of climate change. These include the Ecopath with Ecosim (EwE) model (Christensen et al., 2014), OSMOSE (Shin and Cury, 2001), Atlantis model (Fulton et al., 2011), and linear inverse model (Legendre et al., 2013). One of the most widely used ecosystem model and food web network analysis tools for marine, estuarine, and other ecosystems worldwide is EwE (Christensen et al., 2008). Ecopath was originally used to build coral reef ecosystems (Polovina, 1984) and was later developed into the EwE software (Christensen et al., 1992; Christensen et al., 2005). Although there are more than 500 models which used the EwE model, less than 70 EwE models have focused on the coral reef ecosystem owing to its complexity. Most previous studies focus on the static structure of the ecosystem, with a lesser focus on the impact of a single factor on the coral reef ecosystem, and the comprehensive impact of multiple factors is not well examined (Colléter et al., 2015; Argüelles-Jiménez et al., 2020). For example, by the end of the century, ocean warming would lead to a reduction in the total standing biomass of 1.00%, 8.00%, and 44.00% in RCP2.6 (low greenhouse gas emissions), RCP4.5 (medium greenhouse gas emissions), and RCP8.5 (high greenhouse gas emissions) in the coral reef ecosystem in Brazil, respectively, and change the ecosystem structure to promote low trophic level functional groups, and cause algal increase during coral decrease (Capitani et al., 2022). The biomass of the Red Sea coral reef ecosystem would decrease with an increase in fishing effort, except for those developed by beach seines, consisting of low trophic level fishes (Tesfamichael et al., 2016). The coral-algal phase shifts on coral reef ecosystem would result in reduced biodiversity and ecosystem maturity in Raja Ampat Archipelago in Eastern Indonesia, and the landing of traditional targeted species would greatly reduce (Answorth et al., 2015). In recent years, some studies have reported the combined impacts of overfishing and climate change on large marine ecosystems or estuarine ecosystems. For example, large-scale declines in biomass under climate change in the South China Sea (SCS), and a 99.00% decline in biomass compared to the levels in 2000 of 17 functional groups were predicted under baseline fishing and the RCP8.5 scenario (Teh et al., 2019). The combined effects of climate change and fishing will reduce the biomass in the Pearl River Estuary (PRE) ecosystem (Zeng et al., 2019). However, there is a lack of studies on the combined effects of ocean warming and fishing on coral reef ecosystems, which hinders our forward-looking management.

Xisha Islands are located in the north-central part of the SCS and at the northern edge of the "coral triangle" with the highest biodiversity worldwide (Allen, 2008; Huang et al., 2008). Coral reefs of Xisha Islands are a typical oceanic worldwide, as well as the oldest and most precious coral reefs in China (Huang et al., 2008), and one of the main fishing grounds for reef fisheries in the SCS (Li et al., 2007). Recently, Xisha Islands coral reef (XICR) ecosystem has faced threats of ocean warming and overfishing (Shi et al., 2008; Liu et al., 2021; Wang et al., 2022), leading to a 16.28% reduction in coral reef coverage (Zuo et al., 2020), a decline in fish productivity, diversity, and large fish populations (Li, 2020), and an explosion in the crown of thorns (*Acanthaster planci*) (Li et al., 2019). In addition, the sea surface temperature (SST) of Xisha Islands rises faster than that of the Zhongsha and Nansha Islands (Zuo et al., 2015), and the ecosystem here has weak resistance to external disturbances (Hong et al., 2021). Although a few studies have examined the effects of global warming on corals in the SCS, for example, the potential threat of global warming to coral growth was explored in Xisha Islands and Nansha Islands (Shi et al., 2008), and the remote sensing image records of coral reefs in the SCS responding to climate warming in the past 40 years were analyzed (Liu, 2020), the fate of coral reef ecosystems in the SCS under climate change and fishing remains unknown.

In this study, we developed the Ecopath and Ecosim models using continuous underwater monitoring data for Xisha Islands from 2009 to 2020, and projected trends under different scenarios up to the 2050s. The main objectives were to (1) explore the food web structure of coral reef ecosystem in the SCS and its differences compared to other regions (2) study the

combined effects of ocean warming and fishing on the coral reef ecosystem and identify factors exerting greater influence. This study is the first to examine the effects of global change on coral reef ecosystems in the SCS. Through this study, we aimed to provide a scientific basis for the conservation and management of coral reef ecosystems in the SCS in the context of global change in the future.

2 Materials and methods

2.1 Study area

Xisha Islands are located at 15°46′N–17°08′N and 111°11′E –112°54′E (Figure 1). It is one of the archipelagos with the largest land area (approximately 10 km^2) and the largest number of islands in the SCS (Li et al., 2002). It comprises Yongle and Xuande islands, with 26 islands and sandbanks, 11 underwater reefs, shoal reefs, and sandy beaches. The climate is tropical monsoon, with an annual average SST of 27.50°C. The highest temperature is from May to September (average 29.90°C), and the lowest is from December to February of the following year (average 24.80°C). The transparency of seawater is usually greater than 15 m and can even exceed 30 m. The environmental conditions are suitable for the growth of coral communities (Zuo et al., 2020). The biological resources on Xisha Island are very rich and this region serves as important fishing grounds for coral reef fisheries in the SCS (Li et al., 2007). The island also supports high biodiversity, with 643 fish species, 409 coral species, and 1570 benthic species (Li et al., 2002; Huang et al., 2018; Qiu et al., 2022).

2.2 Food web modeling

The Ecopath with Ecosim (EwE) model (Christensen and Pauly, 1992; Walters et al., 1997; Walters et al., 2000) was used to estimate the model for XICR ecosystem. This model combines a static (Ecopath) and a time dynamic model (Ecosim). The Ecopath model can be used to describe the state of an ecosystem at a given time, and Ecosim is used to simulate the temporal dynamics of a food web under environmental disturbances and fishing (Christensen et al., 2005).

2.2.1 Ecopath

To reduce the complexity of the food web, individuals or groups of species were assigned to similar functional groups or guilds, which share similar ecological parameters, such as growth and consumption rates, diet composition, and predators. Ecopath assumes that the production of each functional group is equal to the consumption due to predation, fishing mortality, biomass accumulation, and migration. The following equations describe the Ecopath model:

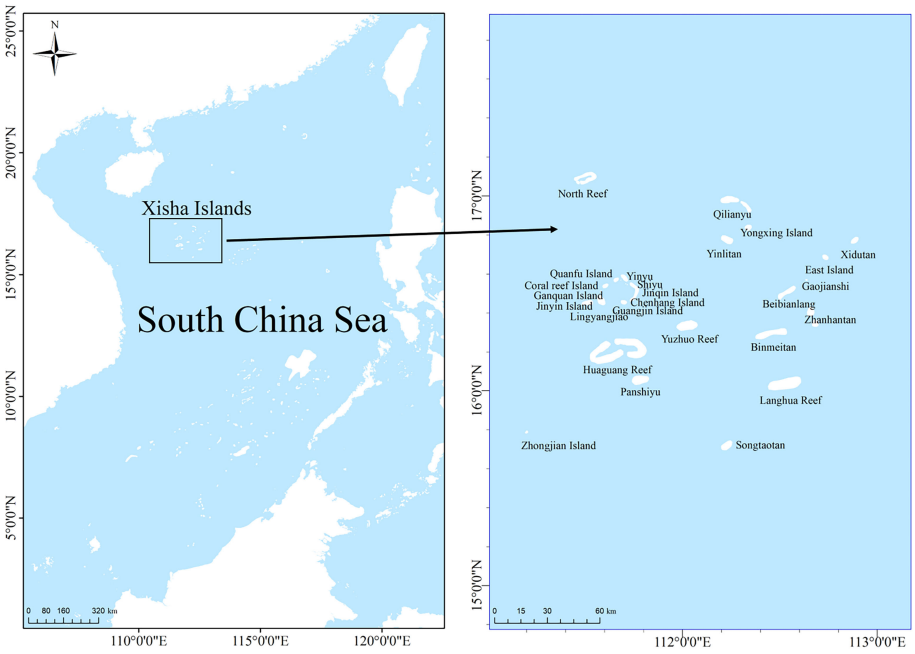

FIGURE 1
Map of the study area of Xisha Islands, South China Sea.

$$B_i \times \left(\frac{P}{B}\right)_i \times EE_i - E_i = \sum B_j \times \left(\frac{Q}{B}\right)_j \times DC_{ij} + Y_i + B_i \times BA_i \quad (1)$$

where B_i is the biomass of the prey species (i) of group i; $(P/B)_i$ is the production/biomass ratio for i; EE_i is the ratio of production to consumption for group i; E_i stands for the net emigration of I; B_j is the biomass of consumers (j) of group i; $(Q/B)_j$ is the ratio of consumption to biomass per unit of j; DC_{ji} is the proportion of i in j's diet; Y_i is the fishery catch of group I; and BA_i is the biomass accumulation of group I.

$$Q = P + R + U \quad (2)$$

To satisfy the energy flow balance among the functional groups of the ecosystem, each functional group should satisfy the second equation, where Q is consumption, P is production, R is respiration, and U is unassimilated food.

2.2.2 Ecosim

Ecosim enables dynamic simulation at the ecosystem level by inheriting key parameters from Ecopath (Christensen et al., 2008). The following equation describes the Ecosim model.

$$\frac{dB_i}{dt} = g_i \times \sum_j Q_{ji} - \sum_j Q_{ij} + I_i - (MO_i + e_i) \times B_i \quad (3)$$

where dB_i/dt is the growth rate of the biomass of group i in time interval dt; g_i is the estimated net growth efficiency based on P/B and Q/B; MO_i is the estimated natural mortality based on the ecotrophic efficiency; e_i is the emigration rate; I_i is the immigration rate. The two summations of Equation (3) estimate consumption rates, the first is the total consumption of group i and the second is predation by its predators on group i.

2.3 Model parameterization

The Ecopath model was built to simulate the coral reef ecosystem of Xisha Islands and was used as the basis for Ecosim. The aquatic ecosystem is very complex, aggregating species into function group is a way to reduce the complex of food web, each function group is conformed according to species traits that are most relevant to define their ecological role. Twenty-three functional groups were defined according to the ecology, taxonomy, feeding or phylogeny characteristics of organisms in the coral reef ecosystem in Xisha Islands, the latest literature in the same area (Hong et al., 2021), and the fish resource survey conducted in Xisha Islands (Sun et al., 2005; Wang et al., 2011), ranging from primary producers to herbivorous fish and Sharks, which basically covered the energy flow process of each trophic level of the ecosystem. The biomass of fish and benthos functional groups were estimated using diving data from Underwater Visual Census (UVC) conducted in 2009, whereas the biomass of other functional groups was got from studies in the SCS (Huang et al., 2009; Hong et al., 2021) and other coral reef model (Du et al., 2020). The P/B, Q/B and EE values of each functional group were mainly acquired from the Qilianyu coral reef model, which lies in the same region (Hong et al., 2021). Diet composition was derived from our feeding studies, stable isotope analysis, and FishBase (https://www.fishbase.se/). The catch data was obtained from comprehensive estimation through interviews and discussions with fishers. Detailed parameters are listed in Table 1.

2.4 Addressing uncertainty in input data

The Ecosampler module in EwE model is used to analyze the impact of uncertainty of input parameters on model output parameters (Steenbeek et al., 2018). We used the Monte Carlo sampling method built in Ecosampler to set a 20% uncertainty for the B, P/B, Q/B and EE parameters of the functional group, and randomly generate 500 rebalanced XICR Ecopath models.

2.5 Simulating ocean warming effects in Ecosim

Ecosim allows us to explore the effects of climate change and human activities on ecosystems over long time scales by fitting time series data. In this study, the time series contained reference data and driving data. The reference data consisting of the biomass of eight fish functional groups was obtained through diving surveys in 2009–2020. The driving data consisted of data on chlorophyll a concentrations, and was obtained from National Oceanic and Atmospheric Administration (https://www.noaa.gov/). In the EwE model, the forcing function was used to express the species' responses to temperature change. It was assumed that the predicted temperature preferences of the species conform to a Gaussian distribution. The Gaussian function was the best statistical fit for the temperature survival curve of fish eggs in the North Atlantic (Dahlke et al., 2020). The species has the highest growth rate at the preferred temperature. Temperatures lower or higher than the optimal will cause a decrease in biomass and productivity (Zeng et al., 2019). In this study, the preferred temperatures of species in Xisha Islands ecosystem were calculated according to previous studies (Day et al., 2018) and FishBase (https://www.fishbase.se/).

SST was obtained from the GFDL-ESM4 (https://esgf-node.llnl.gov/search/cmip6/). It contains historical data (1990–2014) and future simulation data (2015–2100). This study used SSP126 (low radiation forcing scenario) and SSP585 (high radiation forcing scenario) as two climate scenarios. SST selected the r1i1p1f1 model, the spatial resolution contained 15°46′–17°08′ N, 111°11′–112°54′ E, the accuracy was 1°×1°, and the time resolution was monthly. To improve the credibility of future

TABLE 1 Basic input and estimated (bold) parameters for the functional groups in the coral reef model of the XICR ecosystem.

	Functional group	Trophic level	Biomass	P/B	Q/B	Ecotrophic Efficiency	Fishery
1	Sharks	**3.76**	0.10[a]	0.25[c]	4.72[c]	**0.19**	
2	Sea birds	**3.47**	0.37[b]	0.38 [b]	63.95 [b]	**0.62**	
3	Turtle	**2.82**	0.02[b]	0.14[c]	3.50 [b]	**0.71**	0.0020
4	Large carnivorous fish	**3.53**	0.55	0.67[c]	11.52 [c]	**0.77**	0.20
5	Medium carnivorous fish	**3.43**	2.01	0.99[c]	8.50 [c]	**0.93**	2.5
6	Small carnivorous fish	**3.25**	3.09	4.12[c]	13.50 [c]	**0.80**	0.80
7	Omnivorous fish	**2.87**	1.94	4.50[c]	16.30 [c]	**0.74**	1.80
8	Scraping grazers	**2.75**	1.64	2.20 [c]	15.10[c]	**0.88**	0.20
9	Detrital fish	**2.25**	2.95	2.34 [b]	8.33 [b]	**0.85**	
10	Herbivorous fish	**2.19**	6.86	2.54[c]	21.50[c]	**0.77**	1.50
11	Butterflyfish	**2.91**	1.52	4.54[c]	6.72[c]	**0.72**	
12	Coral reef	**2.25**	**17.75**	3.00[c]	10.00 [c]	0.70[c]	
13	Giant triton	**3.34**	0.69[c]	1.22 [c]	4.08 [c]	**0.95**	0.80
14	Crustaceans	**2.78**	4.30 [b]	5.65 [c]	28.50 [c]	**0.82**	0.50
15	Crown-of-thorns starfish	**3.16**	**13.85**	1.20[c]	5.00[c]	0.30 [c]	
16	Other echinoderms	**2.00**	3.04	2.43	8.15[c]	**0.93**	0.50
17	Bivalve	**2.48**	8.50	2.51[c]	5.62[c]	**0.82**	0.50
18	Other invertebrates	**2.20**	**48.73**	3.66[c]	17.75 [b]	0.95[c]	6.00
19	Zooplankton	**2.11**	**3.23**	76.00[c]	253.00 [c]	0.90 [c]	
20	Phytoplankton	**1.00**	8.817 [c]	231.00[c]		**0.35**	
21	Sea grass	**1.00**	52.00 [c]	13.76 [b]		**0.46**	
22	Algae	**1.00**	**36.16**	10.20 [b]		0.31 [b]	
23	Detritus	**1.00**	315.00			**0.23**	

[a](Huang et al., 2009); [b](Du et al., 2020); [c](Hong et al., 2021).
The bold values represent the estimated output from the model.

forecast data, the deviation of the climate model data was corrected according to the retrieved SST based on MODIS data. The retrieved SST data were obtained from the National Oceanic and Atmospheric Administration (https://www.noaa.gov/). The average value of the processed temperature was considered the final SST. The SST in Xisha Islands is projected to increase by approximately 0.47 °C and 1.17 °C under SSP126 and SSP585 in 2050, respectively (Figure 2). Based on this, normalized preference indices for different environmental temperatures were calculated, and biomass dynamics were simulated based on the forcing function and projected SST from 2009 to 2050.

2.6 Simulating fishing effects in Ecosim

Three fishing scenarios were simulated to explore the potential effects of fishing on the Xisha Reef ecosystem. Given that the current global fishing capacity may be 1.5 to 2.5 times the level required to maximize sustainable fishing (Porter, 1998; Sumaila et al., 2012), fishing efforts may need to be reduced by 40 to 60% (World Bank, 2017). In the study of the SCS, the fishing effort in 2100 was simulated to be 50% lower than that in 2010, and the rate of decline was approximately 0.56% per year (Teh et al., 2019). According to this rate, the fishing effort is expected to decline by approximately 20% by 2050. Considering factors such as population and economic constraints, the amount of fishing effort cannot be reduced suddenly, and referring to the study conducted on the Pearl River Estuary (Zeng et al., 2019), we chose the strategy of year by year reduction, to reduce the fishing effort by 20% in 2050 compared with 2009. At the same time, in order to explore the impact of increased effort on the ecosystem, we increased the fishing effort by 20% in the same manner. Thus, the fishing effort in 2009 was set to 100%, and the relative effort in 2050 was set to 80%, 100%, and 120% of 2009, which represented the low, medium, and high fishing scenarios, respectively.

3 Results

3.1 Ecopath model outputs

The sensitivity analysis of the input parameters of the Ecopath model is based on 500 Monte Carlo simulations of Ecosampler embedded in the software. It showed that the

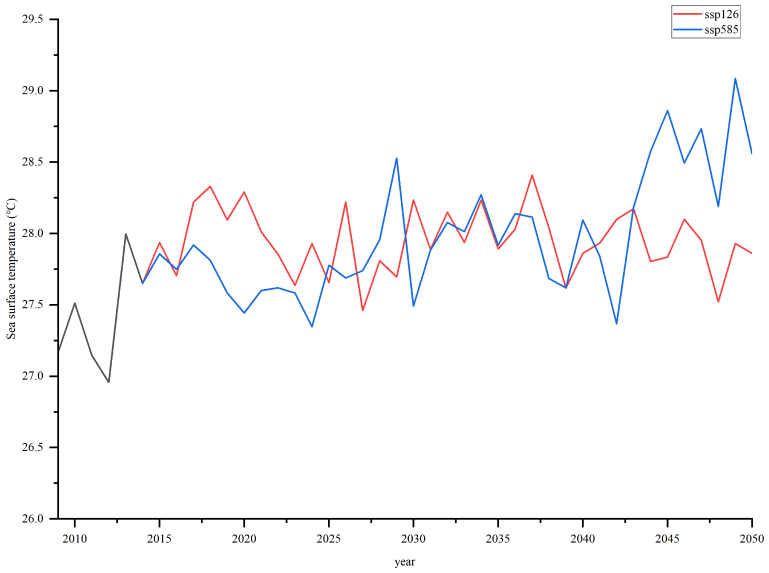

FIGURE 2
Sea surface temperature (°C) in Xisha Islands for the two scenarios (SSP126 and SSP585) in 2009–2050.

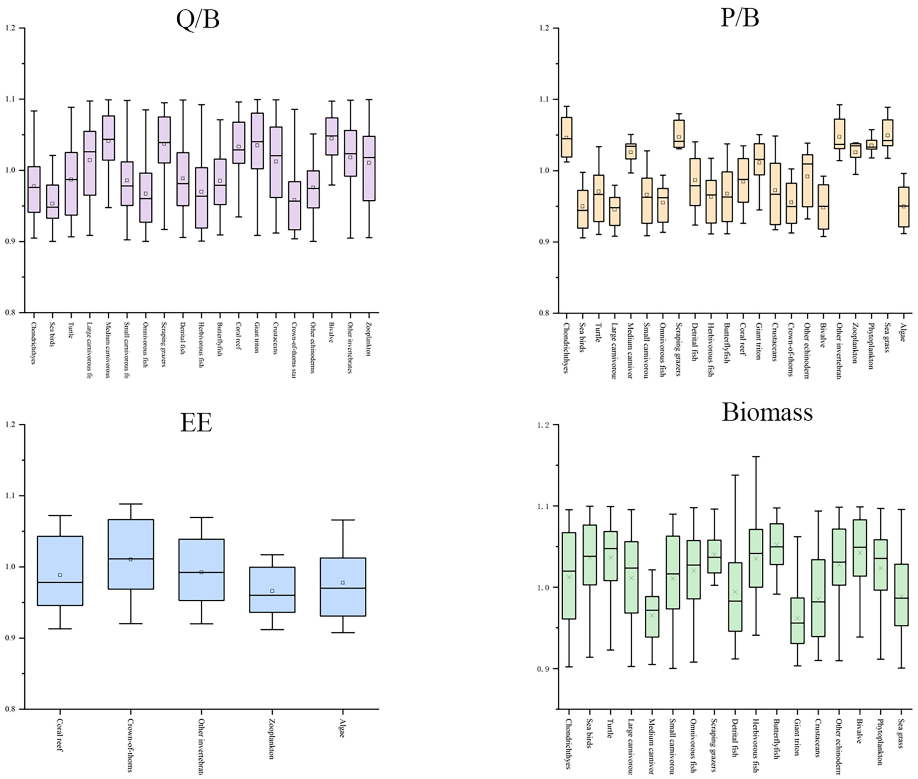

FIGURE 3
Relative perturbation of the four Ecopath parameters (B, P/B, EE, Q/B) of all samples.

average perturbations of EE, P/B, and Q/B were less than 10%, and the disturbance of biomass was less than 12% (Figure 3). The Ecopath model output showed that the trophic level (TL: refers to the level of organisms in the food chain of the ecosystem.) of the XICR ecosystem was 1–3.76, and cartilaginous fish had the highest TL (3.76), followed by large carnivorous fish (3.53), and the level of the coral reef fish functional groups was 2.19–3.53. The energy flows of 23 functional groups in the XICR ecosystem were merged into four TLs through trophic level aggregation, and the total flow of each trophic level decreased with an increase in the nutrient level. The total energy flow of TL I and II accounts for 66.05% and 27.51% of the total energy flow, respectively, and the total energy flow of TL III–IV accounts for 6.44%, conforming to the ecological energy pyramid law. In the XICR ecosystem, the food web comprises grazing and detritus food chains, with 40.00% of the total energy directly derived from detritus and 60.00% from primary producers. A grazing food chain dominates the current ecosystem.

3.2 Projected changes in biomass

Non-producer biomass through the food web increased from 2009 to 2050 for SSP126 and SSP585 in the low and medium fishing scenarios, while the biomass of non-producers projected a decrease for the two ocean warming scenarios in the high fishing scenarios (Figure 4). In the SSP126 scenario, the model expected that the biomass of non-producers would increase by 1.80% and 0.46% for low and medium fishing intensities, respectively, while it would decrease by 1.52% for high fishing effort. In the SSP585 scenario, the biomass of non-producers was predicted to increase by 1.65% and 0.29% for low and medium fishing intensities, respectively, while the predicted ocean warming would lead to a 1.32% decrease in the high fishing effort between 2009 and 2050. Neither SSP126 nor SSP585 caused more than a 2.00% change in the biomass of non-producers in all fishing scenarios. The increase in high trophic level functional groups led to an increase in non-producer biomass, such as large carnivorous fish, medium-carnivorous fish, and sea birds. However, the fishing intensity was predicted to be the primary factor determining changes in biomass.

3.3 Projected changes in catch

Ecosim predicted a decline in fishery catches from 2009 to 2050 for SSP126 and SSP585 across all fishing efforts (Figure 5). In the SSP126 scenario, compared with the baseline scenario, fishery catches were expected to decrease by 11.53, 2.62, and 4.73% for low, medium, and high fishing efforts by 2050, respectively. In the SSP585 scenario, compared with the baseline, the model projected that the fishery catches of the XICR ecosystem would decrease by 12.26, 3.78, and 4.78% for low, medium, and high fishing efforts by 2050, respectively. Fishing intensity was predicted to be the main factor

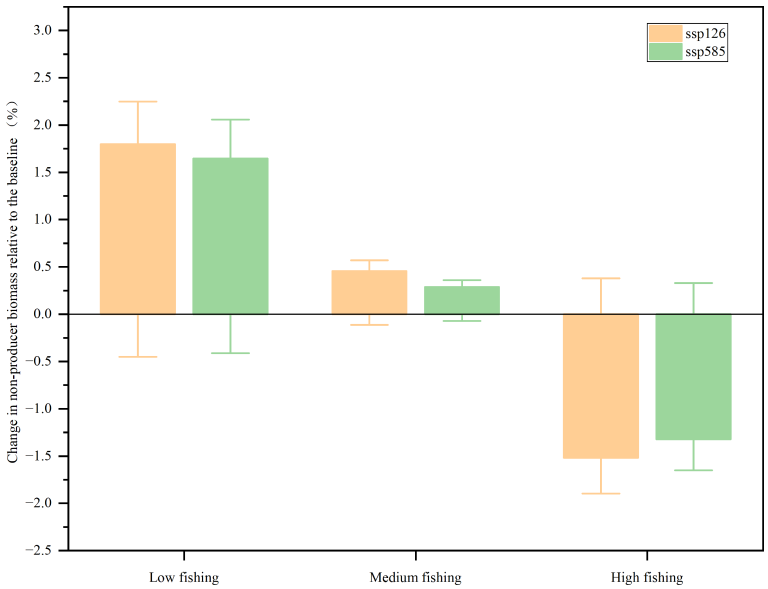

FIGURE 4
Changes in non-producer biomass relative to the baseline (%).

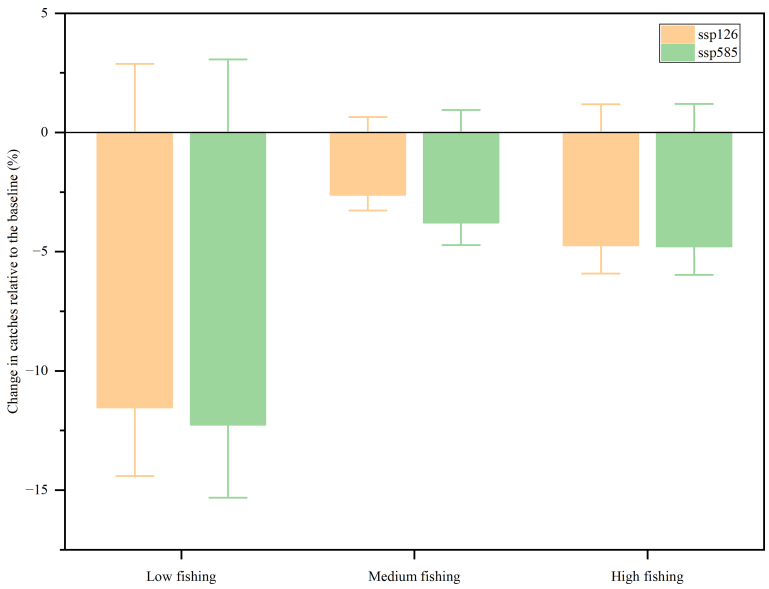

FIGURE 5
Changes in fishery catches relative to the baseline (%).

determining the future catches of the XICR ecosystem. The results showed that catches decreased more at low fishing intensity than at medium and high fishing intensities. Simultaneously, ocean warming was predicted to change the total fishery catch by no more than 1.20% in either the SSP126 or SSP585 scenarios.

3.4 Projected changes in the food web structure

Unlike the biomass of non-producers, the transfer efficiency of the coral reef ecosystem of Xisha Islands decreased for all scenarios, but the magnitude was different (Figure 6). The model assumed that ocean warming (SSP126 and SSP585) had little effect on the transfer efficiency because there was no significant difference between SSP126 and SSP585 in each fishing intensity scenario. In contrast, the fishing intensity was predicted to be a major determinant of future transfer efficiency because there were obvious differences between low, medium, and high fishing intensity settings. In the low fishing scenario, compared to 2009, SSP126 and SSP585 decreased by 0.49% and 0.43%, respectively, whereas in the medium fishing effort scenario, the transfer efficiency was predicted to decrease by 0.37% and 0.43%, and in the high fishing intensity scenario, it decreased by 2.41% and 2.35% under SSP126 and SSP585, respectively. There was a slight difference between the low and medium fishing scenarios. However, in the high fishing scenario, the transfer efficiency for SSP126 and SSP585 decreased by 2.41% and 2.35%, respectively.

In the SSP126 scenario, the change in trophic level of catch (TLC) was projected to decrease by 0.42% and 5.74% under medium and high fishing intensity, respectively (Figure 7). However, under low fishing intensity, it would increase by 1.94% by 2050 compared with the baseline. The model expected that the change in the trophic level of the community (TLcom) would increase under low and medium fishing intensity, while TLcom was predicted to decrease (0.32%) under high fishing intensity. In the SSP585 scenario, TLC would increase (1.64%) under low fishing intensity while decreasing by 0.84% and 6.01% under medium and high fishing efforts, respectively. Notably, the model projected that the impact of fishing intensities on TLC and TLcom was more prominent than that of ocean warming.

In the SSP126 scenario, changes in Kempton's Q were more evident than those in the Shannon index (Figure 8). The model expected that by 2050, the fishing intensity would lead to an increase by 9.90% and 0.18%, higher than the baseline under low and medium fishing efforts, respectively. However, there was a decrease (24.73%) under high-intensity irradiation. The Shannon index was not expected to change by > 1% in all settings. The results showed that it would increase by 0.72% and 0.45% under low and medium fishing intensity, respectively, whereas it would decrease by 0.27% under high fishing effort. The changes in Kempton's Q and Shannon index in the SSP585 scenario were similar to those in

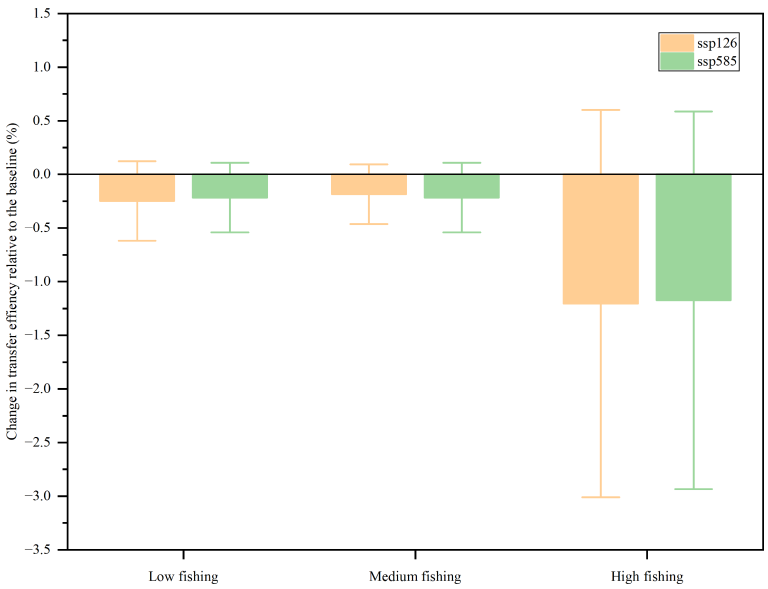

FIGURE 6
Change in transfer efficiency relative to the baseline (%).

SSP126; however, the degree of change was higher than that in the SSP126 scenario. The model predicted that by 2050, Kempton's Q in the SSP585 would increase by 11.96% compared with the baseline under low fishing intensity, whereas it would decrease by 0.47% and 26.50% under medium and high fishing efforts, respectively. The Shannon index was projected to increase by 0.49% and 0.18% for low and medium fishing intensities, respectively, whereas it decreased slightly from 100.00% to 99.51% under high fishing effort. Fishing intensities were predicted to be the most important factor in determining future changes in Kempton's Q and Shannon indices.

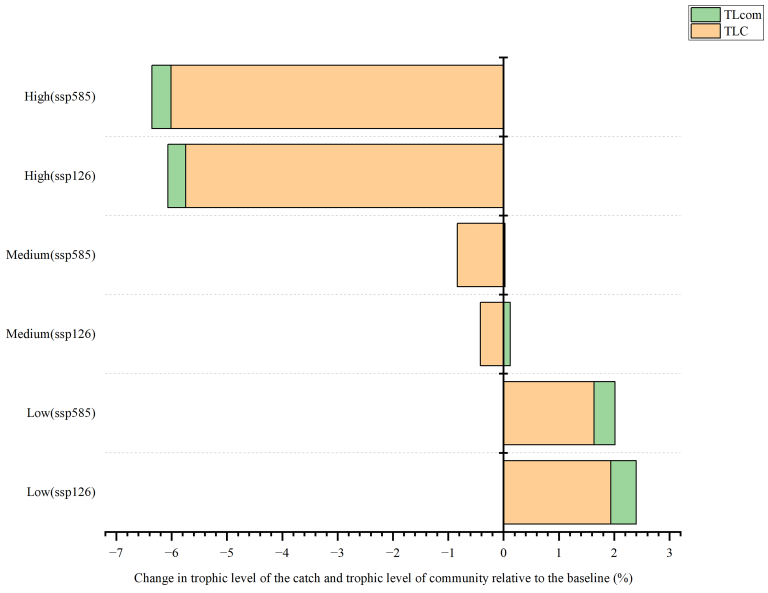

FIGURE 7
Changes in trophic levels of catch and community relative to the baseline (%).

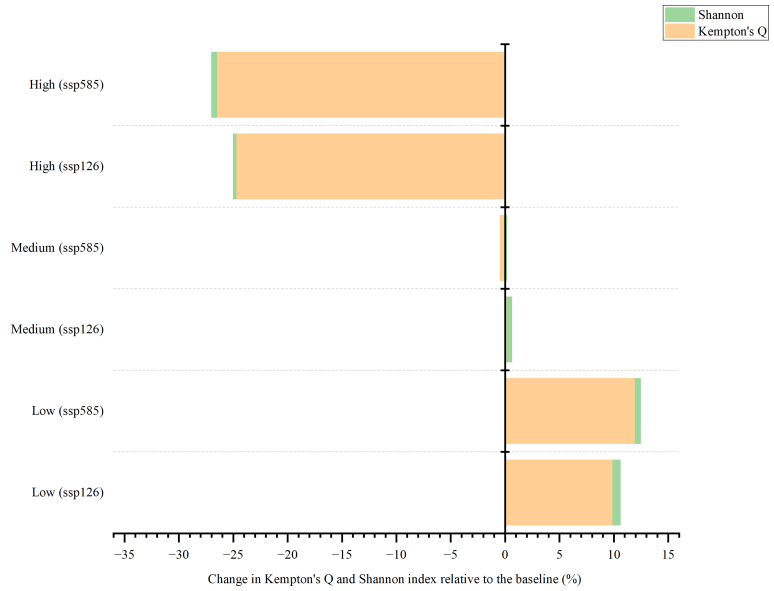

FIGURE 8
Change in Kempton's Q and Shannon indices from 2009 to 2050.

The total standing biomass through the food web varied for the different scenarios (Figure 9). In SSP126, the total standing biomass was projected to decrease by 0.27% under medium fishing intensity and by 1.19% under high fishing effort, whereas it would increase by 0.43% under low fishing intensity. In the SSP585 scenario, the total ecosystem standing biomass was predicted to increase by 0.33%, 0.07%, and 0.80% for low, medium, and high fishing efforts, respectively.

4 Discussion

The biomass of this study area is similar to that in the East Brazil Large Marine Ecosystem (Freire et al., 2008), slightly higher than that of Qilianyu Islands (Hong et al., 2021) and Lembeh Strait (Chen et al., 2009), but much lower than that of the Abrolhos region (Rocha et al., 2007). The study area of Abrolhos has been protected since 1983 and is expected to have higher biomass. The total system throughput was 7937 t/km^2/year, similar to the study in Qilianyu Islands coral reef ecosystem but lower than that of other coral reef ecosystems in Table 2. However, the study area of Xisha Islands is larger than that of the other study areas, with an area of approximately 5×10^5 km^2. The System Omnivory Index (SOI) of the XICR ecosystem was 0.24, whereas it was 0.22 in the Qilainyu model, indicating the TL of functional groups in the XICR did not change obviously, showing that the connection between organisms in XICR food web is more complex. Moreover, the mean trophic level of the catch of XICR is lower than other ecosystems, indicating that the area is greatly affected by fishing. In addition, the total primary production/total respiration (TPP/TR) is an indicator of ecosystem maturity (Odum, 1969; Christensen, 1995), with a range of 0.80–3.2, indicated more maturity when near 1 (Christensen and Pauly, 1992). TPP/TR of XICR ecosystem was 2.47, while the values of the Lembeh Strait and East Brazil Large Marine Ecosystem were 1.48 and 6.60, respectively (Chen et al., 2009; Freire et al., 2008). However, TPP/TR has great variability, it needs more indicators such as macro-descriptors or development attributes to measure the maturity (Argüelles-Jiménez et al., 2020; Arguelles-Jimenez et al., 2021).

Ocean warming can influence the ingestion, digestion, absorption, and assimilation of marine organisms because it requires extra energy to regain homeostasis and endure extreme temperature events (Volkoff et al., 2020; Shahjahan, 2022). In addition, ocean warming can reduce the reproductive capacity of fishes (Rummer et al., 2017). Our results showed that by 2050, the total biomass of fish would decrease, and the biomass of fish with low thermal niches would decrease under the high emission scenario. This phenomenon may be because marine fishes respond to ocean warming by changing their distribution, usually to higher latitudes and deeper waters (Cheung et al., 2013). Ocean warming also directly affects coral reefs, possibly because coral reefs usually live close to the upper limits of their thermal tolerance, and even small temperature increases can lead to bleaching and mortality (DeCarlo et al., 2019). Coral biomass decreased by 0.23% under SSP585, and when coral was lost, algal

FIGURE 9
Changes in biomass and energy flows within the XICR ecosystem food web for ocean warming and fishing. **(A)**, food web of baseline ecosystem (2009). **(B)**, food web of the Xisha ecosystem for the SSP585-High fishing scenario (2050). Each circle represents a functional group, and its size represents the biomass. Functional groups of food webs are represented by trophic levels and are linked by relationships between predators and prey.

biomass increased, leading to a decrease in biodiversity and ecosystem maturity; additionally, the biomass of small-bodied fish would increase, implying that there would be higher productivity on reefs, although the total fish landed would be reduced (Ainsworth et al., 2015). In our study, the total production was predicted to increase, whereas the total catch showed a decrease in all scenarios.

The XICR ecosystem has also been affected by ocean warming. The evenness of the ecosystem was projected to change by 2050, and the evenness of the high trophic species would also shift, especially in the high emission scenario. The Shannon index would not shift considerably, but Kempton's Q index would be influenced by ocean warming, consistent with the study on the Pearl River Estuary (PRE). A study on PRE ecosystem predicted changes in the ecosystem under the dual pressure of climate change and fishing using the EwE model (Zeng et al., 2021). The results indicated that the Shannon index was slightly influenced by climate change, whereas Kempton's Q index was predicted to show a different pattern (Zeng et al., 2019). Ocean variables, including ocean warming, net primary production, dissolved oxygen, and ocean acidification, were predicted to shift the Shannon index during small events, while ocean warming was forecasted to cause a large decrease in the Kempton's Q index (Zeng et al., 2019). These changes indicate that the XICR ecosystem structure will change by 2050, leading to a reduction in the resilience of the coral reef

TABLE 2 System statistics were obtained from the Ecopath model of XICR and other models of coral reef ecosystems.

Parameter	This study	Hong et al., 2021	Chen et al., 2019	Freire et al., 2008	Arias-Gonzalez 2004	Rocha et al., 2007	Units
Sum of all consumption	2415	2478	2154		20496		t/km^2/year
Sum of all exports	1866	2083	588.8		3783		t/km^2/year
Sum of all respiratory flows	1254	1251	1164		12360		t/km^2/year
Sum of all flows into detritus	2402	2738	893.2		11397		t/km^2/year
Total system throughput	7937	8551	4800	23042	48037	43394	t/km^2/year
Sum of all production	3774	3773	2282	10364	20180	13119	t/km^2/year
Mean trophic level of the catch	2.63	2.54	3.35	3.40	3.45		
Gross efficiency (catch/net p.p.)	0.0051		0.0019		0.000079		
Calculated total net primary production	3095		1722	8375	1589	9150	t/km^2/year
Total primary production/total respiration	2.47		1.48	6.60		0.60	
Net system production	1841	1932	558.8		3529		t/km^2/year
Total primary production/total biomass	13.91	19.07	8.79	37.60	15.60	5.60	
Total biomass/total throughput	0.03	0.02	0.04	0.01		0.04	/year
Total biomass (excluding detritus)	222.50	171.00	1960	222.50	1019	1640	t/km^2
Total catch	15.30	15.30	3.22	0.13	1.25		t/km^2/year
Connectance Index	0.31	0.36	0.42				
System Omnivory Index	0.24	0.22	0.35	0.21		0.16	
Total market value	15.90		3.22				
Total shadow value			0				
Total value			3.22				
Total fixed cost			0				
Total variable cost			2.58				
Total cost			2.58				
Profit			0.64				
Study area	500000		215.00	1075		7.00	km^2

ecosystem. Changes in the ecosystem structure can alter the function of coral reef ecosystems (Dulvy et al., 2004; Inagaki et al., 2020). One of the main indicators of the degeneration of coral reef ecosystems is a significant increase in the biomass of macroalgae (Jackson et al., 2001; Kramer, 2003; Acosta et al., 2013), which confirms our findings. Our results predicted that coral biomass would decrease whereas algal biomass would increase in the SSP585 scenario.

Overfishing can affect the biomass of coral reef ecosystems, especially the biomass of large fish and scraping grazers, which are indicators of the health of the ecosystem (McClanahan et al., 2014; Lefcheck et al., 2021). Reducing large predators and competitors alters nutrient profiles, often increasing the number of prey species (Steneck, 1998). In our model, the results predicted that when the fishing effort was reduced (in the low fishing scenario), there would be a small increase in biomass (0.33%), similar to that observed in a previous study in the East China Sea (ECS). Research in the ECS, including 24 functional groups, simulated the impact of the seasonal fishing moratorium (SFM) from 1997 to 2018 (Xu et al., 2022). Compared with no SFM, the biomass of the ECS increased by 67.12% by 2018 with SFM. The fishing policy of the ECS is seasonal and more reasonable, which may be the reason for the larger gap between the growth amplitudes of the XICR and ECS. A significant increase (SOI increased from 0.13 to 0.18) in the ECS ecosystem maturity indicates a slow recovery of the ECS

ecosystem in the past two decades (Xu et al., 2022). In our study, the SOI was predicted to decrease from 0.25 (high fishing intensity) to 0.24 (low fishing intensity). This suggests that the ecosystem can recover to some extent by reducing fishing intensity. Furthermore, the ecosystem can be repaired better through seasonal fishing moratoriums.

Overfishing can also cause ecological problems. With the increase in fishing effort, the biomass of crown of thorns starfish, which is a large predator of coral reefs, has increased by 1.71% under high fishing effort. In healthy coral reef ecosystems, the density of thorn of crowns usually does not exceed one per hectare (Wabnitz et al., 2010). One crown of thorns can eat approximately 0.1 m^2 of healthy coral on average every day (Babcock et al., 2016; Li et al., 2019). When the density exceeds 30 per hectare, the coral biomass cannot meet the predation demand of the crown of thorns, leading to an imbalance in the coral reef ecosystem (Wabnitz et al., 2010). Coral reefs damaged by the crown of thorns cannot recover to their pre-outbreak levels, even over a long period (Li et al., 2019). Therefore, fishing effort should be controlled to keep the biomass of crown of thorns from exploding in large numbers.

Our findings also suggest that there is a risk of ecosystem degeneration due to ocean warming and overfishing, consistent with the findings of recent studies (Burke et al., 2011; Blowes et al., 2019; Bryndum et al., 2019), especially in coral reef ecosystems where human activities are exacerbating the degradation caused by ocean warming (Hughes et al., 2017; Beyer et al., 2018; Capitani et al., 2022). In this case, TPP/TR would decrease by 0.40%, and SOI would decrease by 4.17% in the SSP585-High fishing scenario, indicating that the maturity of the XICR ecosystem would continue to decrease with increasing dual pressure of ocean warming and fishing.

Reducing fishing intensities can ease the impact of ocean warming on most fish functional groups (McClanahan et al., 2014). However, the biomass of some species will also decrease under low fishing effort because they may have higher fishing mortality (Zeng et al., 2019). In this study, the total biomass of the XICR ecosystem was 220.7 t/km^2 in the SSP585-high fishing scenario, whereas it was 224.2 t/km^2 in the SSP585-low fishing scenario, and the increase in fish biomass was mainly concentrated in functional groups composed of non-economic fish, such as butterflyfish and detrital fish. Several studies have also suggested that fishing activities could aggravate the effects of ocean warming and prolong the recovery time of species (Brander, 2007; Kirby et al., 2009; McClanahan et al., 2014; Zeng et al., 2019). In addition, fishing can remove large and older species, increasing age-truncated or juvenile populations in ecosystems (McOwen et al., 2015; Zeng et al., 2019), which can increase the sensitivity of ecosystems to ocean warming (Zeng et al., 2019). One study found that there are mainly small fish species in the XICR ecosystem, and the density of grouper and parrotfish with high food value is low (Yang et al., 2018), which aggravates the impact of climate warming on the ecosystem.

It should be noted that there were some uncertainties in this study. First, the tradeoff between simplicity and complexity is a source of uncertainty. To solve the variability in functional groups and reduce uncertainty, each species is classified into functional groups based on traits, such as individual size, diet, and habitat (Milessi et al., 2010). EwE is advised to divide species into multi-stanza groups (sub-groups), making their dynamics more realistic and providing insights into stock-recruitment relationships, especially the top predators (Christensen et al., 2008; Du et al., 2020). However, we did not define the groups representing life stages or stanzas for species with complex trophic ontogeny in this study owing to a lack of data, which may be uncertain in this model. Twenty-three functional groups are far from enough for complex coral reef ecosystem, the future research can combine diving survey data and net fishing data through cooperation with other fisheries research institute, in order to obtain more biodiversity data and more functional groups, not only the Chondrichthyes, but also the multi-stanza of the main functional groups. Second, some input parameters derived from other ecosystems are relatively more uncertain. For example, the biomass of sharks and phytoplankton was based on previous studies in the SCS (Huang et al., 2009; Hong et al., 2021). Sensitivity analysis showed that biomass has more influence on Ecosim results. To improve the accuracy of the model prediction, historical comparison data were used to reduce the differences between the historical observations and model predictions (Christensen et al., 2008). However, in this study, full historical comparison data were only available for a small number of functional groups, and the normalized change in chlorophyll in Xisha from 2009 to 2021 was applied in our model. The third uncertainty is associated with an incomplete understanding of species' response to ocean warming and their interaction with fishing. In this model, the forcing function used in the ocean warming simulations were linearized and simplified, and the major impacts were related to the growth of the species. The impacts of ocean warming are more complex and extensive because of the complexity of the relationship between coral and temperature (Hughes et al., 2007). Coral bleaching and mortality were not considered in this study, which is another uncertainty in our study. This study was a preliminary attempt to understand the impact of ocean warming and fishing on the coral reef ecosystem of Xisha Islands. To make the study more comprehensive and representative, more environmental parameters, such as pH, dissolved oxygen, and net primary productivity, will be considered in future studies, and the fishing scenario will be revised according to existing fishing policies and trends in fishing effort.

5 Conclusions

We simulated the impacts of environmental stressors (ocean warming) and human activity (fishing) on the XICR ecosystem in the SCS. We identified four reliable ecosystem trends under the impacts of ocean warming and fishing. (1) In the XICR ecosystem, the grazing food chain had a higher energy source than the detrital food chain. (2) Ocean warming will seriously affect tropical reef ecosystems through biomass decline. (3) Fishing has a greater impact on the Xisha coral reef ecosystem than that of ocean warming. (4) The impact of ocean warming can be mitigated by reducing the fishing intensity.

Data availability statement

The original contributions presented in the study are included in the article/supplementary material. Further inquiries can be directed to the corresponding authors.

Author contributions

XZ: Conceptualization, methodology, software, writing. YL: Investigation, data curation. JD: Conceptualization, funding acquisition, methodology, writing, supervision. SQ: Investigation, data curation. BX: Investigation, data curation. WC: Investigation, data curation. JW: Investigation, data curation. WH: Formal analysis, data curation. ZW: Investigation, data curation. BC: Resources, data curation, supervision. All authors contributed to the article and approved the submitted version.

Funding

This work was financially supported by the National Natural Science Foundation of China (grant numbers 42176153 and 41676096), Xiamen Youth Innovation Fund (grant number 3502Z20206096).

Acknowledgments

We thank Lingyan Xu, Qian Peng, and Qifang Wang for the help in the process of this study, and we thank the two reviewers for their constructive comments which greatly improved this paper.

Conflict of interest

The authors declare that the research was conducted in the absence of any commercial or financial relationships that could be construed as a potential conflict of interest.

Publisher's note

References

Acosta, G., Rodriguez, F. A., Hernandez, R. C., and Arias, J. E. (2013). Additive diversity partitioning of fish in a Caribbean coral reef undergoing shift transition. *PloS One* 8, 11. doi: 10.1371/journal.pone.0065665

Ainsworth, C. H., and Mumby, P. J. (2015). Coral–algal phase shifts alter fish communities and reduce fisheries production. *Global Change Biol.* 21, 165–172. doi: 10.1111/gcb.12667

Allen, G. R. (2008). Conservation hotspots of biodiversity and endemism for indo-pacific coral reef fishes. *Aquat. Conservation-Marine Freshw. Ecosystems.* 18, 541–556. doi: 10.1002/aqc.880

Arguelles-Jimenez, J., Alva-Basurto, J. C., Perea-Espana, H., Zetina-rejon, M. J., and Arias-Gonzalez, J. E. (2020). The measurement of ecosystem development in Caribbean coral reefs through topological indices. *Ecol. Indicators* 110, 11. doi: 10.1016/j.ecolind.2019.105866

Arguelles-Jimenez, J., Rodriguez-Zaragoza, F. A., Gonzalez-Gandara, C., Alva-Basurto, J. C., Arias-Gonzalez, J. E., Hernandez-Landa, R., et al. (2021). Functional developmental states of the greater Caribbean coral reefs. *Ecol. Indicators* 121, 107170. doi: 10.1016/j.ecolind.2019.105866

Arias-Gonzalez, J. E., Nunez-Lara, E., Gonzalez-Salas, C., and Galzin, R (2004). Trophic models for investigation of fishing effect on coral reef ecosystems. *Ecological Modelling.* 172, 197-212. doi: 10.1016/j.ecolmodel.2003.09.007

Babcock, R. C., Dambacher, J. M., Morello, E. B., Plaganyi, E. E., Hayes, K. R., Sweatman, H. P. A., et al. (2016). Assessing different causes of crown-of-Thorns starfish outbreaks and appropriate responses for management on the great barrier reef. *PloS One* 11 (12), e0169048. doi: 10.1371/journal.pone.0169048

Bellwood, D. R., Hughes, T. P., Folke, C., and Nystrom, M. (2004). Confronting the coral reef crisis. *Nature.* 429, 827–833. doi: 10.1038/NATURE02691

Bellwood, D. R., Hughes, T. P., and Hoey, A. S. (2006). Sleeping functional group drives coral-reef recovery. *Curr. Biol.* 16, 2434–2439. doi: 10.1016/j.cub.2006.10.030

Beyer, H. L., Kennedy, E. V., Beger, M., ChenN, C. A., Cinner, J. E., Darling, E. S., et al. (2018). Risk-sensitive planning for conserving coral reefs under rapid climate change. *Conserv. Letters.* 11, 10. doi: 10.1111/conl.12587

Blowes, S. A., Supp, S. R., Antao, L. H., Bates, A., Bruelheide, H., Chase, J. M., et al. (2019). The geography of biodiversity changes in marine and terrestrial assemblages. *Science.* 366, 339. doi: 10.1126/science.aaw1620

Brander, K. M. (2007). Global fish production and climate change. *Proc. Natl. Acad. Sci. U S A.* 104, 19709–19714. doi: 10.1073/pnas.0702059104

Bruno, J. F., and Selig, E. R. (2007). Regional decline of coral cover in the indo-pacific: Timing, extent, and subregional comparisons. *PloS One* 2(8), e711. doi: 10.1371/journal.pone.0000711

Bryndum, A., Tittensor, D. P., Blanchard, J. L., Cheung, W. W. L., Coll, M., Galbraith, E. D., et al. (2019). Twenty-first-century climate change impacts on marine animal biomass and ecosystem structure across ocean basins. *Global Change Biol.* 25, 459–472. doi: 10.1111/gcb.14512

Burke, L. M., Reytar, K., Spalding, M., and Perry, A. L. (2011). Coral reefs at risk. *Ethics Medics.* 83 (12), 130. doi: 10.1029/EO083i012p00130-03

Capitani, L., De Araujo, J. N., Vieira, E. A., Angelini, R., and Longo, G. O. (2022). Ocean warming will reduce standing biomass in a tropical Western Atlantic reef ecosystem. *Ecosystems.* 25, 843–857. doi: 10.1007/s10021-021-00691-z

Chen, B. H., Zhou, Q. L., and Yang, S. Y. (2009). Impacts of climate changes on marine biodiversity. *J. Oceanography Taiwan Strait.* 28 (3), 437–444.

Cheung, W. W. L., Watson, R., and Pauly, D. (2013). Signature of ocean warming in global fisheries catch. *Nature.* 497, 365. doi: 10.1038/nature12156

Christensen, V. (1995). ECOSYSTEM MATURITY - TOWARDS QUANTIFICATION. *Ecol. Modelling.* 77, 3–32. doi: 10.1016/0304-3800(93)E0073-C

Christensen, V., Coll, M., Piroddi, C., Steenbeek, J., Buszowski, J., and Pauly, D. (2014). A century of fish biomass decline in the ocean. *Mar. Ecol. Prog. Series.* 512, 155–166. doi: 10.3354/meps10946

Christensen, V., and Pauly, D. (1992). Ecopath II–a software for balancing steady-state ecosystem models and calculating network characteristics. *Ecol. Model.* 61 (3-4), 169–185. doi: 10.1016/0304-3800(92)90016-8

Christensen, V., Walters, C. J., and Pauly, D. (2005). Ecopath with ecosim: A user's guide. fish. centre. univ. br. Columbia. *Vancouver.* 154, 31.

Christensen, V., Walters, C. J., Pauly, D., and Forrest, R. (2008). Ecopath with ecosim version 6 user guide. *Lenfest Ocean Futures Project.* 235.

Colléter, M., Valls, A., Guitton, J., Gascuel, D., Pauly, D., and Christensen, V. (2015). Global overview of the applications of the ecopath with ecosim modeling approach using the EcoBase models repository. *Ecol. Modelling.* 302, 42–53. doi: 10.1016/j.ecolmodel.2015.01.025

Dahlke, F. T., Wohlrab, S., Butzin, M., and Portner, H. O. (2020). Thermal bottlenecks in the life cycle define climate vulnerability of fish. *Science* 369, 65. doi: 10.1126/science.aaz3658

David, D., and Degani, G. (2011). Temperature affects brain and pituitary gene expression related to reproduction and growth in the Male blue gouramis, trichogaster trichopterus. *J. Exp. Zoology Part a-Ecological Integr. Physiol.* 315A, 203–214. doi: 10.1002/jez.663

Day, P. B., Stuart, R. D., Edgar, G. J., and Bates, A. E. (2018). Species' thermal ranges predict changes in reef fish community structure during 8 years of extreme temperature variation. *Diversity Distributions.* 24, 1036–1046. doi: 10.1111/ddi.12753

DeCarlo, T. M., Harrison, H. B., Gajdzik, L., Alaguarda, D., Rodolfo-Metalpa, R., D'Olivo, J., et al. (2019). Acclimatization of massive reef-building corals to consecutive heatwaves. *Proc. R. Soc. B-Biological Sci.* 286, 7. doi: 10.1098/rspb.2019.0235

Dulvy, N. K., Freckleton, R. P., and Polunin, N. V. C. (2004). Coral reef cascades and the indirect effects of predator removal by exploitation. *Ecol. Letters.* 7, 410–416. doi: 10.1111/j.1461-0248.2004.00593.x

Du, J. G., Makatipu, P. C., Tao, L. S. R., Pauly, D., Cheung, W. W. L., Peristiwady, T., et al. (2020). Comparing trophic levels estimated from a tropical marine food web using an ecosystem model and stable isotopes. *Estuar. Coast. Shelf Science.* 233, 13. doi: 10.1016/j.ecss.2019.106518

Eddy, T. D., Bernhardt, J. R., Blanchard, J. L., Cheung, W. W. L., Colleter, M., Pontavice, H., et al. (2021). Energy flow through marine ecosystems: Confronting transfer efficiency. *Trends Ecol. Evo.* 36 (1), 76–86. doi: 10.1016/j.tree.2020.09.006

Fisher, R., O'Leary, R. A., Low-Choy, S., Mengersen, K., Knowlton, N., Brainard, R. E., et al. (2015). Species richness on coral reefs and the pursuit of convergent global estimates. *Curr. Biol.* 25, 500–505. doi: 10.1016/j.cub.2014.12.022

Freire, K. M. F., Christensen, V., and Pauly, D. (2008). Description of the East Brazil Large marine ecosystem using a trophic model. *Scientia Marina.* 72, 477–491.

Fulton, E. A., Link, J. S., Kaplan, I. C., Savina-Rolland, M., Johnson, P., Ainsworth, C., et al. (2011). Lessons in modeling and management of marine ecosystems: the Atlantis experience. *Fish Fisheries.* 12, 171–188. doi: 10.1111/j.1467-2979.2011.00412.x

Gibert, J. P. (2019). Temperature directly and indirectly influences food web structure. *Sci. Rep.* 9, 5312. doi: 10.1038/s41598-019-41783-0

Hong, X., Chen, Z., Zhang, J., Jiang, Y., Gong, Y., Cai, Y., et al. (2021). Analysis of ecological carrying capacity of reefs organisms enhancement in qilanyu islands based on ecopath model. *Trop. Oceanography.* 41 (01), 15–27. doi: 10.11978/2020156(in Chinese with English abstract

Huang, H. (2018). *Coral reef atlas of xisha islands* (Beijing: Science Press).

Huang, Z., Chen, Z., and Zeng, X. (2009). Species composition and resources density of Chondrichthyes in the continental shelf of northern south China Sea. *Ocean ographyin Taiwan Strait.* 28 (1), 38–44. doi: 10.3969/j.issn.1000-8160.2009.01.007(in Chinese with English abstract

Huang, H., Dong, Z., and Lian, J. (2008). Establishment of nature reserve of coral reef ecosystem on the xisha islands. *Trop. Geography.* 28 (6), 540–544. doi: 10.3969/j.issn.1001-5221.2008.06.010(in Chinese with English abstract

Hu, W., Chen, B., Arnupap, P., Zhang, D., Liu, X., Gu, H., et al. (2020). Ecological vulnerability assessment of coral reef: A case study of Si Chang island, Thailand. *Chin. J. Ecology.* 39 (03), 979–989. doi: 10.13292/j.1000-4890.202003.029 (in Chinese with English abstract

Hughes, T. P., Baird, A. H., Bellwood, D. R., Card, M., Connolly, S. R., Folke, C., et al. (2003). Climate change, human impacts, and the resilience of coral reefs. *Science.* 301, 929–933. doi: 10.1126/science.1085046

Hughes, T. P., Barnes, M. L., Bellwood, D. R., Cinner, J. E., Cumming, G. S., Jackson, J. B. C., et al. (2017). Coral reefs in the anthropocene. *Nature.* 546, 82–90. doi: 10.1038/nature22901

Hughes, T. P., Rodrigues, M. J., Bellwood, D. R., Ceccarelli, D., Hoegh, O., Mccook, L., et al. (2007). Phase shifts, herbivory, and the resilience of coral reefs to climate change. *Curr. Biol.* 17, 360–365. doi: 10.1016/j.cub.2006.12.049

Inagaki, K. Y., Pennino, M. G., Floeter, S. R., Hay, M. E., and Longo, G. O. (2020). Trophic interactions will expand geographically but be less intense as oceans warm. *Global Change Biol.* 26, 6805–6812. doi: 10.1111/gcb.15346

Jackson, J. B. C., Kirby, M. X., Berger, W. H., Bjorndal, K. A., Boysford, L. W., Bourque, B. J., et al. (2001). Historical overfishing and the recent collapse of coastal ecosystems. *Science.* 293, 629–638. doi: 10.1126/science.1059199

Kirby, R. R., Beaugrand, G., and Lindley, J. A. (2009). Synergistic effects of climate and fishing in a marine ecosystem. *Ecosystems* 12, 548–561. doi: 10.1007/s10021-009-9241-9

Kramer, P. A. (2003). Synthesis of coral reef health indicators for the western Atlantic: Results of the AGRRA progra-2000). *Atoll Res. Bul.*, 496, 1–58. doi: 10.5479/si.00775630.496-3.1

Lefcheck, J. S., Edgar, G. J., Stuart-Smith, R. D., Bates, A. E., Waldock, C., Brandl, S. J., et al. (2021). Species richness and identity both determine the biomass of global reef fish communities. *Nat. Commun.* 12 (1), 1. doi: 10.1038/s41467-021-27212-9

Legendre, L., and Niquil, N. (2013). Large-Scale regional comparisons of ecosystem processes: Methods and approaches. *J. Marine. Syst.* 109, 4–21. doi: 10.1016/j.jmarsys.2011.11.021

Li, Y. (2020). *Biodiversity and biological characteristics of dominant fish species of typical reef fishes in south China sea* (Shanghai, China: Shanghai Ocean University).

Li, Y., Jia, X., and Chen, G. (2007). *Coral reef fish resources in the south China Sea* (Beijing: Ocean Press).

Liu, J. (2020). *Response of coral reefs and islands in the south China sea to climate warming in the past 40 years recorded by remote sensing images* (Guangxi, China: Guangxi University).

Liu, X., Shi, Q., Tao, S., Yang, H., Zhang, X., and Zhou, S. (2021). The growth rate of coral porites at the zhongbei ansha of the zhongsha atoll and its response to seawater temperature change in the past 165 years. *Trop. Oceanogr.* 41(5), 64-73. doi: 10.11978/2021159

Li, X., and Wang, Y. (2002). Comparison between benthos of nansha islands and xisha islands ,south china sea. *Studia Marina Sinica.* 44, 74–79.

Li, Y., Wu, Z., Liang, J., Chen, S., and Zhao, M. (2019). Analysis on the outbreak period and cause of acanthaster planci in xisha islands in recent 15 years. *Sci. Bulletin.* 64 (33), 3478–3484. doi: 10.1360/TB-2019-0152(in Chinese with English abstract

McClanahan, T. R., Graham, N. A. J., and Darling, E. S. (2014). Coral reefs in a crystal ball: predicting the future from the vulnerability of corals and reef fishes to multiple stressors. *Curr. Opin. Environ. Sustainability.* 7, 59–64. doi: 10.1016/j.cosust.2013.11.028

McOwen, C. J., Cheung, W. W. L., Rykaczewski, R. R., Watson, R. A., and Wood, L. J. (2015). Is fisheries production within Large marine ecosystems determined by bottom-up or top-down forcing? *Fish Fisheries.* 16, 623–632. doi: 10.1111/faf.12082

Milessi, A. C., Danilo, C., Laura, R. G., Daniel, C., Sellanes, J., and Rodriguze, L. (2010). Trophic mass-balance model of a subtropical coastal lagoon, including a comparison with a stable isotope analysis of the food-web. *Ecol. Modelling.* 221, 2859–2869. doi: 10.1016/j.ecolmodel.2010.08.037

Miloslavich, P., and Klein, E. (2005). *Caribbean Marine biodiversity: the known and unknown* Lancaster, PA: Des Tech Publishers Press

Odum, E. P. (1969). The strategy of ecosystem development. *Science.* 164, 262–270. doi: 10.1126/science.164.3877.262

Pandolfi, J. M., Bradbury, R. H., Sala, E., Hughes, T. P., Bjorndal, K. A., Cooke, R. G., et al. (2003). Global trajectories of the long-term decline of coral reef ecosystems. *Science.* 301, 955–958. doi: 10.1126/science.1085706

Pilling, G., Sheppard, C., Davy, S., and Grahamet, N. (2017). *The biology of coral reefs (Second edition)* (Oxford: Oxford University Press).

Polovina, J. J. (1984). Model of a coral reef ecosystem i. the ECOPATH model and its application to French frigate shoals. *Coral reefs.* 3, 1–11. doi: 10.1007/BF00306135

Porter, G. (1998). *Estimating overcapacity in the global fishing fleet* Washington, DC: WWF Press

Qiu, S., Liu, X., Chen, B., Wang, Y., Liao, J., and Du, J. (2022). Reef fish diversity and community pattern of the xisha islands, south China Sea. *Mar. Environ. Science.* 41 (3), 395–401. doi: 10.13634/j.cnki.mes.2022.03.012(in Chinese with English abstract

Reaka-Kudla, M. L. (1997). *The global biodiversity of coral reefs: A comparison with rain forests* (Washington, D.C: Joseph Henry Press).

Rocha, G., Rossi-Wongtschowski, C., Pires-Vanin, A., and Soares, L. (2007). Trophic models of são sebastião channel and continental shelf systems, SE Brazil. *Panam J. Aquat Sci.* 2, 149–162.

Rummer, J. L., and Munday, P. L. (2017). Climate change and the evolution of reef fishes: past and future. *Fish Fisheries.* 18, 22–39. doi: 10.1111/faf.12164

Shahjahan, M., Islam, M. J., Hossain, M. T., Mishu, M. A., Hasan, J., and Brown, C. (2022). Blood biomarkers as diagnostic tools: An overview of climate-driven stress responses in fish. *Sci. Total Environment.* 843, 156910. doi: 10.1016/j.scitotenv.2022.156910

Shi, X., Liu, Y., Chen, T., and Yu, K. (2008). The potential threats of global warming on corals living in the xisha islands. *Trophical Geography.* 04, 342–345, 368. doi: ckni:sun:rddd.0.2008-04-011(in Chinese with English abstract

Shin, Y. J., and Cury, P. (2001). Exploring fish community dynamics through size-dependent trophic interactions using a spatialized individual-based model. *Aquat. Living Resour.* 14, 65–80. doi: 10.1016/S0990-7440(01)01106-8

Simth, S. V. (1978). Coral-reef area and the contributions of reefs to processes and resources of the world's oceans. *Nature.* 273, 225–226. doi: 10.1038/273225a0

Spalding, M., Ravilous, C. R., and Green, E. P. (2001). *World atlas of coral reefs*; California: University of California Press.

Steenbeek, J., Corrales, X., Platts, M., and Coll, M. (2018). Ecosampler: A new approach to assessing parameter uncertainty in ecopath with ecosim. *Softwarex.* 7, e40542 198–204. doi: 10.1016/j.softx.2018.06.004

Steneck, R. S. (1988). *Herbivory on coral reefs: A synthesis*. Queensland: James Cook University Press.

Sumaila, U. R., Cheung, W., Dyck, A., Gueye, K., Huang, L., Lam, V., et al. (2012). Benefits of rebuilding global marine fisheries outweigh costs. *PloS One* 7 (7). doi: 10.1371/journal.pone.0040542

Sun, D., Lin, Z., Qiu, Y., and Wang, X. (2005). Fish fauna of coral reef waters of the xisha islands. *South China Fisheries Science.* 1 (5), 18–25.

Teh, L. S. L., Cashion, T., Alava Saltos, J. J., Cheung, W. W. L., and Sumaila, U. R. (2019). Status, trends, and the future of fisheries in the East and south China seas. *Fisheries Centre Res. Rep.* 27 (1), 101.

Tesfamichael, D., and Pauly, D. (2016). An exploration of ecosystem-based approaches for the management of red Sea fisheries. *Springer Netherlands.*, 111–113. doi: 10.1007/978-94-017-7435-2_9

Volkoff, H., and Ronnestad, I. (2020). Effects of temperature on feeding and digestive processes in fish. *Temperature (Austin Tex.).* 7, 307–320. doi: 10.1080/23328940.2020.1765950

Wabnitz, C. C. C., Balazs, G., Beavers, S., Bjorndal, K. A., Bolten, A. B., Christensen, V., et al. (2010). Ecosystem structure and processes at kaloko honokohau, focusing on the role of herbivores, including the green sea turtle chelonia mydas, in reef resilience. *Mar. Ecol. Prog. Series.* 420, 27–U392. doi: 10.3354/meps08846

Walters, C., Christensen, V., and Pauly, D. (1997). Structuring dynamic models of exploited ecosystems from trophic mass-balance assessments. *Rev. Fish Biol. Fisheries.* 7, 139–172. doi: 10.1023/A:1018479526149

Walters, C., Pauly, D., Christensen, V., and Kitchell, J. F. (2000). Representing density dependent consequences of life history strategies in aquatic ecosystems: EcoSim II. *Ecosystems.* 3, 70–83. doi: 10.1007/s100210000011

Wang, X., Du, F., Lin, Z., Sun, D., Qiu, Y., and Huang, S. (2011). Fish species diversity and community pattern in coral reefs of the xisha islands, south China Sea. *Biodiversity Science.* 19 (4), 463–469.

Wang, T., Liu, Y., Quan, Q., Xioa, Y., Wu, P., and Li, C. (2022). Species composition characteristics analysis of qilianyu reef fishes of xisha islands. *J. Fishery Sci. China* 29 (1), 102–117. doi: 10.12264/JFSC2021-0122(in Chinese with English abstract

Williams, G. J., and Graham, N. A. J. (2019). Rethinking coral reef functional futures. *Funct. Ecology.* 33, 942–947. doi: 10.1111/1365-2435.13374

World bank (2017). *The sunken billions revisited: progress and challenges in global marine fisheries* (Washington, D.C: WB Press).

Xu, L., Song, P., Wang, Y., Xie, B., Huang, L., LI, Y., et al. (2022). Estimating the impact of a seasonal fishing moratorium on the East China Sea ecosystem from 1997 to 2018. *Front. Mar. Science.* 9. doi: 10.3389/fmars.2022.865645

Yang, W., Hu, J., Lin, B., Huang, H., and Liu, M. (2018). Species diversity of coral reef fishes in zhaoshu island waters, xisha islands. *J. Xiamen Univ. (Natural Science)* 57 (6), 819–825. doi: 10.6043/j.issn.0438-0479,201807002(in Chinese with English abstract

Zeng, Z., Cheung, W. W. L., Li, S. Y., Hu, J. T., and Wang, Y. (2019). Effects of climate change and fishing on the pearl river estuary ecosystem and fisheries. *Rev. Fish Biol. Fisheries.* 29, 861–875. doi: 10.1007/s11160-019-09574-y

Zhang, L., Takahashi, D., Hartvig, M., and Andersen, K. H. (2017). Food-web dynamics under climate change. *Proc. R. Soc. B: Biol. Sci.* 284, 20171772. doi: 10.1098/rspb.2017.1772

Zheng, X., Zhang, H., Chen, B., and Yu, W. (2021). Advance of indicator system for the evaluation of coral reef restoration effectiveness. *Appl. Oceanography.* 40 (1), 126–139. doi: 10.3969/J

Zuo, X., Su, F., Wang, Q., Wang, C., Jiang, H., and Shi, W. (2020). Thermal stress temporary refugia under global change for coral reefs in the south China Sea islands. *Scientia Geographica Sinica.* 40 (5), 814–822. doi: 10.13249/j.cnki.sgs.2020.05.016

Zuo, X., Su, F., Wu, W., Chen, Z., and Shi, W. (2015). Spatial and temporal variability of thermal stress to china's coral reefs in south China Sea. *Chin. Geographical Sci.* 25 (2), 159–173. doi: 10.1007/s11769-015-0741-6

frontiers | Frontiers in Marine Science

TYPE Original Research
PUBLISHED 15 December 2022
DOI 10.3389/fmars.2022.1065358

OPEN ACCESS

EDITED BY
Hongsheng Yang,
Institute of Oceanology (CAS), China

REVIEWED BY
Chenguang Feng,
Northwestern Polytechnical University, China
Mohamed Alsafy,
Alexandria University, Egypt
Usha Kumari,
Banaras Hindu University, India

*CORRESPONDENCE
Jie Zhang
zhangjie@ioz.ac.cn
Yuan Mu
muy@eastern-himalaya.cn

SPECIALTY SECTION
This article was submitted to Global Change and the Future Ocean, a section of the journal Frontiers in Marine Science

RECEIVED 09 October 2022
ACCEPTED 23 November 2022
PUBLISHED 15 December 2022

CITATION
Hu W, Mu Y, Wei C, Gai Y and Zhang J (2022) From morphological to ecological adaptation of the cornea in Oxudercinae fishes.
Front. Mar. Sci. 9:1065358.
doi: 10.3389/fmars.2022.1065358

From morphological to ecological adaptation of the cornea in Oxudercinae fishes

Wenxian Hu[1,2], Yuan Mu[3]*, Chuanyu Wei[1], Yulin Gai[4] and Jie Zhang[2]*

[1]Erhai Watershed Ecological Environment Quality Testing Engineering Research Center of Yunnan Provincial Universities, Erhai Research Institute, West Yunnan University of Applied Sciences, Dali, China, [2]Key Laboratory of Animal Ecology and Conservation Biology, Institute of Zoology, Chinese Academy of Sciences, Beijing, China, [3]Institute of Eastern-Himalaya Biodiversity Research, Dali University, Dali, China, [4]Institute of Ecology, China West Normal University, Nanchong, China

The outer cornea plays an important role in animal adaptation and survival in different environments. however, research on the morphological and ecological adaptation of corneal structure in amphibious fishes is limited. In this study, scanning electron microscopy (SEM) was used to evaluate the microstructure and adaptation of corneal epithelial cells in Oxudercinae. The results showed that the corneas of Oxudercinae species possess microridges, microvilli, and microplicae, as well as different numbers of epithelial cells. The morphological structure of corneal epithelial cells, observed by collecting samples and comparing the results with previous results, also showed different adaptive characteristics for moving between water and land. Further analyses revealed significant differences in epithelial cell density ($F_{4, 22} = 5.436$, $P=0.003$) and microridge width ($F_{4, 22} = 8.392$, $P<0.001$) among species with different levels of aquatic dependence. In addition, significant negative correlations of epithelial cell density with microridge width and separation width were confirmed ($P<0.05$). Interestingly, significant negative correlations of habitat type with cell density and microridges were uncovered, as well as a positive correlation between habitat type and separation width ($P<0.05$). The results indicated that the corneal structure of Oxudercinae species has characteristics of adaptation to an amphibious lifestyle.

KEYWORDS

oxudercinae, corneal epithelial cells, amphibian fish adaptation, epithelial cell density, microstructure

Introduction

Understanding the mechanisms by which organisms adapt to changing environments has long been one of the central goals of ecology (Reuter and Peichl, 2008; Savolainen et al., 2013). Due to differences in habitat heterogeneity, fish species diversity is greatly influenced by the evolutionary transition between marine and

terrestrial environments (Vega and Wiens, 2012). As changes in the light condition (floodplains transition to deep water, or diurnal to nocturnal), the environment becomes darker, and fishes show unique sensory, motor, and respiratory systems that evolved *via* adaptation to different bathymetric habitats, especially in regard to vision (Hu et al., 2022; Derbalah et al., 2022). Independent adaptation to different aquatic niches across fishes has been accompanied by widespread changes in the visual structures, systems, and mechanisms for coping with different light conditions (Graham, 1997; Simmich et al., 2012). The morphology of vertebrate corneal epithelial cells is affected by various environmental conditions, showing variation in cell types, densities, and microstructures, which play an important role in visual imaging (Collin and Collin, 2000a; Collin and Collin, 2000b; Subramanian et al., 2008; Simmich et al., 2012).

Vertebrate corneal epithelial cells are mainly irregularly pentagonal or hexagonal and contain many microstructures, such as microvilli, microplicae, microridges and microholes (Collin and Collin, 2006; Hu et al., 2016). It has been shown that aquatic and terrestrial vertebrates have different corneal epithelia; moreover, in some amphibious species, the densities of the superior and inferior surfaces of the cornea are significantly different (Mass and Supin, 2007; Subramanian et al., 2008). Previous studies have shown that the epithelium of marine organisms tends to have a higher cell density; conversely, nonaquatic vertebrates have a relatively low cell density on their corneas, through which the fishes can remove water efficiently (Collin and Collin, 2000b). Of the microstructures, microridges are the least efficient at increasing the surface area of cell membranes, and they are often found in highly permeable subsurface environments (mainly in the marine environment) (Simmich et al., 2012). By increasing the surface area of the cells, microvilli make it easier for oxygen and other nutrients to enter the cells, as well as assist in water transport and nutrient metabolism; these microstructures are essential for terrestrial vertebrates, as they maintain the intrinsic shape of the tear film and enable clear vision in the air (Beuerman and Pedroza, 1996). Microplicae are considered an intermediate form between microvilli and microridges and serve to support cellular morphology with increased osmotic exchange in the superficial layer of the cornea (Murdy, 1989; Jaafar and Larson, 2008). Both microstructures require continuous protection by mucus secretions after the evaporation of water. Microholes allow mucus to be secreted onto the corneal surface (Collin and Collin, 2006). It has been confirmed that structural changes are related to selection pressures in different habitats, such as desiccation and abrasion in terrestrial environments and infection in aquatic environments (Subramanian et al., 2008). In Collin et al.'s study, these four microstructures were found to be adapted to the specific habitat of each taxon (Collin and Collin, 2000b). Further studies revealed microstructural changes in the corneas of four-eyed fish (*Anableps anableps*), and the adaptation patterns of vision-related genes were related to their specific habitat (Avery and Bowmaker, 1982; Owens et al., 2009; Simmich et al., 2012). For a better understanding of how vision evolved to adapt to amphibious environments, it is important to study the physiological characteristics of species with both aquatic and terrestrial vision.

The subfamily Oxudercinae, consisting of 10 genera and 41 species, is a special group showing sharply divergent habitats from aquatic to terrestrial environments. These fishes are mostly found in intertidal mangrove or muddy mudflat areas in tropical, subtropical, and temperate seas (Ishimatsu and Gonzales, 2011). Mudskippers are representative taxa and are the largest group of amphibious teleost fishes, with unique adaptations enabling them to live on mudflats (Nursall, 1981; Burggren, 1997; Sayer, 2005). As a result of adaptation to specific amphibious habitats, their corneal development has special genetic and structural characteristics (Hu et al., 2016), and the cornea-related COL8A2 gene has undergone adaptive evolution (Hu et al., 2022). In addition, different species in this taxon show different degrees of adaptation to amphibious life due to habitat differentiation (Takita et al., 1999; You et al., 2014). Intertidal mudflats are one of the most drastically changing environments in terms of salinity, temperature, and oxygen level, leading to several adaptations in mudskippers. However, there is still a lack of understanding of the corneal adaptation of Oxudercinae to different habitats. To elucidate the adaptation of corneal characteristics of amphibious fishes, we characterized the corneal morphology and histology of five species of Oxudercinae in amphibious habitats. Through correlation analysis, we further investigated the relationships between the histological characteristics of fish eyes and their habitats to provide a reference for further studying the visual adaptation mechanisms allowing movement between aquatic and terrestrial environments.

Materials and methods

Acquisition and treatment of specimens

Specimens sampled from Riau Sumatra, Indonesia and Xiapu, China, were divided into five groups: *Pseudapocryptes elongatus* (5 individuals), *Oxuderces dentatus* (5 individuals), *Scartelaos histophorus* (6 individuals), *Boleophthalmus pectinriostris* (7 individuals), and *Periophthalmus magnuspinnatus* (6 individuals). The specimens were deposited in National Animal Collection Resource Center, Institute of Zoology, Chinese Academy of Sciences (CAS). The examined specimens are listed in Table 1, including individual number and aspects of size, such as total length, head length and eye diameter, measured using a 032102 digital Vernier caliper (exploit 200 mm, precision 0.1 mm).

The specimens were mature, although their exact ages were unknown. All the individuals were in good health prior to euthanasia, showing no evidence of ocular disease or abnormality. Specimens were euthanized with tricaine mesylate (MS-222) in accordance with ethical guidelines under

TABLE 1 Basic information of the individual number and size of specimens.

Species	Collection Location	Collection Time	Number & Preservation	Total Length (mm)	Head Length (mm)	Head Height (mm)	Head Width (mm)	Eye Diameter (mm)
Ps. elongatus	Riau Sumatra, Indonesia	2012.9.16	5	60.2-185.3	12.2-27.1	5.2-10.5	5.2-11.1	2.9-4.5
O. dentatus	Fujian Xiapu, China	2014.12.2	5	95.2-110.3	20.2-22.1	6.9-8.8	8.7-12.0	1.7-2.5
S. histophorus	Fujian Xiapu, China	2014.12.2	6	105.2-140.4	18.1-24.3	9.2-12.1	8.2-14.1	2.0-2.8
B. pectinriostris	Fujian Xiapu, China	2014.12.2	7	151.3-165.1	31.4-33.5	15.2-17.1	14.5-17.1	5.7-7.2
P. magnuspinnatus	Hebei Nanpu, China	2014.12.2	6	73.2-120.1	13.2-25.2	9.3-17.1	10.0-17.1	2.6-3.7

Experimental Animal Ethical Approval Number AEI-04-03-2014 ratified by the Institute of Zoology, Chinese Academy of Sciences. The dose of immersion was 400 ppm for 10 minutes.

After observing the location and shape of the eyes through a ZEISS STEISV II microscope, the right eye of the specimen was removed intact, and the cornea of each individual was stripped, fixed in Karnovsky's fixative (2.5% glutaraldehyde, 2% paraformaldehyde, 0.1 M sodium cacodylate buffer, 2% sucrose and 0.1% calcium chloride, pH 7.2) and then rinsed in 0.1 M sodium cacodylate buffer. The corneas were postfixed in 1% osmium tetroxide and rinsed in 0.1 M cacodylate buffer, followed by a water rinse and alcohol dehydration in a graded series. Cornea samples were desiccated with a critical point desiccator (LEICAEMCPP 300). When completely dry, the samples were mounted on 10-mm aluminum stubs. The mounted samples were coated with 12-15 nm of gold-palladium in a sputter coater (HITA-CHI E-1010) and examined under a scanning electron microscope (SEM, HITACHI S-3000N). Higher-magnification images were recorded digitally all around the cornea. With the fish eyes in a natural open state, the corneas were observed and compared in the middle, upper and lower areas. To ensure the effectiveness of the photos, more than 5 photos were taken at multiple locations in each area to record information, as shown in Figure 1.

Because the corneas of the fish were enlarged many times under a scanning electron microscope (the magnification range of the images used in this paper was 2000-24000 times), the actual area of the picture can be calculated by the plotting scale and the side length of the original image as recorded by the scanning electron microscope. For cell counting, the method adopted in this study was similar to the cell counting plate method, in which each picture was treated as a counting cell in the middle of a cell plate. Because of the obvious cell boundaries in the picture, all the cells in the picture could be counted. For incomplete cells at the edge of the image, only the cells on the left and upper sides (including cells pressed against the line) were counted, and the cells pressed against the lines on the lower and right sides of the image were omitted to reduce the count error. ArcGIS 10 software was used to count the number of cells in each picture and measure the size of the picture. According to the picture scale, the density of corneal epithelial cells in each picture was calculated, and then the corneal density in each area of each specimen was obtained by averaging the data of multiple pictures.

The cell types and microstructures in the images were determined by observing the electron microscope images. ArcGIS 10 software was also used to measure the width and spacing of the microcrest. According to the picture scale, the measured distance was converted, and then the microcrest width and microcrest spacing of each area of each specimen were obtained by averaging the data of multiple points and multiple pictures.

Data analysis

We compared the two positions (upper, lower) of the naturally exposed cornea (Figure 1). In a specified area of each region, the cell type and microstructures were described. The number of cells was determined and converted into density at cell number per mm^2, and microridge width and separation were measured using ArcGIS 10. Differences in cell density, microridge width and microridge separation among species were analyzed by one-way analysis of variance (ANOVA). Differences between upper and lower regions within the same species were tested by paired-samples t test using IBM SPSS (Kirkpatrick and Feeney, 2013). All the results are shown as the mean ± standard deviation (SD) (Table S1). To better understand the relationship between habitat type and phylogeny and further explore the correlations between locomotory mode and corneal traits, we obtained the phylogenetic tree and locomotory features of Oxudercinae according to Steppan et al. (2022) (Figure 2). The habitat assignments for the degree of water dependence of different Oxudercinae species were as follows: 1 = mud swimmers

10.3389/fmars.2022.1065358

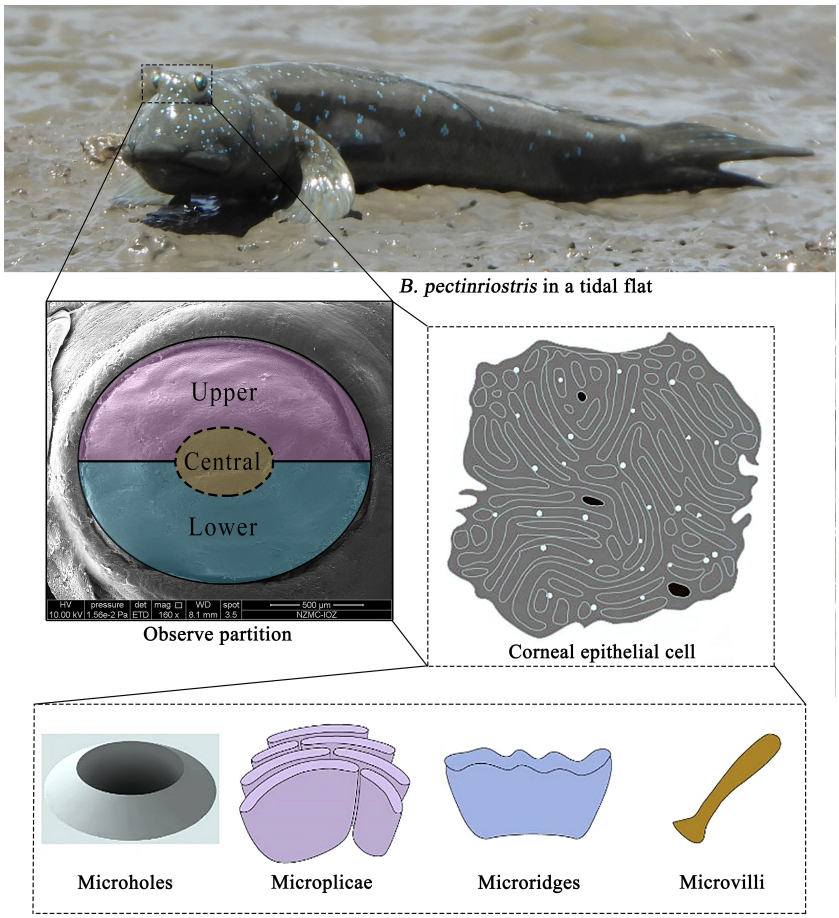

FIGURE 1
Observation sites on the cornea and microstructure model.

(generally eel-like, no substantial use of pectoral fins), 2 = pectoral-aided mud swimmers (generally eel-like with either reported sculling or semilobed fins but the inability to fully lift the body), and 3 = terrestrially crutchers (short, stout bodies with fully developed lobe fins) (Table S2). Then, the correlation analysis was carried out in IBM SPSS (Kirkpatrick and Feeney, 2013). To exclude false positives as much as possible, Bonferroni correction was implemented.

Results

Type and microstructure of epithelial cells

The corneal cell types and cellular microstructures of five fishes were observed by using scanning electron microscopy; detailed descriptions are provided below.

Ps. elongatus corneal epithelial cells are shown in Figures 3A, B, where cell borders were evident, microridges were clear and continuous, microridge widths and gaps could be measured, and microholes, microplicae, and microvilli were observed (Figures 3C, D). However, in *Ps. elongatus*, morphologically specific micropores appeared in the form of a complex subcircular arrangement surrounded by microvilli of varying lengths, composed of 5-8 individual micropores. The cell type was microridge cells.

As shown in Figures 4A, B, the corneal epithelial cells of *O. dentatus* were clearly demarcated from each other, with loose gaps and measurable gap widths, only a very small number of continuous microridges, and distinct cell borders. There were microholes, microplicae and microvilli (Figure 4B). The cell type was microplicae cells. Taste buds or other kinds of sensory structures may be shown in Figures 4C, D, which were observed on the surface of the cornea for the first and time in our experiment.

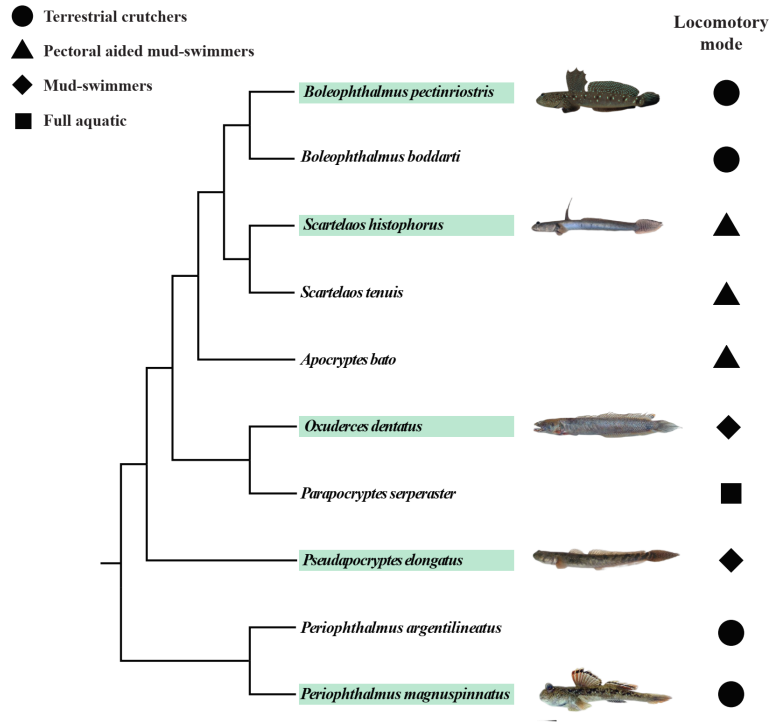

FIGURE 2
The phylogeny and locomotory modes of subfamily Oxudercinae obtained and adapted from Steppan et al. (2022). The images of fish are from "The Mudskipper: http://www.themudskipper.org/". The species in the green boxes are the ones that we examined in this study.

In *S. histophorus*, corneal epithelial cells were observed as the ridge type. The border of corneal epithelial cells was clear (Figures 5A, B). Microplicae, microvilli and microridges were observed under high magnification, but without microholes (Figures 5C, D). The cell type was microridge cells.

In *B. pectinirostris*, the border of corneal epithelial cells was clear (Figure 6A). Cells were differentiated into diverse structures inside as the ridge type, reticular type, and ridge-reticular type (Figures 6A, B, D). Microridges, microplicae, microvilli and microholes were observed under high magnification (Figures 6B, C).

In *P. magnuspinnatus*, ridge-type and reticular-type cells were observed (Figures 7A, B). The corneal epithelial cells also contained four types of microstructures: microridges, microplicae, microvilli and microholes (Figures 7B–D). Compared with those of *B. pectinirostris*, the microridges of corneal epithelial cells of *P. magnuspinnatus* were rough with more microplicae and microvilli. The corneal epithelial cell surface is characterized by fragmentation and a compact structure. On the inferior side of the cornea of *P. magnuspinnatus*, some areas covered with microholes were observed (Figure 7C).

Based on the SEM results, there appeared to be differences among taxa in terms of microholes. No microholes were observed in *S. histophorus*, and similar small numbers of microholes were found in *B. pectinriostris* and *O. dentatus*. An increased number of microholes was observed in *Ps. elongatus*. *P. magnuspinnatus* was found to have the highest numbers of microholes among the five fishes. Additionally, there were also differences in the types of cells (Table 2).

Comparison of the microstructure of corneal epithelial cells in various taxa

By using the SEM results above combined with those of Collin et al. (Collin and Collin, 2006), a comparison was performed against the corneal density, microstructure, and cell type of six species other than the five fish species examined in this study, including *Acanthopagrus butcheri*, *Neoceratodus forsteri*, *Ambystoma mexicanum*, *Xenopus laevis*, *Crocodilus porosus*, and *Ctenophorus ornatus*. In terms of cell types, microridge cells were observed in *A. butcheri*, *Ps. elongatus*, *S. histophorus*, *B. pectinriostris* and *C. ornatus*. Microplicae cells were found in *O. dentatus*, *B. pectinriostris*, *P. magnuspinnatus*, *X. laevis* and *C. ornatus*. Reticular cells were observed in *B. pectinriostris*, *P. magnuspinnatus* and *A. mexicanum*. In adult *B. pectinriostris* and *A. mexicanum*, a mixture of microridge cells

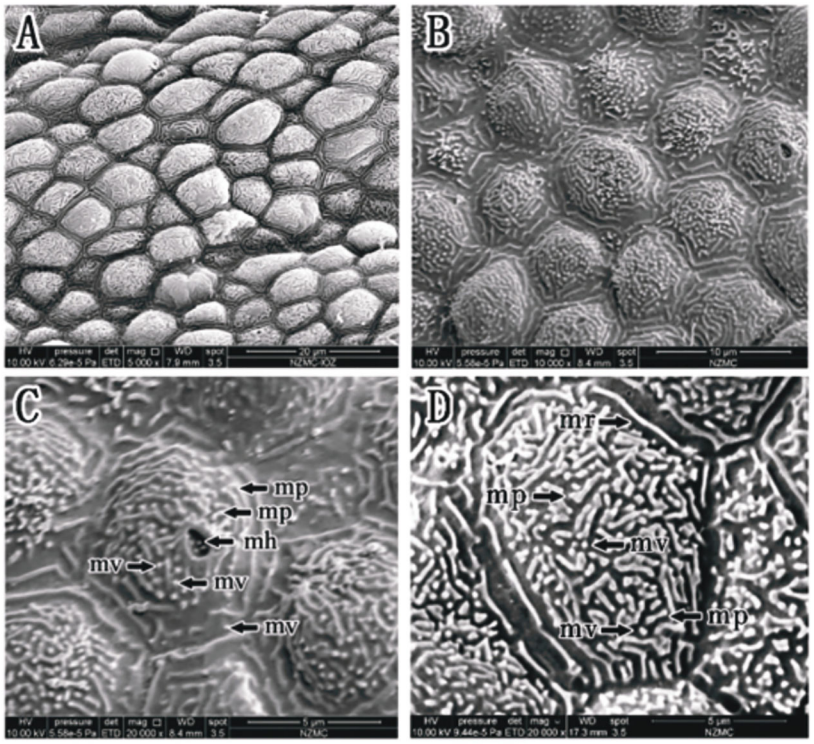

FIGURE 3
(A–D) Corneal epithelial cells of *Ps. elongatus* under an SEM. Microridge cell type **(A, B)**. Microplicae, microridge, microvilli and microholes **(B–D)**. (mp, microplicae; mv, microvilli; mh, microholes; mr, microridge).

and reticular cells was observed. Microstructures such as microridges, microplicae, microholes and microvilli appeared to be present and absent in a variety of taxa (Table 2).

Epithelial cell density

The epithelial cell densities of the 5 Oxudercinae species varied between 29632 ± 7766 cells per mm^2 in *B. pectinriostris* and 52861 ± 10664 cells per mm^2 in *O. dentatus* (Figure 7; Table S1), and the difference was significant ($F_{4, 22} = 5.436$, P=0.003). The trends in cell density in the upper and lower regions within species, as well as the overall trends, were similar and significantly different (up: $F_{4, 22} = 4.690$, P=0.007; down: $F_{4, 22} = 4.157$, P=0.012). In addition, the differences between the upper region and the lower region of the corneas in the other four species were not significant (Figure 8), except in *S. histophorus* (t=3.373, P=0.028).

Microridge width (nm) and separation width (nm)

Our results showed that the microridge width of corneal epithelial cells differed significantly among the 5 species of Oxudercinae. Microridge widths were significantly higher in *Ps. elongatus* and *B. pectinriostris* than in *O. dentatus, S. histophorus* and *P. magnuspinnatus* ($F_{4, 22} = 8.392$, P<0.001; Figure 8). The trends of microridge widths in the upper region and the lower region among species were similar to the trends of total microridge widths. Microridge width was significantly different among the 5 species in the upper region ($F_{4, 22} = 7.419$, P=0.001) but not in the lower region ($F_{4, 22} = 1.671$, P=0.193). Additionally, there were no significant differences between the upper and lower regions within species (Figure 9).

The separation width trend was similar to the microridge width trend but slightly different from the microridge width trend, as there was no significant difference between the various groups ($F_{4, 22} = 2.350$, P=0.086; Figure 9). A similar pattern of microridge widths was observed in both upper regions and lower regions, and this trait did not significantly differ from total microridge width across species (upper: $F_{4, 22} = 2.397$, P=0.081; lower: $F_{4, 22} = 1.392$, P=0.269). The separation widths of the upper region and lower region did not show significant differences within species (Figure 10).

Interestingly, further analyses revealed significant negative correlations of cell density with microridge width and separation width (Figures 11A, B). To exclude false positive statistics as

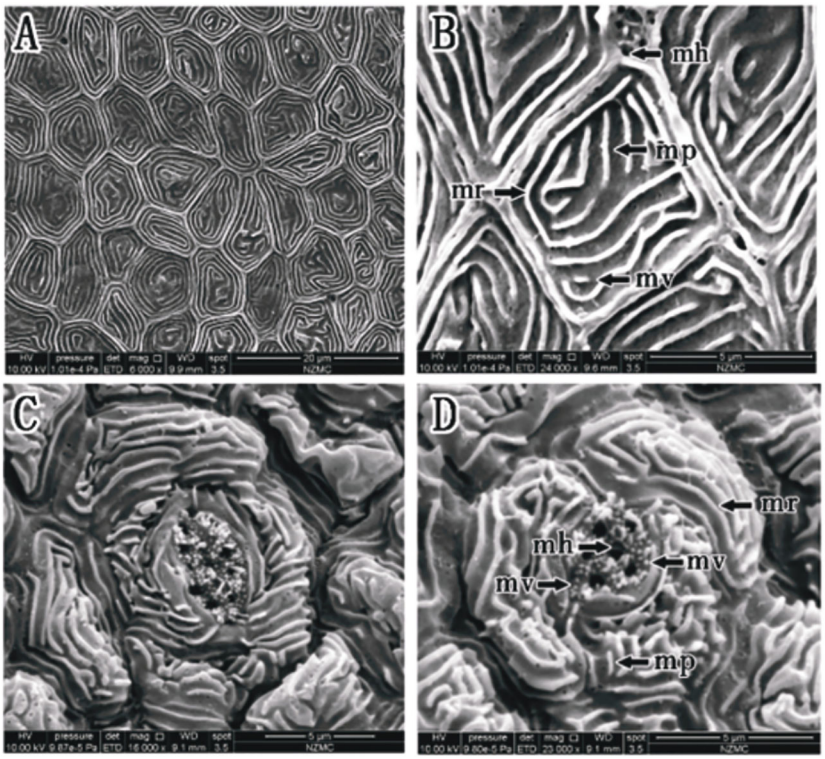

FIGURE 4
(A–D) Corneal epithelial cells of *O. dentatus* under an SEM. Microplicae cell type **(A, B)**. Microplicae, microridge, microvilli and microholes **(B)**. (mp, microplicae; mv, microvilli; mh, microholes; mr, microridge). Taste buds or sensory structures **(C, D)**.

much as possible, we further performed Bonferroni correction (α = 0.01). However, no significant differences were found (Figure 11A: P=0.024, Figure 11B: P=0.012).

Correlation analysis between locomotory mode state and cell density, microridge width, and separation width

The results of correlation analyses showed significant negative correlations between locomotory mode and cell density and between locomotory mode and microridge width (Figures 12A, B); however, there was a significant positive correlation between locomotory mode and separation width (Figure 12C). After Bonferroni correction (α = 0.01), only the correlation between locomotory mode and microridge width was significant (Figure 12B: P=0.005). The other two correlations were not significant (Figure 12A: P=0.027, Figure 12C: P=0.012).

Through a literature review and field observations, we generated detailed descriptions of the preferences and locomotory mode for each species in our study.

O. dentatus: A small warm-water nearshore fish living in saltwater and freshwater zones of estuaries and low-tide areas of nearshore tidal flats; individuals often crawl or jump on mud flats with developed pectoral fin muscle stalks. They can adapt to a wide range of temperatures and salinities and settle in caves. They are sensitive in vision and hearing and usually come out of the cave during the day when the tide is low. When they are slightly frightened, they dive back into the water or drill into the cave (Wu and Zhong, 2008). Adults are more common in the lower part of the tidal flat, while smaller individuals usually appear at the depth of the tidal flat (Murdy, 1989).

Ps. elongatus: Adult individuals are more common in the lower mudflats and creeks; the subadults are mostly found in mangroves, aquatic areas and recluse in neap tide pools of subtidal zones (Bucholtz and Meilvang, 2005). During the dry season, when the tide pools are depleted, this species can aestivate in vertical burrows approximately 60 cm deep (Hora, 1936; Swennen et al., 1995). According to Murdy (1989), *P. elongatus* can breathe air through the gills, oropharyngeal epithelium, operculum epithelium, and skin and is capable of short-term survival out of water. We observed the fish not only breathing air in shallow water but also making brief crawls on the mudflat surface. This fish is highly halogenic (Bucholtz et al., 2009). It is a benthic omnivore, feeding mainly on phytoplankton and small invertebrates. It jumps out of shallow water (the head part of the body jumps out of the water) and

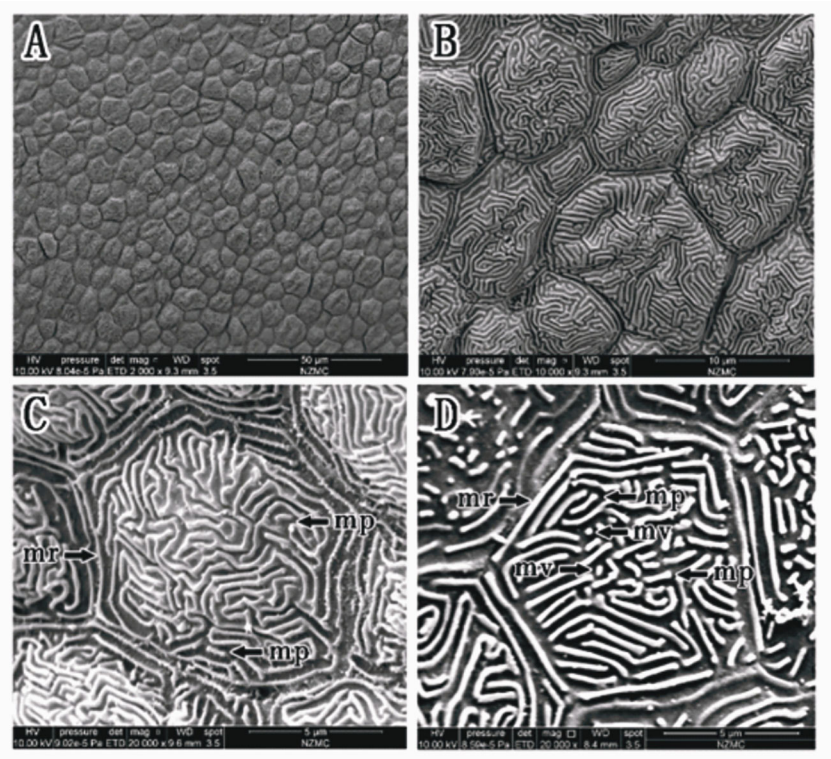

FIGURE 5
(A–D) Corneal epithelial cells of *S. histophorus* under an SEM. Microridge cell type **(B, C)**. Microplicae, microridges and microvilli **(C, D)**. (mp, microplicae; mv, microvilli; mh, microholes; mr, microridge).

moves its head from side to side to scrape and filter mud, similarly to *Boleophthalmus* (Swennen et al., 1995; Bucholtz and Meilvang, 2005; Bucholtz et al., 2009).

S. histophorus: A small warm-water fish living in saltwater and freshwater zones of estuaries. During low tide, larger individuals are more common in the lower areas of tidal flats or below the mean sea level, while smaller individuals are usually found in upper areas, such as the respiratory root zone of mangrove forests (Polgar and Bartolino, 2010) and riverbanks (Milward, 1974). They can adapt to various environmental conditions during relatively low tides, such as mudflats, tidal pools with varying degrees of dryness, or areas where plant debris and respiratory roots are mixed (Milward, 1974; Ansell et al., 1993). They leave burrows to breed at low tide. The males use their tails to stand to attract females to their burrows to lay eggs (Milward, 1974; Townsend and Tibbetts, 2005).

P. magnuspinnatus: This species is found in intertidal mudflats with taller vegetation, in mangrove respiratory root zones, and on coastal tidal flats near estuaries. During winter in temperate regions, it lives in caves (Murdy, 1989). In Korea, the active season is from late April to early September. The active season is slightly shorter than that of *P. modestus* living in the same area (Baeck et al., 2008). In contrast, *P. magnuspinnatus* makes long-term use of its burrowing sites throughout its active season (Baeck et al., 2008).

B. pectinriostris: This species lives in the open area of coastal mudflats. The largest individuals are found only in the lower unvegetated mudflats, while smaller individuals show a more irregular distribution and enter the respiratory root zone of mangroves along the entrance of temporary bays in the open areas of mudflats (Polgar and Bartolino, 2010). In winter, groups in southern Japan hibernate at the bottom of caves, and they can adapt to various environmental conditions during relatively low tide, handle broad temperature and salt conditions and show short-term amphibious habits with strong vitality (Takegaki et al., 2006). This fish is very sensitive to sound and movement. Individuals drill holes or escape into mangrove trees as soon as they encounter signs of enemies, which plays an important role in maintaining the survival and reproduction of the population. The species lives in damp holes. The skin and tail have an auxiliary respiratory function, and individuals can leave the water to forage for a period of time. In the nonreproductive season, they usually live alone in caves and go into seclusion or under water at high tide. During the

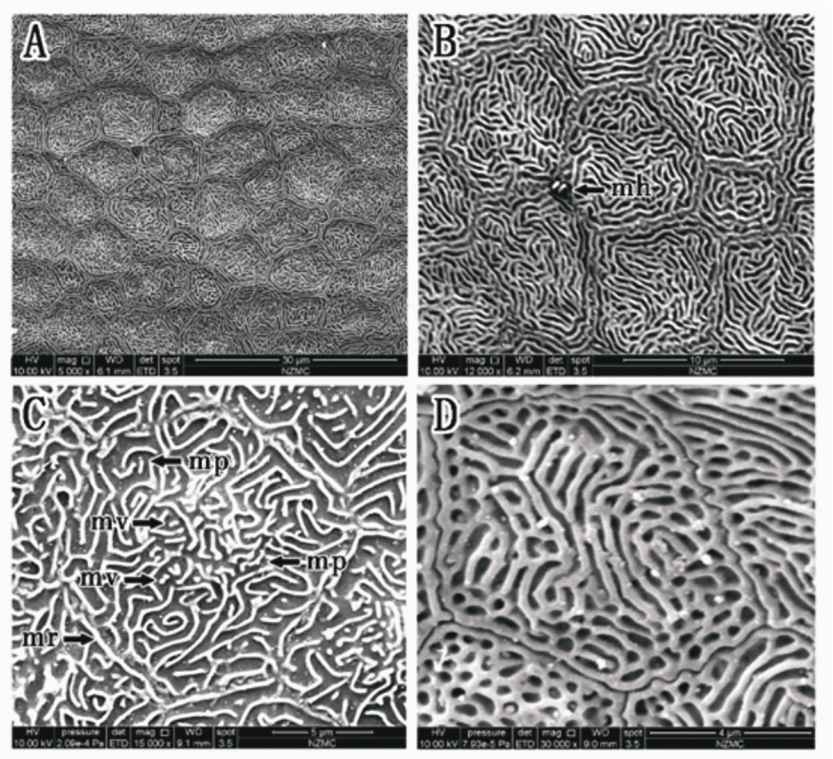

FIGURE 6
(A–D) Corneal epithelial cells of **(B)** *pectinriostris* under an SEM. Microridge cell type **(A)**; Microplicae cell type **(C)**; Reticular cell **(D)**; Mixed cell (Microridge and Reticular) **(D)**. Microplicae, microridges, microvilli and microholes **(B, C)**. (mp, microplicae; mv, microvilli; mh, microholes; mr, microridge).

reproductive period, male and female adult fish live together, spawn and fertilize in the channels. Viscous eggs adhere to the cave wall or substrate by attaching silk, and the male fish gear protects the eggs. Cave dwelling and reproduction can reduce the threat of natural disasters and enemy organisms and improve their survival ability.

Discussion

Diversity of habitat taxa appeared to affect cell density

In general, aquatic vertebrates have a denser corneal epithelium than terrestrial vertebrates (Collin and Collin, 2000a; Mass and Supin, 2007), which is thought to be an adaptation to differences between air and aquatic osmotic stress (Collin and Collin, 2000a; Collin and Collin, 2006). Our results partly showed a similar trend (Figure 12A). Additionally, cell density decreases as the osmotic stress placed on the cornea decreases among aquatic vertebrates (Kröger, 1992; Collin and Collin, 2006). Marine vertebrates maintain proper osmotic levels because the higher epithelial cell density aids in salt transport and water uptake. In contrast, a relatively low epithelial cell density contributes to corneal water removal in nonaquatic vertebrates (Collin and Collin, 2006). It was suggested that different aquatic and terrestrial habitats, as well as different osmotic pressures in aquatic environments, could influence corneal morphological adaptation.

Our results showed that corneal epithelial dependence on aquatic environments decrease, and corneal epithelial density declines (Figures 7A, B, 11A), which are consistent with previous findings. From marine to estuarine or freshwater to terrestrial environments, there is a progressive decrease in epithelial cell density in vertebrates (Collin and Collin, 2000a; Collin and Collin, 2000b). Three species (*P. magnuspinnatus*, *B. pectinriostris*, and *O. dentatus*) showed a higher cell density on the lower region of the cornea than on the upper region of the cornea (Figure 8). Similar findings were obtained in a previous study of 'four-eyed fish' (*A. anableps*), which further confirmed that osmotic pressure influences the distribution of cell density in the cornea (Owens et al., 2009; Simmich et al., 2012). Additionally, the negative relationship between cell density and locomotory mode (or habitat) further confirmed the

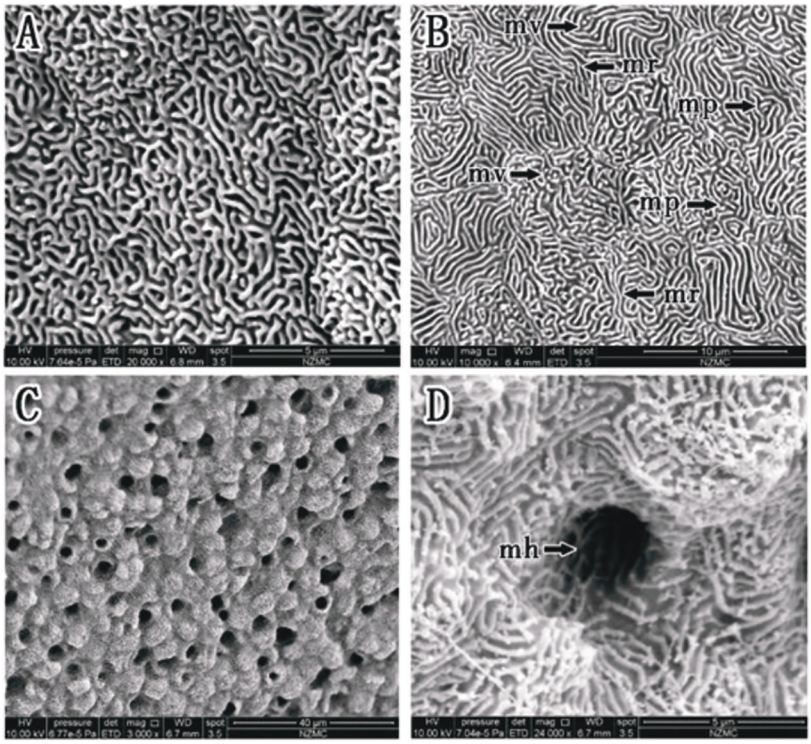

FIGURE 7
(A–D) Corneal epithelial cells of *P. magnuspinnatus* under SEM. Microridge cell type **(B)**; Microplicae cell type **(B)**; Microplicae, microridge, microvilli and microholes **(B–D)**. (mp, microplicae; mv, microvilli; mh, microholes; mr, microridge).

decreasing tendency. However, due to the differences in corneal epithelial cell density between the upper region and lower region, subadult *S. histophorus* live in terrestrial habitats, while the adults prefer lower, wet areas. The cell density of *S. histophorus* was high in the upper region but low in the lower region (Figure 7B), which was in contrast to the trend of changes in *A. anableps* as well as the other three species in Oxudercinae (Collin and Collin, 2006; Simmich et al., 2012). Generally, it can be concluded that the density of epithelial cells in Oxudercinae is affected by dependence on the aquatic environment (Davies et al., 2012; Hauser et al., 2017; Hauser and Chang, 2017). Further investigation is required to determine the distribution and structural characteristics of corneal epithelial cells.

The adaptation of cellular microprojections and their microstructures

Mudskippers live in a wide range of habitats, from shallow water to intertidal flats and supralittoral zones, which is the most drastically changing intertidal environment in terms of moisture content, salinity, temperature, and oxygen level. Coastal and intertidal habitats are at the forefront of anthropogenic influence and environmental change, especially global warming (Wolfe et al., 2020). The change of the intertidal ambient (such as temperature, humidity, oxygen content, etc.) will lead to the corresponding change of the biodiversity pattern and the adaptation mechanism of the species living in the area (Bates et al., 2018; Vafeiadou et al., 2018). To adapt to various aquatic and terrestrial environments, the cornea, an important visual structure, has evolved various adaptive features, including changes in cell density, microridges, microplicae, microholes, and microvilli. Previous studies have shown that *Periophthalmus*, *Boleophthalmus*, and *Scartelaos* have evolutionarily adaptive traits related to vision (Ansell et al., 1993; You et al., 2014; DA, 2017; You et al., 2018; Hu et al., 2022).

The corneal surface in the vertebrate eye features microprojections formed by folds of the epithelial cell membranes. These microprojections increase the surface area available for the transport of nutritional and waste products across the cell surface (Collin and Collin, 2000a). Superficial epithelial cells are covered by numerous microprojections (microridges, microvilli, microplicae, and microholes) (Collin and Collin, 2000b; Collin et al., 2021). In different habitats, the

10.3389/fmars.2022.1065358

TABLE 2 The comparison of corneal epithelial cell microstructures and cell types among different species.

SpeciesMicrostructural typesand cell types	*Acanthopagrus butcheri*	*Neoceratodus forsteri*	*Ps. elongatus*	*O. dentatus*	*S. histophorus*	*B. pectinirostris*	*P. magnuspinnatus*	*Ambystoma mexicanum*	*Xenopus laevis*	*Crocodilus porosus*	*Ctenophorus ornatus*
Microridge	*	–	*	*	*	*	*	–	–	–	*
Microplicae	–	–	*	*	*	*	*	*	*	–	*
Microhole	–	*	*	*	–	*	*	*	*	–	*
Microvilli	–	*	*	*	*	*	*	–	–	*	*
Microridge cell	*	–	*	–	*	*	*	–	–	–	*
Microplicae cell	–	–	–	*	–	*	*	–	*	–	*
Reticular cell	–	–	–	–	–	*	–	*	–	–	–
Mixed cell (Microridge and Reticular)	–	–	–	–	–	*	–	*	–	–	–

(*): present, (–): absent. Information on fishes other than the 5 species of Oxudercinae was obtained from the research of Collin and Collin, 2006.

corneal microstructure and cellular morphology of these vertebrates have evolved corresponding adaptations. The clear interspecific differences in corneal surface structure suggested adaptive plasticity in the composition and stabilization of the cornea in various aquatic environments.

Collin and Collin (2006) found that microridges narrowed as the dependence on the aquatic environment decreased (from water to land). Moreover, it has been shown that the fingerprint-like patterns of corneal microridges are a ubiquitous feature of marine teleosts, covering many types of sensory epithelia. In other words, terrestrial vertebrates, with a less stringent requirement for a physically stable tear film, feature microplicae and/or microvilli in place of microridges (Collin and Collin, 2000a; Collin and Collin, 2000b; Collin and Collin, 2006). In this study, microridge widths of fish in the Oxudercinae subfamily showed a trend similar to that reported by Collin and Collin. As shown in Table 2, the microridges disappeared in animals that were typically terrestrial or amphibious, while the structures could still be found in the typically aquatic *A. butcheri* and an amphibious group of Oxudercinae. On the other hand, between the microplicae, there were numerous holes or pits (microholes), which were found only in terricolous species, such as *C. ornatus* and amphibians, as well as amphibious mudskippers that are usually exposed to air. Generally, corneal microstructures might be influenced by the external environment. Further studies are needed to confirm whether corneal epithelial cell density also affects microstructures.

In terms of cell type, microridge cells were observed in fishes with aquatic characteristics, namely, *A. butcheri*, *Ps. elongatus*, *S. histophorus*, and *B. pectinriostris*; microridges are among the least efficient microstructures for increasing the surface area of the cell membrane (Hu et al., 2016). Reticular cells were another type of cell with a strong secretion function that appeared in *B. pectinriostris*, *P. magnuspinnatus*, and *A. mexicanum*. This suggested that corneal secretions were higher in these three species, facilitating the maintenance of moist eyes. Both microridge cells and reticular cells were found in adult *B. pectinriostris* and *A. mexicanum* at the same time, which suggested that these mixed cell types enhanced the adaptive capacity of eyes in terrestrial environments. Further research is required to determine whether they have any functions other than those associated with osmolality, mucus secretion, and substance exchange.

Conclusion

The amphibious traits of Oxudercinae species are necessary for living under relatively dry conditions on land. This phenomenon suggests that the vision of this group may have special mechanisms in amphibious environments. According to

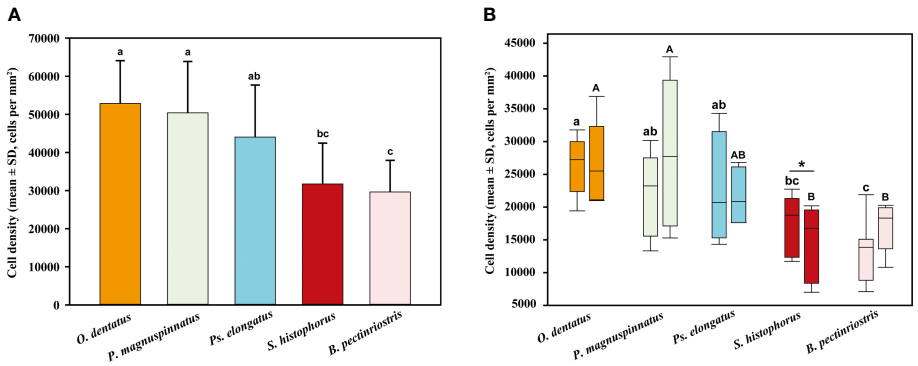

FIGURE 8
Comparison of epithelial cell density among different Oxudercinae species (the order of corneal epithelial cell densities for the five fish species is shown in **(A)**; the upper and lower cell densities are shown in **(B)**.

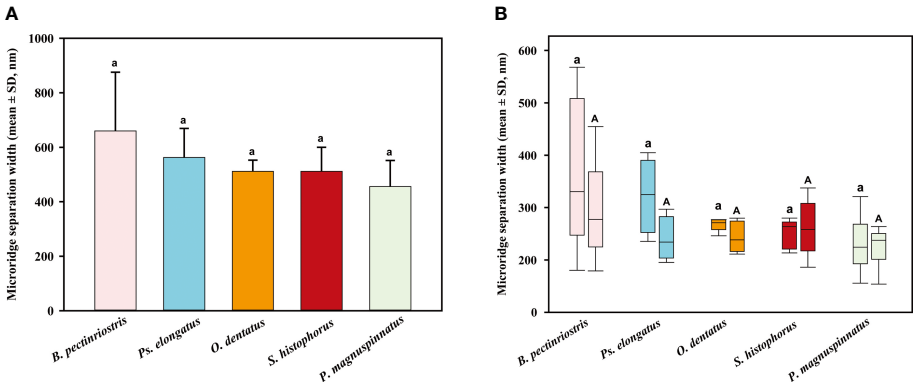

FIGURE 9
The comparison of microridge width among different Oxudercinae species (the order of corneal epithelial microridge widths for the five fish species is shown in **(A)**; the upper and lower microridge widths are shown in **(B)**.

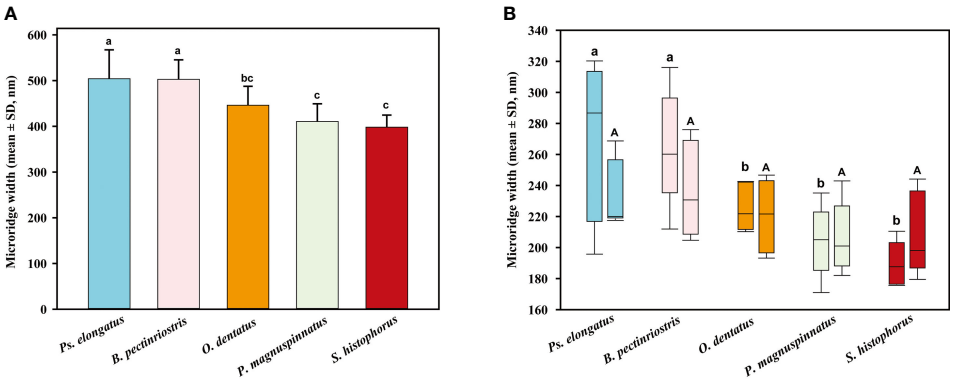

FIGURE 10
The comparison of microridge separation width among different Oxudercinae species (the order of corneal epithelial microridge separation widths for the five fish species is shown in **(A)**; the upper and lower microridge separation widths are shown in **(B)**.

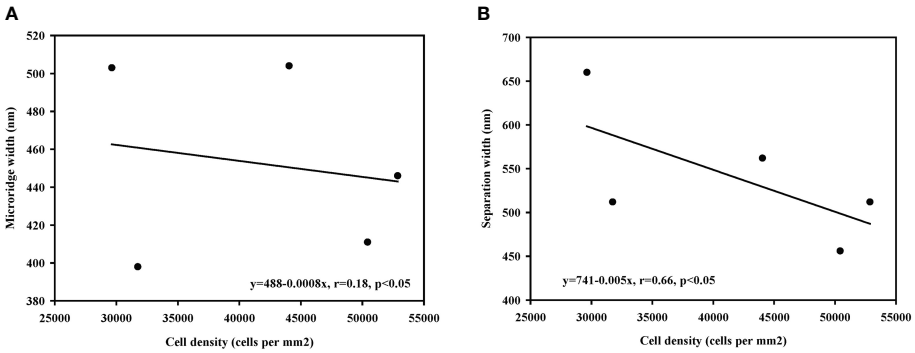

FIGURE 11
The correlation between cell density and width among different Oxudercinae species. (Cell density vs. microridge width in **(A)**; cell density vs. microridge separation width in **(B)**.

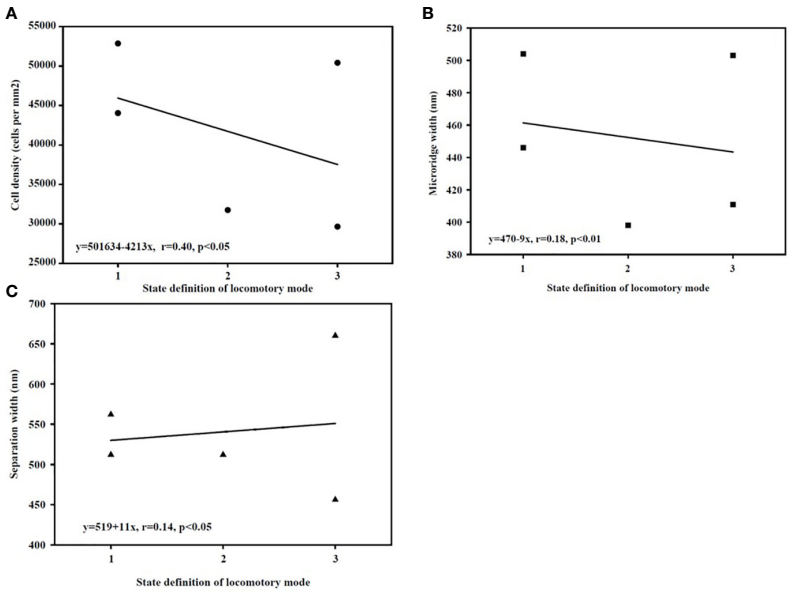

FIGURE 12
(A–C) The correlation between locomotory mode state and corneal epithelial data. [(Locomotory mode vs. cell density **(A)**; locomotory mode vs. microridge width **(B)**; locomotory mode vs. microridge separation width **(C)**].

our results, there were microstructures such as microridges, microvilli, and microplicae on the corneal epithelium of Oxudercinae species with different numbers of epithelial cells. In the amphibious habitats to which Oxudercinae species are adapted, the corneal structure has evolved. Adaptive changes have been observed in the corneal epithelium of mudskippers with amphibious characteristics as a result of differences in the level of dependence on the aquatic environment. With increasing dependence, the corneal epithelial cell density tended to decrease, and the microridge width narrowed. More studies will be required to investigate the relationships between the width of microridges and the separation, function and adaptability of corneal cells.

Data availability statement

The original contributions presented in the study are included in the article/Supplementary Material. Further inquiries can be directed to the corresponding authors.

Ethics statement

The animal study was reviewed and approved by Laboratory Animal Welfare Ethics Review Committee, Institute of Zoology, Chinese Academy of Sciences. The approval number: AEI-04-03-2014.

Author contributions

WH participated in the determination of research and writing ideas, designed and completed the experiment of fish physiology and scanning electron microscopy, completed the data collection and manuscript writing of this part, and completed the manuscript submission. YM participated in the determination of research and writing ideas and completed the data collection, manuscript writing, and paper improvement. JZ provided overall guidance to the research and writing ideas and participated in the writing of the whole manuscript. YG participated in the discussion and paper revision. CW participated in the writing and modification of part of the manuscript. All authors contributed to the article and approved the submitted version.

Funding

Grants supporting this research were received from the Erhai Watershed Ecological Environment Quality Testing Engineering Research Center of Yunnan Provincial Universities to WH and YM (No. DXDGCZX03), from the start-up projects on high-level talent introduction of Dali University to YM (No. KY1916101940), and from the Chinese Academy of Sciences (XDA19050202) to JZ.

Acknowledgments

We thank Shengguo Chen for helping collect specimens and for support in the field. Appreciate for JSPS Invitation Fellowship Programs for Research in Japan to JZ.

Conflict of interest

The authors declare that the research was conducted in the absence of any commercial or financial relationships that could be construed as a potential conflict of interest.

Publisher's note

All claims expressed in this article are solely those of the authors and do not necessarily represent those of their affiliated organizations, or those of the publisher, the editors and the reviewers. Any product that may be evaluated in this article, or claim that may be made by its manufacturer, is not guaranteed or endorsed by the publisher.

Supplementary material

The Supplementary Material for this article can be found online at: https://www.frontiersin.org/articles/10.3389/fmars.2022.1065358/full#supplementary-material

References

Ansell, A., Gibson, R., Barnes, M., and Clayton, D. (1993). Mudskippers. *Oceanogr. Mar. Biol. Ann. Rev.* 31, 507–577.

Avery, J. A., and Bowmaker, J. K. (1982). Visual pigments in the four-eyed fish, *Anableps*. *Nature.* 298, 62–63. doi: 10.1038/298062a0

Baeck, G. W., Takita, T., and Yang, H. Y. (2008). Lifestyle of Korean mudskipper *Periophthalmus magnuspinnatus* with reference to a congeneric species *Periophthalmus modestus*. *Ichthyol. Res.* 55, 43–52. doi: 10.1007/s10228-007-0009-y

Bates, A. E., Helmuth, B., Burrows, M. T., Duncan, M. I., Garrabou, J., Guy-Haim, T., et al. (2018). Biologists ignore ocean weather at their peril. *Nature* 560, 299–301. doi: 10.1038/d41586-018-05869-5

Beuerman, R. W., and Pedroza, L. (1996). Ultrastructure of the human cornea. *Microsc. Res. Tech.* 33, 320–335. doi: 10.1002/(sici)1097-0029(19960301)33:4<320::aid-jemt3>3.0.co;2-t

Bucholtz, R. H., and Meilvang, A. S. (2005). *Biology and utilization of the mudskipper pseudapocryptes elongatus in the Mekong river delta, with aspects on other mudskippers in the area* (Denmark: Department of Marine Ecology and Centre for Tropical Ecosystem Research, University of Aarhus).

Bucholtz, R. H., Meilvang, A. S., Cedhagen, T., Christensen, J. T., and Macintosh, D. J. (2009). Biological observations on the mudskipper *Pseudapocryptes elongatus* in the Mekong delta, Vietnam. *J. World Aquac. Soc* 40, 711–723. doi: 10.1111/j.1749-7345.2009.00291.x

Burggren, W. W. (1997). *Air-breathing fishes: Evolution, diversity, and adaptation* (San Diego, CA: Academic Press).

Collin, H. B., and Collin, S. P. (2000a). The corneal surface of aquatic vertebrates: microstructures with optical and nutritional function? *Philos. Trans. R. Soc Lond. B. Biol. Sci.* 355, 1171–1176. doi: 10.1098/rstb.2000.0661

Collin, S. P., and Collin, H. B. (2000b). A comparative SEM study of the vertebrate corneal epithelium. *Cornea.* 19, 218–230. doi: 10.1097/00003226-200003000-00017

Collin, S. P., and Collin, H. B. (2006). The corneal epithelial surface in the eyes of vertebrates: environmental and evolutionary influences on structure and function. *J. Morphol.* 267, 273–291. doi: 10.1002/jmor.10400

Collin, H. B., Ratcliffe, J., and Collin, S. P. (2021). The functional anatomy of the cornea and anterior chamber in lampreys: insights from the pouched lamprey, *Geotria australis* (Geotriidae, Agnatha). *Front. Neuroanat.* 15. doi: 10.3389/fnana.2021.786729

DA, C. (2017). "Feeding behavior: a review," in *Fishes out of water: Biology and ecology of mudskippers*. Eds. Z. Jaafar and E. O. E. Murdy (Boca Raton: CRC Press.).

Davies, W., Collin, S. P., and Hunt, D. M. (2012). Molecular ecology and adaptation of visual photopigments in craniates. *Mol. Ecol.* 21, 3121–3158. doi: 10.1111/j.1365-294X.2012.05617.x

Derbalah, A., El-Gendy, S. A., Alsafy, M. A., and Elghoul, M. (2022). Micro-morphology of the retina of the light-adapted African catfish (*Clarias gariepinus*). *Microsc. Res. Tech.*, 1–8. doi: 10.1002/jemt.24252

Graham, J. B. (1997). *Air breathing fishes: Evolution, diversity and adaptation* (San Diego, CA: Academic Press).

Hauser, F. E., and Chang, B. S. (2017).). insights into visual pigment adaptation and diversity from model ecological and evolutionary systems. *Curr. Opin. Genet. Dev.* 47, 110–120. doi: 10.1016/j.gde.2017.09.005

Hauser, F. E., Ilves, K. L., Schott, R. K., Castiglione, G. M., López-Fernández, H., and Chang, B. S. W. (2017). Accelerated evolution and functional divergence of the dim light visual pigment accompanies cichlid colonization of central America. *Mol. Biol. Evol.* 34, 2650–2664. doi: 10.1093/molbev/msx192

Hora, S. L. (1936). Ecology and bionomics of the gobioid fishes of the gangetic delta. *Int. Congr. Zool.* 12, 841–863.

Hu, W. X., Mu, Y., Lin, F., Li, X., and Zhang, J. (2022). New insight into visual adaptation in the mudskipper cornea: from morphology to the cornea-related *COL8A2* gene. *Front. Ecol. Evol.* 10. doi: 10.3389/fevo.2022.871370

Hu, W. X., Zhang, J., and Kang, B. (2016). Structure and function of corneal surface of mudskipper fishes. *Fish Physiol. Biochem.* 42, 1481–1489. doi: 10.1007/s10695-016-0234-2

Ishimatsu, A., and Gonzales, T. T. (2011). "Mudskippers: front runners in the modern invasion of land," in *The biology of gobies*. Eds. R. A. Patzner, J.L.V. Tassell, M. Kovačić and B. G. Kapoor (Enfield, NH: Science Publishers Inc), 609–638.

Jaafar, Z., and Larson, H. K. (2008). A new species of mudskipper, *Periophthalmus takita* (Gobiidae: Oxudercinae), from Australia, with a key to the genus. *Zoolog. Sci.* 25, 947. doi: 10.2108/zsj.25.946

Kirkpatrick, L. A., and Feeney, B. C. (2012). *A simple guide to IBM SPSS statistics for version 20.0.* (Student ed. Wadsworth, Cengage Learning, Belmont).

Kröger, R. H. H. (1992). Methods to estimate dispersion in vertebrate ocular media. *J. Opt. Soc Am. A.* 9, 1486–1490. doi: 10.1364/josaa.9.001486

Mass, A. M., and Supin, A. Y. (2007). Adaptive features of aquatic mammals' eye. *Anat. Rec. (Hoboken)* 290, 701–715. doi: 10.1002/ar.20529

Milward, N. E. (1974). *Studies of the taxonomy, ecology, and physiology of Queensland mudskippers* (Australia: University of Queensland).

Murdy, E. O. (1989). A taxonomic revision and cladistic analysis of the oxudercine gobies (Gobiidae: Oxudercinae). *Rec. Aust. Mus. Suppl.* 11, 1–93. doi: 10.3853/j.0812-7387.11.1989.93

Nursall, J. R. (1981). Behavior and habitat affecting the distribution of five species of sympatric mudskippers in Queensland. *Bull. Mar. Sci.* 31, 730–735.

Owens, G. L., Windsor, D. J., Mui, J., and Taylor, J. S. (2009). A fish eye out of water: ten visual opsins in the four-eyed fish, *Anableps anableps*. *PloS One* 4, e5970. doi: 10.1371/journal.pone.0005970

Polgar, G., and Bartolino, V. (2010). Size variation of six species of oxudercine gobies along the intertidal zone in a Malayan coastal swamp. *Mar. Ecol. Prog. Ser.* 409, 199–212. doi: 10.3354/meps08597

Reuter, T., and Peichl, L. (2008). "Structure and function of the retina in aquatic tetrapods," in *Sensory evolution on the threshold: Adaptations in secondarily aquatic vertebrates*. Eds. J. G. M. Thewissen and S. Nummela (Berkeley: University of California Press), 149–172. doi: 10.1525/9780520934122-011

Savolainen, O., Lascoux, M., and Merilä, J. (2013). Ecological genomics of local adaptation. *Nat. Rev. Genet.* 14, 807–820. doi: 10.1038/nrg3522

Sayer, M. D. J. (2005). Adaptations of amphibious fish for surviving life out of water. *Fish Fish.* 6, 186–211. doi: 10.1111/jfb.12270

Simmich, J., Temple, S. E., and Collin, S. P. (2012). A fish eye out of water: epithelial surface projections on aerial and aquatic corneas of the 'four-eyed fish' *Anableps anableps*. *Clin. Exp. Optom.* 95, 140–145. doi: 10.1111/j.1444-0938.2011.00701.x

Steppan, S. J., Meyer, A. A., Barrow, L. N., Alhajeri, B. H., Al-Zaidan, A. S. Y., Gignac, P. M., et al. (2022). Phylogenetics and the evolution of terrestriality in mudskippers (Gobiidae: Oxudercinae). *Mol. Phylo. Evol.* 169, 107416. doi: 10.1016/j.ympev.2022.107416

Subramanian, S., Ross, N. W., and MacKinnon, S. L. (2008). Comparison of antimicrobial activity in the epidermal mucus extracts of fish. *Comp. Biochem. Physiol. B. Biochem. Mol. Biol.* 150, 85–92. doi: 10.1016/j.cbpb.2008.01.011

Swennen, C., Ruttanadakul, N., Haver, M., Piummongkol, S., Prasertsongskum, S., Intanai, I., et al. (1995). The five sympatric mudskippers (Teleostei: Gobioidea) of pattani area, southern Thailand. *Nat. Hist. Bull. Siam. Soc* 42, 109–129.

Takegaki, T., Fujii, T., and Ishimatsu, A. (2006). Overwintering habitat and low-temperature tolerance of the young mudskipper *Boleophthalmus pectinirostris*. *Nihon-suisan-gakkai-shi* 72, 880–885. doi: 10.2331/suisan.72.880

Takita, T., Agusnimar,, and Ali, A. B. (1999). Distribution and habitat requirements of oxudercine gobies (Gobiidae: Oxudercinae) along the straits of malacca. *Ichthyol. Res.* 46, 131–138. doi: 10.1007/BF02675431

Townsend, K. A., and Tibbetts, I. R. (2005). Behaviour and sexual dimorphism of the blue mudskipper, *Scartelaos histophorus* (Pisces: Gobiidae). *P. R. Soc Queensland.* 112, 53–62.

Vafeiadou, A. M., Bretaña, B. L. P., Van Colen, C., Dos Santos, G. A. P., and Moens, T. (2018). Global warming-induced temperature effects to intertidal tropical and temperate meiobenthic communities. *Mar. Environ. Res.* 142, 163–177. doi: 10.1016/j.marenvres.2018.10.005

Vega, G. C., and Wiens, J. J. (2012). Why are there so few fish in the sea? *Proc. Biol. Sci.* 279, 2323–2329. doi: 10.1098/rspb.2012.0075

Wolfe, K., Nguyen, H. D., Davey, M., and Byrne, M. (2020). Characterizing biogeochemical fluctuations in a world of extremes: a synthesis for temperate intertidal habitats in the face of global change. *Glob. Change Biol.* 26 (7), 3858–3879. doi: 10.1111/gcb.15103

Wu, H. L., and Zhong, J. S. (2008). *FAUNA SINICA: PISCES, ORDER PERCIFORMES, SUBORDER GOBIOIDEI* (Beijing: Science Press).

You, X. X., Bian, C., Zan, Q. J., X. Xu, X., Liu, J., Chen, J. M., et al. (2014). Mudskipper genomes provide insights into the terrestrial adaptation of amphibious fishes. *Nat. Commun.* 5, 5594. doi: 10.1038/ncomms6594

You, X. X., Sun, M., Li, J., Bian, C., Chen, J. M., Yi, Y. H., et al. (2018). Mudskippers and their genetic adaptations to an amphibious lifestyle. *Anim. (Basel)* 8, 24. doi: 10.3390/ani8020024

frontiers | Frontiers in Marine Science

TYPE Original Research
PUBLISHED 16 December 2022
DOI 10.3389/fmars.2022.992319

OPEN ACCESS

EDITED BY
Hongsheng Yang,
Chinese Academy of Sciences (CAS), China

REVIEWED BY
Burke Hales,
Oregon State University, United States
Liqiang Zhao,
Guangdong Ocean University, China
Friedrich Buchholz,
University of Hamburg, Germany

*CORRESPONDENCE
Laura Ramajo
laura.ramajo@ceaza.cl

SPECIALTY SECTION
This article was submitted to Global Change and the Future Ocean, a section of the journal Frontiers in Marine Science

RECEIVED 12 July 2022
ACCEPTED 01 December 2022
PUBLISHED 16 December 2022

CITATION
Ramajo L, Sola-Hidalgo C, Valladares M, Astudillo O and Inostroza J (2022) Size matters: Physiological sensitivity of the scallop *Argopecten purpuratus* to seasonal cooling and deoxygenation upwelling-driven events. *Front. Mar. Sci.* 9:992319. doi: 10.3389/fmars.2022.992319

Size matters: Physiological sensitivity of the scallop *Argopecten purpuratus* to seasonal cooling and deoxygenation upwelling-driven events

Laura Ramajo[1,2,3]*, Camila Sola-Hidalgo[1,4], María Valladares[1], Orlando Astudillo[1,2] and Jorge Inostroza[1]

[1]Centro de Estudios Avanzados en Zonas Áridas (CEAZA), Coquimbo, Chile, [2]Departamento de Biología Marina, Facultad de Ciencias del Mar, Universidad Católica del Norte (UCN), Coquimbo, Chile, [3]Center for Climate and Resilience Research (CR2), Santiago Chile, [4]ONG Jáukén, Santiago, Chile

Environment imposes physiological constraints which are life-stage specific as growth-maintenance and/or growth-reproduction energetic requirements are size and volume-dependent. The scallop *Argopecten purpuratus*, one of the most important bivalve species subjected to fishery and aquaculture along the Humboldt Current System, inhabits spaces affected by continuous changes in temperature, pH, oxygen, and food availability driven by remote and local oceanographic processes. Specifically, in Chile, this species is mainly cultured in central-north Chile where is permanently affected by upwelling events of dissimilar intensity and duration which generate local conditions of acidification, deoxygenation, and cooling with different magnitudes. However, to date, it remains unknown how this economic valuable resource is physiologically affected throughout its life cycle by the continuous environmental changes driven by upwelling events of different intensities and duration along the year. Here, for the first time, *A. purpuratus* life-stage physiological sensitivity was assessed at a seasonal scale through a year-field experiment where growth, calcification, and survivorship were evaluated. Our study shows how seasonal differences in the upwelling phenology (here measured as changes in temperature, dissolved oxygen, pH, and primary productivity, but also as the number, duration, and intensity of cooling and de-oxygenation events) notably impacted the *A. purpuratus* physiological performance from juvenile to adult life-stages. This was especially noticeable during the *spring* season which showed the most intense cooling and deoxygenation events driven by stronger favorable-upwelling winds and the lowest growth and gross calcification rates (the highest decalcification rates) where adult stages showed the lowest performance. On the other hand, *A. purpuratus* survivorship was not significantly affected by upwelling intensity which would be providing evidence of the high physiological flexibility and

well-locally adapted is this species to fluctuating and occasional stressful environmental conditions. Our results are significantly relevant in the climate change context as some upwelling systems are at risk to change shortly (i.e., an upwelling intensification in frequency and intensity) as a consequence of changes in the atmospheric pressures that modulate favourable-upwelling winds. These changes may certainly increase the climate related-risks of the entire socio-ecological systems related to the fishery and aquaculture of *A. purpuratus* along the Humboldt Current System.

KEYWORDS

shellfish aquaculture, Humboldt Current System, climate change, upwelling intensification, physiological impacts, ocean deoxygenation, ocean acidification, cooling

1 Introduction

Physiological performance is highly dependent on environmental conditions (Thomsen et al., 2015; Byrne, 2012). Elevated temperatures increase organism's metabolic rates accelerating growth and sexual maturity, while when habitat temperatures exceed the organism tolerance thresholds can promote the rapid deterioration of cellular processes (Pörtner, 2008). Also, low seawater pH values can cause hypercapnia with cascading effects on multiple physiological responses of diverse taxa, being specifically detrimental in calcifiers as shell precipitation and shell integrity are highly dependent on pH and carbonate concentration conditions (e.g., Kroeker et al., 2013; Ramajo et al., 2016; Ramajo et al., 2020). Indeed, lower pH levels result in lower calcification rates, increasing shell malformations (Waldbusser et al., 2015) and shell mechanical changes (e.g., weaker shells) (Zhao et al., 2020; Lagos et al., 2021) which also may increase the vulnerability to predation, parasitism, and/or stress by wave action (Gazeau et al., 2013; MacLeod and Poulin, 2015; Gaylord et al., 2015). Likewise, critical physiological processes such as respiration are dependent on the flux of oxygen (Seibel, 2011) where low oxygen availability is usually related to reduced growth and low reproduction success, altered behavior patterns, and increased risk of predation with resulting lower survivorship for many marine species (Breitburg et al., 2018).

Moreover, physiological sensitivity to environmental changes is life-stage specific (Talmage and Gobler, 2010; Baumann et al., 2012). Early life-stages such as larvae or juveniles usually show lower energy reserves and smaller tolerance limits making them more sensitive than adults to higher temperatures (e.g., Truebano et al., 2018), decreasing pH levels (e.g., Kroeker et al., 2013; Wessel et al., 2018), and hypoxic conditions (e.g., Clark and Gobler, 2016). Also, growth-maintenance and/or growth-reproduction *trade-offs* are more evident when organisms get older as maintenance, growth, and reproduction related-costs are size and volume-dependent (Bayne and Newell, 1983; Kooijman, 2000; Thompson and MacDonald, 2006; Chauvaud et al., 2012). In particular, for calcifying organisms, some physiological *trade-offs* emerge as a consequence of the higher energetic requirements needed for biomineralization and calcification processes including carbonate precipitation and shell organic and periostracum production (Palmer, 1981; Trussell and Smith, 2000; Clark et al., 2020; Ramajo et al., 2019; Ramajo et al., 2020) which could represent up to 75-410% of the energy invested for growth and reproduction (Palmer, 1981).

The scallop *Argopecten purpuratus* is one of the most important bivalve species subjected to fishery and aquaculture along the Peruvian and Chilean Humboldt Current System (Yáñez et al., 2017). Historical *A. purpuratus* landings show an important variability as a consequence of changes in environmental conditions (Lagos et al., 2016; Yáñez et al., 2017) with significant impacts on Chilean and Peruvian markets (von Brand et al., 2016). Previous experimental and field studies on this resource show significant sensitivity to changes in temperature, pH, oxygen, and food availability (Lagos et al., 2016; Ramajo et al., 2016; Lardies et al., 2017; Ramajo et al., 2019; Ramajo et al., 2020; Avendaño and Cantillánez, 2022) which is particularly important in Chile as this scallop species is mostly cultured (i.e., Tongoy Bay) under the effects of one of the most active upwelling centers on the Chilean coast (Figueroa and Moffat, 2000; Rutllant and Montecino, 2002; Aravena et al., 2014; Rahn and Garreaud, 2014). Environmental conditions at Tongoy Bay have important physiological impacts on *A. purpuratus* juveniles (Ramajo et al., 2020), especially during the upwelling season (spring-summer) when the intensity and duration of upwelling events are higher (Moraga-Opazo et al., 2011; Bravo et al., 2016). However, to date, remains unknown which is the life-stage *A. purpuratus* sensitivity to changes in the environmental conditions driven by the seasonal upwelling cycle. This missing information is

significantly relevant in the climate change context as some Eastern Boundary Upwelling Systems (EBUS) are at risk to change shortly (i.e., an upwelling intensification as a consequence of changes in the frequency and intensity) which could also favor local ocean acidification and deoxygenation (see Garreaud and Muñoz, 2005; Aravena et al., 2014; Sydeman et al., 2014; Rykaczewski et al., 2015; IPCC, 2021). Certainly, potential changes in the upwelling phenology may threaten the fishery and aquaculture scallop industry and the related-socioecological system along the Humboldt Current System (Lluch-Cota et al., 2014; Bakun et al., 2015; Ramajo et al., 2020; IPCC, 2021).

Based on that, here was assessed, for the first time, the level of physiological sensitivity of different life-stages of *A. purpuratus* at a seasonal scale in the context of upwelling. To do that, a year-field experiment was performed in Tongoy Bay where physiological responses (growth, calcification, and survivorship) were evaluated in a large range of scallop sizes (from the juvenile to adult stages) aiming to capture how seasonal changes in the upwelling phenology (number of events, duration, and intensity) could be modulating the physiological performance and fitness of this economical valuable resource for the fishery and shellfish aquaculture along the Humboldt Current System.

2 Material and methods

2.1 Study site

Tongoy Bay, in north-central Chile, is a key place for the culture of the scallop *Argopecten purpuratus*. This bay is located just north of Punta Lengua de Vaca (PLV), one of the most important and active upwelling centers that modulate environmental conditions on the central-north Chilean coast (Figueroa and Moffat, 2000; Rutllant and Montecino, 2002; Rahn and Garreaud, 2014) (Figure 1A). Previous studies have determined that Tongoy Bay shows a semi-permanent upwelling regime with higher upwelling intensities during the austral spring-summer seasons (Moraga-Opazo et al., 2011; Bravo et al., 2016). By the year, seasonal differences in the upwelling phenology provoke important oceanographic, biogeochemical, and environmental heterogeneity in the

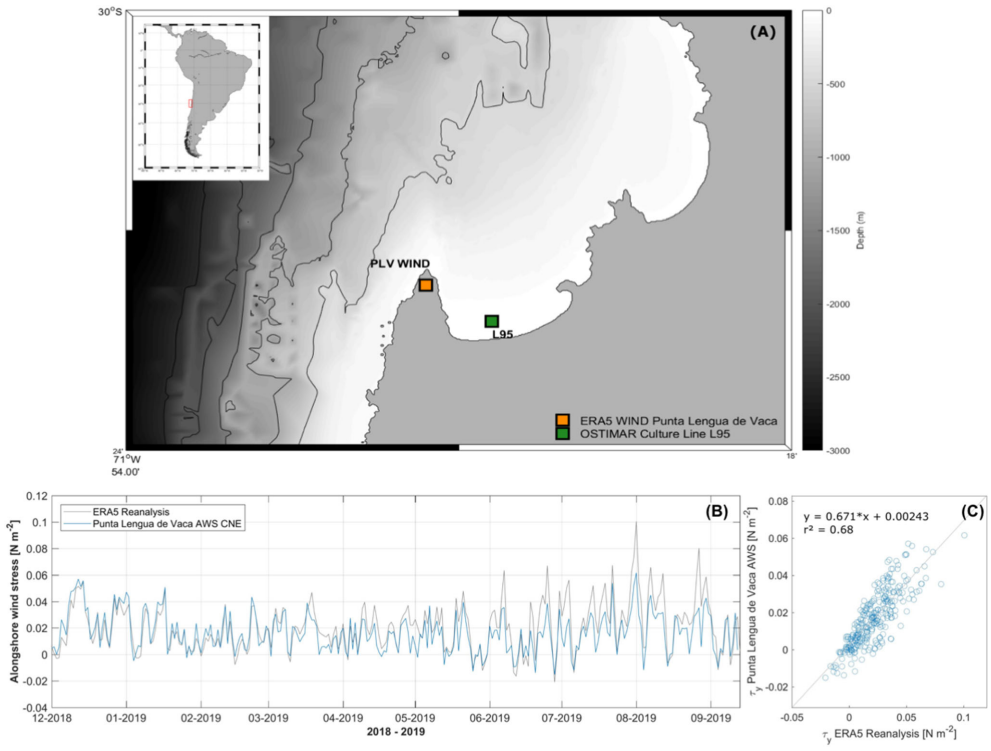

FIGURE 1
Study site and wind conditions. **(A)** Tongoy Bay coastal area with positions of the experiment (green) (culture line L95) and the location of the automatic weather station (AWS) placed close to the upwelling centre Punta Lengua de Vaca (PLV) (orange). **(B)** Validation of ERA5 reanalysis alongshore wind component with the *in situ* PLV-AWS data from 2018 to 2019. **(C)** Least-square linear regression between ERA5 reanalysis and AWS alongshore wind data.

nearby coastal areas (Torres et al., 1999; Torres and Ampuero, 2009; Ramajo et al., 2020). As a consequence of this seasonal pattern and upwelling, Tongoy Bay shows along the year high fluctuations in terms of temperature (10.6°C - 19.7°C), pH (7.6 - 8.1), oxygen concentrations (1.45 - 4.17 ml L^{-1}) (Ramajo et al., 2019; Ramajo et al., 2020), and primary productivity (ranging from 2.40 to 10.45 mg m^{-3}) (Rutllant and Montecino, 2002; Ramajo et al., 2020).

2.2 Organismal collection and experimental design

Wild scallops from Tongoy Bay (30°16'S; 71°35'W), with no shell damage and parasite presence (Basilio et al., 1995), were provided by the scallop aquaculture company OSTIMAR S.A. The experimental design consisted of four analogous field experiments (hereafter, *seasonal experiments*) that aimed to determine how seasonal environmental changes are modulated by upwelling phenological changes (i.e. a semi-permanent upwelling regime with lower intensity during the autumn and winter months, and higher intensity during spring-summer seasons, Thiel et al., 2007; Torres and Ampuero, 2009; Rahn and Garreaud, 2014) and may be affecting different life-stages (from juveniles to adults) of the scallop *A. purpuratus* at Tongoy Bay. To do that, around 180 scallops were used in each *seasonal experiment* with a body-size range between 10 to 90 mm (Figure S1). After collection, experimental scallops were transported under-insulated conditions to the laboratory and labeled with numbered tags glued onto the shells allowing their identification during the experiment. After that, between 100 - 120 scallops (hereafter, *alive scallops*) were maintained in aquaria under controlled conditions (14°C, pH_{NBS} near 8.0, and >90% of oxygen saturation). In addition, ~ 60 scallops were sacrificed and their soft parts were removed, and shells were kept for the experiment (hereafter, *empty shells*). For both, *alive scallops* and *empty shells*, the maximum shell size (length and width), and the shell buoyant weight were recorded at the initial time (Figure S1). After that, *alive scallops* and *empty shells* were randomly distributed in 4 *pearl nets* (i.e. common culture structures used by the aquaculture industry to avoid denso-dependency issues). Each *pearl net* was composed of 2 different nets separated by less than 25 cm between them. Each *pearl net* contained 30 *alive scallops* and 30 *empty shells* (see Figure 2). The four experimental *pearl nets* were located in the culture line number L95 belonging to OSTIMAR S.A (30°16'49.4''S; 71°34'03.7''W) (Figure 1A) at 9 m depth. Each *alive scallop* and each *empty shell* were considered independent replicates. The four *seasonal experiments* followed similar experimental protocols. The *Summer* experiment was carried out between January to March 2019, the *Autumn* experiment between March to July 2019, *Winter* from July to October 2019, and the *Spring* experiment from October 2019 to

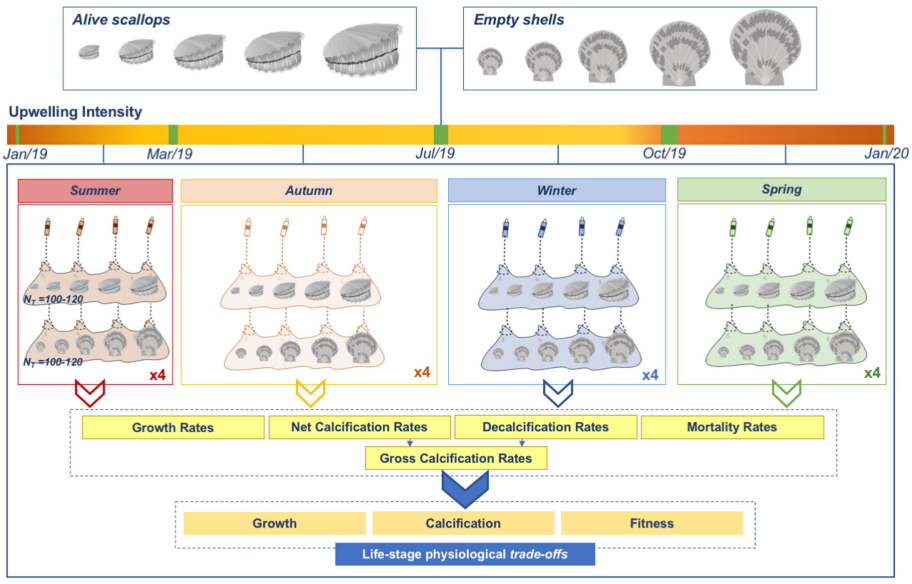

FIGURE 2
Experimental design. General scheme of the experimental design used where *alive scallops* and *empty shells* were exposed to four different *seasonal experiments* (*Summer, Autumn, Winter*, and *Spring*) from January 2019 to January 2020. Four *pearl nets* composed of 2 nets containing between 100-120 *alive scallops* and *empty shells* were used by *seasonal experiment*. At the end of each experiment, growth, net calcification, decalcification, and gross calcification rates were determined, and mortality was recorded. The intensity of the upwelling is based on the environmental data monitored during the experiments (i.e. higher intensity is shown as orange).

January 2020 (see Figure 2). At the end of each *seasonal experiment*, *pearl nets* with *alive scallops* and *empty shells* were removed from the L95 and transported to the laboratory where shell size (maximum length and width) and buoyant weight were measured. At the end of each *seasonal experiment*, all *alive scallops* were sacrificed (not returned to the field).

2.3 Environmental conditions at Tongoy Bay

Tongoy Bay environmental conditions, at high and low frequencies, were monitored during the four *seasonal experiments*. High-frequency (each 15 min) temperature and dissolved oxygen (DO) conditions were registered by using HOBO U26 Dissolved Oxygen Data Loggers (ONSET®) which were attached to the experimental *pearl nets*. According to the manufacturer's instructions, every six months the oxygen logger membranes were replaced with new ones. Anti-fouling sensor maintenance, as well as, data downloading from each sensor were performed at the end of each *seasonal experiment*. At low frequency (weekly), pH_{NBS} conditions were determined by collecting water samples through a NISKIN bottle (5L vol). Three water samples per depth were analyzed within 60 min after water collection using a Metrohm 780 Meter (Metrohm®) connected to a combined electrode (Aquatrode Plus with Pt1000, Metrohm®). The electrode was calibrated using three NBS buffers (Metrohm®) at 25°C before each measurement. In addition, surface chlorophyll-*a* (Chl-*a*) by each *seasonal experiment* was obtained through 8-day composites of Moderate Resolution Imaging Spectroradiometer (MODIS-Aqua) 4km products retrieved from NASA (http://oceancolor.gsfc.nasa.gov) comprising an area limited by 30.6° - 30°S and 71.9°W to the coast. MODIS Chl-*a* data were averaged at a monthly scale and then averaged for each *seasonal experiment*. Finally, the intensity and variability of wind-driven coastal upwelling were obtained from ERA5 reanalysis (https://rda.ucar.edu/datasets/ds633.0/) at PLV during the experiment. PLV is representative of the environmental conditions occurring at Tongoy Bay as it was recently observed by Ramajo et al. (2020) (see also Figure 1A). Reanalysis dataset was validated against available continuous 10m wind data from an Automatic Weather Station (AWS) at the same geographic location between December 2018 to September 2019 (see Figure 1B). Daily alongshore wind magnitude measured by the AWS at PLV and ERA5 reanalysis showed a high and significant correlation (*Pearson* correlation: R^2 = 0.68, *P*-value = 0.000) (see Figure 1C).

2.4 Growth, calcification, and mortality

Growth rates (GR), net calcification rates (NCRs), decalcification rates (DCRs), and gross calcification rates (GCR) were estimated for all *seasonal experiments*. GRs estimations correspond to the difference in the total area of *alive scallops* (estimated as an ellipsoid from shell maximum length and width measurements) divided by the number of days that the experiment lasted. *Empty shells* were used to estimate size differences in DCRs for each *seasonal experiment* (see Figure S2). Previous studies have found that low pH conditions generate corrosive and undersaturated carbonate conditions which are responsible for shell layers dissolution and higher decalcification rates (i.e., Waldbusser et al., 2011; Langer et al., 2014). Both NCRs and DCRs were estimated by using the buoyant weight technique (Davies, 1989). Buoyant weight data was converted into shell dry weight (DW) using the seawater density (average conditions at Tongoy Bay, salinity = 34‰, temperature = 14°C), and the density of calcite (2.71 g cm^{-3}) (see Ramajo et al., 2019). Finally, NCRs and DCRs were computed as the change in the shell dry (DW) weight goes by between two different periods (i.e. duration of each *seasonal experiment*). Lastly, GCRs for each *alive scallop* and *seasonal experiment* were determined by subtracting DCRs from the NCRs. All physiological rates (i.e. GRs, NCR, DCRs, and GCRs) are shown as non-normalized and body-size normalized. Dead organisms were counted at the end of each *seasonal experiment*, and mortality rates were estimated as the percentage of dead organisms per day (% d^{-1}).

2.5 Data analyses

Environmental and biogeochemical seawater properties (i.e. pH_{NBS}, temperature and DO), based on the mean state (± standard error, SE) and their variability (coefficient of variation, CV) were established for the four *seasonal experiments*.

Upwelling was characterized by calculating alongshore wind stress ($\tau_{alongshore}$) after rotating ERA5 daily wind vectors to align them approximately with the direction of the coast (Equation 1).

$$\tau_{alongshore} = \rho_a \times C_d \times |v|v \qquad \text{Eq. (1)}$$

where ρ_{air} is air density (assumed constant at 1.22 kg m^{-3}), C_d is the drag coefficient varying with v, and v is the meridional alongshore wind component.

Further, across-shelf Ekman transport (M, units = m^2 s^{-1} per meter of the coast) was computed following:

$$M = \frac{1}{\rho_w f}\tau_{alongshore} \qquad \text{Eq. (2)}$$

where ρ_w is the water density (assumed constant at 1024 kg m^{-3}), f is the Coriolis parameter (s^{-1}), and τ is the alongshore wind stress. Positive values of M indicate onshore transport due to downwelling favorable winds, while negative values imply offshore transport caused by upwelling favorable winds (Bakun, 1975). Posteriorly, following Tapia et al. (2009) and Ramajo et al. (2020) methodologies, the impact of upwelling on temperature changes (i.e. cooling) and DO conditions (i.e. deoxygenation) at Tongoy Bay were estimated.

The present study spans one entire year in a semi-permanent upwelling region encompassing upwelling, downwelling favorable winds, and relaxation periods (Rahn and Garreaud, 2014), some extra methodological modifications to Ramajo et al. (2020) were implemented to properly attribute cooling and de-oxygenating events to upwelling. To do that, first, we defined a threshold of alongshore wind stress of 5m s^{-1} in the equatorward direction (see Cury and Roy, 1989; García-Reyes et al., 2014). Secondly, to highlight the synoptic variability dominance in upwelling systems (Renault et al., 2009), a 30-day running mean was subtracted from the daily average time series of seawater temperature and DO. Daily anomalies in temperature and DO time series were used to quantify the number, duration, and intensity of the different cooling and de-oxygenations episodes recorded during each *seasonal experiment* (Figure 5A) (for further details, see Ramajo et al., 2020).

Average specific differences in GRs, NCRs, DRs, and GCRs (non- and body-size normalized), as well as, the size distribution of alive and dead scallops after each *seasonal experiment* were evaluated by using Kruskal Wallis and Dunn tests. The role of the tested factors (*Size* and *Season)* for all physiological rates was addressed by using hierarchical linear mixed-effects models (e.g., Ramajo et al., 2020). *Size* and *Season* and the two-way interaction between these were modeled as fixed effects. Random effects at the individual level were employed to control for potential organismal effects. Restricted maximum likelihood (REML) was used to fit the model for each physiological rate (GRs, NCRs, DRs, and GCRs), as well as, to calculate unbiased estimates of parameter variance and standard error according to the general model:

$$y = Xb + X0 + Za + e$$

where y is the vector of the observations (i.e., physiological rates), b and 0 is the vector of fixed effects (i.e., *Size* and *Season*), a is the vector of random effects (i.e., individuals), *e* represents the residual effects, and X and Z are the corresponding incidence matrices. Linear mixed-effects models were estimated by using the *lme4* package. The *AFEX package* was used to obtain parameter *P*-values for the linear mixed-effects models using the Kenward-Roger approximation for degrees of freedom. Optimal models were identified as those yielding the greatest number of significant (P< 0.05) fixed effects. Variance and standard deviation of the random effect (individual) are also reported. Differences in mortality (i.e. number of dead scallops) were determined by using Poisson regressions. Finally, to identify potential associations between environmental variables and physiological rates measured, Pearson correlation analyses were carried out, and multivariate comparisons between all physiological rates and environmental variables were assessed using redundancy analysis (RDA). Before RDA analyses, environmental variables and physiological rates were standardized (from zero to one). RDA analysis was carried out using the vegan package. All these analyses were carried out on R software (version 3.5.0).

3 Results

3.1 Seasonal environmental variability at Tongoy Bay

During 2019 at Tongoy Bay, coastal upwelling conditions (i.e. negative Ekman transport, M) dominated the year-round experimental study showing an increasing intensity from summer towards the *spring* season (observed in mean and minimum values) exhibiting a maximum mean of -0.43 m^2 s^{-1} in the *winter* season. On the other hand, downwelling favorable conditions (i.e., positive Ekman transport, M) were mostly observed during the *autumn* season. Regarding upwelling relaxation events (i.e., Ekman transport close to zero), these were observed throughout the year on a synoptic time scale (~1 to 16 days) (Figure 3A; Table 1).

Surface Chl-*a* at Tongoy Bay presented maximum values during the *spring* and the lowest concentrations during the *autumn* and *winter* months (Figure 4; Figure S3).

In terms of variability (here measured as CV, %), temperature and pH exhibited a decline towards *winter* with a subsequent rise in *spring*. Maximum variability in temperature and pH was found during *spring and summer*, with temperature CV peaking in spring and pH CV in summer (Figures 3B, D; Table 1). DO variability increased from *summer* to *spring*, with a maximum in *winter* (Figure 3C; Table 1).

The number and duration of cooling and de-oxygenation events showed differences among *seasonal experiments* and were highly correlated with Ekman transport magnitude ((Figures 5B–D)) revealing a negative relationship between M and temperature and DO conditions (Figures 3A–D). A slight increase in the number and duration of cooling and de-oxygenation events was observed from *summer* to *winter* then showing a little reduction during the *spring* season. *Winter* presented the highest number of cooling and de-oxygenation events, as well as, the longest duration compared with the rest of the *seasons*. However, *spring* and *summer* exhibited the highest intensity and cooling and de-oxygenation rates (Figures 5E–H).

3.2 Growth and calcification

Both, average non-body-size normalized and body-size normalized GRs showed significant differences among the different *seasonal experiments* (Kruskal-Wallis test: χ^2 = 24.86, *P*-value< 0.001, and χ^2 = 50.58, *P*-value = 0.000, respectively). Average GRs (non-body-size normalized) showed similar values between the *summer*, *autumn*, and *winter* seasons (*Dunn's test*: *P*-value = 1.000), however a significant reduction in the GRs was detected during the *spring* in comparison with *summer (Dunn's test*: *P*-value = 0.000), *autumn* (*Dunn's test*: *P*-value = 0.000) and *winter* (*Dunn's test*: P-value< 0.001) (see Figure 6A). On the other hand, average normalized body-size GRs showed a different trend with a visible

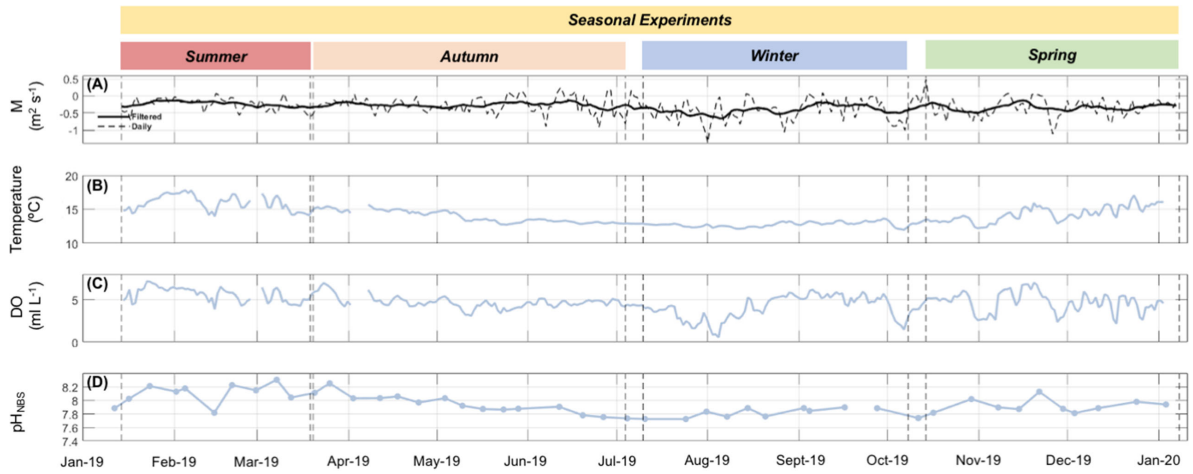

FIGURE 3
Field Conditions. **(A)** Daily averaged and high-pass filtered time series of Ekman transport at PLV, in segmented and continuous lines, respectively. Daily and weekly time series of **(B)** seawater temperature, **(C)** dissolved oxygen (DO), and **(D)** pH_{NBS} at Tongoy Bay (9 m depth). Vertical segmented lines separate the four *seasonal experiments*.

decreasing trend from the *summer* to the *spring*. Normalized body-size GRs were significantly higher during the *summer* in comparison with the *winter* (*Dunn's test*: *P*-value = 0.001) and *spring* seasons (*P*-value = 0.000). No significant differences were found between *summer* and *autumn* (*P*-value = 0.080), as well as between *autumn* and *winter* (*Dunn's test*: *P*-value = 0.844) (see Figure 6B). Linear mixed models controlled for the random effects of individuals confirmed that the scallops' size (*P*-value< 0.001),

TABLE 1 Tongoy Bay environmental conditions.

Environmental Varisable	*Seasonal Experiments* (Jan 2019 – Jan 2020)			
	Summer (Jan – Mar)	*Autumn* (Mar – Jul)	*Winter* (Jul – Oct)	*Spring* (Oct – Jan)
Ekman Transport (M) (m^2 s^{-1})				
Mean (± SE)	-0.23 ± 0.02	-0.26 ± 0.02	-0.43 ± 0.03	-0.33 ± 0.03
Max - Min	0.08 – -0.71	0.25 – -0.92	0.10 – -1.38	0.51 – -1.12
Temperature (° C)				
Mean (± SE)	15.93 ± 0.14	13.90 ± 0.08	12.76 ± 0.04	14.31 ± 0.12
Max - Min	17.79 – 13.98	15.67 – 12.73	13.66 – 11.97	17.04 – 12.22
CV (%)	7.04	6.21	2.9	7.85
Dissolved Oxygen (DO) (ml L^{-1})				
Mean (± SE)	5.61 ± 0.10	4.68 ± 0.07	4.06 ± 0.15	4.70 ± 0.13
Max - Min	7.16 – 3.88	6.96 – 3.10	6.18 – 0.55	6.99 – 2.16
CV (%)	14.86	15.08	35.24	25.61
pH_{NBS} (25° C)				
Mean (± SE)	8.117 ± 0.048	7.959 ± 0.036	7.818 ± 0.021	7.919 ± 0.031
Max - Min	8.301 – 7.814	8.249 – 7.751	7.895 – 7.722	8.125 – 7.809
CV (%)	1.77	1.7	0.91	1.23

Ekman transport (M), temperature, dissolved oxygen (DO), and pH_{NBS} were recorded during the different seasonal experiments at Tongoy Bay. Variability for each variable was estimated by the Coefficient of Variation (CV, %).

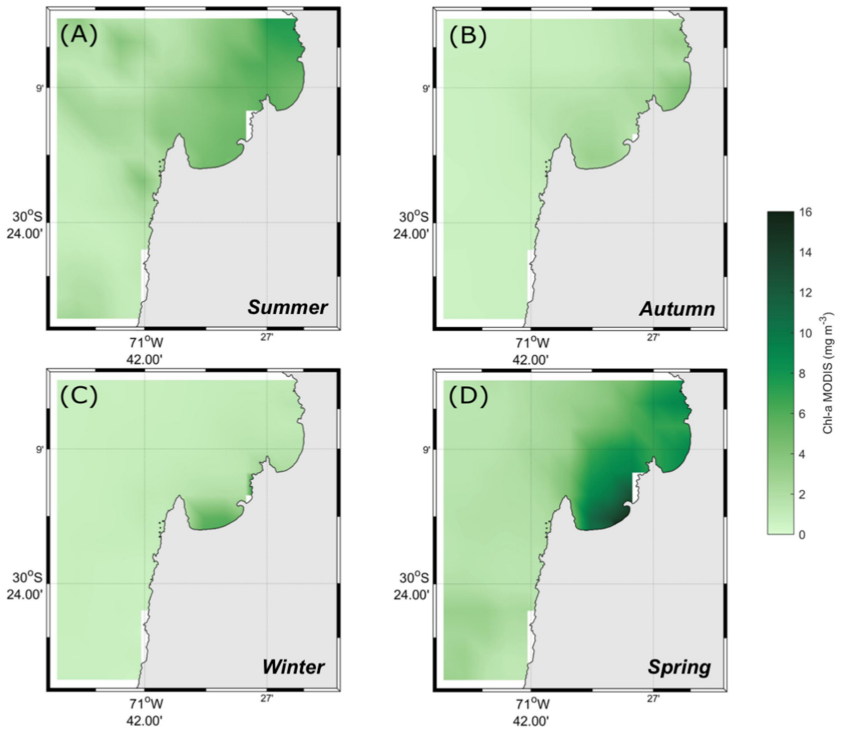

FIGURE 4
Chlorophyll-*a* variability. Seasonally-averaged Chl-*a* fields derived from MODIS-Aqua 8-day composites for each *seasonal experiment*.. **(A)** Summer, **(B)** Autumn, **(C)** Winter, and **(D)** Spring season.

season (i.e., the environmental conditions occurring during each *seasonal experiment)* (*P*-value< 0.037), and the interaction between size and *season* (*P*-value = 0.030) predicted significantly the GRs observed (Figure 7A; Table 2).

Both average NCR (non-normalized and normalized body-size) showed significant differences among the different *seasonal experiments* (*Kruskal-Wallis's test*: $\chi 2 = 13.17$, *P*-value = 0.004, and $\chi 2 = 29.77$, *P*-value = 0.000, respectively). Non-normalized body-size NCRs did not show a clear pattern along the year-round experiment showing similar values during the *autumn* (Dunn test: *P*-value = 1.000), *winter* (*Dunn's test*: *P*-value = 1.000), and *spring* (*Dunn's test*: *P*-value = 1.000) However, non-normalized body-size NCRs were significantly lower in *summer* in comparison with *autumn* (*Dunn's test*: *P*-value = 0.011), and *winter* (*Dunn's test*: *P*-value = 0.0120) (see Figure 6C). On the other hand, normalized body-size NCRs showed a clear pattern with decreasing values from *summer* to *spring* (Figure 6D), presenting significant lower values during *spring* in comparison with *autumn* (*Dunn's test*: *P*-value< 0.001) and *winter* (*Dunn's test*: *P*-value< 0.001). Normalized body-size NCRs were also higher during *summer* in comparison with *winter* (*Dunn's test*: *P*-value = 0.016). No significant differences were found between *autumn* and *summer* (Dunn test: *P*-value = 1.000) and *winter* (*Dunn's test*: *P*-value = 0.330), as well as between *winter* and *spring* (*Dunn's test*: *P*-value = 0.054) (see Figure 6D).

Linear mixed models controlled for the random effects of individuals confirmed that both seasons (i.e., environmental conditions occurring at each *seasonal experiment*) and *size* factors predicted significantly the NCRs observed (*Size* x *Season*; *P*-value= 0.002) (Figure 7; Table 2).

DRs in *alive scallops* (non-body-size and normalized body-size) showed significant differences among the *seasonal experiments* (*Kruskal-Wallis's test*: $\chi 2 = 211.58$, *P*-value = 0.000, and $\chi 2 = 211.11$, *P*-value = 0.000, respectively), being significantly higher during the *spring* (see Figures 6E, F). Linear mixed models controlled for the random effects of individuals confirmed that the interaction between *size* and season factors predicted significantly the DRs observed (*P*-value< 0.011) (see Figure 7; Table 2).

Both, non- and normalized body-size GCRs were significantly different among the different *seasonal experiments* (*Kruskal-Wallis's test*: $\chi 2 = 102.07$, *P*-value = 0.000, and $\chi 2 = 93.96$, *P*-value = 0.000, respectively). *Spring* season showed the lowest GCRs in comparison with *summer*, *autumn*, and *winter* seasons in both non-normalized (Dunn test: *P*-value = 0.000) and normalized body-size GCRs (*Dunn`s test*: *P*-value = 0.000) (Figures 6G, H). GCRs (non-normalized and normalized body-size) did not show significant differences between the *autumn*, *winter*, and *summer* seasons (*Dunn`s tests*: P-value< 0.05 for all combinations). Linear mixed models controlled for the random effects of individuals confirmed

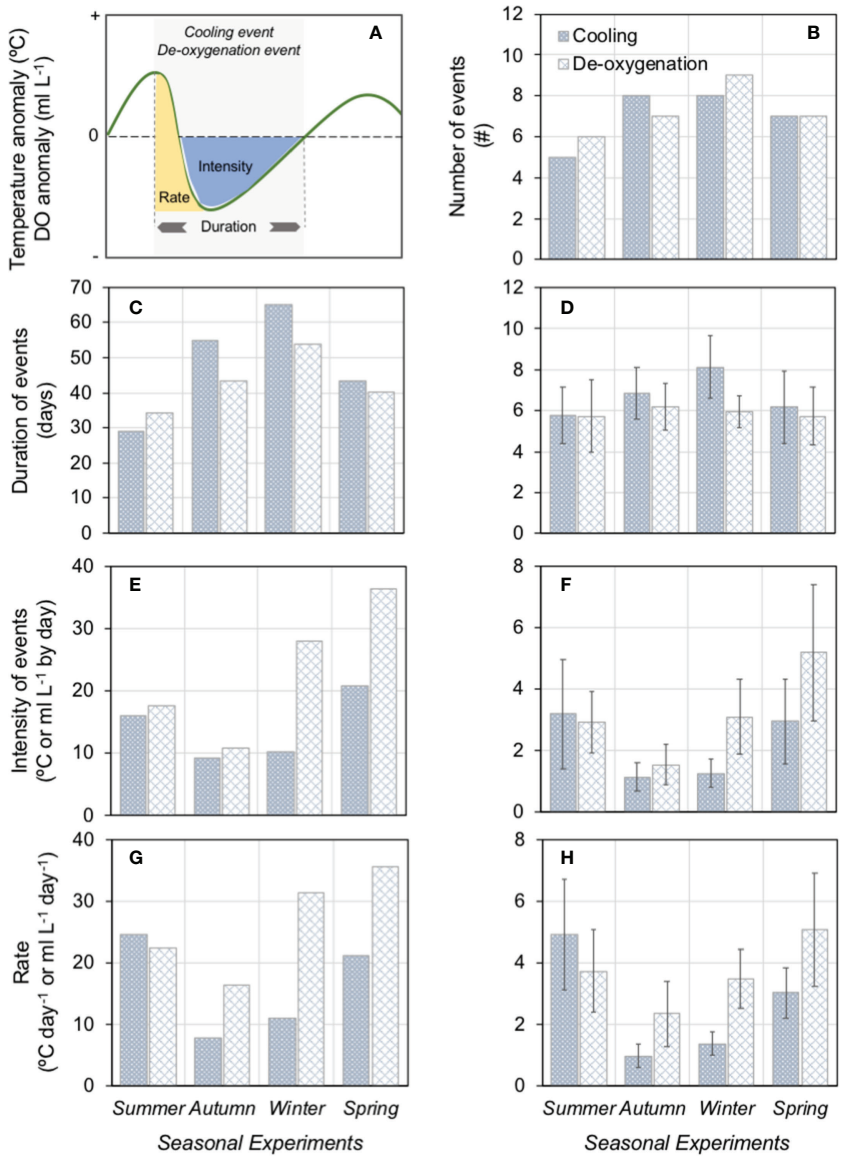

FIGURE 5
Cooling and de-oxygenation at Tongoy Bay. **(A)** Scheme of the methodology used to determine the upwelling impact on cooling and de-oxygenation events based on thermal and dissolved oxygen anomalies (see section 2.1 for further details). Number **(B)**; accumulated **(C)** and mean **(D)** duration; accumulated **(E)** and mean **(F)** intensity (as an integrated anomaly); accumulated **(G)** and mean **(H)** rate (as integrated cooling/deoxygenation) of events registered each *seasonal experiment*. Data in D, F, and H are means ± SE.

that *size* (*P*-value< 0.001), *season* (i.e., the environmental conditions occurring during each *seasonal experiment*) (*P*-value = 0.023), and the interaction between *size* and *season* factors (*P*-value = 0.001) predicted significantly the GCRs observed (Figure 7; Table 2).

3.3 Mortality

Higher mortality rates were found during the *spring* and *summer* seasons which corresponded to the 57% and 35% of initial experimental scallops used for each *seasonal experiment*, respectively. On average, dead scallops in *summer* and *spring* seasons mortalities occurred in those organisms with larger sizes (88.65 and 92.97 mm maximum shell length, respectively) (see Figure 8A). However, mortality rates (Poisson regression: $\chi 2$ = 4.3825, *P*-value = 0.223) and size of the dead scallops (Kruskal-Wallis test: $\chi 2$ = 7.6931, *P*-value = 0.053) did not show any significant difference among the *seasonal experiments* (Figure 8B).

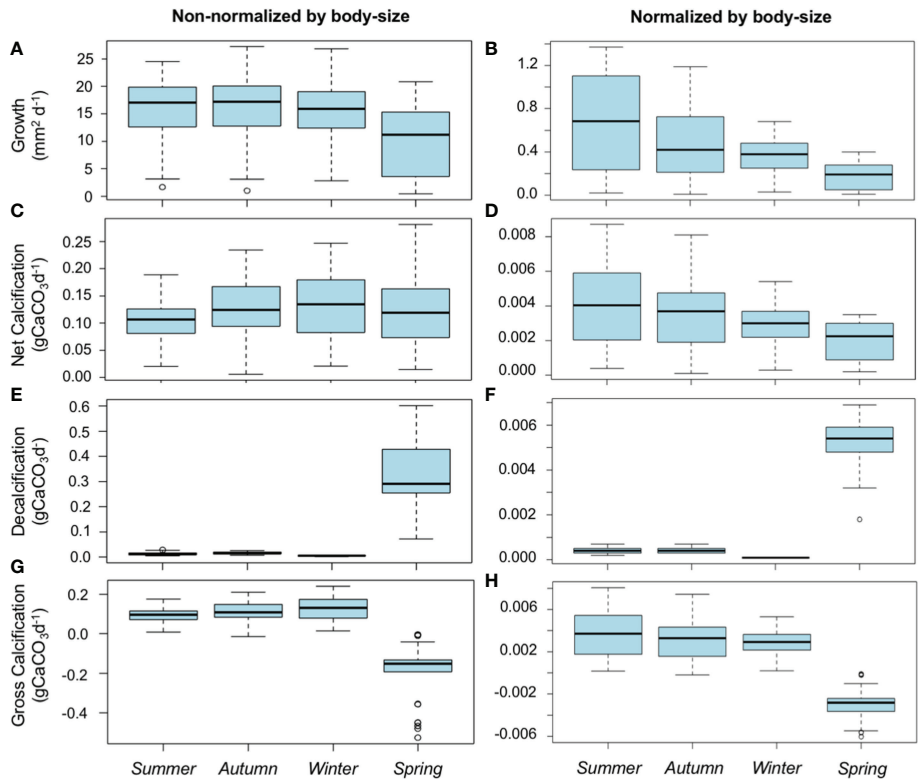

FIGURE 6
A. *purpuratus* physiological rates. Average non-normalized and normalized body-size growth **(A, B)**, net calcification **(C, D)**, decalcification **(E, F)**, and gross calcification rates **(G, H)** were recorded during the four *seasonal experiments*. Data shown are mean ± SE.

3.4 Interaction between environmental conditions and scallop physiology

High collinearity between environmental conditions recorded at each *seasonal experiment* and physiological *A. purpuratus* performance was corroborated by the RDA analyses (Figure 9A). The two main components explained, in total, more than 99% of the observed variance (89.8% of Component RDA1 and 9.96% of Component RDA2). Ekman transport, pH, DO and temperature were all highly correlated (RDA2), while Chl-*a* showed a higher load along the RDA1 axis, and thus, a lower correlation with the variables previously mentioned (Figure 9A).

In particular, strong negative and significant correlations were found between Ekman transport and the temperature, DO, and pH levels of Tongoy Bay. On the other hand, pH and DO showed stronger positive and significant correlations. Weak correlation values were observed (positive and significant) between temperature and pH and DO. Chl-*a* showed a positive and significant correlation with Ekman transport, as well as a negative and significant correlation with DO and pH values.

Related to physiological responses, GRs showed a positive and significant correlation with NCR and GCRs, and a negative and significant correlation with DRs. NCRs showed a negative and significant correlation with DRs, and a positive and significant correlation with GCRs. GCRs and DCs showed a significant and strong negative correlation

Finally, strong correlations were found between the environmental variables (Ekman transport, temperature, DO, pH, and Chl-*a*) and *A. purpuratus* physiological responses (GRs, NCRs, DCs, and GCRs) (Figure 9B). GRs and NCRs showed significant positive correlations with DO and pH, while this correlation was negative with Ekman transport and Chl-*a*, and null with temperature. DRs showed significant and positive correlations with temperature and Chl-*a* values, however, no significant correlations were observed between DRs with DO, pH, and Ekman transport. GCRs showed a negative significant correlation with Ekman transport, temperature, and Chl-*a* values, and positive with pH values.

4 Discussion

Marine environmental conditions are modulated by remote and local drivers that alter, at multiple spatiotemporal scales, several physical, chemical, biological and socio-ecological processes (e.g., Bakun et al., 2015; Sprogis et al., 2018). Environmental fluctuations have important effects on the physiological performance of marine

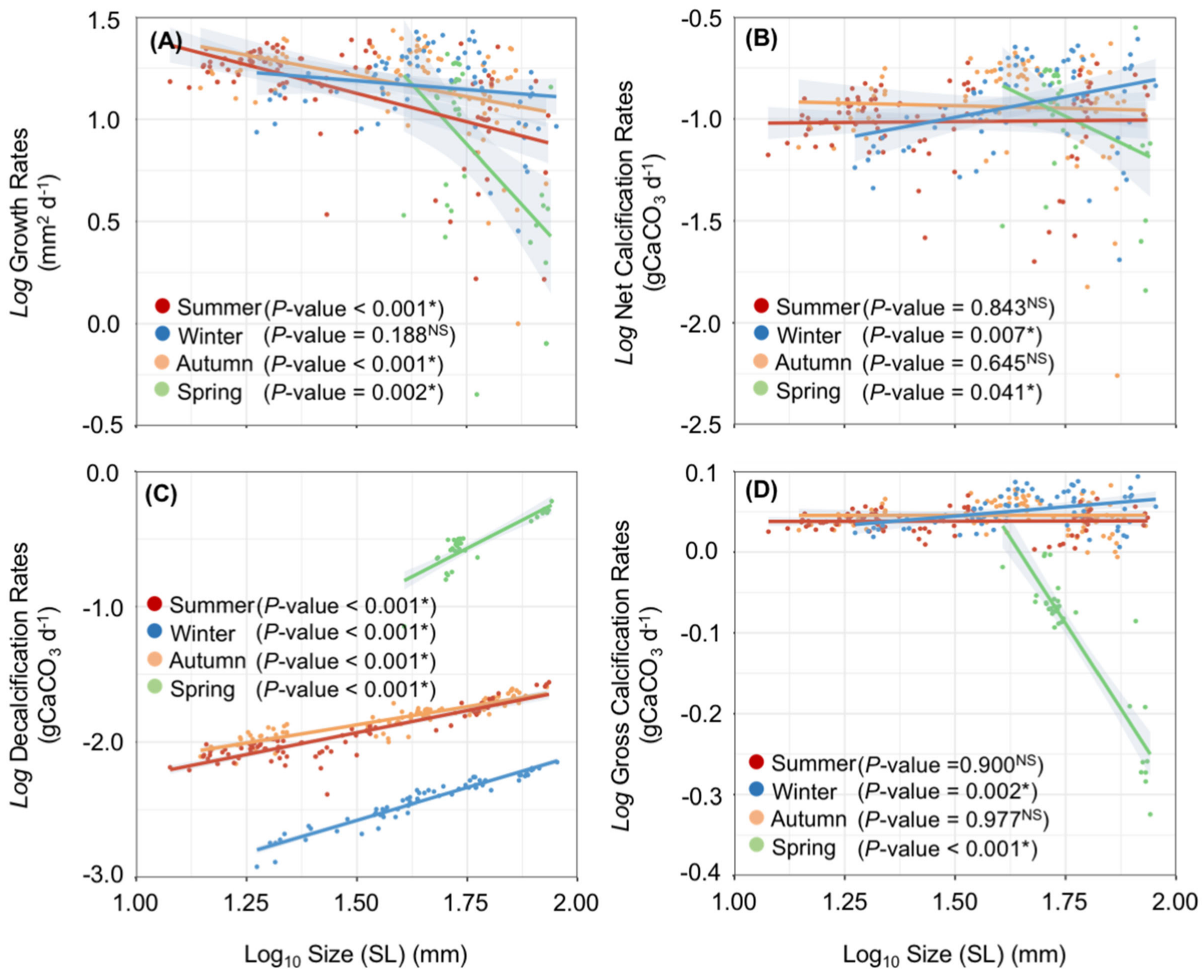

FIGURE 7
Size-related physiological performance. Growth **(A)**, net calcification**(B)**, decalcification **(C)**, and gross calcification rates **(D)** rates by shell maximum large (SL) were recorded during the four seasonal experiments. Regression P-values are shown for each season and physiological trait. * = P-value< 0.05; NS = Not significant.

organisms with significant consequences on the ecosystem structure and functioning, as well as, on the state of the socio-ecological systems (SES) related to fisheries or aquaculture (Sprogis et al., 2018; Bertrand et al., 2020). Our study shows the major role of upwelling shaping the annual physiological performance and fitness of the scallop *A. purpuratus*, one of the most important resources subjected to fishery and aquaculture along the Humboldt Current System.

Tongoy Bay, in central-north Chile, is the main location where the scallop *A. purpuratus* is cultured in Chile. This area is permanently affected by changes in seawater temperature, dissolved oxygen, pH, and primary productivity as a consequence of the upwelling transport forced by coastal wind patterns (e.g., Ramajo et al., 2020). The magnitude of environmental changes is modulated by the seasonal and intra-seasonal variability of the local atmospheric forcing controlling the phenological upwelling pattern (i.e., number, intensity, and duration of upwelling, relaxation, and downwelling events). Seasonal differences in upwelling phenology (here measured as changes in temperature, oxygen pH, and primary productivity, but also as the number, duration, and intensity of cooling and de-oxygenation events) affected the physiological performance and fitness of the different *A. purpuratus* life-stages tested. *Spring* and *summer* experimental periods showed higher intensities of cooling and deoxygenation events which, on average, produced lower growth and gross calcification rates (higher decalcification rates), especially in *A. purpuratus* adults. On the other hand, although higher mortalities were recorded under more intense upwelling periods (*spring* and *summer)*, environmental conditions driven by upwelling did not significantly affect the *A. purpuratus* survivorship confirming the high physiological flexibility and well-locally-adaptation of this species to the fluctuating and stressful environmental conditions imposed by upwelling (Lagos et al., 2016; Ramajo et al., 2016; Ramajo et al., 2020).

TABLE 2 Growth and Calcification.

Fixed Effects	Estimates	CI	*P*-value
Growth Rate (mm^2 d^{-1})			
Intercept	25.05	21.36 – 28.74	**<0.001**
Size	-0.21	-0.29 – -0.14	**<0.001**
Season	-1.43	-2.78 – -0.09	**0.037**
Size × *Season*	0.03	0.00 – 0.06	**0.030**
Random Effects	**Variance**	**SD**	
Individual	5.20	2.28	
Net Calcification Rate ($gCaCO_3$ d^{-1})			
Intercept	0.15	0.12 – 1.01	**<0.001**
Size	0.00	-0.00 – 0.00	0.071
Season	-0.02	-0.03 – -0.01	**0.004**
Size × *Season*	0.00	0.00 – 0.00	**0.002**
Random Effects	**Variance**	**SD**	
Individual	0.00	0.00	
Decalcification Rate ($gCaCO_3$ d^{-1})			
Intercept	-0.08	-0.15 – -0.01	**0.027**
Size	0.00	0.00 – -0.01	**<0.001**
Season	0.02	-0.01 – 0.04	0.225
Size × *Season*	0.00	-0.00 – -0.00	**0.011**
Random Effects	**Variance**	**SD**	
Individual	0.00	0.00	
Gross Calcification Rate ($gCaCO_3$ d^{-1})			
Intercept	0.23	0.15 – 0.31	**<0.001**
Size	0.00	-0.01 – 0.00	**<0.001**
Season	-0.03	-0.06 – -0.00	**0.023**
Size × Season	0.00	0.00 – 0.00	**0.001**
Random Effects	**Variance**	**SD**	
Individual	0.00	0.00	

Summary of statistical parameters for linear mixed-effects models for growth rates, net calcification rates, decalcification rates, and gross calcification rates. Relative variance of the random effects (individual) is shown. Bold texts show significant P-values at $\alpha = 0.05$.

It is known that upwelling, forced by the alongshore southerly favourable-winds, provokes a replacement of surface seawater by deeper water masses (Chapman, 1996; Bravo et al., 2016) which are colder, richer in nutrients and pCO_2 (low pH), and poor in oxygen concentrations (Huyer, 1983; Garcia-Reyes et al., 2015, Ramajo et al., 2020; Kämpf and Chapman, 2016). Alongshore upwelling-favourable winds at PLV (nearest upwelling center to Tongoy Bay) had significant effects on Tongoy Bay's environmental and biogeochemical conditions during the experiment, where the highest strength of upwelling (i.e., more negative Ekman transport values) occurred during the *winter* and *spring* months. Environmental conditions recorded during 2019-2020 partially agrees with previous studies that show year-round upwelling activity, peaking during the spring season at 30°S (Strub et al., 1998; Torres et al., 1999; Rutllant and Montecino, 2002; Torres and Ampuero, 2009; Aravena et al., 2014; Rahn and Garreaud, 2014). However, climate change is forcing shifts in major atmospheric high-pressure Hadley cells that trigger an intensification and a change of the intraseasonal variability of the alongshore favourable-upwelling winds (Lu et al., 2007; Rykaczewski et al., 2015; Schneider et al., 2017)

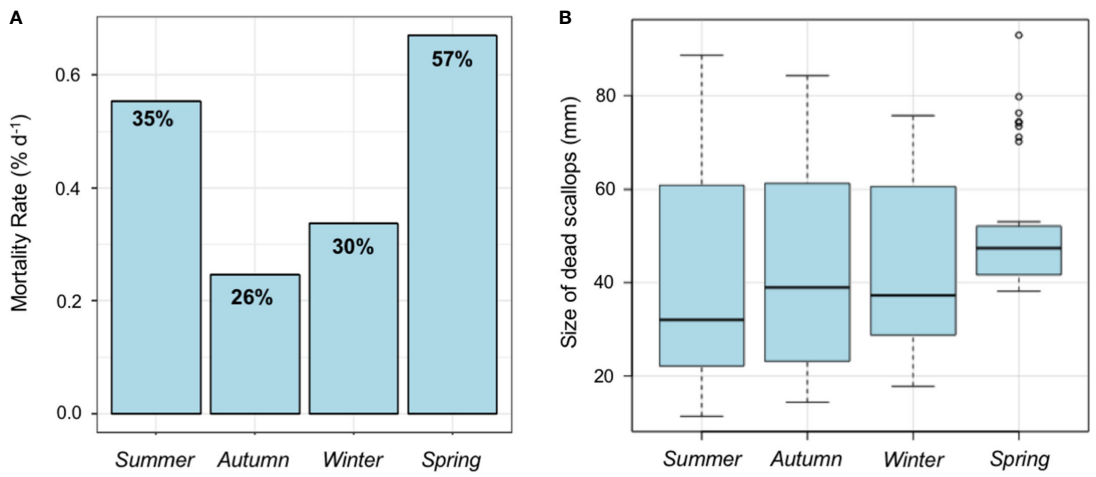

FIGURE 8
Mortality. **(A)** Mortality rates (% d^{-1}) and percentage of dead scallops recorded, and **(B)** size of dead scallop *A. purpuratus* recorded at the end of each *seasonal experiment*.

particularly, in the poleward part of the Humbolt Current System (e.g., Aguirre et al., 2018; Aguirre et al., 2021; Belmadani et al., 2014) which may be explaining why intense upwelling events occurred during the *winter* season.

Major Ekman transport values (M) were significantly correlated with lower seawater temperatures, DO and pH values, and higher Chl-*a* concentrations similar to those recently observed at Tongoy Bay by Ramajo et al. (2020). Annual seawater temperature pattern followed the solar radiation annual cycle with higher mean values recorded in *summer* and *spring*, and lower in *winter* months. However, the *summer* and *spring* months presented higher temperature variability with values ranging between 12-13°C to 18° C. Higher temperature values can be explained by the higher solar radiation occurring during the *summer* and *spring* months, while lower temperatures can be attributed to the higher cooling rates associated with upwelling events of higher intensity observed at Tongoy Bay. The lowest dissolved oxygen and pH average values were recorded in the *winter* months when Ekman transport values were higher. *Winter* and *spring* months showed a high number of de-oxygenation events with higher duration and intensity. Moreover, the

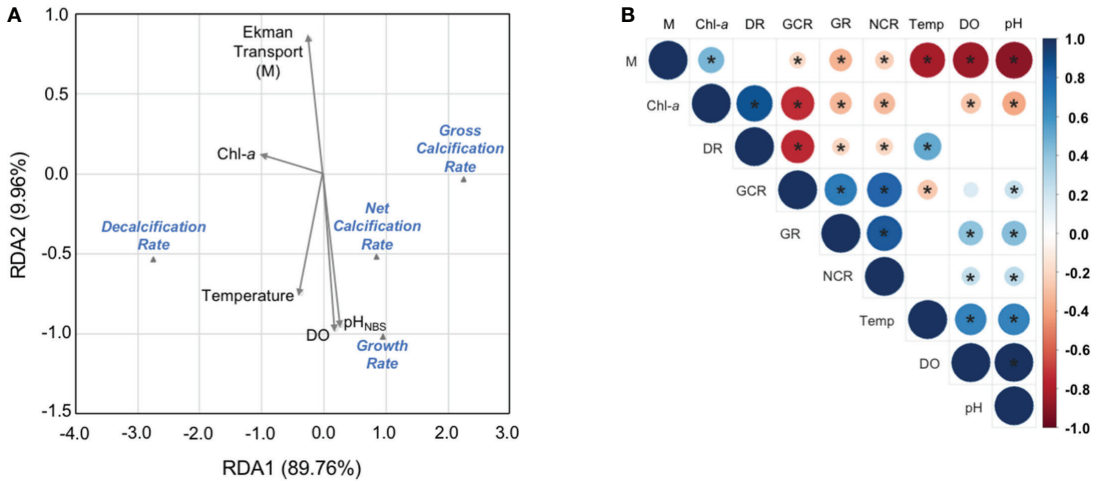

FIGURE 9
Environment and physiology. **(A)** Correlation matrix of environmental variables of Tongoy Bay with *A. purpuratus* physiological rates. Significance values at a = 0.05 are shown by asterisks (*P*-value< 0.05). **(B)** Redundancy analysis (RDA) for environmental variables (i.e. Ekman transport, temperature, DO, and pH_{NBS}) with *A. purpuratus* physiological rates (i.e. GRs, NCRs, DCRs, and GCRs).

higher speed of loss of dissolved oxygen in the water column (i.e., upwelling rate) recorded in the *winter* and *spring* seasons may be explaining the higher variability in oxygen conditions. On average, seasonal pH values were also highly correlated with higher Ekman transport values. This agrees with previous studies that determine that multiple processes such as organic matter remineralization, high oxygen consumption, and dissolved inorganic carbon (DIC) production occur at deeper depths making upwelled waters poor in oxygen and rich pCO_2 concentrations (low pH) (Umasangaji et al., 2021). Average seasonal surface Chl-*a* at Tongoy Bay also responded to the radiation and temperature annual cycle (highest values recorded in *summer* and *spring* seasons). However, during the *winter* months, when stronger upwelling-favourable winds were recorded at PLV, a peak of Chl-*a* (with values ranging between 0.6 and 18.6 mg m^{-3}) was registered. This agrees with several studies across different upwelling systems showing how nearshore productivity is coupled to local upwelling conditions (e.g., Daneri et al., 2012; Du and Peterson, 2014; Aguirre et al., 2021).

Upwelling generates important coastal environmental fluctuations at local and larger scales as a consequence of deep upwelled waters properties (i.e., colder, hypoxic-anoxic, acidic) which, in many cases, can cause physiological constraints for marine biota. Paradoxically, these areas highlight by their high productivity, high biodiversity, and significant socio-economical contributions to humans (Carr et al., 2002; Chavez and Messié, 2009; Yáñez et al., 2017). In particular, the Humboldt Current System is recognized as one of the most productive areas on a global scale (300 gC/m^2 per year, Kämpf and Chapman, 2016) holding one of the highest fisheries worldwide (Chavez et al., 2008). Only in Chile in 2018, 3.7 million tons of fish (including mollusks and crustaceans) were captured with a value of USD 11,544.1 million being aquaculture responsible for 91% of this value (OECD, 2021). In particular, scallop aquaculture in Chile is an important socioeconomic activity whose production reached 7,600 tones in 2018 (SERNAPESCA, 2019) being exported to multiple international target markets (e.g. Spain, France, Singapore, and Brazil), and contributing to more than US$5.5 million to the Chilean's export basket (Yáñez et al., 2017). However, to date, the culture of *A. purpuratus* in Chile is completely carried out in the natural environment being highly vulnerable to environmental fluctuations and climate change impact-drivers.

Our study show how *A. purpuratus* physiology was significantly altered by seasonal environmental conditions which were modulated by the presence and intensity of favourable-upwelling winds. The lowest *A. purpuratus* performance (lowest GRs and GCRs) occurred during the *spring* season when upwelling generated an elevated number and intense cooling and de-oxygenation events resulting in rapid losses of temperature and oxygen in the water column. Environment imposes biological constraints (e.g., major energy requirement) which are especially notorious when habitat conditions reach values near (or out) of the physiological tolerance ranges of species (Pörtner, 2008). In particular, cold stress has significant consequences from molecular to major physiological scales affecting cellular processes, development, metabolism, growth, and swimming capacities, among others (Pernet et al., 2007; Boroda et al., 2020). In addition, oxygen levels below physiological thresholds impact the performance, fitness, and behavior of the majority of marine taxa (e.g., Vaquer-Sunyer and Duarte, 2008). Previous studies on *A. purpuratus* show higher survivorship and growth under higher temperatures (Arntz et al., 2006) in agreement with Waller (1969) who described this species as warmed-adapted due to its tropical/sub-tropical origin. Also, more recent studies show how *A. purpuratus* is also seriously affected by hypoxia (e.g., lower growth and net calcification rates), especially when low oxygen conditions are also accompanied by changes in temperature or pH conditions (i.e., see Aguirre-Velarde et al., 2016; Ramajo et al., 2019; Ramajo et al., 2020). Indeed, multiple studies warn that low pH values are physiologically stressful for the majority of calcifying biota (Kroeker et al., 2013) affecting particularly calcification and metabolic rates, shell growth, and larval development among others (Kroeker et al., 2013). However, *A. purpuratus* living at Tongoy Bay seems to be highly adapted to acidified conditions (i.e., higher growth and calcification rates, see Ramajo et al., 2016) which have been attributed to acclimatization and local adaptation processes (Ramajo et al., 2016; Ramajo et al., 2019). Still, the magnitude and direction of changes in physiological responses to pH fluctuations depend greatly on temperature, oxygen, or food availability conditions (Ramajo et al., 2016; Lagos et al., 2016; Ramajo et al., 2019; Ramajo et al., 2020) which could explain the lowest GCRs observed during *spring* months when pH did not show the lowest values of the year, but oxygen and temperature showed important reductions.

Nevertheless, *A. purpuratus* was not only exposed to the most intense cooling and de-oxygenation events during the *spring* season but also to the most rapid reductions in temperature (cooling rate) and oxygen concentrations (de-oxygenation rate). Certainly, this had serious consequences on the physiological performance of this species (lowest GR and GCRs, and higher DRCs). Coping responses to physiological stress in marine organisms can take many shapes as they depend on the direction, duration, magnitude, and velocity of the environmental changes (Kristensen et al., 2020). In particular, the velocity of environmental changes is extremely relevant from the point of view of evolutionary processes and the expression of biological mechanisms, but also in the current context of climate change where unprecedented rapid changes are occurring in all world oceans (i.e., climate velocities, e.g., Brito-Morales et al., 2018).

Lower physiological performance during *spring* can be also explained by the annual environmental cycle as a continuous decrease in temperature, oxygen, and pH occurring from *summer* to *winter*, where *winter* also showed the lowest average temperatures, and oxygen and pH values. Continuous environmental changes and previous stressful conditions may have affected the total *A. purpuratus* energetic budget, and thus the ability to express physiological mechanisms to cope with

rapid changes in temperature and oxygen during *spring*. Fluctuating and stressful environmental conditions foster the expression of biological mechanisms that require high consumption of energy (Hendriks et al., 2015; Ramajo et al., 2020) which also promote the energetic requirements re-allocation and the apparition of physiological *trade-offs*, lower physiological performance, and decreased fitness (e.g., Pan et al., 2015). This may be explaining the steady decay in GRs, NCRs and GCRs observed during the experiment. On the other hand, food supply could also explain why *A. purpuratus* fitness was not affected during the *summer* and *spring* months, as both seasons also presented the highest food availability conditions (i.e., higher Chl-*a* concentrations). Previous studies have observed and suggested that *A. purpuratus* can increase its feeding rates under low pH (Ramajo et al., 2016) and after intense upwelling events to recover from physiological stressful conditions (see Ramajo et al., 2020).

Energetic demands for maintenance and reproduction change across sizes and ages (Kooijman, 2000). Thus, it can be expected that not all life-stages cope equally with environmental fluctuations as different life-stages present different necessities in terms of food, oxygen availability, and calcium carbonate supply (Baumann et al., 2012). Our study shows how seasonal physiological responses of *A. purpuratus* were significantly modulated by the size (age) (Table 1), especially when environmental conditions pose a physiologically stressful scenario with rapid cooling and deoxygenation/corrosive rates (i.e., *Spring* season, see Figure 7). *Size* seems to be a key factor explaining the thermal tolerances of *A. purpuratus* which may explain different results among previous studies. Meanwhile, Arntz et al. (2006) and Lagos et al. (2016) studies detected a higher tolerance of *A. purpuratus* under higher than lower temperatures, Ramajo et al. (2019) concluded that *A. purpuratus* seems to be a species better adapted to cold than warmer conditions. These differences among studies may be attributed to differences in the life-stages tested as Arntz et al. (2006) and Lagos et al. (2016) studies were performed on larvae or adult organisms, while Ramajo et al. (2019) experiment was accomplished on juveniles. A similar physiological pattern has been observed to compare the physiological performance of juveniles and adults to changes in pH (see Ramajo et al., 2016; Lagos et al., 2016). Unfortunately, to date, no studies addressing the oxygen availability impact among different *A. purpuratus* life-stages have been yet performed.

The lower physiological performance observed in *A. purpuratus* adult stages as a consequence of more intense upwelling conditions occurring during the spring season may have additional impacts on aquaculture production as the scallop industry in Tongoy Bay mainly relies on natural larvae captured from the natural environment. Although *A. purpuratus* gametes release can occur throughout the year, this is more active in the austral spring and summer seasons when higher food availability (Chl-*a* concentrations) is present due to nutrients supplied by upwelling (Avendaño et al., 2008). However, unusual intense upwelling events and related stressful conditions could have important impacts on the reproductive *A. purpuratus* conditions (i.e., gamete release, spawning time, as well as egg production and larval survivorship). Multiple studies in bivalve species show how temperature, pH, and oxygen conditions modulate multiple reproductive adult traits including larvae availability and their survivorship (i.e., Kroeker et al., 2013; Breitburg et al., 2018). In particular, for *A. purpuratus*, studies performed by Cantillánez et al. (2005, 2006, 2008) and Avendaño et al. (2005) show how dates of spawning events occur under higher water temperatures and food availability conditions. Here, although *A. purpuratus* reproductive-related traits were not addressed, our results (i.e., lower performance in older scallops) suggest that intense cooling and deoxygenation/corrosive conditions driven by intense upwelling events may constrain reproductive *A. purpuratus* cycle due to growth-maintenance-reproduction *trade-offs* which are more evident in older stages as energetic costs are size and volume-dependent (see the introduction for references).

In brief, our study concludes that physiological sensitivity to isolated environmental variables is not able to entirely explain the seasonal physiological performance of *A. purpuratus*. Upwelling imposes differential physiological pressures across *A. purpuratus* life-stages, where the combination of intensity and the velocity of the changes, as well as the food availability, modulated the performance and the energy available to cope with uninterrupted (and sometimes stressful) environmental conditions. This highlight the necessity of considering marine upwelling habitats as highly complex and heterogenous environmental entities where fluctuations ranges (and not only average values), the speed of changes, and the nature of the interaction (antagonist, synergistic, additive) among environmental variables need to be considered to make better projections about the future of fisheries and shell marine aquaculture (SMA) developed in EBUS (Henson et al., 2017; Kristensen et al., 2020). In particular, this is highly relevant along the Humboldt Current System, as the coastal invertebrates' catches have shown sustained growth since 1950, and specifically, SMA is a growing productive activity with an elevated socio-economic impact on the region and worldwide (FAO 2005-2021; Gutiérrez et al., 2017). However, to date, understanding how SMA in this region will cope with future climate conditions driven by changes in upwelling, ocean acidification, or ocean deoxygenation as a consequence of climate change is not completely understood as it requires an adequate comprehension of the environmental dynamics of marine systems, as well as, better knowledge about the physiological tolerance of the species and their different life-stages to heterogeneous conditions.

Data availability statement

The raw data supporting the conclusions of this article will be made available by the authors, without undue reservation.

Author contributions

LR designed and conceived the study. CS-H, MV, JI, and LR conducted the experiment. LR, MV, and JI registered and measured the environmental data. MV and OA provided wind data and upwelling index estimations. LR, CS-H, and MV analyzed the data. LR, CS-H, and MV prepared the manuscript. All authors contributed to the article and approved the submitted version.

Funding

This study was funded by FONDECYT Project #3170156 to LR. LR and CS-H acknowledge the support from the "Center for the study of multiple drivers on marine socio-ecological systems (MUSELS) from the Ministerio de Economía, Fomento y Turismo. OA acknowledges the support from FONDECYT project #11190999. LR, MV, OA, and JI acknowledge the support from ANID-CENTROS REGIONALES R20F0008 (CEAZA). LR acknowledges the support from FONDAP/ANID 15110009, and grants PID2020-116660GB-I00 (Ministerio de Ciencia e Innovación, Spain), grupo RNM-938, B-RNM-265-UGR18 and P20_00207 (Junta de Andalucía, Spain).

Acknowledgments

We are very grateful to Julia Godoy, Pamela Tapia, Christian Tapia from OSTIMAR S.A., and Tongoy local school (Liceo Carmen Rodríguez Henriquez) for their support during the experiments. We thank Carolina Fernández, Paul Watt-Arévalo, Manuel Núñez, Marco A. Lardies, Bernardo Broitman, William Farias, and Fernanda Oyarzún for their support and help during the study. Finally, we want to acknowledge Cristian Duarte and Loretto Contreras for their valuable comments and suggestions while the research was conducted. Scientific illustrations in the figures are courtesy of the Integration and Application Network (http://ian.umces.edu/symbols), University of Maryland Center for Environmental Science.

Conflict of interest

The authors declare that the research was conducted in the absence of any commercial or financial relationships that could be construed as a potential conflict of interest.

Publisher's note

Supplementary material

The Supplementary Material for this article can be found online at: https://www.frontiersin.org/articles/10.3389/fmars.2022.992319/full#supplementary-material

References

Aguirre, C., García-Loyola, S., Testa, G., Silva, D., and Farias, L. (2018). Insight into anthropogenic forcing on coastal upwelling off south-central Chile. *Elem. Sci. Anth.* 6 (1), 59. doi: 10.1525/elementa.314

Aguirre-Velarde, A., Jean, F., Thouzeau, G., and Flye-Sainte-Marie, J. (2016). Effects of progressive hypoxia on oxygen uptake in juveniles of the Peruvian scallop, *Argopecten purpuratus* (Lamarck 1819). *Aquaculture* 451, 385–389. doi: 10.1016/j.aquaculture.2015.07.030

Aguirre, C., Garreaud, R., Belmar, L., Farías, L., Ramajo, L., and Barrera, F. (2021). High-Frequency Variability of the Surface Ocean Properties Off Central Chile During the Upwelling Season. *Front. Mar. Sci.* doi: 10.3389/fmars.2021.702051

Aravena, G., Broitman, B., and Stenseth, N. C. (2014). Twelve years of change in coastal upwelling along the central-northern coast of Chile: spatially heterogeneous responses to climatic variability. *PloS One* 9 (2), e90276. doi: 10.1371/journal.pone.0090276

Arntz, W. E., Gallardo, V. A., Gutiérrez, D., Isla, E., Levin, L. A., Mendo, J., et al (2006). El Niño and similar perturbation effects on the benthos of the Humboldt, California, and Benguela Current upwelling ecosystems. *Adv. Geosci.* 6, 243–265. doi: 10.5194/adgeo-6-243-2006

Avendaño, M., and Cantillánez, M. (2022). *Argopecten purpuratus* (Mollusca, pectinidae) post-El niño 1997-98 response in la rinconada marine reserve (Antofagasta, Chile). *Lat. Am. J. Aquat. Res.* 50 (2), 168–180. doi: 10.3856/vol50-issue2-fulltext-2776

Avendaño, M., Cantillánez, M., Le Pennec, M., and Thouzeau, G. (2008). Reproductive and larval cycle of the scallop argopecten purpuratus (Ostreoida: Pectinidae), during El niño-la niña events and normal weather conditions in antofagasta, Chile. *Rev. Biología Trop.* 56 (1), 121–132.

Avendaño, M., Cantillánez, M., and Peña, J. (2006). Effect of immersion time of culthch on spatfall of the scallop argopecten purpuratus (Lamarck 1819) in the marine reserve at la rinconada, antofagasta, Chile. *Aquacul. Int.* 14, 267–283. doi: 10.1007/s10499-005-9033-y

Avendaño, M., Cantillánez, M., Rodríguez, L., Zúñiga, O., Escribano, R., and Oliva, M. (2005). *Crecimiento y estructura demográfica de Argopecten purpuratus en la reserva marina La Rinconada* (Antofagasta, Chile: Ciencias marina). 31 (3), 491–503.

Bakun, A., Black, B. A., Bograd, S. J., García-Reyes, M., Miller, A. J., Rykaczewki, R. R., et al (2015). Anticipated effects of climate change on coastal upwelling ecosystems. *Curr. Clim. Change Rep.* 1, 85–93. doi: 10.1007/s40641-015-0008-4

Bakun, A. (1975). *Daily and weekly upwelling indices, west coast of North Americ-73* (U.S: Department of Commerce), 114. Available at: https://repository.library.noaa.gov/view/noaa/15387.

Basilio, C. D., Cañete, J. I., and Rozbaczylo, N. (1995). Polydora sp. (Spionidae), un poliqueto perforador de las valvas del ostión argopecten purpuratus (Bivalvia: Pectinidae) en bahía tongoy, Chile. *Rev. Biología Marina* 30, 71–77. doi: 10.4067/S0718-19572001000100009

Baumann, H., Talmage, S. C., and Gobler, J. (2012). Reduced early life growth and survival in a fish in direct response to increased carbon dioxide. *Nat. Clim. Change* 2, 38–41. doi: 10.1038/nclimate1291

Bayne, B. L., and Newell, R. C. (1983). Physiological Energetics of Marine Molluscs. Eds. Saleuddin, A. S. M, and Wilbur, K. M. B. T.-T. M. (Academic press), 407–515. doi: 10.1016/B978-0-12-751404-8.50017-7

Belmadani, A., Echevin, V., Codron, F., Takahashi, K., and Junquas, C. (2014). What dynamics drive future wind scenarios for coastal upwelling off Peru and Chile? *Clim. Dyn.* 43, 1893–1914. doi: 10.1007/s00382-013-2015-2

Bertrand, A., Lengaigne, M., Takahashi, K., Avadi, A., Poulain, F., and Harrod, C (2020). *El Niño southern oscillation (ENSO) effects on fisheries and aquaculture. FAO fisheries and aquaculture technical paper no. 660* (Rome: FAO). doi: 10.4060/ca8348en

Boroda, A. V., Kipryushina, Y. O., and Odintsova, N. A. (2020). The effects of cold stress on mytilus species in the natural environment. *Cell Stress Chaperones* 25 (6), 821–832. doi: 10.1007/s12192-020-01109-w

Bravo, L., Ramos, M., Astudillo, O., Dewitte, B., and Goubanova, K. (2016). Seasonal variability of the ekman transport and pumping in the upwelling system off central-northern Chile (∼ 30° s) based on a high-resolution atmospheric regional model (WRF). *Ocean Sci.* 12 (5), 1049–1065. doi: 10.5194/os-12-1049-2016

Breitburg, D., Levin, L. A., Oschlies, A., Grégoire, M., Chaves, F. P., Conley, D. J., et al (2018). Declining oxygen in the global ocean and coastal waters. *Science* 359 (6371), eaam7240. doi: 10.1126/science.aam7240

Brito-Morales, I., García-Molinos, J., Schoeman, D. S., Burrows, M. T., Poloczanska, E. S., Brown, C. J., et al (2018). Climate Velocity Can Inform Conservation in a Warming World. *Trends Ecol. Evol.* 33 (6), 441–457. doi: 10.1016/j.tree.2018.03.009

Byrne, M. (2012). Global change ecotoxicology: Identification of early life history bottlenecks in marine invertebrates, variable species responses and variable experimental approaches. *Mar. Environ. Res* 76, 3–15. doi: 10.1016/j.marenvres.2011.10.004

Cantillánez, M., Avendaño, M., Thouzeau, G., and Le Pennec, M. (2005). Reproductive cycle of argopecten purpuratus (Bivalvia: Pectinidae) in la rinconada marine reserve, (Antofagasta, chile): response to environmental effects of El niño and la niña. *Aquaculture* 246, 181–195. doi: 10.1016/j.aquaculture.2004.12.031

Carr, M.-E., Strub, P. T., Thomas, A. C., and Blanco, J. L. (2002). Evolutions of the 1996–1999 la niña and El niño conditions off the western coast of south America: a remote sensing perspective. *J. Geophys. Res.* 108 (C12), 3236. doi: 10.1029/2001JC001183

Chapman, P. (1996). Upwelling in the ocean: Modern processes and ancient records. *Limnology Oceanography* 41. doi: 10.4319/lo.1996.41.7.1585

Chauvaud, L., Patry, Y., Jolivet, A., Cam, E., Le Goff, C., Strand, Ø., et al (2012). Variation in size and growth of the great scallop pecten maximus along a latitudinal gradient. *PloS One* 7 (5), e37717. doi: 10.1371/journal.pone.0037717

Chavez, F. P., and Messié, M. (2009). A comparison of eastern boundary upwelling ecosystems. *Prog. Oceanogr.* 83, 80–96. doi: 10.1016/j.pocean.2009.07.032

Chavez, F. P., Bertrand, A., Guevara-Carrasco, R., Soler, P., and Csirke, J. (2008). The Northern Humboldt Current System: ocean dynamics, ecosystem processes, and fisheries. *Prog. Oceanogr* 79, 95–105. doi: 10.1016/j.pocean.2008.10.012

Clark, M. S., Peck, L. S., Arivalagan, J., Backeljau, T., Berland, S., Cardoso, J. C., et al (2020). Deciphering mollusc shell production: the roles of genetic mechanisms through to ecology, aquaculture and biomimetics. *Biol. Rev.* 95 (6), 1812–1837. doi: 10.1111/brv.12640

Clark, H. R., and Gobler, C. J. (2016). Diurnal fluctuations in CO2 and dissolved oxygen concentrations do not provide a refuge from hypoxia and acidification for early-life-stage bivalves. *Mar. Ecol. Prog. Ser.* 558, 1–14. doi: 10.3354/meps11852

Cury, P., and Roy, C. (1989). Optimal environmental window and pelagic fish recruitment success in upwelling areas. *Can. J. Fish. Aquat. Sci.* 46 (4), 670–680. doi: 10.1139/f89-086

Daneri, G., Lizárraga, L., Montero, P., González, H. E., and Tapia, ,. F. J. (2012). Wind forcing and short-term variability of phytoplankton and heterotrophic bacterioplankton in the coastal zone of the Concepción upwelling system (Central Chile). *Prog. Oceanography* 92–95, 92–96. doi: 10.1016/j.pocean.2011.07.013

Davies, P. S. (1989). Short-term growth measurements of corals using an accurate buoyant weighing technique. *Mar. Biol.* 101, 389–395. doi: 10.1007/BF00428135

Du, X., and Peterson, W. T. (2014). Seasonal Cycle of Phytoplankton Community Composition in the Coastal Upwelling System Off Central Oregon in 2009. *Estuaries Coasts* 37, 299–311. doi: 10.1007/s12237-013-9679-z

Falvey, M., and Garreaud, R. D. (2009). Regional cooling in a warming world: Recent temperature trends in the southeast pacific and along the west coast of subtropical south america, (1979–2006). *J. Geophys. Res.: Atmospheres* 114 (D4), D04102. doi: 10.1029/2008JD010519

FAO (2005-2021). "World inventory of fisheries. Subsidies and trade distortion. Issues Fact Sheets," in *Text by Audun Lem* (Rome: FAO Fisheries Division [online]).

Figueroa, D., and Moffat, C. (2000). On the influence of topography in the induction of coastal upwelling along the Chilean coast. *Geophys. Res. Lett.* 27 (23), 3905–3908. doi: 10.1029/1999GL011302

García-Reyes, M., Largier, J. L., and Sydeman, W. J. (2014). Synoptic-scale upwelling indices and predictions of phyto- and zooplankton populations. *Prog. Oceanogr.* 120, 177–188. doi: 10.1016/j.pocean.2013.08.004

García-Reyes, M., Sydeman, W. J., Schoeman, D. S., Rykaczewski, R. R., Black, B. A., Smit, A. J., et al (2015). Under Pressure: Climate Change, Upwelling, and Eastern Boundary Upwelling Ecosystems. *Front. Mar. Sci.* doi: 10.3389/fmars.2015.00109

Garreaud, R., and Muñoz, R. C. (2005). The low-level jet off the west coast of subtropical south America: Structure and variability. *Monthly Weather Rev.* 133 (8), 2246–2261. doi: 10.1175/MWR2972.1

Gaylord, B., Kroeker, K. J., Sunday, J. M., Anderson, K. M., Barry, J. P., Brown, N. E., et al (2015). Ocean acidification through the lens of ecological theory. *Ecology* 96 (1), 3–15. doi: 10.1890/14-0802.1

Gazeau, F., Parker, L. M., Comeau, S., Gattuso, J. P., O'Connor, W. A., Martin, S., et al (2013). Impacts of ocean acidification on marine shelled molluscs. *Mar. Biol.* 160, 2207–2245. doi: 10.1007/s00227-013-2219-3

Gutiérrez, D., Akester, M., and Naranjo, L. (2017). Productivity and Sustainable Management of the Humboldt Current Large Marine Ecosystem under climate change. *Environ. Dev.* 17, 126–144. doi: 10.1016/j.envdev.2015.11.004

Hendriks, I. E., Duarte, C. M., Olsen, Y. S., Steckbauer, A., Ramajo, L., Moore, T. S., et al (2015). Biological mechanisms supporting adaptation to ocean acidification in coastal ecosystems. *Estuarine Coast. Shelf Sci.* 152, A1–A8. doi: 10.1016/j.ecss.2014.07.019

Henson, S., Beaulieu, C., Ilyina, T., John, J. G., Long, M., Séférian, R., et al (2017). Rapid emergence of climate change in environmental drivers of marine ecosystems. *Nat. Commun.* 8, 14682. doi: 10.1038/ncomms14682

Huyer, A. (1983). Coastal upwelling in the California current system. *Prog. Oceanogr.* 12, 259–284. doi: 10.1016/0079-6611(83)90010-1

IPCC (2021). "Climate Change 2021: The Physical Science Basis. Contribution of Working Group I to the Sixth Assessment Report of the Intergovernmental Panel on Climate Change,". Eds. V. Masson-Delmotte, P. Zhai, A. Pirani, S. L. Connors, C. Péan, S. Berger, et al (Cambridge, United Kingdom and New York, NY, USA: Cambridge University Press). doi: 10.1017/9781009157896

Kämpf, J., and Chapman, P. (2016). *Upwelling systems of the world. A scientific journey to the most productive marine ecosystems* (Switzerland: Springer International Publishing). doi: 10.1007/978-3-319-42524-5

Kooijman, S (2000). *Dynamic Energy and Mass Budgets in Biological Systems* (2nd ed.). Cambridge: Cambridge University Press. doi: 10.1017/CBO9780511565403

Kristensen, T. N., Ketola, T., and Kronholm, I. (2020). Adaptation to environmental stress at different timescales. *Ann. N.Y. Acad. Sci.* 1476, 5–22. doi: 10.1111/nyas.13974

Kroeker, K. J., Kordas, R. L., Crim, R., Hendriks, I. E., Ramajo, L., Singh, G. S., et al (2013). Impacts of ocean acidification on marine organisms: quantifying sensitivities and interaction with warming. *Glob Change Biol* 19, 1884–1896. doi: 10.1111/gcb.12179

Lagos, N. A., Benítez, S., Duarte, C., Lardies, M. A., Broitman, B. R., Tapia, C., et al (2016). Effects of temperature and ocean acidification on shell characteristics of argopecten purpuratus: implications for scallop aquaculture in an upwelling-influenced area. *Aquacult. Environ. Interact.* 8, 357–370. doi: 10.3354/aei00183

Lagos, N. A., Benítez, S., Grenier, C., Rodriguez-Navarro, A. B., García-Herrera, C., Abarca-Ortega, A., et al (2021). Plasticity in organic composition maintains biomechanical performance in shells of juvenile scallops exposed to altered temperature and pH conditions. *Sci. Rep.* 11, 24201. doi: 10.1038/s41598-021-03532-0

Langer, G., Nehrke, G., Baggini, C., Rodolfo-Metalpa, R., Hall-Spencer, J. M., and Bijma, J. (2014). Limpets counteract ocean acidification induced shell corrosion by thickening of aragonitic shell layers. *Biogeosciences* 11, 7363–7368. doi: 10.5194/bg-11-7363-2014

Lardies, M. A., Benitez, S., Osores, S., Vargas, C. A., Duarte, C., Lohrmann, K. B., et al (2017). Physiological and histopathological impacts of increased carbon dioxide and temperature on the scallops argopecten purpuratus cultured under upwelling influences in northern Chile. *Aquaculture* 479, 455–466. doi: 10.1016/j.aquaculture.2017.06.008

Lluch-Cota, S. E., Hoegh-Guldberg, O., Karl, D., Pörtner, H. O., Sundby, S., and Gattuso, J. P. (2014). "Cross-chapter box on uncertain trends in major upwelling ecosystems," in *Climate change 2014: Impacts, adaptation, and vulnerability. part a: Global and sectoral aspects. contribution of working group II to the fifth assessment report of the intergovernmental panel of climate change*. Eds. C. B. Field, V. R. Barros, D. J. Dokken, K. J. Mach and M. D. Mastrandrea (Cambridge, Uk: New York, NY: Cambridge University Press), 149–151.

Lu, J., Vecchi, G. A., and Reichler, T. (2007). Expansion of the Hadley cell under global warming. *Geophys. Res. Lett.* 34, L06805. doi: 10.1029/2006GL028443

MacLeod, C. D., and Poulin, R. (2015). Interactive effects of parasitic infection and ocean acidification on the calcification of a marine gastropod. *Marine Ecology Progress Series*. 537, 137–150. doi: 10.1016/j.ijpara.2015.02.007

Moraga-Opazo, J., Valle-Levinson, A., Ramos, M., and Pizarro-Koch, M. (2011). Upwelling-triggered near-geostrophic recirculation in an equatorward facing embayment. *Continental Shelf Res.* 31 (19-20), 1991–1999. doi: 10.1016/j.csr.2011.10.002

OECD (2021). "The Organization for Economic Cooperation and Developmen)," in *Fisheries and Aquaculture in Chile January 2021* (Paris (France: . OECD Review of Fisheries Country Notes).

Palmer, A. R. (1981). Do carbonate skeletons limit the rate of body growth? *Nature* 292 (5819), 150–152. doi: 10.1038/292150a0

Pan, T. C. F., Applebaum, S. L., and Manahan, ,. D. T. (2015). Experimental ocean acidification alters the allocation of metabolic energy. *Proc. Natl. Acad. Sci.* 112 (15), 4696–4701. doi: 10.1073/pnas.1416967112

Pernet, F., Tremblay, R., Comeau, L., and Guderley, H. (2007). Temperature adaptation in two bivalve species from different thermal habitats: energetics and remodelling of membrane lipids. *J. Exp. Biol.* 210 (17), 2999–3014. doi: 10.1242/jeb.006007

Pörtner, H. (2008). Ecosystem effects of ocean acidification in times of ocean warming: a physiologist's view. *Mar. Ecol. Prog. Ser.* 373, 203–217. doi: 10.3354/meps07768

Rahn, D. A., and Garreaud, R. D. (2014). A synoptic climatology of the near-surface wind along the west coast of south America. *Int. J. Climatol.* 34 (3), 780–792. doi: 10.1002/joc.3724

Ramajo, L., Prado, L., Rodriguez-Navarro, A. B., Lardies, M. A., Duarte, C. M., and Lagos, N. A. (2016). Plasticity and trade-offs in physiological traits of intertidal mussels subjected to freshwater-induced environmental variation. *Mar. Ecol. Prog. Ser.* 553, 93–109. doi: 10.3354/meps11764

Ramajo, L., Fernández, C., Núñez, Y., Caballero, P., Lardies, M. A., and Poupin, M. J. (2019). Physiological responses of juvenile Chilean scallops (Argopecten purpuratus) to isolated and combined environmental drivers of coastal upwelling. *ICES J. Mar. Sci.* 76 (6), 1836–1849. doi: 10.1093/icesjms/fsz080

Ramajo, L., Valladares, M., Astudillo, O., Fernández, C., Rodríguez-Navarro, B. A., Watt-Arévalo, P., et al (2020). Upwelling intensity modulates the fitness and physiological performance of coastal species: Implications for the aquaculture of the scallop argopecten purpuratus in the Humboldt current system. *Sci. Total Environ* 745, 140949. doi: 10.1016/j.scitotenv.2020.140949

Renault, L., Dewitte, B., Falvey, M., Garreaud, R., Echevin, V., and Bonjean, F. (2009). Impact of atmospheric coastal jet off central Chile on sea surface temperature from satellite observations, (2000–2007). *J. Geophys. Res.* 114, C08006. doi: 10.1029/2008JC005083

Rutllant, J., and Montecino, V. (2002). Multiscale upwelling forcing cycles and biological response off north-central Chile. *Rev. Chil. Hist. Natural* 75 (217), e231. doi: 10.4067/S0716-078X2002000100020

Rykaczewski, R. R., Dunne, J. P., Sydeman, W. J., García-Reyes, M., Black, B. A., and Bograd, S. J. (2015). Poleward displacement of coastal upwelling-favorable winds in the ocean's eastern boundary currents through the 21st century. *Geophys. Res. Lett.* 42, 6424–6431. doi: 10.1002/2015GL064694

Schneider, W., Donoso, D., Garcés-Vargas, J., and Escribano, R. (2017). Water-column cooling and sea surface salinity increase in the upwelling region off central Chile driven by a pole-ward displacement of the south pacific high. *Prog. Oceanogr.* 151, 38–48. doi: 10.1016/j.pocean.2016.11.004

Seibel, B. A. (2011). Critical oxygen levels and metabolic suppression in oceanic oxygen minimum zones. *J. Exp. Biol.* 214 (2), 326–336. doi: 10.1242/jeb.049171

SERNAPESCA (2019) *Desembarque total*. Available at: http://www.sernapesca.cl/sites/default/files/2019_0301_desembarque_total.pdf (Accessed December 9, 2022).

Sprogis, K. R., Christiansen, F., Wandres, M., and Bejder, L. (2018). El Niño southern oscillation influences the abundance and movements of a marine top predator in coastal waters. *Glob Change Biol.* 24, 1085–1096. doi: 10.1111/gcb.13892

Strub, P. T., Shillington, F. A., James, C, and Weeks, S. J. (1998). Satellite comparison of the seasonal circulation in the Benguela and California current systems. *South African Journal of Marine Science*, 19 (1), 99-112. doi: 10.2989/025776198784126836

Sydeman, W. J., García-Reyes, M., Schoeman, D. S., Rykaczewski, R. R., Thompson, S. A., Black, B. A., et al (2014). Climate change and wind intensification in coastal upwelling ecosystems. *Science* 345 (6192), 77–80. doi: 10.1126/science.1251635

Talmage, S. C., and Gobler, ,. C. J. (2010). Effects of past, present, and future ocean carbon dioxide concentrations on the growth and survival of larval shellfish. *Proc. Natl. Acad. Sci.* 107 (40), 17246–17251. doi: 10.1073/pnas.0913804107

Tapia, F. J., Navarrete, S. A., Castillo, M., Menge, B. A., Castilla, J. C., Largier, J., et al (2009). Thermal indices of upwelling effects on inner-shelf habitats. *Prog. Oceanography* 83, 278–287. doi: 10.1016/j.pocean.2009.07.035

Thiel, M., et al (2007) *The Humboldt current system of northern and central Chile*. Available at: https://www.webofscience.com/wos/WOSCC/full-record/000252476600006.

Thompson, R. J., and MacDonald, B. A. (2006). "Chapter 8 Physiological integrations and energy partitioning," in S. E. Shumway and F. S. Parsons Eds. *Scallops: Biology, Ecology and Aquaculture*. (Elsevier), 35, 493–520. doi: 10.1016/S0167-9309(06)80035-9

Thomsen, J., Haynert, K., Wegner, K.M., and Melzner, F. (2015). Impact of seawater carbonate chemistry on the calcification of marine bivalves. *Biogeosciences* 12, 4209–4220. doi: 10.5194/bg-12-4209-2015

Torres, R., and Ampuero, P. (2009). Strong CO2 outgassing from high nutrient low chlorophyll coastal waters off central Chile (30 s): The role of dissolved iron. *Estuarine Coast. Shelf Sci.* 83 (2), 126–132. doi: 10.1016/j.ecss.2009.02.030

Torres, R., Turner, D. R., Silva, N., and Rutllant, J. (1999). High short-term variability of CO2 fluxes during an upwelling event off the Chilean coast at 30 s. *Deep Sea Res. Part I: Oceanogr. Res. Papers* 46 (7), 1161–1179. doi: 10.1016/S0967-0637(99)00003-5

Truebano, M., Fenner, P., Tills, O., Rundle, S. D., and Rezende, E. L. (2018). Thermal strategies vary with life history stage. *J. Exp. Biol.* 221 (8), jeb171629. doi: 10.1242/jeb.171629

Trussell, G. C., and Smith, L. D. (2000). Induced defenses in response to an invading crab predator: an explanation of historical and geographic phenotypic change. *Proc. Natl. Acad. Sci.* 97 (5), 2123–2127. doi: 10.1073/pnas.040423397

Umasangaji, H., and Ramili, Y. (2021). "Mini review: Characteristics of upwelling in several coastal areas in the world," in *IOP Conference Series: Earth and Environmental Science*, Vol. 890. 012004 (IOP Publishing). doi: 10.1088/1755-1315/890/1/012004

Vaquer-Sunyer, R., and Duarte, C. M. (2008). Thresholds of hypoxia for marine biodiversity. *Proc Natl Acad Sci U S A*. doi: 10.1073/pnas.0803833105

von Brand, E., Abarca, A., Merino, G. E., and Stotz, W. (2016). "Scallop fishery and aquaculture in Chile: A history of developments and declines," in *Scallop, biology, ecology, aquaculture and fisheries*. Eds. S. E. Shumway and J. G. (Oxford: Elsevier), 1047–1072. doi: 10.1016/B978-0-444-62710-0.00026-2

Waldbusser, G. G., Hales, B., Langdon, C. J., Haley, B. A., Schrader, P., Brunner, E. L., et al (2015). Ocean acidification has multiple modes of action on bivalve larvae. *PloS One* 10 (6), e0128376. doi: 10.1371/journal.pone.0128376

Waldbusser, G. G., Voigt, E. P., Bergschneider, H., Green, M. A., and Newell, R. I. E. (2011). Biocalcification in the Eastern oyster (Crassostrea virginica) in relation to long-term trends in Chesapeake bay pH. *Estuaries Coasts* 34, 221–231. doi: 10.1007/s12237-010-9307-0

Waller, T. R. (1969). The evolution of the *Argopecten gibbus* stock (Mollusca: Bivalvia), with emphasis on the Tertiary and Quaternary species of eastern North America. *Memoir (The Paleontological Society)* 3, i–125.

Wessel, N., Martin, S., Badou, A., Dubois, P., Huchette, S., Julia, V., et al (2018). Effect of CO2–induced ocean acidification on the early development and shell mineralization of the European abalone (Haliotis tuberculata). *J. Exp. Mar. Biol. Ecol* 508, 52–63. doi: 10.1016/j.jembe.2018.08.005

Yáñez, E., Lagos, N.A., Norambuena, R., Silva, C., Letelier, J., Muck, K.-P., et al (2017). Impacts of climate change on marine fisheries and aquaculture in Chile. *Climate Change Impacts Fish. Aquacult.: A Global Anal.* 1 (1), 239–342. doi: 10.1002/9781119154051.ch10

Zhao, X., Han, Y., Chen, B., Xia, B., Qu, K., and Liu, G. (2020). CO2-driven ocean acidification weakens mussel shell defense capacity and induces global molecular compensatory responses. *Chemosphere* 243, 125415. doi: 10.1016/j.chemosphere.2019.125415

frontiers | Frontiers in Marine Science

TYPE Data Report
PUBLISHED 23 December 2022
DOI 10.3389/fmars.2022.1094814

OPEN ACCESS

EDITED BY
Jonathan Y.S. Leung,
University of Adelaide, Australia

REVIEWED BY
Chunlin Wang,
Ningbo University, China
Kai Liao,
Ningbo University, China

*CORRESPONDENCE
Lina Sun
sunlina@qdio.ac.cn

SPECIALTY SECTION
This article was submitted to Global Change and the Future Ocean, a section of the journal Frontiers in Marine Science

RECEIVED 10 November 2022
ACCEPTED 07 December 2022
PUBLISHED 23 December 2022

CITATION
Huo D, Su F, Zhang L, Yang H and Sun L (2022) Temperature and dissolved oxygen influence the immunity, digestion, and antioxidant level in sea cucumber *Apostichopus japonicus*. *Front. Mar. Sci.* 9:1094814. doi: 10.3389/fmars.2022.1094814

Temperature and dissolved oxygen influence the immunity, digestion, and antioxidant level in sea cucumber *Apostichopus japonicus*

Da Huo[1,2,3,4,5], Fang Su[1,2,3,4,5,6], Libin Zhang[1,2,3,4,5,6], Hongsheng Yang[1,2,3,4,5,6,7] and Lina Sun[1,2,3,4,5,6]*

[1]CAS Key Laboratory of Marine Ecology and Environmental Sciences, Institute of Oceanology, Chinese Academy of Sciences, Qingdao, China, [2]Laboratory for Marine Ecology and Environmental Science, Qingdao National Laboratory for Marine Science and Technology, Qingdao, China, [3]Center for Ocean Mega-Science, Chinese Academy of Sciences,, Qingdao, China, [4]CAS Engineering Laboratory for Marine Ranching, Institute of Oceanology, Chinese Academy of Sciences, Qingdao, China, [5]Shandong Province Key Laboratory of Experimental Marine Biology, Qingdao, China, [6]University of Chinese Academy of Sciences, Beijing, China, [7]The Innovation of Seed Design, Chinese Academy of Sciences, Wuhan, China

KEYWORDS

echinoderm, heat stress, hypoxia, environmental stress, immune response, oxidative stress

Introduction

Aquatic species naturally live in water environment, therefore stress brought on by alterations in the environmental conditions directly affects them (Huo et al., 2021). The growth, survival and distribution of marine organisms are largely influenced by environmental factors like water temperature and dissolved oxygen (DO) (Coutant, 1985; Gobler et al., 2014). By the end of the century, it is expected that global temperatures will rise by at least 2°C, but ocean DO concentrations will drop by 4-7% (Matear and Hirst, 2003; Hoegh-Guldberg et al., 2007). Since oxygen becomes less soluble as temperature rises, heat stress and hypoxic stress frequently coexist (Huo et al., 2020).

The sea cucumber *Apostichopus japonicus* is an echinoderm with considerable commercial and ecological significance (Huo et al., 2020). As an aquatic poikilothermal animal, the physiological activities (*i.e.*, digestive function, immunity, and antioxidant defense) of sea cucumber are directly influenced by water temperature and dissolved oxygen. The suitable temperature range for *A. japonicus* growth is between 15°C and 18°C (Dong et al., 2006), and when the temperature exceeds 26°C and persists for more than 10 days, massive mortality would occur in farmed sea cucumbers. Moreover, hypoxia is typically seen as occurring when dissolved oxygen levels drop

below 2 mg·L^{-1} (Wu, 2002). An earlier study illustrated that *A. japonicus* could survive at hypoxic condition (2 mg·L^{-1}) in a short time, but its physical status and movement would be affected (Huo et al., 2018). The *A. japonicus* mainly relies on non-specific immunity, and the humoral immune response is one of its main defense reactions (Shao et al., 2018). The coelomic fluid of *A. japonicus* is similar to lymphatic fluid, and the cells inside work together with various humoral immune factors to form an immune response. Therefore, it is necessary to investigate the variations of enzyme activity in the coelomic fluid of *A. japonicus* to reveal how that species reacts to environmental challenges.

The activity of digestive enzymes is one of the most commonly used indicators to evaluate the digestive capacity, nutritional biochemistry and physiological status of the organism (Zhang et al., 2014). *A. japonicus* would reduce feeding and the digestive tract would be degraded when water temperature increases and dissolved oxygen decreases (Xu et al., 2015; Huo et al., 2018), and the digestive functions were potentially negatively affected (Huo et al., 2018). Therefore, the digestive function of *A. japonicus* may be altered under environmental stress, and to investigate this change, we could check digestive enzyme activities.

Environmental stresses could lead to an increase in reactive oxygen species (ROS) in the organism (Das and Roychoudhury, 2014). To avoid the damage caused by ROS, organisms have evolved various types of antioxidant systems, including non-enzymatic antioxidants represented by vitamin C and vitamin E and enzymatic antioxidants represented by superoxide dismutase (SOD) and catalase (CAT) (Tan et al., 2020). The antioxidant enzyme family members are widely distributed in the organism and regulate ROS levels thus acting as antioxidants and play crucial roles in response to stress. It is necessary to identify the changes of antioxidant enzymes in *A. japonicus* under adverse environment. In this study, 16 enzymes related to immune defense, digestive function, and antioxidant level were measured to reveal the physiological response characteristics in *A. japonicus* exposed to environmental stress. Our findings would provide insight into the response and adaptation of sea cucumber under the context of global climate change.

Methods

Experimental *A. japonicus* were collected from the coast of Weihai, China, with a wet weight of 90-110 g. One-week acclimatation in a tank containing aeration sand-filtered seawater at a temperature of 16 ± 0.5°C before the formal experiment. The normal control (NC) group was maintained at a temperature of 16°C with sufficient aeration; the high temperature (HT) group (heat stress group) was maintained at a temperature of 26°C with sufficient aeration; the low dissolved oxygen (LO) group (hypoxic stress group) was maintained at a temperature of 16°C and dissolved oxygen concentration of 2 mg·L^{-1}; the high temperature and low dissolved oxygen (HL) group (heat combined with hypoxic stress group) maintains at a temperature of 26°C and a DO concentration of 2 mg·L^{-1}. The equipment used for temperature and DO change, and the changing rate were same with the previous study (Huo et al., 2020). Five replicates were set in each group and cultured in separate tanks during the experiment. After 48h exposure, the coelomic fluid of each *A. japonicus* was collected by sterile syringe and rapidly frozen in liquid nitrogen, and then transferred to a refrigerator at -80°C for storage.

A total of 16 enzyme activities involving immunity, digestion and antioxidant ability were measured in this study, including acid phosphatase (ACP), alkaline phosphatase (AKP) and lysozyme (LZM), lipase (LPS), α-amylase (AMS), pepsin (PEP), trypsin (TRY), SOD, glutathione peroxidase (GSH-PX), CAT, succinate dehydrogenase (SDH), lactate dehydrogenase (LDH), total antioxidant capacity (T-AOC), malondialdehyde (MDA), peroxidase (POD), and phenol oxidase (PPO). All enzyme activities were determined within one month of sampling the coelomic fluid samples, and the commercial kits used in this study were purchased from Nanjing Jiancheng Biological Research Institute (Nan Jing, China) and tested according to the instructions. Specifically, the kit number for the enzymes assay were listed in Table S1. The obtained data were statistically analyzed by SPSS19 software (IBM Corp., Armonk, NY, USA). The significance of the differences between the treated and comparison groups for each enzyme was analyzed by *t*-test and the statistical significance threshold was set at $P < 0.05$. Bar graphs were plotted using Prism7 software (GraphPad Software Inc., USA).

Data description

As the immune response in *A. japonicus* is a typical non-specific immune response, enzymes like ACP, AKP, and LZM may be able to aid in the complete destruction of foreign compounds after they have passed through the organism's first line of defense (Wang et al., 2015). In this study, the activity of the three enzymes related to immune defense was measured (Figure 1). Compared with the normal environmental condition, the activity of ACP was significantly higher in *A. japonicus* under hypoxic stress ($P < 0.05$), and the changes of AKP activity were not significant under the three environmental stresses; the activity of LZM was significantly higher in *A. japonicus* under heat combined with hypoxic stress ($P < 0.05$). This could be that more adenosine triphosphate (ATP) was needed to maintain normal metabolic level when *A. japonicus* exposed to environment stress, and the inorganic phosphate required for ATP synthesis can be produced by the hydrolysis of phosphate by ACP and AKP (Zheng et al., 2014). The results suggested that supply of potential metabolic high energy demand was

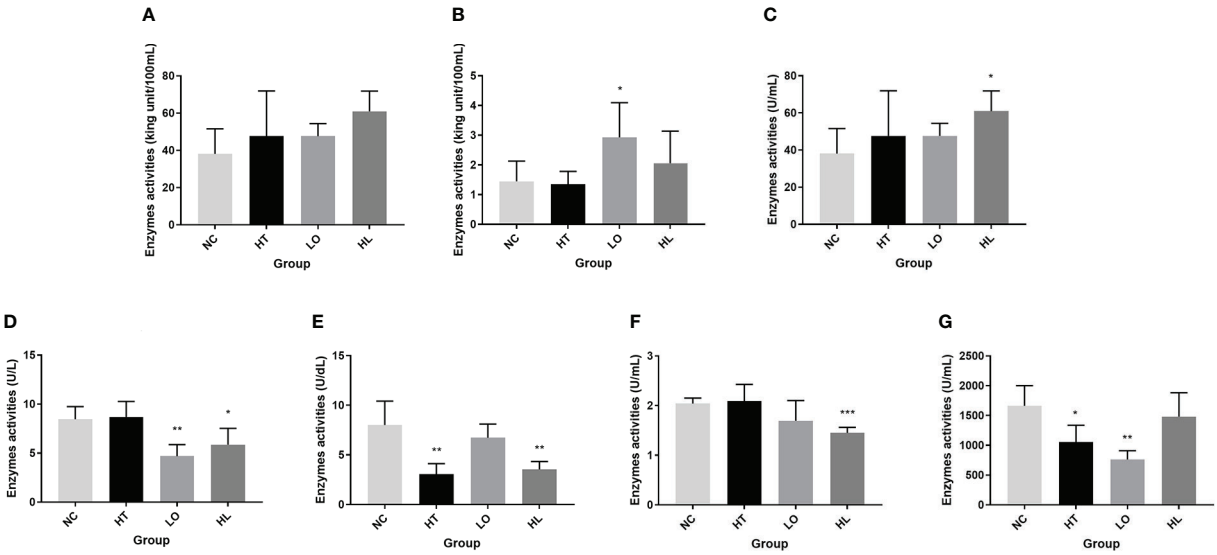

FIGURE 1
Activities of immune and digestive enzymes in *A. japonicus* under environmental stresses **(A)**. alkaline phosphatase (AKP); **(B)** acid phosphatase (ACP); **(C)** lysozyme (LZM); **(D)** lipase (LPS); **(E)** α-amylase (AMS); **(F)** pepsin (PEP); and **(G)** trypsin (TRY); *: $P < 0.05$; **: $P < 0.01$; ***: $P < 0.001$).

enhanced, thus providing more energy to adapt to the adversity. Lysozyme is an important innate immune factor widely present in the endothelial cells and body fluids of echinoderms that kills germs and shields against bacterial infection (Canicatti and Roch, 1989). The increased LZM activity suggested that phagocytic activity of phagocytes may be elevated. A high temperature also caused an increase in serum lysozyme levels in Atlantic halibut *Hippoglossus hippoglossus* L. (Langston et al., 2002). According to the findings, the immune defense mechanisms were induced in *A. japonicus* in response to environmental stress, the organism's defense against foreign substances was enhanced.

In this study, four enzymes related to digestive function were selected for activity measurement, including LPS, AMS, PEP and TRY. The results showed that the LPS activity was significantly reduced under hypoxia ($P < 0.01$) and heat combined with hypoxic stress ($P < 0.05$); AMS activity was highly significantly reduced under heat and heat combined with hypoxic stress ($P < 0.01$); PEP activity was extremely significantly reduced under heat combined with hypoxic stress ($P < 0.001$); and TRY activity was significantly reduced under heat stress ($P < 0.05$) and hypoxic stress ($P < 0.01$) (Figure 1). In the previous of yellowtail kingfish *Seriola lalandi*, TRY, LPS and AMS enzyme activities were altered by temperature but did not seem to be impacted by dissolved oxygen concentration (Bowyer et al., 2014); PEP and AMS activities also significantly changed by temperature in the leopard coral grouper *Plectropomus leopardus* (Sun et al., 2015). Under environmental stress, *A. japonicus* undergoes degeneration of the intestine and respiratory tree (Xu et al., 2015; Huo et al., 2018), and may even occur evisceration. Substantial changes in these digestive organs are also responsible for the decrease in digestive enzyme secretion and activity. The decrease in digestion-related enzyme activities in *A. japonicus* under environmental stress indicated that there was a negative impact of environmental stress on the digestive function of *A. japonicus*.

Environmental stress may lead to an increase in ROS, which could oxidize cellular components and damage cell membrane. The imbalance between the production and clearance of ROS will cause oxidative stress (Halliwell and Gutteridge, 2001; Kong et al., 2012). To assess the oxidative stress response of *A. japonicus* under environmental stress, nine enzyme activities were measured in this study (Figure 2), including SOD, GSH-PX, CAT, SDH, LDH, MDA, POD, PPO, and T-AOC. The T-AOC was significantly reduced under heat and heat combined with hypoxic stress ($P < 0.05$); SOD was significantly reduced, and MDA were extremely significantly increased under hypoxia and heat combined with hypoxic stress ($P < 0.001$). These suggested that oxidative stress brought on by environmental stress results in lipid peroxidation and caused oxidative damage to organisms. SDH activity was significantly reduced heat combined with hypoxic stress ($P < 0.05$), suggesting that aerobic oxidation capacity was suppressed, and the tricarboxylic acid cycle was impacted. POD and PPO activity were significantly increased under heat stress; the activity of CAT was significantly reduced under all three types of environmental stresses. PPO could oxidize phenolic substrates to unstable quinones (Cerenius et al., 2008); POD has the property of catalyzing the oxidation

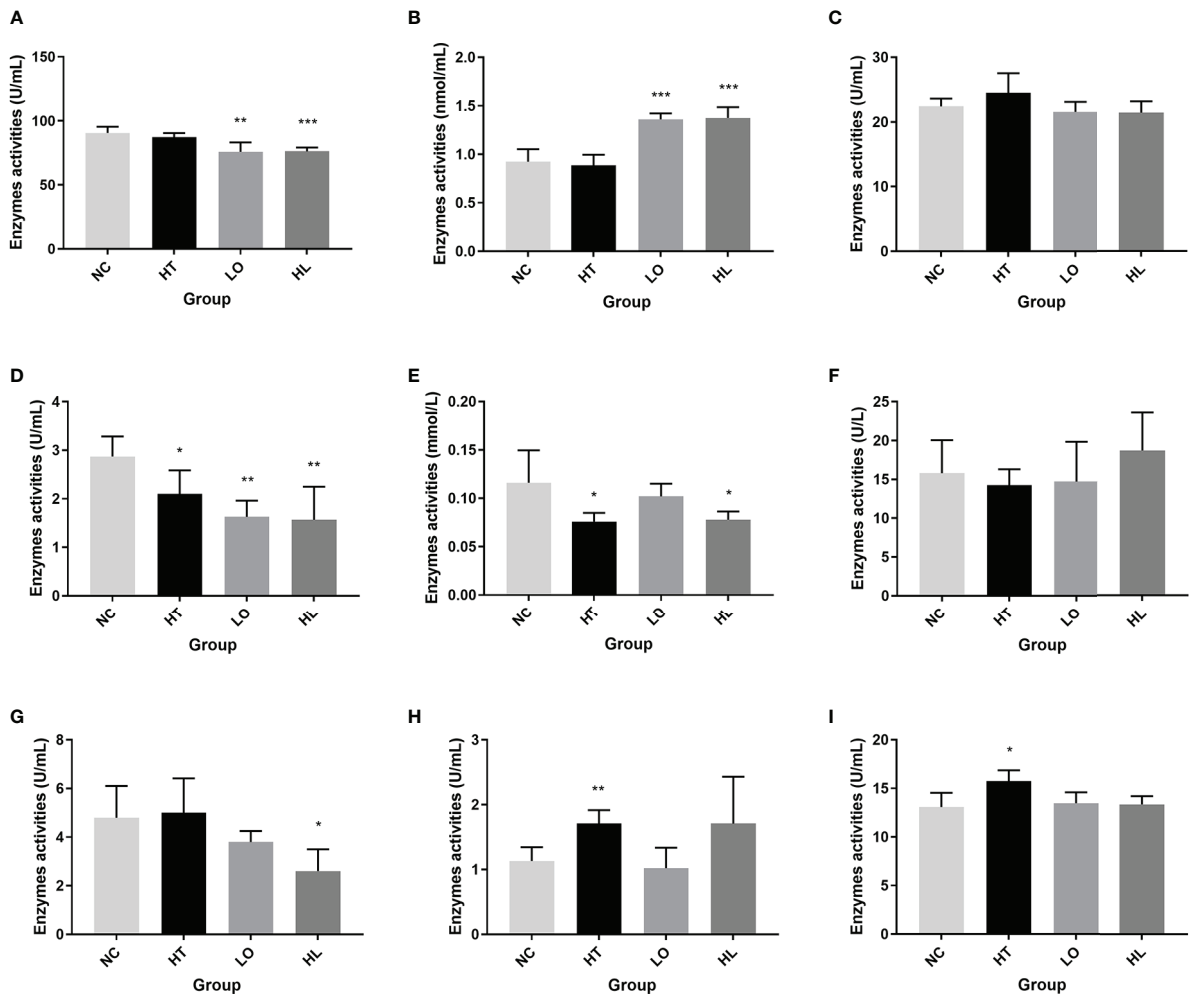

FIGURE 2
Activities of antioxidative enzymes in *A. japonicus* under environmental stresses **(A)**. superoxide dismutase (SOD); **(B)** malondialdehyde (MDA); **(C)** glutathione peroxidase (GSH-PX); **(D)** catalase (CAT); **(E)** total antioxidant capacity (T-AOC); **(F)** lactate dehydrogenase (LDH); **(G)** succinate dehydrogenase (SDH); **(H)** peroxidase (POD); and **(I)** phenol oxidase (PPO); *: $P < 0.05$; **: $P < 0.01$; ***: $P < 0.001$).

reaction between hydrogen peroxide (H_2O_2) and hydrogen donors (Şişecioğlu et al., 2010), and CAT could catalyze the intracellular hydrogen peroxide decomposition (Wang et al., 2016). Therefore, by altering their activity to reduce the cell damage caused by excessive free radicals, *A. japonicus* could adapt to the adversity. The activity of GSH-PX and LDH did not significantly change; It is possible that these two enzymes did not play such crucial role in the oxidative stress defense in *A. japonicus*. It is also possible that these two indicators are not sensitive to environmental stress in *A. japonicus* coelomic fluid. The oxidation status influenced by environmental changes has been reported in aquatic animals, including the shrimp *Litopenaeus vannamei* (Liu et al., 2015), the crab *Paralomis granulosa* (Romero et al., 2011), the fish *Carassius auratus* (Sun et al., 2012), *Micropterus salmoides* (Sun et al., 2020) and the scallop *Chlamys farreri* (Chen et al., 2007). For example, the results of decreased SOD and CAT were in accordance of the crucian carp *Carassius auratus* in hypoxic condition (Sun et al., 2012). Increased T-AOC and GSH-Px activities were also found in heat-stressed largemouth bass *Micropterus salmoides* (Sun et al., 2020). It was suggested that various environmental stresses resulted in varing degrees of oxidative stress response, and these enzymes with altered activity may be vital in protecting *A. japonicus* from oxidative damage.

To conclude, the coelomic fluid is an important component in sea cucumbers to defense against undesirable environments. When exposed to the environmental stress, digestive function was suppressed, immune system was induced, and the antioxidant enzymes changed in varying degrees in *A. japonicus*. The integrated regulation of immunity, digestion, oxidative stress, and other associated enzymes is a series of adaptive mechanisms made by the *A. japonicus* to adapt to the extreme environment.

Our results provide a better understanding of how the *A. japonicus* survives in adversity in the context of global change.

Data availability statement

The original contributions presented in the study are included in the article/Supplementary Material. Further inquiries can be directed to the corresponding author.

Ethics statement

Since culture commercial sea cucumber were used, ethical review and approval not required.

Author contributions

DH: Conceptualization, Investigation, Data curation, Methodology, Validation, Project administration, Funding acquisition, Writing - original draft, Writing - review & editing. FS: Validation, Writing - review & editing. LZ: Supervision, Writing - review & editing. HY: Supervision, Funding acquisition, Writing - review & editing. LS: Formal analysis, Funding acquisition, Writing - review & editing. All authors contributed to the article and approved the submitted version.

Funding

This work was supported by the National Natural Science Foundation of China (grant numbers 42106106, 42030408), Postdoctoral Innovative Talents Support Program of Shandong Province (grant number SDBX2020006), the Major Scientific and Technological Innovation Projects in Shandong Province (grant number 2019JZZY010812), Shandong Provincial Natural Science Foundation (grant number ZR2021QD013), Special Research Assistant Project of Chinese Academy of Sciences, Qingdao Postdoctoral Applied Research Project (grant number 2020170), Youth Innovation Promotion Association CAS (grant number 2019209).

Conflict of interest

The authors declare that the research was conducted in the absence of any commercial or financial relationships that could be construed as a potential conflict of interest.

Publisher's note

All claims expressed in this article are solely those of the authors and do not necessarily represent those of their affiliated organizations, or those of the publisher, the editors and the reviewers. Any product that may be evaluated in this article, or claim that may be made by its manufacturer, is not guaranteed or endorsed by the publisher.

Supplementary material

The Supplementary Material for this article can be found online at: https://www.frontiersin.org/articles/10.3389/fmars.2022.1094814/full#supplementary-material

References

Bowyer, J. N., Booth, M. A., Qin, J. G., D'Antignana, T., Thomson, M. J., and Stone, D. A. (2014). Temperature and dissolved oxygen influence growth and digestive enzyme activities of yellowtail kingfish *Seriola lalandi* (Valenciennes 1833). *Aquaculture Res.* 45 (12), 2010–2020. doi: 10.1111/are.12146

Canicatti, C., and Roch, P. (1989). Studies on *Holothuria polii* (Echinodermata) antibacterial proteins. i. evidence for and activity of a coelomocyte lysozyme. *Cell. And Mol. Life Sci.* 45, 756–759. doi: 10.1007/BF01974579

Cerenius, L., Lee, B. L., and Söderhäll, K. (2008). The proPO-system: pros and cons for its role in invertebrate immunity. *Trends Immunol.* 29, 263–271. doi: 10.1016/j.it.2008.02.009

Chen, M., Yang, H., Delaporte, M., and Zhao, S. (2007). Immune condition of *Chlamys farreri* in response to acute temperature challenge. *Aquaculture* 271 (1-4), 479–487. doi: 10.1016/j.aquaculture.2007.04.051

Coutant, C. C. (1985). Striped bass, temperature, and dissolved oxygen: a speculative hypothesis for environmental risk. *Trans. Am. Fisheries Soc.* 114 (1), 31–61. doi: 10.1577/1548-8659(1985)114<31:SBTADO>2.0.CO;2

Das, K., and Roychoudhury, A. (2014). Reactive oxygen species (ROS) and response of antioxidants as ROS-scavengers during environmental stress in plants. *Front. Environ. Sci.* 2, 53. doi: 10.3389/fenvs.2014.00053

Dong, Y., Dong, S., Tian, X., Wang, F., and Zhang, M. (2006). Effects of diel temperature fluctuations on growth, oxygen consumption and proximate body composition in the sea cucumber apostichopus japonicus selenka. *Aquaculture* 255 (1-4), 514–521. doi: 10.1016/j.aquaculture.2005.12.013

Gobler, C. J., DePasquale, E. L., Griffith, A. W., and Baumann, H. (2014). Hypoxia and acidification have additive and synergistic negative effects on the growth, survival, and metamorphosis of early life stage bivalves. *PloS One* 9 (1), e83648. doi: 10.1371/journal.pone.0083648

Halliwell, B., and Gutteridge, J. M. C. (2001). *Free radicals in biology and medicine* (New York: Oxford University Press Inc).

Hoegh-Guldberg, O., Mumby, P. J., Hooten, A. J., Steneck, R. S., Greenfield, P., Gomez, E., et al. (2007). Coral reefs under rapid climate change and ocean acidification. *Science* 318, 1737–1742. doi: 10.1126/science.1152509

Huo, D., Sun, L., Ru, X., Zhang, L., Lin, C., Liu, S., et al. (2018). Impact of hypoxia stress on the physiological responses of sea cucumber *Apostichopus japonicus*: respiration, digestion, immunity and oxidative damage. *PeerJ* 6, e4651. doi: 10.7717/peerj.4651

Huo, D., Sun, L., Storey, K. B., Zhang, L., Liu, S., Sun, J., et al. (2020). The regulation mechanism of lncRNAs and mRNAs in sea cucumbers under global

climate changes: Defense against thermal and hypoxic stresses. *Sci. Total Environ.* 709, 136045. doi: 10.1016/j.scitotenv.2019.136045

Huo, D., Sun, L., Sun, J., Lin, C., Liu, S., Zhang, L., et al. (2021). Emerging roles of circRNAs in regulating thermal and hypoxic stresses in *Apostichopus japonicus* (Echinodermata: Holothuroidea). *Ecotoxicol. Environ. Saf.* 228, 112994. doi: 10.1016/j.ecoenv.2021.112994

Kong, X., Wang, S., Jiang, H., Nie, G., and Li, X. (2012). Responses of acid/alkaline phosphatase, lysozyme, and catalase activities and lipid peroxidation to mercury exposure during the embryonic development of goldfish *Carassius auratus*. *Aquat. Toxicol.* 120-121, 119–125. doi: 10.1016/j.aquatox.2012.05.005

Langston, A. L., Hoare, R., Stefansson, M., Fitzgerald, R., Wergeland, H., and Mulcahy, M. (2002). The effect of temperature on non-specific defence parameters of three strains of juvenile Atlantic halibut (*Hippoglossus hippoglossus* l.). *Fish Shellfish Immunol.* 12 (1), 61–76. doi: 10.1006/fsim.2001.0354

Liu, H. L., Yang, S. P., Wang, C. G., Chan, S. M., Wang, W. X., Feng, Z. H., et al. (2015). Effect of air exposure and resubmersion on the behavior and oxidative stress of pacific white shrimp *Litopenaeus vannamei*. *North Am. J. Aquaculture* 77 (1), 43–49. doi: 10.1080/15222055.2014.955157

Matear, R. J., and Hirst, A. C. (2003). Long-term changes in dissolved oxygen concentrations in the ocean caused by protracted global warming. *Global Biogeochemical Cycles* 17, 1125. doi: 10.1029/2002GB001997

Romero, M. C., Tapella, F., Sotelano, M. P., Ansaldo, M., and Lovrich, G. A. (2011). Oxidative stress in the subantarctic false king crab paralomis granulosa during air exposure and subsequent re-submersion. *Aquaculture* 319 (1-2), 205–210. doi: 10.1016/j.aquaculture.2011.06.041

Şişecioğlu, M., Gülçin, L., Çankaya, M., Atasever, A., Kaya, H. B., and Ozdemir, H. (2010). Purification and characterization of peroxidase from Turkish black radish (*Raphanus sativus* l.). *J. Medicinal Plants Res.* 4, 1187–1196. doi: 10.5897/JMPR10.071

Shao, Y., Che, Z., Xing, R., Wang, Z., Zhang, W., Zhao, X., et al. (2018). Divergent immune roles of two fucolectin isoforms in *Apostichopus japonicus*. *Dev. Comp. Immunol.* 89, 1–6. doi: 10.1016/j.dci.2018.07.028

Sun, H., Li, J., Tang, L., and Yang, Z. (2012). Responses of crucian carp *Carassius auratus* to long-term exposure to nitrite and low dissolved oxygen levels. *Biochem. Systematics Ecol.* 44, 224–232. doi: 10.1016/j.bse.2012.06.011

Sun, Z., Xia, S., Feng, S., Zhang, Z., Rahman, M. M., Rajkumar, M., et al. (2015). Effects of water temperature on survival, growth, digestive enzyme activities, and body composition of the leopard coral grouper plectropomus leopardus. *Fisheries Sci.* 81 (1), 107–112. doi: 10.1007/s12562-014-0832-9

Sun, J. L., Zhao, L. L., Liao, L., Tang, X. H., Cui, C., Liu, Q., et al. (2020). Interactive effect of thermal and hypoxia on largemouth bass (Micropterus salmoides) gill and liver: Aggravation of oxidative stress, inhibition of immunity and promotion of cell apoptosis. *Fish Shellfish Immunol.* 98, 923–936. doi: 10.1016/j.fsi.2019.11.056

Tan, K., Zhang, B., Zhang, H., Ma, H., Li, S., and Zheng, H. (2020). Enzymes and non-enzymatic antioxidants responses to sequential cold stress in polymorphic noble scallop *Chlamys nobilis* with different total carotenoids content. *Fish Shellfish Immunol.* 97, 617–623. doi: 10.1016/j.fsi.2019.12.063

Wang, C., Wang, X., Wang, P., Chen, B., Hou, J., Qian, J., et al. (2016). Effects of iron on growth, antioxidant enzyme activity, bound extracellular polymeric substances and microcystin production of microcystis aeruginosa FACHB-905. *Ecotoxicol. Environ. Saf.* 132, 231–239. doi: 10.1016/j.ecoenv.2016.06.010

Wang, J. H., Zhao, L. Q., Liu, J. F., Wang, H., and Xiao, S. (2015). Effect of potential probiotic rhodotorula benthica D30 on the growth performance, digestive enzyme activity and immunity in juvenile sea cucumber *Apostichopus japonicus*. *Fish Shellfish Immunol.* 43, 330–336. doi: 10.1016/j.fsi.2014.12.028

Wu, R. S. (2002). Hypoxia: from molecular responses to ecosystem responses. *Mar. pollut. Bull.* 45 (1-12), 35–45. doi: 10.1016/S0025-326X(02)00061-9

Xu, D., Sun, L., Liu, S., Zhang, L., and Yang, H. (2015). Histological, ultrastructural and heat shock protein 70 (HSP70) responses to heat stress in the sea cucumber *Apostichopus japonicus*. *Fish Shellfish Immunol.* 45, 321–326. doi: 10.1016/j.fsi.2015.04.015

Zhang, H. C., Zhu, J. Y., Chen, Z. Q., and Lin, M. (2014). Variation of the activity of digestive enzymes involved in *Apostichopus japonicus* with different sizes. *J. Quanzhou Normal Univ* 32 (2), 27–30. doi: 10.16125/j.cnki.1009-8224.2014.02.019

Zheng, H., Li, B., Rong, X., Liao, M., Chen, G., Zhang, Z., et al. (2014). Effects of salinity and dissolved oxygen variation on the non-specific immune response of *Apostichopus japonicus*. *Prog. Fishery Sci.* 118–124. doi: 10.3969/j.issn.1000-7075.2014.01.017

frontiers | Frontiers in Marine Science

TYPE Original Research
PUBLISHED 13 January 2023
DOI 10.3389/fmars.2022.1108330

OPEN ACCESS

EDITED BY
Hongsheng Yang,
Institute of Oceanology (CAS), China

REVIEWED BY
Yunwei Dong,
Ocean University of China, China
Liqiang Zhao,
Guangdong Ocean University, China

*CORRESPONDENCE
Mauricio J. Carter
mauricio.carter@unab.cl

SPECIALTY SECTION
This article was submitted to Global Change and the Future Ocean, a section of the journal Frontiers in Marine Science

RECEIVED 25 November 2022
ACCEPTED 30 December 2022
PUBLISHED 13 January 2023

CITATION
Carter MJ, García-Huidobro MR, Aldana M, Rezende EL, Bozinovic F, Galbán-Malagón C and Pulgar JM (2023) Upper thermal limits and risk of mortality of coastal Antarctic ectotherms. *Front. Mar. Sci.* 9:1108330. doi: 10.3389/fmars.2022.1108330

Upper thermal limits and risk of mortality of coastal Antarctic ectotherms

Mauricio J. Carter [1*], M. Roberto García-Huidobro [2], Marcela Aldana [2], Enrico L. Rezende [3], Francisco Bozinovic [3], Cristóbal Galbán-Malagón [4] and José M. Pulgar [1]

[1]Departamento de Ecología y Biodiversidad, Facultad de Ciencias de la Vida, Universidad Andrés Bello, Santiago, Chile, [2]Centro de investigación e Innovación para el Cambio Climático, Facultad de Ciencias, Universidad Santo Tomás, Santiago, Chile, [3]Departamento de Ecología, Center of Applied Ecology and Sustainability (CAPES), Facultad de Ciencias Biológicas, Pontificia Universidad Católica de Chile, Santiago, Chile, [4]Center for Genomics, Ecology & Environments (GEMA), Universidad Mayor, Santiago, Chile

Antarctic marine animals face one of the most extreme thermal environments, characterized by a stable and narrow range of low seawater temperatures. At the same time, the Antarctic marine ecosystems are threatened by accelerated global warming. Determining the upper thermal limits (CT_{max}) is crucial to project the persistence and distribution areas of the Antarctic marine species. Using thermal death time curves (TDT), we estimated CT_{max} at different temporal scales from 1 minute to daily and seasonal, the predict vulnerability to the current thermal variation and two potential heatwave scenarios. Our results revealed that CT_{max} at 1 min are far from the temperature present in the marine intertidal area where our study species, showing Echinoderm species higher CT_{max} than the Chordata and Arthropods species. Simulations indicated that seasonal thermal variation from the intertidal zone contributed to basal mortality, which increased after considering moderate scenarios of heatwaves (+2°C) in the Shetland Archipelago intertidal zone. Our finding highlighted the relevance of including exposure time explicitly on the CT_{max} estimates, which deliver closer and more realistic parameters according to the species that may be experiencing in the field.

KEYWORDS

upper thermal limits, heatwave, Antarctic peninsula, marine ectotherms, temperature mortality

Introduction

Global warming (GW) poses one of the greatest threats to biodiversity (Pecl et al., 2017), leading by anthropogenic activities that are likely to increase the frequency of mean temperatures and extreme heatwaves in regions such as the Antarctic continent (Robinson et al., 2020; González-Herrero et al., 2022; Turner et al., 2022). Polar areas such as Antarctica Peninsula have experienced the increasing effect of GW due to anthropogenic activities worldwide affecting surface seawater temperature variation in the last 50 years to about ~ 2°C

(Meredith and King, 2005; Cook et al., 2016; Morley et al., 2020). These extreme zones are also characterized by marine species adapted to relatively stable and isolated conditions, which are harmed due to the increased temperature associated with GW (Peck, 2018). The increased seawater temperature and their impact on Antarctic animals, represent an ideal scenery to understand the impact of increased GW on habitats and species adapted to low temperatures.

Because the shape of thermal performance is determined by multiple sensitive biological rates (Lefevre et al., 2021), this biological phenomenon is ultimately linked with the thermal limits for life and death in ectotherms experience. Also, thermal windows that a species can successfully tolerate providing a good insight into the thermal niche of taxa (Rezende et al., 2014), helping determine species distribution modeling and predict response to GW (Sunday et al., 2012; Liao et al., 2021; Ørsted et al., 2022). Determining the consequences of GW on Antarctic marine communities is crucial to building a detailed description of the organismal performance in challenger thermal conditions, which aids in predicting the thermal tolerance responses from species under thermal stress (Sinclair et al., 2016). Based on the intimate nature of intensity and time of exposition that thermal stress had, Thermal Death Time curves (TDTs) have been explicitly formalized to evaluate the impact of time on the critical response to thermal stress (Rezende et al., 2014; Jørgensen et al., 2021). Recently, a detailed description of upper thermal limits from 39 ectotherm marine species belonging to the Antarctic ecosystem has revealed differences in thermal sensitivity among taxa (Molina et al., 2022). This approach using TDTs explicitly considers exposure time to thermal stress on an ecological scale. This remarkable methodological tool allows for specifying relevant temporal windows of thermal stress. Then, the risk of extirpation due to the temperature increment in bounded time, such as extreme heatwave events, may be determined (Hobday et al., 2016; Hobday et al., 2018). For animals that inhabit outer regions, thermal sensitivity is an urgent need due to assessing the magnitude of time effects to obtain a precise estimate of CT_{max} (Peralta-Maraver and Rezende, 2021), which is valuable information to predict temperature mortality in field conditions (Rezende et al., 2020).

Southern ocean species inhabitant constantly cold environments characterized by thermal stenothermality (Peck, 2005), and slight differences in thermal environment can be enough to cause differences between species (Bilyk and DeVries, 2011; Sandersfeld et al., 2017), populations (Morley et al., 2009), and spatial distribution (Morley et al., 2010). Several phenomena, such as interspecific differences, trophic levels position, and body size variation, significantly affect thermal limits (Peck et al., 2009). The mismatch with the upper thermal limits and the temperature that Antarctic animals experience in the field (Peck et al., 2009; Beers and Jayasundara, 2015) may be attributable to sub-estimated the effect of exposure time in the experimental trial (Molina et al., 2022). According to the evidence above, this work aims to evaluate the upper thermal limits of seven marine ectotherm Antarctic species (Chordata 3 spp., Arthropoda 2 spp., and Echinodermata 2 spp.), standardizing by the exposition time (T_{ko} 1 min) making the measures comparable among experimental trial and species (Rezende et al., 2014). Thus, based on *in situ* records of seawater intertidal temperature variation (Kuklinski and Balazy, 2014), and an analytic approach to evaluate risk of mortality to Antarctic marine species (Molina et al., 2022), we quantify vulnerability to the current condition of thermal variation and two scenarios (+2°C 10 days and 30 days) of moderate heatwaves (Hobday et al., 2016) that those ectotherm species may experience in field conditions.

Methods

Animal collection

Fieldwork was carried out in January 2020 in the lower intertidal zone off the South Shetland Island, Fildes Bay, King George Island (62°11'S, 58°59'W). A total of 20 Antarctic juvenile fishes were collected from three species *Harpagifer antarcticus* (12), *Trematomus newnesi* (6) and *Lepidonotothem nudifrons* (2), and 14 arthropods individuals from two species *Bovallia gigantea* (4), and *Glyptonotus antarcticus* (10), and 19 echinoderms from two species *Odontaster validus* (9) and *Sterechinus neumayeri* (10). All animals were caught using a 12-inch aquarium fish net and hands turning over rocks off the intertidal zone. After, animals were immediately deposited in coolers with constant aeration and carried alive to the laboratories infrastructures of Instituto Antártico Chileno (INACH) in Escudero Antarctic Scientific Station. This laboratory facility includes several 50 L tanks with circulating and filtered, aerated seawater. The animals were transferred to aquariums with seawater at a controlled temperature (1 ± 0.3°C), salinity of 33 (± 0.5) psu, under natural photoperiod, and no feeding. These conditions were maintained for at least 48 hours to allow them to be acclimated to captivity conditions before undergoing the thermal trials. All animals were kept in separated 50 L aquariums during captivity before the thermal trials.

TDT curves to CT_{max}

All animals individually were subjected to a temperature ramp, to fishes and arthropods with an increment of 0.07°C min^{-1} and echinoderms, a ramp of 0.08°C min^{-1}. The experimental trial stopped when animals presented signals of thermic stress such as loss of equilibrium, defined as the inability of fish and arthropods to maintain dorso-ventral orientation for at least 1 min (Beitinger et al., 2000), and to echinoderms loss of adhesion to the surface of the metabolic chamber or showed lack of evident movement of tube feet or spines (Peck et al., 2009). These procedures were repeated until all individuals were measured during the experiment time. At the end of trail routines, all individuals were euthanized using an overdose of BZ20, following bioethics protocols of Universidad Andres Bello, and body mass and length were recorded using a caliper and analytical balance.

To obtain a proper estimate that reflects both upper thermal critic temperature and exposition time, we combine the CT_{max} observation (i.e., the temperature that would result in knockdown or death) from the ramping experiment with the respective recorded time (t). Using these two parameters (CT_{max} and t), we build the thermal death time (TDT) curves (eq. 1) (Rezende et al., 2014) to estimates Standardized T_{ko} ranges.

$$T_{ko} = CT_{max} - z\text{Log}_{10}t, \quad (1)$$

To thermal sensitivity parameter (z), which describes how thermal tolerance decays with the duration of the heat challenge (i.e., the net reduction in T_{ko} resulting from a tenfold increase in exposure time), we used the z estimates from Antarctic ectotherm marine species nearly related with the species studied here (Molina et al., 2022).Then, we mapped this slope back onto the experimental estimated of T_{ko} and standardized t to estimate the expected tolerance temperature at t = 1 minute, 10 days, and 30 days (eq. 1) on a species-specific basis. Then we built a single TDT per individual per the seven species considered in this study, obtained a total of 53 curves (Figure 1B).

Predicting thermal mortality

Combining standardized T_{ko} from the experimental essay with thermal sensitivity reported in literature and field temperatures in Antarctica, we were able to determine if these organisms could be experiencing thermal mortality under the current condition as well as two moderate marine heatwaves episodes scenarios (Hobday et al., 2016).

Thermal scenarios were built using temperature data obtained temperatures with a 1-min resolution from these datasets *via* interpolation and calculated the 'instantaneous mortality' associated with these temperatures as described in (Rezende et al., 2020). Intertidal temperature records were obtained from 12 dataloggers covering the whole tidal range of Admiralty Bay, King George Island, with a resolution of 5 min between December 2010 and March 2011 (Kuklinski and Balazy, 2014). Because the main goal of this analysis is to determine if current recorded temperatures can lead to thermal mortality in Antarctica, we selected these locations as they are representative of warmer waters within the Western Antarctic Peninsula (Barnes and Peck, 2008) and used records from the austral summer between December and March in subsequent analyses. With the interpolated temperature data with a 1-min resolution at hand, we estimated the predicted thermal mortality for an 'average' individual organism belonging to each of seven species of chordate, arthropod, and echinoderm. As explained in detail elsewhere (Rezende et al., 2020), this procedure involved (1) using the mean CT_{max} and z to obtain a generic TDT for each species, (2) simulating the tolerance landscape from these TDTs assuming that knockdown times at each measurement temperature are normally distributed with CV = 0.25 (CV = standard deviation [SD]/mean) [see Supplementary Information in (Rezende et al., 2020)], and then (3) running the dynamic.landscape function combines the tolerance landscapes with the ambient temperature records to estimate the predicted mortality under these field conditions. We performed simulations for all species under three contrasting scenarios. First, under the highly variable thermal conditions, with the temperature data from the 12 data loggers deployed in the intertidal zone and assuming that animals recover when the temperatures drop at night (this is accomplished by calculating daily survival iteratively and resetting the survival curve at 00:00). Second, under two scenarios of a moderate marine heatwave as is described in (Hobday et al., 2016), with an average increment of seawater of +2° C for a period of 10 days and 30 days. As vulnerability indices, we calculated each species' average mortality across days along loggers for the intertidal records (n = 12 loggers per species). All analyses were performed in R environment (R Development Core Team, 2019)

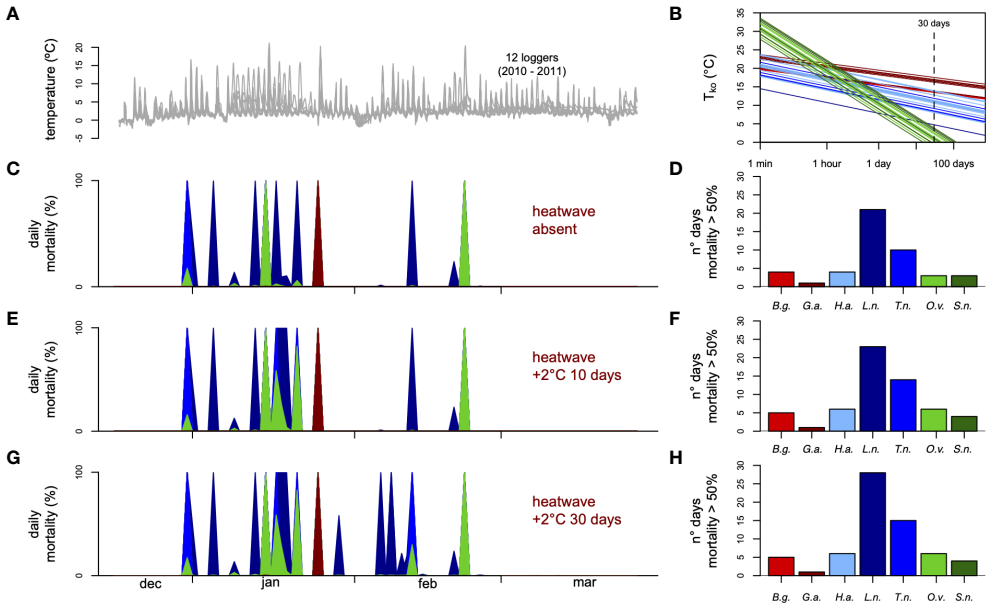

FIGURE 1
Simulated mortality combining the thermal tolerance landscape reconstructed for the seven species and high-resolution environmental temperatures recorded in the **(A)** intertidal zone, **(B)** using the thermal-death time (TDT) curves obtained with these *CT*max and *z* parameters from three mayor taxa (Chordata, Arthropods and Echinoderms) (Molina et al., 2022). Note that values crossing the TDT curves at 1 min and 30 days correspond to standardized T_{ko}. Simulated mortality procedure by Rezende et al. (Rezende et al., 2020) assumed that organisms could recover every 24 h from an acute heat stress in the intertidal **(C)** and two scenarios of heatwaves event (**E, G**). Bar plots show sum of days which mortality overpassed 50% to the daily basis of **(D)** current intertidal thermal condition and the two scenarios of heatwave events (**F, H**). *B.g.*, *Bovallia gigantea* (red); *G.a.*, *Bovallia gigantea* (dark red); *H.a.*, *Harpagifer antarcticus* (light blue); *L.n.*, *Lepidonotothem nudifrons* (dark blue); *T.n.*, *Trematomus newnesi* (blue); *O.v.*, *Odontaster validus* (green); *S.n.*, *Sterechinus neumayeri* (dark green).

Results

Thermal tolerance and TDTs estimates

Body sizes (fresh weight) of animals collected ranged between 0.88 - 37.1 g. Echinoderms (*Odontaster validus* and *Sterechinus neumayeri*) were the bigger animals measured with a body size mean of 18.34 ± 8.84SD and ranged between 5.49 – 37.1 g., followed by Chordata (*Harpagifer antarcticus*, *Trematomus newnesi* and *Lepidonotothem nudifrons*) animals with a body size mean of 8.84 ± 5.22SD and ranged between 2.38 – 25.25 g., and Arthropoda (*Bovallia gigantea*, and *Glyptonotus antarcticus*) with a body size mean of 3.58 ± 1.54SD and ranged between 0.88 – 6.049 g. Having a rough estimate of upper thermal limits with the dynamic essay and the thermal sensitivity obtained from Molina et al. (Molina et al., 2022), we then proceeded to calculate expected T_{ko} following 1 min exposure to compare among the major taxa which species belong at the same temporal scale. The mixed model ANOVA with phylum as a random effect revealed significant differences among Echinoderms, Chordata, and Arthropod species ($F_{2,4}$ = 57.95, p = 0.011). Pairwise comparison indicated differences between Echinoderms and Chordata (t = -10.291, p = 0.0011) and Arthropods species (t = -5.766, p = 0.0011), and absence of differences between Arthropods and Chordata (t = 2.787, p = 0.1024). The Echinoderm species showed higher T_{ko} 1 min with *S. neumayeri* 31.18 ± 2.10SD and *O. validus* 30.65 ± 1.29SD, followed by Arthropods species *G. antarticus* with 22.42 ± 1.21 and *B. gigantea* 19.81 ± 0.14SD, and Chordata species *H. antarticus* 21.04 ± 1.86SD, *L. nudifrons* 17.57 ± 4.33SD and *T. newnesi* 19.08 ± 1.59SD.

Predicted mortality in the field

We estimated predicted daily mortalities over 100 days during the Austral summer for the intertidal zones. Our simulations suggest that current temperatures can elicit some thermal mortality depending on the TDT profiles of different species. In our field thermal stress scenario (Figure 1A), mortality surpassed 50% on five occasions for arthropods *B. gigantea* (4) and *G. antarticus* (1), 35 occasions for chordates *L. nudifrons* (4), *H. antarticus* (21), *T. newnesi* (10), and 6 for echinoderms *O. validus* (3) and *S. neumayeri* (3) and all these instances involved primarily loggers at higher tide locations (Figures 1C, D). Accordingly, the mean daily mortality estimated per logger differed significantly across species based on regular analysis of variance ($F_{6,77}$ = 6.45, p = 6.34 x 10^{-6}), suggesting that one arthropod (*B. gigantea*) and chordates are more susceptible to high-temperature fluctuations than other species. Note that, even though pairwise differences between species were not always statistically significant (Figure 1), the inclusion of loggers with less extreme temperatures decreases the statistical power of this analysis as mortality in these circumstances is nearly zero for all groups. For simulations assuming heatwaves with sea water warming of +2°C by a duration of at 10 days and 30 day the increment in days when mortality surpassed 50% was over of 29% and 42% respectively (Figures 1E, G), in both cases mainly driven by increment in mortality to *B. gigantea* (1 day both scenarios), *L. nudifrons* (2 days both scenarios), *H. antarticus* (2 days and 7 days respectively), *T. newnesi* (4 days and 5 days respectively), *O. validus* (3 days both scenarios) and *S. neumayeri* (2 days both scenarios) (Figures 1G, H). Similarly, mean predicted daily mortality differed significantly between species (F6,77 = 6.475, p = 1.47 × 10^{-5}), once again supporting differences in susceptibility to warm waters between groups (Figure 1).

Discussion

Precise estimates of upper thermal limits are essential to determine the impact of GW on Antarctic species, either because they have evolved in habitant characterized by narrow and extreme thermal environments or because their habitats are changing rapidly (Morley et al., 2020). Here, we combined an experimental essay on Antarctic organisms with thermal sensitivity to build an accurate and comparable estimate of upper thermal limits through the taxa. Our results evidence a clear difference in thermal tolerance among Arthropods Chordata and Echinoderms, as well as the relevance of distinguishing the time effect (i.e., T_{ko} 1 min, T_{ko} 1 day and 30 days) on the vulnerability to warming conditions (Richard et al., 2012; Molina et al., 2022). In addition, under the tolerance landscape framework (Rezende et al., 2020), we showed that temperature variation from the intertidal area did affect the predicted mortality to the studied species, though in different intensities depending on the taxa. Also, conservative scenarios of extreme marine warming events (heatwaves) during an Austral summer at the Antarctic archipelago did impact predicted mortality (Figure 1A), showing the vulnerability of the Antarctic marine species to GW on an ecological scale.

According to previous evidence about thermal tolerance to Antarctic species (Peck et al., 2009), we found that estimators of thermal limits such as CT_{max} are above the temperature these animals experience in natural conditions. Our approach explicitly followed a correction by time exposure and used estimates of thermal sensitivity to Antarctic species (Molina et al., 2022). It is one step forward because TDT curves allow building an estimate of time scale with ecological significance, either daily, monthly, or seasonally temporal window (Figure 1B). That is important because the role of exposure time in determining temperature tolerance is a perspective little studied in the literature (Lefevre et al., 2021), but essential if we want to evaluate the impact of GW on Antarctic species (Morley et al., 2020). For instance, our study is the first to show evidence of upper thermal limits to Malacostraca Arthropods such as the amphipodan *Bovallia gigantea* and the isopoda *Glyptonotus antarticus*. Despite the interspecific difference among Antarctic arthropods, our findings cover the wide range of thermal limits reported in the literature, from 32.5°C to 6.7°C (Lahdes et al., 1993; Peck, 2004; Peck et al., 2009; Peck et al., 2010; Toullec et al., 2020). Also, our results on Chordata animals such as *Harpafiger antarcticus*, *Lepidonotothen nudriforns*, and *Trematomus newnesi* are according to the wide range of upper thermal limits Antarctic nototenids from 21.58°C to 5°C (Somero and

DeVries, 1967; Peck et al., 2009; Beers and Sidell, 2011; Bilyk and DeVries, 2011; Joyce et al., 2018). Likewise, the Echinoderms *Odontaster validus* and *Sterechinus neumayeri* showed upper thermal limits, as reported previously, in a range of 24.7°C to 10.9° C (Peck et al., 2009; Peck et al., 2010; Morley et al., 2012). Undoubtedly, species comparison allows us to visualize the diversity of the thermal tolerance capacity that Antarctic species must possess, which underpins different physiological architectures. However, discrepancies in methodological approaches and traits evaluated may obscure another phenomenon in the variation in thermal tolerance limits (Williams et al., 2016), making it difficult to build proper interspecific comparisons. Comparison among species that inhabit the same environments may differ in physiological strategies to cope with environmental thermal stress, constrained to a specific ecological scale (Peck, 2011; Byers, 2020). Therefore, physiological and genetic mechanisms are needed to understand the variation in thermal tolerance and distinguish phenotypic thermal strategy from adapting to extreme and cold Antarctic habitats, including physiological, molecular mechanisms (González-Aravena et al., 2021; Saravia et al., 2021), and behavioral responses influenced changes in distribution ranges (Morley et al., 2010).

Predicting ectotherm species' response to GW is key to understanding the global anthropic effect on biodiversity (Pecl et al., 2017). Identified as an anthropic global driver affecting the polar marine ecosystem, such as in the Antarctic peninsula, where increments until 2°C on the current pattern of temperatures are expected shortly (Hellmer et al., 2017; Moffat and Meredith, 2018). Here, the higher variation in temperature records to the intertidal zone may be linked with a daily higher sensibility to the tidal pattern experienced in this coastal area (Figure 1), which has been described as an extended pattern along the marine coast (Byers, 2020; Liao et al., 2021). As an atmospheric event to date, heatwaves have been related to the Antarctic continent (Robinson et al., 2020; González-Herrero et al., 2022; Turner et al., 2022), and the recurrence of extreme marine heatwaves worldwide (Hobday et al., 2018) makes it possible to expect those events around Antarctica. Due to that, GW heatwaves in marine ecosystems affect the biological communities (Paganini et al., 2014; Hobday et al., 2016; Roberts et al., 2019; Magel et al., 2020), and exposure time is urgently needed to quantify the effect of thermal stress on organismal performance (Williams et al., 2016; Lefevre et al., 2021). We used TDT curves that use the exposure time linked with thermal limits (Rezende et al., 2014), which combine real-time scales to thermal stress, allowing us to predict the effect of thermal variation in the ecological scale (Rezende et al., 2020). We modeled mortality in a window of 24 hours along with the 100 days considered from the Austral summer, then the relevant time scale of T_{ko} built from TDTs curve was from 1 to 1440 minutes to estimate mortality. The cumulated effect on a daily scale was enough to produce mortality, and this rise when moderate heatwaves (Hobday et al., 2018) were considered into de daily variation (Figure 1). Based on the higher thermal sensitivity (z) of the echinoderm *O.validatus* (T_{ko} 1 min = 30.65; T_{ko} 1 day = 10.41) and *S. neumayeri* (T_{ko} 1 min = 31.18; T_{ko} 1 day = 10.93), this mayor taxa seems to be better adapted to future warming events, which may be linked with the sessile condition and less capabilities to escape to local thermal stress (Sunday et al., 2011; Molina et al., 2022). Although lower thermal sensitivity may impact long-term response from the three Chordata *L. nudrifrons* (T_{ko} 1 min = 17.57; T_{ko} 1 day = 10.91), *H.antarticus* (T_{ko} 1 min = 21.04; T_{ko} 1 day = 14.39), *T. newnesi* (T_{ko} 1 min = 19.81; T_{ko} 1 day = 13.15) and the two Arthropods *B. gigantea* (T_{ko} 1 min = 19.81; T_{ko} 1 day = 15.61) and *G. antarticus* (T_{ko} 1 min = 22.41; T_{ko} 1 day = 18.20), the lower temperature which those species responded to the experimental thermal challenge, determine higher vulnerability to increment of temperature in a daily scale and its cumulative effect on the entire Austral summer intertidal area as well as the effects of the moderate heatwave.

In overview, precise predictions of the Antarctic fauna responses to global warming are a priority to conservation and decision-makers because of the pristine condition of the continent and the evolutionary and ecological process that has built its unique biological diversity. Our finding reveals that Antarctic marine species may be under thermal stress under less temperature but on a more extended time scale, such heatwaves events, indeed, temperatures that may be organisms experienced at the current time in the wild. In line, differences among species are influenced by the thermal sensitivity parameter (Rezende et al., 2014), which summary the phenotypic response to the thermal difference in a specific time (minutes). We interpreted these interspecific differences as a consequence of the morphological, physiological, and behavioral adaptations that distinguish the species studied to face thermal stress in the Antarctic marine ecosystem as consequences of global warming due to human activities worldwide.

Data availability statement

The datasets presented in this study can be found in online repositories. The names of the repository/repositories and accession number(s) can be found below: https://datadryad.org/stash/share/CdFIhwoocjOslligf5dzjb9OjJa2V7EzLtiqxyuPokw.

Ethics statement

The animal study was reviewed and approved by Comité de Bioética, Universidad Andrés Bello.

Author contributions

MC: Conceptualization, Investigation, Writing – original draft, Writing – review & editing, Visualization, Data curation. MRG-H: Investigation, Writing – review & editing. MA: Writing- Reviewing and Editing. ER: Writing- Reviewing and Editing, Funding acquisition. FB:

Writing- Reviewing and Editing. CG-M: Writing- Reviewing and Editing, Funding acquisition. JP: Supervision, Writing- Reviewing and Editing, Resources, Funding acquisition. All authors contributed to the article and approved the submitted version.

Funding

MC thanks the support of UNAB DI 10.20/Reg grants. MRG-H acknowledges the support of ANID Grand No. PAI77190031 and FONDECYT 11220593 grants. MA acknowledges the support of FONDECYT 1220866 grants. FB acknowledge ANID PIA/BASAL FB0002. CG-M thanks the support of FONDECYT 11150548 and 1210946, INACH RT12-17 and ANID PIA/INACH ACT192057 grants. JP thanks the support by INACH RT09-18 and FONDECYT 1200813 grants.

Conflict of interest

The authors declare that the research was conducted in the absence of any commercial or financial relationships that could be construed as a potential conflict of interest.

Publisher's note

References

Barnes, D. K. A., and Peck, L. S. (2008). Vulnerability of Antarctic shelf biodiversity to predicted regional warming. *Clim. Res.* 37, 149–163. doi: 10.3354/cr00760

Beers, J. M., and Jayasundara, N. (2015). Antarctic Notothenioid fish: What are the future consequences of "losses" and "gains" acquired during long-term evolution at cold and stable temperatures? *J. Exp. Biol.* 218, 1834–1845. doi: 10.1242/jeb.116129

Beers, J. M., and Sidell, B. D. (2011). Thermal tolerance of Antarctic notothenioid fishes correlates with level of circulating hemoglobin. *Physiol. Biochem. Zool.* 84, 353–362. doi: 10.1086/660191

Beitinger, T. L., Bennett, W. A., and McCauley, R. W. (2000). Temperature tolerances of north American freshwater fishes exposed to dynamic changes in temperature. *Environ. Biol. Fishes* 58, 237–275. doi: 10.1023/A:1007676325825

Bilyk, K. T., and DeVries, A. L. (2011). Heat tolerance and its plasticity in Antarctic fishes. *Comp. Biochem. Physiol. - A Mol. Integr. Physiol.* 158, 382–390. doi: 10.1016/j.cbpa.2010.12.010

Byers, J. E. (2020). Effects of climate change on parasites and disease in estuarine and nearshore environments. *PloS Biol.* 18, 1–12. doi: 10.1371/journal.pbio.3000743

Cook, A. J., Holland, P. R., Meredith, M. P., Murray, T., Luckman, A., and Vaughan, D. G. (2016). Ocean forcing of glacier retreat in the western Antarctic peninsula. *Science* 353, 283–286. doi: 10.1126/science.aae0017

González-Aravena, M., Rondon, R., Font, A., Cárdenas, C. A., Toullec, J. Y., Corre, E., et al. (2021). Low transcriptomic plasticity of Antarctic giant isopod glyptonotus antarcticus juveniles exposed to acute thermal stress. *Front. Mar. Sci.* 8. doi: 10.3389/fmars.2021.761866

González-Herrero, S., Barriopedro, D., Trigo, R. M., López-Bustins, J. A., and Oliva, M. (2022). Climate warming amplified the 2020 record-breaking heatwave in the Antarctic peninsula. *Commun. Earth Environ.* 3, 1–9. doi: 10.1038/s43247-022-00450-5

Hellmer, H. H., Kauker, F., Timmermann, R., and Hattermann, T. (2017). The fate of the southern weddell sea continental shelf in a warming climate. *J. Clim.* 30, 4337–4350. doi: 10.1175/JCLI-D-16-0420.1

Hobday, A. J., Alexander, L. V., Perkins, S. E., Smale, D. A., Straub, S. C., Oliver, E. C. J., et al. (2016). A hierarchical approach to defining marine heatwaves. *Prog. Oceanogr.* 141, 227–238. doi: 10.1016/j.pocean.2015.12.014

Hobday, A. J., Oliver, E. C. J., Sen Gupta, A., Benthuysen, J. A., Burrows, M. T., Donat, M. G., et al. (2018). Categorizing and naming marine heatwaves. *Oceanography* 31, 162–173. doi: 10.5670/oceanog.2018.205

Jørgensen, L. B., Malte, H., Ørsted, M., Klahn, N. A., and Overgaard, J. (2021). A unifying model to estimate thermal tolerance limits in ectotherms across static, dynamic and fluctuating exposures to thermal stress. *Sci. Rep.* 11, 1–14. doi: 10.1038/s41598-021-92004-6

Joyce, W., Axelsson, M., Egginton, S., Farrell, A. P., Crockett, E. L., and O'Brien, K. M. (2018). The effects of thermal acclimation on cardio-respiratory performance in an Antarctic fish (Notothenia coriiceps). *Conserv. Physiol.* 6, 1–12. doi: 10.1093/conphys/coy069

Kuklinski, P., and Balazy, P. (2014). Scale of temperature variability in the maritime Antarctic intertidal zone. *J. Sea Res.* 85, 542–546. doi: 10.1016/j.seares.2013.09.002

Lahdes, E. O., Kivivuori, L. A., and Lehti-Koivunen, S. M. (1993). Thermal tolerance and fluidity of neuronal and branchial membranes of an antarctic amphipod (Orchomene plebs); a comparison with a baltic isopod (Saduria entomon). *Comp. Biochem. Physiol. – Part A Physiol.* 105, 463–470. doi: 10.1016/0300-9629(93)90420-9

Lefevre, S., Wang, T., and McKenzie, D. J. (2021). The role of mechanistic physiology in investigating impacts of global warming on fishes. *J. Exp. Biol.* 224, jeb238840. doi: 10.1242/jeb.238840

Liao, M., Li, G., Wang, J., Marshall, D. J., Hui, T. Y., Ma, S., et al. (2021). Physiological determinants of biogeography: The importance of metabolic depression to heat tolerance. *Glob. Change Biol.* 27, 2561–2579. doi: 10.1111/gcb.15578

Magel, J. M. T., Dimoff, S. A., and Baum, J. K. (2020). Direct and indirect effects of climate change-amplified pulse heat stress events on coral reef fish communities. *Ecol. Appl.* 30, 1–15. doi: 10.1002/eap.2124

Meredith, M. P., and King, J. C. (2005). Rapid climate change in the ocean west of the Antarctic peninsula during the second half of the 20th century. *Geophys. Res. Lett.* 32, 1–5. doi: 10.1029/2005GL024042

Moffat, C., and Meredith, M. (2018). Shelf-ocean exchange and hydrography west of the Antarctic peninsula: A review. *Philos. Trans. R. Soc A Math. Phys. Eng. Sci.* 376, 20170164. doi: 10.1098/rsta.2017.0164

Molina, A. N., Pulgar, J. M., Rezende, E. L., and Carter, M. J. (2023). Heat tolerance of marine ectotherms in a warming Antarctica. *Glob. Change Biol.* 29, 179–88. doi: 10.1111/gcb.16402

Morley, S. A., Abele, D., Barnes, D. K. A., Cárdenas, C. A., Cotté, C., Gutt, J., et al. (2020). Global drivers on southern ocean ecosystems: Changing physical environments and anthropogenic pressures in an earth system. *Front. Mar. Sci.* 7. doi: 10.3389/fmars.2020.547188

Morley, S. A., Griffiths, H. J., Barnes, D. K. A., and Peck, L. S. (2010). South Georgia: A key location for linking physiological capacity to distributional changes in response to climate change. *Antarct. Sci.* 22, 774–781. doi: 10.1017/S0954102010000465

Morley, S. A., Hirse, T., Pörtner, H. O., and Peck, L. S. (2009). Geographical variation in thermal tolerance within southern ocean marine ectotherms. *Comp. Biochem. Physiol. - A Mol. Integr. Physiol.* 153, 154–161. doi: 10.1016/j.cbpa.2009.02.001

Morley, S. A., Martin, S. M., Bates, A. E., Clark, M. S., Ericson, J., Lamare, M., et al. (2012). Spatial and temporal variation in the heat tolerance limits of two abundant southern ocean invertebrates. *Mar. Ecol. Prog. Ser.* 450, 81–92. doi: 10.3354/meps09577

Ørsted, M., Jørgensen, L. B., and Overgaard, J. (2022). Finding the right thermal limit: a framework to reconcile ecological, physiological and methodological aspects of CTmax in ectotherms. *J. Exp. Biol.* 225, jeb244514. doi: 10.1242/jeb.244514

Paganini, A. W., Miller, N. A., and Stillman, J. H. (2014). Temperature and acidification variability reduce physiological performance in the intertidal zone porcelain crab petrolisthes cinctipes. *J. Exp. Biol.* 217, 3974–3980. doi: 10.1242/jeb.109801

Peck, L. S. (2004). Physiological flexibility: The key to success and survival for Antarctic fairy shrimps in highly fluctuating extreme environments. *Freshw. Biol.* 49, 1195–1205. doi: 10.1111/j.1365-2427.2004.01264.x

Peck, L. S. (2005). Prospects for survival in the southern ocean: Vulnerability of benthic species to temperature change. *Antarct. Sci.* 17, 497–507. doi: 10.1017/S0954102005002920

Peck, L. S. (2011). Organisms and responses to environmental change. *Mar. Genomics* 4, 237–243. doi: 10.1016/j.margen.2011.07.001

Peck, L. S. (2018). Antarctic Marine biodiversity: Adaptations, environments and responses to change. *Oceanogr. Mar. Biol.* 56, 105–236. doi: 10.1201/9780429454455-3

Peck, L. S., Clark, M. S., Morley, S. A., Massey, A., and Rossetti, H. (2009). Animal temperature limits and ecological relevance: Effects of size, activity and rates of change. *Funct. Ecol.* 23, 248–256. doi: 10.1111/j.1365-2435.2008.01537.x

Peck, L. S., Morley, S. A., and Clark, M. S. (2010). Poor acclimation capacities in Antarctic marine ectotherms. *Mar. Biol.* 157, 2051–2059. doi: 10.1007/s00227-010-1473-x

Pecl, G. T., Araújo, M. B., Bell, J. D., Blanchard, J., Bonebrake, T. C., Chen, I. C., et al. (2017). Biodiversity redistribution under climate change: Impacts on ecosystems and human well-being. *Science* 355, eaai9214. doi: 10.1126/science.aai9214

Peralta-Maraver, I., and Rezende, E. L. (2021). Heat tolerance in ectotherms scales predictably with body size. *Nat. Clim. Change* 11, 58–63. doi: 10.1038/s41558-020-00938-y

R Development Core Team (2019). *R: a language and environment for statistical computing* (Vienna, Austria: R Foundation for Statistical Computing). Available at: http://www.rproject.org.

Rezende, E. L., Bozinovic, F., Szilágyi, A., and Santos, M. (2020). Predicting temperature mortality and selection in natural drosophila populations. *Science* 369, 1242–1245. doi: 10.1126/science.aba9287

Rezende, E. L., Castañeda, L. E., and Santos, M. (2014). Tolerance landscapes in thermal ecology. *Funct. Ecol.* 28, 799–809. doi: 10.1111/1365-2435.12268

Richard, J., Morley, S. A., Thorne, M. A. S., and Peck, L. S. (2012). Estimating long-term survival temperatures at the assemblage level in the marine environment: Towards macrophysiology. *PloS One* 7, e34655. doi: 10.1371/journal.pone.0034655

Roberts, S. D., Van Ruth, P. D., Wilkinson, C., Bastianello, S. S., and Bansemer, M. S. (2019). Marine heatwave, harmful algae blooms and an extensive fish kill event during 2013 in south Australia. *Front. Mar. Sci.* 6. doi: 10.3389/fmars.2019.00610

Robinson, S. A., Klekociuk, A. R., King, D. H., Pizarro Rojas, M., Zúñiga, G. E., and Bergstrom, D. M. (2020). The 2019/2020 summer of Antarctic heatwaves. *Glob. Change Biol.* 26, 3178–3180. doi: 10.1111/gcb.15083

Sandersfeld, T., Mark, F. C., and Knust, R. (2017). Temperature-dependent metabolism in Antarctic fish: Do habitat temperature conditions affect thermal tolerance ranges? *Polar Biol.* 40, 141–149. doi: 10.1007/s00300-016-1934-x

Saravia, J., Paschke, K., Oyarzún-Salazar, R., Cheng, C. H. C., Navarro, J. M., and Vargas-Chacoff, L. (2021). Effects of warming rates on physiological and molecular components of response to CTMax heat stress in the Antarctic fish harpagifer antarcticus. *J. Therm. Biol.* 99, 103021. doi: 10.1016/j.jtherbio.2021.103021

Sinclair, B. J., Marshall, K. E., Sewell, M. A., Levesque, D. L., Willett, C. S., Slotsbo, S., et al. (2016). Can we predict ectotherm responses to climate change using thermal performance curves and body temperatures? *Ecol. Lett.* 19, 1372–1385. doi: 10.1111/ele.12686

Somero, G. N., and DeVries, A. L. (1967). Temperature tolerance of some Antarctic fishes. *Science* 156, 257–258. doi: 10.1126/science.156.3772.258

Sunday, J. M., Bates, A. E., and Dulvy, N. K. (2011). Global analysis of thermal tolerance and latitude in ectotherms. *Proc. R. Soc B Biol. Sci.* 278, 1823–1830. doi: 10.1098/rspb.2010.1295

Sunday, J. M., Bates, A. E., and Dulvy, N. K. (2012). Thermal tolerance and the global redistribution of animals. *Nat. Clim. Change* 2, 686–690. doi: 10.1038/nclimate1539

Toullec, J. Y., Cascella, K., Ruault, S., Geffroy, A., Lorieux, D., Montagné, N., et al. (2020). Antarctic Krill (Euphausia superba) in a warming ocean: thermotolerance and deciphering Hsp70 responses. *Cell Stress Chaperones* 25, 519–531. doi: 10.1007/s12192-020-01103-2

Turner, J., Lu, H., King, J. C., Carpentier, S., Lazzara, M., Phillips, T., et al. (2022). An extreme high temperature event in coastal East Antarctica associated with an atmospheric river and record summer downslope winds. *Geophys. Res. Lett.* 49, 1–11. doi: 10.1029/2021GL097108

Williams, C. M., Buckley, L. B., Sheldon, K. S., Vickers, M., Pörtner, H. O., Dowd, W. W., et al. (2016). Biological impacts of thermal extremes: mechanisms and costs of functional responses matter. *Integr. Comp. Biol.* 56, 73–84. doi: 10.1093/icb/icw013

frontiers | Frontiers in Marine Science

TYPE Original Research
PUBLISHED 02 February 2023
DOI 10.3389/fmars.2023.1101725

OPEN ACCESS

EDITED BY
Hongsheng Yang,
Institute of Oceanology, Chinese Academy of Sciences (CAS), China

REVIEWED BY
Yi Yang,
Hainan University, China
Xinran Li,
Foshan University, China

*CORRESPONDENCE
Chenglin Li
lcl_xh@hotmail.com

SPECIALTY SECTION
This article was submitted to Global Change and the Future Ocean, a section of the journal Frontiers in Marine Science

RECEIVED 18 November 2022
ACCEPTED 09 January 2023
PUBLISHED 02 February 2023

CITATION
Yao L, Zhao B, Wang Q, Jiang X, Han S, Hu W and Li C (2023) Contribution of the TGFβ signaling pathway to pigmentation in sea cucumber (*Apostichopus japonicus*). *Front. Mar. Sci.* 10:1101725. doi: 10.3389/fmars.2023.1101725

Contribution of the TGFβ signaling pathway to pigmentation in sea cucumber (*Apostichopus japonicus*)

Linlin Yao[1], Bin Zhao[1], Qi Wang[1], Xuyang Jiang[2], Sha Han[1], Wei Hu[1] and Chenglin Li[1]*

[1]Shandong Key Laboratory of Intelligent Marine Ranch (under preparation), Marine Science Research Institute of Shandong Province (National Oceanographic Center, Qingdao), Qingdao, China, [2]Department of Breeding Technology, Country Conson CSSC (Qingdao) Ocean Technology CO., Ltd, Qingdao, China

Pigmentation mediated by the transforming growth factor β (TGFβ) signaling pathway is a key trait for understanding environmental adaptability and species stability. In this study, TGFβ signaling pathway members and their expression patterns in different color morphs of the sea cucumber *Apostichopus japonicus* were evaluated. Using a bioinformatics approach, 22 protein sequences of TGFβ signaling pathway members in *A. japonicus* were classified, including 14 that were identified for the first time in the species, including 7 ligands, 6 receptors, and 1 R-Smad. We further evaluated mRNA expression data for different color morphs and pigmentation periods. These results support the hypothesis that both subfamilies of the TGFβ superfamily, i.e., the TGFβ/activin/Nodal and BMP/GDF/AMH subfamilies, are involved in the regulation of pigmentation in *A. japonicus*. The former subfamily was complete and contributes to the different color morphs. The BMP/GDF/AMH subfamily was incomplete. BMP2/4-induced differentiation of white adipocytes was regulated by the BMP2/4–ACVR2A–Smad1 signaling pathway. These findings provide insight into the TGFβ family in early chordate evolution as well as the molecular basis of color variation in an economically valuable species.

KEYWORDS

TGFβ signaling pathway, regulatory mechanism, pigmentation, *Apostichopus japonicas*, gene family divergence

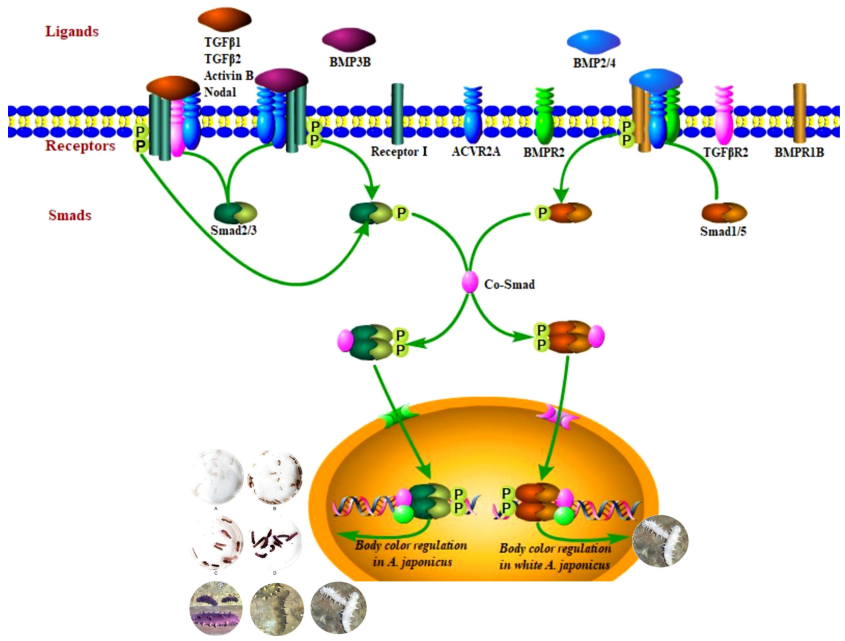

GRAPHICAL ABSTRACT

1 Introduction

The sea cucumber *Apostichopus japonicus* is a commercially important marine species in China (Chen et al., 2022). Color variation, one of the most important characteristics of *A. japonicus*, plays a significant role in determining market price (Kang et al., 2011) and is an important trait for breeding. In China, this species is mainly green, and purple and white morphs are very rare and highly valuable (Bai et al., 2016). Extensive studies have shown that the growth and development of sea cucumber are affected by various environmental factors, such as temperature and salinity (Chen et al., 2007; Wang et al., 2007; Ji et al., 2008). There are significant differences in the tolerance of sea cucumbers with different body colors to environmental factors (Bao, 2008; Guo et al., 2020; Li et al., 2020). For example, purple *A. japonicus* has a wider temperature range and stronger salt tolerance, while the white morph has a higher temperature tolerance but narrower range of salinity tolerance than those of the green morph (Zhao et al., 2018; Zhu et al., 2013).

Pigmentation is a tractable and relevant trait for understanding key issues in evolutionary biology such as adaptation, speciation and the maintenance of balanced polymorphisms (Henning et al., 2013).Substantial recent research has focused on the identification of genetic pathways that determine pigmentation variation (Hubbard et al., 2010; Henning et al., 2013). Studies of animal models have found that the TGFβ signaling pathway mediates many biological processes, such as pigmentation, tissue and organ development, and stress resistance (Cheng, 2008; Hubbard et al., 2010). Recent structural, biochemical, and cellular studies have provided significant insight into the mechanisms underlying TGFβ signaling. In brief, a TGFβ ligand initiates signaling by binding to and bringing together type I and type II receptor on the cell surface. This allows receptor II to phosphorylate receptor I, which then regulates target gene expression by the phosphorylation of Smad proteins. The number and type of TGFβ family members have been evaluated in model organisms, ranging from worms and flies to mammals (Massagué and Chen, 2000; Patterson and Padgett, 2000; ten Dijke et al., 2000). Six conserved cysteine residues characteristic of the TGFβ family are encoded by 6 open reading frames in worms, 9 in flies, and 42 in humans (Linton et al., 2001).

Although studies of the TGFβ family in non-model organisms are increasing, relatively little is known about functional changes and divergence in expression patterns between invertebrates and vertebrates (Lapraz et al., 2007; Weiss and Attisano, 2013; Zheng et al., 2018). Echinoderms, which first appeared in the early Cambrian period (Bottjer et al., 2006), occupy a critical phylogenetic position for understanding the origin of chordates (Lowe et al., 2015). The radiation of echinoderms was believed to be responsible for the Mesozoic Marine Revolution (Signor and Brett, 1984). In particular, sea cucumbers are an outstanding representative of the phylum, as they have survived ice ages and are considered “living fossils” (Bottjer et al., 2006). Despite the importance of pigmentation mediated by the TGFβ signaling pathway (Cheng, 2008; Hubbard et al., 2010; Henning et al., 2013), few studies have evaluated the TGFβ signaling pathway in sea cucumbers. Only 14 ligands (some sharing the same name), 6 receptors, and 2 R-Smads have been recorded in GenBank. In

addition, some loci have informal names, such as Sj-BMP2/4 (accession no. PIK56114.1 and BAC53989.1), and some were not classified in detail, e.g., putative TGFβ (accession no. PIK61515.1). Accordingly, their functions and roles in morphs with different body colors are unclear. This can be explained, in part, by poor sampling of genomes (Sodergren et al., 2006; Cameron et al., 2015; Hall et al., 2017; Sun et al., 2017; Zhang et al., 2017). In this study, the types and quantities of TGFβ signaling pathway members in *A. japonicus* were characterized for the first time and expression levels in different color morphs and developmental stages were evaluated, providing an important basis for analyses of functions of TGFβ signaling in invertebrates.

2 Materials and methods

2.1 Sequence analysis

All TGFβ ligand receptors and Smad protein sequences of *A. japonicus* available on NCBI were obtained and compared using BLAST (Basic Local Alignment Search Tool) (Tables 1–3). Multiple sequence alignments were analyzed using the ClustalW Multiple Alignment program (http://www.ebi.ac.uk/clustalw/). Separate trees were generated based on ligand, receptor, and SMAD amino acid sequences using the neighbor-joining (NJ) algorithm within MEGA version 7.0. The reliability of the tree was assessed by 1000 bootstrap repetitions.

2.2 Animals

2.2.1 Sea cucumbers of different color morphs

Healthy sea cucumbers aged 2 years and weighing 120 ± 10 g were collected from green, purple, and white cultivated populations (Figure 1). The purple and white morphs are genetically stable and have been bred by our research team for nearly 20 years.

2.2.2 Purple sea cucumber at different developmental stages

9 purple sea cucumbers with a body weight of >180 g were screened as the parent population. Artificial labor was stimulated by drying in the shade and running water (20.5°C). Male individuals were removed from the incubator immediately after ejaculation. All parents were removed when the egg density was 20–30 eggs/mL. Then, the water temperature was increased to 21.0 ± 0.2°C for incubation. During the incubation period, the incubator was agitated once an hour, and micro-aerated continuously for 24 h to ensure an even distribution of fertilized eggs. Marine red yeast was fed to early auricularia after hatching. When 10% to 20% of doliolaria formed, a corrugated plate frame after disinfection was placed as the attachment matrix. After the larvae were attached, they were gradually transitioned to artificial compound feed. The feeding amount was 0.5% to 2% of the body weight. Juveniles were randomly selected every 3 days after the larvae developed to pentactula and were placed in a Petri dish to observe the change in body color. The pigmentation stage was defined at the point at which 80% of individuals were completely pigmented.

2.3 mRNA expression of TGFβ signaling pathway genes mRNA in *A. japonicas*

9 body walls from each sample of different color morphs and purple sea cucumber at different developmental stages were peeled away carefully, flash-frozen in liquid nitrogen, and stored at −80°C for subsequent total RNA extraction. Specific primers for BMP2/4, ACVR2A, Smad1, TGFβR2, Smad2/3, and grb2 (a housekeeping gene used as an internal reference) based on known *A. japonicus* sequences (Table 4) were designed using Oligo 7.0. Primers were synthesized by Invitrogen Biotechnology Co., Ltd. (Shanghai, China). TRIzol Reagent was used to isolate total RNA from the body walls according to the manufacturer's instructions (Invitrogen, Waltham, MA, USA) and contaminating genomic DNA was eliminated using RNase-free DNase (Takara, Tokyo, Japan). The RNA samples were reverse-transcribed using the Prime Script RT-PCR Kit (Takara, Tokyo, Japan). Equal amounts of cDNA were used for real-time quantitative RT-PCR using in a PikoReal 96-well RT-PCR System (Thermo Scientific., Waltham, MA, USA). Amplification was performed in a total volume of 10 μL, containing 5 μL of 2× SYBR Green master Mix, 1 μL of diluted cDNA, 0.4 μL of each primer, and 3.2 μL of PCR-grade water. The PCR cycling conditions were 95°C for 5 min followed by 35 cycles of 95°C for 15 s, 60°C for 30 s, and 72°C for 1 min, and a final elongation step at 72°C for 7 min. Each sample was run in triplicate along with the internal control gene (grb2). The PCR products were visualized on a UV-transilluminator after electrophoresis on a 1.5% agarose gel containing ethidium bromide.

2.4 Statistical analysis

Statistical analyses were performed using GraphPad Prism 5.0, and all data were assessed using one-way ANOVA. Differences in means between groups were assessed using Tukey's honestly significant difference test for *post hoc* multiple comparisons. All data are expressed as the mean ± standard deviation (SD). Values of $p < 0.05$ indicated a statistically significant difference.

3 Results

3.1 Phylogenetic analysis based on ligand sequences

In a phylogenetic tree based on amino acid sequences from multiple TGFβ ligands, the ligands of the same type formed clusters. The phylogenetic tree is shown in Figure 2 and the corresponding sequences are shown in Table 1. According to the phylogenetic tree, 14 known TGFβ ligands from *A. japonicus* were assigned to 7 classes: TGFβ1, TGFβ2, Nodal, Activin/Inhibin, BMP2/4, BMP3, and GDF8 (Growth Differentiation Factor 8, alternative name myostatin (de Caestecker, 2004)). Notably, TGFβ2 of *A. japonicus* was classified as TGFβ2 but was also closely related to TGFβ3. The BMP2/4 cluster contained BMP2A, BMP2, BMP, and Sj-BMP2/4 of *A. japonicus*. BMP3/3B of *A. japonicus* was classified into BMP3. Putative activin BX1 and putative inhibin beta C chain-like of *A. japonicus* were included in the Activin/Inhibin cluster.

TABLE 1 Ligand protein sequences included in the present study.

Accession no.	Protein name	Species
PIK34829.1	**putative TGFβ1 like**	**Apostichopus japonicus**
QHG11580.1	**putative TGFβ1X1**	**Apostichopus japonicus**
PIK56215.1	**putative TGFβ1X1**	**Apostichopus japonicus**
XP_029964045.1	TGFβ1X2	Salarias fasciatus
XP_041850924.1	TGFβ1X1	Melanotaenia boesemani
XP_031614329.1	TGFβ1	Oreochromis aureus
XP_033486555.1	TGFβ1X1	Epinephelus lanceolatus
XP_040902844.1	TGFβ1	Toxotes jaculatrix
XP_033851930.2	TGFβ1X1	Acipenser ruthenus
XP_035241816.1	TGFβ1X1	Anguilla anguilla
XP_026865903.2	TGFβ1X2	Electrophorus electricus
XP_036440909.1	TGFβ1X1	Colossoma macropomum
KAG9273341.1	TGFβ1X1	Astyanax mexicanus
PIK45926.1	**BMP2A**	**Apostichopus japonicus**
PIK48439.1	**BMP2**	**Apostichopus japonicus**
PIK57098.1	**BMP**	**Apostichopus japonicus**
AAF19841.1	BMP2/4	Branchiostoma belcheri
QYF06707.1	BMP2/4	Holothuria scabra
PIK56114.1	**Sj-BMP2/4**	**Apostichopus japonicus**
BAC53989.1	**Sj-BMP2/4**	**Apostichopus japonicus**
AAD28038.1	BMP2/4	Lytechinus variegatus
ACA04460.1	BMP2/4	Strongylocentrotus purpuratus
ABG00199.1	BMP2/4	Paracentrotus lividus
BBC77411.1	BMP2/4	Temnopleurus reevesii
PIK37799.1	**BMP3/3B**	**Apostichopus japonicus**
KAF3695343.1	BMP3	Channa argus
XP_033946079.1	BMP3	Pseudochaenichthys georgianus
XP_007425424.1	BMP3	Python bivittatus
XP_042727338.1	BMP3	Lagopus leucura
XP_021252303.1	BMP3	Numida meleagris
PIK42868.1	**TGFβ family member nodal**	**Apostichopus japonicus**
ACF32774.1	Nodal	Heliocidaris erythrogramma
ACF32773.1	Nodal	Heliocidaris tuberculata
XP_036937551.1	Nodal2	Acanthopagrus latus
XP_034426535.1	Nodal2	Hippoglossus hippoglossus
KFM00388.1	Nodal	Aptenodytes forsteri
XP_035248296.1	Nodal	Anguilla anguilla
RXN30610.1	Nodal	Labeo rohita
QYF06711.1	GDF8	Holothuria scabra
AJQ81037.1	**GDF8**	**Apostichopus japonicus**

(Continued)

TABLE 1 Continued

Accession no.	Protein name	Species
XP_013394669.1	GDF8	Lingula anatina
XP_014253049.1	GDF8	Cimex lectularius
XP_046672106.1	GDF8	Homalodisca vitripennis
RWS12911.1	GDF8	Dinothrombium tinctorium
XP_023223240.1	GDF8	Centruroides sculpturatus
QYF06710.1	inhibin	Holothuria scabra
PIK34215.1	**putative inhibin beta C chain-like**	**Apostichopus japonicus**
QYF06712.1	activin	Holothuria scabra
PIK48233.1	**putative activin B X1**	**Apostichopus japonicus**
XP_037927328.1	INHβB	Teleopsis dalmanni
XP_022218905.1	INHβA	Drosophila obscura
XP_017154392.1	INHβA	Drosophila miranda
XP_002028363.1	INHβA	Drosophila persimilis
XP_033236864.1	INHβA	Drosophila pseudoobscura
QYF06713.1	TGFβ2	Holothuria scabra
PIK61515.1	**putative TGFβ2**	**Apostichopus japonicus**
XP_022090565.1	TGFβ2	Acanthaster planci
XP_038073348.1	TGFβ2	Patiria miniata
BCB62973.1	TGFβ	Patiria pectinifera
XP_041467929.1	TGFβ2	Lytechinus variegatus
XP_030855505.1	TGFβ2	Strongylocentrotus purpuratus
QAV52899.1	TGFβ	Mesocentrotus nudus
XP_041951915.1	TGFβ3	Alosa sapidissima
XP_042562890.1	TGFβ3	Clupea harengus
XP_039597176.1	TGFβ3	Polypterus senegalus
XP_028678165.1	TGFβ3	Erpetoichthys calabaricus
XP_042593951.1	TGFβ2	Cyprinus carpio
KAA0709699.1	TGFβ2	Triplophysa tibetana
XP_039388520.1	TGFβ2X2	Mauremys reevesii
XP_037751639.1	TGFβ2	Chelonia mydas
XP_005307005.1	TGFβ2	Chrysemys picta bellii
XP_003800184.1	TGFβ2X2	Otolemur garnettii
XP_008825028.1	TGFβ2	Nannospalax galili
CAA40672.1	TGFβ2	Mus musculus
XP_021016320.1	TGFβ2X2	Mus caroli

3.2 Phylogenetic analysis of receptors

In a phylogenetic tree based on amino acid sequences from multiple TGFβ receptors proteins, each type of receptor assembled in a cluster. The phylogenetic tree is shown in Figure 3 and corresponding sequences are shown in Table 2. According to the phylogenetic tree, six TGFβ receptors from *A. japonicus* were classified into six classes: TGFβR2 [transforming growth factor beta receptor 2, alternative name TβR2 (Hart et al., 2002)], TGFβR3 (transforming growth factor beta receptor 3, alternative name TβR3), BMPR1B [bone morphogenetic protein

TABLE 2 Receptor protein sequences included in the present study.

Accession no.	Protein name	Species
XP_026886611.2	TβR2	Electrophorus electricus
TSK92904.1	TβR2	Bagarius yarrelli
XP_017324951.1	TβR2	Ictalurus punctatus
XP_026802727.2	TβR2	Pangasianodon hypophthalmus
PIK56848.1	**putative TβR2**	**Apostichopus japonicus**
XP_033116886.1	TβR2	Anneissia japonica
XP_030828751.1	TβR2	Strongylocentrotus purpuratus
XP_038058105.1	TβR2	Patiria miniata
XP_033624779.1	TβR2	Asterias rubens
PIK56867.1	**putative TβR3**	**Apostichopus japonicus**
CAC5417350.1	TβR3	Mytilus coruscus
CAG2237547.1	TβR3	Mytilus edulis
XP_038129033.1	TβR3	Cyprinodon tularosa
XP_040482976.1	TβR3X2	Ursus maritimus
XP_036901372.1	TβR3X1	Sturnira hondurensis
XP_025893663.1	TβR3	Nothoprocta perdicaria
XP_005238531.1	TβR3X1	Falco peregrinus
XP_040466106.1	TβR3X2	Falco naumanni
PIK46054.1	**putative BMPR2**	**Apostichopus japonicus**
XP_033099609.1	BMPR2	Anneissia japonica
XP_790983.2	BMPR2	Strongylocentrotus purpuratus
XP_041459768.1	BMPR2	Lytechinus variegatus
XP_033624844.1	BMPR2	Asterias rubens
XP_038058132.1	BMPR2	Patiria miniata
XP_022088502.1	BMPR2	Acanthaster planci
PIK52453.1	**putative ACVR2AX2**	**Apostichopus japonicus**
XP_030828527.1	ACVR2A	Strongylocentrotus purpuratus
XP_041458652.1	ACVR2A	Lytechinus variegatus
XP_038079379.1	ACVR2AX1	Patiria miniata
XP_033624296.1	ACVR2A	Asterias rubens
XP_042301709.1	ACVR2AX2	Sceloporus undulatus
XP_032880604.1	ACVR2AX2	Amblyraja radiata
XP_043550051.1	ACVR2AX1	Chiloscyllium plagiosum
XP_041056629.1	ACVR2A	Carcharodon carcharias
XP_022103314.1	ACVR1X4	Acanthaster planci
XP_033113857.1	ACVR1X4	Anneissia japonica
PIK59495.1	**putative ACVR1**	**Apostichopus japonicus**
NXL14502.1	ACVR1	Setophaga kirtlandii
NWI57693.1	ACVR1	Calyptomena viridis
NXY49840.1	ACVR1	Ceuthmochares aereus

(Continued)

TABLE 2 Continued

Accession no.	Protein name	Species
NXB24442.1	ACVR1	Rhagologus leucostigma
NP_001383423.1	ACVR1	Gallus gallus
KFP78435.1	ACVR1	Apaloderma vittatum
XP_032435030.1	BMPR1BX3	Xiphophorus hellerii
XP_005795012.2	BMPR1B	Xiphophorus maculatus
XP_027890208.1	BMPR1BX3	Xiphophorus couchianus
PIK51009.1	**putative BMPR1B**	**Apostichopus japonicus**
XP_797469.4	BMPR1B	Strongylocentrotus purpuratus
XP_041485680.1	BMPR1B	Lytechinus variegatus
XP_033644308.1	BMPR1B	Asterias rubens
XP_038060789.1	BMPR1B	Patiria miniata
XP_022089444.1	BMPR1B	Acanthaster planci

TABLE 3 Smad protein sequences included in the present study.

Accession no.	full name	Species
XP_041459990.1	Smad4X1	Lytechinus variegatus
XP_030827838.1	Smad4X1	Strongylocentrotus purpuratus
XP_033109387.1	Smad4X2	Anneissia japonica
XP_033646664.1	Smad4X1	Asterias rubens
XP_022081844.1	Smad4X1	Acanthaster planci
XP_038058605.1	Smad4X1	Patiria miniata
XP_032649614.1	Smad4	Chelonoidis abingdonii
XP_035384718.1	Smad4	Electrophorus electricus
XP_030421567.1	Smad4X1	Gopherus evgoodei
XP_035314530.1	Smad4X1	Cricetulus griseus
XP_016004267.1	Smad4X1	Rousettus aegyptiacus
XP_030885493.1	Smad4	Leptonychotes weddellii
XP_033127281.1	Smad6	Anneissia japonica
ADW95340.1	Smad6	Paracentrotus lividus
XP_798238.2	Smad6	Strongylocentrotus purpuratus
XP_022083936.1	Smad6	Acanthaster planci
XP_038077875.1	Smad6	Patiria miniata
XP_026878186.2	Smad6b	Electrophorus electricus
XP_015996485.2	Smad6X1	Rousettus aegyptiacus
XP_003500538.2	Smad6X1	Cricetulus griseus
XP_032621963.1	Smad6	Chelonoidis abingdonii
XP_030434864.1	Smad6	Gopherus evgoodei
XP_016003943.1	Smad7X1	Rousettus aegyptiacus
XP_007644509.3	Smad7X1	Cricetulus griseus
XP_032637417.1	Smad7X1	Chelonoidis abingdonii

(Continued)

TABLE 3 Continued

Accession no.	full name	Species
XP_030423387.1	Smad7X1	Gopherus evgoodei
XP_033124235.1	Smad3	Anneissia japonica
XP_041460773.1	Smad3	Lytechinus variegatus
XP_033624249.1	Smad3X1	Asterias rubens
XP_022083075.1	Smad3X2	Acanthaster planci
XP_038076479.1	Smad3X1	Patiria miniata
XP_006749953.1	Smad3	Leptonychotes weddellii
XP_026860560.1	Smad3a	Electrophorus electricus
XP_015996478.1	Smad3	Rousettus aegyptiacus
XP_007639432.2	Smad3X1	Cricetulus griseus
XP_028706267.1	Smad3X1	Macaca mulatta
XP_030434068.1	Smad3X1	Gopherus evgoodei
XP_032620241.1	Smad3	Chelonoidis abingdonii
XP_035391548.1	Smad2X1	Electrophorus electricus
XP_032654336.1	Smad2X1	Chelonoidis abingdonii
XP_003501086.1	Smad2X1	Cricetulus griseus
XP_006738743.2	Smad2	Leptonychotes weddellii
XP_028693529.1	Smad2X2	Macaca mulatta
XP_036085916.1	Smad2X1	Rousettus aegyptiacus
PIK47643.1	**mothers against decapentaplegic-like protein 1**	**Apostichopus japonicus**
XP_032620791.1	Smad1X2	Chelonoidis abingdonii
XP_030420831.1	Smad1X2	Gopherus evgoodei
XP_036089426.1	Smad1X1	Rousettus aegyptiacus
XP_030895811.1	Smad1	Leptonychotes weddellii
XP_026859416.1	Smad5	Electrophorus electricus
XP_032631983.1	Smad5	Chelonoidis abingdonii
XP_030428443.1	Smad5	Gopherus evgoodei
XP_003503786.1	Smad5	Cricetulus griseus
XP_014996357.1	Smad5X1	Macaca mulatta
XP_015993196.1	Smad5	Rousettus aegyptiacus
XP_022079499.1	Smad5X2	Acanthaster planci
XP_033632185.1	Smad5	Asterias rubens
XP_038055290.1	Smad5	Patiria miniata
XP_041455371.1	Smad5	Lytechinus variegatus
XP_030836187.1	Smad5	Strongylocentrotus purpuratus
ACU12852.1	Smad1	Paracentrotus lividus
PIK47644.1	**Smad1**	**Apostichopus japonicus**

FIGURE 1
Green, purple and white *A. japonicus*.

TABLE 4 Oligonucleotide primers for *A. japonicus*.

Gene	Accession no.	Primer sequence	
BMP2/4	AB057451.1	Forward	5'- CCAAAAGGCAGAAAAGCA -3'
		Reverse	5'- ACCCACAATGGCAAAGTC -3'
ACVR2A	BSL78_25911	Forward	5'- ACAGAGAAGCGTGGTGAAG -3'
		Reverse	5'- GGTAGTCATAGAGGGAGCCA -3'
Smad1	BSL78_15508	Forward	5'- ATTCTCCTTTACCAGTCCAGTT -3'
		Reverse	5'- AGCCTTCTCCAGTTCTTCC -3'
TβR2	BSL78_06251	Forward	5'- GAGCCGAAAGAAGACAGAAC -3'
		Reverse	5'- TATCGTAGAGGGAAGGACTCA -3'
Smad 2/3	BSL78_11878	Forward	5'- GCTACCGCCTCCATCTTT -3'
		Reverse	5'- CCTCCATACTGTTGTCATTGG -3'
grb2	C112121_gl_il	Forward	5'- ATCTTTCACATATTGCGAGCCAG -3'
		Reverse	5'- ATGACCATTCCGATGCCCTAA -3'

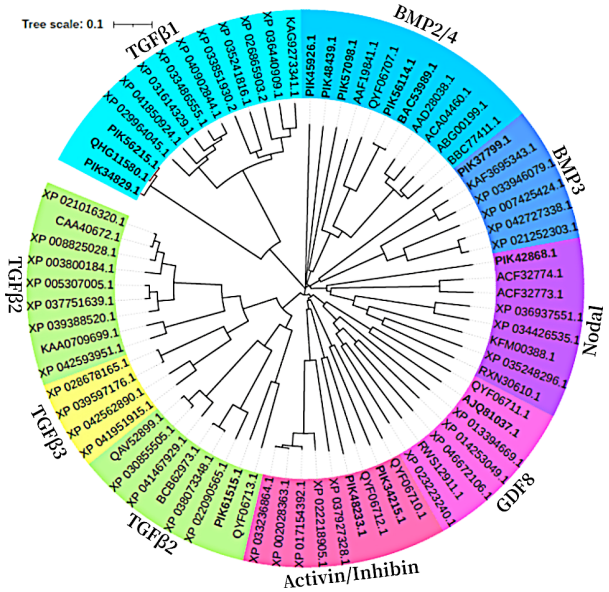

FIGURE 2
Phylogenetic analysis of the 14 ligands proteins compared to other species.

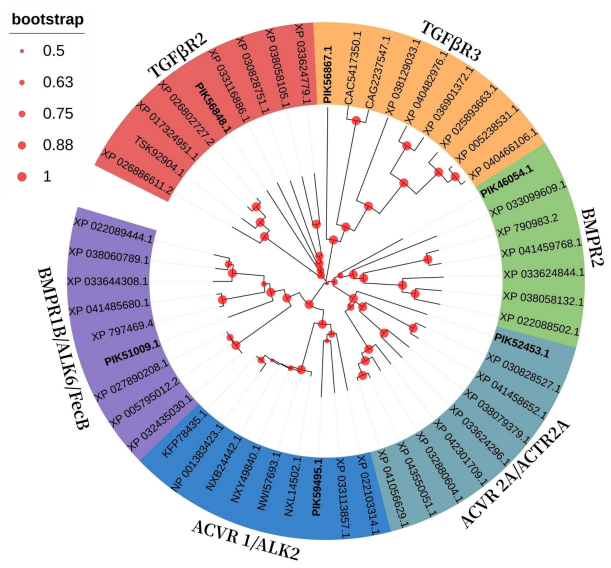

FIGURE 3
Phylogenetic analysis of the 6 receptors proteins compared to other species.

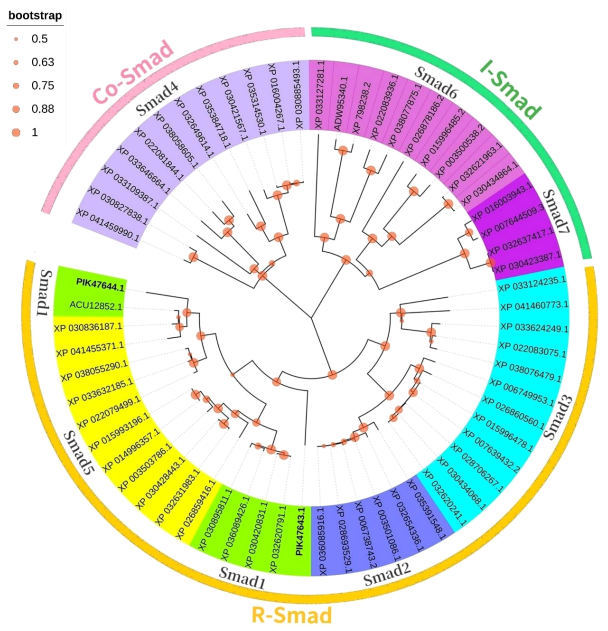

FIGURE 4
Phylogenetic analysis of the 2 Smads proteins compared to other species.

receptor type 1B, alternative name ALK6, FecB (Li et al., 2021)], BMPR2 (bone morphogenetic protein receptor type 2), ACVR1 [activin receptor type 1, alternative name ACTR1, ALK2 (Lee et al., 2017)], and ACVR2A [activin receptor type 2A, alternative name ACTR2A (Bondulich et al., 2017)].

3.3 Phylogenetic analysis of Smads

In a phylogenetic tree based on amino acid sequences of multiple Smads, the each type of Smad assembled in a cluster. The phylogenetic tree is shown in Figure 4 and the corresponding sequences are shown in Table 3. According to the phylogenetic tree, two kinds of known R-Smads from *A. japonicus* were classified into one class, the Smad1 class. Notably, they were closely related to Smad5.

3.4 mRNA levels of TGFβ signaling pathway genes in *A. japonicus* color morphs

Three different color morphs of *A. japonicus* are shown in Figure 1. mRNA levels of TGFβ signaling pathway genes in *A. japonicus* with different colors are shown in Figure 5. Compared to levels in green *A. japonicus*, the mRNA expression levels of all TGFβ signaling pathway genes were much higher in purple *A. japonicus*, with significant differences in TGFβR2 and Smad2/3 levels between morphs ($p < 0.05$). The mRNA expression levels of BMP2/4, ACVR2A, Smad1, and TGFβR2 of the purple individuals were significantly lower than those in the white morph ($p < 0.05$), with no difference in Smad 2/3 ($p > 0.05$).

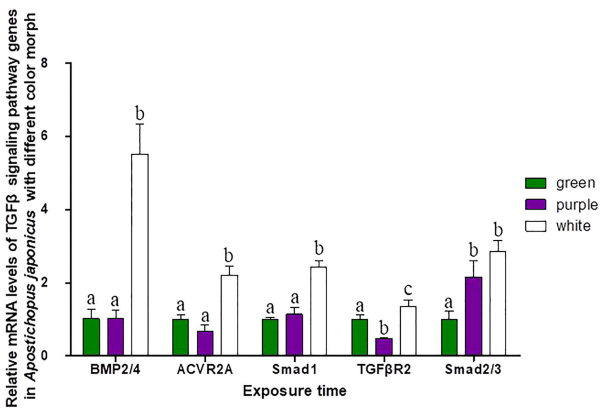

FIGURE 5
Relative mRNA levels of TGFβ signaling pathway genes in *A. japonicus* of different body colors. Means followed by different lower-case letters are significantly different at *P*<0.05.

3.5 mRNA levels of TGFβ signaling pathway genes during pigmentation in *A. japonicus*

The pigmentation process in purple sea cucumber was divided into four stages: A, B, C, and D (Figure 6). mRNA levels of TGFβ signaling pathway genes at each stage are shown in Figure 7. BMP2/4 and Smad2/3 levels did not differ among pigmentation stages in *A. japonicus* ($p > 0.05$). Compared to levels at stage A, the mRNA expression of ACVR2A was lower at stage C and higher at stage D. The mRNA expression levels of Smad1 and TGFβR2 were significantly higher at stages B and C than at stage A. As time progressed, the expression level of TGFβR2 began to decrease, with lower levels at stage D than at stages B and C.

4 Discussion

The TGFβ superfamily consists of over 50 structurally related ligands and can be divided into two subfamilies based on sequence similarity and the specific signaling pathways they activate: the TGFβ/activin/Nodal subfamily and BMP/GDF/AMH (anti-Mullerian hormone) subfamily (Shi and Massagué, 2003; Massagué, 2012; Miyazono et al., 2018). These have been described in a large number of studies of TGFβ superfamily ligand, receptor, and R-Smad interactions in various species (Piek et al., 1999; Attisano and Wrana, 2002; de Caestecker, 2004; Schilling et al., 2008; Romano et al., 2012) and were detected in the sea cucumber genome (Tables 1–3) . Ligand–receptor–R-Smad interactions in *A. japonicus* were inferred, as shown in Table 5, and putative TGFβ-mediated signaling pathways in *A. japonicus* are shown in Graphical Abstract. In the first subfamily, ligands (TGFβ1, TGFβ2, Activin B, Inhibin, and Nodal), Receptor II (TGFβR2 and ACVR2A/ACTR2A), and R-Smads (Smad2, 3) were found in *A. japonicus*. In the second subfamily, ligands (BMP2, BMP4, BMP3, and BMP3B), Receptor I (BMPR1B/ALK6), Receptor II (ACVR2A/ACTR2A and BMPR2), and R-Smad (Smad1, 5 and Smad2, 3) were found in *A. japonicus*.

The TGFβ signaling pathway is considered a good marker for the evolution of animal genomes (Long, 2019). Three TGFβ isoforms are known in mammals (Derynck et al., 1985; Van Obberghen-Schilling et al., 1987; ten Dijke et al., 1988; Miller et al., 1989a; Miller et al., 1989b) and in birds (TGFβ2, β3, and β4) (Jakowlew et al., 1988a; Jakowlew et al., 1988c; Jakowlew et al., 1988b; Jakowlew et al., 1990), two in amphibians (TGFβ2 and TGFβ5) (Kondaiah et al., 1990; Rebbert et al., 1990), and four in fish (TGFβ1, β2, β3 and β6) (Funkenstein et al., 2010). In the

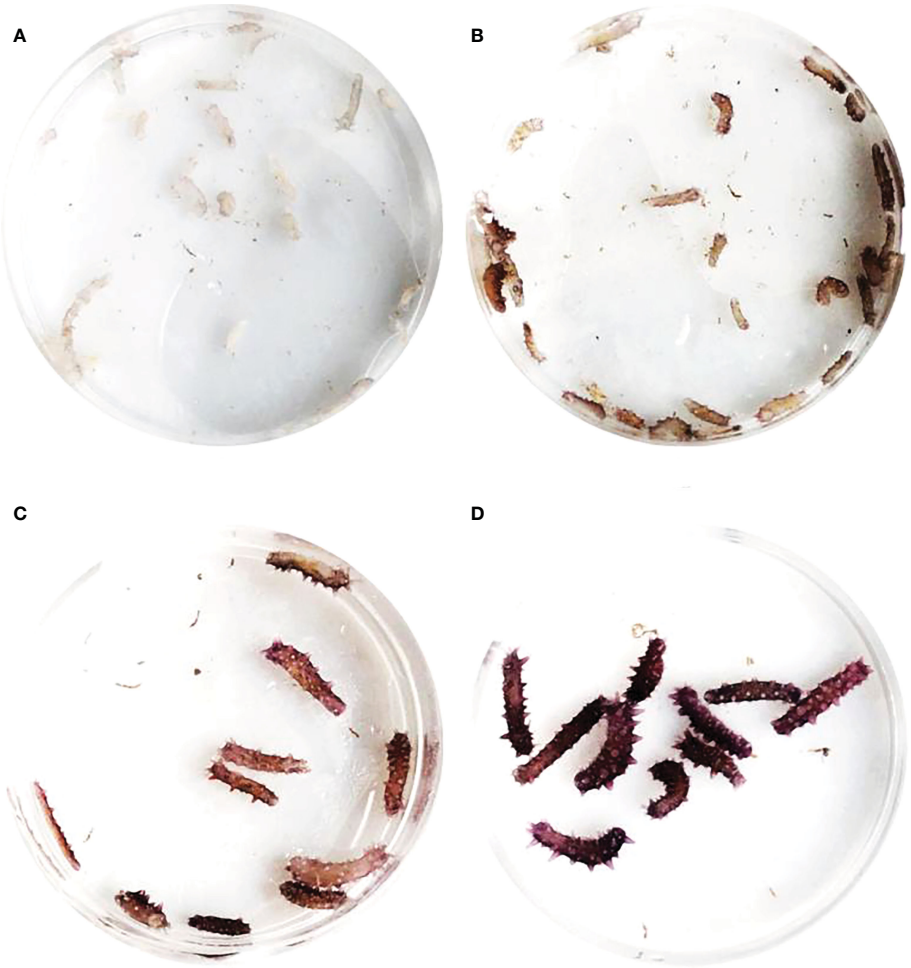

FIGURE 6
Pigmentation stages of purple *A. japonicus*.

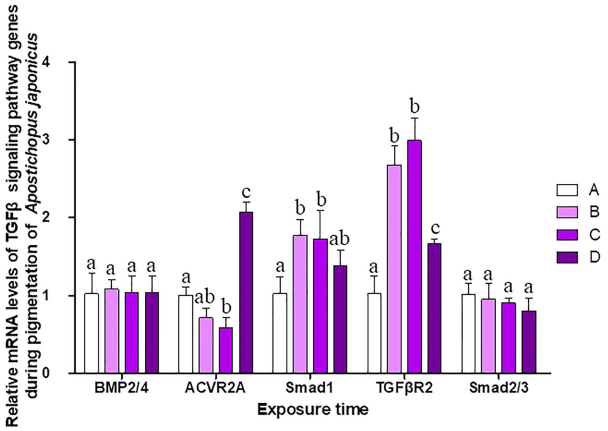

FIGURE 7
Relative mRNA levels of TGFβ signaling pathway genes during different pigmentation stages of purple *A. japonicus*. Means followed by different lowercase letters are significantly different at $P<0.05$.

present study, two TGFβ ligand isoforms (TGFβ1 and TGFβ2) were identified in *A. japonicus* (Figure 2). A BLAST search against GenBank entries (putative TGFβ1 like, PIK34829.1, putative TGFβ1X1, PIK56215.1, and putative TGFβ1X1, QHG11580.1) revealed high amino acid sequence homology with TGFβ1 (Figure 2 and Table 1). It is worth noting that although TGFβ2 was classified as TGFβ2, it was closely related to TGFβ3 (Figure 2 and Table 1). Activin is the dimer of β-subunits, activin A (β_A-β_A), activin B (β_B-β_B), and activin AB (β_A-β_B). Inhibin A, B, C are dimers composed of an α-subunit associated with β_A, β_B, and β_C (Burger, 1988; Mellor et al., 2000; Ushiro et al., 2006). Accordingly, the putative activin BX1 and putative inhibin beta C chain-like of *A. japonicus* clustered in the Activin/Inhibin cluster on the phylogenetic tree and showed a relatively low identity (Figure 2 and Table 1). The TGFβ family member nodal of *A. japonicus* were assigned to the Nodal cluster (Figure 2 and Table 1). In summary, sea cucumber possessed the complete TGFβ/activin/Nodal ligand subfamily.

Although no typical receptor I was found in the TGFβ/activin/Nodal subfamily (Table 5), significant differences in the mRNA expression levels of TGFβR2, ACVR2A, and Smad2/3 were detected in sea cucumbers with different body colors (Figure 5). Expression levels of TGFβR2 during different pigmentation stages of purple *A. japonicus* were significantly higher than those during the unpigmented period; however, the expression levels of Smad2/3 did not differ significantly ($p > 0.05$) (Figure 7). This indicates that TGFβR2 is involved in the regulation of the coloration process of *A. japonicus*; however, its specific regulatory mechanism is still unclear. TGFβR2 and Smad2/3 also differ significantly between peripheral blood lymphocytes of patients with systemic lupus erythematosus and a normal control group (Sun et al., 2013). When ACVR2A function is reduced in melanocytes, gray hair develops (Han et al., 2012). These findings are consistent with the higher expression of ACVR2A in the white morph than in the other color morphs of *A. japonicus*. More broadly, there are ethnic differences in TGFβ signaling in African American and Caucasian skin (Fantasia et al., 2013). Taken together, these studies support the hypothesis that the TGFβ/activin/Nodal subfamily is involved in the regulation of body color of *A. japonicas*.

The second subfamily involved BMP/GDF/AMH. BMP is the largest subfamily of TGFβ ligands. In the current study, two BMPs, BMP2/4 and BMP3, were found. The BMPs (PIK57098.1) of *A. japonicus* were classified as BMP2/4. Sj-BMP2/4 was recorded in GenBank with two different accession numbers (PIK56114.1 and BAC53989.1). A Blast

TABLE 5 TGFβ superfamily ligand-receptor-Smad specificity.

Subfamily	Ligand	Receptor I	Receptor II	R-Smad
TGFβ/activin/Nodal	TGFβ1	no records	TGFβR2	Smad2, 3
	TGFβ2	no records	TGFβR2	Smad2, 3
	Activin B	no records	ACVR2A/ACTR2A	Smad2, 3
	Inhibin	No type I receptor	ACVR2A	no specific R-Smads
	Nodal	no records	ACVR2A/ACTR2A	Smad2, 3
BMP/GDF/AMH	BMP2	BMPR1B/ALK6	ACVR2A/ACTR2A and BMPR2	Smad1, 5
	BMP4	BMPR1B/ALK6	ACVR2A/ACTR2A and BMPR2	Smad1, 5
	BMP3	No type I receptor	no records	no records
	BMP3B	no records	ACVR2A/ACTR2A	Smad2, 3

analysis showed that the two proteins were highly homologous (query cover: 100%, identity: 99.29%). *A. japonicus* and *Stichopus japonicus* are two different names for the same species (Chang et al., 2009). Accordingly, Sj-BMP2/4 corresponds to BMP2/4 of *A. japonicus*. In this study, the mRNA expression of BMP2/4 did not differ among pigmentation stages of purple *A. japonicus* (Figure 7). However, BMP2/4 expression was significantly higher in the white morph than in the green and purple morphs (Figure 5), suggesting that BMP2/4 is closely related to formation of the white body color. Numerous studies have shown that BMP2 and BMP4 can induce stem cells to differentiate into adipocytes and to differentiate into white adipocytes (Ahrens et al., 1993; Wang et al., 1993; Sottile and Seuwen, 2000; Bowers and Lane, 2007; Gomes et al., 2012). White sea cucumbers are uniformly white on the dorsal and ventral sides, while purple and green sea cucumbers have obvious color differences, i.e., the dorsal side is darker than the ventral side (Figures 1, 6). The specificity of BMP2/4 was receptor I (BMPR1B)–receptor II (ACVR2A and BMPR2)–R-Smad (Smad1,5). In *A. japonicus*, their expression levels in white sea cucumber were significantly higher than those in the purple and green sea cucumbers (Figure 5). These results suggest that the BMP2/4-induced differentiation of white adipocytes in *A. japonicus* is regulated by this signaling pathway. Functional tests, including gain- or loss-of-function assays, using exogenous BMPs or BMP antagonists are necessary to validate the roles of this pathway in *A. japonicus*. In the GDF gene family, only GDF8 was detected in *A. japonicus* (Figure 2 and Table 1). There was no record of AMH in sea cucumber. Accordingly, the BMP/GDF/AMH ligand subfamily in sea cucumber is incomplete.

5 Conclusions

In summary, 14 TGFβ signaling pathway members were identified in *A. japonicus* for the first time, including 7 ligands, 6 receptors, and 1 R-Smad. Detailed phylogenetic and gene expression analyses support the hypothesis (Graphical Abstract) that both subfamilies of the TGFβ superfamily were involved in the regulation of pigmentation in different color morphs of *A. japonicus*. The TGFβ/activin/Nodal subfamily was complete and contributed to the regulation of different color morphs. The BMP/GDF/AMH subfamily was incomplete, and the BMP2/4-induced differentiation of white adipocytes was regulated by the BMP2/4–ACVR2A–Smad1 signaling pathway.

Data availability statement

The original contributions presented in the study are included in the article/supplementary material. Further inquiries can be directed to the corresponding author.

Author contributions

LY and CL conceived and designed the experiments. Material preparation, data collection and analysis were performed by LY, BZ, QW, XJ, SH, WH. The first draft of the manuscript was written by LY and all authors commented on previous versions of the manuscript. All authors contributed to the article and approved the submitted version.

Funding

This study was supported by the Shandong Provincial Natural Science Foundation (ZR2022QC183), Key R&D Plan of Shandong Province (2021TZXD008), National Key Research and Development Program "Blue Granary Scientific and Technological Innovation" (2018YFD0901602).

Conflict of interest

Author XJ was employed by the company Country Conson CSSC Qingdao Ocean Technology CO., Ltd.

The remaining authors declare that the research was conducted in the absence of any commercial or financial relationships that could be construed as a potential conflict of interest.

Publisher's note

References

Ahrens, M., Ankenbauer, T., Schröder, D., Hollnagel, A., Mayer, H., and Gross, G. (1993). Expression of human bone morphogenetic proteins-2 or-4 in murine mesenchymal progenitor C3H10T½ cells induces differentiation into distinct mesenchymal cell lineages. *DNA Cell Biol.* 12 (10), 871–880. doi: 10.1089/dna.1993.12.871

Attisano, L., and Wrana, J. L. (2002). Signal transduction by the TGF-β superfamily. *Science* 296 (5573), 1646–1647. doi: 10.1126/science.1071809

Bai, Y., Zhang, L., Xia, S., Liu, S., Ru, X., Xu, Q., et al. (2016). Effects of dietary protein levels on the growth, energy budget, and physiological and immunological performance of green, white and purple color morphs of sea cucumber, apostichopus japonicus. *Aquaculture.* 437, 297–303. doi: 10.1016/j.aquaculture.2015.08.021

Bao, J. (2008). *Effects and mechanism of environment on growth of green and red sea cucumber, apostichopus japonicus* (Ocean University of China).

Bondulich, M. K., Jolinon, N., Osborne, G. F., Smith, E. J., Rattray, I., Neueder, A., et al. (2017). Myostatin inhibition prevents skeletal muscle pathophysiology in huntington's disease mice. *Sci. Rep.* 7 (1), 1–14. doi: 10.1038/s41598-017-14290-3

Bottjer, D. J., Davidson, E. H., Peterson, K. J., and Cameron, R. A. (2006). Paleogenomics of echinoderms. *Science.* 314 (5801), 956–960. doi: 10.1126/science.1132310

Bowers, R. R., and Lane, M. D. (2007). A role for bone morphogenetic protein-4 in adipocyte development. *Cell Cycle* 6 (4), 385–389. doi: 10.4161/cc.6.4.3804

Burger, H. G. (1988). Inhibin: definition and nomenclature, including related substances. *J. Endocrinol.* 117 (2), 159–160. doi: 10.1677/joe.0.1170159

Cameron, R. A., Kudtarkar, P., Gordon, S. M., Worley, K. C., and Gibbs, R. A. (2015). Do echinoderm genomes measure up? *Mar. Genomics* 22, 1–9. doi: 10.1016/j.margen.2015.02.004

Chang, Y., Feng, Z., Yu, J., and Ding, J. (2009). Genetic variability analysis in five populations of the sea cucumber stichopus (Apostichopus) japonicus from China, Russia, south Korea and Japan as revealed by microsatellite markers. *Mar. Ecol.* 30 (4), 455–461. doi: 10.1111/j.1439-0485.2009.00292.x

Cheng, K. C. (2008). Skin color in fish and humans: Impacts on science and society. *Zebrafish* 5 (4), 237–242. doi: 10.1089/zeb.2008.0577

Chen, Y., Gao, F., Liu, G., Shao, L., and Shi, G. (2007). The effects of temperature, salinity and light cycle on the growth and behavior of apostichopus japonicus. *J. Fisheries China* 31 (5), 687–691. doi: 1000-0615(2007)05-0687-05

Chen, J., Lv, Z., and Guo, M. (2022). Research advancement of apostichopus japonicus from 2000 to 2021. *Front. Mar. Sci.*, 1595. doi: 10.3389/fmars.2022.931903

de Caestecker, M. (2004). The transforming growth factor-β superfamily of receptors. *Cytokine Growth factor Rev.* 15 (1), 1–11. doi: 10.1016/j.cytogfr.2003.10.004

Derynck, R., Jarrett, J. A., Chen, E. Y., Eaton, D. H., Bell, J. R., Assoian, R. K., et al. (1985). Human transforming growth factor-β complementary DNA sequence and expression in normal and transformed cells. *Nature* 316 (6030), 701–705. doi: 10.1038/316701a0

Fantasia, J., Lin, C. B., Wiwi, C., Kaur, S., Hu, Y., Zhang, J., et al. (2013). Differential levels of elastin fibers and TGF-β signaling in the skin of caucasians and African americans. *J. Dermatol. Sci.* 70 (3), 159–165. doi: 10.1016/j.jdermsci.2013.03.004

Funkenstein, B., Olekh, E., and Jakowlew, S. B. (2010). Identification of a novel transforming growth factor-β (TGF-β6) gene in fish: regulation in skeletal muscle by nutritional state. *BMC Mol. Biol.* 11 (1), 1–16. doi: 10.1186/1471-2199-11-37

Gomes, S. P., Deliberador, T. M., Gonzaga, C. C., Klug, L. G., Oliveira, L., Urban, A. C., et al. (2012). Bone healing in critical-size defects treated with immediate transplant of fragmented autogenous white adipose tissue. *J. Craniofacial Surg.* 23 (5), 1239–1244. doi: 10.1097/SCS.0b013e31825da9d9

Guo, Z., Wang, Z., Hou, X., and Zhang, H. (2020). Comparative study on genetic structure of three color variants of the sea cucumber (apostichopus japonicus) based on mitochondrial and ribosomal genes. *J. Shandong Univ. (Natural Science)* 55 (11), 7. doi: 10.6040/j.issn.1671-9352.0.2020.231

Hall, M. R., Kocot, K. M., Baughman, K. W., Fernandez-Valverde, S. L., Gauthier, M. E., Hatleberg, W. L., et al. (2017). The crown-of-thorns starfish genome as a guide for biocontrol of this coral reef pest. *Nature* 544 (7649), 231–234. doi: 10.1038/nature22033

Han, R., Beppu, H., Lee, Y. K., Georgopoulos, K., Larue, L., Li, E., et al. (2012). A pair of transmembrane receptors essential for the retention and pigmentation of hair. *Genesis* 50 (11), 783–800. doi: 10.1002/dvg.22039

Hart, P. J., Deep, S., Taylor, A. B., Shu, Z., Hinck, C. S., and Hinck, A. P. (2002). Crystal structure of the human TβR2 ectodomain–TGF-β3 complex. *Nat. Struct. Biol.* 9 (3), 203–208. doi: 10.1038/nsb766

Henning, F., Jones, J. C., Franchini, P., and Meyer, A. (2013). Transcriptomics of morphological color change in polychromatic Midas cichlids. *BMC Genomics* 14 (1), 171–171. doi: 10.1186/1471-2164-14-171

Hubbard, J. K., Uy, J., Hauber, M. E., Hoekstra, H. E., and Safran, R. J. (2010). Vertebrate pigmentation: from underlying genes to adaptive function. *Trends Genet.* 26 (5), 231–239. doi: 10.1016/j.tig.2010.02.002

Jakowlew, S. B., Dillard, P. J., Kondaiah, P., Sporn, M. B., and Roberts, A. B. (1988a). Complementary deoxyribonucleic acid cloning of a novel transforming growth factor-beta messenger ribonucleic acid from chick embryo chondrocytes. *Mol. Endocrinol. (Baltimore Md.)* 2 (8), 747–755. doi: 10.1210/mend-2-8-747

Jakowlew, S. B., Dillard, P. J., Sporn, M. B., and Roberts, A. B. (1988b). Complementary deoxyribonucleic acid cloning of a messenger ribonucleic acid encoding transforming growth factor β 4 from chicken embryo chondrocytes. *Mol. Endocrinol.* 2 (12), 1186–1195. doi: 10.1210/mend-2-12-1186

Jakowlew, S. B., Dillard, P. J., Sporn, M. B., and Roberts, A. B. (1988c). Nucleotide sequence of chicken transforming growth factor-beta 1 (TGF-beta 1). *Nucleic Acids Res.* 16 (17), 8730. doi: 10.1093/nar/16.17.8730

Jakowlew, S. B., Dillard, P. J., Sporn, M. B., and Roberts, A. B. (1990). Complementary deoxyribonucleic acid cloning of an mRNA encoding transforming growth factor-β2 from chicken embryo chondrocytes. *Growth Factors* 2 (2), 123–133. doi: 10.3109/08977199009071499

Ji, T., Dong, Y., and Dong, S. (2008). Growth and physiological responses in the sea cucumber, apostichopus japonicus selenka: Aestivation and temperature. *Aquaculture* 283 (1), 180–187. doi: 10.1016/j.aquaculture.2008.07.006

Kang, J. H., Yu, K. H., Park, J. Y., An, C. M., Jun, J. C., and Lee, S. J. (2011). Allele-specific PCR genotyping of the HSP70 gene polymorphism discriminating the green and red color variants sea cucumber (Apostichopus japonicus). *J. Genet. Genomics* 38 (8), 351–355. doi: 10.1016/j.jgg.2011.06.002

Kondaiah, P., Sands, M. J., Smith, J. M., Fields, A., Roberts, A. B., Sporn, M. B., et al. (1990). Identification of a novel transforming growth factor-beta (TGF-beta 5) mRNA in xenopus laevis. *J. Biol. Chem.* 265 (2), 1089–1093. doi: 10.1016/S0021-9258(19)40162-2

Lapraz, F., Duboc, V., and Thierry, L. (2007). A genomic view of TGF-β signal transduction in an invertebrate deuterostome organism and lessons from the functional analyses of nodal and BMP2/4 during sea urchin development. *Signal Transduction.* 7 (2), 187–206. doi: 10.1002/sita.200600125

Lee, H., Chong, D. C., Ola, R., Dunworth, W. P., Meadows, S., Ka, J., et al. (2017). Alk2/ACVR1 and Alk3/BMPR1A provide essential function for bone morphogenetic protein–induced retinal angiogenesis. *Arteriosclerosis thrombosis Vasc. Biol.* 37 (4), 657–663. doi: 10.1161/ATVBAHA.116.308422

Li, J., Liu, J., Cao, X., Wang, F., Li, J., Zheng, L., et al. (2020). Effects of light intensity on growth, digestion and immunity of green, white and purple sea cucumber apostichopus japonicus selenka. *J. Dalian Ocean Univ.* 35 (02), 184–189. doi: 10.16535/j.cnki.dlhyxb.2019-057

Linton, L. M., Birren, B. W., and Lander, E. (2001). International human genome sequencing consortium. *Nature* 409 (6822), 860–921. doi: 10.1038/35057062

Li, H., Xu, H., Akhatayeva, Z., Liu, H., Lin, C., Han, X., et al. (2021). Novel indel variations of the sheep FecB gene and their effects on litter size. *Gene* 767, 145176. doi: 10.1016/j.gene.2020.145176

Long, J. (2019). *Bioinformatic analysis of TGF-β signaling pathway members and their expression in Nile tilapia* (Southwest University).

Lowe, C. J., Clarke, D. N., Medeiros, D. M., Rokhsar, D. S., and Rokhsar, J. (2015). The deuterostome context of chordate origins. *Nature*. 520 (7548), 456–465. doi: 10.1038/nature14434

Massagué, J. (2012). TGFβ signalling in context. *Nat. Rev. Mol. Cell Biol.* 13 (10), 616–630. doi: 10.1038/nrm3434

Massagué, J., and Chen, Y. (2000). Controlling TGF-β signaling. *Genes Dev.* 14 (6), 627–644. doi: 10.1101/gad.14.6.627

Mellor, S. L., Cranfield, M., Ries, R., Pedersen, J., Cancilla, B., Kretser, D. D., et al. (2000). Localization of activin βA-, β b-, andβ c-subunits in human prostate and evidence for formation of new activin heterodimers ofβ c-subunit. *J. Clin. Endocrinol. Metab.* 85 (12), 4851–4858. doi: 10.1210/jcem.85.12.7052

Miller, D. A., Lee, A., Matsui, Y., Chen, E. Y., Moses, H. L., and Derynck, R. (1989a). Complementary DNA cloning of the murine transforming growth factor-β3 (TGFβ3) precursor and the comparative expression of TGFβ3 and TGFβ1 messenger RNA in murine embryos and adult tissues. *Mol. Endocrinol.* 3 (12), 1926–1934. doi: 10.1210/mend-3-12-1926

Miller, D. A., Lee, A., Pelton, R. W., Chen, E. Y., Moses, H. L., and Derynck, R. (1989b). Murine transforming growth factor-β2 cDNA sequence and expression in adult tissues and embryos. *Mol. Endocrinol.* 3 (7), 1108–1114. doi: 10.1172/JCI67521

Miyazono, K., Katsuno, Y., Koinuma, D., Ehata, S., and Morikawa, M. (2018). Intracellular and extracellular TGF-β signaling in cancer: some recent topics. *Front. Med.* 12 (4), 387–411. doi: 10.1007/s11684-018-0646-8

Patterson, G. I., and Padgett, R. W. (2000). TGFβ-related pathways: roles in caenorhabditis elegans development. *Trends Genet.* 16 (1), 27–33. doi: 10.1242/dev.00863

Piek, E., Heldin, C., and Dijke, P. T. (1999). Specificity, diversity, and regulation in TGF-β superfamily signaling. *FASEB J.* 13 (15), 2105–2124. doi: 10.1096/fasebj.13.15.2105

Rebbert, M. L., Bhatiadey, N. , and Dawid, I. B. (1990). The sequence of TGF-beta 2 from xenopus laevis. *Nucleic Acids Res.* 18 (8), 2185. doi: 10.1093/nar/18.8.2185

Romano, V., Raimondo, D., Calvanese, L., D'Auria, G., Tramontano, A., and Falcigno, L. (2012). Toward a better understanding of the interaction between TGF-β family members and their ALK receptors. *J. Mol. modeling* 18 (8), 3617–3625. doi: 10.1007/s00894-012-1370-y

Schilling, S. H., Hjelmeland, A. B., Rich, J. N., and Wang, X. (2008). 3 TGF-β: A multipotential cytokine. *Cold Spring Harbor Monograph. Arch.* 50, 45–77. doi: 10.1101/087969752.50.45

Shi, Y., and Massagué, J. (2003). Mechanisms of TGF-β signaling from cell membrane to the nucleus. *cell* 113 (6), 685–700. doi: 10.1016/s0092-8674(03)00432-x

Signor, P. W., and Brett, C. E. (1984). The mid-Paleozoic precursor to the mesozoic marine revolution. *Paleobiology* 10 (2), 229–245. doi: 10.1017/S0094837300008174

Sodergren, E., Weinstock, G. M., Davidson, E. H., Cameron, R. A., Gibbs, R. A., Angerer, R. C., et al. (2006). The genome of the sea urchin strongylocentrotus purpuratus. *Science* 314 (5801), 941–952. doi: 10.1126/science.1133609

Sottile, V., and Seuwen, K. (2000). Bone morphogenetic protein-2 stimulates adipogenic differentiation of mesenchymal precursor cells in synergy with BRL 49653 (rosiglitazone). *FEBS Lett.* 475 (3), 201–204. doi: 10.1016/s0014-5793(00)01655-0

Sun, B., Tan, Y., Hong, X., and Liu, D. (2013). Expressions of TGFβR2 and Smad2 in peripheral lymphocytes in patients with systemic lupus erythematosus. *J. Pract. Med* 29 (8), 1255–1257. doi: 10.3969/j.issn.1006-5725.2013.08.019

Sun, J., Zhang, Y., Xu, T., Zhang, Y., Mu, H., Zhang, Y., et al. (2017). Adaptation to deep-sea chemosynthetic environments as revealed by mussel genomes. *Nat. Ecol. Evol.* 1 (5), 121. doi: 10.1038/s41559-017-0121

ten Dijke, P., Hansen, P., Iwata, K. K., Pieler, C., and Foulkes, J. G. (1988). Identification of another member of the transforming growth factor type beta gene family. *Proc. Natl. Acad. Sci.* 85 (13), 4715–4719. doi: 10.1073/pnas.85.13.4715

ten Dijke, P., Miyazono, K., and Heldin, C.-H. (2000). Signaling inputs converge on nuclear effectors in TGF-β signaling. *Trends Biochem. Sci.* 25 (2), 64–70. doi: 10.1016/s0968-0004(99)01519-4

Ushiro, Y., Hashimoto, O., Seki, M., Hachiya, A., Shoji, H., and Hasegawa, Y. (2006). Analysis of the function of activin betaC subunit using recombinant protein. *J. Reprod. Dev.* 52 (4), 487–495. doi: 10.1262/jrd.17110. 0604200034-0604200034.

Van Obberghen-Schilling, E., Kondaiah, P., Ludwig, R. L., Sporn, M. B., and Baker, C. C. (1987). Complementary deoxyribonucleic acid cloning of bovine transforming growth factor-β1. *Mol. Endocrinol.* 1 (10), 693–698. doi: 10.1210/mend-1-10-693

Wang, E. A., Israel, D. I., Kelly, S., and Luxenberg, D. P. (1993). Bone morphogenetic protein-2 causes commitment and differentiation in C3Hl0T1/2 and 3T3 cells. *Growth factors* 9 (1), 57–71. doi: 10.3109/08977199308991582

Wang, G., Zhu, W., Li, Z., and Fu, R. (2007). Effects of water temperature and salinity on the growth of apostichopus japonicus. *Shandong Science*. 20 (3), 6–9. doi: 10.3969/j.issn.1002-4026.2007.03.002

Weiss, A., and Attisano, L. (2013). The TGFbeta superfamily signaling pathway. *Wiley Interdiscip. Reviews: Dev. Biol.* 2 (1), 47–63. doi: 10.1002/wdev.86

Zhang, X., Sun, L., Yuan, J., Sun, Y., Gao, Y., Zhang, L., et al. (2017). The sea cucumber genome provides insights into morphological evolution and visceral regeneration. *PloS Biol.* 15 (10), e2003790. doi: 10.1371/journal.pbio.2003790

Zhao, B., Hu, W., Li, C., and Han, S. (2018). Effects of temperature and salinity survival, growth, and coloration of juvenile apostichopus japonicus selenta. *Oceanologia Limnologia Sin.* 36 (5), 1835–1842. doi: 10.11693/hyhz20170800211

Zheng, S., Long, J., Liu, Z., Tao, W., and Wang, D. (2018). Identification and of TGF-β signaling pathway members in twenty-four animal species and expression in tilapia. *Int. J. Mol. Sci.* 19 (4), 1154. doi: 10.3390/ijms19041154

Zhu, H., Kong, L., Li, Q., Wang, Y., and Zhao, Q. (2013). *Effects of Salinity,Temperature and stocking density on the growth and srvival of white race Sea Cucumber(Apostichopus japonicus) larvae* (Periodical of Ocean University of China). doi: 10.16441/j.cnki.hdxb.2013.07.006

frontiers | Frontiers in Marine Science

TYPE Original Research
PUBLISHED 03 February 2023
DOI 10.3389/fmars.2023.1109691

OPEN ACCESS

EDITED BY
Juan D. Gaitan-Espitia,
The University of Hong Kong, Hong Kong SAR, China

REVIEWED BY
James Scott Maki,
Marquette University, United States
Ming Cong,
Yantai University, China

*CORRESPONDENCE
Chenggang Lin
linchenggang@qdio.ac.cn

SPECIALTY SECTION
This article was submitted to Global Change and the Future Ocean, a section of the journal Frontiers in Marine Science

RECEIVED 28 November 2022
ACCEPTED 24 January 2023
PUBLISHED 03 February 2023

CITATION
Zhang C, Zhang L, Li L, Mohsen M, Su F, Wang X and Lin C (2023) RNA sequencing provides insights into the effect of dietary ingestion of microplastics and cadmium in the sea cucumber *Apostichopus japonicus*. *Front. Mar. Sci.* 10:1109691. doi: 10.3389/fmars.2023.1109691

RNA sequencing provides insights into the effect of dietary ingestion of microplastics and cadmium in the sea cucumber *Apostichopus japonicus*

Chenxi Zhang[1,2,3,4,5,6], Libin Zhang[1,2,3,4,5], Lingling Li[6], Mohamed Mohsen[1,2,3,4,5], Fang Su[1,2,3,4,5], Xu Wang[1,2,3,4,5] and Chenggang Lin[1,2,3,4,5]*

[1]CAS Key Laboratory of Marine Ecology and Environmental Sciences, Institute of Oceanology, Chinese Academy of Sciences, Qingdao, China, [2]Laboratory for Marine Ecology and Environmental Science, Qingdao National Laboratory for Marine Science and Technology, Qingdao, China, [3]Center for Ocean Mega-Sciences, Chinese Academy of Sciences, Qingdao, China, [4]CAS Engineering Laboratory for Marine Ranching, Institute of Oceanology, Chinese Academy of Sciences, Qingdao, China, [5]Shandong Province Key Laboratory of Experimental Marine Biology, Qingdao, China, [6]College of Environment and Safety Engineering, Qingdao University of Science and Technology, Qingdao, China

Introduction: Microplastics (MPs) and cadmium (Cd) are persistent pollutants in aquatic environments. Sea cucumbers are susceptible to MPs and Cd due to their feeding behavior.

Methods: This study, based on Illumina sequencing, compared the transcriptomes of *A. japonicus* before and after Cd and/or MPs exposure. Additionally, we detected the changes of catalase (CAT), and superoxide dismutase (SOD) activity, glutathione (GSH), and malondialdehyde (MDA) content in sea cucumbers.

Results and Discussion: High concentration of MPs caused the increase of SOD activity. High concentration combined treatment resulted in significant up regulation of these four indicators in *A. japonicus* and had the largest number of differential expression genes (DEGs) reaching 1,618 DEGs, consisting of 789 up regulated along with 829 down regulated DEGs. Transcriptome results showed that Cd induced up regulation of intestinal FAS associated death domain protein (FADD) expression, which may cause apoptosis and inflammation. The increase of intestinal putative heparan sulfate 2-O-sulfotransferase in cadmium treatment groups provided a mechanism for host defense. The imbalance of expression of the NOD-like receptor (NLR) family inflammatory bodies and caspase 6 in the microplastic treatment group also led to the inflammatory reaction in the intestine of sea cucumber. Gene Ontology (GO) and Kyoto Encyclopedia of Genes and Genomes (KEGG) pathway analysis showed that in the process of fatty acid metabolism, MPs and Cd showed antagonistic effects, mainly in the inconsistent expression of Stearoyl CoA Ddesaturase (SCD1) protein. The significant changes of Toll interacting protein (TOLLIP) and E-selectin (SELE) in all Cd and MPs treatment

groups may indicate the key immune response genes of sea cucumber to Cd exposure and MPs exposure. These genes were involved in the immune defense of sea cucumber exposed to different levels of Cd and MPs. This study provided insights into the mechanism of dietary MPs and Cd intake in an economically and ecologically important invertebrate species.

KEYWORDS

microplastics, cadmium, sea cucumber, combined toxicity, RNA sequencing

1 Introduction

In recent years, there has been widespread concern about environmental pollution caused by the rapid accumulation of plastic debris in the natural environment (Auta et al., 2017; Liao and Yang, 2020). Tiny plastic fragments, fibers, and particles, known as Microplastics (MPs) (1 μm to 5 mm in diameter), are the main form of marine plastic debris (Thompson et al., 2004). MPs are small and easily ingested by predators living in the water column and sediments. The presence of MPs has been demonstrated in zooplankton, fish, crabs, shrimps, echinoderms including sea urchins, sea cucumbers and even marine mammals. (Daniel et al., 2020; Feng et al., 2020; Plee and Pomory, 2020; Taha et al., 2021; Zantis et al., 2021; Zhang et al., 2021). Ingested MPs may accumulate in the digestive tract of aquatic animals and in severe cases even obstruct the digestive tract, resulting in decreased feeding motility and feeding rate (Md Amin et al., 2020). MPs have been shown to cause a variety of negative effects on living organisms, including mechanical damage to digestive organs, inflammatory responses, causing oxidative stress, and alterations in enzyme production and metabolism (Wright et al., 2013; Welden and Cowie, 2016; Lei et al., 2018). Plastics are usually complex mixtures composed of polymers, residual monomers, and chemical additions (Zettler et al., 2013).

Furthermore, the organic matter, bacteria and chemical contaminants adsorbed by MPs increase their complexity (Carbery et al., 2020; Liu et al., 2022; Mohsen et al., 2022). Due to their physicochemical properties, surface characteristics, small particle size, large specific surface area and hydrophobicity, MPs have the potential to adsorb other harmful pollutants such as heavy metals in the surrounding environment (Vedolin et al., 2018; Wang et al., 2020). Heavy metals are classified as harmful to living organisms even at low concentrations due to their high toxicity and carcinogenicity (Akhbarizadeh et al., 2018). MPs and heavy metals are persistent pollutants in aquatic environments due to their bioaccumulation and biomagnification in the food chain (Kim et al., 2017). The accumulation of heavy metals in organisms may destroy enzyme activity, lead to oxidative damage, and affect biological growth and metabolism. In addition, these heavy metals are often concentrated and amplified in organisms at higher levels of the food chain, particularly in the benthos (Boyd and Massaut, 1999; Esmaeilzadeh et al., 2017; Kovacevic et al., 2020). These organisms may become food for humans and then threaten human health. Cd is poorly degradable and highly soluble in lipids, and when ingested by living organisms, it will be enriched in living organisms and not easily decomposed and excreted (Rainbow, 2003). The investigation found that the median concentration of Cd was higher on the microplastics than in the corresponding sediment (Mohsen et al., 2019a). According to another report, MPs can change the bioavailability of heavy metals in environmental media (Zhang et al., 2020). Among marine organisms, considering the combined effects of MPs and heavy metals, the most common organisms studied include phytoplankton algae, invertebrates, and fish (Qiao et al., 2019; Fernandez et al., 2020; Lin et al., 2020). Previous studies have shown that both MPs and heavy metals could show toxic effects on organisms, and their combination may produce three effects, namely synergistic, antagonistic, or potentiating effects (Bhagat et al., 2021).

Sea cucumber (*Apostichopus japonicus*) has a high market value and medicinal properties. It is an important economic species in the north of China (Fu et al., 2005). Sea cucumbers prefer to inhabit the sea floor where there is a high content of organic matter such as algae (Purcell et al., 2014; Ru et al., 2019). The concentration of metals in sediments is usually much higher than in water. Sediments can be a source of chemicals in the water column and also adversely affect sediment-dwelling organisms through direct toxicity (Roussiez et al., 2006; Dane and Sisman, 2020). The feeding nature of sea cucumbers make them more susceptible to heavy metals and MPs in the sediment (Jiang et al., 2013; Yokoyama, 2013). The environmental pollution problem is especially prominent because coastal industrial effluents and domestic effluents are largely discharged offshore, causing great harm to the sea cucumber cultivation industry along the coast (Khan et al., 2019). In addition, sea cucumbers, as sediment and suspension feeders, can be effective as a bioindicator of environmental pollution (Mohsen et al., 2020; Parra-Luna et al., 2020).

The intestine not only plays a role in absorption of nutrients, but is also the main route for toxic substances to enter the body (Ling et al., 2018; Dane and Sisman, 2020). The ingestion of sediments by sea cucumbers could lead to the unselected entry of MPs and Cd from sediments into the gut. The intestine is the first tissue to be affected by contaminants present in ingested foods, and many studies have been conducted on the effects of heavy metals on its histological changes (Joshy et al., 2022). It is not clear how the intestine of sea cucumber responds to MPs and heavy metal stresses at the molecular level. With high-throughput precision and reproducibility, transcriptome sequencing technology is a useful tool for studying aquatic animal growth, development, the immune system against disease, stress

physiology, and other functional processes. To help understand the intrinsic molecular processes of the gut in the face of Cd and MPs stress, we determined the transcriptome changes of its gut by using Illumina HiSeq 2500 sequencing technology. Additionally, we examined the status of oxidative stress enzymes. The findings of the present study are important for further understanding the mechanisms of adaptation of echinoderms to Cd and MPs of the environment, and thus, provide references for the cultivation and food safety of sea cucumber.

2 Materials and methods

2.1 Animal collection

Healthy sea cucumbers weighing 25.54 ± 2.24 g were selected as experimental animals. They were purchased from the Shandong Tonghe Marine Technology Co., Ltd. (Dongying, China). They were randomly divided into seven groups of five in parallel, each with 10 sea cucumbers, and reared in a 120 L (length × width × height: 70 cm × 50 cm × 35 cm) breeding boxes, maintained with ample blast gas and half water changed every 24 h. They were given a period of 2 weeks to acclimate before the start of the experiment. Throughout the rearing process, the breeding box water inlets were filtered with a 74 μm silk sieve. The seawater used in the experiment met the first-class conditions of the seawater quality standard (GB 3097-1997). We maintained a 12 h - 12 h light-dark illumination regime throughout the study. Further information is presented in 2.3 Experimental setup.

2.2 Test diets

Polyethylene glycol terephthalate (PET) microplastic particles of about 150 μm diameter were purchased from the Hangzhou Hongyuan Polymer Technology Co., Ltd. (Hangzhou, China), and sequentially sieved through stainless steel sieves with mesh diameters of 180 μm and 150 μm. The density of the MPs was about 1.37/(g/cm^3). The chemicals used ($CdCl_2·2.5H_2O$; analytical grade)) were purchased from the Shanghai Wokai Biotechnology Co., Ltd. (Shanghai, China). $CdCl_2·2.5H_2O$ was prepared into 5g/L Cd standard solution with ultrapure water. The composition of the experimental diets are shown in Table 1. The actual Cd and MPs concentrations were 0.49mg/kg, 46.2mg/kg, 0.0194g/kg (about 1000 microplastic particles/kg), 1.9358g/kg (about 100000 microplastic particles/kg) dry weight, respectively. They were separately passed through a grinder and pelleted through 3mm diameter extruder. The diets dried at 45 °C for 24 hours and stored in -20°C for further use.

2.3 Experimental setup

Three hundred fifty sea cucumber were randomly divided into seven groups, five parallel in each group (n = 10), and the diet exposure experiment was conducted for 30 days. Seven groups included one control group and six experimental groups. The experimental group included three environmentally relevant treatment groups (approximate natural sediment pollutant concentrations): LH (environmentally relevant concentration Cd group) with 0.5 mg/kg Cd; LM (environmentally relevant concentration MPs group) with 1000 microplastic particles/kg; and LHM (combined group with environmentally relevant concentrations of Cd and MPs) with 0.5 mg/kg Cd + 1,000 microplastic particles/kg (Mohsen et al., 2019; Wu et al., 2022) and three high concentration treatment groups (one hundred times the concentration of both pollutants in natural sediments): HH (high concentration Cd group) with 50 mg/kg Cd; HM (high concentration MPs group) with 100,000 microplastic particles/kg; and HHM (combined group with high concentrations of Cd and MPs) with 50 mg/kg Cd + 100,000 microplastic particles/kg. The ranges of the parameters were as follows: water temperature 14 ± 1°C, pH 8.3 ± 0.2, salinity 30 ± 1, dissolved oxygen 10.2 ± 0.3 mg O_2/l. In the experiment periods, sea cucumbers were fed at an amount of 3% of their body weight once a day at 16:00. We set a blank environmental control breeding box to exclude the entry of MPs in the environment. After the test, no MPs

TABLE 1 Ingredient composition of the experimental diets (g/kg).

Ingredients	Treatments						
	CK	LH	HH	LM	HM	LHM	HHM
Sargassum	185	185	185	185	185	185	185
Spirulina	26.25	26.25	26.25	26.25	26.25	26.25	26.25
Oyster shell	26.25	26.25	26.25	26.25	26.25	26.25	26.25
Scallop skirt	12.5	12.5	12.5	12.5	12.5	12.5	12.5
Sea mud	660	660	660	660	660	660	660
Starch	90	90	90	89.98	88	89.98	88
MPs	0	0	0	0.02	2.00	0.02	2.00
TOTAL	1000	1000	1000	1000	1000	1000	1000
Cd standard solution (ml)	0	0.1	10	0	0	0.1	10
H_2O (ml)	50	49.9	40	50	50	49.9	40

CK, control group; LH, environmentally relevant concentration Cd group; LM, environmentally relevant concentration MPs group; LHM, Combined group with environmentally relevant concentrations of Cd and MPs; HH, High concentration Cd group; HM, High concentration MPs group; HHM, Combined group with high concentrations of Cd and MPs.

similar to the MPs used in this experiment were found in control breeding box.

2.4 Detection of indicators related to oxidative stress

After exposure, a total of 35 sea cucumbers (five replicates per group) were collected and dissected on ice. The body coelomic fluid and intestinal tract were quickly frozen with liquid nitrogen, and placed in an Ultra-low temperature freezer for storage until testing. The detection kit was purchased from Nanjing Jiancheng Bioengineering Institute (Jiangsu, China). After thawed, the coelomic fluid was centrifuged at 425 × g for 10 mins at 4°C, and the levels of CAT, SOD and GSH were measured at wavelengths of 405 nm, 450 nm and 405 nm using a microplate reader (Thermo Scientific, Waltham, MA, USA), respectively. After the intestinal sample was thawed, a portion of the sample was weighed and added to normal saline (saline volume: tissue mass, 9:1). It was then homogenized in a centrifuge tube to obtain a 10% tissue homogenate solution, centrifuged at 956 × g for 10 min at 4°C, and the MDA content in the supernatant was determined using a microplate reader at a wavelength of 532 nm. Protein concentrations were measured using the bicinchoninic acid microplate method and a detection kit purchased from the Nanjing Jiancheng Bioengineering Institute (Nanjing, China).

2.5 RNA isolation and Illumina sequencing

Total RNA was extracted using TRIzol reagent kit (Invitrogen, Carlsbad, CA, USA) according to the manufacturer's protocol. RNA quality was assessed on an Agilent 2100 Bioanalyzer (Agilent Technologies, Palo Alto, CA, USA) and checked using RNase free agarose gel electrophoresis. After total RNA was extracted, eukaryotic mRNA was enriched by Oligo(dT) beads, while prokaryotic mRNA was enriched by removing rRNA by Ribo-ZeroTM Magnetic Kit (Epicentre, Madison, WI, USA). Then the enriched mRNA was fragmented into short fragments using fragmentation buffer and reverse transcripted into cDNA with random primers. Second-strand cDNA were synthesized by DNA polymerase I, RNase H, dNTP, and buffer. Then the cDNA fragments were purified with QiaQuick PCR extraction kit (Qiagen, Venlo, The Netherlands), end repaired, poly(A) added, and ligated to Illumina sequencing adapters. The ligation products were size selected by agarose gel electrophoresis, PCR amplified, and sequenced using Illumina HiSeq 2500 by Gene Denovo Biotechnology Co. (Guangzhou, China). The raw reads were deposited into the National Center for Biotechnology Information (NCBI) Sequence Read Archive (SRA) database (accession number: PRJNA907491).

2.6 Bioinformatics analysis

To get high quality clean reads, reads were further filtered by fastp (version 0.18.0) (Chen et al., 2018). Short reads alignment tool Bowtie2 (version 2.2.8) was used for mapping reads to ribosome RNA (rRNA) database (Langmead and Salzberg, 2012). The rRNA mapped reads were then removed. The remaining clean reads were further used in assembly and gene abundance calculation. An index of the reference genome was built, and paired-end clean reads were mapped to the reference genome using HISAT2. 2.4. RNAs differential expression analysis was performed by DESeq2 software between two different groups (and by edgeR between two samples) (Robinson et al., 2010; Love et al., 2014; Kim et al., 2015). The Gene Ontology (GO) enrichment analysis along with the Kyoto Encyclopedia of Genes and Genomes (KEGG) enrichment analyses for DEGs were performed taking false discovery rate (FDR) ≤ 0.05 as a threshold.

2.7 Real-time PCR validation

To validate the RNA-sequencing results, six genes were randomly selected for real-time PCR. Primers were designed for optimal performance using primer 5 (Supplementary Table 4). Total RNA was extracted from the respiratory tree, the same tissue used for the construction of the RNA-seq profile, by using a MiniBEST Universal RNA Extraction Kit (Takara, Shiga, Japan). A SYBR Green® real-time PCR assay (SYBR PrimeScript™ RT-PCR Kit II, TaKaRa) with an Eppendorf Mastercycler® ep realplex (Eppendorf, Hamburg, Germany) were used for examining the mRNA expression levels, and NADH was used as a reference gene for internal standardization (Zhang et al., 2022). Quantitative real-time PCR was conducted in 20 μL using SYBR Master Mix (TaKaRa, Kusatsu, Japan). The PCR was conducted at 95°C for 90 s, followed by 40 cycles at 95°C for 5 s, 60°C for 15 s, and 72°C for 20 s. Then, a melting curve analysis was performed to assess the specificity of qPCR amplification. Each gene was repeated three technique replications and $2^{-\triangle\triangle CT}$ method was used for analyzing relative quantification (Schmittgen and Livak, 2008).

2.8 Statistical analysis

The results of the experiments are presented as the means ± SD. CAT, SOD, and MDA were analyzed using the one-way analysis of variance (ANOVA) with multiple comparisons for significant differences between treated and control groups, raw data were diagnosed for their normality of distribution by Shapiro-Wilk test. Meanwhile, two-way ANOVA was used to evaluate the interactive effect of pollutant type and pollutant concentration on the parameters of oxidative stress of sea cucumber. Statistical analyses were performed using GraphPad Prism version 8.0. A value of $P < 0.05$ was considered significant. The genes with the parameter of $P \leq 0.05$ and absolute fold change ≥ 2 were considered differentially expressed genes.

3 Results

3.1 Oxidative stress related indicators

The effects of different treatment methods on catalase (CAT), superoxide dismutase (SOD) activity, glutathione (GSH) content, and

malondialdehyde (MDA) content of sea cucumber are shown in the Figure 1. In the environmental concentration exposure experiment, the LH group significantly increased the SOD enzyme activity ($P < 0.001$) and the LHM group significantly increased the content of MDA ($P < 0.05$). In the high concentration treatment group, the activity of CAT in the HH and HHM groups was significantly increased, compared with that in the CK group ($P < 0.05$). The SOD activity was significantly increased in HH; HM and HHM groups ($P < 0.001$). The content of GSH in HH and HHM groups was significantly increased ($P < 0.01$), and the content of MDA was significantly increased in HH and HHM groups ($P < 0.01$). The concentration and type of pollutants showed significant interaction on the three oxidative stress indicators of SOD, GSH and MDA($P < 0.01$) (Table 2).

3.2 Transcriptome assembly and annotation

A total of 35 cDNA libraries were constructed in this study. For data quality assurance, raw data were data filtered before information analysis to reduce analytical interference from invalid data. First, we quality controlled the resulting raw reads using fastp, and filtered low quality data to obtain clean reads (Supplementary Table 1) (Chen et al., 2018). RNA-seq generated 35,986,062–62,000,734 high quality clean reads (Supplementary Table 2). We then aligned clean reads to the ribosomal database of that species using the short reads alignment tool Bowtie2, removed reads mapping to the ribosome on the alignment without allowing mismatches, and retained unmapped reads were used for subsequent transcriptome analysis (Langmead and Salzberg, 2012). Using hisat2 software, we developed reference genome-based alignment analysis. We mapped 25,301,750–44,342,913 reads (67.35%–75.63% of clean reads) to the genome of *A. japonicus* (Supplementary Table 3).

3.3 Identification of differentially expressed genes

To reveal the mechanism of how *A. japonicus* responds to MPs and Cd stress, we performed differential gene expression analysis ($P < 0.05$) in the CK intestine relative to the LH, LM, and LHM intestines of the environmental concentration treated group and the HH, HM, and

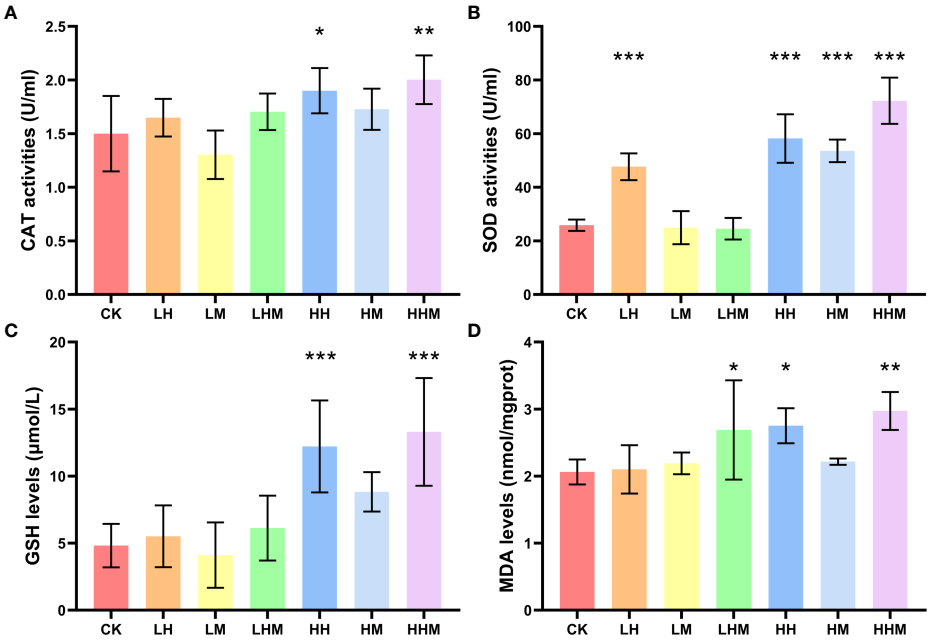

FIGURE 1
(A) Catalase (CAT) and **(B)** Superoxide dismutase (SOD) activities, **(C)** glutathione (GSH) and **(D)** Malondialdehyde (MDA) contents of *A. japonicus* at the end of the toxic exposure experiment. Asterisks (*) represent significant differences between treatments and the control group (CK) at the same developmental stage (*$P < 0.05$, **$P < 0.01$, ***$P < 0.001$). CK: control group; LH: environmentally relevant concentration Cd group; LM: environmentally relevant concentration MPs group; LHM: Combined group with environmentally relevant concentrations of Cd and MPs; HH: High concentration Cd group; HM: High concentration MPs group; HHM: Combined group with high concentrations of Cd and MPs.

TABLE 2 The interactive effect of pollutant type and pollutant concentration on the parameters of oxidative stress of sea cucumber.

Two-way ANOVA	CAT	SOD	GSH	MDA
pollutant concentration	*	***	***	*
pollutant type	*	***	**	**
Interaction	ns	***	**	**

Asterisks (*) represent significant differences between treatments and the control group (CK) at the same developmental stage (*$P < 0.05$, **$P < 0.01$, ***$P < 0.001$).

HHM intestines of the high concentration group. In environmentally relevant concentration groups, there were 1107 DEGs in the LH group, consisting of 452 up regulated along with 655 down regulated DEGs; 1240 DEGs in LM group, consisting of 493 up regulated along with 747 down regulated DEGs; and 1091 DEGs in the LHM group, consisting of 518 up regulated along with 573 down regulated DEGs. In the high concentration group, there were 1,173 DEGs in the HH group, consisting of 505 up regulated along with 668 down regulated DEGs; 1,094 DEGs in the HM group, consisting of 419 up regulated along with 675 down regulated DEGs. The HHM group had the largest number of DEGs reaching 1618, consisting of 789 up regulated along with 829 down regulated DEGs (Figure 2). Figure 3 shows the top 10 DEGs with the highest fold change values under the six group treatments.

3.4 Gene ontology enrichment analysis of differentially expressed genes

To gain insights into the biological roles of the DEGs, we performed a Gene ontology (GO) categories enrichment analysis. The GO enrichment data denoted that DEGs were classified into Biological Processes (BPs), Cellular Components (CCs), and Molecular Functions (MFs) three major functional categories. In the LH vs CK group, the most significantly enriched terms of DEGs in BPs, MFs and CCs three major functional categories are DNA-dependent DNA replication, magnesium chelatase activity, and replication fork; in the LM vs CK group, the most significantly enriched terms are interneuron axon guidance, extracellular matrix structural constituent, and basolateral plasma membrane; for LHM vs CK group, the most significantly enriched terms of are regulation of atrial cardiac muscle cell action potential, heme binding, and extracellular region; in the HH vs CK group, the most significantly enriched terms are mesonephric tubule formation, ADP binding, and NLS-dependent protein nuclear import complex; in the HM vs CK group, the most significantly enriched terms are Group II intron splicing, aspartic-type endopeptidase activity, and anchored component of membrane; and for HHM vs CK group, the most significantly enriched terms of DEGs in BPs, MFs and CCs three major functional categories are anchored component of membrane, oxidoreductase activity, and microbody.

3.5 Kyoto encyclopedia of genes and genomes enrichment analysis of differentially expressed genes

To further investigate the function of these DEGs, we mapped all these DEGs into the KEGG database. Hypergeometric tests with a P value cutoff of 0.05 was used as the criteria for pathway detection. After mapping to the KEGG database, the results in CK vs. LH, CK vs. LM, CK vs. LHM, CK vs. HH, CK vs. HM, and CK vs HHM groups showed that these DEGs were successfully annotated and assigned to 277, 239, 247, 233, 253, and 294 pathways, respectively. The most significant KEGG pathways in the LH, LM, LHM, HH, HM, HHM groups were DNA replication, pancreatic secretion, biosynthesis of unsaturated fatty acids, other glycan degradation, complement and coagulation cascades, and fatty acid metabolism, respectively. Figures 4, 5 demonstrates the top 20 most significantly altered pathways, with the most differentially gene containing pathways in cancer, metabolic pathways, arachidonic acid metabolism, MAPK

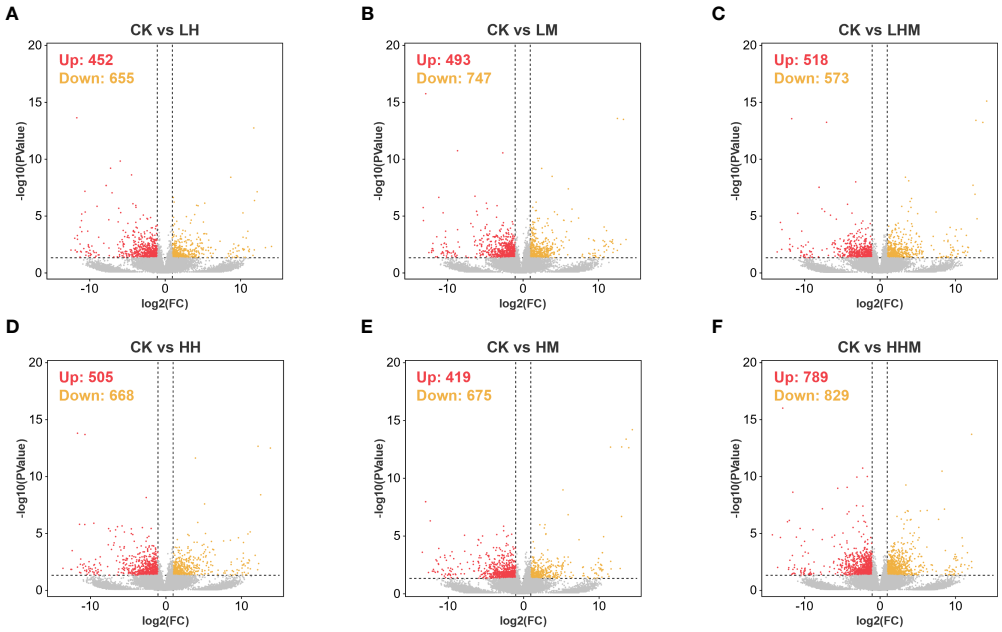

FIGURE 2
Differential expression genes (DEGs) were identified in the intestine of **(A)** japonicus after exposure. Volcano plots of DEGs in **(A)** CK vs. LH, **(B)** CK vs. LM, **(C)** CK vs. LHM, **(D)** CK vs. HH, **(E)** CK vs. HM, and **(F)** CK vs. HHM. Red dots designate up regulated genes, and orange dots designate down regulated genes. CK: control group; LH: environmentally relevant concentration Cd group; LM: environmentally relevant concentration MPs group; LHM: Combined group with environmentally relevant concentrations of Cd and MPs; HH: High concentration Cd group; HM: High concentration MPs group; HHM: Combined group with high concentrations of Cd and MPs.

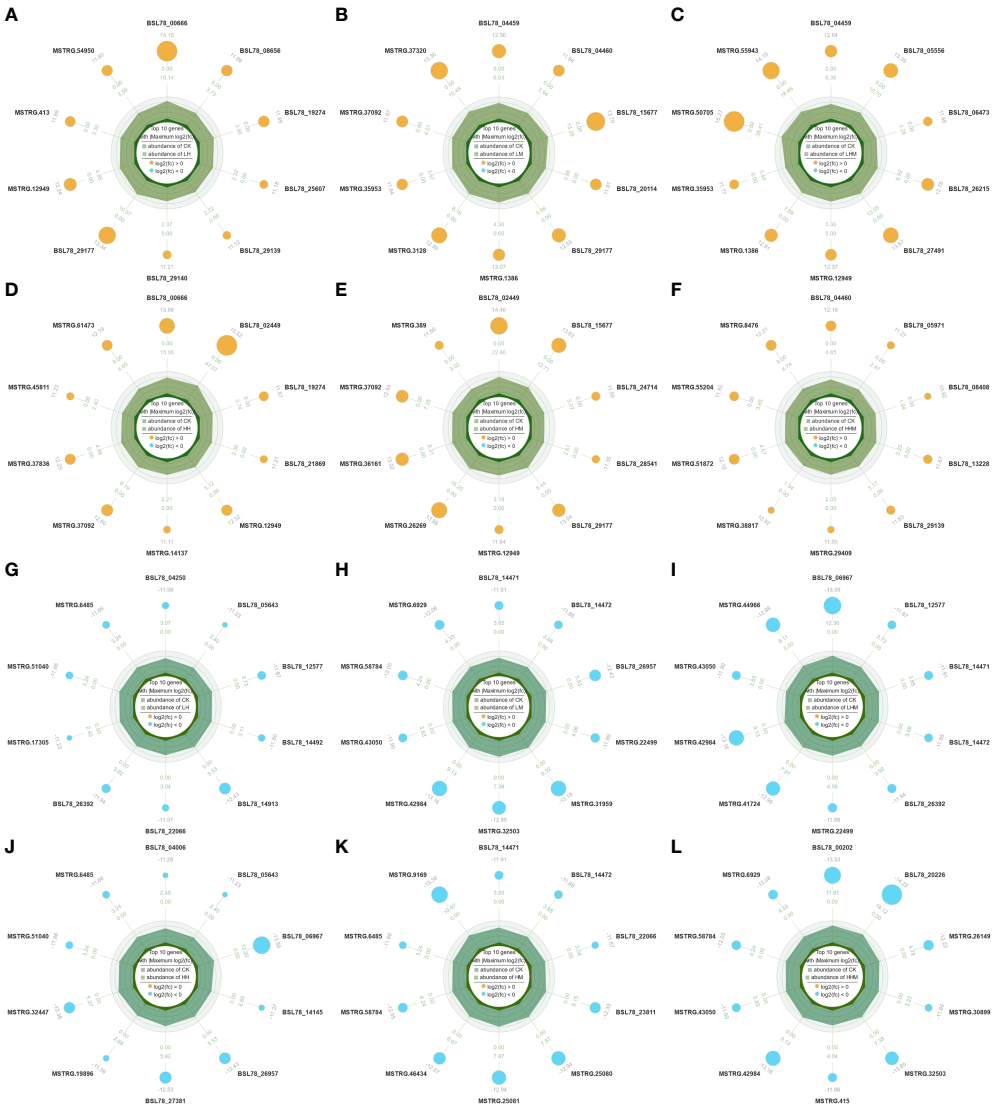

FIGURE 3
Radar map of the first 10 significantly up regulated differentially expressed genes in **(A)** CK vs. LH, **(B)** CK vs. LM, **(C)** CK vs. LHM, **(D)** CK vs. HH, **(E)** CK vs. HM, and **(F)** CK vs. HHM. Radar map of the first 10 significantly down regulated differentially expressed genes in **(G)** CK vs. LH, **(H)** CK vs. LM, **(I)** CK vs. LHM, **(J)** CK vs. HH, **(K)** CK vs. HM, and **(L)** CK vs. HHM. CK: control group; LH: environmentally relevant concentration Cd group; LM: environmentally relevant concentration MPs group; LHM: Combined group with environmentally relevant concentrations of Cd and MPs; HH: High concentration Cd group; HM: High concentration MPs group; HHM: Combined group with high concentrations of Cd and MPs.

signaling pathway, arachidonic acid metabolism, and metabolic pathways in CK vs. LH, CK vs. LM, CK vs. LHM, CK vs. HH, CK vs. HM, and CK vs. HHM, respectively. For better clarity and concise presentation, we analyzed the union of the top 20 GO terms and KEGG pathways in the environmentally relevant concentration and high concentration treatment groups, respectively (Figures 4–7). See Supplementary Figures 2-13 for specific significance and other information of these terms and pathways.

3.6 Targeted gene analysis

By comparing the genes of all treatment groups containing Cd treatments, we found 30 DEGs in common. To clarify the function of these 30 DEGs, they were subjected to KEGG enrichment and found to be significantly enriched in a total of three pathways in lipid metabolism, glycan biosynthesis and metabolism and immune system. Similarly, in the DEGs Venn plots of all the MPs treated groups, 27 DEGs were found (Figure 8). We performed KEGG enrichment analysis and found that it was significantly enriched in a total of seven pathways including endocrine system, immune system, digestive system, glycan biosynthesis and metabolism, lipid metabolism, endocrine and metabolic disease, and infectious disease: bacterial. MPs and Cd treatment had significant effects on lipid metabolism and immune system. In the Cd treatment group, three lipid metabolism pathways of fatty acid elongation, biosynthesis of unsaturated fatty acids, and steroid household biosynthesis changed significantly. In the MPs treatment group, the steroid hormone biosynthesis pathway of lipid metabolism changed. Toll-like receptor signaling pathway and complex and coordination cascades pathways were significantly enriched in the immune system of Cd and microplastic treatment groups, respectively. In addition, MPs also

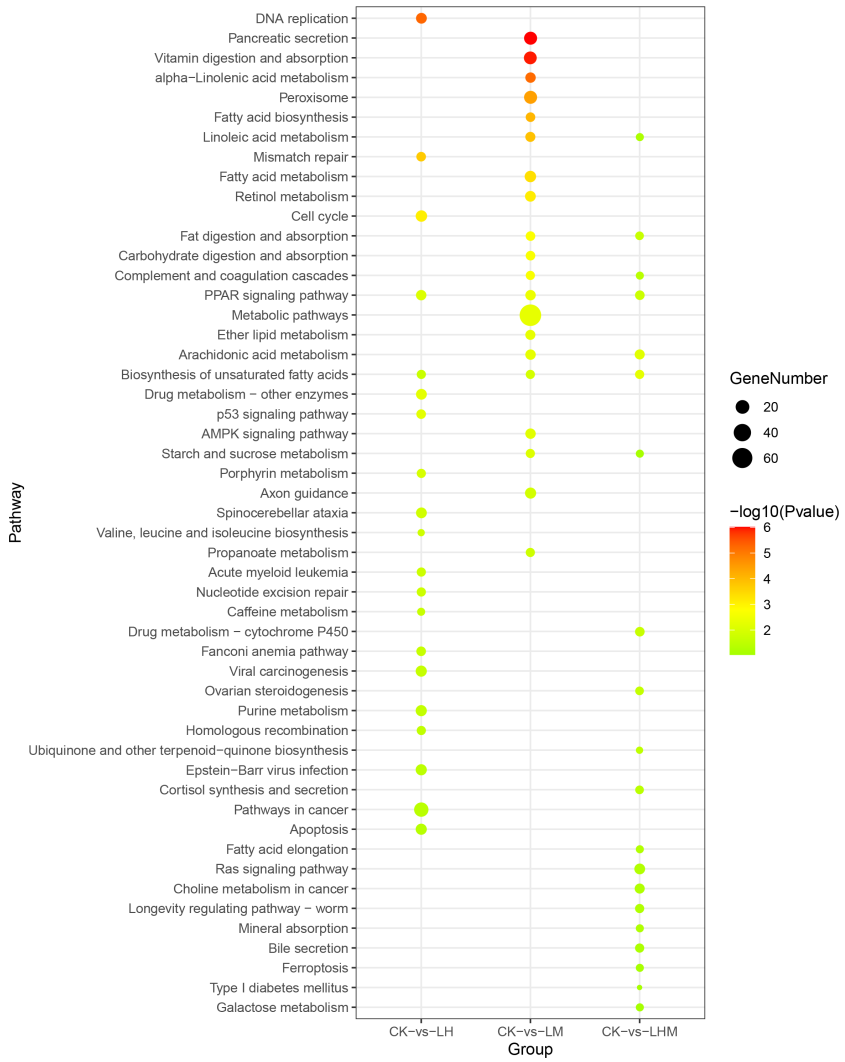

FIGURE 4
Top 20 KEGG pathways enrichment of DEGs in CK vs. LH, CK vs. LM, and CK vs. LHM. CK: control group; LH: environmentally relevant concentration Cd group; LM: environmentally relevant concentration MPs group; LHM: Combined group with environmentally relevant concentrations of Cd and MPs.

caused changes in cortisol synthesis and secret, prolactin signaling pathway, and ovarian steroidogenesis endocrine system pathways.

3.7 Real-time PCR validation

In order to verify the gene expression profile identified by RNA Seq, six DEGs were selected to verify the correctness of transcriptome analysis (BSL78_01257, BSL78_04100, BSL78_07802, BSL78_08543, BSL78_12019, BSL78_20141). The relative expression level of mRNA was further detected by qRT-PCR. These data were congruent with RNA-seq data in terms of the variation trend (Figure 9), demonstrating the accuracy and reliability of the RNA-seq investigation.

4 Discussion

The pollution of MPs in the water column often has a great visual impact on people, but the transfer of MPs from the water column to the sediment environment has a huge impact on benthos. Sediment environment is considered as a long-term sink of MPs (Cozar et al., 2014; Avio et al., 2017). Heavy metal pollution in sediment environment is also an important environmental pollution problem (Hanebuth et al., 2018). The feeding characteristics of sea cucumber as deposit feeders or suspension feeders will cause it to be in the complex pollution environment of MPs and heavy metals (Roberts et al., 2000; Taylor et al., 2016). In our study, sea cucumbers were exposed to MPs and Cd under simulated environmental concentrations and severe pollution. We detected their indicators related to oxidative stress, and used RNA-Seq technology to build the gene expression profile of the intestine most vulnerable to these two pollutants. The changes of catalase (CAT) and superoxide dismutase (SOD) enzyme activities and the contents of glutathione (GSH) and malondialdehyde (MDA) mainly occurred in the high concentration treatment group. The transcriptome sequencing results showed that the MPs and Cd caused the intestinal inflammatory reaction of sea cucumber and affected the immune system and endocrine system.

FIGURE 5
Top 20 KEGG pathways enrichment of DEGs in CK vs. HH, CK vs. HM, and CK vs. HHM. CK: control group; HH: High concentration Cd group; HM: High concentration MPs group; HHM: Combined group with high concentrations of Cd and MPs.

4.1 Changes of indexes related to oxidative stress

In the process of evolution, organisms have formed an effective antioxidant defense system including antioxidant enzymes and non-enzymatic antioxidants. In the present study these parameters were not severely affected by the treatment of pollutants at environmentally relevant concentrations, and the absence of oxidative stress at this concentration may be due to the protective effect of the gut, which sequestered Cd more than liver and muscle (Hani et al., 2018).

SOD, CAT enzyme activities and GSH, MDA contents were significantly increased in the high concentration Cd treatment group. Heavy metals can damage organisms through various pathways including ROS generation, weakening of the antioxidant defense, enzyme inactivation, oxidative stress and some of them have selective binding to specific macromolecules (Balali-Mood et al., 2021). When aquatic invertebrates are exposed to heavy metals, animals respond by activating detoxification mechanisms (Wenli et al., 2008). But with increasing concentration or time of exposure, Cd may exceed the detoxification limit of the organism. Cd will bind to macromolecular proteins (such as various enzymes) in the body, resulting in toxic effects.

In this study, high concentrations of MPs caused an increase in SOD activity. Current research has found that the toxic effects of MPs on marine organisms are affected by various factors. The size, concentration, and type will affect the accumulation and distribution of MPs in organisms to a certain extent, and then have different toxic effects on organisms (Kim et al., 2021). The MPs used in this study are large in size (Supplementary Figure 1), the defecation cycle of *A. japonicus* is short, and the large-sized MPs stay in the intestine for a short time, so they have less impact. Overall, micron-sized MPs can be efficiently excreted in the form of fecal pellets. However, it is important to note that smaller MPs, such as nano-sized MPs, may have retention times longer than 24 hours or even days (Jeong et al., 2018).

Combined exposure to high concentrations of experimental groups did not cause more severe oxidative stress in this study, however, some studies have shown that the interaction between

FIGURE 6
Top 20 Gene Ontology (GO) terms enrichment of DEGs in CK vs. LH, CK vs. LM, and CK vs. LHM. CK: control group; LH: environmentally relevant concentration Cd group; LM: environmentally relevant concentration MPs group; LHM: Combined group with environmentally relevant concentrations of Cd and MPs.

MPs and heavy metals may greatly affect the bioaccumulation and toxicity of heavy metals (Barboza et al., 2018). MPs can aggravate copper toxicity in zebrafish liver and gut by inhibiting copper ion transport while enhancing oxidative stress, resulting in elevated levels of malondialdehyde (MDA) and metallothionein (MT), and decreased levels of superoxide dismutase (SOD) (Qiao et al., 2019). When MPs and heavy metals coexist, the toxicity to organisms changes, and even the toxicity trend of the same substance may vary due to the functional groups and other characteristics of MPs (Kim et al., 2017).

4.2 Function classification of DEGs

Among the top 10 genes with significant difference between each experimental group and the control group (Figure 2), gene BSL78_00666 was significantly up regulated in LH and HH treatment groups, which may be related to the synthesis of FAS-associated death domain protein (FADD). FADD is a central mediator of death receptor-initiated apoptosis that directly activates the caspase-8 protease (Chinnaiyan et al., 1995; Kim et al., 2003). In addition, overexpression of FADD complex may cause apoptosis and inflammation (Salaun et al., 2007). Abnormal inflammatory reaction is an important link of cell and tissue damage caused by heavy metals (Fagerberg et al., 2017). Cd has always been considered as a kind of xenobiotics related to inflammation, because it can induce complex inflammatory reactions in a variety of cell types (Anka et al., 2022). After Cd exposure for 9 weeks, the expression of two enzymes associated to inflammation, cyclooxygenase type 2 (COX-2), and iNOS in mice increased significantly. Chronic Cd nephrotoxicity is associated with overexpression of COX-2 and iNOS (Morales et al., 2006).

Gene BSL78_19274 was significantly up regulated in LH and HH treatment groups, which was related to the synthesis of heparan sulfate 2-O-sulfotransferase. Heparin sulfate is a glycosaminoglycan sulfate, which can facilitate neutrophil recruitment based on the reduction of neutrophil infiltration in mice (Axelsson et al., 2012). Cytokines (TNF-α, IL-1, and others), L- and P-selectins, and chemokines bind to therapeutic heparin and purified heparan sulfate, suggesting the importance of heparan sulfate in inflammation (Ley et al., 1991; Wang et al., 2002). Neutrophil recruitment and exosmosis at the inflammatory site provide a mechanism for host defense. The up-regulation of this gene indicated the response mechanism of sea cucumber in response to the inflammation caused by Cd exposure.

Gene BSL78_29177 was significantly up regulated in LH, LM and HM treatment groups, which may be related to the activation of NLRC4 inflammatory bodies. The NLR family inflammatory bodies are activated by various exogenous and endogenous drugs,

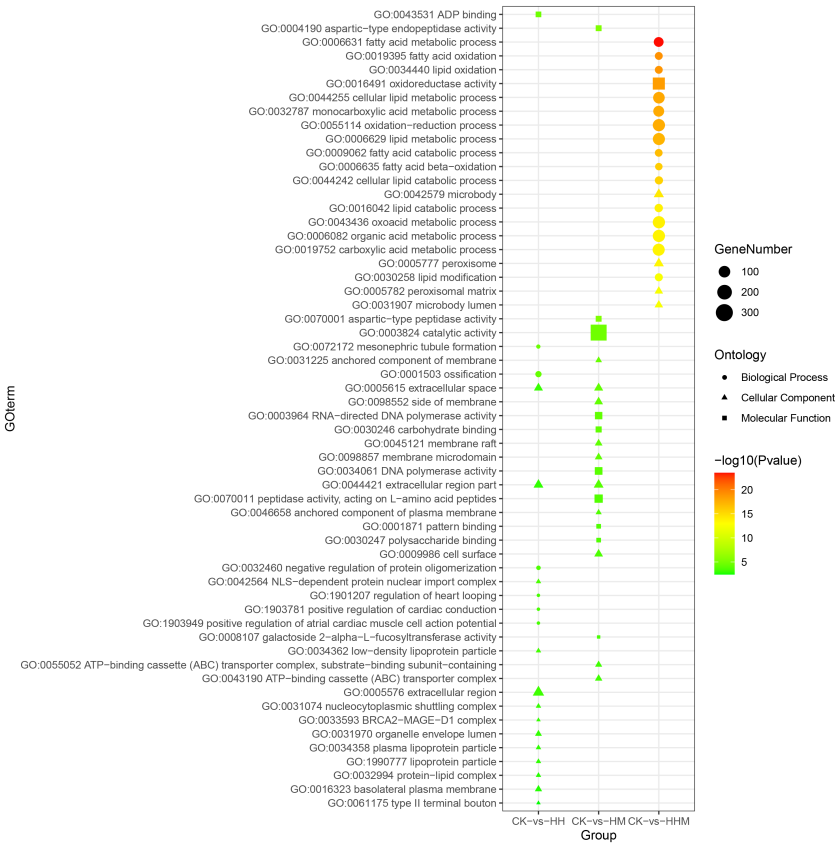

FIGURE 7
Top 20 Gene Ontology (GO) terms enrichment of DEGs in CK vs. HH, CK vs. HM, and CK vs. HHM. CK: control group; HH: High concentration Cd group; HM: High concentration MPs group; HHM: Combined group with high concentrations of Cd and MPs.

and then promote and enhance the inflammatory response. NLRC4 inflammatory corpuscles are considered to be the main promoter of Hemophagocytic lymphohistiocytosis (Schulert and Cron, 2020; Tomasik and Basak, 2022). Hemophagocytic lymphohistiocytosis is a disease characterized by immune system damage associated with excessive inflammation. Excessive release of proinflammatory cytokines triggers pathological systemic inflammation, which ultimately leads to multiple organ failure (Hayden et al., 2016). A total of 1% to 4% of polystyrene Pparticles ingested in the intestine are believed to migrate into the blood. Transferring nano plastics into the blood may cause local inflammation or cause allergic reaction in the tissues (Sass et al., 1990; Hwang et al., 2020).

CASP6 (BSL78_15677) gene was significantly up regulated in LM and HM groups. Caspases are a family of intracellular cysteine proteases that play an important role in tissue homeostasis by regulating inflammation and apoptosis. The disorder of these proteases can lead to inflammatory diseases, neurodegenerative diseases, and cancer (Creagh et al., 2003). Intracellular protease caspase-6 (CASP6) regulates neuronal apoptosis and axonal degeneration. Higher levels of Casp6 activity are associated with lower cognitive ability (Albrecht et al., 2007; Berta et al., 2014). MSTRG.12949 and MSTRG.6485 showed significant changes in expression in multiple treatment groups, which may be an important gene for intestinal response to pollutants. However, their annotation is unknown.

4.3 Gene ontology and Kyoto encyclopedia of genes and genomes enrichment analysis of differentially expressed genes

GO enrichment and KEGG enrichment analysis provided biological variations and molecular mechanisms possibly participate in detoxification of MPs and Cd in sea cucumber. Among the GO enrichment items, there were few items shared by the combined treatment group and the single MPs and Cd treatment group. Only DNA integration (GO: 0015074) was significantly enriched in LM and LHM treatment groups. In the high concentration treatment, the two entries of extracellular space (GO: 0005615) and extracellular region part (GO: 0044421) were significantly enriched in the HH and HM treatment groups. These results indicated that the toxic effects of MPs and Cd on sea cucumber were complex, and the effects of mixed exposure of the two pollutants were not simple addition effects.

In the environmental related concentration treatment group, the differentially expressed genes in LM, LH, and LHM treatment groups were significantly enriched in Peroxisome proliferator activated receptor (PPAR) signaling pathway and biosynthesis of unsaturated fat acids pathway. PPAR can regulate the metabolism of many cells, regulate the transcription of target genes, and play a very important role in various metabolic processes (Ma et al., 2017). PPAR signaling pathway is closely related to lipid metabolism. Stearoyl CoA Desaturase (SCD1) and acyl CoA oxidase (ACO) are important proteins in PPAR signaling pathway, which play a regulatory role

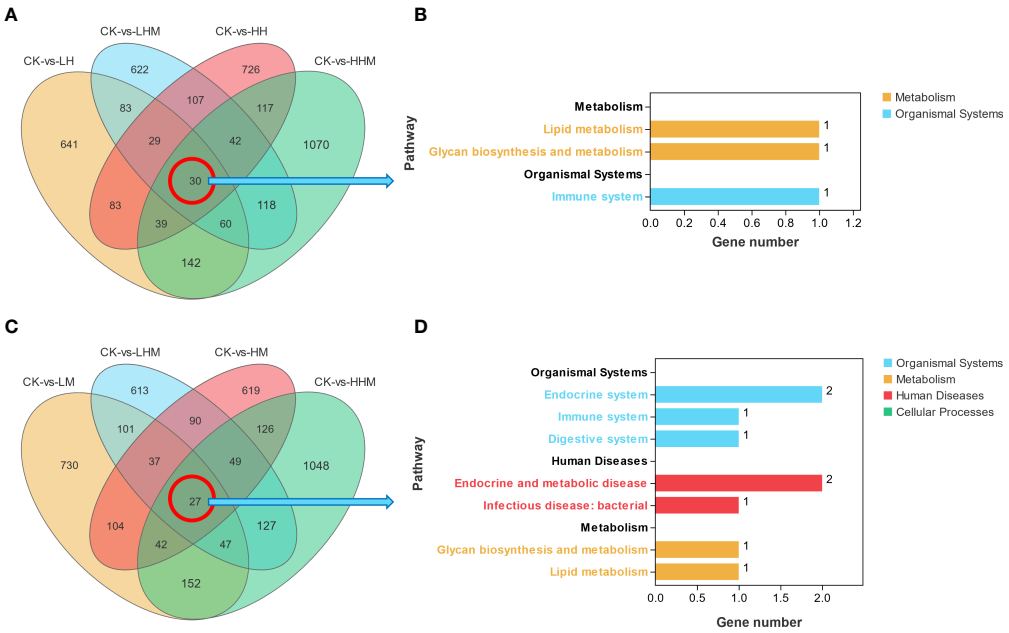

FIGURE 8
Wayne map of common differentially expressed genes (DEGs) in **(A)** Cd and **(C)** microplastic treatment groups. Enrichment of KEGG pathway by **(B)** Cd and **(D)** microplastic treatment groups target DEGs. CK: control group; LH: environmentally relevant concentration Cd group; LM: environmentally relevant concentration MPs group; LHM: Combined group with environmentally relevant concentrations of Cd and MPs; HH: High concentration Cd group; HM: High concentration MPs group; HHM: Combined group with high concentrations of Cd and MPs.

in fatty acid composition. SCD1 is the rate-limiting enzyme of biosynthesis of monounsaturated fatty acids. It plays an important role in *de novo* synthesis of fatty acids (Dumas and Ntambi, 2017; Tracz-Gaszewska and Dobrzyn, 2019). LM treatment may have a negative effect on fatty acid metabolism of sea cucumber. Interestingly, after LH treatment, SCD1 and long chain acyl CoA synthase (ACS) were up regulated, and LH treatment promoted the metabolism of fatty acids to some extent. It may be related to the detoxification of pollutants by organisms themselves. SCD1 protein is located on the endoplasmic reticulum membrane and mainly controls the endoplasmic reticulum stress response. The increase of saturated phospholipid components leads to the destruction of the endoplasmic reticulum, which activates the endoplasmic reticulum stress response. The stress reaction can be repaired by supplementing unsaturated fatty acids (Borradaile et al., 2006; Peng et al., 2011).

MPs and Cd play an antagonistic role in the metabolism of fatty acids at low concentrations. Similarly, in biosynthesis of unsaturated fatty acids pathway, there were more up regulated genes after LH treatment and more down regulated genes after LM treatment. Furthermore, the arachidonic acid metabolism pathway was significantly enriched in the LM and LHM treatment groups. In addition, the linoleic acid metabolism pathway and the starch and

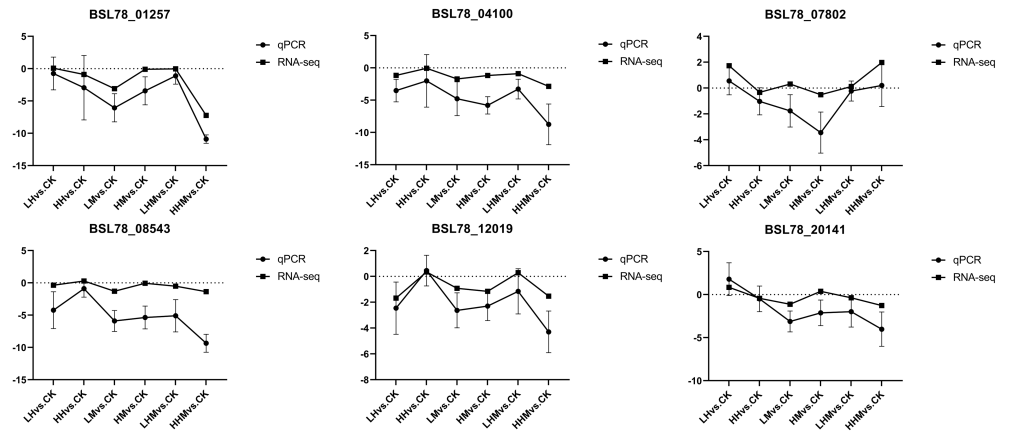

FIGURE 9
Relative expression of 6 selected genes differentially expressed after treatment. CK: control group; LH: environmentally relevant concentration Cd group; LM: environmentally relevant concentration MPs group; LHM: Combined group with environmentally relevant concentrations of Cd and MPs; HH: High concentration Cd group; HM: High concentration MPs group; HHM: Combined group with high concentrations of Cd and MPs.

sucrose metabolism pathway were both enriched in the LM and LHM groups. Further analysis of DEGs enriched in the pathway showed that after LM treatment, DEGs in the linoleic acid metabolism and arachidonic acid metabolism pathways were mainly down regulated, while DEGs in the starch and sucrose metabolism pathways were up regulated. After LHM treatment, DEGs in the linoleic acid metabolism and radionic acid metabolism pathways were up regulated, and those in the starch and sucrose metabolism were down regulated. In our study, MPs inhibited lipid metabolism, promoted carbohydrate metabolism, and antagonized Cd. It is speculated that MPs may have a significant impact on intestinal metabolism related pathways. Metabolic pathways are also significantly enriched in HM and HHM groups. Similarly, ingesting MPs can affect the metabolism of fish by changing the proportion of triglycerides and cholesterol in the blood and the distribution of cholesterol in muscle and liver tissues (Jovanovic, 2017). It will also affect the induction or inhibition of enzymes related to lipid metabolism, as well as the changes of hormone levels related to lipid metabolism, leading to changes in triglyceride and cholesterol levels (Banaee et al., 2019).

In addition, the complex and coagulation cascades pathway was significantly enriched in LM and LHM groups. In LM, the completion component (3b/4b) receiver 1 (CR1) was up regulated. In LHM, the completion factor H (CFH) and completion component (3b/4b) receiver 1 (CR1) were up regulated. Similarly, this pathway was significantly enriched in HM and HHM treatment groups, and most of the genes were up regulated. Complement factor H (CFH), a multifunctional soluble complement regulatory protein, can bind to a variety of pathogens and play a crucial role in host innate immune defense. CFH is also an important regulator of immune cells. It can regulate the phagocytosis of monocytes/macrophages and the production of inflammatory factors (Abdul-Aziz et al., 2016). CFH plays an important role in protecting host cells against damage mediated by disturbance of completion system and normal function of immune cells (Roy et al., 2016). CFH also aids non-inflammatory clearance of damaged cells and cell debris. These results may be related to the physical damage of MPs to the intestine (Jozsi et al., 2022). Simple chemical forces can produce nanoscale particles from PS particles and cause direct cell damage. Absorbed MPs and nanomaterials with a diameter less than 1.5 μm can directly damage cells (Mattsson et al., 2017; Sharma and Chatterjee, 2017).

4.4 Analysis of target functional genes related to immune response

Analysis of common differential genes in all Cd-containing treatment groups showed that gene *BSL78_29595* is enriched to Toll-like receiver signaling pathway. The Toll interacting protein (TOLLIP) is an inhibitor of TLR4 signal pathway. On one hand, it can interact with interleukin 1 receptor associated kinase 4 (IRAK4) in TLR4-MYD88 dependent signal pathway, and inhibit the phosphorylation of IRAK4, thereby inhibiting the activation of the downstream of TLR4 signal pathway (Burns et al., 2000). On the other hand, TOLLIP interacts with TLR2, TLR4, and IL-1R receptor to inhibit the occurrence of natural immune response activated by LPS (Bulut et al., 2001). In Toll-like signaling pathway, TOLLIP plays a negative regulatory role and inhibits the occurrence of Toll signaling pathway. Recent studies have shown that TOLLIP negative regulation of TLR4 signaling pathway may help to limit the production of excessive cytokines during inflammation and various pathogenic infections (Zhang and Ghosh, 2002; Shibolet and Podolsky, 2007). Therefore, TOLLIP seems to be a key regulatory factor involved in the initiation and maintenance of inflammatory process in TLR4 mediated inflammatory process (Didierlaurent et al., 2006; Kowalski and Li, 2017). Kim et al. (2020) knockdown of TOLLIP expression by RNA interference, RM treated activated macrophages showed augmented expression of inflammatory mediators (pro-inflammatory cytokines, NO, inducible nitric oxidase, and cyclooxygenase-2, and surface molecules) and restored the expression of MAPK and NF-κB signals inhibited by RM treatment (Kim et al., 2020). In this study, TOLLIP plays an important role in the negative regulation of the intestinal tract of sea cucumber on Cd-induced inflammation.

High concentrations of MPs or toxic substances adsorbed by MPs may cause acute damage to the human intestinal tract, inflammation of the inner wall of the intestinal tract, and a sharp decline in the amount of intestinal mucus (Wright and Kelly, 2017). Intestinal immune system disorder can recruit inflammatory cells to release inflammatory mediators, causing tissue damage and dysfunction. Among them, cell adhesion molecules play an important role in intestinal immune response and inflammation process.

The SELE gene encodes E-selectin, which is found in cytokine-stimulated endothelial cells and is thought to be responsible for the accumulation of leukocytes at sites of inflammation by mediating the adhesion of cells to the vascular wall (Li et al., 2021). Inflammatory factor interleukin-1 (IL-1), tumor necrosis factor-α (TNF-α), bacterial lipopolysaccharide (LPS) stimulated endothelial cells, the expression of E-selectin increased significantly, which can increase the permeability of blood vessel surface, promote the activation of inflammatory cells, and mediate the occurrence of inflammation (McEver, 2015). Similarly, high concentrations of polystyrene MPs/NPs may induce intestinal inflammation due to the disorder of zebrafish intestinal microbiota. The proinflammatory cytokines were significantly up regulated in the 1 mg/L NPS treatment group. The correlation between intestinal microbiota composition and immune related genes showed that the change of intestinal microbiota comparison was positively correlated with the expression of immune cytokines. Different amounts of MPs can increase the secretion of pro-inflammatory cytokine IL-1α in serum (Li et al., 2020). Different amounts of MPs can also increase the secretion of proinflammatory cytokines IL-1α in mice serum, but the amount of each MPs will affect the secretion of specific cytokines. High concentrations of MPs tend to induce intestinal inflammation by activating TLR4 signal transduction (Li et al., 2020). MPs are considered as foreign substances, which can stimulate the immune response of fish or inhibit the immune function by inducing immunotoxicity, i.e., MPs can affect the immunity of fish through a variety of mechanisms. However, a detailed study of the immune response of fish after MP exposure is needed (Kim et al., 2021).

5 Conclusions

In conclusion, the oxidative stress of sea cucumber was mainly influenced by Cd. Although the high concentration of MPs also caused a certain increase in SOD activity, this effect may not cause substantial damage to the sea cucumber. This study is the first to report the transcriptome information of *A. japonicus* intestine after combined exposure to Cd and MPs. In the environmental concentration group, 1,107, 1,240, and 1,091 DEGs were identified respectively in LH, LM, and LHM groups, and 1,173, 1,094 and 1,618 DEGs were identified, respectively, in HH, HM and HHM groups in the high concentration group. Cd-induced up-regulation of intestinal FAS associated death domain protein (FADD) expression may cause apoptosis and inflammation. At the same time, the increase of intestinal putative heparan sulfate 2-O-sulfotransferase in LH and HH treatment groups provides a mechanism for host defense. The imbalance of expression of NLR family inflammatory bodies and CASP6 in the MPs treatment group also led to the inflammatory reaction in the intestine of sea cucumber. GO and KEGG pathway analysis showed that the mixed toxicity of MPs and Cd was not a simple additive effect. In the process of fatty acid metabolism, MPs and Cd showed antagonistic effects, mainly in the inconsistent expression of SCD1 protein. MPs and Cd also showed antagonistic effects in lipid metabolism and carbohydrate metabolism pathways. The significant up-regulation of completion factor H after MPs treatment may be related to the physical damage caused by microplastics. The significant changes of TOLLIP and SELE in all Cd and MPs treatment groups may indicate the key immune response genes of sea cucumber to Cd exposure and MPs exposure. These genes are involved in the immune defense of sea cucumber exposed to different levels of Cd and MPs. These findings indicated that the exposure of MPs and Cd caused oxidative stress in sea cucumber, inflammatory reaction in the intestine, and activated the intestinal immune defense system. The results of this study will provide clues for the molecular process of the combined toxicity of MPs and Cd.

Data availability statement

The data presented in the study are deposited in the NCBI Sequence Read Archive repository, accession number PRJNA907491.

Author contributions

CZ: Conceptualization, Investigation, Formal analysis, Writing – original draft, Writing – review & editing. LZ: Funding acquisition, Writing – review & editing. LL: Writing – review & editing. MM: Writing – review & editing. FS: Methodology. XW: Formal analysis. CL: Writing – review & editing, Resources, Funding acquisition, Supervision. All authors contributed to the article and approved the submitted version

Funding

This work was supported by the National Natural Science Foundation of China (42176106; 31960225; 32150410376) and the Shandong Provincial Key R&D Program, China (2022RZB07051).

Conflict of interest

The authors declare that the research was conducted in the absence of any commercial or financial relationships that could be construed as a potential conflict of interest.

Publisher's note

All claims expressed in this article are solely those of the authors and do not necessarily represent those of their affiliated organizations, or those of the publisher, the editors and the reviewers. Any product that may be evaluated in this article, or claim that may be made by its manufacturer, is not guaranteed or endorsed by the publisher.

Supplementary material

The Supplementary Material for this article can be found online at: https://www.frontiersin.org/articles/10.3389/fmars.2023.1109691/full#supplementary-material

References

Abdul-Aziz, M., Tsolaki, A. G., Kouser, L., Carroll, M. V., Al-Ahdal, M. N., Sim, R. B., et al. (2016). Complement factor h interferes with mycobacterium bovis BCG entry into macrophages and modulates the pro-inflammatory cytokine response. *Immunobiology* 221 (9), 944–952. doi: 10.1016/j.imbio.2016.05.011

Akhbarizadeh, R., Moore, F., and Keshavarzi, B. (2018). Investigating a probable relationship between microplastics and potentially toxic elements in fish muscles from northeast of Persian gulf. *Environ. pollut.* 232, 154–163. doi: 10.1016/j.envpol.2017.09.028

Albrecht, S., Bourdeau, M., Bennett, D., Mufson, E. J., Bhattacharjee, M., and LeBlanc, A. C. (2007). Activation of caspase-6 in aging and mild cognitive impairment. *Am. J. Pathol.* 170 (4), 1200–1209. doi: 10.2353/ajpath.2007.060974

Anka, A. U., Usman, A. B., Kaoje, A. N., Kabir, R. M., Bala, A., Arki, M. K., et al. (2022). Potential mechanisms of some selected heavy metals in the induction of inflammation and autoimmunity. *Eur. J. Inflammation* 20. doi: 10.1177/1721727X221122719

Auta, H. S., Emenike, C. U., and Fauziah, S. H. (2017). Distribution and importance of microplastics in the marine environment: A review of the sources, fate, effects, and potential solutions. *Environ. Int.* 102, 165–176. doi: 10.1016/j.envint.2017.02.013

Avio, C. G., Gorbi, S., and Regoli, F. (2017). Plastics and microplastics in the oceans: From emerging pollutants to emerged threat. *Mar. Environ. Res.* 128, 2–11. doi: 10.1016/j.marenvres.2016.05.012

Axelsson, J., Xu, D., Kang, B. N., Nussbacher, J. K., Handel, T. M., Ley, K., et al. (2012). Inactivation of heparan sulfate 2-o-sulfotransferase accentuates neutrophil infiltration during acute inflammation in mice. *Blood* 120 (8), 1742–1751. doi: 10.1182/blood-2012-03-417139

Balali-Mood, M., Naseri, K., Tahergorabi, Z., Khazdair, M. R., and Sadeghi, M. (2021). Toxic mechanisms of five heavy metals: Mercury, lead, chromium, cadmium, and arsenic. *Front. Pharmacol.* 12. doi: 10.3389/fphar.2021.643972

Banaee, M., Soltanian, S., Sureda, A., Gholamhosseini, A., Haghi, B. N., Akhlaghi, M., et al. (2019). Evaluation of single and combined effects of cadmium and micro-plastic particles on biochemical and immunological parameters of common carp (Cyprinus carpio). *Chemosphere* 236, 124335. doi: 10.1016/j.chemosphere.2019.07.066

Barboza, L. G. A., Vieira, L. R., Branco, V., Carvalho, C., and Guilhermino, L. (2018). Microplastics increase mercury bioconcentration in gills and bioaccumulation in the liver, and cause oxidative stress and damage in dicentrarchus labrax juveniles. *Sci. Rep.* 8 (1), 15655. doi: 10.1038/s41598-018-34125-z

Berta, T., Park, C. K., Xu, Z. Z., Xie, R. G., Liu, T., Lu, N., et al. (2014). Extracellular caspase-6 drives murine inflammatory pain *via* microglial TNF-alpha secretion. *J. Clin. Invest.* 124 (3), 1173–1186. doi: 10.1172/JCI72230

Bhagat, J., Nishimura, N., and Shimada, Y. (2021). Toxicological interactions of microplastics/nanoplastics and environmental contaminants: Current knowledge and future perspectives. *J. Hazard. Mater.* 405, 123913. doi: 10.1016/j.jhazmat.2020.123913

Borradaile, N. M., Han, X. L., Harp, J. D., Gale, S. E., Ory, D. S., and Schaffer, J. E. (2006). Disruption of endoplasmic reticulum structure and integrity in lipotoxic cell death. *J. Lipid Res.* 47 (12), 2726–2737. doi: 10.1194/jlr.M600299-JLR200

Boyd, C. E., and Massaut, L. (1999). Risks associated with the use of chemicals in pond aquaculture. *Aquacult. Eng.* 20 (2), 113–132. doi: 10.1016/S0144-8609(99)00010-2

Bulut, Y., Faure, E., Thomas, L., Equils, O., and Arditi, M. (2001). Cooperation of toll-like receptor 2 and 6 for cellular activation by soluble tuberculosis factor and borrelia burgdorferi outer surface protein a lipoprotein: Role of toll-interacting protein and IL-1 receptor signaling molecules in toll-like receptor 2 signaling. *J. Immunol.* 167 (2), 987–994. doi: 10.4049/jimmunol.167.2.987

Burns, K., Clatworthy, J., Martin, L., Martinon, F., Plumpton, C., Maschera, B., et al. (2000). Tollip, a new component of the IL-1RI pathway, links IRAK to the IL-1 receptor. *Nat. Cell Biol.* 2 (6), 346–351. doi: 10.1038/35014038

Carbery, M., MacFarlane, G. R., O'Connor, W., Afrose, S., Taylor, H., and Palanisami, T. (2020). Baseline analysis of metal(loid)s on microplastics collected from the Australian shoreline using citizen science. *Mar. Pollut. Bull.* 152, 110914. doi: 10.1016/j.marpolbul.2020.110914

Chen, S. F., Zhou, Y. Q., Chen, Y. R., and Gu, J. (2018). Fastp: an ultra-fast all-in-one FASTQ preprocessor. *Bioinf.* 34 (17), 884–890. doi: 10.1093/bioinformatics/bty560

Chinnaiyan, A. M., Orourke, K., Tewari, M., and Dixit, V. M. (1995). FADD, a novel death domain-containing protein, interacts with the death domain of FAS and initiates apoptosis. *Cell* 81 (4), 505–512. doi: 10.1016/0092-8674(95)90071-3

Cozar, A., Echevarria, F., Gonzalez-Gordillo, J. I., Irigoien, X., Ubeda, B., Hernandez-Leon, S., et al. (2014). Plastic debris in the open ocean. *Proc. Natl. Acad. Sci. U. S. A.* 111 (28), 10239–10244. doi: 10.1073/pnas.1314705111

Creagh, E. M., Conroy, H., and Martin, S. J. (2003). Caspase-activation pathways in apoptosis and immunity. *Immunol. Rev.* 193 (1), 10–21. doi: 10.1034/j.1600-065X.2003.00048.x

Dane, H., and Sisman, T. (2020). A morpho-histopathological study in the digestive tract of three fish species influenced with heavy metal pollution. *Chemosphere* 242, 125212. doi: 10.1016/j.chemosphere.2019.125212

Daniel, D. B., Ashraf, P. M., and Thomas, S. N. (2020). Abundance, characteristics and seasonal variation of microplastics in Indian white shrimps (Fenneropenaeus indicus) from coastal waters off Cochin, kerala, India. *Sci. Total. Environ.* 737, 139839. doi: 10.1016/j.scitotenv.2020.139839

Didierlaurent, A., Brissoni, B., Velin, D., Aebi, N., Tardivel, A., Kaslin, E., et al. (2006). Tollip regulates proinflammatory responses to interleukin-1 and lipopolysaccharide. *Mol. Cell. Biol.* 26 (3), 735–742. doi: 10.1128/MCB.26.3.735-742.2006

Dumas, S., and Ntambi, J. M. (2017). Co-Conspirators in a new mechanism for the degradation of 9-desaturase. *J. Biol. Chem.* 292 (49), 19987–19988. doi: 10.1074/jbc.H117.801936

Esmaeilzadeh, M., Karbassi, A. R., and Bastami, K. D. (2017). Antioxidant response to metal pollution in phragmites australis from anzali wetland. *Mar. pollut. Bull.* 119 (1), 376–380. doi: 10.1016/j.marpolbul.2017.03.030

Fagerberg, B., Borne, Y., Barregard, L., Sallsten, G., Forsgard, N., Hedblad, B., et al. (2017). Cadmium exposure is associated with soluble urokinase plasminogen activator receptor, a circulating marker of inflammation and future cardiovascular disease. *Environ. Res.* 152, 185–191. doi: 10.1016/j.envres.2016.10.019

Feng, Z., Wang, R., Zhang, T., Wang, J., Huang, W., Li, J., et al. (2020). Microplastics in specific tissues of wild sea urchins along the coastal areas of northern China. *Sci. Total. Environ.* 728, 138660. doi: 10.1016/j.scitotenv.2020.138660

Fernandez, B., Santos-Echeandia, J., Rivera-Hernandez, J. R., Garrido, S., and Albentosa, M. (2020). Mercury interactions with algal and plastic microparticles: Comparative role as vectors of metals for the mussel, mytilus galloprovincialis. *J. Hazard. Mater.* 396, 122739. doi: 10.1016/j.jhazmat.2020.122739

Fu, X. Y., Xue, C. H., Miao, B. C., Li, Z. J., Gao, X., and Yang, W. G. (2005). Characterization of proteases from the digestive tract of sea cucumber (*Stichopus japonicus*): High alkaline protease activity. *Aquaculture* 246 (1-4), 321–329. doi: 10.1016/j.aquaculture.2005.01.012

Hanebuth, T. J. J., King, M. L., Mendes, I., Lebreiro, S., Lobo, F. J., Oberle, F. K., et al. (2018). Hazard potential of widespread but hidden historic offshore heavymetal (Pb, zn) contamination (Gulf of cadiz, Spain). *Sci. Total Environ.* 637, 561–576. doi: 10.1016/j.scitotenv.2018.04.352

Hani, Y. M. I., Turies, C., Palluel, O., Delahaut, L., Gaillet, V., Bado-Nilles, A., et al. (2018). Effects of chronic exposure to cadmium and temperature, alone or combined, on the threespine stickleback (*Gasterosteus aculeatus*): Interest of digestive enzymes as biomarkers. *Aquat. Toxicol.* 199, 252–262. doi: 10.1016/j.aquatox.2018.04.006

Hayden, A., Park, S., Giustini, D., Lee, A. Y. Y., and Chen, L. Y. C. (2016). Hemophagocytic syndromes (HPSs) including hemophagocytic lymphohistiocytosis (HLH) in adults: A systematic scoping review. *Blood Rev.* 30 (6), 411–420. doi: 10.1016/j.blre.2016.05.001

Hwang, J., Choi, D., Han, S., Jung, S., Choi, J., and Hong, J. (2020). Potential toxicity of polystyrene microplastic particles. *Sci. Rep.* 10 (1), 7391. doi: 10.1038/s41598-020-64464-9

Jeong, C.-B., Kang, H.-M., Lee, Y. H., Kim, M.-S., Lee, J.-S., Seo, J. S., et al. (2018). Nanoplastic ingestion enhances toxicity of persistent organic pollutants (POPs) in the monogonont rotifer brachionus koreanus *via* multixenobiotic resistance (MXR) disruption. *Environ. Sci. Technol.* 52 (19), 11411–11418. doi: 10.1021/acs.est.8b03211

Jiang, S. H., Dong, S. L., Gao, Q. F., Wang, F., and Tian, X. L. (2013). Comparative study on nutrient composition and growth of green and red sea cucumber, apostichopus japonicus (Selenka 1867), under the same culture conditions. *Aquacult. Res.* 44 (2), 317–320. doi: 10.1111/j.1365-2109.2011.03033.x

Joshy, A., Sharma, S. R. K., Mini, K. G., Gangadharan, S., and Pranav, P. (2022). Histopathological evaluation of bivalves from the southwest coast of India as an indicator of environmental quality. *Aquat. Toxicol.* 243, 106076. doi: 10.1016/j.aquatox.2022.106076

Jovanovic, B. (2017). Ingestion of microplastics by fish and its potential consequences from a physical perspective. *Integr. Environ. Assess. Manage.* 13 (3), 510–515. doi: 10.1002/ieam.1913

Jozsi, M., Barlow, P. N., and Meri, S. (2022). Editorial: Function and dysfunction of complement factor h. *Front. Immunol.* 12. doi: 10.3389/fimmu.2021.831044

Khan, M. I., Zahoor, M., Khan, A., Gulfam, N., and Khisroon, M. (2019). Bioaccumulation of heavy metals and their genotoxic effect on freshwater mussel. *Bull. Environ. Contam. Toxicol.* 102 (1), 52–58. doi: 10.1007/s00128-018-2492-4

Kim, D., Chae, Y., and An, Y. J. (2017). Mixture toxicity of nickel and microplastics with different functional groups on daphnia magna. *Environ. Sci. Technol.* 51 (21), 12852–12858. doi: 10.1021/acs.est.7b03732

Kim, W. S., Kim, K., Byun, E. B., Song, H. Y., Han, J. M., Park, W. Y., et al. (2020). RM, a novel resveratrol derivative, attenuates inflammatory responses induced by lipopolysaccharide *via* selectively increasing the tollip protein in macrophages: A partial mechanism with therapeutic potential in an inflammatory setting. *Int. Immunopharmacol.* 78, 106072. doi: 10.1016/j.intimp.2019.106072

Kim, D., Landmead, B., and Salzberg, S. L. (2015). HISAT: A fast spliced aligner with low memory requirements. *Nat. Methods* 12 (4), 357–U121. doi: 10.1038/NMETH.3317

Kim, P. K. M., Park, S. Y., Koty, P. P., Hua, Y., Luketich, J. D., and Billiar, T. R. (2003). Fas-associating death domain protein overexpression induces apoptosis in lung cancer cells. *J. Thorac. Cardiovasc. Surg.* 125 (6), 1336–1342. doi: 10.1016/S0022-5223(02)73227-3

Kim, J. H., Yu, Y. B., and Choi, J. H. (2021). Toxic effects on bioaccumulation, hematological parameters, oxidative stress, immune responses and neurotoxicity in fish exposed to microplastics: A review. *J. Hazard. Mater.* 413, 125423. doi: 10.1016/j.jhazmat.2021.125423

Kovacevic, M., Jovanovic, Z., Andrejic, G., Dzeletovic, Z., and Rakic, T. (2020). Effects of high metal concentrations on antioxidative system in phragmites australisgrown in mine and flotation tailings ponds. *Plant Soil* 453 (1-2), 297–312. doi: 10.1007/s11104-020-04598-x

Kowalski, E. J. A., and Li, L. W. (2017). Toll-interacting protein in resolving and non-resolving inflammation. *Front. Immunol.* 8. doi: 10.3389/fimmu.2017.00511

Langmead, B., and Salzberg, S. L. (2012). Fast gapped-read alignment with bowtie 2. *Nat. Methods* 9 (4), 357–U354. doi: 10.1038/NMETH.1923

Lei, L. L., Wu, S. Y., Lu, S. B., Liu, M. T., Song, Y., Fu, Z. H., et al. (2018). Microplastic particles cause intestinal damage and other adverse effects in zebrafish danio rerio and nematode caenorhabditis elegans. *Sci. Total Environ.* 619, 1–8. doi: 10.1016/j.scitotenv.2017.11.103

Ley, K., Cerrito, M., and Arfors, K. E. (1991). SULFATED POLYSACCHARIDES INHIBIT LEUKOCYTE ROLLING IN RABBIT MESENTERY VENULES. *Am. J. Physiol.* 260 (5), 1667–1673. doi: 10.1152/ajpheart.1991.260.5.H1667

Liao, Y. L., and Yang, J. Y. (2020). Microplastic serves as a potential vector for cr in an in-vitro human digestive model. *Sci. Total Environ.* 703, 134805. doi: 10.1016/j.scitotenv.2019.134805

Li, B. Q., Ding, Y. F., Cheng, X., Sheng, D. D., Xu, Z., Rong, Q. Y., et al. (2020). Polyethylene microplastics affect the distribution of gut microbiota and inflammation development in mice. *Chemosphere* 244, 125492. doi: 10.1016/j.chemosphere.2019.125492

Ling, S. C., Luo, Z., Chen, G. H., Zhang, D. G., and Liu, X. (2018). Waterborne zn influenced zn uptake and lipid metabolism in two intestinal regions of juvenile goby synechogobius hasta. *Ecotoxicol. Environ. Saf.* 148, 578–584. doi: 10.1016/j.ecoenv.2017.10.064

Lin, W., Su, F., Lin, M. Z., Jin, M. F., Li, Y. H., Ding, K. W., et al. (2020). Effect of microplastics PAN polymer and/or Cu2+ pollution on the growth of chlorella pyrenoidosa. *Environ. pollut.* 265, 114985. doi: 10.1016/j.envpol.2020.114985

Liu, S., Chen, N., and Yang, X. (2022). Research progress on adsorption-desorption characteristics of organic pollutants by microplastics and their combined toxic effects. *Ecol. Environ. Sci.* 31 (3), 610–620. doi: 10.16258/j.cnki.1674-5906.2022.03.020

Li, N., Xiao, H. H., Shen, J. L., Qiao, X. M., Zhang, F. J., Zhang, W. B., et al. (2021). SELE gene as a characteristic prognostic biomarker of colorectal cancer. *J. Int. Med. Res.* 49 (4). doi: 10.1177/03000605211004386

Love, M. I., Huber, W., and Anders, S. (2014). Moderated estimation of fold change and dispersion for RNA-seq data with DESeq2. *Genome Biol.* 15 (12), 550. doi: 10.1186/s13059-014-0550-8

Mattsson, K., Johnson, E. V., Malmendal, A., Linse, S., Hansson, L. A., and Cedervall, T. (2017). Brain damage and behavioural disorders in fish induced by plastic nanoparticles delivered through the food chain. *Sci. Rep.* 7, 11452. doi: 10.1038/s41598-017-10813-0

Ma, Z. G., Yuan, Y. P., Zhang, X., Xu, S. C., Wang, S. S., and Tang, Q. Z. (2017). Piperine attenuates pathological cardiac fibrosis *Via* PPAR-gamma/AKT pathways. *EBioMedicine* 18, 179–187. doi: 10.1016/j.ebiom.2017.03.021

McEver, R. P. (2015). Selectins: initiators of leucocyte adhesion and signalling at the vascular wall. *Cardiovasc. Res.* 107 (3), 331–339. doi: 10.1093/cvr/cvv154

Md Amin, R., Sohaimi, E. S., Anuar, S. T., and Bachok, Z. (2020). Microplastic ingestion by zooplankton in terengganu coastal waters, southern south China Sea. *Mar. pollut. Bull.* 150, 110616. doi: 10.1016/j.marpolbul.2019.110616

Mohsen, M., Lin, C. G., Hamouda, H. I., Al-Zayat, A. M., and Yang, H. S. (2022). Plastic-associated microbial communities in aquaculture areas. *Front. Mar. Sci.* 9. doi: 10.3389/fmars.2022.895611

Mohsen, M., Wang, Q., Zhang, L., Sun, L., Lin, C., and Yang, H. (2019). Microplastic ingestion by the farmed sea cucumber apostichopus japonicus in China. *Environ. pollut.* 245, 1071–1078. doi: 10.1016/j.envpol.2018.11.083

Mohsen, M., Wang, Q., Zhang, L., Sun, L., Lin, C., and Yang, H. (2019a). Heavy metals in sediment, microplastic and sea cucumber apostichopus japonicus from farms in China. *Mar. pollut. Bull.* 143, 42–49. doi: 10.1016/j.marpolbul.2019.04.025

Mohsen, M., Zhang, L. B., Sun, L. N., Lin, C. G., Wang, Q., and Yang, H. S. (2020). Microplastic fibers transfer from the water to the internal fluid of the sea cucumber *Apostichopus japonicus*. *Environ. pollut.* 257, 113606. doi: 10.1016/j.envpol.2019.113606

Morales, A. I., Vicente-Sanchez, C., Jerkic, M., Santiago, J. M., Sanchez-Gonzalez, P. D., Perez-Barriocanal, F., et al. (2006). Effect of quercetin on metallothionein, nitric oxide synthases and cyclooxygenase-2 expression on experimental chronic cadmium nephrotoxicity in rats. *Toxicol. Appl. Pharmacol.* 210 (1-2), 128–135. doi: 10.1016/j.taap.2005.09.006

Parra-Luna, M., Martin-Pozo, L., Hidalgo, F., and Zafra-Gomez, A. (2020). Common sea urchin (Paracentrotus lividus) and sea cucumber of the genus holothuria as bioindicators of pollution in the study of chemical contaminants in aquatic media. a revision. *Ecol. Indic.* 113, 106185. doi: 10.1016/j.ecolind.2020.106185

Peng, G., Li, L. H., Liu, Y. B., Pu, J., Zhang, S. Y., Yu, J. H., et al. (2011). Oleate blocks palmitate-induced abnormal lipid distribution, endoplasmic reticulum expansion and stress, and insulin resistance in skeletal muscle. *Endocrinol.* 152 (6), 2206–2218. doi: 10.1210/en.2010-1369

Plee, T. A., and Pomory, C. M. (2020). Microplastics in sandy environments in the Florida keys and the panhandle of Florida, and the ingestion by sea cucumbers (Echinodermata: Holothuroidea) and sand dollars (Echinodermata: Echinoidea). *Mar. pollut. Bull.* 158, 111437. doi: 10.1016/j.marpolbul.2020.111437

Purcell, S. W., Lovatelli, A., and Pakoa, K. (2014). Constraints and solutions for managing pacific island sea cucumber fisheries with an ecosystem approach. *Mar. Policy* 45, 240–250. doi: 10.1016/j.marpol.2013.11.005

Qiao, R., Lu, K., Deng, Y., Ren, H., and Zhang, Y. (2019). Combined effects of polystyrene microplastics and natural organic matter on the accumulation and toxicity of copper in zebrafish. *Sci. Total. Environ.* 682, 128–137. doi: 10.1016/j.scitotenv.2019.05.163

Rainbow, P. S. (2003). Trace metal concentrations in aquatic invertebrates: why and so what? *Environ. pollut.* 121 (3), 489–489. doi: 10.1016/S0269-7491(02)00445-1

Roberts, D., Gebruk, A., Levin, V., and Manship, B. A. D. (2000). Feeding and digestive strategies in deposit-feeding holothurians. *Oceanogr. Mar. Biol.* 38, 257–310.

Robinson, M. D., McCarthy, D. J., and Smyth, G. K. (2010). edgeR: a bioconductor package for differential expression analysis of digital gene expression data. *Bioinformatics* 26 (1), 139–140. doi: 10.1093/bioinformatics/btp616

Roussiez, V., Ludwig, W., Monaco, A., Probst, J. L., Bouloubassi, I., Buscail, R., et al. (2006). Sources and sinks of sediment-bound contaminants in the gulf of lions (NW Mediterranean sea): A multi-tracer approach. *Cont. Shelf Res.* 26 (16), 1843–1857. doi: 10.1016/j.csr.2006.04.010

Roy, D., Grenier, D., Segura, M., Mathieu-Denoncourt, A., and Gottschalk, M. (2016). Recruitment of factor h to the streptococcus suis cell surface is multifactorial. *Pathog.* 5 (3), 47. doi: 10.3390/pathogens5030047

Ru, X. S., Zhang, L. B., Li, X. N., Liu, S. L., and Yang, H. S. (2019). Development strategies for the sea cucumber industry in China. *J. Oceanol. Limnol.* 37 (1), 300–312. doi: 10.1007/s00343-019-7344-5

Salaun, B., Rorner, P., and Lebecque, S. (2007). Toll-like receptors' two-edged sword: when immunity meets apoptosis. *Eur. J. Immunol.* 37 (12), 3311–3318. doi: 10.1002/eji.200737744

Sass, W., Dreyer, H. P., and Seifert, J. (1990). RAPID INSORPTION OF SMALL PARTICLES IN THE GUT. *Am. J. Gastroenterol.* 85 (3), 255–260.

Schmittgen, T. D., and Livak, K. J. (2008). Analyzing real-time PCR data by the comparative C(T) method. *J. Nat. Protoc.* 3 (6), 1101–1108. doi: 10.1038/nprot.2008.73

Schulert, G. S., and Cron, R. Q. (2020). The genetics of macrophage activation syndrome. *Genes Immun.* 21 (3), 169–181. doi: 10.1038/s41435-020-0098-4

Sharma, S., and Chatterjee, S. (2017). Microplastic pollution, a threat to marine ecosystem and human health: a short review. *Environ. Sci. pollut. Res.* 24 (27), 21530–21547. doi: 10.1007/s11356-017-9910-8

Shibolet, O., and Podolsky, D. K. (2007). TLRs in the gut. IV. negative regulation of toll-like receptors and intestinal homeostasis: addition by subtraction. *Am. J. Physiol-Gastr. L.* 292 (6), G1469–G1473. doi: 10.1152/ajpgi.00531.2006

Taha, Z. D., Md Amin, R., Anuar, S. T., Nasser, A. A. A., and Sohaimi, E. S. (2021). Microplastics in seawater and zooplankton: A case study from terengganu estuary and offshore waters, Malaysia. *Sci. Total. Environ.* 786, 147466. doi: 10.1016/j.scitotenv.2021.147466

Taylor, M. L., Gwinnett, C., Robinson, L. F., and Woodall, L. C. (2016). Plastic microfibre ingestion by deep-sea organisms. *Sci. Rep.* 6, 33997. doi: 10.1038/srep33997

Thompson, R. C., Olsen, Y., Mitchell, R. P., Davis, A., Rowland, S. J., John, A. W., et al. (2004). Lost at sea: where is all the plastic? *Science* 304 (5672), 838. doi: 10.1126/science.1094559

Tomasik, J., and Basak, G. W. (2022). Inflammasomes-new contributors to blood diseases. *Int. J. Mol. Sci.* 23 (15), 8129. doi: 10.3390/ijms23158129

Tracz-Gaszewska, Z., and Dobrzyn, P. (2019). Stearoyl-CoA desaturase 1 as a therapeutic target for the treatment of cancer. *Cancers* 11 (7), 948. doi: 10.3390/cancers11070948

Vedolin, M. C., Teophilo, C. Y. S., Turra, A., and Figueira, R. C. L. (2018). Spatial variability in the concentrations of metals in beached microplastics. *Mar. pollut. Bull.* 129 (2), 487–493. doi: 10.1016/j.marpolbul.2017.10.019

Wang, L. C., Brown, J. R., Varki, A., and Esko, J. D. (2002). Heparin's anti-inflammatory effects require glucosamine 6-o-sulfation and are mediated by blockade of l- and p-selectins. *J. Clin. Invest.* 110 (1), 127–136. doi: 10.1172/JCI200214996

Wang, Q. J., Zhang, Y., Wangjin, X. X., Wang, Y. L., Meng, G. H., and Chen, Y. H. (2020). The adsorption behavior of metals in aqueous solution by microplastics effected by UV radiation. *J. Environ. Sci.* 87, 272–280. doi: 10.1016/j.jes.2019.07.006

Welden, N. A. C., and Cowie, P. R. (2016). Long-term microplastic retention causes reduced body condition in the langoustine, nephrops norvegicus. *Environ. pollut.* 218, 895–900. doi: 10.1016/j.envpol.2016.08.020

Wenli, M., Lan, W., Yongji, H., and Yao, Y. (2008). Tissue-specific cadmium and metallothionein levels in freshwater crab sinopotamon henanense during acute exposure to waterborne cadmium. *Environ. Toxicol.* 23 (3), 393–400. doi: 10.1002/tox.20339

Wright, S. L., and Kelly, F. J. (2017). Plastic and human health: A micro issue? *Environ. Sci. Technol.* 51 (12), 6634–6647. doi: 10.1021/acs.est.7b00423

Wright, S. L., Thompson, R. C., and Galloway, T. S. (2013). The physical impacts of microplastics on marine organisms: A review. *Environ. pollut.* 178, 483–492. doi: 10.1016/j.envpol.2013.02.031

Wu, Z., Dong, Y., Liu, R., Liu, L., Gao, J., Song, W., et al. (2022). Assessment of heavy metal contamination in surface sediments off the dongying coast, bohai Sea. *Mar. pollut. Bull.* 180, 113826. doi: 10.1016/j.marpolbul.2022.113826

Yokoyama, H. (2013). Growth and food source of the sea cucumber apostichopus japonicus cultured below fish cages - potential for integrated multi-trophic aquaculture. *Aquaculture* 372, 28–38. doi: 10.1016/j.aquaculture.2012.10.022

Zantis, L. J., Carroll, E. L., Nelms, S. E., and Bosker, T. (2021). Marine mammals and microplastics: A systematic review and call for standardisation. *Environ. pollut.* 269, 116142. doi: 10.1016/j.envpol.2020.116142

Zettler, E. R., Mincer, T. J., and Amaral-Zettler, L. A. (2013). Life in the "Plastisphere": Microbial communities on plastic marine debris. *Environ. Sci. Technol.* 47 (13), 7137–7146. doi: 10.1021/es401288x

Zhang, G. L., and Ghosh, S. (2002). Negative regulation of toll-like receptor-mediated signaling by tollip. *J. Biol. Chem.* 277 (9), 7059–7065. doi: 10.1074/jbc.M109537200

Zhang, S. W., Han, B., Sun, Y. H., and Wang, F. Y. (2020). Microplastics influence the adsorption and desorption characteristics of cd in an agricultural soil. *J. Hazard. Mater.* 388, 121775. doi: 10.1016/j.jhazmat.2019.121775

Zhang, S. Y., Ru, X. S., Su, F., Liang, W. K., Zhang, L. B., and Yang, H. S. (2022). Use of quantitative real-time PCR to select reference genes in the testis and ovary of apostichopus japonicus during the breeding period. *Aquacult. Rep.* 22, 101010. doi: 10.1016/j.aqrep.2022.101010

Zhang, T., Sun, Y., Song, K., Du, W., Huang, W., Gu, Z., et al. (2021). Microplastics in different tissues of wild crabs at three important fishing grounds in China. *Chemosphere* 271, 129479. doi: 10.1016/j.chemosphere.2020.129479

frontiers | Frontiers in Marine Science

TYPE Original Research
PUBLISHED 03 February 2023
DOI 10.3389/fmars.2023.1089482

OPEN ACCESS

EDITED BY
Juan D. Gaitan-Espitia,
The University of Hong Kong, Hong Kong SAR China

REVIEWED BY
Petra Heinz,
University of Vienna, Austria
Wojciech Majewski,
Institute of Paleobiology (PAS), Poland

*CORRESPONDENCE
Yanli Lei
leiyanli@qdio.ac.cn
Tiegang Li
tgli@fio.org.cn

SPECIALTY SECTION
This article was submitted to Global Change and the Future Ocean, a section of the journal Frontiers in Marine Science

RECEIVED 04 November 2022
ACCEPTED 24 January 2023
PUBLISHED 03 February 2023

CITATION
Li Q, Lei Y, Li H and Li T (2023) Distinct responses of abundant and rare foraminifera to environmental variables in the Antarctic region revealed by DNA metabarcoding.
Front. Mar. Sci. 10:1089482.
doi: 10.3389/fmars.2023.1089482

Distinct responses of abundant and rare foraminifera to environmental variables in the Antarctic region revealed by DNA metabarcoding

Qingxia Li[1], Yanli Lei[1,3,4,5]*, Haotian Li[1] and Tiegang Li[2,4]*

[1]Laboratory of Marine Organism Taxonomy and Phylogeny, Center for Ocean Mega-Science, Institute of Oceanology, Chinese Academy of Sciences, Qingdao, China, [2]Key Laboratory of Marine Sedimentology and Environmental Geology, First Institute of Oceanography, Ministry of Natural Resources, Qingdao, China, [3]Southern Marine Science and Engineering Guangdong Laboratory (Zhuhai), Zhuhai, China, [4]Pilot National Laboratory for Marine Science and Technology (Qingdao), Qingdao, China, [5]University of Chinese Academy of Sciences, Beijing, China

The Antarctic region plays a key role in regulating the Earth's climate and contains a unique record of environmental change. Foraminifera, a group of shell-bearing protists, are widely used as paleoenvironmental proxies. However, core-based reconstructions of Antarctic paleoenvironments are often hindered by the lack of foraminiferal fossil record. Foraminiferal ancient DNA provides new avenues for understanding environmental change, but the correlation between molecular ecological features of foraminifera and environmental conditions remains poorly understood. Here, we obtained surface sediment samples from the Southern Ocean at water depths ranging from 50 to 4399 m and measured eight environmental variables. We generated a DNA metabarcoding dataset of foraminifera and presented the first assessment of relationships between foraminiferal molecular diversity and environmental variables in the Antarctic region. The results showed that the alpha diversity of whole community and abundant subcommunity was positively correlated with water depth and negatively correlated with temperature, chlorophyll a and pheophytin a, while the alpha diversity of rare subcommunity had no linear correlation with the above environmental variables. Both rare and abundant foraminiferal subcommunities exhibited distance-decay relationships, but only the beta diversity of rare subcommunity showed a significant positive correlation with water depth. This study reveals contrasting biogeographical patterns of abundant and rare foraminifera and their different correlations with Antarctic environmental variables, holding promise to provide more proxies for reconstructing past environments using foraminiferal ancient DNA and more information for predicting the impact of future environmental changes on polar biodiversity.

KEYWORDS

foraminifera, polar region, environmental change, paleoenvironmental reconstruction, biogeographical pattern

1 Introduction

The Antarctic region contains multiple extreme environmental conditions, including low temperatures, freeze-thaw cycles, ultra-oligotrophic conditions, wind abrasion and high radiation levels (Rosa et al., 2020). Its surrounding ocean current, the Antarctic Circumpolar Current, is the largest current in the world and interacts with the Pacific, Atlantic, and Indian Oceans through deep-water circulations (Barker and Thomas, 2004). Such a unique environment in the Antarctic region shapes its diverse and unusual marine fauna (Griffiths, 2010) and provides an exceptional field laboratory for studying the relationship between biological communities and environmental variability. However, research on Antarctic biodiversity has been largely limited by the relative inaccessibility of the region due to its remoteness, thick ice sheets and harsh weather conditions (Griffiths, 2010). The Southern Ocean seafloor covers an area of 34.8 million km^2, of which over 85% are deeper than 1000 m (Clarke and Johnston, 2003), but most benthic samples taken for investigations are from depths of less than 500 m (Griffiths, 2010). Compared with its shallow-water benthic communities, little is known about benthic biodiversity in the vast deep-sea area of the Southern Ocean (Janosik and Halanych, 2010; Brandt and Gutt, 2011).

Foraminifera, a group of shell-bearing protists, are significant components of the marine ecosystem in the Antarctic region (Mikhalevich, 2004). They can rapidly respond to environmental changes because of their unicellular organization and relatively short life cycles, and their hard shells can be preserved as fossils in marine sediments across geological timescales (Goldstein, 1999; Bouchet et al., 2012). For these reasons, foraminifera become efficient proxies for reconstructing past environmental conditions (Gooday, 2003). The study of foraminifera in the Antarctic region can date back to the nineteenth century, but ecological investigations of foraminifera are mostly based on the morphological characters of their calcareous, agglutinated, or organic tests (Majewski, 2010). Molecular techniques offer an alternative approach to assess foraminiferal diversity in marine environments (Pawlowski et al., 2002). Habura et al. (2004) revealed unexpected foraminiferal diversity in the sediment samples collected from shallow Antarctic stations using DNA sequencing method. With the advent of ultra-deep sequencing technology, Lecroq et al. (2011) assessed foraminiferal richness using Illumina sequencing technology and unveiled hidden diversity of early monothalamous lineage in deep-sea sediments of the Southern Ocean. These findings revealed the immense richness of unexplored foraminiferal phylotypes and improved understanding of foraminiferal diversity in the Antarctic region.

The application of foraminifera in previous paleoenvironmental studies was mainly based on their fossil tests. However, most calcareous foraminifera in the Antarctic region are limited to relatively shallow water depths, whereas below the carbonate compensation depth (CCD), foraminiferal assemblages are dominated by agglutinated taxa, which are poorly preserved in fossil record and are of little use for paleoenvironmental studies (Majewski et al., 2018).

Ancient DNA (aDNA) provides new ways to reconstruct past environmental changes using foraminifera (Pawłowska et al., 2016). Numerous studies report the preservation of foraminiferal aDNA in marine sediments over thousands of years (Lejzerowicz et al., 2013; Pawłowska et al., 2014; Szczuciński et al., 2016). Recently, Pawłowska et al. (2020) retrieved aDNA sequences of the planktonic foraminifera *Neogloboquadrina pachyderma* from a 140,000-year-old sediment core and found that the genomic variations of *N. pachyderma* could reflect the palaeoceanographic changes. Additionally, foraminiferal aDNA has been shown to be a useful complementary indicator of palaeotsunami deposits, especially in the absence of foraminiferal tests (Szczuciński et al., 2016). However, our knowledge of the biogeographical patterns and driving mechanisms of foraminifera and the environmental information documented in foraminiferal DNA data remains insufficient.

Biological communities are normally composed of abundant and rare species (Logares et al., 2014), but previous molecular ecological studies on foraminifera have mostly focused on the whole community and rarely compared the ecological properties of abundant and rare taxa. Increasing studies have shown that abundant and rare subcommunities tend to have contrasting biogeographical patterns and different environmental responses, which are seen in both prokaryotes and eukaryotes, such as marine microeukaryotes (Logares et al., 2014), pelagic bacteria (Liu et al., 2015), planktic eukaryotes (Xue et al., 2018), benthic bacteria (Jiao et al., 2017; Hou et al., 2020). In-depth analysis of the biogeographical patterns of abundant and rare foraminifera and their responses to environmental variables has the potential to provide more accurate proxies for future reconstruction of paleoenvironments using foraminiferal ancient DNA.

In this study, we collected surface sediment samples from ten sites between 50 to 4399 m in the Southern Ocean and obtained a DNA metabarcoding dataset of foraminifera using high-throughput sequencing technology. The specific goals of this study are listed as follows: (1) to analyze the ecological characteristics of foraminiferal assemblages in the Antarctic region based on DNA data; (2) to compare and determine the biogeographical patterns and driving mechanisms of abundant and rare foraminiferal subcommunities in the Antarctic region; (3) to separately assess the correlations of whole community, abundant and rare subcommunities with multiple environmental variables in the Antarctic region.

2 Materials and methods

2.1 Study sites and sediment collection

We collected sediment samples from ten sites between 50 to 4399 m in the Southern Ocean based on the 34th Chinese Antarctic Scientific Expedition from January to February 2018 onboard the R/V "Xiangyanghong 01" (Table S1). The study areas are in the convergence region of the Weddell Sea and the Scotia Sea, close to the Antarctic Peninsula (Figure 1). Four sites (ANT01 to ANT04) with water depths ranging from 50 m to 340 m are situated on the South Orkney Plateau. Three sites (ANT05, ANT06 and ANT07) with water depths ranging from 440 m to 1052 m are close to the King George Island, the largest island of the South Shetland Islands archipelago. ANT08 (2551 m) and ANT09 (3389) belong to the Weddell Sea, near the east side of the South Orkney Plateau.

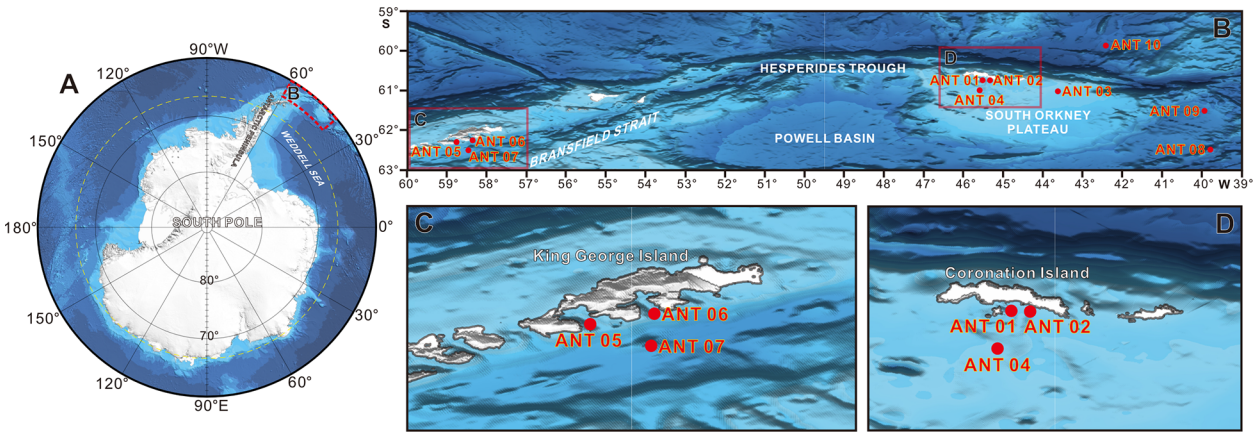

FIGURE 1
Location of the ten sampling sites in the Antarctic region.

ANT10 is the deepest of all study sites, with a water depth of over 4300 m, and it is close to the north of the South Orkney Plateau, belonging to the Scotia Sea. At each site, one sediment sample was collected using a box corer (0.5 × 0.5 × 0.84 m^3), and undisturbed 0-1 cm surface sediments were recovered from the box corer with a clean spoon. We took three subsamples from one sediment sample and separately transferred them to a sealable polyethylene bag. All samples were frozen at −80° C on board until further processing.

2.2 Measurement of physicochemical properties

Eight environmental variables were measured for each sample, including water depth, temperature, salinity, chlorophyll a (Chl a), pheophytin a (Pheo a), total nitrogen (TN), total carbon (TC) and total organic carbon (TOC). The water depth, *in situ* temperature and salinity were measured using a shipborne Sea-Bird Electronics 911plus Conductivity-Temperature-Depth (CTD) profiler. The obtained CTD data were processed using the standard processing procedure of SBE Company. The concentrations of Chl a and Pheo a in sediment samples were analyzed using a Turner Designs (Model II) fluorometer (Trilogy, USA). Total nitrogen, total carbon and total organic carbon in the samples were determined by a vario MACRO cube elemental analyzer (Elementar, Germany).

2.3 DNA extraction, PCR amplification and illumina sequencing

Total environmental DNA (eDNA) was extracted from ca. 0.25 g sediment using DNeasy PowerSoil kit (QIAGEN, Germany) and three eDNA extracts were required for each subsample. The foraminiferal-specific 37F hypervariable region of 18S rRNA gene was amplified using the foraminiferal-specific primers s14F3 and s17 following the amplification reaction volume and PCR program described by Li et al. (2020). For Illumina sequencing, tagged forward and reverse primers with 6-nt sequences appended at their 5′-end were used to multiplex multiple samples into a single library. A unique combination of tagged primers was designed for each subsample. PCR products were detected by agarose gel electrophoresis and purified with E.Z.N.A Gel Extraction Kit (Omega Bio-Tek, USA). The sequencing libraries were prepared with TruSeq DNA PCR-Free Sample Preparation Kit (Illumina, USA) following the manufacturer's protocol and assessed using the Agilent Bioanalyzer 2100 system. The Illumina HiSeq 2500 platform was used to sequence libraries and generated 250 bp paired-end reads. The datasets presented in this study can be found in online repositories. The names of the repository/repositories and accession number(s) can be found below: BioProject, PRJNA908891.

2.4 Quality control and processing of sequencing data

After we obtained raw paired-end reads from the Illumina sequencing platform, we performed data processing as described by Li et al. (2020). We demultiplexed raw paired-end reads to samples based on their unique barcodes. Low-quality paired-end reads were discarded, and the barcode and primer sequences of the remaining reads were cut off. We merged paired-end reads using FLASH (Magoč and Salzberg, 2011), and filtered the spliced reads using QIIME (Caporaso et al., 2010) according to its quality-controlled process. Denoising on the retained reads was performed using the UNOISE3 algorithm in USEARCH (Edgar, 2016) and the correct biological sequences (representative sequences of OTUs) were picked out. All effective reads were clustered into OTUs with the otutab command in USEARCH according to the representative sequences of OTUs, and taxonomic assignment of OTUs was performed based on the Protist Ribosomal Reference (PR^2) database (Guillou et al., 2013) using BLAST. Specific parameters and more detailed information on data processing can be found in Li et al. (2020). Planktonic foraminiferal OTUs and the OTUs that could not be assigned to foraminifera were discarded from the dataset. The OTUs that were assigned to foraminifera but had an identity value below 90% were placed into the group of Unknown Foram. The retained OTUs were classified as abundant or rare in relation to their relative abundance in all sites. The OTUs occupied >0.1% of total reads were defined as "abundant taxa" (Logares et al., 2014; Liu et al., 2015; Wang et al., 2021), those with

reads proportions <0.01% were defined as "rare taxa" (Zhao et al., 2021), and the remaining OTUs were defined as "intermediate taxa".

2.5 Statistical analysis

Proportions of OTUs and reads belonging to different taxonomic groups at the class level (Figure 2) and taxonomic composition at the order level in the ten sites (Figure S2) were visualized using the R package ggplot2 (Wickham, 2016). The variation trends of the seven environmental factors along water depth were shown in Figure 3, and their correlations with water depth were analyzed by the Spearman's Rank Correlation Test. The phylotype richness was represented by the number of observed OTUs. Shannon index and phylotype richness were selected as indicators of alpha diversity (α-diversity) referring to previous studies (Zeng et al., 2019; Li et al., 2020; Kang et al., 2021). The correlations between Shannon index and phylotype richness and water depth (Figure 4A) and temperature (Figure 4B) were tested by Pearson correlation statistic and visualized using OriginPro 9.0 software packages (OriginLab Corporation, USA). Before calculating two α-diversity indices, we normalized the data of each sample corresponding to the sample with the least reads. A mantel test was conducted using the R package vegan to determine the relationship between the Bray-Curtis dissimilarity and water depth, geographic distance and environmental factors (Chl a and Pheo a) (Figure 5). Variation partitioning analysis (VPA) was used to evaluate the proportion of community variation explained by water depth and temperature in abundant and rare subcommunities (Figure S3). Beta diversity (β-diversity) of abundant and rare subcommunities was partitioned into two components: nestedness and species turnover by applying Baselga's approach to assess their contribution to community dissimilarities (Table S3).

3 Results

3.1 Overview of sequencing data

In our study, a total of 898,437 effective reads were clustered into 1322 initial OTUs. After taxonomic assignment, 35 OTUs that could not find a hit in the PR^2 database and 14 OTUs which were attributed to planktonic foraminifera were removed (Table S2). Finally, 1273 OTUs representing 894,160 reads were retained for downstream analysis. Among the 1273 OTUs that were assigned to benthic foraminifera, 410 OTUs had a sequence similarity of less than 90% to the reference sequences in the PR^2 database and were placed to the group of Unknown Foram, 471 OTUs were assigned to the paraphyletic clade monothalamiids, 344 OTUs were assigned to the class Globothalamea, 35 OTUs were assigned to the class Tubothalamea, and 13 OTUs were a part of Foraminifera-X.

3.2 General composition and distribution patterns of foraminiferal assemblages

Among the 1273 OTUs, 121, 541 and 611 OTUs were placed to the abundant taxa, intermediate taxa and rare taxa, representing 724650, 139798 and 29712 reads, respectively. The abundant taxa

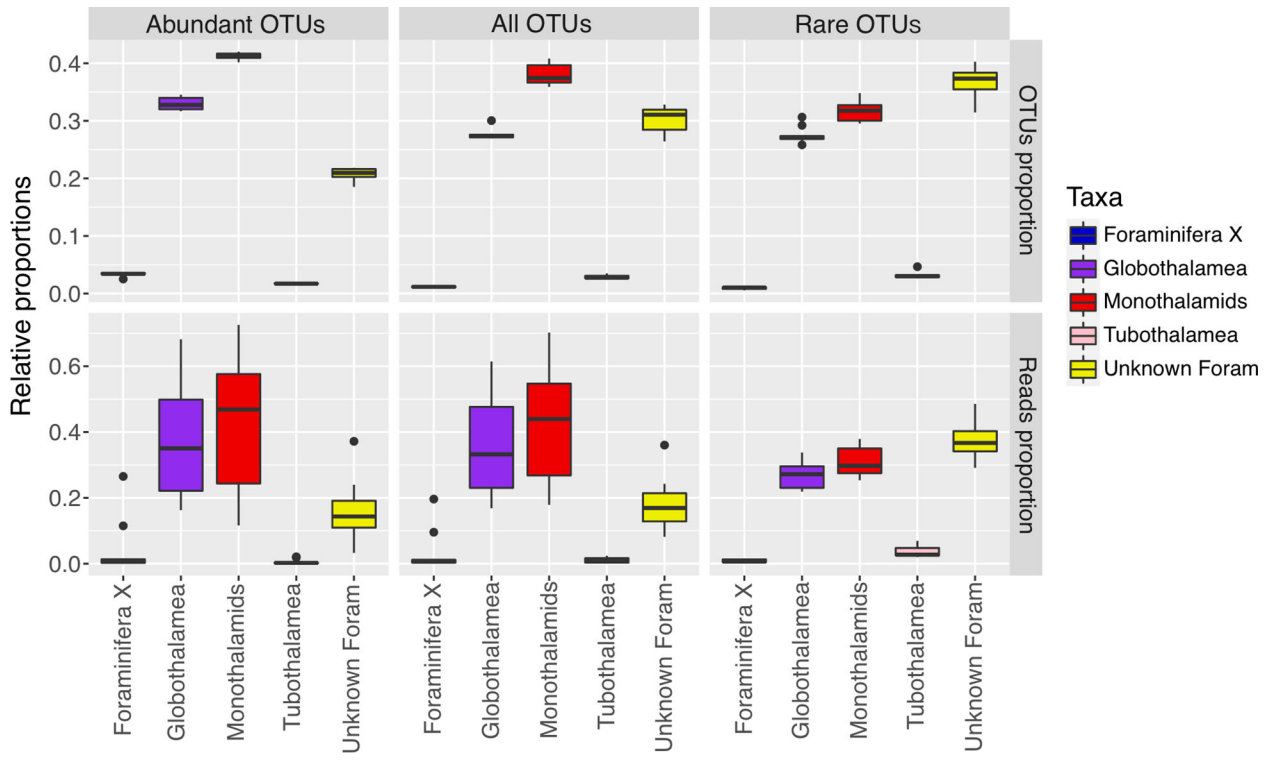

FIGURE 2
Proportions of OTUs and reads assigned to different taxonomic groups at the class level in abundant, rare and all taxa.

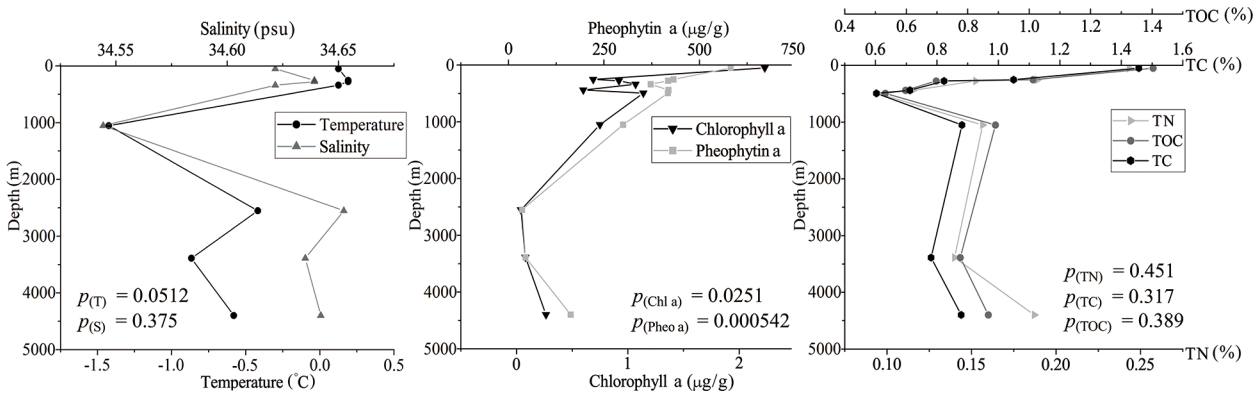

FIGURE 3
Profiles of bottom seawater temperature, salinity, and concentrations of chlorophyll a, pheophytin a, total nitrogen, total carbon and total organic carbon in the sediment samples. The correlations between the seven environmental variables with water depth were analyzed by the Spearman's Rank Correlation Test. The results of statistical significance tests are shown at the bottom of each panel.

accounted for 9.5% of all OTUs but occupied 81.0% of reads. Conversely, the rare taxa constituted the highest proportion of OTUs (48.0%), while their reads contributed to only 3.3% of total reads (Figure S1). Abundant and rare foraminiferal taxa exhibited distinct compositional differences at the class level (Figure 2). For abundant taxa, soft-shelled monothalamous foraminifera occupied the highest proportion of both OTUs (41%) and reads (42%), with only 20% of OTUs and 16% of reads belonging to the group of Unknown Foram. However, for rare taxa, 37% of OTUs and 37% of reads were placed to the group of Unknown Foram.

Abundant and rare foraminiferal subcommunities showed different distribution patterns. For abundant subcommunity, the ten sites had obviously different taxonomic composition at the order level (Figure S2). In ANT01, ANT04, ANT05, ANT08 and ANT09, monothalamiids accounted for the highest proportion of reads (over 55%), while in ANT02, ANT03, ANT06 and ANT10, most reads were assigned to the order Rotaliida. For rare subcommunity, the ten sites showed similar taxonomic composition at the order level. The Unknown Foram occupied the highest proportion of reads (37%), followed by monothalamous foraminifera (31%), and only about 18% of reads were assigned to the order Rotaliida in rare taxa.

3.3 Correlations between foraminiferal diversity and environmental variables

In our study area, the water temperature varied between -1.43°C and 0.20°C, and the salinity varied between 34.54 psu and 34.64 psu. The water temperature and salinity showed complex and similar trends along water depth from 50 to 4399 m, reaching the lowest value at the depth of about 1000 m. The concentrations of sediment Chl a and Pheo a were negatively correlated with water depth. Concentrations of TN, TC and TOC first decreased sharply with water depth from 50 m to 495 m, and then slowly increased with water depth (Figure 3).

Alpha diversity of foraminiferal communities was estimated by phylotype richness and Shannon index. For whole community and abundant subcommunity, their two α-diversity indices had positive correlations with water depth (Figure 4A) and negative correlations with temperature (Figure 4B). In addition, the correlations between the two α-diversity indices of whole community and water depth and temperature were significant ($p < 0.01$), whilst only phylotype richness of abundant subcommunity showed significant correlations with the above two environmental variables ($p < 0.01$). No linear correlations were observed between the two α-diversity indices of rare subcommunity with water depth and temperature. Except for water depth and temperature, Phylotype richness and Shannon index of whole community and abundant subcommunity were also negatively correlated with Chl a and Pheo a (Table 1). There was no linear correlation between foraminiferal alpha diversity and TN, TOC, and TC (Table 1).

3.4 Effects of environmental variables on foraminiferal community structure

The results of mantel test showed that the beta diversity of whole community, abundant and rare subcommunities had different relationships with geographic distance, water depth, and environmental factors (Figure 5). The Bray-Curtis dissimilarity of whole community was positively correlated with water depth (R = 0.207, $p = 0.017$), geographic distance (R = 0.1638, $p < 0.01$) and environmental factors (R = 0.2888, $p < 0.01$). The Bray-Curtis dissimilarity of abundant subcommunity was significantly correlated with environmental factors (R = 0.2636, $p < 0.01$), weakly correlated with geographic distance (R = 0.1444, $p = 0.023$), but not correlated with water depth (R = 0.1422, $p = 0.064$). The Bray-Curtis dissimilarity of rare subcommunity had significant correlations with water depth (R = 0.3087, $p < 0.01$) and environmental factors (R = 0.2115, $p < 0.01$), and had a weak correlation with geographic distance (R = 0.1134, $p = 0.032$).

The results of VPA showed that water depth and temperature had a greater impact on the abundant subcommunity than on the rare subcommunity (Figure S3). More than 7% of the community variations in the abundant subcommunity could be explained by water depth and temperature, while only 2.4% of community variations in the rare subcommunity could be explained by these two environmental variables. Water depth explained 2.3% and 0.2%

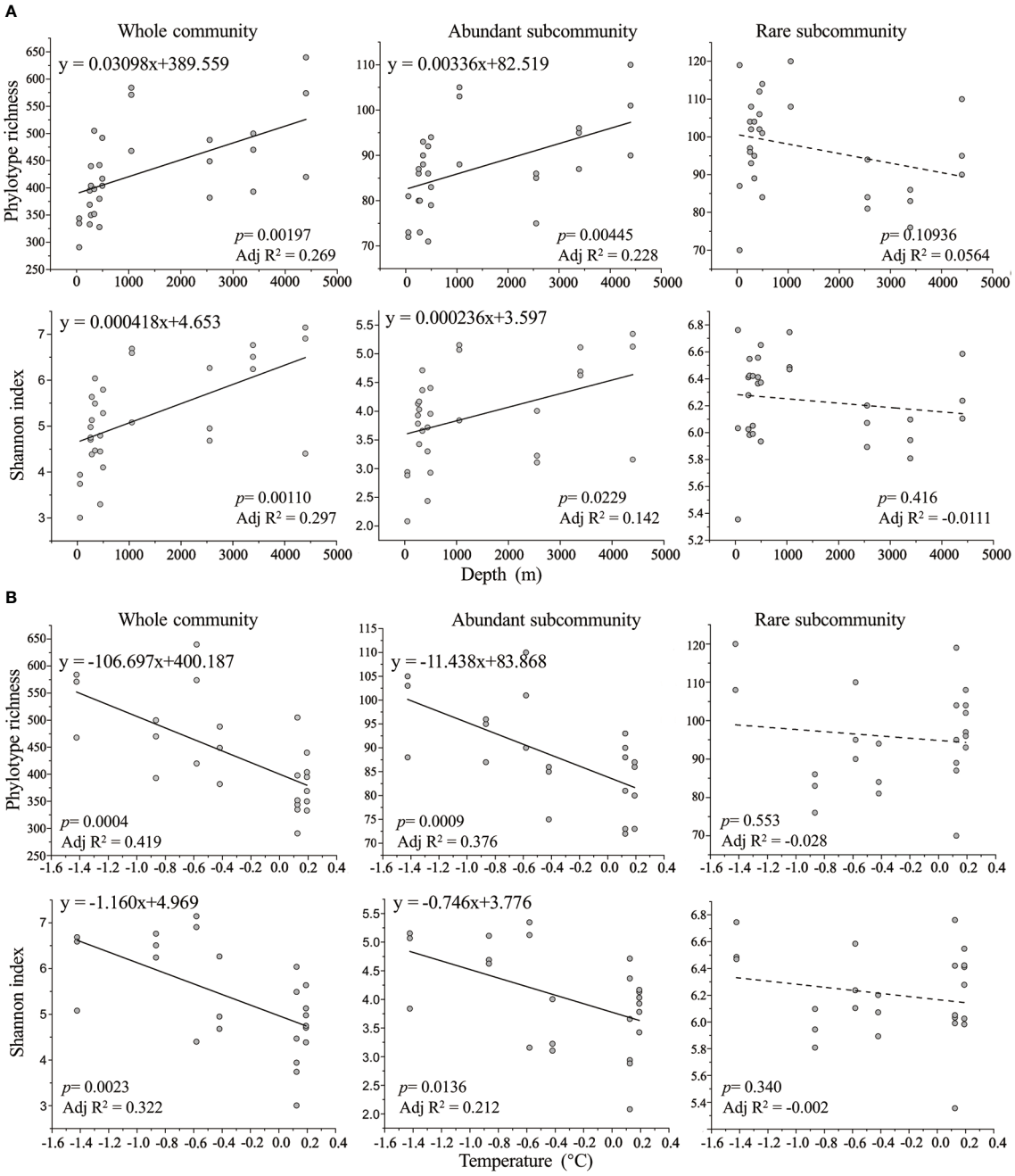

FIGURE 4
The correlations between foraminiferal alpha diversity estimated by phylotype richness and Shannon index and water depth **(A)** and temperature **(B)**.

of the community variations for abundant subcommunity and rare subcommunity, respectively. Temperature contributed 1.9% and 0.9% of the community variations for abundant subcommunity and rare subcommunity, respectively. Partitioning of β-diversity showed that the β-diversity (Beta.SOR) of abundant and rare subcommunities was shaped by different components (Table S3). The contribution of nestedness (Beta.NES = 0.4747) was two times more than that of spatial turnover (Beta.SIM = 0.2470) to β-diversity in abundant subcommunity, while nestedness component accounted for less than 1% of β-diversity for rare subcommunity and spatial turnover accounted for a great percentage (98.06%).

4 Discussion

4.1 Contrasting biogeographical patterns of abundant and rare foraminiferal subcommunities

Numerous studies have shown that abundant and rare bacterial subcommunities differ remarkably in diversity (Mo et al., 2018), community composition (Wang et al., 2020), distribution patterns (Jiao et al., 2017), driving mechanisms (Liu et al., 2015) and relationships with key environmental factors (Hou et al., 2020;

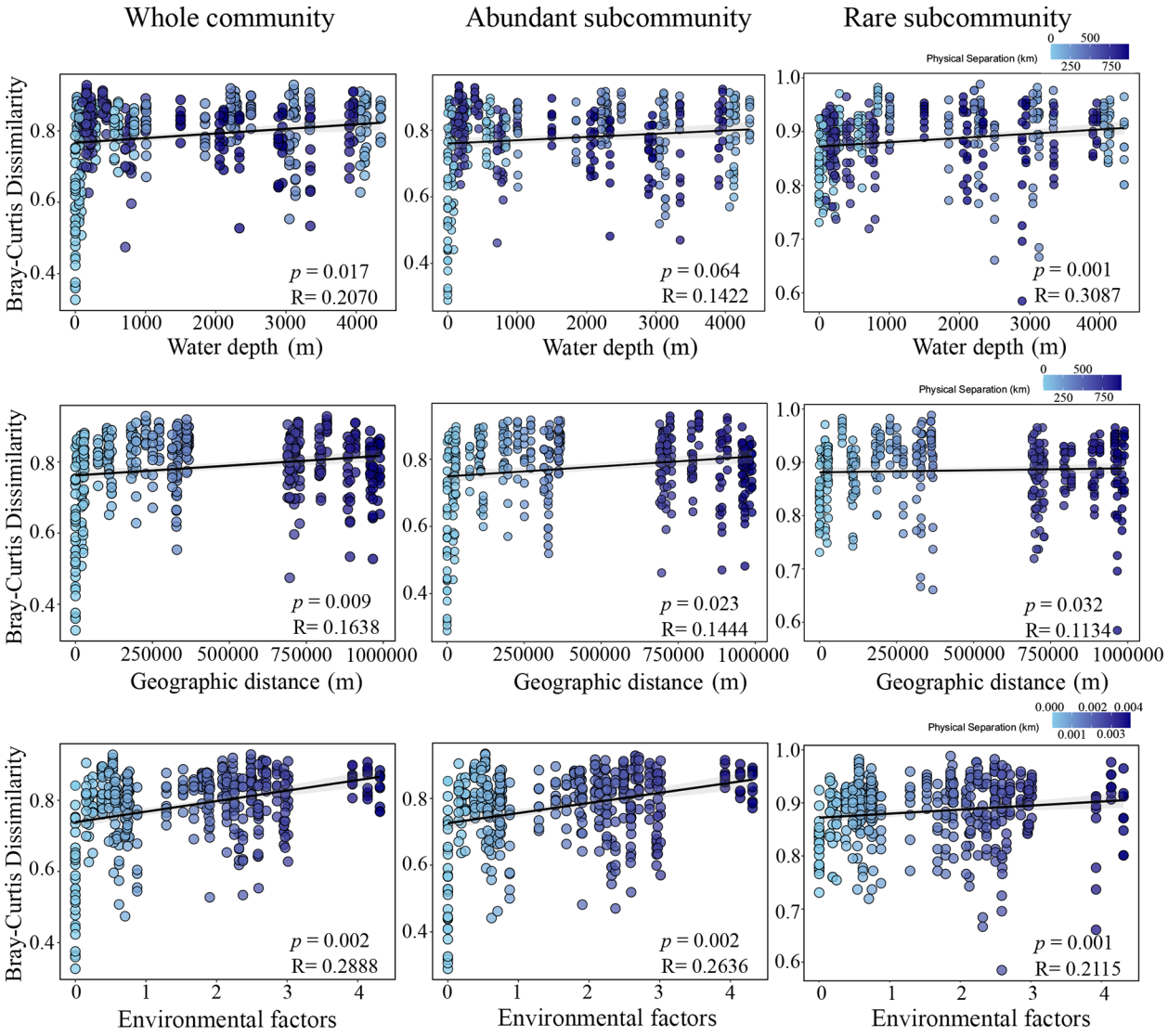

FIGURE 5
Mantel test results between Bray-Curtis dissimilarity of whole community, abundant and rare subcommunities with water depth, geographic distance and environmental factors (chlorophyll a and pheophytin a).

Wang et al., 2021). Likewise, some studies have also confirmed the differences between abundant and rare eukaryotic subcommunities in structuring patterns (Logares et al., 2014) and ecological mechanisms (Xue et al., 2018).

Although the ecological study of foraminifera has a long history, the associated differences in diversity patterns and driving forces between abundant and rare foraminifera are still unclear. In this study, we compared the molecular diversity, taxonomic composition, distribution patterns and driving mechanisms of abundant and rare foraminifera in the Antarctic region based on a DNA metabarcoding dataset for the first time. Our results showed that the abundant taxa accounted for 9.5% of all OTUs representing 81.0% of all reads and the rare taxa accounted for 48.0% of all OTUs representing 3.3% of all reads (Figure S1), which indicated that rare taxa comprised a majority of foraminiferal community diversity in the Antarctic region. Abundant and rare foraminiferal subcommunities exhibited distinct differences in taxonomic composition, with the former dominated by soft-shelled monothalamous foraminifera and the latter by unclassified foraminifera (Figure 2), suggesting that a large proportion of rare foraminifera remain unexplored or that their DNA sequences are highly divergent from the reference sequences in the PR^2 database. This result is not surprising since the Antarctic region is known for having a high rate of new species discoveries (Kaiser et al., 2009; Holzmann et al., 2022) and foraminifera are notorious for their high intragenomic variability (Weber and Pawlowski, 2014; Majewski et al., 2021). We also found that abundant and rare foraminiferal subcommunities had obviously different distribution patterns in the Antarctic region. Abundant foraminiferal taxa were more unevenly distributed across all sites than the rare taxa at the order level (Figure S2). Furthermore, our findings suggested that the mechanisms shaping β-diversity of abundant and rare foraminiferal subcommunities were different (Table S3). For abundant subcommunity, its β-diversity was driven by nestedness component, which is normally caused by species loss because of passive sampling, selective extinction, selective colonization, or habitat nestedness (Wang et al., 2010). However,

TABLE 1 Pearson correlations between two α-diversity indices (phylotype richness and Shannon index) and eight environmental variables.

	Phylotype richness						Shannon index					
	All		Abundant		Rare		All		Abundant		Rare	
	R	*p*	R	*p*	R	*p*	R	*p*	R	*p*	R	*p*
Depth	0.542	**0.002***	0.505	**0.004***	-0.298	0.109	0.567	**0.001***	0.414	**0.023**	-0.154	0.416
T	-0.667	**0.0004***	-0.635	**0.0009***	-0.128	0.553	-0.593	**0.002***	-0.497	**0.014**	-0.204	0.340
Salinity	-0.326	0.120	0.363	0.081	-0.480	**0.018**	-0.158	0.462	-0.242	0.254	-0.388	0.061
Chl a	-0.456	**0.011**	-0.411	**0.024**	0.127	0.504	-0.561	**0.001***	-0.454	**0.012**	-0.002	0.992
Pheo a	-0.502	**0.005***	-0.424	**0.020**	0.339	0.067	-0.617	**0.0003***	-0.441	**0.015**	0.181	0.339
TN	-0.187	0.380	-0.097	0.652	-0.135	0.530	-0.217	0.309	-0.189	0.375	-0.192	0.369
TOC	-0.272	0.198	-0.166	0.440	-0.173	0.419	-0.284	0.179	-0.259	0.221	-0.236	0.268
TC	-0.384	0.064	-0.294	0.163	-0.154	0.473	-0.402	0.051	-0.373	0.073	-0.230	0.280

* indicates significant correlations at 0.01 level.
The bold value indicates a correlation at 0.05 level.

the β-diversity of rare subcommunity was driven by spatial turnover, which usually results from species replacement because of environmental sorting or spatial and historical constraints (Baselga, 2010). Our study is the first attempt to synthetically analyze the community characteristics of abundant and rare foraminifera in the Antarctic region and reveals their differences in biogeographical patterns. Our findings suggest that abundant and rare foraminiferal taxa may occupy distinct ecological niches and play different roles in community stability. Distinguishing these two subcommunities in future studies may help to expand our understanding of foraminiferal community dynamics.

4.2 Different responses of abundant and rare subcommunities to environmental variables

Our results showed that both water depth and temperature had clearly different effects on abundant and rare foraminiferal subcommunities in the Southern Ocean (Figures 4, 5). The foraminiferal alpha diversity of abundant subcommunity was positively correlated with water depth (Figure 4A) and negatively correlated with temperature (Figure 4B), whilst no linear correlation existed between alpha diversity of rare subcommunity and these two environmental variables (Figure 4). In addition, the results of mantel test showed that the Bray-Curtis dissimilarity of abundant subcommunity was independent of water depth ($p = 0.064$), but the Bray-Curtis dissimilarity of rare subcommunity had a significant correlation with water depth ($p < 0.01$).

Antarctica and the surrounding Southern Ocean are facing complex environmental changes, and their native biota are now challenged by environmental changes (Convey and Peck, 2019). The most immediate threats to Antarctic biota are consequences of increased temperature and altered sea ice (Chown et al., 2012). Although the Intergovernmental Panel on Climate Change (IPCC) aims to limit average global warming to 2°C by the end of this century, current trends of global temperature increase, sea level rise, and ice loss are at the upper end of the IPCC's more pessimistic scenarios (Peters et al., 2013; Siegert et al., 2020). The Antarctic Peninsula has already warmed by more than 2°C in the 20th century, with some areas experiencing average annual temperature increases of 3°C or more between 1951 and 2011 (Turner et al., 2014). The native biota in the Antarctic region has adapted to the region's extreme conditions over many millions of years (Convey and Peck, 2019) and they are more sensitive to temperature variation and much less able to survive elevated temperatures than marine groups elsewhere (Peck and Conway, 2000). Our results showed that the foraminiferal alpha diversity of whole community and abundant subcommunity decreased significantly ($p < 0.01$) with increasing temperature despite the temperature separation between ten sites being less than 2°C (Figure 3). Antarctic temperature is closely coupled with global sea level (Rohling et al., 2009; Pattyn and Morlighem, 2020). Our results demonstrated that water depth had significant correlations with the beta diversity of rare subcommunity, as well as the alpha diversity of whole community and abundant subcommunity, implying that sea level rise may have an impact on the diversity and community composition of native Antarctic foraminifera, especially those living in shallow waters. This study reveals the different effects of environmental variables on abundant and rare foraminiferal subcommunities and suggests that these two subcommunities may respond differently to future environmental changes, which could lead to subversive changes in Antarctic foraminifera assemblages.

4.3 Effects of environmental variables on foraminiferal community

In this study, we collected surface sediment samples from the Southern Ocean at water depths ranging from 50 to 4399 m and comprehensively analyzed the relationships between foraminiferal diversity and eight measured environmental variables. Our results showed that the foraminiferal alpha diversity was positively correlated with water depth (Figure 4A) and negatively correlated with temperature, chlorophyll a and pheophytin a (Figure 4B; Table 1). Foraminiferal diversity and species distribution are influenced by a

variety of environmental factors, such as temperature, salinity, sediment type, primary productivity, organic matter fluxes to the sea floor, water currents and water masses (Murray, 1991). The deep sea contains different environmental settings and the parameters affecting benthic foraminifera tend to vary with bathymetry, therefore the bathymetric distribution of deep-sea foraminifera is considered to reflect the combined effects of various environmental factors closely related to water depth, rather than water depth itself (Gooday, 2003). In our study, temperature, chlorophyll a, pheophytin a, total organic carbon, total carbon and total nitrogen all varied with increasing water depth (Figure 3), so it is hard to quantify the direct effect of individual parameters on foraminiferal diversity.

The organic matter flux to the seafloor is thought to be a crucial parameter for benthic foraminiferal assemblages (Morigi et al., 2001). Although our analysis showed no linear correlation between foraminiferal alpha diversity and total organic carbon, total carbon and total nitrogen (Table 1), it does not mean that TOC, TC and TN had no effect on foraminiferal alpha diversity. Species diversity is believed to have a parabolic relationship with productivity and food supply in deep-sea and other ecosystems (Levin et al., 2001). This may explain why no linear correlations were found between foraminiferal alpha diversity and TOC, TC and TN. The VPA results of our study suggested that the proportion of community variation explained by a single environmental factor was low under the condition of constraining other environmental variables. For example, temperature alone contributed only 1.9% and 0.9% of the community variations for abundant subcommunity and rare subcommunity, respectively (Figure S3). The complex patterns of bathymetry, sea-ice cover, sediment types, surface productivity and water mass characteristics in the Antarctic region make it difficult to untangle the factors underlying the foraminiferal biogeographical patterns, which may be the result of multiple interrelated drivers.

4.4 Future application of foraminiferal DNA for polar paleoenvironmental reconstruction

Polar regions play a key role in maintaining the stability of the global climate system (Anisimov et al., 2001). Meanwhile, climate change in the polar regions is projected to be one of the largest and fastest on the Earth, and will lead to continuing increases in surface temperatures, losses of sea ice and tundra, and warming of permafrost in the Arctica and Antarctica (Turner et al., 2007). These changes will have significant impacts on global climate system and human society. Long-time-scale reconstruction of polar environmental changes will greatly improve our understanding of future climate and environmental changes, and thus better predict and respond to these changes.

Previous paleoenvironmental analyses have been largely based on the fossil record of foraminifera, ignoring the vast amount of foraminiferal DNA accumulated on the deep-sea floor (Lejzerowicz et al., 2013). Foraminiferal aDNA opens new avenues for understanding and reconstructing past environments using foraminifera (Pawłowska et al., 2020). Pawłowska et al. (2016) reported that the analysis of foraminiferal aDNA, with a focus on the non-fossilized monothalamous species, well supported the reconstruction of climate-driven environmental changes over the last millennium in Hornsund Fjord (Svalbard) based on sedimentological and micropaleontological records. The Antarctic region is dominated by cold conditions with thick ice and snow, which is conducive to the long-term preservation of DNA and provides good materials for foraminiferal aDNA study. However, the molecular ecology of benthic foraminifera in the Antarctic region is still poorly studied. In this study, we analyzed the biogeographical patterns of foraminifera based on the obtained DNA metabarcoding dataset and presented the first comprehensive assessment of relationships between ecological diversity of foraminifera and environmental conditions in the Antarctic region. Furthermore, we demonstrated that abundant and rare foraminiferal subcommunities had significantly different correlations with water depth and temperature, and we established equations between α-diversity indices of whole community and abundant subcommunity and water depth and temperature, which may provide additional proxies for future polar paleoceanography using foraminiferal aDNA.

5 Conclusions

In summary, this study was the first attempt to comprehensively analyze the ecological characteristics of foraminifera in the Antarctic region and their correlations with key environmental variables based on the eDNA metabarcoding dataset. The Antarctic foraminiferal community consists of a small number of abundant taxa and a high proportion of rare taxa, the former dominated by monothalamous foraminifera and the latter dominated by unclassified foraminifera. The alpha diversity of whole community and abundant subcommunity had positive correlations with water depth and negative correlations with temperature, Chl a and Pheo a, while no linear correlation was observed between the alpha diversity of rare subcommunity and these environmental variables. Both abundant and rare subcommunities showed distance-decay patterns, but the effect of water depth on the beta diversity of rare subcommunity was more significant than that of abundant subcommunity. Partitioning of beta diversity suggested that abundant and rare subcommunities were shaped by nestedness and turnover components, corresponding to two antithetic processes: species loss and species replacement, respectively. This study clearly reveals the contrasting biogeographical patterns of abundant and rare foraminifera in the Antarctic region and their different correlations with environmental variables, which may provide useful information and more accurate proxies for future reconstruction of polar paleoenvironments using foraminifera aDNA.

Data availability statement

The datasets presented in this study can be found in online repositories. The names of the repository/repositories and accession number(s) can be found below: BioProject, PRJNA908891.

Author contributions

QL, YL and TL conceived and designed the study. TL collected the samples. QL and HL performed the molecular experiments and

bioinformatics analysis. QL, YL, HL and TL interpreted the data and wrote the manuscript. All authors contributed to the article and approved the submitted version.

Funding

This work received financial supports from the following projects: the Strategic Priority Research Program of the Chinese Academy of Sciences (XDB42000000); the Marine S&T Fund of Shandong Province for Pilot National Laboratory for Marine Science and Technology (Qingdao) (No.2022QNLM050203; 2021WHZZB0804); National Natural Science Foundation of China (Grant No. 41976058).

Acknowledgments

Special thanks are due to Prof. Dr. Zhimin Jian (Tongji University, China) for many supports and instructions to the first corresponding author in foraminiferal research.

Conflict of interest

The authors declare that the research was conducted in the absence of any commercial or financial relationships that could be construed as a potential conflict of interest.

Publisher's note

All claims expressed in this article are solely those of the authors and do not necessarily represent those of their affiliated organizations, or those of the publisher, the editors and the reviewers. Any product that may be evaluated in this article, or claim that may be made by its manufacturer, is not guaranteed or endorsed by the publisher.

Supplementary material

The Supplementary Material for this article can be found online at: https://www.frontiersin.org/articles/10.3389/fmars.2023.1089482/full#supplementary-material

References

Anisimov, O., Fitzharris, B., Hagen, J. O., Jefferies, R., Marchant, H., Nelson, F., et al. (2001). "Polar regions (Arctic and Antarctic)." in *Climate Change: Impacts, Adaptation and Vulnerability. The Contribution of Working Group II of the Intergovernmental Panel on Climate Change, Third Assessment Review*, Eds. J. J. McCarthy, O. Canziani, N. Leary, D. J. Dokken and K. White (Cambridge: Cambridge University Press), 801–841.

Barker, P. F., and Thomas, E. (2004). Origin, signature and palaeoclimatic influence of the Antarctic circumpolar current. *Earth Sci. Rev.* 66, 143–162. doi: 10.1016/j.earscirev.2003.10.003

Baselga, A. (2010). Partitioning the turnover and nestedness components of beta diversity. *Glob. Ecol. Biogeogr.* 19, 134–143. doi: 10.1111/j.1466-8238.2009.00490.x

Bouchet, V. M. P., Alve, E., Rygg, B., and Telford, R. J. (2012). Benthic foraminifera provide a promising tool for ecological quality assessment of marine waters. *Ecol. Indic.* 23, 66–75. doi: 10.1016/j.ecolind.2012.03.011

Brandt, A., and Gutt, J. (2011). "Biodiversity of a unique environment: The southern ocean benthos shaped and threatened by climate change," in *Biodiversity hotspots*. Eds. F. Zachos and J. Habel (Berlin, Heidelberg: Springer), 503–526.

Caporaso, J. G., Kuczynski, J., Stombaugh, J., Bittinger, K., Bushman, F. D., Costello, E. K., et al. (2010). QIIME allows analysis of high-throughput community sequencing data. *Nat. Methods* 7, 335–336. doi: 10.1038/nmeth.f.303

Chown, S. L., Lee, J. E., Hughes, K. A., Barnes, J., Barrett, P. J., Bergstrom, D. M., et al. (2012). Challenges to the future conservation of the Antarctic. *Science* 337, 158–159. doi: 10.1126/science.1222821

Clarke, A., and Johnston, N. M. (2003). Antarctic Marine benthic diversity. *Oceanogr. Mar. Biol.* 41, 47–114.

Convey, P., and Peck, L. S. (2019). Antarctic Environmental change and biological responses. *Sci. Adv.* 5, eaaz0888. doi: 10.1126/sciadv.aaz0888

Edgar, R. C. (2016). UNOISE2: improved error-correction for illumina 16S and ITS amplicon sequencing. *BioRxiv*. 081257. doi: 10.1101/081257

Goldstein, S. T. (1999). "Foraminifera: a biological overview," in *Modern foraminifera*. Eds. B. K. Sen Gupta (Dordrecht: Springer), 37–55.

Gooday, A. J. (2003). Benthic foraminifera (Protista) as tools in deep-water palaeoceanography: environmental influences on faunal characteristics. *Adv. Mar. Biol.* 46, 1–90. doi: 10.1016/S0065-2881(03)46002-1

Griffiths, H. J. (2010). Antarctic Marine biodiversity – what do we know about the distribution of life in the southern ocean? *PLoS One* 5, e11683. doi: 10.1371/journal.pone.0011683

Guillou, L., Bachar, D., Audic, S., Bass, D., Berney, C., Bittner, L., et al. (2013). The protist ribosomal reference database (PR^2): A catalog of unicellular eukaryote small Sub-unit rRNA sequences with curated taxonomy. *Nucleic Acids Res.* 41 (Database issue), D597–D604. doi: 10.1093/nar/gks1160

Habura, A., Pawlowski, J., Hanes, S. D., and Bowser, S. S. (2004). Unexpected foraminiferal diversity revealed by small-subunit rDNA analysis of Antarctic sediment. *J. Eukaryot Microbiol.* 51, 173–179. doi: 10.1111/j.1550-7408.2004.tb00542.x

Holzmann, M., Gooday, A. J., Majewski, W., and Pawlowski, J. (2022). Molecular and morphological diversity of monothalamous foraminifera from south Georgia and the Falkland islands: Description of four new species. *Eur. J. Protistol.* 85, 125909. doi: 10.1016/j.ejop.2022.125909

Hou, J., Wu, L., Liu, W., Ge, Y., Mu, T., Zhou, T., et al. (2020). Biogeography and diversity patterns of abundant and rare bacterial communities in rice paddy soils across China. *Sci. Total Environ.* 730, 139116. doi: 10.1016/j.scitotenv.2020.139116

Janosik, A. M., and Halanych, K. M. (2010). Unrecognized Antarctic biodiversity: A case study of the genus odontaster (Odontasteridae; asteroidea). *Integr. Comp. Biol.* 50, 981–992. doi: 10.1093/icb/icq119

Jiao, S., Chen, W., and Wei, G. (2017). Biogeography and ecological diversity patterns of rare and abundant bacteria in oil-contaminated soils. *Mol. Ecol.* 26, 5305–5317. doi: 10.1111/mec.14218

Kaiser, S., Barnes, D. K. A., Sands, C. J., and Brandt, A. (2009). Biodiversity of an unknown Antarctic Sea: Assessing isopod richness and abundance in the first benthic survey of the amundsen continental shelf. *Mar. Biodiv* 39, 27–43. doi: 10.1007/s12526-009-0004-9

Kang, E., Li, Y., Zhang, X., Yan, Z., Wu, H., Li, M., et al. (2021). Soil pH and nutrients shape the vertical distribution of microbial communities in an alpine wetland. *Sci. Total Environ.* 774, 145780. doi: 10.1016/j.scitotenv.2021.145780

Lecroq, B., Lejzerowicz, F., Bachar, D., Christen, R., Esling, P., Baerlocher, L., et al. (2011). Ultra-deep sequencing of foraminiferal microbarcodes unveils hidden richness of early monothalamous lineages in deep-sea sediments. *PNAS* 108, 13177–13182. doi: 10.1073/pnas.1018426108

Lejzerowicz, F., Esling, P., Majewski, W., Szczuciński, W., Decelle, J., Obadia, C., et al. (2013). Ancient DNA complements microfossil record in deep-sea subsurface sediments. *Biol. Lett.* 9, 20130283. doi: 10.1098/rsbl.2013.0283

Levin, L. A., Etter, R. J., Rex, M. A., Gooday, A. J., Smith, C. R., Pineda, J., et al. (2001). Environmental influences on regional deep-sea species diversity. *Annu. Rev. Ecol. Syst.* 32, 51–93. doi: 10.1146/annurev.ecolsys.32.081501.114002

Li, Q., Lei, Y., Morard, R., Li, T., and Wang, B. (2020). Diversity hotspot and unique community structure of foraminifera in the world's deepest marine blue hole – Sansha Yongle Blue Hole. *Sci. Rep.* 10, 10257. doi: 10.1038/s41598-020-67221-0

Liu, L., Yang, J., Yu, Z., and Wilkinson, D. M. (2015). The biogeography of abundant and rare bacterioplankton in the lakes and reservoirs of China. *ISME J.* 9, 2068–2077. doi: 10.1038/ismej.2015.29

Logares, R., Audic, S., Bass, D., Bittner, L., Boutte, C., Christen, R., et al. (2014). Patterns of rare and abundant marine microbial eukaryotes. *Curr. Biol.* 24, 813–821. doi: 10.1016/j.cub.2014.02.050

Magoč, T., and Salzberg, S. L. (2011). FLASH: fast length adjustment of short reads to improve genome assemblies. *Bioinformatics* 27, 2957–2963. doi: 10.1093/bioinformatics/btr507

Majewski, W. (2010). Benthic foraminifera from West Antarctic fiord environments: An overview. *Pol. Polar Res.* 31, 61–82. doi: 10.4202/ppres.2010.05

Majewski, W., Bart, P. J., and McGlannan, A. J. (2018). Foraminiferal assemblages from ice-proximal paleo-settings in the Whales Deep Basin, eastern Ross Sea, Antarctica. *Palaeogeogr. Palaeoclimatol. Palaeoecol.* 493, 64–81. doi: 10.1016/j.palaeo.2017.12.041

Majewski, W., Holzmann, M., Gooday, A. J., Majda, A., Mamos, T., and Pawlowski, J. (2021). Cenozoic climatic changes drive evolution and dispersal of coastal benthic foraminifera in the Southern Ocean. *Sci. Rep.* 11, 19869. doi: 10.1038/s41598-021-99155-6

Mikhalevich, V. I. (2004). The general aspects of the distribution of Antarctic foraminifera. *Micropaleontology* 50, 179–194. doi: 10.2113/50.2.179

Mo, Y., Zhang, W., Yang, J., Lin, Y., Yu, Z., and Lin, S. (2018). Biogeographic patterns of abundant and rare bacterioplankton in three subtropical bays resulting from selective and neutral processes. *ISME J.* 12, 2198–2210. doi: 10.1038/s41396-018-0153-6

Morigi, C., Jorissen, E. J., Gervais, A., Guichard, S., and Borsetti, A. M. (2001). Benthic foraminiferal faunas in surface sediments off NW Africa: Relationship with organic flux to the ocean floor. *J. Foraminiferal Res.* 31, 350–368. doi: 10.2113/0310350

Murray, J. W. (1991). *Ecology and palaeoecology of benthic foraminifera* (Harlow: Longman Scientific and Technical).

Pattyn, F., and Morlighem, M. (2020). The uncertain future of the Antarctic ice sheet. *Science* 367, 1331–1335. doi: 10.1126/science.aaz5487

Pawłowska, J., Lejzerowicz, F., Esling, P., Szczuciński, W., Zajączkowski, M., and Pawlowski, J. (2014). Ancient DNA sheds new light on the Svalbard foraminiferal fossil record of the last millennium. *Geobiology* 12, 277–288. doi: 10.1111/gbi.12087

Pawłowska, J., Wollenburg, J. E., Zajączkowski, M., and Pawlowski, J. (2020). Planktonic foraminifera genomic variations reflect paleoceanographic changes in the Arctic: evidence from sedimentary ancient DNA. *Sci. Rep.* 10, 15102. doi: 10.1038/s41598-020-72146-9

Pawłowska, J., Zajączkowski, M., Łącka, M., Lejzerowicz, F., Esling, P., and Pawlowski, J. (2016). Palaeoceanographic changes in Hornsund Fjord (Spitsbergen, Svalbard) over the last millennium: new insights from ancient DNA. *Clim. Past* 12, 1459–1472. doi: 10.5194/cp-12-1459-2016

Pawlowski, J., Fahrni, J. F., Brykczynska, U., Habura, A., and Bowser, S. S. (2002). Molecular data reveal high taxonomic diversity of allogromiid foraminifera in Explorers Cove (McMurdo Sound, Antarctica). *Polar Biol.* 25, 96–105. doi: 10.1007/s003000100317

Peck, L. S., and Conway, L. Z. (2000). The myth of metabolic cold adaptation: oxygen consumption in stenothermal Antarctic bivalves. *Geological Society London Special Publications* 177, 441–450. doi: 10.1144/GSL.SP.2000.177.01.29

Peters, G. P., Andrew, R. M., Boden, T., Canadell, J. G., Ciais, P., Le Quéré, C., et al. (2013). The challenge to keep global warming below 2 °C. *Nat. Clim Chang* 3, 4–6. doi: 10.1038/nclimate1783

Rohling, E., Grant, K., Bolshaw, M., Roberts, A. P., Siddall, M., Hemleben, Ch., et al. (2009). Antarctic temperature and global sea level closely coupled over the past five glacial cycles. *Nat. Geosci.* 2, 500–504. doi: 10.1038/ngeo557

Rosa, L. H., da Silva, T. H., Ogaki, M. B., Pinto, O. H. B., Stech, M., Convey, P., et al. (2020). DNA metabarcoding uncovers fungal diversity in soils of protected and non-protected areas on Deception Island, Antarctica. *Sci. Rep.* 10, 21986. doi: 10.1038/s41598-020-78934-7

Siegert, M., Alley, R. B., Rignot, E., Englander, J., and Corell, R. (2020). Twenty-first century sea-level rise could exceed IPCC projections for strong-warming futures. *One Earth* 3, 691–703. doi: 10.1016/j.oneear.2020.11.002

Szczuciński, W., Pawłowska, J., Lejzerowicz, F., Nishimura, Y., Kokociński, M., Majewski, W., et al. (2016). Ancient sedimentary DNA reveals past tsunami deposits. *Mar. Geol.* 381, 29–33. doi: 10.1016/j.margeo.2016.08.006

Turner, J., Barrand, N. E., Bracegirdle, T. J., Convey, P., Hodgson, D. A., Jarvis, M., et al. (2014). Antarctic climate change and the environment: an update. *Polar Rec.* 50, 237–259. doi: 10.1017/S0032247413000296

Turner, J., Overland, J. E., and Walsh, J. E. (2007). An Arctic and Antarctic perspective on recent climate change. *Int. J. Climatol.* 27, 277–293. doi: 10.1002/joc.1406

Wang, J., Wang, Y., Li, M., Xu, L., He, N., Yan, P., et al. (2021). Differential response of abundant and rare bacterial subcommunities to abiotic and biotic gradients across temperate deserts. *Sci. Total Environ.* 763, 142942. doi: 10.1016/j.scitotenv.2020.142942

Wang, Y., Bao, Y., Yu, M., Xu, G., and Ding, P. (2010). BIODIVERSITY RESEARCH: Nestedness for different reasons: the distributions of birds, lizards and small mammals on islands of an inundated lake. *Divers. Distrib.* 16, 862–873. doi: 10.1111/j.1472-4642.2010.00682.x

Wang, Y., Ye, F., Wu, S., Wu, J., Yan, J., Xu, K., et al. (2020). Biogeographic pattern of bacterioplanktonic community and potential function in the Yangtze river: Roles of abundant and rare taxa. *Sci. Total Environ.* 747, 141335. doi: 10.1016/j.scitotenv.2020.141335

Weber, A. A.-T., and Pawlowski, J. (2014). Wide occurrence of SSU rDNA intragenomic polymorphism in foraminifera and its implications for molecular species identification. *Protist* 165, 645–661. doi: 10.1016/j.protis.2014.07.006

Wickham, H. (2016). *ggplot2 – elegant graphics for data analysis. 2nd ed.* (Springer-Verlag New York: Media).

Xue, Y., Chen, H., Yang, J. R., Liu, M., Huang, B., and Yang, J. (2018). Distinct patterns and processes of abundant and rare eukaryotic plankton communities following a reservoir cyanobacterial bloom. *ISME J.* 12, 2263–2277. doi: 10.1038/s41396-018-0159-0

Zeng, Q., An, S., Liu, Y., Wang, H., and Wang, Y. (2019). Biogeography and the driving factors affecting forest soil bacteria in an arid area. *Sci. Total Environ.* 680, 124–131. doi: 10.1016/j.scitotenv.2019.04.184

Zhao, F., Wang, Y., Zheng, S., Zhao, R., Lin, M., and Xu, K. (2021). Patterns and drivers of microeukaryotic distribution along the North Equatorial Current from the Central Pacific Ocean to the South China Sea. *Mar. pollut. Bull.* 165, 112091. doi: 10.1016/j.marpolbul.2021.112091

frontiers | Frontiers in Marine Science

TYPE Original Research
PUBLISHED 24 February 2023
DOI 10.3389/fmars.2023.1109523

OPEN ACCESS

EDITED BY
Juan D. Gaitan-Espitia,
The University of Hong Kong, Hong Kong SAR ,China

REVIEWED BY
Marcelo Lagos,
The University of Hong Kong, Hong Kong SAR, China
Chuanxin Qin,
South China Sea Fisheries Research Institute (CAFS), China

*CORRESPONDENCE
Yanli Tang
tangyanli@ouc.edu.cn
Tao Zhang
tzhang@qdio.ac.cn

SPECIALTY SECTION
This article was submitted to Global Change and the Future Ocean, a section of the journal Frontiers in Marine Science

RECEIVED 27 November 2022
ACCEPTED 02 February 2023
PUBLISHED 24 February 2023

CITATION
Yu H, Fang G, Rose KA, Lin J, Feng J, Wang H, Cao Q, Tang Y and Zhang T (2023) Effects of habitat usage on hypoxia avoidance behavior and exposure in reef-dependent marine coastal species. *Front. Mar. Sci.* 10:1109523. doi: 10.3389/fmars.2023.1109523

Effects of habitat usage on hypoxia avoidance behavior and exposure in reef-dependent marine coastal species

Haolin Yu[1,2,3,4], Guangjie Fang[5], Kenneth A. Rose[6], Jiazheng Lin[7], Jie Feng[8], Haiyan Wang[9], Qingxian Cao[10], Yanli Tang[7]* and Tao Zhang[1,2,3,4]*

[1]Chinese Academy of Sciences (CAS) Key Laboratory of Marine Ecology and Environmental Sciences, Institute of Oceanology, Chinese Academy of Sciences, Qingdao, China, [2]Laboratory for Marine Ecology and Environmental Science, Qingdao National Laboratory for Marine Science and Technology, Qingdao, China, [3]CAS Engineering Laboratory for Marine Ranching, Institute of Oceanology, Chinese Academy of Sciences, Qingdao, China, [4]Shandong Province Key Laboratory of Experimental Marine Biology, Qingdao, China, [5]Fishery Resources and Ecology Research Department, Zhejiang Marine Fisheries Research Institute, Zhoushan, China, [6]Horn Point Laboratory, University of Maryland Center for Environmental Science, Cambridge, MD, United States, [7]College of Fisheries, Ocean University of China, Qingdao, China, [8]North China Sea Marine Forecasting Center of State Oceanic Administration, Qingdao, China, [9]Department of Marine Organism Taxonomy & Phylogeny, Institute of Oceanology, Chinese Academy of Sciences, Qingdao, China, [10]Guangxi Institute of Oceanography, Nanning, China

Reef habitat in coastal ecosystems is increasingly being augmented with artificial reefs (ARs) and is simultaneously experiencing increasing hypoxia due to eutrophication and climate change. Relatively little is known about the effects of hypoxia on organisms that use complex habitat arrangements and how the presence of highly preferred AR habitat can affect the exposure of organisms to low dissolved oxygen (DO). We performed two laboratory experiments that used video recording of behavioral movement to explore 1) habitat usage and staying duration of individuals continuously exposed to 3, 5, and 7 mg/L dissolved oxygen (DO) in a complex of multiple preferred and avoided habitat types, and 2) the impact of ARs on exposure to different DO concentrations under a series of two-way replicated choice experiments with or without AR placement on the low-oxygen side. Six common reef-dependent species found in the northeastern sea areas of China were used (i.e., rockfish *Sebastes schlegelii* and *Hexagrammos otakii*, filefish *Thamnaconus modestus*, flatfish *Pseudopleuronectes yokohamae*, sea cucumber *Stichopus japonicus*, and crab *Charybdis japonica*). Results showed that lower DO levels decreased the usage of preferred habitats of the sea cucumber and the habitat-generalist filefish but increased the habitat affinity to preferred habitat types for the two habitat-specific rockfishes. Low DO had no effect on the crab's habitat usage. In the choice experiment, all three fish species avoided 1 mg/L, and the rockfish *S. schlegelii* continued to avoid the lower DO when given choices involving pairs of 3, 5, and 7 mg/L, while *H. otakii* and the flatfish showed less avoidance. The availability of ARs affected exposure to low DO for the habitat-preferring rockfishes but was not significant for the flatfish. This study provides information for assessing the ecological effects and potential for adaptation through behavioral movement for key reef-dependent species under the increasing overlap of ARs and hypoxia anticipated in the future.

KEYWORDS

habitat usage, hypoxia, behavioral response, reef-dependent species, hypoxia avoidance, exposure to low oxygen

Introduction

The frequency and extent of hypoxia, which is typically defined as the dissolved oxygen (DO) concentration of less than 2 mg/L, are rapidly increasing in coastal areas around the world (Diaz and Rosenberg, 2008; Breitburg et al., 2018), and this trend is predicted to continue and likely accelerate into the future under climate change (Weiland et al., 2012; Rabalais and Turner, 2019). Hypoxia in river-influenced coastal areas typically results from eutrophication (increasing nitrogen and phosphorous) generated by point and non-point sources that accompany the human development of watersheds (Caddy, 1993; Steckbauer et al., 2011; Watson, 2016; Domenici et al., 2017). Nutrients stimulate primary and secondary production in surface waters that subsequently sink and decompose, with the associated decline in oxygen, in the bottom layer that is isolated from oxygen inputs due to vertical stratification of the water column (Steckbauer et al., 2011). Hypoxia often occurs during the summer months (warm conditions) when primary production is high from the spring influx of nutrients and vertical stratification has been established. DO increases again in the fall as production decreases and increasing mixing of the water column breaks down or weakens the stratification (Wei et al., 2021b).

Hypoxia causes direct effects on individuals that can translate into localized and population-level responses (Rose et al., 2009). Direct effects from exposure to low DO concentrations result in increased mortality (including massive mortality events), reduced growth, lowered reproduction (Diaz and Rosenberg, 2008), and altered behavior (Wannamaker and Rice, 2000; Vaquer-Sunyer and Duarte, 2008; Rasmuson et al., 2021). Mortality generally occurs with hypoxia, while sublethal effects can occur at DO concentrations up to 4 mg/L (Hrycik et al., 2017).

Hypoxia also causes indirect effects on individuals. Low DO can affect the prey and predators of the species of interest, which then, even without direct exposure, affect growth and mortality (David and David, 2000). Major indirect effects occur from the avoidance movement in response to hypoxia exhibited by many mobile species to reduce their exposure to low DO (Craig, 2012; Lagos et al., 2015; Jorissen and Nugues, 2021; LaBone et al., 2021). Avoidance results in indirect effects because it is not the exposure to DO that causes physiological effects but rather the consequences of individuals being forced to move to less preferred locations and habitats where mortality, growth, and reproduction would be different than if they were able to inhabit the avoided areas (Eby and Crowder, 2002; LaBone et al., 2021).

Reef-dependent species are especially susceptible to hypoxia because they show an affinity for specific habitats that are not uniformly available and, to various degrees, may be reluctant to simply move. Many reef-oriented species therefore exhibit complex ecological responses that emerge from specific differences in behavior and how the spatial arrangement of the reefs allows for connectivity and intersects with the spatially and temporally variable patterns of hypoxia (Rasmuson et al., 2021).

The increasing use of artificial reefs to augment fisheries and the increasing frequency and extent of hypoxia will lead to more situations of overlap between artificial reefs and hypoxia. For example, the summer hypoxic zones in the northern Gulf of Mexico are well-known, and the use of oil and gas platforms that are converted to artificial reefs after they no longer are operational often overlaps with the hypoxic areas (Bianchi et al., 2010). Artificial reef habitats are commonly deployed to restore some of the functioning of degraded habitats in coastal areas (Lemoine et al., 2019). Engineering devices have been proposed with artificial reefs to alleviate local hypoxia, like generating artificial downwelling flow and regionally changing hydrodynamic conditions (Fan et al., 2019).

Laboratory experiments have been extensively used to quantify the effects of low DO on growth, mortality, reproduction, avoidance, and other (e.g., foraging) behaviors (Wu, 2002; Domenici et al., 2007; Portner and Peck, 2010). These experiments have focused on varying DO, sometimes also varying other environmental variables (e.g., temperature, salinity, acidification) in multi-factor designs (Gunderson et al., 2016; Breitburg et al., 2019). What has not been explored in detail is how hypoxia affects the behavior and exposure of individuals in complex habitats and how this differs among reef-dependent species that exhibit highly specific habitat affinities. Habitat assessment based on a field survey of reef-dependent species demonstrated species-specific preferences under normoxic conditions (Yu et al., 2020). Whether hypoxia would cause relatively simple shifts of individuals among reefs that are predictable from species information on preferences and swimming behavior is not known (e.g., generalist good swimming species move to nearby reefs). Such information is difficult to infer from field studies where individuals are affected by multiple factors and hypoxia is often temporally and spatially dynamic.

In this paper, we used a laboratory experiment approach to explore the behavioral responses of reef-dependent fish and invertebrate species to independently manipulated habitat complexity and DO. We performed two laboratory experiments and analyzed the video-recorded movement behavior of representative reef-dependent species in tanks with complex scaled-reduced habitats under different DO concentrations. AR habitat was included as part of the complex habitat and was a factor in the experiments. Behavioral responses to habitat usage, staying duration, and the influence of AR were quantified to assess how species differences in affinities for habitat types and avoidance behavior interact with low DO to affect their exposure. Specifically, Experiment I examined how DO concentration affected the use of preferred habitat types. Experiment II explored how the presence of AR habitat affected avoidance and thereby exposure to low DO. We discuss the implications of the results on the ability of the species to adapt *via* movement behavior to conditions when habitat use overlaps with hypoxia.

Materials and methods

Experiments were conducted between 24 September and 30 October 2020, at the laboratory of the Tianyuan aquaculture company, Shandong, China. Our study adheres to the policies relating to animal experiments and welfare (e.g., EU Directive 2010/63/EU for animal experiments; ASAB/ABS guidelines), and all experiments are approved by the Institutional Animal Care and Use Committee of Ocean University of China.

Animal selection and description

Yu et al. (2022) grouped the epibenthic reef-dependent species found in a reef area located in Bohai, China, into six archetypes based on their shared responses to the environmental variables of temperature, DO, substrate type, and distance to the nearest reef. The six archetypes simplified the spatial distribution responses of multiple species to environmental conditions and ARs and offered representative reef-dependent species as indicators of community response. We used the member species in the three reef-associated archetypes to select six species (juvenile-stage) to conduct our experiments: rockfish *Sebastes schlegelii* and *Hexagrammos otakii* and crab *Charybdis japonica* from the dominant reef-dependent species archetype; sea cucumber *Stichopus japonicus* from the reef-neighbor archetype; and filefish *Thamnaconus modestus* and flatfish *Pseudopleuronectes yokohamae* from the DO-independent reef-neighbor archetype. The average length and weight of individuals of the test species were typical for their juvenile life stages (Supplementary Table S1). Five of the six species (not *P. yokohamae*) that represented all three reef-associated archetypes were used in Experiment I. Two species (*S. schlegelii* and *H. otakii*) from the reef-dependent species archetype and *P. yokohamae* from the DO-independent archetype were used in Experiment II.

Except for the crab *C. japonica* that was purchased from Penglai Fisheries Wholesale Market (Shandong, China), the other species were obtained from organisms bred in the facilities of the Tianyuan Aquaculture Company. All species were kept separate for 7 days. Fish and sea cucumber were fed a commercial diet (Shandong Oriental Ocean Sci-Tech Co. Ltd., Yantai, China) and the crab was fed fresh shellfish twice daily. Feeding of the experimental organisms was stopped 48 h before the experiments began. Experimental seawater was extracted from a coastal underground source and filtered by sand filtration for the experiments. The water quality of the experimental water was nearly identical to the water quality of their culturing water (pH 7.88 ± 0.1; temperature 18.61 ± 0.44°C; DO 7.73 ± 0.2 mg/L; salinity 31.13 ± 0.17).

Experimental set-up and procedure

Different experimental tanks were utilized for two experiments (Figure 1). Details of the experiments are provided in Supplementary—Section 1.2.1. We designed a 120 × 120 × 50 cm regular hexagon uncovered apparatus as the experimental tank for Experiment I (Figure 1A). The tank was constructed from polymethyl methacrylate (PMMA) and divided into six triangle sections using a transparent PMMA bottom clapboard (2.5 cm in height and 0.5 cm in width). We placed five artificially-simulated habitats (i.e., artificial reef [AR], boulder, rubble, gravel, and sand) in sections of the tank and left one section empty (blank).

The experimental tank for Experiment II was an 80 × 30 × 30 cm PMMA uncovered rectangular chamber with a 0.5 cm-thick PMMA plate inserted in the middle to establish two sections that were maintained at different DO levels (Figure 1B). We set the height off the bottom of the liftable bottom plate to 6 cm to ensure all species could easily swim back and forth between the sections. In addition, three AR monomers, identical to Experiment I, were selected to be place horizontally in the lower oxygen section to enable detection of any interference of AR on the hypoxia-avoidance capacity of the species.

Lighting was provided by a fixed incandescent light bulb (100 lx, 2 m in height), and a Huawei XiaoTun Camera (1080P, 1.8 m in height) mounted above each experimental tank was used to record the locations of everyone within the treatment sections of the tanks. Water depth was maintained at 30 cm, and nitrogen and air were bubbled to the bottom of the tank to control the target DO

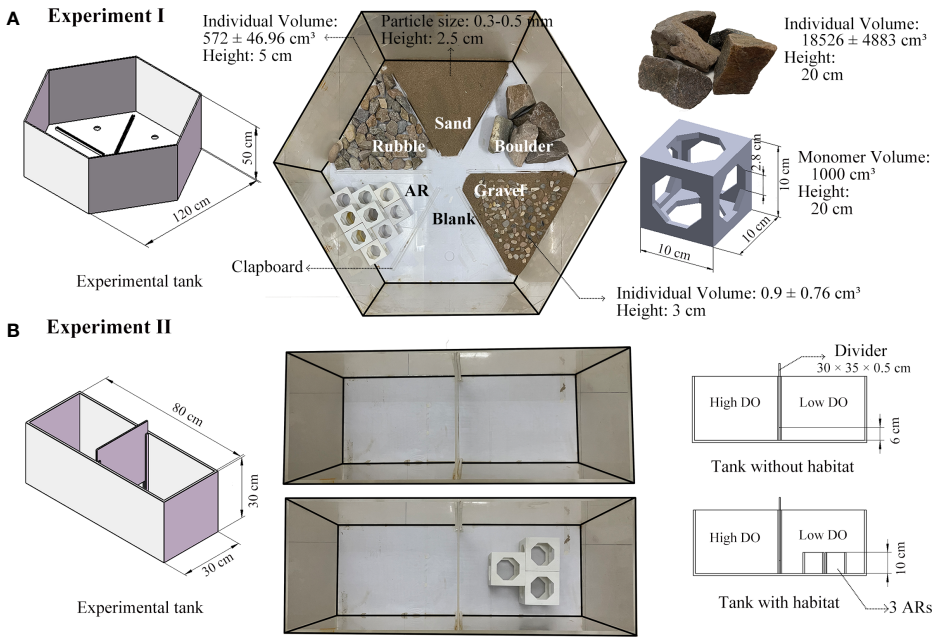

FIGURE 1
Design of the tanks used in the laboratory experiments. **(A)**, regular hexagon apparatus of Experiment I with artificially-configured versions of the five habitats and one blank area; **(B)**, rectangle channel apparatus of Experiment II with and without artificial reefs placed in the low-oxygen side.

concentration of ±0.4 mg/L (Wannamaker and Rice, 2000). DO concentration in the tanks was monitored by Taiwan Hengxin AZ-8403 dissolved oxygen meters at the start and end of each of the experiments. DO readings were taken in each section (habitat area) in Experiment I and along the side at 5 cm from the bottom and water surface in Experiment II.

Experiment I—Habitat usage

Experiment I (left side of Figure 2) was conducted under three DO levels (7, 5, and 3 mg/L) and repeated eight times (replicates) for sea cucumber *S. japonicus* and crab *C. japonica* and four times for each of the three fish species (Table 1). Thirty individuals were used in each trial (defined as a specific DO treatment in a replicate), except for 20 individuals in each trial used for *H. otakii*. Once the DO concentration reached the target level, 20 or 30 individuals were released into the central area of the tanks. Organisms were allowed to acclimatize for 30 min, and then video recording went for 1 to 12 h, depending on the species. A new central area within a 15 cm radius of the center of the apparatus was added for sea cucumber and crab to accommodate their slower-swimming behavior compared to fish. Details of the difference in the number of species and experimental design are provided in Supplementary—Section 1.2.2.

A parallel set of control experiments was designed and implemented to assess the spatial preferences of each species for areas within the experimental tank. All habitats were removed from the tank, and the oxygen level was set at the normoxia (7 mg/L) condition (Table 1). The five species demonstrated no significant differences in sections when all were blank habitats (Supplementary Tables S2, S3).

Experiment II—Hypoxic avoidance

In Experiment II (right side of Figure 2), we set up various pairwise combinations of different DO concentrations between the two sides of the rectangle chamber (1 vs. 3, 1 vs. 5, 1 vs. 7, 3 vs. 5, 3 vs. 7, and 5 vs. 7 mg/L, Table 2). Experiment II was divided into two parts: one part did not include AR habitat and was used to measure the hypoxia-avoidance capacity of each species when only DO vary, and the second part then included placing three AR monomers on the lower-oxygen side to explore how having a preferred habitat type (AR) affected the hypoxia-avoidance capacity (Table 2). Both parts (with and without ARs) were replicated six times. Individuals were held for 30 minutes in the same-design apparatus with normoxic conditions on both sides before their introduction to the testing tank.

Once the target DO concentrations were reached on each side of the tank and the 30-minute acclimatization was completed, the central divider was lifted to create the bottom channel for passage. The five acclimatized fish were then gently introduced into the bottom channel with a small diddle net. Recording started 5 min after fish introduction, and recording was for 15 min (10 min for the 1 vs. 7 mg/L DO combination). The relatively short duration ensured that starting and ending DO concentrations varied less than 0.4 mg/L from the target DO levels.

Behavior observations and parameter calculations

For both experiments and each species, we analyzed the video recording of each trial and accumulated the results over replicates.

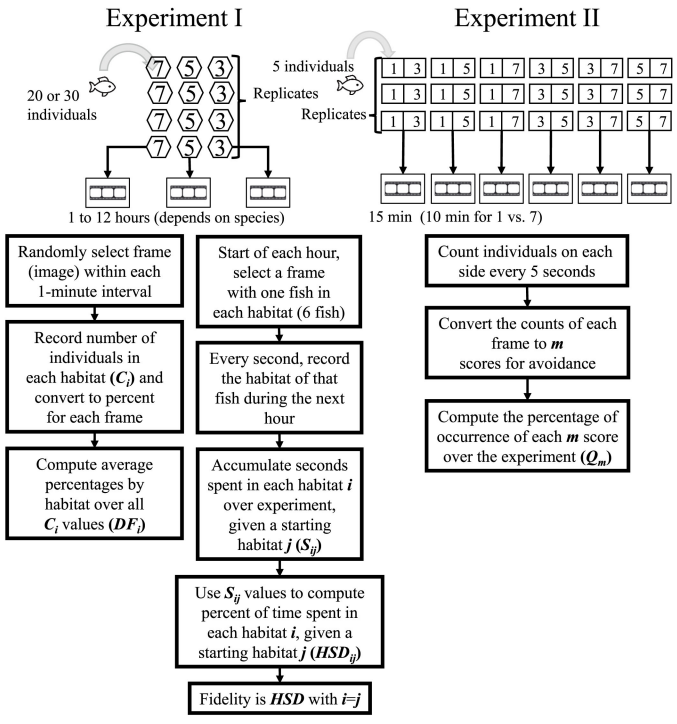

FIGURE 2
Flow chart of the design and analysis for Experiment I (left side) and Experiment II (right side).

TABLE 1 Design of Experiment I and the control version.

Experiment	Species	DO (mg/L)	Habitat categories	Duration of each trial (h)	Number of replicates	Number of individuals in each trial
Experiment I	*Stichopus japonicus*	7, 5, 3	AR, boulder, rubble, gravel, sand, blank	3	8	30
	Charybdis japonica	7, 5, 3	AR, boulder, rubble, gravel, sand, blank	1	8	30
	Hexagrammos otakii	7, 5, 3	AR, boulder, rubble, gravel, sand, blank	12	4	20
	Sebastes schlegeli	7, 5, 3	AR, boulder, rubble, gravel, sand, blank	12	4	30
	Thamnaconus modestus	7, 5, 3	AR, boulder, rubble, gravel, sand, blank	12	4	30
Control	*Stichopus japonicus*	7	All blank	3	8	30
	Charybdis japonica	7	All blank	1	8	30
	Hexagrammos otakii	7	All blank	6	2	20
	Sebastes schlegeli	7	All blank	6	2	30
	Thamnaconus modestus	7	All blank	6	2	30

Distribution frequency (DF_i) was estimated and measured from video recordings for each trial; Habitat Staying Duration (HSD_{ij}) and Habitat Fidelity (HSD_{ii}) were also measured for the three fish species. Light condition was 100 lx for all trials.

The recordings had 24 frames (images) every second and we sampled images from those frames for analyses.

Experiment I—Habitat usage

Two metrics were calculated for the experiment with habitat types present and the control experiment with empty sections. For convenience, we refer to the sections in the control experiment by the habitat types of the version of the experiment that used habitat. This is even though no habitat was present.

The first metric was the percent of individuals by habitat type, denoted DF_i, i = 1, 2, 3, 4, 5, 6. This refers to AR, boulder, rubble, gravel, sand, and blank. First, we randomly selected an image (frame) from each 1-minute interval. The number of individuals in each habitat (section) was counted (C_i) for each selected frame and converted to a percentage based on the total number of individuals present. The number of C values for a species in a specific treatment was therefore the duration of the treatment (minutes) × number of replicates. Distribution frequency (DF_i, expressed as a percent) was then computed for each of the six habitat types in a treatment as the average of the C_i values for that habitat type (Figure S1).

The second metric of habitat staying duration (HSD_{ij}) was calculated from the same recordings as the first metric and for the fish species only. HSD reflected the movement trajectory of individuals among the habitats. At the start of an hour, we selected a frame that had at least one individual in each of the six sections and treated that as their starting habitat. j = 1, 2, 3, 4, 5, 6 refers to the starting habitat as AR, boulder, rubble, gravel, sand, and blank. We then followed that individual in frames every second and recorded what habitat it was in for the rest of that hour. This was then repeated (one individual in each of the six starting habitats) for every hour of the experiment. The cumulative seconds spent by each individual over replicates (S_{ij}) was determined. The number of S values for a species that individuals starting in each habitat

TABLE 2 Design of Experiment II. Light condition was 100 lx for all trials.

Species	Pairwise DO combinations (mg/L)	Duration of each trial (min)	Number of replicates	Number of individuals in each trial
Hexagrammos otakii *Sebastes schlegeli* *Pseudopleuronectes yokohamae*	1 vs 3	15	6	5
	1 vs 5	15	6	5
	1 vs 7	10	6	5
	3 vs 5	15	6	5
	3 vs 7	15	6	5
	5 vs 7	15	6	5

The experiment used three ARs on the side with the lower DO concentration. The control version repeated the experiment without the ARs present.

spent in each of the six habitats was the duration of the one-hour treatment (12 h) × four replicates or 48 values, and S_{ij} values were then used to calculate the percent of total seconds (HSD_{ij}, Figure S2). Habitat fidelity was the special case of the habitat staying duration computed for when the starting habitat used the cumulative seconds spent in that same habitat (i.e., HSD_{ii}).

Experiment II—Hypoxic avoidance

A metric that categorized the degree of avoidance for the lower DO choice (Q_m) was used in the experiment with AR present and the control version that had no ARs. The number of individuals on each side of the tank was recorded from a frame selected every 5 s and categorized into the behavior codes (denoted m) that used how the five individuals were split between the sections (Table 3). Thus, there were 15 min × 12 images per minute × six replicates, or 1,080 values of m for each species in each treatment. These values of m were then converted to the percent of the values (Q_m) accounted for by each of the six possible values of m (Figure S3). For statistical analysis and labeling of figures, we then further categorized the six behavior codes into three hypoxia-avoidance capacity categories: strong (m = 1, 2), weak (m = 3), and no capacity (m = 4, 5, 6).

Statistical analysis

The behavior metrics of DF_i and HSD_{ii} (fidelity only, $I = j$) from Experiment I and the 3-category version of degree of avoidance from Experiment II were analyzed using the Kruskal–Wallis test ($\alpha = 0.05$) followed by a Nemenyi *post-hoc* pairwise comparison (Table 4). For Experiment I, the tests were to assess the effect of the three DO concentrations (on usage DF_i and fidelity HSD_{ii}) for each habitat type and were done separately for the experiment with three DO levels and for the control for each species. Also, we tested DF_i across habitats given the same DO levels for the experiment with three DO levels and for the control for each species (see Supplementary Tables S2–S8). For Experiment II, the tests were to compare the "strong," "weak," and "no" avoidance capacity categories for each pair-wise combination of lower and higher DO and were done separately for when ARs are present and for when they are absent (control) for each species. Significant differences were reported using letters on the figures to denote differences (a, b, c; A, B, C for the control results of Experiment II). All analyses were conducted using the R program (v. 4.1.0) with the "PMCMRplus," "tidycerse," and "circlize" packages.

TABLE 3 Use of the number of individuals on each side of the tank in each frame to assign a degree of avoidance category (m) to the frame and categories of avoidance capacity.

m	Number of individuals on the low and high DO sides	Categories of avoidance capacity
1	0 on low and 5 on high	Strong
2	1 on low and 4 on high	Strong
3	2 on low and 3 on high	Weak
4	3 on low and 2 on high	No
5	4 on low and 1 on high	No
6	5 on low and 0 on high	No

Results

Preferred habitats under normoxia and no ARs

Frequency percentages from Experiment I under the normoxic condition (7 mg/L DO) indicated the preferred habitats and movement characteristics for each species. Four species (i.e., sea cucumber *S. japonicus*, crab *C. japonica*, and two rockfishes *H. otakii* and *S. schlegelii*) similarly preferred boulder, AR, and rubble habitats, while the filefish *T. modestus* had a strong preference for the blank area followed by AR (black bars in Figures 3, 4). More detailed results of habitat preferences are documented in Supplementary—Section 2.1. In the control of Experiment I (no ARs and other habitats), rockfish *H. otakii* indicated the highest dependence on its starting position, followed by *S. schlegelii*, while *T. modestus* showed relatively equal constant staying durations among all habitats (Supplementary—Section 2.2 and Figure S4).

Low DO effects on habitat usage

Distribution frequency

Overall, lower DO concentrations decreased the use of preferred habitats (AR, boulder, and rubble areas) by the sea cucumber *S. japonicus* (Figure 3A) and the preferred habitats (blank and AR areas) of the filefish *T. modestus* (Figure 4C). In contrast, lower DO increased the dependence on complex habitats (AR, boulders, rubble) of the two rockfish species *S. schlegelii* and *H. otakii* (Figures 4A, B). DO concentration had no significant influence on how the crab *C. japonica* used its preferred habitats (Figure 3B).

Examining the results in more detail, the distribution frequency of sea cucumber decreased in the AR, boulder, and rubble habitats with decreasing DO concentration (Figure 3A). The highest percent frequencies were observed under the normoxic condition (7 mg/L), while the lowest frequencies occurred under the lowest (3 mg/L) DO concentration. Percent frequencies for 7 mg/L and 3 mg/L were: 38 versus 5.5% in boulders, 32 versus 5% in rubble, and 19 versus 1.1% in ARs. These were reduced below 5 mg/L, and especially below 3 mg/L. Most individuals congregated in the center of the tank under low oxygen conditions, which resulted in no differences in distribution frequency related to DO for the less preferred habitats (p >0.05, Supplementary Table S4).

Crabs showed the same habitat preferences as the sea cucumber, but crab usage of habitat types was not significantly affected by low DO conditions (Figure 3B; Supplementary Table S5). Lowered DO concentrations did not significantly influence the distribution frequencies of their preferred usage levels (p >0.05, Figure 3B), with the exception of sand.

Both rockfish species (Figures 4A, B) showed the highest use of ARs and rubble at 5 mg/L, with use being lower for 3 and 7 mg/L (p <0.05, Supplementary Tables S6, S7). This resulted in a dome shape for the bars in Figures 4A, B. However, for the remaining habitats, including the

TABLE 4 Testing metrics from Experiments I and II using the Kruskal–Wallis test followed by Nemenyi pairwise comparison.

Experiment	Metric	Three DO levels (Exp. I) or AR present (Exp. II)	Results	Control versions	Results
I	DF_i	Effect of DO (given a habitat type)	Figures 3, Figure 4	Effect of blank sections under 7 mg/L	Tables S2, S3
		Effect of habitat type (given a DO)	Tables S4–S8		
	HSD_{ii}	Effect of DO	Figures 5–Figure 7	Effect of blank sections under 7 mg/L	Figure S4
II	3 categories of *m* values	Differences among the categories for each pairwise combination with ARs present	Figures 8–Figure 10	Differences among the categories for each pairwise combination without ARs	Figures 8–Figure 10

preferred habitat of boulders, the two rockfish species showed different or even opposite responses. Use of boulder increased from 22 to 28% with decreasing DO (from 7 to 3 mg/L) for *H. otakii*, while the use of boulder decreased from 29 to 20% with *S. schlegelii*. Among the less preferred habitats, a mix of patterns of dome-shaped, no differences, and increasing or decreasing usage was observed.

The final species, *T. modestus*, showed a habitat usage response to low oxygen that differed from the other species (Figure 4C). *T. modestus* showed the weakest preferences for the habitat types, with the blank option getting the most use for all DO concentrations. Habitat use of blank was similar (although p <0.05) at about 35% for 7 and 3 mg/L (Supplementary Table S8). While use was generally low for other habitats, decreasing DO (7 mg/L versus 3 mg/L) caused a decrease in usage of ARs (from 21 to 16%) and an increased use of boulders (from 6.7 to 11%). Other habitats showed little dependence on DO concentration.

Staying duration

In general, low DO concentrations affected the staying duration of habitats for the two rockfish species that showed a high degree of preference for specific habitats. This was compared to a small DO effect observed for the generalist filefish *T. modestus*.

The staying duration in the preferred habitats of both rockfish species was increased by lower DO concentrations, but with some differences. Both species showed the same increase in staying duration with low DO in a preferred habitat. Staying duration from 7 to 3 mg/L increased in AR (77 to 88%) and boulder for *H. otakii* (p <0.05, Figures 5A, B). Similarly, staying duration increased moderately in AR and in rubble for *S. schlegelii* (Figure 6C). However, duration in rubble showed no differences for *H. otakii* (Figure 5C), and *S. schlegelii* showed reduced duration in boulders (Figure 6B).

For the filefish *T. modestus*, lower DO concentrations showed only slight effects on staying duration, with the highest staying duration in the blank area under all DO conditions, followed by the second-most usage in its other preferred habitat of AR (Figure 7). The staying duration in the AR area was higher under 3 mg/L (34%) than under 5 and 7 mg/L DO (20% and 28%, p <0.05, Figure 7A).

Exposure to low DO concentrations

Avoidance without ARs

All three species avoided 1 mg/L, as shown by the gray bars (indicating no AR present) being to the left in the three top panels (i.e., all panels that included 1 mg/L in Figures 8–10). When given choices involving pairs of 3, 5, and 7 mg/L, the rockfish *S. schlegelii* continued to avoid the lower DO (gray bars remain to the left in Figure 9), while *H. otakii* and the flatfish *P. yokohamae* showed less avoidance (gray bars shifted to the right in the three bottom panels of Figures 8, 10). *S. schlegelii* showed a significantly strong capacity to

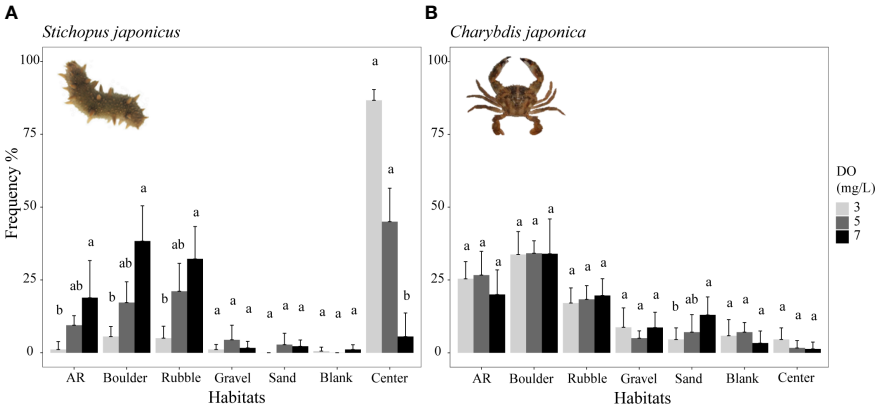

FIGURE 3
Mean distribution frequency percentage of sea cucumber *Stichopus japonicus* from reef-neighbor archetype **(A)** and crab *Charybdis japonica* from dominant reef-dependent archetype **(B)** in each habitat under three DO levels of Experiment I. Data are expressed as the mean ± SEs and analyzed by the Kruskal–Wallis test, followed by a *post-hoc* multiple comparison test between three DO levels in the same habitat (α = 0.05). Significant differences are indicated by different letters.

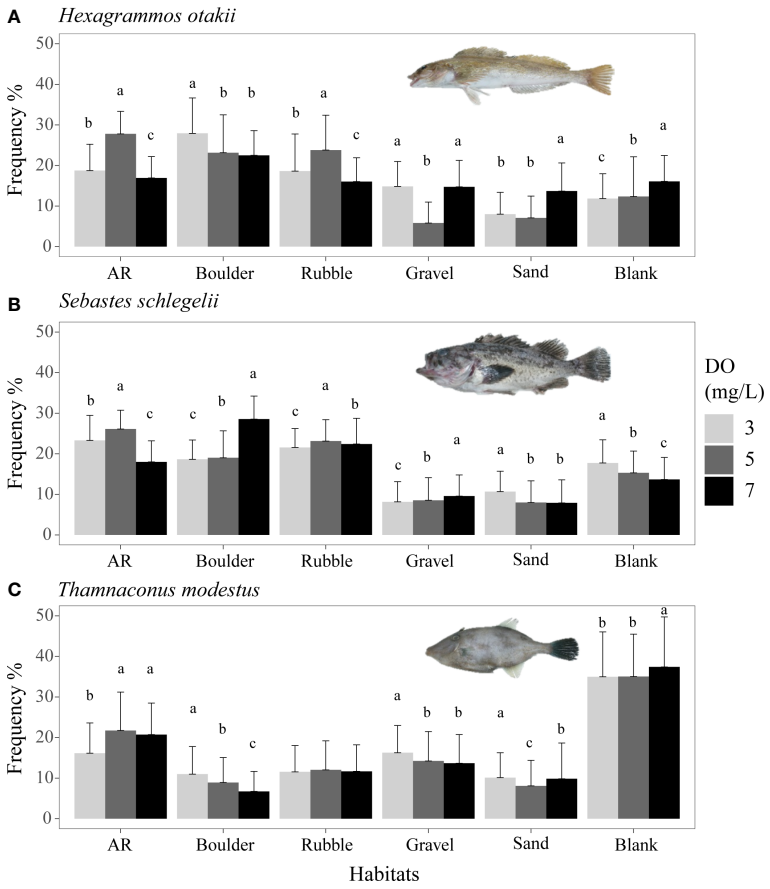

FIGURE 4
Mean distribution frequency of rockfish *Hexagrammos otakii* **(A)** and *Sebastes schlegelii* **(B)** both from dominant reef-dependent archetype, and filefish *Thamnaconus modestus* from DO-independent reef-neighbor archetype **(C)** for each habitat under three DO concentrations of Experiment I. These results are from Experiment I. Data were analyzed by the Kruskal–Wallis test, followed by a *post-hoc* multiple comparison test comparing the three DO levels in each habitat (α = 0.05). Significant differences are indicated by different letters.

avoid low oxygen in all DO combinations (p <0.05), with the frequency of the strong-capacity groups (behavior groups m = 1 and 2) being 79% to 100% (Figure 9). *H. otakii* showed a significantly higher frequency of strong avoidance (m = 1 and 2) in certain combinations: 78% (1 versus 3 mg/L), 56% (1 versus 5), and 83% (1 versus 7) (Figure 8), but showed no significant difference in avoidance between 3 versus 5, 3 versus 7, and 5 versus 7 mg/L DO combinations. This is seen as the gray bars being centered and spread out over the behavior groups in the lower three panels of Figure 8. The flatfish *P. yokohamae* also demonstrated avoidance like *H. otakii*: strong capacity to avoid 1 mg/L but "weak" or "no" capacity to avoid low oxygen in the trials including 3, 5, and 7 mg/L. As with *H. otakii*, the avoidance of *P. yokohamae* also showed gray bars to the left for the top 3 panels and centered and spread out for the lower three panels (Figure 10).

Avoidance with ARs

Overall, the availability of ARs affected avoidance, and therefore exposure to low DO concentrations, for the habitat-preferring rockfishes but was not a significant factor affecting exposure for the flatfish.

The presence of ARs caused *H. otakii* and *S. schlegelii* to reduce their avoidance capacity. However, *H. otakii* continued avoidance in the presence of ARs at 1 versus 3 mg/L and 1 versus 5 mg/L, but increased its exposure when the lowest DO was 3 or 5 (black bars in Figure 8). The decrease in avoidance at 1 versus 7 is inconsistent with the general pattern of *H. otakii* continuing to avoid very low DO.

S. schlegelii increased its exposure to low DO with the presence of ARs at all levels of DO, even when the lowest DO was 1 mg/L (black bars to the right of gray bars in all panels, Figure 9). There was also an exception with *S. schlegelii* with ARs causing increased avoidance capacity at 5 versus 7. In this case, as opposed to the exception with 1 versus 7 for *H. otakii*, the consequences of higher exposure to lower DO concentrations are small because 5 mg/L is still high enough for minimal physiological effects. Finally, the avoidance of the flatfish *P. yokohamae* was unaffected by the presence of ARs (gray and black bars showed the same pattern from left to right in each panel, Figure 10).

Discussion

Effects of low DO on fish have focused on growth, mortality, reproduction, and behavioral responses of individuals in laboratory experiments (Shimps et al., 2005; Portner and Peck, 2010; Wang et al., 2016; French and Wahl, 2018). Some exploration of interactions

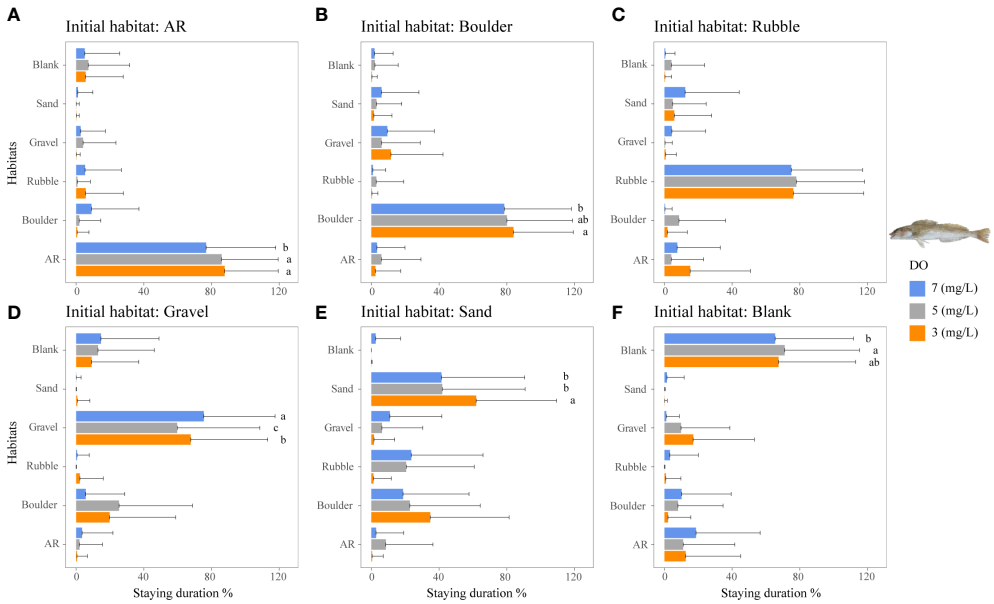

FIGURE 5
Mean staying duration percentage of the rockfish *H. otakii* from dominant reef-dependent archetype under the three DO concentrations of Experiment I. Data for the special case of staying duration that used the time spent in the same habitat type as the individual was started from (i.e., fidelity) were analyzed by the Kruskal–Wallis test, followed by a *post-hoc* multiple comparison test comparing the three DO levels (α = 0.05). Significant differences are indicated by different letters. **(A–F)** Initial starting habitat is from AR, boulder, rubble, gravel, sand, and blank, respectively.

between DO and temperature (Roman et al., 2019) using a variety of endpoints such as growth and mortality (McNeill and Perry, 2006; McBryan et al., 2013; Marcek et al., 2020). There are a few examples of how habitat usage and affinity can be altered by low DO and how habitat can influence avoidance of low DO. In the field, both cases involve how habitat and avoidance behavior combine to determine how individuals use their preferred habitats and their exposure to low DO concentrations. Our experiments were designed to directly address movement behavior as the interplay between habitat usage and avoidance of low DO.

Our results showed several important species differences in how reef-dependent species behaviorally respond and use preferred habitats under low DO. In Experiment I, lower DO concentrations decreased the usage of preferred habitats by the sea cucumber (AR,

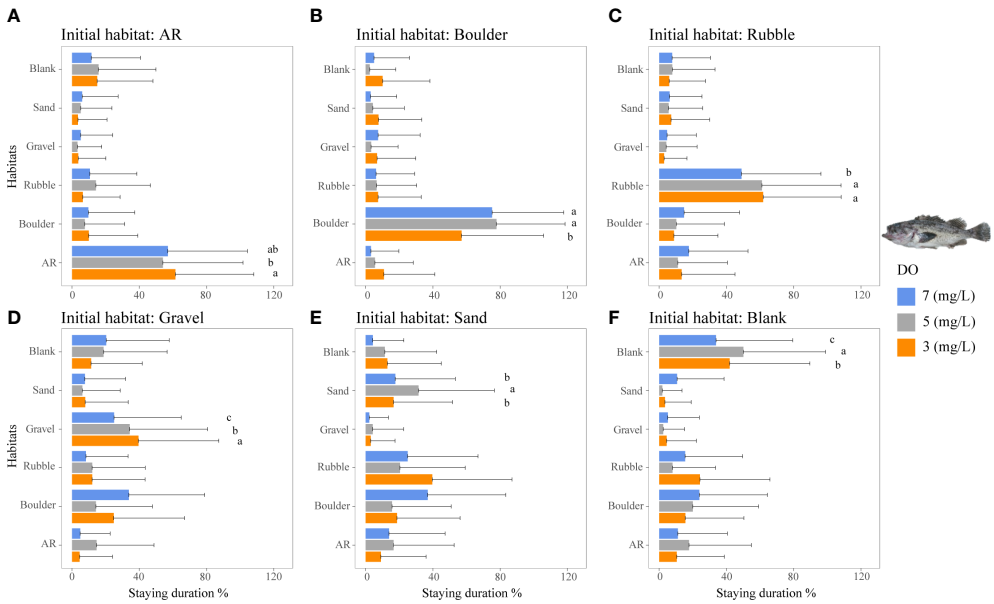

FIGURE 6
Mean staying duration percentage of the rockfish *S. schlegelii* from dominant reef-dependent archetype under the three DO concentrations of Experiment I. Data for the special case of staying duration that used the time spent in the same habitat type as the individual was started from (i.e., fidelity) were analyzed by the Kruskal–Wallis test, followed by a *post-hoc* multiple comparison test comparing the three DO levels (α = 0.05). Significant differences are indicated by different letters. **(A–F)** Initial starting habitat is from AR, boulder, rubble, gravel, sand, and blank, respectively.

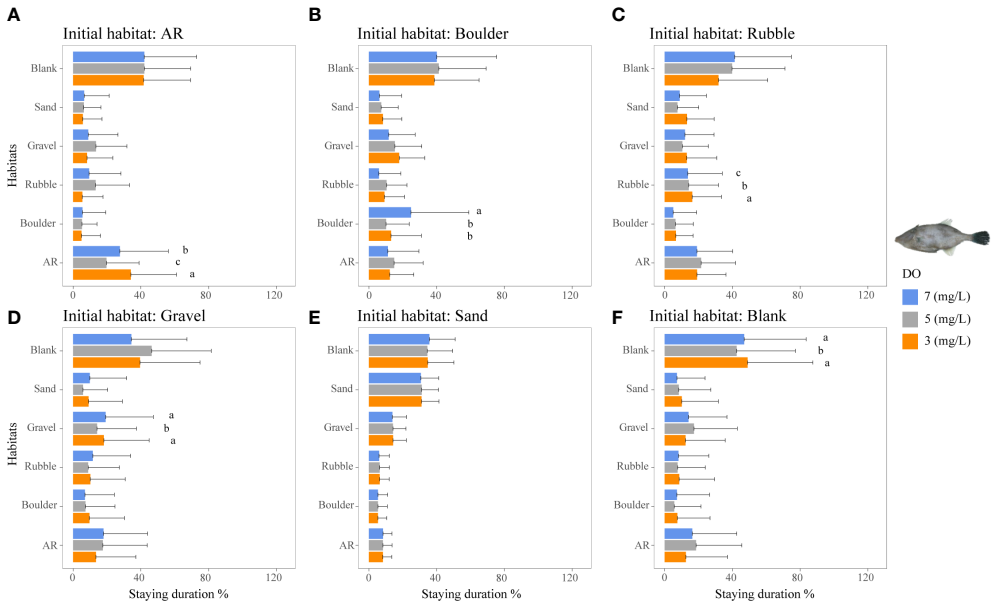

FIGURE 7
Mean staying duration percentage of the filefish *T. modestus* from DO-independent reef-neighbor archetype for the three DO concentrations in Experiment I. Data for the special case of staying duration that used the time spent in the same habitat type as the individual was started from (i.e., fidelity) were analyzed by the Kruskal–Wallis test, followed by a *post-hoc* multiple comparison test comparing the three DO levels (α = 0.05). Significant differences are indicated by different letters. **(A–F)** Initial starting habitat is from AR, boulder, rubble, gravel, sand, and blank, respectively.

boulders, and rubble areas) and by the filefish (blank and AR areas) but increased the dependence on preferred habitats (AR, boulders, and rubble) for the two rockfish species. Low DO did not affect how the crab species used their habitats. The low oxygen effect was much stronger for the two rockfishes that showed a high degree of preference for specific habitats compared to the relatively small DO effect for the generalist filefish. Experiment II showed that all three species examined avoided hypoxic water (1 mg/L DO). Differences among species arose with choices between moderate (3 and 5 mg/L) and high DO concentrations (7 mg/L). The rockfish *S. schlegelii* continued to avoid lower DO when given choices involving pairs of 3, 5, and 7 mg/L. In contrast, *H. otakii* and the flatfish showed weaker avoidance of lower DO concentrations. As with habitat usage in Experiment I, the effects of low DO on avoidance in Experiment II were stronger for the two rockfish species with strong habitat preferences than for the more generalist flatfish.

Effects of hypoxia on habitat usage

Hypoxia had the most significant impact on habitat usage for the sea cucumber, *S. japonicus*. When the DO was decreased to 3 mg/L, many sea cucumbers lost their moving ability and gathered in the initial introduced position in the tank. This phenomenon is consistent with Zhou et al. (2018), who explored how hypoxia affects the behavior of the sea cucumber, *Apostichopus japonicus*. At the other extreme, the habitat usage by the crab *C. japonica* was not influenced by low DO, which may be related to its strong hypoxia tolerance, flexible usage of various habitat types like rock and sand (Yatsuya and Matsumoto, 2021), and its territorial nature (Fowler and McLay, 2013; Yu et al., 2020). Zhu et al. (2022) examined how complex habitats can reduce the territorial behavior of crabs. After the crabs were introduced into the tank, we observed some transitory fighting and competitive behavior for territory in the gravel, sand, and blank habitat sections; some individuals would hide in the crevices of the boulders or bury themselves in the sand. All or some combination of these traits would lead to the crab being unresponsive to low DO.

Fish may exhibit a range of physiological responses as adaptations to hypoxic conditions (Domenici et al., 2017). For example, some species exposed to low DO accelerate oxygen uptake by the gills to facilitate systemic blood transport (Randall, 1982; Richards, 2009). While these adaptive measures provide short-term relief from the effects of hypoxia, if hypoxia persists, fish may decrease their metabolic rate by reducing aerobic activities (Claireaux and Lefrançois, 2007; Pörtner and Farrell, 2008). Studies have demonstrated the limiting effects of hypoxia on fish swimming behavior, such as decreased swim speed and reduced caudal fin swing frequency (Domenici et al., 2017; Messina-Henríquez et al., 2022). This reduction in mobility and physiology (Jones, 1971; Jourdan-Pineau et al., 2010) may have contributed to the increased stay duration of the reef fish species observed in Experiment I. The two rockfish species displayed strong preferences for their preferred habitats. The staying duration of the less mobile *H. otakii* in AR habitat (highly preferred) increased with lower DO concentrations. Approximately 5 mg/L DO showed the largest use values for ARs, but 3 mg/L DO had the longest staying duration. The persistence to use AR under 3 mg/L could be due to the relatively large *H. otakii* occupying sufficient spaces to impede other individuals from swimming into the AR section. While low DO also increased the staying duration of the more mobile *S. schlegelii*, they showed a range of responses in other preferred habitats.

The behavioral responses of fish to hypoxia may include a trade-off between reducing swimming activity to reduce oxygen demand and increasing swimming activity to move to more oxygenated waters

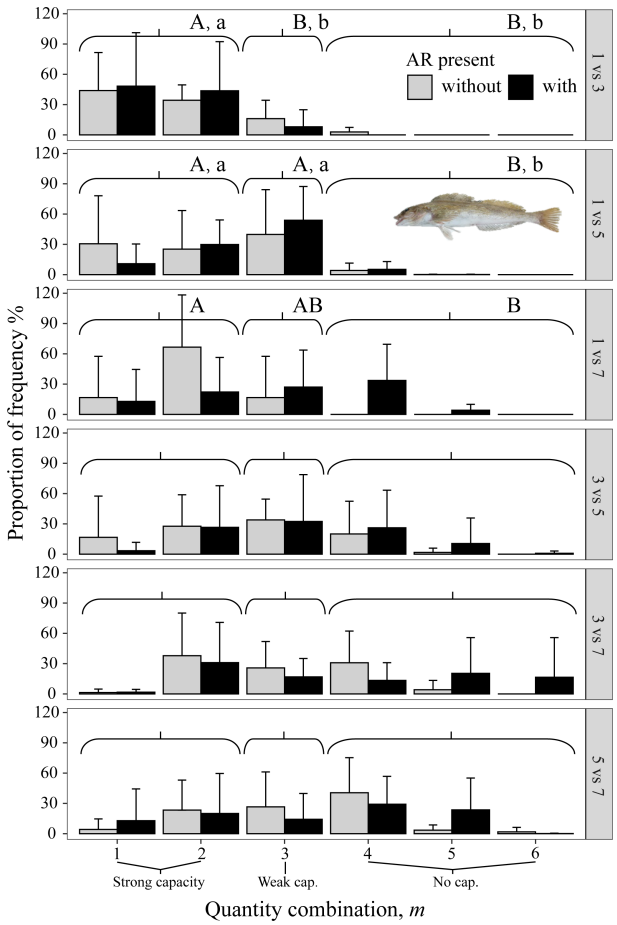

FIGURE 8
Mean percent of each of the six possible values for *m* that codes the degree of avoidance of the lower DO side for rockfish *H. otakii* from dominant reef-dependent archetype in Experiment II, with ARs present in the lower DO side (black bars) and without ARs (gray bars). Each panel shows the results for each pairwise combination of low DO in one side and higher DO on the other side of the tank. Data were analyzed by the Kruskal–Wallis test, followed by a *post-hoc* multiple comparison test comparing the three categories of avoidance capacity: strong (*m* = 1 and 2), weak (*m* = 3), and none (*m* = 4, 5, and 6) across DO levels for each pairwise DO combination (α = 0.05). Significant differences are indicated by different letters (lower case for ARs present and upper case for control).

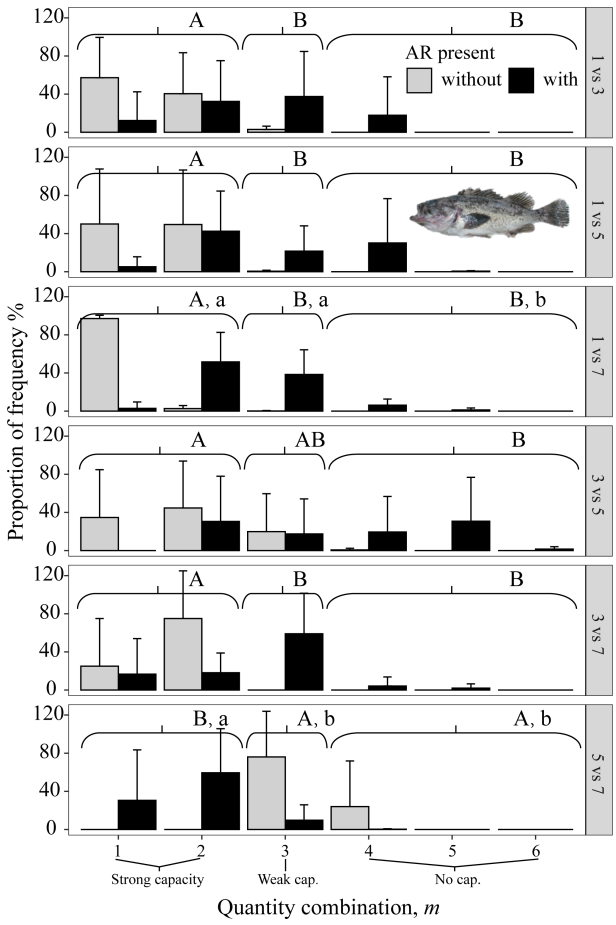

FIGURE 9
Mean percent of each of the six possible values for *m* that codes the degree of avoidance of the lower DO side for rockfish *S. schlegelii* from dominant reef-dependent archetype in Experiment II, with ARs present in the lower DO side (black bars) and without ARs (gray bars). Each panel shows the results for each pairwise combination of low DO in one side and higher DO on the other side of the tank. Data were analyzed by the Kruskal–Wallis test, followed by a *post-hoc* multiple comparison test comparing the three categories of avoidance capacity: strong (*m* = 1 and 2), weak (*m* = 3), and none (*m* = 4, 5, and 6) across DO levels for each pairwise DO combination (α = 0.05). Significant differences are indicated by different letters (lower case for ARs present and upper case for control).

(Domenici et al., 2000; Lefrançois et al., 2009; Zhang et al., 2010). How reducing activity to lower metabolism combines with avoidance behavior that involves increasing activity is not well documented and is likely dependent on species and conditions (Diaz and Rosenberg, 1996; Domenici et al., 2007; Herbert et al., 2011). Our experimental results confirmed inter-specific differences in movement responses to hypoxia. In contrast to the rockfish species, the habitat generalist filefish *T. modestus* was curious about the AR area in the tank. Many filefish individuals first touched the AR with their rostral side, swam around the reef two or three times, and then left that section and entered more-open sections like blank, sand, or gravel habitats. After seemingly traversing all habitat types, they sometimes returned to the AR section and repeated without ever entering the interior structure of the AR. Under the 3 mg/L DO condition, only filefish individuals frequently swam to the water surface for breathing, which is consistent with the behavioral characteristics of fish with strong swimming capacity under hypoxic stress (Domenici et al., 2013); the two rockfishes were rarely observed swimming near the water surface.

Effects of artificial reef on exposure to low oxygen

In large-scale sea areas, hypoxic conditions may change gradually and can be distributed in patches (LaBone et al., 2021). A relatively stationary and stable low-oxygen location allows most organisms, especially fish, to avoid this area. In contrast, an uneven spatial distribution of local hypoxic areas or local areas that vary in intensity over time would result in individuals having to constantly respond to changing DO conditions as they swim. Our study examined the effects of the presence of AR, a preferred habitat for many species, on

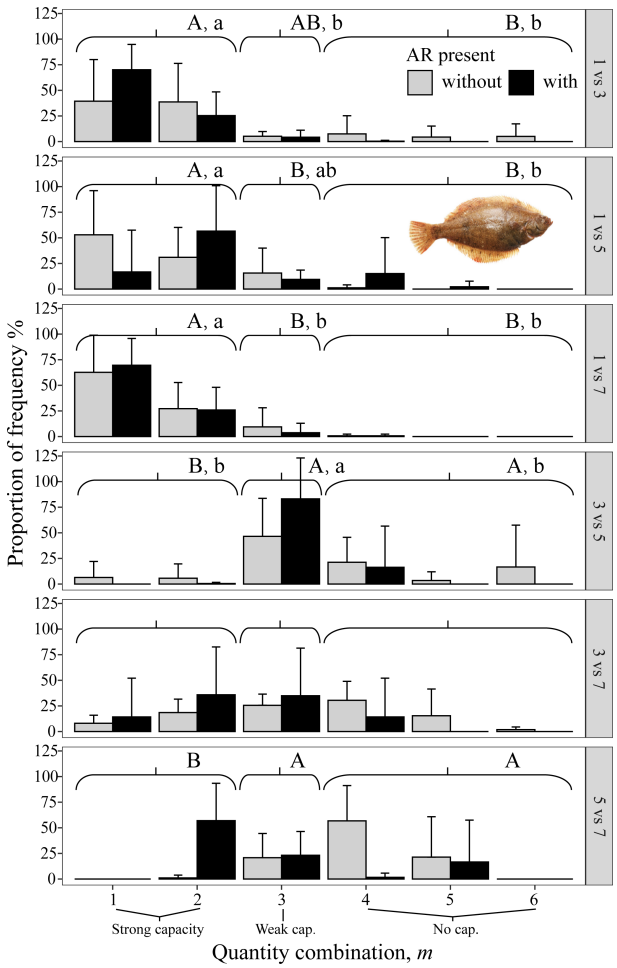

FIGURE 10
Mean percent of each of the six possible values for *m* that codes the degree of avoidance of the lower DO side for the flatfish *P. yokohamae* from DO-independent reef-neighbor archetype in Experiment II, with ARs present in the lower DO side (black bars) and without ARs (gray bars). Each panel shows the results for each pairwise combination of low DO in one side and higher DO on the other side of the tank. Data were analyzed by the Kruskal–Wallis test, followed by a *post-hoc* multiple comparison test comparing the three categories of avoidance capacity: strong (*m* = 1 and 2), weak (*m* = 3), and none (*m* = 4, 5, and 6) across DO levels for each pairwise DO combination (α = 0.05). Significant differences are indicated by different letters (lower case for ARs present and upper case for control).

avoidance when faced with two DO conditions. This implies how ARs affect the exposure of individuals to low DO. We used a range of DO values representative of the values observed in the field.

Many studies have confirmed the hypoxia avoidance behavior of organisms relative to high DO values (Domenici et al., 2007). Less definitive is when individuals are given choices between hypoxia and moderate DO and moderate DO and high DO conditions. Meyer-Gutbrod et al. (2021) investigated the shifts in the vertical distributions of rock reef fish species in the Southern California Channel Islands in response to hypoxia and showed that 19 of 23 species of fish shifted to a shallower depth. Craig (2012) detected aggregation patterns of many species in nearby oxygenated refuge habitats when hypoxia was most severe. Campbell and Rice (2014) also summarized that fish densities may increase in nearshore oxygenated refuges when hypoxic conditions expand.

However, the effects of the presence of preferred habitats on the capacity for hypoxia avoidance are still relatively unknown for many habitat-dependent species. Mitamura et al. (2021) tracked tagged marbled flatfish and found that 36% of the individuals were still distributed in shallow water around an AR despite warm waters. They suggested this phenomenon was related to the high prey conditions associated with ARs. Rasmuson et al. (2021) used an acoustic telemetry array to monitor the movement trajectories of the deacon rockfish (*Sebastes diaconus*) for 11 months at a nearshore rocky reef area. They found that the resident deacon rockfish were resistant to moving away from the local reef area and that hypoxia resulted in individuals using more rugose habitats during the daytime. In our study, we detected that AR influenced the capacity for hypoxia avoidance of the two rockfish species, although to different degrees. The presence of ARs caused *H. otakii* and *S. schlegelii* to reduce their avoidance capacity, with *H. otakii* maintaining strong avoidance at 1 mg/L and diminished avoidance when the lower DO was 3 or 5 mg/L, while the more uniformly reduced avoidance of *S. schlegelii* would generally result in increased exposure. Our results agreed with Rasmuson et al. (2021) and showed that hypoxia directly increased the staying duration of our rockfish species when in AR, boulders, and rubble sections under the light condition, and the capacity of hypoxia avoidance of the rockfishes was influenced (generally reduced) by the presence of ARs. Because we did not use baits in the experimental apparatus, the effect of AR can be viewed as potentially indicative of habitat dependence and avoidance relevant to field conditions.

Responses of reef-dependent species to changing ocean conditions

Documenting how hypoxia affects habitat usage and how the presence of preferred habitat (e.g., ARs) can influence avoidance and therefore exposure can inform future studies and management. Examining the effects of low DO levels on habitat usage allows us to make a precautionary estimate of how low DO may reduce the availability of preferred habitats. Anthropogenic climate change is predicted to increase the frequency and extent of hypoxia (Hughes et al., 2020). Thus, this information can be used to assess changes in habitat, as preferred habitats may decline simultaneously with increasing hypoxia. ARs were preferred for several species in our experiments and are a management tool for enhancing stocks. The presence of ARs weakened the hypoxia-avoidance capacity of the strong habitat-affinity rockfish species, and in different directions for the two species with moderate DO concentrations (i.e., 3 and 5 mg/L). The low oxygen effect was much stronger for the two rockfishes that showed a high degree of preference for specific habitats compared to the relatively small DO effect for the generalist filefish. Experiment II showed that all three fish species examined avoided hypoxic water (1 mg/L DO). Differences among species arose with choices between moderate (3 and 5 mg/L) and high DO concentrations (7 mg/L). Further, crab movement behavior showed little sensitivity to low DO, and some relationships of habitat usage (two rockfish species) were dome-shaped as a function of DO. Anticipating where low DO will occur can ensure the placement of ARs in locations likely to be of high habitat quality in the future. Similarly, knowing how ARs will affect avoidance and exposure to low DO is also useful to select locations

where species are productive. Simultaneous examination of complex habitats and low oxygen is essential to consider the tradeoff between placing AR in the best habitat that may also experience hypoxia versus less optimal habitats with little hypoxia. It is especially important to consider such tradeoffs under likely future climate conditions.

Species may be able to cope with hypoxic stress associated with their habitats through phenotypic plasticity, and extreme types (not the average) of individuals can show more capacity for avoidance and higher tolerance (McBryan et al., 2013). Such variation occurs because of among-individual differences in phenotypes that affect their physiology, behavior, and ability to acclimate. Many teleost fish species associated with coral reefs have been investigated for their variability in physiological tolerance to hypoxia (Nilsson and Östlund-Nilsson, 2004; Nilsson et al., 2010; Wong et al., 2018). Zhu et al. (2013) reviewed the hypoxia adaptation of fish through examination of variation in proteins and signaling pathways. Our results can directly inform the adaptation potential of behavioral movements related to the usage of preferred habitats under hypoxia and avoidance of low DO, so reef managers can consider how hypoxia could affect reef-dependent species distribution and productivity.

Design, location selection, and management of reefs may increasingly have to consider hypoxia as a factor. The behavior of target species, as well as unwanted species (e.g., sea stars) in some cases (Hayes and Sliwa, 2003), can be used with other information to infer the performance of ARs in the planning stages and after deployment. In our experiments, the dependence of the rockfish species on ARs was strengthened under low DO with likely increased exposure to low DO concentrations, while the dependence of the sea cucumber was weakened, but individuals changed their behavior to gather in the center of the tank. Experiment II showed that the presence of ARs reduced the hypoxia-avoidance capacity of the rockfish species for low DO (1 mg/L). but with an important difference at higher DO concentrations: *H. otakii* avoidance was relatively unaffected compared to no AR present, whereas the avoidance of *S. schlegelii* continued to be diminished. ARs to enhance fisheries have been deployed in areas that experience hypoxia. Examples include the northern Gulf of Mexico continental shelf adjacent to the Mississippi River (Rabalais and Turner, 2019), the Gulf of Finland and deep basins of the Baltic Sea (Kõuts et al., 2021), the western Bohai Sea in China (Wei et al., 2019), and the northeastern area off the Changjiang Estuary (Wei et al., 2021a). The ARs in these systems can affect the local trophic dynamics on or in the vicinity of the ARs (Reeves et al., 2018; Plumlee et al., 2020; Wang et al., 2022), and this may also need to be incorporated into assessments of hypoxia effects on reef layouts, locations, and performance. While hypoxic conditions are a major consideration, sublethal DO concentrations are also important. Many laboratory studies document that DO concentrations between 2 and 5 often result in less avoidance (i.e., significant exposure), and individuals show reduced growth and fecundity (Uphoff et al., 2011; LaBone et al., 2021). Our study showed that the presence of ARs would likely increase the exposure of the two rockfish species to 3 mg/L. Therefore, both hypoxia and higher (moderate) DO concentrations should be part of the design and assessment of performance for ARs.

In addition to how AR locations relate to low DO areas, the connectedness among ARs should also be considered. Based on our results (Experiment I) showing the prolonged staying duration by rock fishes in their preferred habitats, we propose that reef managers consider ways to increase the connectivity of ARs between low and high-oxygen areas. Highly connected AR layouts may help rockfish avoid low DO concentrations while maintaining the overall performance of the ARs. The effective distances between AR monomers are determined by the overall ecological connectivity provided by reef monomers, natural reefs, and the spatial distribution of other habitat types (Logan and Lowe, 2018; Reeds et al., 2018). If the effective distances were considered and adjusted at the design of the ARs or by adding strategic new ARs after operation, corridors that encourage movement among ARs under hypoxia could minimize the low DO effects. Additional experiments like Experiment II that have ARs with both low and high DO conditions, combined with ecological modeling (e.g., Campbell et al., 2011), would further aid in designing AR-centric escape corridors.

Conclusion

Continued eutrophication of coastal waters and global climate change will increase the frequency and scope of hypoxic events (Rabalais et al., 2010). Reef-dependent species typically utilize multiple preferred habitat types that are patchily distributed and form a complex seascape of habitats (Rilov et al., 2007; Huntington et al., 2010). Our study confirmed previous results on the habitat preferences of multiple species that use reef habitats to various degrees. Two laboratory experiments explored the effect of low oxygen on habitat utilization when organisms are faced with multiple habitat types and the effect of the presence of ARs on movement behavior related to avoidance capacity. Taken together, this study indicated that hypoxia would increase the habitat dependence of the sea cucumber *S. japonicus*, two rockfishes *S. schlegelii* and *H. otakii*, and the habitat use of the filefish *T. modestus* in more expansive waters but have no significant impact on the crab *C. japonica*. The presence of ARs on the low-oxygen side enhanced the exposure to low DO for the rockfish *S. schlegelii*, followed by *H. otakii*, and slightly influenced the flatfish *P. yokohamae*. Our study adds novel knowledge and evidence to the behavioral responses to hypoxia of reef-dependent species that use complex habitats. The results provide information for assessing the ecological effects and potential for adaptation through behavioral movement for key reef-dependent species under the increasing overlap of ARs and hypoxia anticipated in the future with more ARs being deployed and climate change amplifying hypoxia.

Data availability statement

The original contributions presented in the study are included in the article/Supplementary Material. Further inquiries can be directed to the corresponding authors.

Ethics statement

The animal study was reviewed and approved by Institutional Animal Care and Use Committee of Ocean University of China.

Author contributions

HY came up with the main ideas, conducted all experiments, and wrote the manuscript. GF conducted experiments, offer proposal for the experiment design, and made biological measurements of species. KR offered constructive comments and ideas, instructed to tackle with problems of analysis, revised and edited this manuscript. JL conducted the experiments and look after the experimental species. JF and HW gave constructive ideas and revised the structure and contents of this article. QC offered valuable references and examined statistics test. YT and TZ applied for the research project, offered funds of this study, offered valuable suggestion, and revised this article. All authors listed have made a substantial, direct, and intellectual contribution to the work and approved it for publication.

Funding

This research was supported by the National Key R&D Program of China (2019YFD0901301), the National Natural Science Foundation of China (Grant No. 42106102), the Primary Research and Development Plan of Guangxi Province (Grant No. 2021AB34014), and the Qingdao Postdoctoral Application Research Project (Grant No. QDBSH20220201045). The funders had no role in study design, data collection and analysis, decision to publish, or preparation of the manuscript.

Acknowledgments

We thank all scientific staffs and crew members of the Lab of Marine Fisheries Technology and Yantai Tianyuan Aquaculture Company for their assistance in experiments.

Conflict of interest

The authors declare that the research was conducted in the absence of any commercial or financial relationships that could be construed as a potential conflict of interest.

Publisher's note

Supplementary material

The Supplementary Material for this article can be found online at: https://www.frontiersin.org/articles/10.3389/fmars.2023.1109523/full#supplementary-material

References

Bianchi, T., DiMarco, S., Cowan, J., Hetland, R., Chapman, P., Day, J., et al. (2010). The science of hypoxia in the northern gulf of Mexico: A review. *Sci. Total Environ.* 408, 1471–1484. doi: 10.1016/j.scitotenv.2009.11.047

Breitburg, D. L., Baumann, H., Sokolova, I. M., and Frieder, C. A. (2019). "Multiple stressors -forces that combine to worsen deoxygenation and its effects," in *Ocean deoxygenation: Everyone's problem. causes, impacts, consequences and solutions*. Eds. D. D. A. Laffoley and J. M. Baxter (Gland: IUCN), 225–247.

Breitburg, D. L., Levin, L. A., Oschlies, A., Grégoire, M., Chavez, F. P., Conley, D. J., et al. (2018). Declining oxygen in the global ocean and coastal waters. *Science* 359, eaam7240. doi: 10.1126/science.aam7240

Caddy, J. F. (1993). Toward a comparative evaluation of human impacts on fishery ecosystems of enclosed and semi-enclosed seas. *Rev. Fish. Sci.* 1, 57–95. doi: 10.1080/10641269309388535

Campbell, L. A., and Rice, J. A. (2014). Effects of hypoxia-induced habitat compression on growth of juvenile fish in the neuse river estuary, north Carolina, USA. *Mar. Ecol. Prog. Ser.* 497, 199–213. doi: 10.3354/meps10607

Campbell, M. D., Rose, K. A., Boswell, K., and Cowan, J. (2011). Individual-based modeling of an artificial reef fish community: Effects of habitat quantity and degree of refuge. *Ecol. Model.* 222, 3895–3909. doi: 10.1016/j.ecolmodel.2011.10.009

Claireaux, G., and Lefrançois, C. (2007). Linking environmental variability and fish performance: integration through the concept of scope for activity. *Philos. Trans. R. Soc B-Biol. Sci.* 362, 2031–2041. doi: 10.1098/rstb.2007.2099

Craig, J. K. (2012). Aggregation on the edge: Effects of hypoxia avoidance on the spatial distribution of brown shrimp and demersal fishes in the northern gulf of Mexico. *Mar. Ecol. Prog. Ser.* 445, 75–95. doi: 10.3354/meps09437

David, L. T., and David, B. E. (2000). Effects of hypoxia on an estuarine predator-prey interaction: Foraging behavior and mutual interference in the blue crab callinectes sapidus and the infaunal clam prey mya arenaria. *Mar. Ecol. Prog. Ser.* 196, 221–237. doi: 10.3354/meps196221

Diaz, R. J., and Rosenberg, R. (1996). Marine benthic hypoxia: A review of its ecological effects and the behavioural responses of benthic macrofauna. *Oceanographic literature Rev.* 12, 1250.

Diaz, R. J., and Rosenberg, R. (2008). Spreading dead zones and consequences for marine ecosystems. *Science* 321, 926–929. doi: 10.1126/science.1156401

Domenici, P., Herbert, N. A., Lefrançois, C., Steffensen, J. F., and McKenzie, D. J. (2013). "The effect of hypoxia on fish swimming performance and behaviour," in *Swimming physiology of fish: Towards using exercise to farm a fit fish in sustainable aquaculture*. Eds. A. P. Palstra and J. V. Planas (Berlin, Heidelberg: Springer Berlin Heidelberg Press) 129–159. doi: 10.1007/978-3-642-31049-2_6

Domenici, P., Lefrançois, C., and Shingles, A. (2007). Hypoxia and the antipredator behaviours of fishes. *Philos. Trans. R. Soc B-Biol. Sci.* 362, 2105–2121. doi: 10.1098/rstb.2007.2103

Domenici, P., Steffensen, J. F., and Batty, R. S. (2000). The effect of progressive hypoxia on swimming activity and schooling in Atlantic herring. *J. Fish Biol.* 57, 1526–1538. doi: 10.1111/j.1095-8649.2000.tb02229.x

Domenici, P., Steffensen, J. F., and Marras, S. (2017). The effect of hypoxia on fish schooling. *Philos. Trans. R. Soc B-Biol. Sci.* 372, 236–249. doi: 10.1098/rstb.2016.0236

Eby, L., and Crowder, L. (2002). Hypoxia-based habitat compression in the neuse river estuary: context-dependent shifts in behavioral avoidance thresholds. *Can. J. Fish. Aquat. Sci.* 59, 952–965. doi: 10.1139/F02-067

Fan, W., Pan, D., Xiao, C., Lin, T., Pan, Y., and Chen, Y. (2019). Experimental study on the performance of an innovative tide-induced device for artificial downwelling. *Sustainability* 11 (19), 1–23. doi: 10.3390/su11195268

Fowler, A. E. , and McLay, C. L. (2013). Early stages of a new Zealand invasion by charybdis japonica (A. Milne-Edwards 1861) (Brachyura: Portunidae) from Asia: Population demography. *J. Crustac. Biol.* 33, 224–234. doi: 10.1163/1937240X-00002127

French, C. G., and Wahl, D. H. (2018). Influences of dissolved oxygen on juvenile largemouth bass foraging behaviour. *Ecol. Freshw. Fish* 27, 559–569. doi: 10.1111/eff.12370

Gunderson, A. R., Armstrong, E. J., and Stillman, J. H. (2016). Multiple stressors in a changing world: the need for an improved perspective on physiological responses to the dynamic marine environment. *Annu. Rev. Mar. Sci.* 8, 357–378. doi: 10.1146/annurev-marine-122414-033953

Hayes, K. R., and Sliwa, C. (2003). Identifying potential marine pests–a deductive approach applied to Australia. *Mar. pollut. Bull.* 46, 91–98. doi: 10.1016/S0025-326X(02)00321-1

Herbert, N. A., Skjæraasen, J. E., Nilsen, T., Salvanes, A. G. V., and Steffensen, J. F. (2011). The hypoxia avoidance behaviour of juvenile Atlantic cod (Gadus morhua l.)

depends on the provision and pressure level of an O2 refuge. *Mar. Biol.* 158, 737–746. doi: 10.1007/s00227-010-1601-7

Hrycik, A. R., Almeida, L. Z., and Höök, T. O. (2017). Sub-Lethal effects on fish provide insight into a biologically-relevant threshold of hypoxia. *Oikos* 126, 307–317. doi: 10.1111/oik.03678

Hughes, D., Alderdice, R., Cooney, C., Kuhl, M., Pernice, M., Voolstra, C., et al. (2020). Coral reef survival under accelerating ocean deoxygenation. *Nat. Clim. Change* 10, 296–307. doi: 10.1038/s41558-020-0737-9

Huntington, B. E., Karnauskas, M., Babcock, E. A., and Lirman, D. (2010). Untangling natural seascape variation from marine reserve effects using a landscape approach. *PloS One* 5, e12327. doi: 10.1371/journal.pone.0012327

Jones, D. R. (1971). The effect of hypoxia and anaemia on the swimming performance of rainbow trout (Salmo gairdneri). *J. Exp. Biol.* 55, 541–551. doi: 10.1242/jeb.55.2.541

Jorissen, H., and Nugues, M. M. (2021). Coral larvae avoid substratum exploration and settlement in low-oxygen environments. *Coral Reefs.* 40, 31–39. doi: 10.1007/s00338-020-02013-6

Jourdan-Pineau, H., Dupont-Prinet, A., Claireaux, G., and McKenzie, D. J. (2010). An investigation of metabolic prioritization in the European Sea bass, dicentrarchus labrax. *Physiol. Biochem. Zool.* 83, 68–77. doi: 10.1086/648485

Kõuts, M., Maljutenko, I., Elken, J., Liu, Y., Hansson, M., Viktorsson, L., et al. (2021). Recent regime of persistent hypoxia in the Baltic Sea. *Environ. Res. Commun.* 3, 075004. doi: 10.1088/2515-7620/ac0cc4

LaBone, E. D., Rose, K. A., Justic, D., Huang, H., and Wang, L. (2021). Effects of spatial variability on the exposure of fish to hypoxia: A modeling analysis for the gulf of Mexico. *Biogeosciences* 18, 487–507. doi: 10.5194/bg-18-487-2021

Lagos, M. E., White, C. R., and Marshall, D. J. (2015). Avoiding low-oxygen environments: oxytaxis as a mechanism of habitat selection in a marine invertebrate. *Mar. Ecol. Prog. Ser.* 540, 99–107. doi: 10.3354/meps11509

Lefrançois, C., Ferrari, R. S., Moreira da Silva, J., and Domenici, P. (2009). The effect of progressive hypoxia on spontaneous activity in single and shoaling golden grey mullet liza aurata. *J. Fish Biol.* 75, 1615–1625. doi: 10.1111/j.1095-8649.2009.02387.x

Lemoine, H. R., Paxton, A. B., Anisfeld, S. C., Rosemond, R. C., and Peterson, C. H. (2019). Selecting the optimal artificial reefs to achieve fish habitat enhancement goals. *Biol. Conserv.* 238, 108200. doi: 10.1016/j.biocon.2019.108200

Logan, R. K., and Lowe, C. G. (2018). Residency and inter-reef connectivity of three gamefishes between natural reefs and a large mitigation artificial reef. *Mar. Ecol. Prog. Ser.* 593, 111–126. doi: 10.3354/meps12527

Marcek, B. J., Burbacher, E. A., Dabrowski, K., Winslow, K. P., and Ludsin, S. A. (2020). Interactive effects of hypoxia and temperature on consumption, growth, and condition of juvenile hybrid striped bass. *Trans. Am. Fish. Soc* 149, 71–83. doi: 10.1002/tafs.10210

McBryan, T. L., Anttila, K., Healy, T. M., and Schulte, P. M. (2013). Responses to temperature and hypoxia as interacting stressors in fish: Implications for adaptation to environmental change. *Integr. Comp. Biol.* 53, 648–659. doi: 10.1093/icb/ict066

McNeill, B., and Perry, S. F. (2006). The interactive effects of hypoxia and nitric oxide on catecholamine secretion in rainbow trout (Oncorhynchus mykiss). *J. Exp. Biol.* 209, 4214–4223. doi: 10.1242/jeb.02519

Messina-Henríquez, S., Aguirre, Á., Brokordt, K., Flores, H., Oliva, M., Allen, P. J., et al. (2022). Swimming performance and physiological responses of juvenile cojinoba seriolella violacea in hypoxic conditions. *Aquaculture* 548, 737560. doi: 10.1016/j.aquaculture.2021.737560

Meyer-Gutbrod, E., Kui, L., Miller, R., Nishimoto, M., Snook, L., and Love, M. (2021). Moving on up: Vertical distribution shifts in rocky reef fish species during climate-driven decline in dissolved oxygen from 1995 to 2009. *Glob. Change Biol.* 27, 6280–6293. doi: 10.1111/gcb.15821

Mitamura, H., Nishizawa, H., Mitsunaga, Y., Tanaka, K., Takagi, J., Noda, T., et al. (2021). Attraction of an artificial reef: A migratory demersal flounder remains in shallow water under high temperature conditions in summer. *Environ. Biol. Fishes* 105, 1953–1962. doi: 10.1007/s10641-021-01153-0

Nilsson, G. E., and Östlund-Nilsson, S. (2004). doi: 10.1098/rsbl.2003.0087

Nilsson, G. E., Östlund-Nilsson, S., and Munday, P. L. (2010). Effects of elevated temperature on coral reef fishes: Loss of hypoxia tolerance and inability to acclimate. *Comp. Biochem. Physiol. A-Mol. Integr. Physiol.* 156, 389–393. doi: 10.1016/j.cbpa.2010.03.009

Plumlee, J. D., Dance, K. M., Dance, M. A., Rooker, J. R., TinHan, T. C., Shipley, J. B., et al. (2020). Fish assemblages associated with artificial reefs assessed using multiple gear types in the northwest gulf of Mexico. *Bull. Mar. Sci.* 96, 655–678. doi: 10.5343/bms.2019.0091

Pörtner, H. O., and Farrell, A. P. (2008). Physiology and climate change. *Science* 322, 690–692. doi: 10.1126/science.1163156

Portner, H. O., and Peck, M. (2010). Climate change effects on fishes and fisheries: Towards a cause-and-effect understanding. *J. Fish Biol.* 77, 1745–1779. doi: 10.1111/j.1095-8649.2010.02783.x

Rabalais, N. N., Díaz, R. J., Levin, L. A., Turner, R. E., Gilbert, D., and Zhang, J. (2010). Dynamics and distribution of natural and human-caused hypoxia. *Biogeosciences* 7, 585–619. doi: 10.5194/bg-7-585-2010

Rabalais, N. N., and Turner, R. E. (2019). Gulf of Mexico hypoxia: Past, present, and future. *Limnol. Oceanogr. Bull.* 28, 117–124. doi: 10.1002/lob.10351

Randall, D. (1982). The control of respiration and circulation in fish during exercise and hypoxia. *J. Exp. Biol.* 100, 275–288. doi: 10.1242/jeb.100.1.275

Rasmuson, L. K., Blume, M. T. O., and Rankin, P. S. (2021). Habitat use and activity patterns of female deacon rockfish (Sebastes diaconus) at seasonal scales and in response to episodic hypoxia. *Environ. Biol. Fishes* 104, 535–553. doi: 10.1007/s10641-021-01092-w

Reeds, K. A., Smith, J. A., Suthers, I. M., and Johnston, E. L. (2018). An ecological halo surrounding a large offshore artificial reef: Sediments, infauna, and fish foraging. *Mar. Environ. Res.* 141, 30–38. doi: 10.1016/j.marenvres.2018.07.011

Reeves, D. B., Chesney, E. J., Munnelly, R. T., Baltz, D. M., and Marx, B. D. (2018). Abundance and distribution of reef-associated fishes around small oil and gas platforms in the northern gulf of mexico's hypoxic zone. *Estuaries Coasts* 41, 1835–1847. doi: 10.1007/s12237-017-0349-4

Richards, J. G. (2009). "Chapter 10 metabolic and molecular responses of fish to hypoxia," in *Fish physiology*. Eds. J. G. Richards, A. P. Farrell and C. J. Brauner (Amsterdam, The Netherlands: Academic Press), 443–485. doi: 10.1016/S1546-5098(08)00010-1

Rilov, G., Figueira, W. F., Lyman, S. J., and Crowder, L. B. (2007). Complex habitats may not always benefit prey: Linking visual field with reef fish behavior and distribution. *Mar. Ecol. Prog. Ser.* 329, 225–238. doi: 10.3354/meps329225

Roman, M. R., Brandt, S. B., Houde, E. D., and Pierson, J. J. (2019). Interactive effects of hypoxia and temperature on coastal pelagic zooplankton and fish. *Front. Mar. Sci.* 6. doi: 10.3389/fmars.2019.00139

Rose, K. A., Adamack, A. T., Murphy, C. A., Sable, S. E., Kolesar, S. E., Craig, J. K., et al. (2009). Does hypoxia have population-level effects on coastal fish? musings from the virtual world. *J. Exp. Mar. Biol. Ecol.* 381, S188–S203. doi: 10.1016/j.jembe.2009.07.022

Shimps, E. L., Rice, J. A., and Osborne, J. A. (2005). Hypoxia tolerance in two juvenile estuary-dependent fishes. *J. Exp. Mar. Biol. Ecol.* 325, 146–162. doi: 10.1016/j.jembe.2005.04.026

Steckbauer, A., Duarte, C., Carstensen, J., Vaquer-Sunyer, R., and Conley, D. (2011). Ecosystem impacts of hypoxia: Thresholds of hypoxia and pathways to recovery. *Environ. Res. Lett.* 6, 025003. doi: 10.1088/1748-9326/6/2/025003

Uphoff, J. H., McGinty, M., Lukacovic, R., Mowrer, J., and Pyle, B. (2011). Impervious surface, summer dissolved oxygen, and fish distribution in Chesapeake bay subestuaries: Linking watershed development, habitat conditions, and fisheries management. *North Am. J. Fish Manage.* 31, 554–566. doi: 10.1080/02755947.2011.598384

Vaquer-Sunyer, R., and Duarte, C. M. (2008). Thresholds of hypoxia for marine biodiversity. *Proc. Natl. Acad. Sci.* 105, 15452–15457. doi: 10.1073/pnas.0803833105

Wang, X., Feng, J., Lin, C., Liu, H., Chen, M., and Zhang, Y. (2022). Structural and functional improvements of coastal ecosystem based on artificial oyster reef construction in the bohai Sea, China. *Front. Mar. Sci.* 9. doi: 10.3389/fmars.2022.829557

Wang, S. Y., Lau, K., Lai, K.-P., Zhang, J.-W., Tse, A. C.-K., Li, J.-W., et al. (2016). Hypoxia causes transgenerational impairments in reproduction of fish. *Nat. Commun.* 7, 12114. doi: 10.1038/ncomms12114

Wannamaker, C. M., and Rice, J. A. (2000). Effects of hypoxia on movements and behavior of selected estuarine organisms from the southeastern united states. *J. Exp. Mar. Biol. Ecol.* 249, 145–163. doi: 10.1016/S0022-0981(00)00160-X

Watson, A. (2016). Oceans on the edge of anoxia. *Science* 354, 1529–1530. doi: 10.1126/science.aaj2321

Wei, Q., Wang, B., Yao, Q., Xue, L., Sun, J., Xin, M., et al. (2019). Spatiotemporal variations in the summer hypoxia in the bohai Sea (China) and controlling mechanisms. *Mar. pollut. Bull.* 138, 125–134. doi: 10.1016/j.marpolbul.2018.11.041

Wei, Q., Wang, B., Zhang, X., Ran, X., Fu, M., Sun, X., et al. (2021a). Contribution of the offshore detached changjiang (Yangtze river) diluted water to the formation of hypoxia in summer. *Sci. Total Environ.* 764, 142838. doi: 10.1016/j.scitotenv.2020.142838

Wei, Q., Xue, L., Yao, Q., Wang, B., and Yu, Z. (2021b). Oxygen decline in a temperate marginal sea: Contribution of warming and eutrophication. *Sci. Total Environ.* 757, 143227. doi: 10.1016/j.scitotenv.2020.143227

Weiland, F., van Beek, L., Kwadijk, J., and Bierkens, M. (2012). Global patterns of change in discharge regimes for 2100. *Hydrol. Earth Syst. Sci.* 16, 1047–1062. doi: 10.5194/hess-16-1047-2012

Wong, C. C., Drazen, J. C., Callan, C. K., and Korsmeyer, K. E. (2018). Hypoxia tolerance in coral-reef triggerfishes (Balistidae). *Coral Reefs* 37, 215–225. doi: 10.1007/s00338-017-1649-7

Wu, R. (2002). Hypoxia: From molecular responses to ecosystem responses. *Mar. pollut. Bull.* 45, 35–45. doi: 10.1016/S0025-326X(02)00061-9

Yatsuya, K., and Matsumoto, Y. (2021). Effects of the swimming crab charybdis japonica on sea urchin mesocentrotus nudus grazing: Cage experiments in barren ground and land-based tanks. *Fish. Sci.* 87, 817–826. doi: 10.1007/s12562-021-01555-0

Yu, H., Fang, G., Rose, K. A., Tang, Y., and Song, X. (2022). Examining epibenthic assemblages associated with artificial reefs using a species archetype approach. *Mar. Coast. Fish.* 14, e10206. doi: 10.1002/mcf2.10206

Yu, H., Yang, W., Liu, C., Tang, Y., Song, X., and Fang, G. (2020). Relationships between community structure and environmental factors in xixiakou artificial reef area. *J. Ocean Univ.* 19, 883–894. doi: 10.1007/s11802-020-4298-3

Zhang, J., Gilbert, D., Gooday, A. J., Levin, L., Naqvi, S. W. A., Middelburg, J. J., et al. (2010). Natural and human-induced hypoxia and consequences for coastal areas: Synthesis and future development. *Biogeosciences* 7, 1443–1467. doi: 10.5194/bg-7-1443-2010

Zhou, X., Zhang, X., and Li, W. (2018). Effects of temperature and dissolved oxygen on the survival, activity and the adaptation strategy of metabolism in sea cucumber (Apostichopus japonicus). *J. Fisheries China* 42 (08), 1209–1219.

Zhu, C. D., Wang, Z. H., and Yan, B. (2013). Strategies for hypoxia adaptation in fish species: A review. *J. Comp. Physiol. B* 183, 1005–1013. doi: 10.1007/s00360-013-0762-3

Zhu, B., Zhang, H., Liu, D., Lu, Y., and Wang, F. (2022). Importance of substrate on welfare in swimming crab (Portunus trituberculatus) culture: A territorial behavior perspective. *Aquacult. Rep.* 24, 101113. doi: 10.1016/j.aqrep.2022.101113

frontiers | Frontiers in Marine Science

TYPE Original Research
PUBLISHED 12 June 2023
DOI 10.3389/fmars.2023.1029512

OPEN ACCESS

EDITED BY
Gang Li,
Chinese Academy of Sciences (CAS), China

REVIEWED BY
Pingping Shen,
Yantai University, China
Yan Fang,
Ludong University, China

*CORRESPONDENCE
Xiuxian Song
songxx@qdio.ac.cn

RECEIVED 27 August 2022
ACCEPTED 22 May 2023
PUBLISHED 12 June 2023

CITATION
Zhang Y, Song X and Zhang P (2023) Combined effects of toxic *Karenia mikimotoi* and hypoxia on the juvenile abalone *Haliotis discus hannai*. *Front. Mar. Sci.* 10:1029512. doi: 10.3389/fmars.2023.1029512

Combined effects of toxic *Karenia mikimotoi* and hypoxia on the juvenile abalone *Haliotis discus hannai*

Yue Zhang[1,2], Xiuxian Song[1,2,3,4]* and Peipei Zhang[2]

[1]Laoshan Laboratory, Qingdao, China, [2]CAS Key Laboratory of Marine Ecology and Environmental Sciences, Institute of Oceanology, Chinese Academy of Sciences, Qingdao, China, [3]University of Chinese Academy of Sciences, Beijing, China, [4]Center for Ocean Mega-Science, Chinese Academy of Sciences, Qingdao, China

Eutrophication in aquaculture areas concurrently leads to a high incidence of dissolved oxygen deficiency and toxic algal blooms. The combined effects of hypoxia and typical toxic algae on cultured organisms should be given sufficient consideration. Abalone breeding in China has greatly suffered from hypoxia and toxic *Karenia mikimotoi* blooms for many years. In this study, the individual and combined effects of the toxic dinoflagellate, *K. mikimotoi*, and hypoxia on juvenile abalone were determined based on abalone survival and oxidative stress indicators in their gills, hepatopancreas and hemolymph. The results showed that at a density of 10^6 to 3×10^7 cells/L, *K. mikimotoi* alone had a negligible influence on the survival of juvenile abalone under sufficient dissolved oxygen (DO) conditions. The 24 h-half lethal concentration (LC_{50}) of DO alone for juvenile abalone was 0.75 mg/L in seawater. When *K. mikimotoi* was added at a density of 3×10^6 cells/L, the 24 h-LC_{50} of DO for juvenile abalone significantly increased to 2.59 mg/L, indicating obvious synergistic effects. The individual effects of hypoxia or *K. mikimotoi* on the oxidative stress indicators were limited, and only the superoxide dismutase (SOD) activity in the abalone gills significantly decreased under *K. mikimotoi* stress. However, the combined stress of hypoxia and *K. mikimotoi* led to significant changes in the antioxidant indicators in all tested tissues. The SOD activity in gills and hepatopancreas decreased, while the SOD and catalase (CAT) activity and malondialdehyde (MDA) content in the hemolymph increased due to the combined stress of hypoxia and *K. mikimotoi*. These results illustrated that the synergistic effects of hypoxia and *K. mikimotoi* caused serious oxidative damage in abalone and that the hemolymph exhibited greater sensitivity than did the gills and hepatopancreas. Further investigation found that *K. mikimotoi* increased the oxygen consumption rate in abalone and that hypoxia enhanced the hemolytic toxicity of *K. mikimotoi*. These results revealed that hypoxia and typical toxic algae cause synergistic harm to cultured organisms, which is expected to provide a new understanding of the destructive mechanisms of typical toxic algal blooms in aquacultural areas.

KEYWORDS

hypoxia, *Karenia mikimotoi*, *Haliotis discus hannai*, oxidative stress, synergistic effects

Introduction

Due to climate change and eutrophication, organisms are often threatened by the combined effects of dissolved oxygen (DO) deficiencies and harmful algal blooms (HABs), especially those in aquacultural waters. Global oxygen levels in the ocean and in coastal waters have decreased by 2% annually over the past 50 years, leading to widespread occurrence of hypoxia (Schmidtko et al., 2017). Aquacultural areas are prone to hypoxia due to their high-density farming structure and high organic matter content (Matos et al., 2016; Yang et al., 2021). As aquacultural areas are usually nearshore or in inner bays and involve a weak exchange of water, DO deficiency could occur for a long time. Generally, water with a DO content of less than 2 mg/L is regarded as hypoxic, while in cultured water, biological hypoxia can occur when the DO content is less than 5 mg/L (Gobler and Baumann, 2016; Wu et al., 2016). Hypoxia affects energy metabolism and the immune system, hindering normal physiological activities and even causing the death of organisms. On the other hand, the generally high level of eutrophication in aquacultural waters provides the basis for the formation and maintenance of HABs, making the aquacultural waters a high-frequency area of HABs (Glibert et al., 2005; Heisler et al., 2008). Cultured organisms are threatened by HABs, especially those of toxic dinoflagellates, which can directly poison them. The high density of toxic algae could further aggravate hypoxia through serious oxygen consumption at night and during the decomposition period, making it harder for cultured organisms to survive. Therefore, with this underlying trend of more frequent HAB occurrences and severe hypoxia (Gilbert et al., 2009; Lee et al., 2016; Breitburg et al., 2018), many coastal aquacultural areas have both a high incidence of HABs and hypoxia. The combined effects of hypoxia and toxic algae on cultured organisms should be given sufficient attention.

Karenia mikimotoi is a typical toxic dinoflagellate, and hemolytic toxins are regarded as its main type of poison (Li et al., 2019a; Niu et al., 2021). It was first discovered in Kyoto Bay of Japan in 1935, and then it appeared in many coastal waters around the world, including waters near Japan, South Korea, Britain, France, India, and the US (Li et al., 2019a; Hu et al., 2022). China is the area that was most impacted by *K. mikimotoi* blooms. Since they first appeared in China in 1998, *K. mikimotoi* blooms have occurred more than 120 times and have become an annual disaster; the largest distribution of *K. mikimotoi* was nearly 1.4×10^4 km^2, and its duration ranges from 2 days to 35 days. *K. mikimotoi* blooms usually cause massive amounts of various fish, shellfish and mammals to die, and they have been regarded as the second largest HAB disaster in China (Lv et al., 2019; Chen et al., 2021). Studies have shown that during the outbreak of *K. mikimotoi* blooms, algal cells with large biomasses make their biological oxygen demand much higher than the DO level in seawater, which can lead to the occurrence of hypoxia (O'Boyle et al., 2016). In addition, *K. mikimotoi* blooms occur mostly in spring and summer when seawater stratification is severe, which will further aggravate the formation and deterioration of hypoxia (Brand et al., 2012). Therefore, cultured organisms almost inevitably face the combined effects of *K. mikimotoi* toxicity and hypoxia when *K. mikimotoi* blooms occur in aquacultural areas. However, the combined effect of *K. mikimotoi* and hypoxia on typical cultured organisms still lacks research.

Abalone is a typical gastropod with great economic importance. In 2020, the production of abalone in China reached more than 2 billion tons, accounting for nearly 90% of the world's total abalone production (Fisheries Bureau of the Ministry of Agriculture, 2021). However, the areas of abalone breeding in China are frequently threatened by toxic *K. mikimotoi* blooms, especially at night, when the high density of *K. mikimotoi* cells causes massive consumption of respiratory oxygen, resulting in both toxic and hypoxic effects on abalone. As a kind of nocturnal organism, abalone has a higher oxygen demand at night, which makes abalone more susceptible to the combined effects of toxicity and hypoxia. Indeed, *K. mikimotoi* blooms have caused heavy losses in abalone production many times. For example, *K. mikimotoi* blooms have resulted in countless abalone deaths, with an estimated economic loss of 2.01 billion yuan (approximately $330 million) (Li et al., 2019a). Therefore, using cultured abalone as the research object to investigate the combined effects of *K. mikimotoi* and hypoxia is typical and necessary. By comparing hypoxia stress, *K. mikimotoi* stress, and their combination, the survival rate and oxidative stress indicators in different tissues and organs of abalone were tested to illustrate the combined effects of hypoxia and typical toxic algae. This study is expected to be helpful for understanding the disaster-causing mechanism of typical toxic HAB species.

Materials and methods

Organism culture and preparation

K. mikimotoi was isolated from waters near Fujian Province and preserved at the Institute of Oceanology, Chinese Academy of Sciences, Qingdao, China. The seawater was filtered through a 0.47 μm fiber membrane and heated at 121°C for 30 min, and L1 media without silicate (Guillard and Hargraves, 1993) was then added to the *K. mikimotoi* culture. The salinity of the culture medium was 31 psu. *K. mikimotoi* was cultured at 20 ± 1°C under a light intensity of approximately 50-60 μmol photons/(m^2·s), which was supplied by cool-white fluorescent bulbs on a 12:12 light-dark cycle. The algae used in the experiments were cultured to the mid-to-late exponential growth phase at cell densities of 3.0×10^7 cells/L.

Juvenile abalone *Haliotis discus hannai* was purchased from a breeding facility in Qingdao, China. During the rearing period of the juvenile abalone, the seawater was fully aerated and changed daily, and the juvenile abalone were fed dried kelp. Abalone individuals with similar sizes (shell length 25.72 ± 1.20 mm, weight 1.75 ± 0.30 g) were selected for the experiment after 24 h of starvation.

Survival impact

The experimental container was a plastic rectangular box with a volume of 16 L (0.08 m^2 × 0.2 m). The DO content was set to 0.2-2.0 mg/L, with 0.2 mg/L as a gradient. A DO probe was placed into the box to monitor the DO concentration in real time. To maintain the different DO concentrations, air and pure nitrogen were injected into the box, and an electronic DO controller (Jenco 6308DT, accuracy ± 0.05 mg/L) was used to set the DO concentration, receive the monitoring signal of the DO probe, and adjust the aeration of air and pure nitrogen to maintain the DO concentration at the set DO value. In addition, 20 juvenile abalone were placed in each box to investigate the survival of juvenile abalone under different DO contents for 24 h. The treatments were performed in triplicate, and the 24 h half lethal concentration (LC_{50}) of abalone under hypoxia stress was calculated based on the fitting equation.

To investigate the effects of different densities of *K. mikimotoi* on the survival of abalone, 20 abalone in triplicate were placed in seawater with algal densities of 10^6, 3×10^6, 5×10^6, 10^7, and 3×10^7 cells/L, and the DO content in the seawater was maintained above 8 mg/L through slow aeration. The survival of abalone was observed within 24 h.

To choose a proper *K. mikimotoi* density for exploring the combined effects of density with hypoxia, the density of *K. mikimotoi* blooms in Fujian coastal waters was analyzed; these blooms were chosen because Fujian Province is not only the main area for abalone farming but is also the area most impacted by *K. mikimotoi* blooms. The density of *K. mikimotoi* was chosen to be 3×10^6 cells/L according to the medium density of the *K. mikimotoi* bloom in Fujian Province from 2012 to 2022 (Supplementary Figure 1). The DO content was set as 2-5 mg/L, and the survival of abalone was observed after 24 h. All treatments were performed in triplicate. The abalone was judged to be dead when its gastropod adhesion disappeared and there was no response to multiple stimulations. The temperature of the experimental water was 20 ± 1°C, and a shading curtain was used for shading during the experiment to simulate the dark environment for abalone survival. The 24 h-LC_{50} of abalone under the combined stress of hypoxia and *K. mikimotoi* was calculated through a fitting equation.

Measurements of oxidative stress indicators

The control group (group C), hypoxia treatment group (DO 2 mg/L, group H), *K. mikimotoi* treatment group (*K. mikimotoi* 3×10^6 cells/L, group K), and synthesis treatment group (DO 2 mg/L, *K. mikimotoi* 3×10^6 cells/L, group S) were set in triplicate with the same container described above. Twenty abalone were placed in each box of the group, and one surviving individual (3 abalone per treatment) was randomly selected from each box to sample the oxidative stress indicator at 0 h, 3 h, 6 h, 12 h, 18 h, and 24 h. The hemolymph was collected by cutting longitudinally in the pedal sinus of the foot muscle in the abalone with a sterilized scalpel. Approximately 200 μL of hemolymph was collected from each individual by sterilized syringe. Then, the gills, hepatopancreas and hemolymph of juvenile abalone were collected and stored frozen at -80°C for analysis. Before the assay, the gills and hepatopancreas were homogenized into 10% tissue with phosphate-buffered saline (PBS, pH 7.2-7.4; Solarbio, China) and centrifuged at 4000×g for 10 min, and then the supernatant was used for the experiment. Superoxide dismutase (SOD) was detected by xanthine oxidase method, and one unit of SOD activity was defined as the amount of enzyme required for 1 mg tissue proteins in 1 ml of a reaction mixture SOD inhibition rates to 50%. The catalase (CAT) was detected by ammonium molybdate method, and one unit of CAT activity was defined as 1 mg of tissue protein that consumed 1 μmol H_2O_2 for 1 second. The malondialdehyde (MDA) content was measured by the 2-thiobarbituric acid (TBA) method. The tissue protein content was measured by the Bradford method for the calculation of SOD and CAT activity and MDA content. Both the SOD and CAT activity and the MDA and protein contents were measured by reagent kits (Nanjing Jiancheng Bioengineering Institute, Nanjing, China), determined using an EnSight microplate reader (PerkinElmer, USA) and read at 550 nm, 405 nm, 532 nm and 595 nm, respectively.

Oxygen consumption rate calculation

Two abalone were labeled and placed in a 1 L cell culture bottle without illumination at 20 ± 1°C. The calibrated DO probe was inserted into the water body with DO content above 7 mg/L. After the bottle was sealed, the DO content was recorded every 30 min for 24 h to track the abalone oxygen consumption rate in the seawater. The oxygen consumption rate of the same abalone individuals in seawater with a *K. mikimotoi* density of 3×10^6 cells/L was also tracked as described above. This experiment was conducted in duplicate. The oxygen consumption rate of abalone in the seawater (R) and in the *K. mikimotoi* culture (R') was calculated using the following formula (Ahmed et al., 2008):

$$R = [(I - F)1000(V - v)]/t$$

$$R' = [(I - F - OC_K)1000(V - v)]/t$$

where I is the DO content at the beginning of the experiment; F is the final DO content; V is the volume of the container; v is the volume of abalone; t is the time interval and OC_K is the oxygen consumption of *K. mikimotoi*.

Determination of the hemolytic activity of *K. mikimotoi*

K. mikimotoi was added to the square box at a density of 5×10^6 cells/L. The control group was slowly aerated, the DO content was maintained at 8.5 mg/L, and the DO content of the experimental groups was maintained with the electronic DO controller described above at 3, 2, 1.5, and 1.0 mg/L. After 2 h of treatment, 200 mL of algae fluid was filtered onto a GF/F membrane (0.7 μm), and the

extraction and determination of hemolytic toxins were carried out in parallel for each treatment.

The extraction of hemolytic toxin was performed as follows: Membranes were extracted using a mixed solution of chloroform, methanol and water with a volume ratio of 13:7:5 (v/v). After adding the grinding particles, the mixture was fully ground with a sample preparation system (MP, FastPrep-24) and then centrifuged at 3000 r/min for 10 min. The supernatant was removed for nitrogen blowing at 40°C until it evaporated and was dry. The solution was reconstituted with 1 mL methanol to obtain a crude extract, and then the crude extract was used to dissolve rabbit blood cells (Yuanye, China) for experiments.

The hemolytic toxin was determined as follows: A standard series of digitonin solutions were configured to draw a working curve. A mixture of 0.1 mL of the toxin extract, 0.3 mL of citric acid buffer solution and 1.60 mL of 0.5% (v/v) fresh rabbit red blood was heated in a water bath at 37°C for 30 min and then centrifuged at 800 r/min for 10 min, and the absorbance of the supernatant was measured at 540 nm. The calculation of hemolytic activity was performed according to the industry standard (HY/Y 151-2013), and the hemolytic activity was defined as hemolytic units (HU) which represents 1 ml reaction solution that can dissolve 50% of rabbit blood cells within 30 min at 37°C.

Statistical analysis

The data analysis method of this study was two-way analysis of variance (ANOVA), and Duncan's method was used for *post hoc* multiple comparisons. The data involved in correlation analysis and two-way ANOVA were analyzed and processed with SPSS 22.0, and the graphs were drawn in Origin 9.0.

Results

Survival of abalone

In this study, the effects of different densities of *K. mikimotoi* under sufficient DO content on the survival of abalone were investigated. The results showed that under aeration conditions, the 24-h survival rate of abalone was nearly 100%. When investigating the effect of DO content on abalone, it was found that abalone had a certain tolerance to hypoxia. The 24 h LC_{50} values was 0.75 mg/L according to the logistic models (Figure 1A). When *K. mikimotoi* was present at a density of 3×10^6 cells/L, the 24 h LC_{50} that was calculated by the exponential models increased to 2.59 mg/L (Figure 1B).

Oxidative stress indicators

The changes in CAT activity, SOD activity and MDA content in the gills of abalone under different treatments were tracked. The CAT activity decreased slightly with time, SOD activity exhibited a decreasing tendency first and then increased, with 12 h as the inflection point, while MDA content fluctuated with time (Figure 2). Through statistical analysis, it was found that there was no significant difference in the CAT activity and MDA content among the different treatment groups ($p > 0.05$), and only the SOD enzyme activity was significantly different among the treatment groups ($p< 0.05$) (Table 1). Duncan multiple comparisons showed that hypoxic stress alone did not cause significant changes in SOD enzyme activity in abalone gills, while *K. mikimotoi* stress alone and the combined stress of hypoxia and *K. mikimotoi* caused a significant decrease in SOD activity in abalone gills.

The determination of oxidative stress indicators in the hepatopancreas of abalone in each treatment group showed that the changes in CAT activity and MDA content with time were negligible, and the difference between groups was not significant (Figure 3). Compared with the control group, hypoxia stress, *K. mikimotoi* stress alone and their combination led to a decrease in SOD activity in the hepatopancreas of abalone after 6 h. Through further statistical analysis, it was found that the CAT activity and MDA content in the hepatopancreas of abalone were not significantly affected by time, treatment or their interaction ($p > 0.05$) (Table 2). The SOD activity in the hepatopancreas of abalone was significantly affected by time, and it was found by performing Duncan multiple comparisons that the SOD activity was

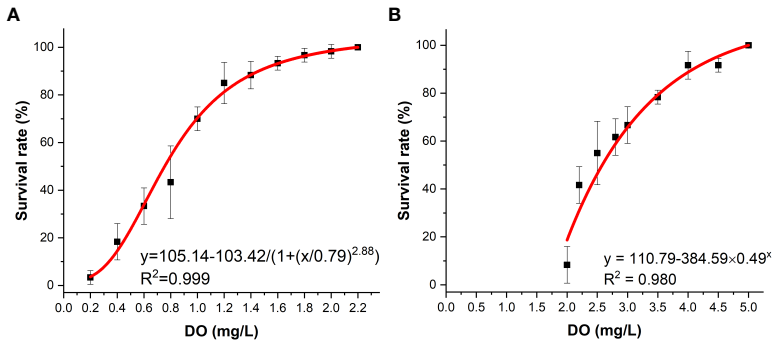

FIGURE 1
Survival of *H. discus hannai* in the seawater system **(A)** and in the K. mikimotoi system **(B)** under different DO contents.

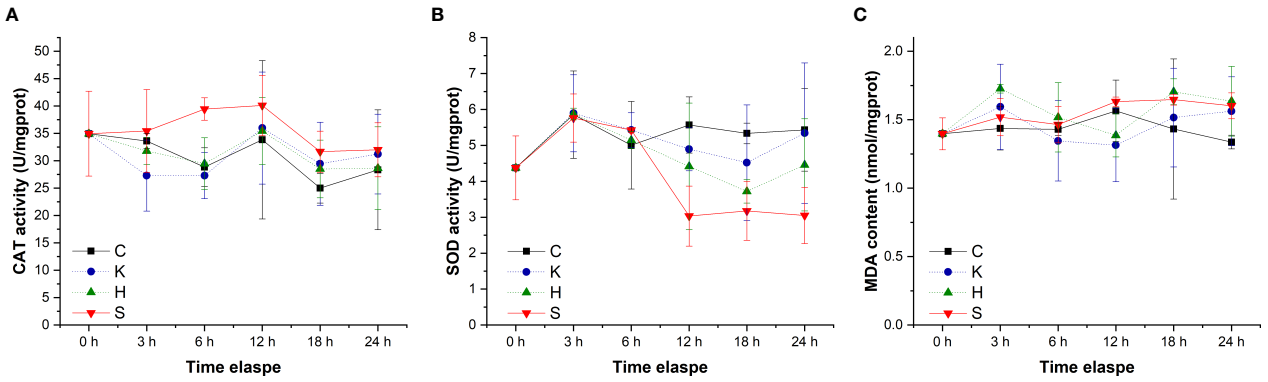

FIGURE 2
Changes in the CAT activity **(A)**, SOD activity **(B)** and MDA content **(C)** in the gills of *H. discus hannai* in different treatment groups. The solid line with black squares represents the control group; the dotted line with blue circles represents the group with the *K. mikimotoi* treatment; the dotted line with green triangles represents the group with the hypoxia treatment; the solid line with inverted triangle represents the group with both the *K. mikimotoi* and the hypoxia treatments.

significantly inhibited by the combined stress of hypoxia and *K. mikimotoi* ($p< 0.05$).

By tracking the oxidative stress indicators of abalone hemolymph, it was found that with the extension of time, the CAT activity in the group C, group K, and group H were relatively stable. When the stresses of hypoxia and *K. mikimotoi* combined, the CAT activity in the abalone hemolymph increased with time, from 34.33 U/mgprot at the beginning to 70.46 U/mgprot at 24 h, which was significantly different from that in the other three groups ($p< 0.05$) (Figure 4). The SOD activity in the abalone hemolymph was slightly lower within 12 h and then slightly higher than that in the control with the hypoxia or *K. mikimotoi* treatment alone, while it was higher than that in the control at all time points due to the combined stress of hypoxia and *K. mikimotoi*. Compared with the control group, in the three experimental groups, the MDA content increased at 3 h, but the MDA content in the abalone hemolymph in the group K and group H decreased to the same level as the control at 6 h, while the MDA content in the abalone hemolymph in group S remained at a high level. Through Duncan multiple comparisons, it was found that hypoxia or *K. mikimotoi* stress alone did not cause significant changes in CAT activity, SOD activity or MDA content in the abalone hemolymph, while their combination resulted in insignificant increases in CAT and SOD activity and MDA content in the abalone hemolymph ($p< 0.05$) (Table 3).

The effects of *K. mikimotoi* on the oxygen consumption rate of abalone

The oxygen consumption rates of the same individuals in the seawater and the *K. mikimotoi* system indicated that *K. mikimotoi* aggravated the consumption of DO in abalone (Figure 5). The oxygen consumption of seawater itself was negligible, and due to low illumination, 1 L of *K. mikimotoi* consumed 0.16 mg of DO within 24 h (Table 4). Through calculation, it was found that the average oxygen consumption rate of abalone in the seawater system was 0.086 ± 0.016 mg/ind/h, and the average oxygen consumption rate in the *K. mikimotoi* system was 0.103 ± 0.008 mg/ind/h, with an increase of more than 20% compared with that in the seawater.

The effects of DO on hemolytic toxins

The results showed that in the control group with sufficient DO, the hemolytic activity of *K. mikimotoi* was 6.64×10^{-6} HU/cell (Figure 6). After hypoxia stress with DO contents of 3 mg/L, 2 mg/L, 1.5 mg/L and 1 mg/L for 2 h, the hemolytic activity of *K. mikimotoi* increased significantly, reaching 7.12×10^{-6} HU/cell, 16.62×10^{-6} HU/cell, 25.65×10^{-6} HU/cell, and 31.35×10^{-6} HU/cell, respectively. A DO content of 2 mg/L and below significantly increased the hemolytic activity of *K. mikimotoi* ($p< 0.05$).

TABLE 1 Summary of two-way ANOVA testing the effects of the treatment and time on CAT and SOD activity and MDA content in the gills of *H. discus hannai* (* represents a significant difference compared with the control, $p< 0.05$).

Sources	df	CAT		SOD		MDA	
		F	*p*	*F*	*p*	*F*	*p*
Time	7	13.756	0.000*	22.450	0.000*	1.434	0.229
Group	3	1.107	0.355	10.889	0.000*	2.114	0.111
Time*Group	21	0.284	0.995	1.866	0.052	0.560	0.890

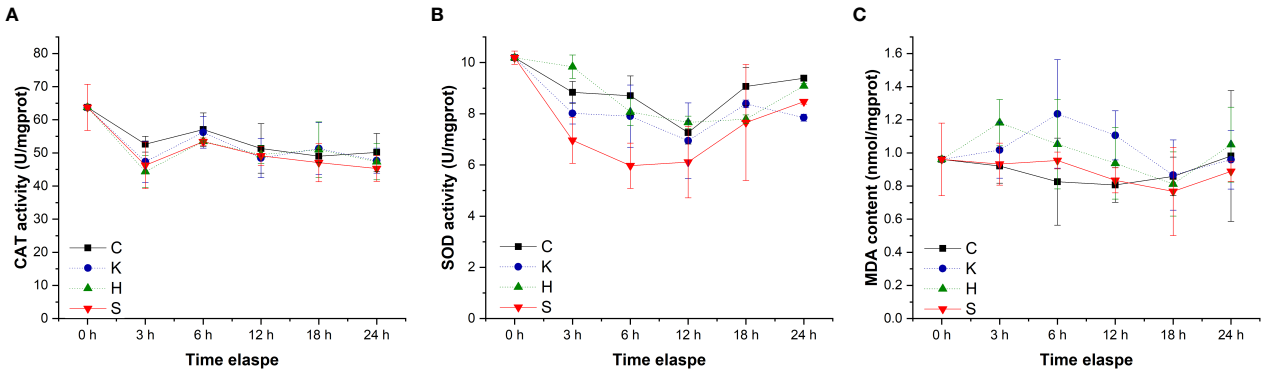

FIGURE 3
Changes in the CAT activity **(A)**, SOD activity **(B)** and MDA content **(C)** in the hepatopancreas of *H. discus hannai* in different treatment groups. The solid line with black squares represents the control group; the dotted line with blue circles represents the group with the *K. mikimotoi* treatment; the dotted line with green triangles represents the group with the hypoxia treatment; the solid line with inverted triangles represents the group with both the *K. mikimotoi* and the hypoxia treatments.

Discussion

Hypoxia tolerance is quite different among species. Compared to fish, shellfish are generally more tolerant to hypoxia, but because of their limited ability to swim, their survival is threatened if the DO content continues to decline. Most bivalves have a strong tolerance to hypoxia. For example, studies have shown that the 20-day LC_{50} values of DO to *Ruditapes philippinarum* and *Chlamys farreri* are 0.57 mg/L and 1.8 mg/L, respectively (Li et al., 2019b; Li et al., 2020). In this study, abalone is a marine gastropod that is widely distributed. Studies have shown that gastropods also have a certain tolerance to hypoxia because they are distributed in the bottom environment, in which the DO levels are relatively low, or live in the intertidal zone, in which exposure to air periodically occurs (Vaquer-Sunyer and Duarte, 2008; Levin et al., 2009). Samuel et al. (2019) investigated the effect of DO content on the survival of *H. fulgens*, and the 24-h LC_{50} of DO content at 26°C was 0.23 ± 0.73 mg/L. Shen (2018) found that the 24-h LC_{50} of DO content to *H. discus hannai* at 20°C was 0.80 mg/L. In this study, the 24-h LC_{50} of DO content in the seawater for abalone was 0.75 mg/L, which was similar to the results of previous studies, indicating that abalone itself has a certain tolerance to hypoxia. Algal blooms are considered to be one of the main causes of marine hypoxia. A hypoxic condition with a DO concentration at 2.2 mg/L was observed in Donegal Bay due to a *K. mikimotoi* bloom (O'Boyle et al., 2016), which was still within a tolerable range for abalone, suggesting that hypoxia alone is not the main cause of massive abalone mortality in the field.

As a typical toxic alga, *K. mikimotoi* can produce hemolytic toxins, fish toxins, cytotoxins, etc. A harmful algal bloom occurs when the density of *K. mikimotoi* exceeds 10^6 cells/L. In recent years, studies have found that the toxic effects of *K. mikimotoi* are the strongest through the direct contact of intact *K. mikimotoi* cells with organisms, and their toxicity depends on the strain (Li et al., 2017; Yan et al., 2022). The algal strain used in this study was isolated from the coast of Fujian. Relevant studies show that this strain poses a certain threat to the survival of a variety of zooplankton and fish, such as turbot *Scophthalmus maximus* and marine medaka *Oryzias melastigma* (Li et al., 2017; Zhang et al., 2022). Lin et al. (2016a) investigated the effect of the *K. mikimotoi* Fujian strain on the survival of *H. discus hannai*. The results showed that at a density of 10^7 cells/L, *K. mikimotoi* caused the 48h survival rate of *H. discus hannai* to be more than 80%. When the *K. mikimotoi* density increased to 3×10^7 cells/L, the survival of *H. discus hannai* decreased to 66.7%. In this study, under an environment with sufficient DO, 3×10^7 cells/L *K. mikimotoi* did not cause the death of juvenile *H. discus hannai* within 24 h. The results of this study and previous studies showed that *K. mikimotoi* had limited effects on the survival of *H. discus hannai* in the short term.

Recent studies have found that when the DO content is sufficient, the toxic effects of *K. mikimotoi* are relatively limited,

TABLE 2 Summary of two-way ANOVA testing the effects of the treatment and time on CAT and SOD activity and MDA content in the hepatopancreas of *H. discus hannai* (* represents a significant difference compared with the control, $p< 0.05$).

Sources	df	CAT		SOD		MDA	
		F	*p*	*F*	*p*	*F*	*p*
Time	7	2.153	0.075	4.894	0.001*	1.440	0.227
Group	3	1.953	0.134	4.545	0.007*	1.660	0.188
Time*Group	21	0.376	0.979	1.105	0.377	0.705	0.767

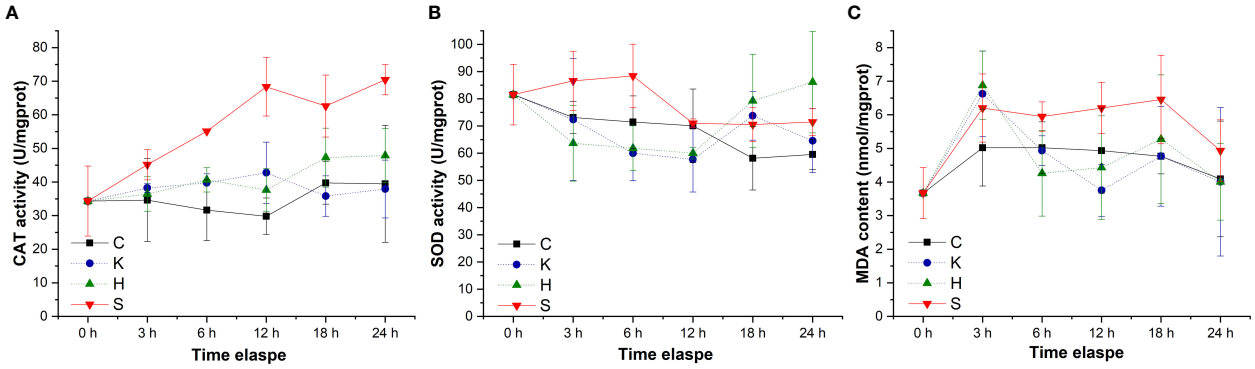

FIGURE 4
Changes in the CAT activity **(A)**, SOD activity **(B)** and MDA contents **(C)** in the hemolymph of *H. discus hannai* in different treatment groups. The solid line with black squares represents the control group; the dotted line with blue circles represents the group with the *K. mikimotoi* treatment; the dotted line with green triangles represents the group with the hypoxia treatment; the solid line with inverted triangles represents the group with both the *K. mikimotoi* and the hypoxia treatments.

while under environments without aeration, *K. mikimotoi* could cause the death of fish and shellfish even at their tolerant DO content (Lin et al., 2016a; Li et al., 2019a). This indicates that the hypoxic environment exacerbates the toxic effects of *K. mikimotoi* on marine organisms. On the basis of previous studies, this study further investigated the effects of *K. mikimotoi* under different degrees of hypoxia on the survival of juvenile abalone by accurately regulating the DO content in water. During the 24 h experimental period, the stress of *K. mikimotoi* at a density of 3×10^6 cells/L alone did not cause the death of juvenile abalone, and the same survival influence was found under hypoxia stress at a DO content of 2 mg/L. When hypoxia and *K. mikimotoi* stress were combined, however, the survival rate of juvenile abalone was significantly reduced to less than 10%. This clearly shows that hypoxia and *K. mikimotoi* have a synergistic effect on the survival of juvenile abalone. Previous studies on the synergistic effects of environmental factors on aquatic organisms have mostly focused on substances such as heavy metals, organic pollutants, pesticides, etc. (Goswami et al., 2014; Zou et al., 2017; Mandich, 2018; Pittura et al., 2018; Tang et al., 2020; Zhang et al., 2021). In recent years, the synergistic effect of typical toxic harmful algae and hypoxia has attracted attention. For example, studies have shown that in freshwater, the stress of hypoxia combined with *Microcystis aeruginosa* caused more serious harm to the gills, stomach, intestine and crystal rod of *Hyriopsis cumingii* than that of a single stress (Hu et al., 2016; Wu et al., 2017). *Karenia brevis* reduced the survival rate of stone crabs by 7.2% in an environment with sufficient DO, while *K. brevis* reduced the 24-h survival rate of stone crabs by 43% in a hypoxic environment, and the stone crabs exhibited obvious hysteresis behavior at the same time (Gravinese et al., 2020). This shows that the synergistic effects of a hypoxic environment and toxic algae may be an important disaster-causing mechanism of typical toxic HABs and is worthy of more research.

All aerobic organisms have antioxidant defense systems to prevent the production of excess reactive oxygen species (ROS), and changes in oxidative stress indicators can reflect the response of organisms to environmental stress. This system consists of enzymes that can be induced by oxidative stress, including SOD and CAT. SOD can remove excess free radicals so that the generation and elimination of free radicals are in a dynamic balance, thereby preventing the damage of free radicals to the organism. CAT can quickly remove the toxic H_2O_2 produced by cell metabolism. MDA is a product of lipid peroxidation. Therefore, changes in SOD and CAT activity and MDA content in organisms are regarded as antioxidative responses to environmental changes. The individual and synergistic effects of hypoxia and *K. mikimotoi* on the gills, hepatopancreas, and hemolymph of juvenile abalone, which are the main organs and tissues involved in respiration, detoxification and immunity, were also investigated in this study. Although the gills, hepatopancreas, and hemolymph are regarded as organs and tissues in abalone that are sensitive to environmental stress, their antioxidant responses to hypoxia stress, *K. mikimotoi* stress, and both of these stresses combined were quite different. Little response was observed with the hepatopancreas and gill tissues to the experimental treatment, and

TABLE 3 Summary of two-way ANOVA testing the effects of the treatment and time on CAT and SOD activity and MDA content in the hemolymph of *H. discus hannai* (* represents a significant difference compared with the control, $p< 0.05$).

Sources	df	CAT		SOD		MDA	
		F	*p*	*F*	*p*	*F*	*p*
Time	7	3.149	0.015*	3.385	0.026*	6.569	0.000*
Group	3	14.392	0.000*	2.782	0.050*	2.807	0.049*
Time*Group	21	1.297	0.241	2.005	0.064	0.778	0.694

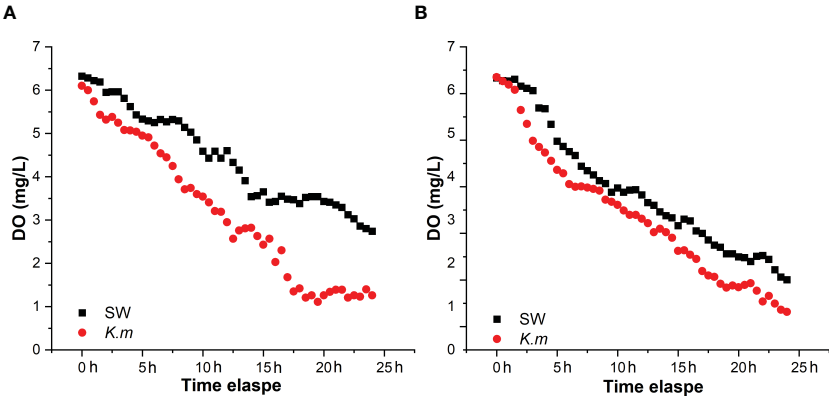

FIGURE 5
DO consumption of *H. discus hannai* in the seawater and *K. mikimotoi* treatment groups in group **(A)** and group **(B)** The black square and the red dot represent the DO value in the seawater and the *K. mikimotoi* culture, respectively.

TABLE 4 Oxygen consumption rates in different systems.

Item	Oxygen consumption rate (OCR)		Average
	Group 1	Group 2	
Seawater	0.000 (mg/h)		
K. mikimotoi	0.007 (mg/h)		
Abalone in seawater	0.074 (mg/ind/h)	0.097(mg/ind/h)	0.086 ± 0.016 (mg/ind/h)
Abalone in *K. mikimotoi*	0.097(mg/ind/h)	0.109(mg/ind/h)	0.103 ± 0.008(mg/ind/h)
Increase in OCR	31.08%	12.37%	20.47%

only the SOD activity of the gills was significantly changed due to *K. mikimotoi* stress. Previous studies have found that *K. mikimotoi* can cause damage to the gills of marine medaka, salmon and other fish (Mitchell and Rodger, 2007; Zhang et al., 2022). In other studies, it was also observed that *K. mikimotoi* at a density of 10^7 cells/L had adverse effects on the microstructure and SOD and CAT activities of abalone gills (Lin et al., 2016b), which indicates that the hemolytic toxins of *K. mikimotoi* cause certain oxidative harm to the respiratory system of abalone. In this study, compared with the gills and hepatopancreas, the hemolymph of abalone was more sensitive to the treatment, especially the synergistic stress of hypoxia and *K. mikimotoi*. Abalone relies on innate immunity, and hemolymph is the main tissue of its immunity, which may be responsible for its sensitivity to environmental stress (Shen et al., 2019). In general, except for SOD activity in the gills of juvenile abalone, no other oxidative stress indicators were found to be significantly different from those of the control after treatment with hypoxia stress or *K. mikimotoi* stress alone. When the stresses of hypoxia and *K. mikimotoi* were combined, their synergistic stress caused significant decrease of the SOD activity in the gills and hepatopancreas of juvenile abalone. Moreover, the stress of hypoxia combined with *K. mikimotoi* affected all the oxidative stress indicators in the hemolymph. The activities of SOD and CAT were significantly enhanced, and the MDA content was significantly increased, showing a top-down oxidative damage process. That is, the large generation of ROS caused the elevation of SOD activity and the accumulation of H_2O_2, and excess H_2O_2 further resulted in an increase in CAT activity and MDA content (Figure 7). The related results of oxidative stress indicators further demonstrated that the

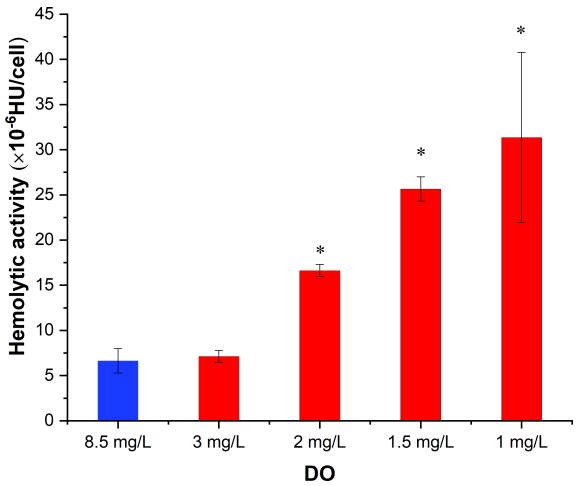

FIGURE 6
Hemolytic activity of *K. mikimotoi* under different DO conditions (* represents a significant difference compared with the control, $p < 0.05$).

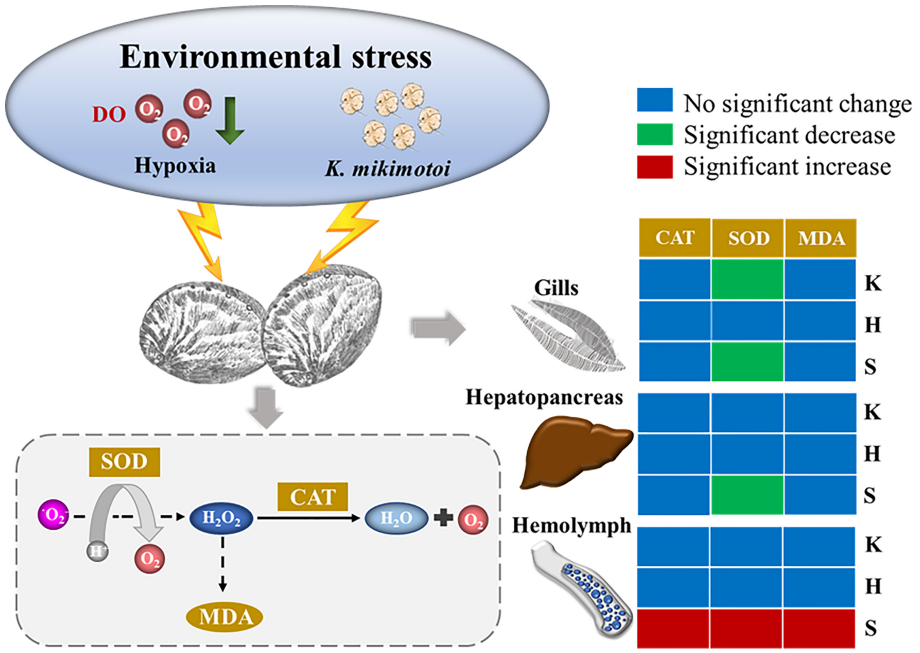

FIGURE 7
Overall schematic figure of the effects of hypoxia (H), *K. mikimotoi* (K) and their synergy (S) on SOD activity, CAT activity and MDA content after24 h of exposure in juvenile abalone. Blue, green and red colors in the box represent no significant change, a significant decrease and a significant increase, respectively.

synergistic effect of hypoxia and *K. mikimotoi* causes serious harm to the immune system of abalone, resulting in the antioxidant system disorder, indicating that the abalone suffered obvious oxidative damage.

To analyze the enhanced pathway of hypoxia and *K. mikimotoi* synergistic toxicity, this study further focused on the interaction between *K. mikimotoi* toxicity and DO content. First, it was found that *K. mikimotoi* could affect the oxygen consumption rate of abalone. Ahmed et al. (2008) estimated that the oxygen consumption rates of *H. discus discus*, *H. gigantea*, *H. madaka* and their hybrids (more than 2 g) were 0.030-0.040 mL/g/h, which equals 0.086-0.114 mg/ind/h. The abalone used in this study was *H. discus hannai* weighed less than 2 g. Considering that the oxygen consumption rate increases with the increase in abalone body weight and varies by species, it is reasonable that the oxygen consumption rate in this study was at 0.086 mg/ind/h on average. Generally, the oxygen consumption rate value of *H. discus hannai* in seawater in this study is consistent with the record in the literature (Ahmed et al., 2008). When *K. mikimotoi* exists, its toxicity could directly damage the gill tissues of fish and shellfish, which may reduce the rate of oxygen utilization by the organism. To maintain normal metabolism, this reduction in rate can be compensated by more consumption. In addition, studies have shown that when organisms are affected by toxic substances such as heavy metals and organic compounds, their respiratory metabolism increases for detoxification (Engel and Fowler, 1979; Unkiewicz-Winiarczyk and Gromysz-Kałkowska, 2012). It is necessary for abalone to participate in more physiological metabolic activities that are related to detoxification, and these activities result in higher consumption of DO.

In addition, in the present study, hypoxia promoted the hemolytic toxicity of *K. mikimotoi*, which made the situation for the abalone even worse. Due to the mysterious composition of the hemolytic toxin in *K. mikimotoi*, the toxicity level of *K. mikimotoi* is usually represented in terms of hemolytic activity. Hemolytic activity is an indicator that can reflect individual cell toxicity and therefore unrelated to algal density. Some studies suggest that toxins are an environmental deterrent that are produced by algal cells; when environmental conditions are unfavorable, algal toxins increase for defense purposes. A large number of studies have shown that a lack of nutrients, such as nitrate and phosphate, as well as the discomfort of light, temperature, pH, etc., can significantly increase toxic algal toxins (Indrasena and Gill, 2000; Wang and Hsieh, 2002; Murata et al., 2006). However, there is still a lack of research on the effects of DO on algal toxins. Although algal cells can generate oxygen through photosynthesis, components for their respiration and metabolism still need to be provided by the external environment, especially under limited light conditions. This means that DO content may be a limiting environmental factor. Based on the results, it is speculated that when the DO content is insufficient, algal cells may be directly stimulated by hypoxia to increase toxin production.

Conclusions

This study confirmed that hypoxia and *K. mikimotoi* caused strong synergistic effects on typical organisms. The synergistic effects of hypoxia and *K. mikimotoi* could significantly decrease SOD activity in gill tissue and hepatopancreas of abalone.

Compared with the gill and hepatopancreas, the hemolymph of the abalone was more sensitive to the synergistic stress of hypoxia and *K. mikimotoi*. The SOD and CAT activity and the MDA content in the hemolymph of the abalone were significantly enhanced, indicating that abalone suffered strong oxidative damage. Further investigation regarding the reason for their synergistic activity showed that *K. mikimotoi* promoted the oxygen consumption rate of juvenile abalone, and hypoxia led to a significant increase in the hemolytic activity of *K. mikimotoi*; these activities may be the essential causes for the synergistic enhancement effects of *K. mikimotoi* combined with hypoxia.

Data availability statement

The original contributions presented in the study are included in the article/Supplementary Material. Further inquiries can be directed to the corresponding author.

Author contributions

YZ contributed to methodology, investigation, formal analysis, writing - original draft. XS contributed to funding acquisition, resources, supervision, writing - review & editing. PZ contributed to methodology and investigation. All authors contributed to the article and approved the submitted version.

Funding

This research was funded by the Intergovernmental Innovation Cooperation Project of the Ministry of Science and Technology, (No. 2022YFE0136400), the National Natural Science Foundation of China (No. 41976148), the Laoshan Laboratory (No. LSKJ202203700), and the Research Start-up Fund Project of the Cross Research Center in the Pilot National Laboratory for Marine Science and Technology (No. JCZX202030).

Acknowledgments

The authors would like to acknowledge Xiaojun Meng and Yuxia Zhong for their assistance.

Conflict of interest

The authors declare that the research was conducted in the absence of any commercial or financial relationships that could be construed as a potential conflict of interest.

Publisher's note

Supplementary material

The Supplementary Material for this article can be found online at: https://www.frontiersin.org/articles/10.3389/fmars.2023.1029512/full#supplementary-material

SUPPLEMENTARY FIGURE 1
The occurrence of *K. mikimotoi* blooms in Fujian Province (China) from 2012 to 2022. **(A)** The columns represents the density of *K. mikimotoi* in each bloom; **(B)** Frequency histogram of *K. mikimotoi* blooms.

References

Ahmed, F., Segawa, S., Yokota, M., and Watanabe, S. (2008). Effect of light on oxygen consumption and ammonia excretion in *Haliotis discus discus*, *H. gigantea*, *H. madaka* and their hybrids. *Aquaculture* 279 (1-4), 160–165. doi: 10.1016/j.aquaculture.2008.03.040

Brand, L. E., Campbell, L., and Bresnan, E. (2012). *Karenia*: the biology and ecology of a toxic genus. *Harmful Algae* 14, 156–178. doi: 10.1016/j.hal.2011.10.020

Breitburg, D. L., Levin, L. A., Oschlies, A., Grégoire, M., Chavez, F. P., Conley, D. J., et al. (2018). Declining oxygen in the global ocean and coastal waters. *Science* 359 (6371), eaam7240. doi: 10.1126/SCIENCE.AAM7240

Chen, B., Wang, K., Guo, H., and Lin, H. (2021). *Karenia mikimotoi* blooms in coastal waters of China from 1998 to 2017. *Estuarine Coast. Shelf Sci.* 249, 107034. doi: 10.1016/j.ecss.2020.107034

Engel, D. W., and Fowler, B. A. (1979). Factors influencing cadmium accumulation and its toxicity to marine organisms. *Environ. Health Perspect.* 28, 81–88. doi: 10.2307/3428908

Fisheries Bureau of the Ministry of Agriculture (2021). *China Fishery Statistical Yearbook*. (Beijing: China Agriculture Press).

Gilbert, D., Rabalais, N. N., Diaz, R. J., and Zhang, J. (2009). Evidence for greater oxygen decline rates in the coastal ocean than in the open ocean. *Biogeosci. Discussions* 7 (5), 2283–2296. doi: 10.5194/bgd-6-9127-2009

Glibert, P., Seitzinger, S., Heil, C., Burkholder, J. A., and Kelly, V. (2005). The role of eutrophication in the global proliferation of harmful algal blooms. *Oceanography* 18 (2), 198–209. doi: 10.5670/oceanog.2005.54

Gobler, C. J., and Baumann, H. (2016). Hypoxia and acidification in ocean ecosystems: coupled dynamics and effects on marine life. *Biol. Lett.* 12 (5), 20150976. doi: 10.1098/rsbl.2015.0976

Goswami, P., Hariharan, G., Godhantaraman, N., and Munuswamy, N. (2014). An integrated use of multiple biomarkers to investigate the individual and combined effect of copper and cadmium on the marine green mussel (*Perna viridis*). *J. Environ. Sci. Health Part A* 49 (13), 1564–1577. doi: 10.1080/10934529.2014.938534

Gravinese, P. M., Munley, M. K., Kahmann, G., Cole, C., Lovko, V., Blum, P., et al. (2020). The effects of prolonged exposure to hypoxia and Florida red tide (*Karenia brevis*) on the survival and activity of stone crabs. *Harmful Algae* 98, 101897. doi: 10.1016/j.hal.2020.101897

Guillard, R. R. L., and Hargraves, P. E. (1993). *Stichochrysis immobilis* is a diatom, not a chrysophyte. *Phycologia* 32 (3), 234–236. doi: 10.2216/i0031-8884-32-3-234.1

Heisler, J., Glibert, P. M., Burkholder, J. M., Anderson, D. M., Cochlan, W., Dennison, W. C., et al. (2008). Eutrophication and harmful algal blooms: a scientific consensus. *Harmful Algae* 8 (1), 3–13. doi: 10.1016/j.hal.2008.08.006

Hu, L., Wang, R., Wang, M., Cannizzaro, J., Garrett, M., Harper, M., et al. (2022). The inactivation effects and mechanisms of *Karenia mikimotoi* by non-metallic elements modified TiO_2 (SNP-TiO2) under visible light. *Sci. Total Environ.* 820, 153346. doi: 10.1016/j.hal.2022.102289

Hu, M., Wu, F., Yuan, M., Liu, Q., and Wang, Y. (2016). Combined effects of toxic cyanobacteria *Microcystis aeruginosa* and hypoxia on the physiological responses of triangle sail mussel *Hyriopsis cumingii*. *J. Hazard. Mater.* 306, 24–33. doi: 10.1016/j.aquatox.2019.05.013

Indrasena, W. M., and Gill, T. A. (2000). Thermal degradation of partially purified paralytic shellfish poison toxins at different times, temperatures, and pH. *J. Food Sci.* 65 (6), 948–953. doi: 10.1111/j.1365-2621.2000.tb09398.x

Lee, Y. G., Jeong, D. U., Lee, J. S., Choi, Y. H., and Lee, M. O. (2016). Effects of hypoxia caused by mussel farming on benthic foraminifera in semi-closed gamak bay, south Korea. *Mar. pollut. Bull.* 109 (1), 566–581. doi: 10.1016/j.marpolbul.2016.01.024

Levin, L. A., Ekau, W., Gooday, A. J., Jorissen, F., Middelburg, J. J., Naqvi, S. W. A., et al. (2009). Effects of natural and human-induced hypoxia on coastal benthos. *Biogeosciences* 6 (10), 2063–2098. doi: 10.5194/bg-6-2063-2009

Li, Q., Sun, S., Zhang, F., Wang, M., and Li, M. (2019b). Effects of hypoxia on survival, behavior, metabolism and cellular damage of Manila clam (*Ruditapes philippinarum*). *PloS One* 14 (4), e0215158. doi: 10.1371/journal.pone.0215158

Li, X., Yan, T., Lin, J., Yu, R., and Zhou, M. (2017). Detrimental impacts of the dinoflagellate *Karenia mikimotoi* in fujian coastal waters on typical marine organisms. *Harmful Algae* 61, 1–12. doi: 10.1016/j.hal.2016.11.011

Li, X., Yan, T., Yu, R., and Zhou, M. (2019a). A review of *Karenia mikimotoi*: bloom events, physiology, toxicity and toxic mechanism. *Harmful Algae* 90, 101702. doi: 10.1016/j.hal.2019.101702

Li, Q., Zhang, F., Wang, M., Li, M., and Sun, S. (2020). Effects of hypoxia on survival, behavior, and metabolism of zhikong scallop *Chlamys farreri* Jones et Preston 1904. *J. Oceanol. Limnol.* 38 (2), 351–363.

Lin, J. N., Yan, T., Zhang, Q. C., Wang, Y. F., Liu, Q., and Zhou, M. J. (2016a). The detrimental impacts of *Karenia mikimotoi* blooms on the abalone haliotis discus hannai in fujian province. *Mar. Environ. Sci.* 35 (1), 27–34.

Lin, J. N., Yan, T., Zhang, Q. C., Wang, Y. F., Liu, Q., and Zhou, M. J. (2016b). Effects of *Karenia mikimotoi* blooms on antioxidant enzymes in gastropod abalone, *Haliotis discus hannai*. *Mar. Sci.* 40, 17–22. doi: 10.11759/hykx20150330001

Lv, S., Cen, J., Wang, J., and Ou, L. (2019). The research *Status quo*, hazard, and ecological mechanisms of *Karenia mikimotoi* red tide in coastal waters of China. *Oceanol. Limnol. Sinica.* 50, 487–484. doi: 10.11693/hyhz20181000255

Mandich, M. (2018). Ranked effects of heavy metals on marine bivalves in laboratory mesocosms: a meta-analysis. *Mar. Pollut. Bull.* 131, 773–781. doi: 10.1016/j.marpolbul.2018.04.068

Matos, C. R., Mendoza, U., Diaz, R., Moreira, M., Belem, A. L., Metzger, E., et al. (2016). Nutrient regeneration susceptibility under contrasting sedimentary conditions from the Rio de Janeiro coast, Brazil. *Mar. Pollut. Bull.* 108 (1-2), 297–302. doi: 10.1016/j.marpolbul.2016.04.046

Mitchell, S., and Rodger, H. (2007). Pathology of wild and cultured fish affected by a *Karenia mikimotoi* bloom in Ireland 2005. *Bulletin-European Assoc. Fish Pathol.* 27 (1), 39–42.

Murata, A., Leong, S. C. Y., Nagashima, Y., and Taguchi, S. (2006). Nitrogen: phosphorus supply ratio may control the protein and total toxin of dinoflagellate *Alexandrium tamarense*. *Toxicon* 48 (6), 683–689. doi: 10.1016/j.toxicon.2006.08.004

Niu, X., Xu, S., Yang, Q., Xu, X., Zheng, M., Li, X., et al. (2021). Toxic effects of the dinoflagellate *Karenia mikimotoi* on zebrafish (*Danio rerio*) larval behavior. *Harmful Algae* 103, 101996. doi: 10.1016/j.hal.2021.101996

O'Boyle, S., McDermott, G., Silke, J., and Cusack, C. (2016). Potential impact of an exceptional bloom of *Karenia mikimotoi* on dissolved oxygen levels in waters off Western Ireland. *Harmful Algae* 53, 77–85. doi: 10.1016/j.hal.2015.11.014

Pittura, L., Avio, C. G., Giuliani, M. E., d'Errico, G., Keiter, S. H., Cormier, B., et al. (2018). Microplastics as vehicles of environmental PAHs to marine organisms: combined chemical and physical hazards to the Mediterranean mussels, *Mytilus galloprovincialis*. *Front. Mar. Sci.* 5. doi: 10.3389/fmars.2018.00103

Samuel, C. L., Norma Yolanda, H. S., Salvador Emilio, L. C., Pedro, C. H., Felipe De Jesus, A. V., and Maria Teresa, S. (2019). Survival and respiration of green abalone (*Haliotis fulgens*) facing very short-term marine environmental extremes. *Mar. Freshw. Behav. Physiol.* 52 (1), 1–15. doi: 10.1080/10236244.2019.1607734

Schmidtko, S., Stramma, L., and Visbeck, M. (2017). Decline in global oceanic oxygen content during the past five decades. *Nature* 542 (7641), 335–339. doi: 10.1038/nature21399

Shen, Y. W. (2018). *Effects of hypoxia stress on survival, immune physiology of abalone (Haliotis discus hannai and its hybrid with h. fulgens) and primary study on molecular basis* (Dissertation, Xiamen:Xiamen University).

Shen, Y., Huang, Z., Liu, G., Ke, C., and You, W. (2019). Hemolymph and transcriptome analysis to understand innate immune responses to hypoxia in pacific abalone. *Comp. Biochem. Physiol. Part D: Genomics Proteomics* 30, 102–112. doi: 10.1016/j.cbd.2019.02.001

Tang, Y., Rong, J., Guan, X., Zha, S., Shi, W., Han, Y., et al. (2020). Immunotoxicity of microplastics and two persistent organic pollutants alone or in combination to a bivalve species. *Environ. Pollut.* 258, 113845. doi: 10.1016/j.envpol.2019.113845

Unkiewicz-Winiarczyk, A., and Gromysz-Kałkowska, K. (2012). Effect of temperature on toxicity of deltamethrin and oxygen consumption by *Porcellio scaber* latr (Isopoda). *Bull. Environ. Contam. Toxicol.* 89 (5), 960–965. doi: 10.1007/s00128-012-0814-5

Vaquer-Sunyer, R., and Duarte, C. M. (2008). Thresholds of hypoxia for marine biodiversity. *Proc. Natl. Acad. Sci.* 105 (40), 15452–15457. doi: 10.1073/pnas.0803833105

Wang, D. Z., and Hsieh, D. P. (2002). Effects of nitrate and phosphate on growth and C2 toxin productivity of *Alexandrium tamarense* CI01 in culture. *Mar. pollut. Bull.* 45 (1-12), 286–289. doi: 10.1016/S0025-326X(02)00183-2

Wu, F., Kong, H., Shang, Y., Zhou, Z., Gul, Y., Liu, Q., et al. (2017). Histopathological alterations in triangle sail mussel (*Hyriopsis cumingii*) exposed to toxic cyanobacteria (*Microcystis aeruginosa*) under hypoxia. *Aquaculture* 467, 182–189. doi: 10.1016/j.aquaculture.2016.05.026

Wu, Z., You, F., Wen, A., Ma, D., and Zhang, P. (2016). Physiological and morphological effects of severe hypoxia, hypoxia and hyperoxia in juvenile turbot (*Scophthalmus maximus* l.). *Aquacult. Res.* 47 (1), 219–227. doi: 10.1111/are.12483

Yan, T., Li, X. D., Tan, Z. J., Yu, R. C., and Zou, J. Z. (2022). Toxic effects, mechanisms, and ecological impacts of harmful algal blooms in China. *Harmful Algae* 111, 102148. doi: 10.1016/j.hal.2021.102148

Yang, B., Gao, X., Zhao, J., Liu, Y., Xie, L., Lv, X., et al. (2021). Potential linkage between sedimentary oxygen consumption and benthic flux of biogenic elements in a coastal scallop farming area, north yellow Sea. *Chemosphere* 273, 129641. doi: 10.1016/j.chemosphere.2021.129641

Zhang, P., Song, X., Zhang, Y., Zhu, J., Shen, H., and Yu, Z. (2022). Assessing the effect of modified clay on the toxicity of *Karenia mikimotoi* using marine medaka (*Oryzias melastigma*) as a model organism. *Toxics* 10 (3), 1–19. doi: 10.3390/jmse9080822

Zhang, X., Wang, X., and Yan, B. (2021). Single and combined effects of phenanthrene and polystyrene microplastics on oxidative stress of the clam (*Mactra veneriformis*). *Sci. Total Environ.* 771, 144728. doi: 10.1016/j.scitotenv.2020.144728

Zou, Y., Xu, Q., Zhang, G., Wang, Y., Liu, C., Zheng, H., et al. (2017). Review on the joint toxicity of microplastics and pesticide pollution. *Asian J. Ecotoxicol.* 4, 25–33. doi: 10.7524/AJE.1673-5897.20170518001

Frontiers in Marine Science

Explores ocean-based solutions for emerging global challenges

The third most-cited marine and freshwater biology journal, advancing our understanding of marine systems and addressing global challenges including overfishing, pollution, and climate change.

Discover the latest Research Topics

See more →

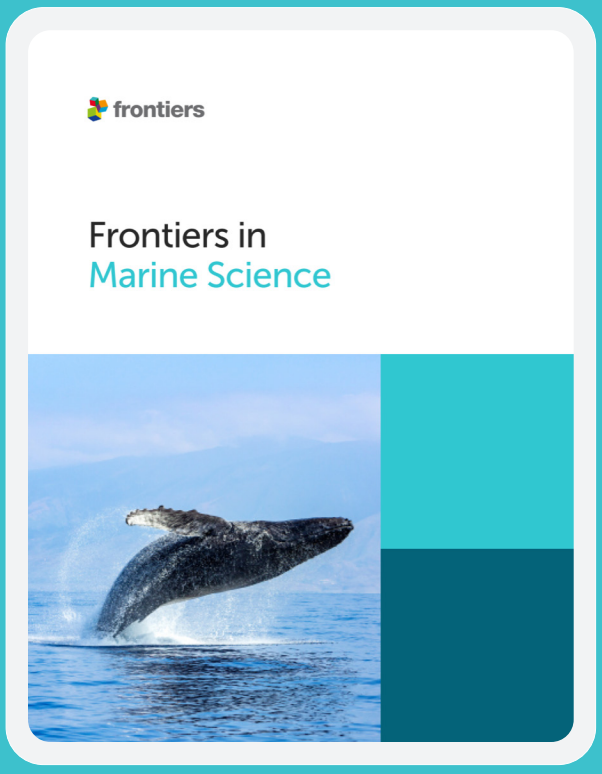

Frontiers

Avenue du Tribunal-Fédéral 34
1005 Lausanne, Switzerland
frontiersin.org

Contact us

+41 (0)21 510 17 00
frontiersin.org/about/contact